87

Advances in Biochemical Engineering/Biotechnology

Series Editor: T. Scheper

Advances in Biochemical Engineering/Biotechnology

Series Editor: T. Scheper

Recently Published and Forthcoming Volumes

Recent Progress of Biochemical and Biomedical Engineering in Japan II
Volume Editor: Kobayashi, T.
Vol. 91, 2004

Recent Progress of Biochemical and Biomedical Engineering in Japan I
Volume Editor: Kobayashi, T.
Vol. 90, 2004

Physiological Stress Responses in Bioprocesses
Volume Editor: Enfors, S.-O.
Vol. 89, 2004

Molecular Biotechnology of Fungal β-Lactam Antibiotics and Related Peptide Synthetases
Volume Editor: Brakhage, A.
Vol. 88, 2004

Biomanufacturing
Volume Editor: Zhong, J.-J.
Vol. 87, 2004

New Trends and Developments in Biochemical Engineering
Vol. 86, 2004

Biotechnology in India II
Volume Editors: Ghose, T. K., Ghosh, P.
Vol. 85, 2003

Biotechnology in India I
Volume Editors: Ghose, T. K., Ghosh, P.
Vol. 84, 2003

Proteomics of Microorganisms
Volume Editors: Hecker, M., Müllner, S.
Vol. 83, 2003

Biomethanation II
Volume Editor: Ahring, B. K.
Vol. 82, 2003

Biomethanation I
Volume Editor: Ahring, B. K.
Vol. 81, 2003

Process Integration in Biochemical Engineering
Volume Editors: von Stockar, U., van der Wielen, L. A. M.
Vol. 80, 2003

Microbial Production of L-Amino Acids
Volume Editors: Faurie, R., Thommel J.
Vol. 79, 2003

Phytoremediation
Volume Editor: Tsao, D. T.
Vol. 78, 2003

Chip Technology
Volume Editor: Hoheisel, J.
Vol. 77, 2002

Modern Advances in Chromatography
Volume Editor: Freitag, R.
Vol. 76, 2002

History and Trends in Bioprocessing and Biotransformation
Vol. 75, 2002

Tools and Applications of Biochemical Engineering Science
Volume Editors: Schügerl, K., Zeng, A.-P.
Vol. 74, 2002

Metabolic Engineering
Volume Editor: Nielsen, J.
Vol. 73, 2001

Biomanufacturing

Volume Editor: Jian-Jiang Zhong

With contributions by
C. Chen · J. Chu · M. B. Gu · H. Honda · B. C. Kim · T. Kobayashi
Y.-M. Koo · A. A. Koutinas · S.-M. Lee · J. Lin · J. Luo · R. J. Mitchell
H. Tabata · Y.-J. Tang · R. Wang · C. Webb · S.-T. Yang · S. Zhang
J.-J. Zhong · Y. Zhuang

Springer

Advances in Biochemical Engineering/Biotechnology reviews actual trends in modern biotechnology. Its aim is to cover all aspects of this interdisciplinary technology where knowledge, methods and expertise are required for chemistry, biochemistry, micro-biology, genetics, chemical engineering and computer science. Special volumes are dedicated to selected topics which focus on new biotechnological products and new processes for their synthesis and purification. They give the state-of-the-art of a topic in a comprehensive way thus being a valuable source for the next 3–5 years. It also discusses new discoveries and applications.

In general, special volumes are edited by well known guest editors. The series editor and publisher will however always be pleased to receive suggestions and supplementary information. Manuscripts are accepted in English.

In references *Advances in Biochemical Engineering/Biotechnology* is abbreviated as *Adv Biochem Engin/Biotechnol* as a journal.

Visit the ABE home page at http://www.springeronline.com

ISSN 0724-6145
ISBN 3-540-20501-2
DOI 10.1007/b95986
Springer-Verlag Berlin Heidelberg New York

Library of Congress Catalog Card Number 72-152360

Springer-Verlag is a part of Springer Science+Business Media

springeronline.com

Printed in Germany

Typesetting: Fotosatz-Service Köhler GmbH, Würzburg
Cover: KünkelLopka GmbH, Heidelberg; design & production GmbH, Heidelberg

Printed on acid-free paper 02/3020mh – 5 4 3 2 1 0

Series Editor

Professor Dr. T. Scheper

Institute of Technical Chemistry
University of Hannover
Callinstraße 3
30167 Hannover, Germany
E-mail: scheper@iftc.uni-hannover.de

Volume Editor

Professor Dr. Jian-Jiang Zhong

State Key Laboratory of Bioreactor Engineering
East China University of Science and Technology
130 Meilong Road
Shanghai 200237, China
E-mail: jjzhong@ecust.edu.cn

Editorial Board

Advances in Biochemical Engineering/Biotechnology Also Available Electronically

For all customers who have a standing order to Advances in Biochemical Engineering/Biotechnology, we offer the electronic version via SpringerLink free of charge. Please contact your librarian who can receive a password for free access to the full articles by registering at:

http://www.springerlink.com

If you do not have a subscription, you can still view the tables of contents of the volumes and the abstract of each article by going to the SpringerLink Homepage, clicking on "Browse by Online Libraries", then "Chemical Sciences", and finally choose Advances in Biochemical Engineering/Biotechnology.

You will find information about the

– Editorial Board
– Aims and Scope
– Instructions for Authors
– Sample Contribution

at http://www.springeronline.com using the search function.

Attention all Users of the "Springer Handbook of Enzymes"

Information on this handbook can be found on the internet at
http://www.springeronline.com

A complete list of all enzyme entries either as an alphabetical Name Index or as the EC-Number Index is available at the above mentioned URL. You can download and print them free of charge.

A complete list of all synonyms (more than 25,000 entries) used for the enyzmes is available in print form (ISBN 3-540-41830-X).

Preface

Biomanufacturing refers to the production of therapeutic proteins in living cells, which can be mammalian, yeast, insect or bacterial cells. The task of a biomanufacturing industry is to develop cost-effective and reproducible biomanufacturing processes. The biopharmaceutical industry is expanding very rapidly, fueled by major advances in the speed of drug discovery (such as genomics technology) and the advent of new, more powerful drugs derived from the sequencing of the human genome. There is a great need for the development of a biotechnology curriculum for the biomanufacturing industry. In this volume, the original biomanufacturing concept is extended by including various production processes such as traditional fermentation and cell culture processes. All chapters reflect recent development in bioproducts manufacturing and bioprocesses for the benefit of human beings.

Historically, medicinal plants and mushrooms have been shown to have profound health promoting benefits, and recent studies are now confirming their medical efficacy and identifying many of the bioactive molecules. Submerged cultivation of plant cells and mushrooms has significant industrial potential while its success on a commercial scale depends on cost compared with existing technology. Chapter 1 describes production of an anticancer drug paclitaxel by utilizing the advantages that plant cells catalyze multiple-step reactions of secondary metabolite biosynthesis and selectively synthesize chiral compounds with polycyclic structures. Several signal transducers such as jasmonates and ethylene inhibitors were used to regulate paclitaxel biosynthesis. In a large-scale culture of *Taxus x media* cells using a two-stage process, the paclitaxel production reached 295 mg per liter. Advances in submerged cultures of mushrooms by taking *Ganoderma lucidum*, which is a popular folk and an oriental medicine used to treat many diseases, as a typical example, are demonstrated in Chapter 2. Its content covers key factors affecting metabolite production, new strategies for enhancing the process efficiency, novel process scale-up as well as modeling.

It is evident that monoclonal antibodies (MAb) are widely used in biomedical research and diagnostics. There are about 25 thousand MAb being produced by cell lines or clones obtained from animals that have been immunized with corresponding antigens. There is a major concern that the current industrial capacity for MAb production may be insufficient to meet the fast growing market for antibody-based therapeutic products. A fibrous-bed bioreactor originally developed for microbial cells was proposed to cultivate hybridoma cells

for long-term continuous production of MAb (Chapter 3). A high MAb productivity of 6.5 gram per liter per day was reached in a repeated batch culture and a good potential of the reactor system for industrial animal cell culture was suggested.

As we know, whether in cell cultures and traditional fermentation processes, there is a close interaction among molecular, cellular and process engineering aspects. This issue so called as multi-scale problems is discussed in Chapter 4 with a focus on industrial fermentation processes. The optimization methodology for studying multi-scale problems in fermentation based on parameter correlation and the scale-up technique for regulating multi parameters in bioprocesses are demonstrated via a couple of typical processes such as penicillin, erythromycin, chlortetracycline, inosine and guanosine fermentation, as well as production of recombinant human serum albumin and a malaria vaccine. In another aspect, because a huge number of biological reactions is always working in intracellular space, the control of such a process is very complicated in deed (Chapter 5). Using the knowledge and experiences of skilled operators (experts) for the process control, fuzzy control was successfully applied to practical industrial productions including pravastatin precursor, vitamin B2, and Japanese sake mashing process in Japan. Furthermore, fuzzy neural network was interestingly proven applicable to biomedical research area such as modeling of complicated causality between electroencephalogram or gene expression profiling data and prognostic prediction.

Related with operation of bioproducts manufacturing processes, environmental protection should never be neglected. It is common knowledge that sustainable development and green processing is essential for the sake of humanity. Increasing efforts are being made to recycle organic waste because of environmental concerns, governmental regulations and economic considerations. The paper sludge generated by waste water treatment unit of paper mills is currently a major concern of the paper industry in many countries. Chapter 6 shows the production of lactic acid from paper sludge using simultaneous saccharification and fermentation (SSF). Compared to batch SSF, the SSF of paper sludge with intermittent feeding produced more lactic acid (162 gram per liter) with a yield of 74% and a productivity of 1.4 gram per liter per hour. A simulated moving bed process was successfully used to separate lactic acid and acetic acid. In Chapter 7, a process leading to the production of a generic fermentation feedstock from wheat was devised and evaluated in terms of efficiency and economics. The process operating cost was estimated to be dependent on the plant capacity, cereal market price, presence and market value of added-value byproducts, labour costs and mode of processing. As human activities have without a doubt had a negative impact on the environment, resulting in the contamination of water, the atmosphere and soil, monitoring and quantifying the degree of pollution is critical. Chapter 8 reviews various whole cell-based biosensors developed using numerous native and recombinant biosensing cells. The application of whole-cell based biosensors to different environmental media is summarized, with distinct attention given to their use in the detection of various stressors including dioxins, endocrine disrupting chemicals and ionizing radiation.

I would like to thank all of the authors for their contributions to this book. The kind advice and much help from Professor Thomas Scheper, Dr. Marion Hertel, Mrs. Ulrike Kreusel and Mrs. Birgit Münch are greatly appreciated. I also acknowledge the support by the National Natural Science Foundation of China (Project no. 20225619) and Cheung Kong Scholars Program of the Ministry of Education of China.

Shanghai, February 2004 Jian-Jiang Zhong

Contents

Adv Biochem Engin/Biotechnol (2004) 7: 1–23
DOI 10.1007/b13538

Paclitaxel Production by Plant-Cell-Culture Technology

Homare Tabata

Life Science Laboratory, Mitsui Chemicals, Inc. 1144, Togo, Mobara-shi, Chiba 297–0017, Japan
E-mail: Homare.Tabata@mitsui-chem.co.jp

Abstract Plant cells catalyze multiple-step reactions of secondary metabolite biosynthesis, and selectively synthesize chiral compounds with polycyclic structures. Taking advantage of this characteristic, we studied the production of the anticancer drug paclitaxel, which is currently produced in limited supply. Callus culture investigations indicate that woody plant medium supplemented with 10^{-5} mol L^{-1} 1-naphthylacetic acid and without the NH_4^+-type ion is the best condition for growth of the callus. The accumulation of paclitaxel and related taxanes in *Taxus* plants is thought to be a biological response to specific external stimuli. Several signal transducers were screened; taxane biosynthesis was strongly promoted by methyl jasmonate (MeJA) and silver thiosulfate (STS) as an anti-ethylene compound. Of ten taxane-type diterpenoids isolated from *T. baccata* suspension-cultured cells treated with MeJA, five have a phenylisoserine side-chain at the C-13 position of the taxane skeleton. Time-course analysis revealed two regulatory steps in taxane biosynthesis: the taxane-ring formation step and the acylation step of the C-13 position. Methyl jasmonate promoted the formation of the taxane-ring. The production of paclitaxel reached a maximum level of 295 mg L^{-1} in a large-scale culture of *T. x media* cells using a two-stage process.

Keywords *Taxus* · Paclitaxel · Taxane · Methyl jasmonate · Silver thiosulfate

List of Abbreviations

MeJA Methyl jasmonate
JA Jasmonic acid
NAA 1-Naphthylacetic acid
ACC 1-Aminocyclopropane-1-carboxylic acid
STS Silver thiosulfate
GGPP Geranylgeranylpyrophosphate
DO Dissolved oxygen
HPLC High-performance liquid chromatography
TPS Tuberose polysaccharides

1 Introduction

Paclitaxel, a complex diterpenoid, has been identified in the bark of *Taxus brevifolia* [1]. Paclitaxel and related taxanes have received considerable attention because of their potential antitumor activity against a variety of tumors, e.g. breast cancer, ovarian cancer, AIDS-related Kaposi's sarcoma, and non-small cell lung cancer [2]. Their mechanism of action, tubulin stabilization by promoting the assembly of microtubules and inhibiting their disassembly, is unique [3]. It was recently reported that paclitaxel has another molecular target besides tubulin; it specifically binds to Bcl-2, a human protein that prevents cells from undergoing apoptosis, providing another potential mechanism by which paclitaxel acts [4]. Paclitaxel and other taxane derivatives might be useful for inhibiting P-glycoprotein, a pump protein responsible for multidrug resistance in tumors [5–7]. Two taxane-type anticancer drugs have been launched – paclitaxel and docetaxel (Fig. 1). In 2000, Bristol–Myers Squibb reported $18.2 billion in annual global sales; three products including paclitaxel exceeded $1.5 billion in annual sales. Current sales of paclitaxel and related taxanes are expected to exceed $2 billion. The history of paclitaxel is summarized in Table 1.

Extraction from natural and cultivated plants, plant cells, and tissue cultures, total synthesis, and semi-synthesis utilizing biosynthetic intermediates are the methods currently used to supply useful compounds isolated from plant sources. It is not realistic, however, to supply paclitaxel by extraction from natural sources because the *Taxus* species plant grows very slowly, and the paclitaxel content is only 0.01% of the dry weight of the bark, in which accumulation is highest [8]. A 100-year-old yew tree might yield just 300 mg of the compound. Other species and other parts of *Taxus* trees also produce paclitaxel and related taxanes [8, 9]. Although paclitaxel has been supplied commercially by semisynthesis using 10-deacetylbaccatin III (Fig. 1) from the needles of *T. wallichiana*, *Taxus* trees have to grow for a long time, which led to a high risk of damage due to weather stress and thus a fluctuating paclitaxel content. Several reports indicate extensive damage to native *Taxus* populations in both China and India resulting from harvesting practices in order to supply paclitaxel and its semisynthetic precursors [10–13]. Total synthesis of paclitaxel has been achieved, but it is not a realistic method of supply because of the cost [14, 15].

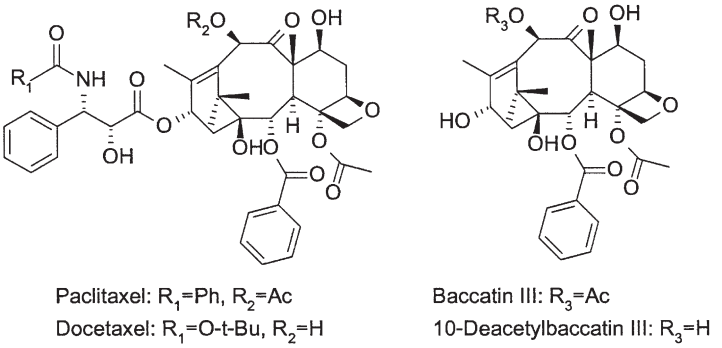

Fig. 1 Structures of paclitaxel, docetaxel, and their biosynthetic intermediates baccatin III and 10-deacetylbaccatin III

Table 1 Paclitaxel history

Year	Events
1963	Anti-tumor activity in the extract of *T. brevifolia* bark tissue was discovered during large-scale screening of 35,000 plants.
1971	Paclitaxel was identified as the active component of anti-tumor activity.
1979	Paclitaxel's unique mechanism, i.e. tubulin stabilization, was identified.
1983	NCI began conducting clinical trials of paclitaxel's safety and its effectiveness against various types of cancer.
1989	Paclitaxel produced partial or complete responses in 30% of previously treated patients with advanced ovarian cancer.
1991	Bristol–Myers Squibb Company is selected by the NCI to be its commercial partner in developing TAXOL injection and signs a CRADA with the NCI.
1992	FDA approved the use of paclitaxel for refractory ovarian cancer. Clinical trials using paclitaxel demonstrated that the drug is effective against advanced breast cancer.
1993	Bristol–Myers Squibb Company ends *T. brevifolia* bark harvesting for the manufacture of TAXOL and begins to develop other renewable sources for the drug.
1994	FDA approved the use of paclitaxel for breast cancer that has recurred within 6 months of completion of initial chemotherapy and for metastatic breast cancer that is not responding to combination chemotherapy.
1995	The semisynthetic form of paclitaxel receives clearance for marketing from the FDA.
1997	FDA approved semisynthetic TAXOL for the second-line treatment of AIDS-related Kaposi's sarcoma. Paclitaxel produced by plant cell culture was approved in Korea and was exported as Genexol by Samyang Genex.
1998	FDA approved semisynthetic TAXOL in combination with cisplatin for first-line treatment of advanced carcinoma of the ovary.
1999	FDA approved semisynthetic TAXOL in combination with cisplatin for first-line treatment of non-small cell lung cancer in patients who are not candidates for potentially curative surgery and/or radiation therapy.

Compared with these methods, plant-cell culture is well-suited to commercial production of paclitaxel. *Taxus* cell culture eliminates the use of the limited natural resource of *Taxus* species, and can provide a stable supply of paclitaxel. Research on the production of paclitaxel and related taxanes has been conducted using species such as *T. brevifolia* [16–18], *T. baccata* [19], *T. cuspidata* [20–24], *T. chinensis* [25–28], *T. canadensis* [23], *T. yunnanensis* [29], and *T. x media* (a cross of *T. baccata* and *T. cuspidata*) [30–32]. Several factors, for example jasmonates, which are listed as chemical and fungal elicitors, up-regulate taxane production.

Two commercial companies, Phyton and Samyang Genex, now produce paclitaxel and related taxanes by large-scale fermentation. Phyton and Bristol–Myers Squibb have been collaborating to establish the commercial feasibility of plant-cell fermentation technology since 1993. In 2002, Phyton announced it had extended its business relationship with Bristol–Myers Squibb by signing a long-term, multimillion-dollar deal to supply paclitaxel. They operate the world's largest facility dedicated to plant-cell fermentation; the capacity is 75,000 L.

2
Undifferentiated cultures

2.1
Callus cultures

Calluses are a proliferating mass of undifferentiated cells. Generally speaking, the selection of the explant species and tissue is important for the production of high taxane-producing calluses. Paclitaxel isolation began with ethanol extraction of *T. brevifolia* bark tissues, because cytotoxic activity was observed in a sample (PR-4960) of stem and bark whereas there was no activity in a sample (PR-4959) of stem and fruit in the USDA collection. Analytical studies of the paclitaxel content of various *Taxus* plant tissues indicate that high levels of paclitaxel are contained in bark tissues.

To form calluses, we selected other proliferous tissues in *Taxus* plants. The paclitaxel content of needles is higher than that of stems, wood, and roots [33]. Furthermore, the paclitaxel content of young needles collected within 2 months after growing new needles and stems is higher than that from old needles and young/old stems. Thus, young needle tissue was selected for callus formation.

The basal medium best suited for cell growth was then screened from 18 mediums used for woody plants, i.e. LS [34], WS [35], CD [36], WP [37], AC [38], IS [39], White [40], Nitch and Nitch [41], SH [42], DK [43], LP [44], BTM [45], Anderson [46], GD [47], B5 [48], Harvey [49], Slankis [50], and SSS [51]. The callus obtained by use of LS medium supplemented with 10^{-5} mol L^{-1} 1-naphthylacetic acid (NAA) turned brownish and its growth was immediately stopped. A whitish callus was collected from the other media, disked (∅6×1 mm), then cultured for 21 days on basal medium. After cultivation, the volume increase was calculated from the numbers of colonies and their sizes.

The results indicated that WP medium was the most suitable basal medium (Fig. 2) and the total concentration of NO_3^- suitable for cell growth was approxi-

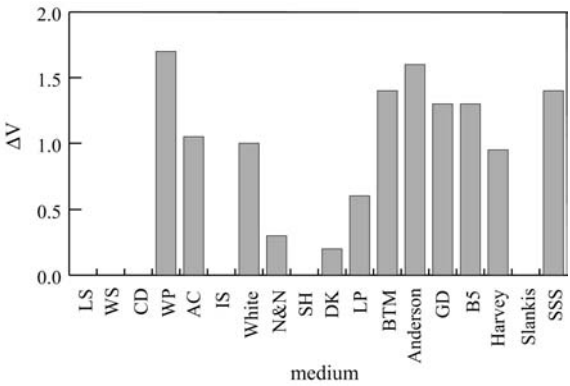

Fig. 2 Comparison of cell proliferation under each basal medium conditions. The volume of increase (ΔV) was calculated by use of the equation $\Delta V = \Sigma 4\pi r^3/3n$ where r is the radius and n the number of colonies

mately 10 mmol L^{-1}. Furthermore, 20 mmol L^{-1} NO_3^- as total nitrate ion was the best concentration for cell proliferation.

2.2 Suspension cultures

Plant-cell-suspension cultures are usually induced from established callus cultures by transferring the callus into liquid medium suitable for cell growth in a suspension. The medium established in callus cultures was basically liquid, and the volume of some of the components was increased or decreased to optimize suspension cell growth.

Suspension cultures of many *Taxus* species were established, and the paclitaxel content in established cell-suspension culture lines was compared. The growth of most *Taxus* species explant is very slow. Unexpectedly, the proliferation of suspended cells was also slow, i.e. three- to five-fold growth in 21 days, in comparison with other plant species. Phenolic compounds, and products of their oxidation, inhibit a variety of enzyme activity, causing damage to cell metabolism [52]. When we first transferred a callus to autoclaved liquid medium that included 3% sucrose, it induced cell darkening. Thereafter, medium solutions were autoclaved before adding the sucrose and the sucrose solution was filtered through a 0.22-μm membrane. After the proliferation of suspension cells was confirmed in small-scale cultures, the culture was slowly scaled-up.

3 Factors regulating paclitaxel biosynthesis

Generally, when plant cells perceive environmental changes via specific receptors or perception mechanisms, they generate biological responses by specific signal-transduction mechanisms. The accumulation of paclitaxel and related taxanes in *Taxus* plants is thought to be a biological response to specific external stimuli

such as natural hormones, nutrients, chemical and fungal elicitors, lights, and wounding stresses. We screened several signal transducers, including plant hormones, polyamines, and chemical and fungal elicitors, for their ability to induce taxane production. Taxane production was strongly promoted by methyl jasmonate (MeJA) and silver thiosulfate (STS).

3.1 Methyl jasmonate and its analogs

Jasmonates have an important role in signal-transduction processes that regulate defense-related genes in plants [53]. These gene products, for example phenylalanine ammonia lyase [54], proteinase inhibitors [53], are basic pathogenesis-related proteins [55, 56] that are mainly involved in healing damaged tissues and in protecting the undamaged tissues against pathogen infection or insect proteases. Activation of these genes by jasmonates often occurs in both wounded and unwounded tissues. Endogenous jasmonic acid (JA) levels increase in response to external stimuli such as wounding, mechanical forces, and pathogen attack [57–60]. Jasmonates also induce the production of some secondary metabolites such as alkaloids in *Catharanthus roseus* and Cinchona seedlings [61], anthocyanins in soybean seedlings [62], rosmarinic acid in *Lithospermum erythrorhizon* cell-suspension cultures [63], sesquiterpene phytoalexin capsidiol in tobacco cell-suspension cultures [64], momilactone A in rice cell-suspension cultures [65], β-thujaplicin in *Cupressus lusitanica* cell-suspension cultures [66], saikosaponin in *Bupleurum falcatum* root cultures [67], and aflatoxin B1 in *Aspergillus parasiticus* [68].

Our screening of stimulants for taxane production indicated that MeJA enhanced the production of paclitaxel and related taxanes. Other stimulators such as abscisic acid and salicylic acid had no effect on the cell growth and the production of taxanes. In contrast, MeJA stimulated the production of taxanes and inhibited cell growth. Paclitaxel accumulated in a dose-dependent manner, with maximal induction at 100 µmol L^{-1} MeJA (Fig. 3a). MeJA promoted the accumulation of paclitaxel and baccatin III (Fig. 1) more strongly than the accumulation of cephalomannine. Jasmonates inhibit the growth of seedlings [69, 70], roots [71], and cell division [72–74]. At 100 µmol L^{-1}, MeJA inhibited the growth by 20 and 25% in *T. x media* suspension cultures. The productivity of paclitaxel reached 110 mg L^{-1} in 14 days.

Cell yield and taxane production in cell-suspension cultures of *T. baccata*, *T. brevifolia*, and *T. x media* are compared in Table 2. After treatment with MeJA the taxane content of each cell culture increased, but the level of the response to MeJA treatment was different in each culture. In control cultures, i.e. cultures that did not contain MeJA, *T. x media* cultures produced the highest taxane levels. In contrast, *T. baccata* and *T. brevifolia* cultures produced little taxane. *T. x media* and *T. baccata* cultures treated with 100 µmol L^{-1} MeJA, produced the highest paclitaxel levels (*T. x media*, 0.606%, 110.3 mg L^{-1} in 14 days), and the highest baccatin III levels (*T. baccata*, 0.245%, 53.6 mg L^{-1} in 14 days). The increase in MeJA-induced taxane in *T. brevifolia* cultures was smaller.

MeJA induces production of paclitaxel in suspension cultures of *T. cuspidata* [21] and *T. canadensis* [23]. Mirjalili et al. examined the kinetics of paclitaxel

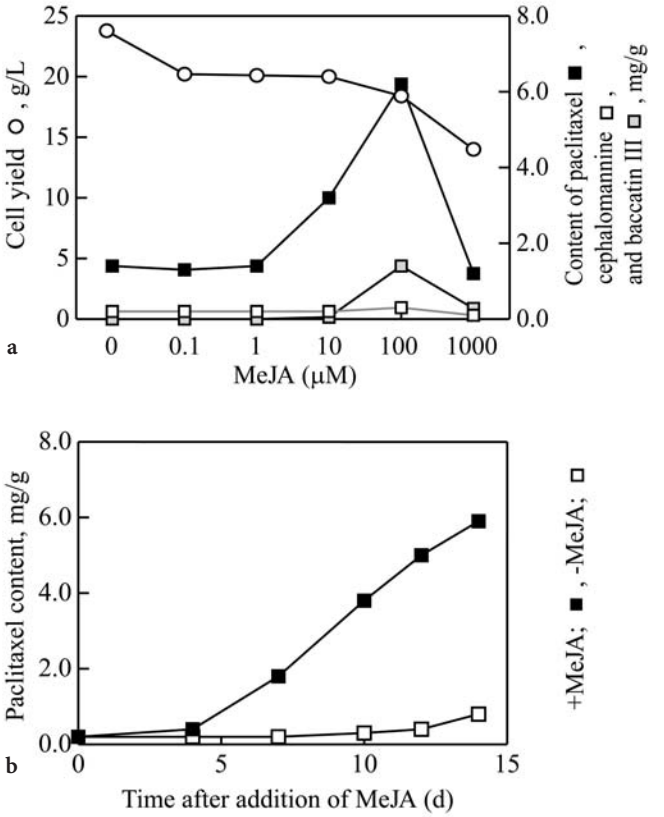

Fig. 3 **a** Effects of MeJA on cell yield and taxane content in cell-suspension cultures of *T. x media*. Each concentration of MeJA was added to the cultures in 2.5 mmol L^{-1} of ethanol mL^{-1} culture medium just after cell inoculation. The cultures were then incubated for 14 days. Data are means of triplicate determinations. **b** Time-course of paclitaxel production in cell-suspension cultures of *T. x media* treated with 100 μmol L^{-1} MeJA

Table 2 Comparison of production of taxanes among *Taxus* species

Species	MeJA (μmol L^{-1})	Cell yield (g L^{-1})	Paclitaxel		Baccatin III	
			(%)	(mg L^{-1})	(%)	(mg L^{-1})
T. baccata	0	24.7±0.7	0.002±0.000	0.4±0.0	0.002±0.000	0.4±0.0
	100	21.0±0.4	0.229±0.009	48.3±2.5	0.245±0.009	53.6±2.2
T. brevifolia	0	18.5±0.4	0.001±0.000	0.2±0.0	n.d.	n.d.
	100	14.6±0.3	0.004±0.000	0.5±0.1	0.005±0.000	0.8±0.1
T. x media	0	23.6±0.2	0.120±0.009	28.2±2.4	0.007±0.000	1.6±0.1
	100	18.2±0.5	0.606±0.022	110.3±4.9	0.139±0.015	25.2±2.6

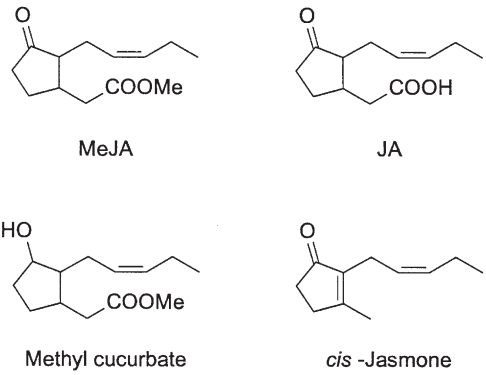

Fig. 4 Structures of MeJA-related compounds

production for different concentrations and combinations of MeJA and ethylene in *T. cuspidata* cultures. Paclitaxel production increased from 0.2 to 3.4 mg L^{-1} after 51 h on treatment with 10 µmol L^{-1} MeJA and 5 ppm ethylene. Treatment with only 10 µmol L^{-1} MeJA increased paclitaxel productivity to 2.7 mg L^{-1}. Ketchum et al. demonstrated the greatest accumulation of paclitaxel, 117 mg L^{-1} within 5 days after adding MeJA to cultures at a final concentration of 200 µmol L^{-1} on day 7 of the culture cycle in *T. canadensis* cultures (C93AD cell line). Furthermore, paclitaxel production due to MeJA treatment was different not only among species but also among cell lines within species. Each cell line required an optimum concentration of MeJA and/or culture conditions. Selection of the highest-responding cell line is more important than selection of the highest responding species.

To determine the structural requirements for promoting paclitaxel production, MeJA-related compounds were added separately to *T. x media* cultures (Fig. 4). Methyl cucurbate and *cis*-jasmone had less effect on cell yield than MeJA and had weak paclitaxel-promoting activity. In contrast, (±)-JA had the strongest activity, almost equal to that of MeJA (Table 3). The results indicate that at least two parts of the MeJA structure are important for the activity – substitution by acetic acid or its ester at the C-1 position and a keto group at the C-3 position.

Table 3 Effects of MeJA-related compounds on cell yield and paclitaxel production in cell-suspension cultures of *T. x media*

Chemical (g L^{-1})	Cell yield (mg L^{-1})	Paclitaxel production (%)	Promoting activity
Control	23.0±0.3	33.0±13.3	0.0
MeJA	15.8±0.6	104.2±8.3	100.0
(±)-JA	18.7±1.2	110.1±9.5	108.3
Methyl cucurbate	20.8±1.2	60.4±9.1	38.4
cis-Jasmone	23.7±0.5	34.0±6.2	1.4

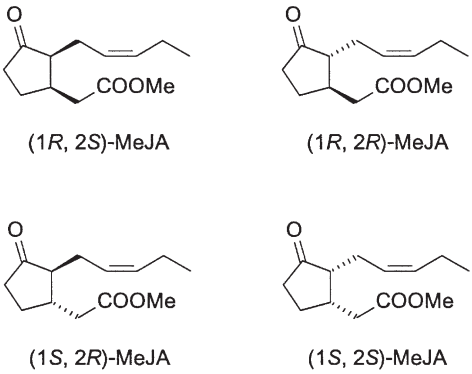

Fig. 5 Structures of four stereoisomers of MeJA

These structural requirements for paclitaxel-promoting activity are similar to those reported for the tuber-inducing activity of compounds in potato plants [75] and for the senescence-promoting activity assayed in oat leaves [76]. *cis*-Jasmone is a well-known component of plant volatiles and its release can be induced by damage such as insect herbivory. Birkett et al. reported that *cis*-jasmone increased levels of (*E*)-β-ocimene production as a result of properties different from those of MeJA [77]. Although *cis*-jasmone has no significant effect on paclitaxel production, it might induce the production of other reported compounds.

MeJA contains two asymmetric centers (C-1 and C-2) that can have *R* or *S* configurations, resulting in four possible stereoisomers (Fig. 5). Commercially available MeJA is a mixture of approximately 5% each of the (1*R*,2*S*)- and (1*S*,2*R*)-*cis* isomers and 45% each of the (1*R*,2*R*)- and (1*S*,2*S*)-*trans* isomers [78]. Yukimune et al. separated these isomers using high-performance liquid chromatography (HPLC) and reported that (1*R*,2*R*)-MeJA had the greatest paclitaxel and baccatin III-promoting activity [79]. (In the original paper, the carbon position number in MeJA was written in relation to the linolenic acid position.) There have been several studies of the biosynthesis of JA [80–84]. (1*R*,2*R*)-JA was biosynthesized from linolenic acid via (1*R*,2*S*)-JA, and was highly stable compared with the (1*R*,2*S*) isomer. The side-chain at the C-2 position on the (1*R*,2*S*) isomer is located on the α-position of the keto group, therefore (1*R*,2*S*)-JA is isomerized to (1*R*,2*R*)-JA.

3.2 Ethylene inhibitors

Among the cultures tested, *T. x media* cultures produced the highest taxane levels (paclitaxel; 0.120%, 28.2 mg L^{-1} in 14 days). In contrast, *T. baccata* cultures produced little (paclitaxel; 0.002%, 0.4 mg L^{-1} in 14 days). This productivity difference was not because of culture medium components or the culture periods. Another important consideration in the culture conditions was the gas components in the headspace of the culture flasks. There have been several studies on the various physiological responses to ethylene. Xu et al. reported that plant de-

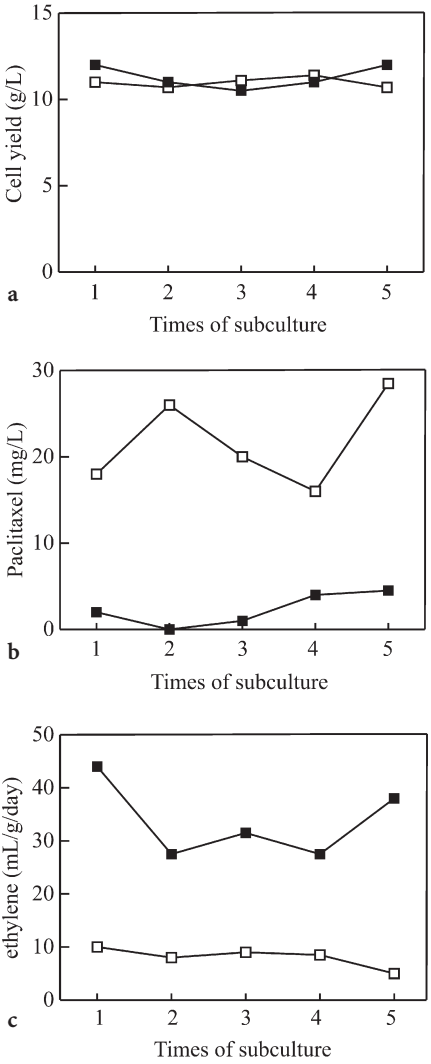

Fig. 6 **a** Stability of cell yield, **b** paclitaxel production, and **c** ethylene evolution in cell-suspension cultures of *T. baccata* and *T. x media*. The cells were subcultured at 14-day intervals and each value was determined on day 14 after inoculation. *Open squares*, *T. x media*; *closed squares*, *T. baccata*

fense genes such as PR-1b and osmotin were synergistically induced by ethylene and MeJA in tobacco seedlings [85]. Ethylene and MeJA induction also resulted in osmotin protein accumulation to levels similar to those induced by osmotic stress. Oldroyd et al. reported that ethylene inhibited the Nod factor signal-transduction pathway in *Medicago truncatula* [86]. In addition, Shoji et al. reported that ethylene suppressed jasmonate-induced gene expression in nicotine biosynthesis [87]. In paclitaxel production in *Taxus* cell-suspension cultures, levels of

ethylene evolution in *T. x media* were consistently three-times higher than in *T. baccata* (Fig. 6) [88]. To assess the possibility of a relationship between ethylene evolution and paclitaxel production, we studied the effect of paclitaxel production by applying Ethrel, an ethylene-releasing agent, to *T. x media* cell-suspension cultures. Paclitaxel production levels decreased, with the amount of inhibition depending on the amount of Ethrel.

Ethylene is derived from L-methionine via *S*-adenosyl-L-methionine and 1-aminocyclopropane-1-carboxylic acid (ACC). ACC is synthesized by ACC-synthase and oxidized by ACC oxidase to ethylene and cyanoformic acid [89, 90]. ACC-synthase is a key enzyme in that ethylene formation is controlled by the expression of ACC-synthase, which can be induced by stress conditions [91–93]. Various kinds of inhibitor, such as aminoethoxyvinylglycine, polyamines, *n*-propyl gallate, and STS, inhibit different reaction steps [94]. Therefore, these inhibitors are candidate inducers of paclitaxel production. The results of feeding experiments indicated that STS promotes paclitaxel production. STS is effective in increasing vase life and preventing bud drop [95]. STS is an ethylene-receptor-binding inhibitor. On the other hand, STS treatment promotes ethylene productivity, because STS activates ethylene biosynthetic pathways [96]. Thus, ethylene does not directly regulate paclitaxel production, but unknown reactions (or compounds) induced by the binding of ethylene to its receptor inhibit the production of paclitaxel in *Taxus* cells.

Pan et al. reported that both the content and production of taxuyunnanine C on suspension cultures of *T. chinensis* were greatly improved by the addition of ethylene [97]. These contrasting results of the effect of ethylene might be due to different cell line properties.

4
Taxanes produced by plant-cell culture

Terpenes [98], sterols [99], flavonoids [100], and lignans [101–103] have been isolated from explants and callus cultures of *Taxus* species. In particular, *Taxus* explants produce not only a taxane-type diterpene – a 6/8/6-membered ring system, to which paclitaxel belongs – but also an 11(15→1)-abeotaxane-type 5/7/6-membered ring system, an 11(15→1),11(10→9)bisabeotaxane-type 5/6/6-membered ring system, a 3,11-cyclotaxane-type 6/5/5/6-membered ring system, a 2(3→20)-abeotaxane-type 6/10/6-membered ring system, and a 3,8-secotaxane-type 6/12-membered ring system [104]. 11(15→1)-Abeotaxanes might be derived from a taxane-type ring system through a Wagner–Meerwein rearrangement of ring A [105], and it has been proposed that 3,11-cyclotaxanes are derived by a concerted $\sigma_s^2+\pi_s^2$ route [106]. 3,8-Secotaxanes might be derived from verticillene by $\Delta^7 \rightarrow \Delta^8$ isomerization [107]. 2(3→20)-abeotaxanes seem to be derived by cyclization of $\Delta^{4(20),7}$-verticillene, which is synthesized from verticillene by $\Delta^3 \rightarrow \Delta^{4(20)}$ isomerization (Fig. 7) [108].

Extracts of *T. baccata* suspension cells treated with MeJA were analyzed by HPLC and liquid chromatography–mass spectrometry. The components of ten major peaks were fractionated and identified by mass spectrometry, ^{1}H and ^{13}C nuclear magnetic resonance, infrared spectral data: 2α,4α-dihydroxy-5β,20-epoxy-1β,7β,9α,10β,13α-pentaacetoxytax-11-ene, 4α,9α-diacetoxy-2α,10β-dibenzoxy-

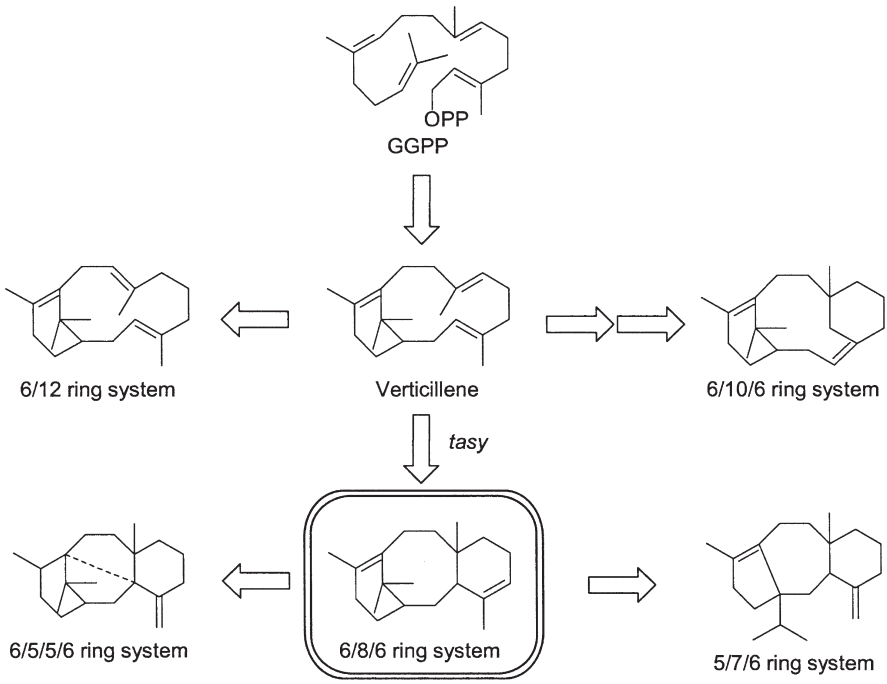

Fig. 7 Hypothetical routes to different ring systems

5β,20-epoxy-1α,7β,13α-trihydroxytax-11-ene, baccatin VI, 10-deacetylbaccatin III, baccatin III, 10-deacetylpaclitaxel, 10-deacetylpaclitaxel C, cephalomannine, paclitaxel, and paclitaxel C, that is, ten products of *Taxus* cell culture that appeared as major peaks on the chromatogram were all classified as taxane-type diterpenes. On the other hand, *Taxus* explants accumulate high concentrations of taxinine, but the results of HPLC analysis indicate that *Taxus* suspension-cultured cells do not produce taxinine. These results clearly indicate that *T. baccata* suspension-cultured cells treated with MeJA mainly produce taxane-type diterpenes. No other detectable diterpenes were produced. The same results were obtained for the production of diterpenes in suspension cultures of *T. x media* treated with MeJA.

Although there have been studies of the production of taxane-type diterpenes such as paclitaxel, baccatin III, and taxuyunnanine C by *Taxus* species cell culture, the production of abeotaxanes in cultured cells is still controversial. Sun et al. reported that 5α,7β,9α,10β,13α-pentahydroxy-4(20),11(12)-taxadiene was converted to two 1(15→11)abeotaxanes (42 and 4% yields) by *Absidia coerula* ATCC 10738a [109]. The partially acetylated substrates 5α,13α-dihydroxy-7β,9α,10β-triacetoxy-4(20),11(12)-taxadiene and 5α-hydroxy-7β,9α,10β-triacetoxy-4(20),11(12)-taxadiene-13-one did not react, however. One interpretation of this finding is that acetyltransferases against the hydroxylated taxanes had high activity in MeJA-treated *Taxus* cells. Actually, polyacetylated taxanes such as baccatin VI were derived from MeJA-treated cells. Another possibility is the biotransforma-

tion of hydroxylated taxanes by mycobionts. A 4(20),11(12)-taxadiene derivative has been converted into an 11(15→1)abeotaxane derivative [110]. Further research is necessary to clarify the correlation between abeotaxane degradation and acetyltransferase activity.

5 Mechanism of paclitaxel production in *T. baccata* cell-suspension cultures

Paclitaxel and related taxanes are classified as diterpenoids, which are C_{20} compounds derived from geranylgeranylpyrophosphate (GGPP). To achieve high production of paclitaxel it is important to determine the regulatory mechanism of paclitaxel production by first clarifying the biosynthetic pathway of endogenous paclitaxel and taxanes produced in *Taxus* cell-suspension cultures. We identified ten taxane compounds derived from *T. baccata* cell-suspension cultures. Of these five had a phenylisoserine side chain at the C-13 position like paclitaxel. There was either a hydroxyl group or an acetoxy group at the C-13 position of the other taxanes.

MeJA-induced paclitaxel production was remarkable in *T. baccata* compared with in *T. x media* or *T. brevifolia*. We therefore checked the time course of taxane production using MeJA-treated *T. baccata* cell-suspension cultures and compared the phenylisoserine side-chain-acylated taxanes with taxanes non-acylated at the C-13 position (Fig. 8).

Regardless of the presence of the phenylisoserine side-chain at the C-13 position, the accumulation of all taxanes increased for 1 week after addition of 100 µmol L^{-1} MeJA. During the second week, the accumulation of taxanes with the phenylisoserine side-chain continued. In contrast, accumulation of non-acylated taxanes containing the phenylisoserine side-chain stopped except for 10-deacetylbaccatin III. In the third week, the accumulation levels of all taxanes without the phenylisoserine side-chain group decreased. In the taxanes with the

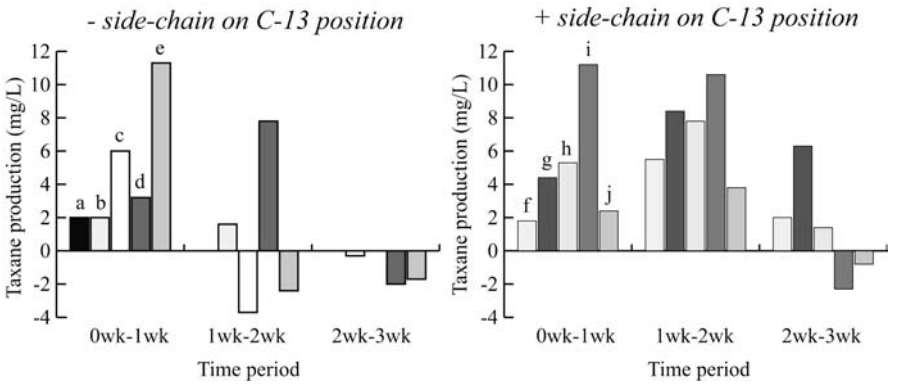

Fig. 8 Time-course of taxane production by MeJA-treated cells. ***a*** 2α,4α-dihydroxy-5β,20-epoxy-1β,7β,9α,10β,13α-pentaacetoxytax-11-ene, ***b*** 4α,9α-diacetoxy-2α,10β-dibenzoxy-5β,20-epoxy-1α,7β,13α-trihydroxytax-11-ene, ***c*** baccatin VI, ***d*** 10-deacetylbaccatin III, ***e*** baccatin III, ***f*** 10-deacetylpaclitaxel, ***g*** 10-deacetylpaclitaxel C, ***h*** cephalomannine, ***i*** paclitaxel, ***j*** paclitaxel C

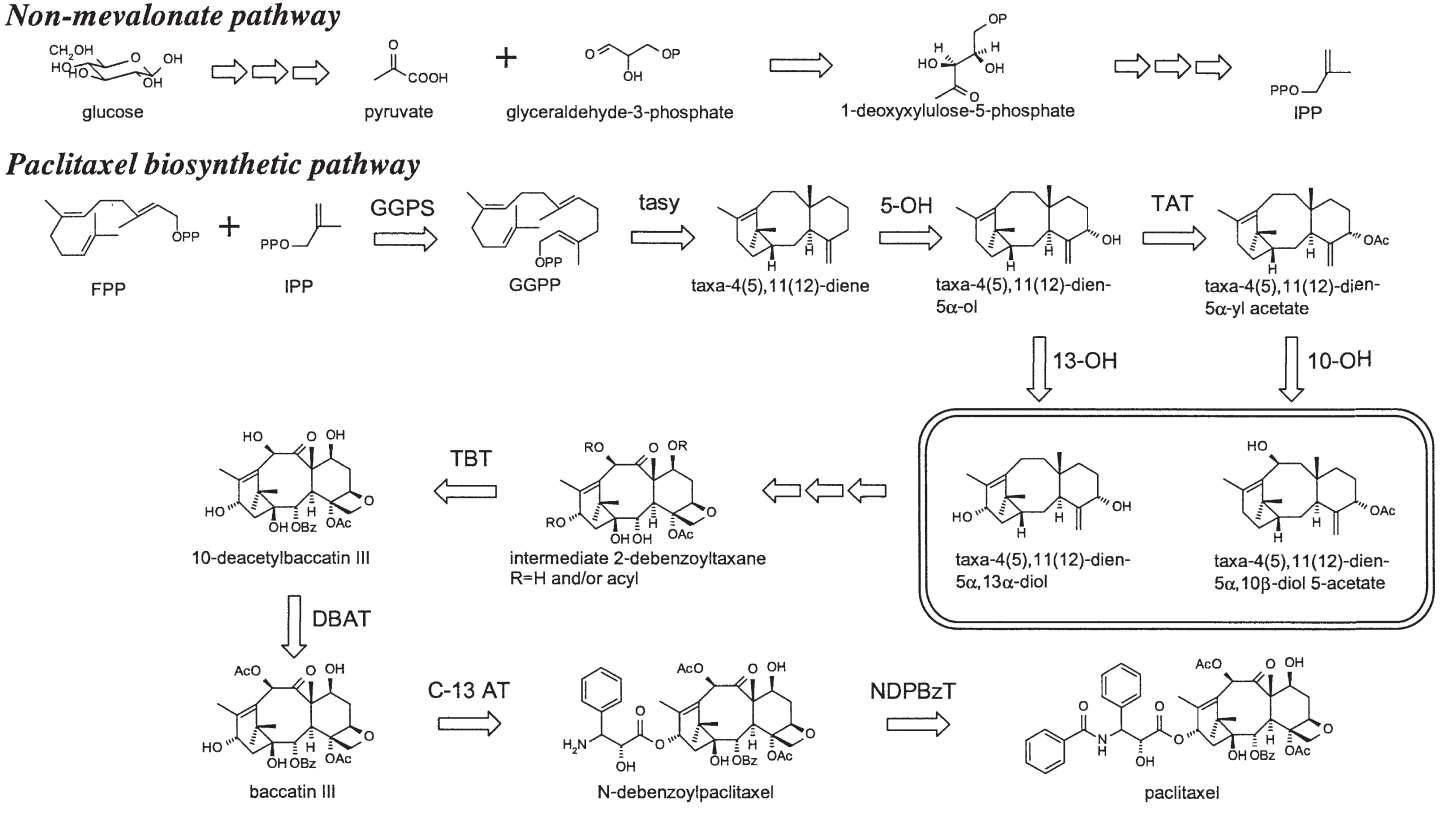

Scheme 1 Biosynthetic pathway of paclitaxel. IPP is synthesized through the non-mevalonate pathway. The taxane skeleton is synthesized by cyclization of GGPP; the genes relating to three steps of hydroxylase reactions and five steps of acyltransferase reactions have been identified. The C-13 phenylisoserine side-chain is synthesized from phenylalanine

phenylisoserine side-chain, the accumulation of 10-deacetylpaclitaxel, 10-deacetylpaclitaxel C, and cephalomannine continued, but the levels decreased, except for those of paclitaxel and paclitaxel C. MeJA stimulates taxane-ring formation and there are two regulatory steps in paclitaxel biosynthesis, i.e. the taxane-ring-formation step and the acylation step of the phenylisoserine side-chain at the C-13 position. Both of these reaction steps were active for 1 week after addition of MeJA, then the activity of taxane-ring formation decreased in contrast with the activity of the acylation step, which continued to be high in the second week and then decreased in the third week.

There have been several studies on the paclitaxel biosynthetic pathway [111–119]. Genes related to the ten steps of paclitaxel biosynthesis have been identified (Scheme 1). In the early steps of the pathway, the supply of GGPP, the universal precursor of diterpenoids, is important for the high production of paclitaxel. In paclitaxel formation GGPP is biosynthesized by electrophilic coupling of farnesyl diphosphate and isopentenyl diphosphate, which are supplied via a non-mevalonate pathway, catalyzed by GGPP synthase. The other important step is the initial cyclization of GGPP by taxadiene synthase to produce taxa-4(5), 11(12)-diene. Hefner et al. reported a rapid increase in steady-state mRNA levels for both GGPP synthase and taxadiene synthase observed 8 h after induction by MeJA, and these levels remained significantly elevated for at least 48 h before declining [111]. After a short induction period the activity levels of both enzymes increased steadily for 48 h, with relatively little change thereafter. For *T. baccata*, GGPP synthase cDNA was cloned and sequenced by polymerase chain reaction-base cloning. Comparison of the deduced amino acid sequence of *T. baccata* and *T. canadensis* GGPP synthases revealed that only two amino acid residues were different from each other in positions unimportant to enzyme activity (Fig. 9).

```
TbGGPS   MAYTAMAAGTQSLQLRTVASYQECNSMRSCFKLTPFKSFHGVNFNVPSLGAANCEIMGHL  60
TcGGPS   ............................................................  60

TbGGPS   KLGSLPYKQCSVSSRSTKTMAQLVDLAETEKAEGKDIEFDFNEYMKSKAVSVDAALDKAI 120
TcGGPS   ............K.................................A.............. 120

TbGGPS   PLEYPEKIHESMRYSLLAGGKRVRPALCIAACELVGGSQDLAMPTACAMEMIHTMSLIHD 180
TcGGPS   ..............................................................  180

TbGGPS   DLPCMDNDDFRRGKPTNHKVFGEDTAVLAGDALLSFAFEHIAVATSKTVPSDRTLRVISE 240
TcGGPS   ............................................................  240
                  I
TbGGPS   LGKTIGSQGLVGGQVVDITSEGDANVDLKTLEWIHIHKTAVLLECSVVSGGILGGATEDE 300
TcGGPS   ............................................................  300

TbGGPS   IARIRRYARCVGLLFQVVDDILDVTKSSEELGKTAGKDLLTDKATYPKLMGLEKAKEFAA 360
TcGGPS   ..........................................................  360
                                  II
TbGGPS   ELATRAKEELSSFDQIKAAPLLGLADYIAFRQN                          393
TcGGPS   ...........................                                393
```

Fig. 9 Amino acid sequence comparison of GGPSs of *T. baccata* and *T. canadensis*. The underlined regions designated I and II are regions that contain highly conserved Asp and Arg residues that have been shown to be important in catalysis [120–123]

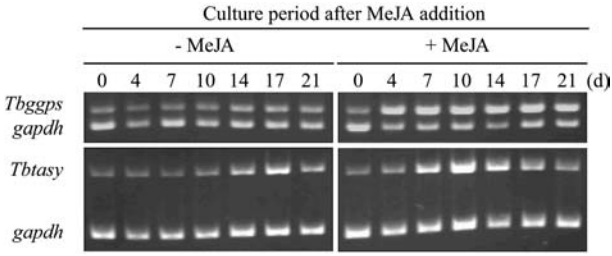

Fig. 10 Effect of MeJA treatment on transcript levels of *Tbggps* and *Tbtasy* in *T. baccata* cell-suspension cultures

The time course of transcriptional levels of GGPP synthase and taxadiene synthase was studied by reverse transcriptase polymerase chain reaction analysis (Fig. 10). The steady-state mRNA level for GGPP synthase increased for 4 days after induction by MeJA, and the level remained constant for at least 21 days. On the other hand, the mRNA level of taxadiene synthase increased 4 days after induction and the level remained significantly elevated for 14 days, then slowly decreased. These results indicate that MeJA induces taxane-ring formation but the transcriptional responses of the biosynthetic genes are different.

6 Large-scale culture

Large-scale plant-cell culture in bioreactors is important technology in the development of a commercial process. The first successful example of commercial production using plant-cell culture technology was shikonin, used as a lipstick component, produced by large-scale culture of *Lithospermum erythrorhizone* suspension cells. In addition, ginseng saponin production by *Panax ginseng* cell culture was developed by Kitasato University and Nitto Denko Corporation, and commercially scaled-up by Nitto Denko in the late 1980s [124]. Over the past few years, there have been several studies of the production of ginseng saponin and polysaccharide in *P. notoginseng* cell-suspension cultures [125–131]. In other cases of commercial production, a research group at Kao reported that suspension culture cells initiated from petals of *Polianthes tuberosa* L. secrete a large amount of polysaccharides (TPS) into the medium. TPS is a basic polymer consisting of Man (*pyranosyl*) and Glc (*pyranosyl*)-UA with side chains of Ara (*furanosyl*) and Gal (*pyranosyl*), and has a high capacity to hold moisture [132]. TPS-containing cosmetics have been available commercially since 1993.

Indeed, shikonin production from cell-suspension cultures of *L. erythrorhizone* and TPS production from cell-suspension cultures of *P. tuberosa* are commercially successful examples, but the total number of successful cases is small, because of the low cost performance, owing to the poor production of useful compounds and the small number of large-scale jar fermenters for plant-cell culture.

6.1
Conditions affecting paclitaxel productivity

For successful large-scale plant-cell-suspension cultures, many factors involved in cell proliferation and the production of useful compounds suitable for large-scale culture must be studied. A major problem is that the conditions required for each plant species differ. Nutrient manipulation and gas composition are particularly important factors for large-scale culture.

In flask-scale culture, selection of the cell line for high production, establishment of the most suitable medium components, including phytohormones, and discovery of stimulators for useful compound production have been studied. In paclitaxel production we selected the *T. x media* cell line, established the most suitable medium by altering the WP medium, and determined that MeJA and STS are the optimum stimulators for paclitaxel production. These materials and conditions must be combined and improved upon for large-scale culture.

The gas composition and the gassing method are important factors for cell viability and useful compound production. Our results indicate that ethylene inhibits paclitaxel production (Figs. 6b, c). There are interactions between the dissolved gases, i.e. ethylene and CO_2. High CO_2 concentrations inhibit ethylene production and ethylene activity [133]. Also, supplementation with CO_2 can maintain a high growth rate of cultured cells [134]. Furthermore, Luo et al. reported that paclitaxel production increased when the dissolved oxygen (DO) level was increased from 20% to 40–60% in a bioreactor with a six-flat-bladed turbine in a cell-suspension culture of *T. chinensis* [135]. In large-scale culture of *Taxus* cells, DO control and CO_2 supplement are very important for high paclitaxel production.

6.2
Culture process

A two-stage culture process has been successful in a number of systems, including production of shikonin [136], anthocyanins [137, 138], and indole alkaloids [139–141]. Thus, we produced a two-stage culture process, i.e. cell proliferation cultures of *Taxus* cells and the MeJA-induced paclitaxel production culture (Fig. 11).

High-density culture is also important for high productivity, leading to low production costs. Thus, the inoculum cell volume was increased from 1 to 3 times

Table 4 High-density culture of *T. x media* cell suspension cultures

Culture apparatus	Relative inoculum size	Cell yield ($g\ L^{-1}$)	Paclitaxel production ($mg\ L^{-1}$)
Shake flask	1	13	90
Jar fermenter	1	13	90
	2	24	190
	3	38	295

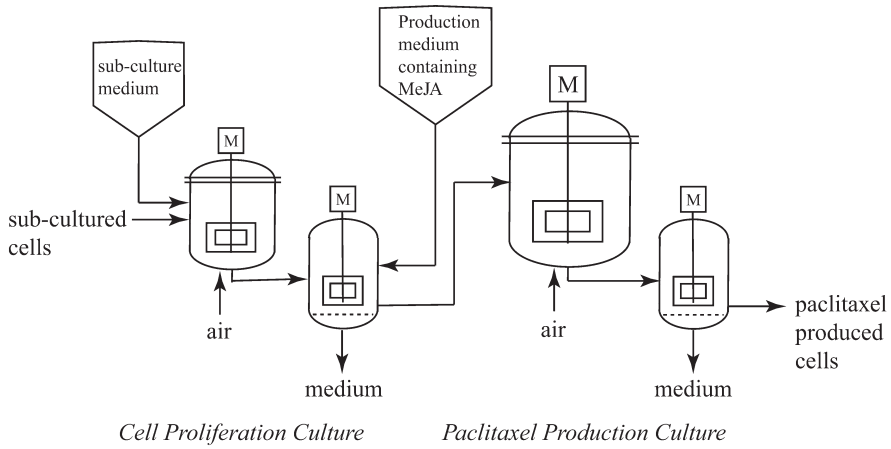

Fig. 11 Two-stage culture process of paclitaxel production

Fig. 12 White precipitate at the bottom of the fermenter

that of the flask-scale culture. The cell volume reached full growth in 14 days; at that time, cell-density was 38 g L^{-1} and the production of paclitaxel in high-densitycultures was three times higher than in normal density cultures (Table 4).

Production of paclitaxel reached 295 mg L^{-1} under high-density culture conditions. Not all of the produced paclitaxel, however, accumulated in the cells. A few days after treatment with MeJA, white precipitates accumulated in the medium. This phenomenon is even more remarkable in a jar fermenter, because white compounds accumulate around the top of the culture medium due to aeration. After the cultivation, cultured medium and cells are transferred to the filter, and the white precipitate remains at the bottom of the fermenter (Fig. 12). The white precipitate consists of taxanes such as paclitaxel, and the concentra-

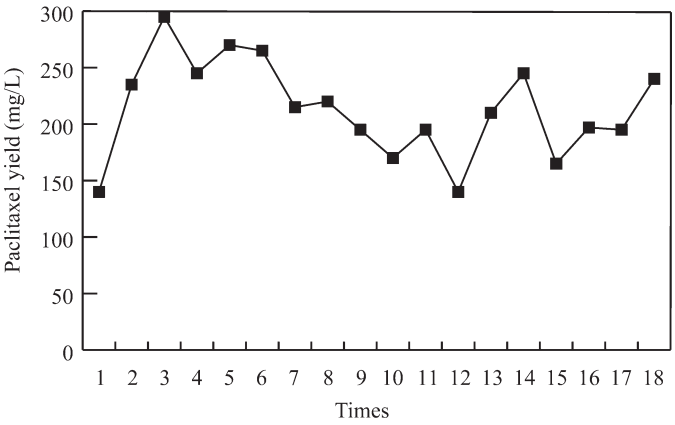

Fig. 13 Variation of yield in 200-L scale production culture

Table 5 Comparison of paclitaxel production in elicited *Taxus* cells

Species	Stimulators	Paclitaxel production (mg L^{-1} day^{-1})	Ref.
T. chinensis	Fungal elicitor	1.5	[28]
T. yunnanensis	La^{3+}	0.4	[29]
T. chinensis	Temperature shift	6.5	[26]
T. canadensis	MeJA	23.4	[23]
T. x media	MeJA	21.1	[32]

tion of paclitaxel in the white precipitate is approximately 30 to 50%. To increase the recovery rate, paclitaxel should be extracted both from the white precipitate and from the cells.

The steady high productivity of paclitaxel is important for commercial purposes. The stability of paclitaxel production under these conditions was studied (Fig. 13). Repeating the cultivation 18 times resulted in stable production of paclitaxel in the range 140 to 295 mg L^{-1}.

Our results indicate that *T. x media* cultured cells produce 21.1 mg L^{-1} paclitaxel per day. This productivity was compared with reported examples (Table 5). Of the few types of stimulator available MeJA is the most effective. MeJA effectively stimulates production of paclitaxel in cell-suspension cultures of several species of the *Taxus* genus. The cell line selected is important for high productivity.

Ketcham et al. recently reported that the 13-acetyl-9-dihydrobaccatin III and baccatin VI produced in elicited cultures accounted for 39 to 62% of the total taxanes [142]. These compounds can serve as precursors of the second-generation paclitaxel derivative 9-dihydropaclitaxel [143, 144].

Acknowledgement The author thanks the Botanical Garden of the Faculty of Agriculture, Hokkaido University, for providing cuttings of *T. baccata* LINN plants, the National Cancer Institute (USA) for providing paclitaxel, baccatin III, and cephalomannine standards, and D.G.I. Kingston of Virginia Polytechnic Institute and State University for providing a standard sample of baccatin III and NMR spectra.

7 References

1. Wani MC, Taylor HL, Wall ME, Coggon P, McPhail AT (1971) J Am Chem Soc 93:2325
2. Rowinsky EK, Cazenave LA, Donehower RC (1990) J Natl Cancer Inst 82:1247
3. Schiff PB, Fant J, Horwitz SB (1979) Nature 277:665
4. Rodi DJ, Janes RW, Sanganee HJ, Holton RA, Makowski L (1999) J Mol Biol 285:197
5. Halder S, Basu A, Croce CM (1997) Cancer Res 57:229
6. Liu Y, Priest DG (1996) Cell Pharmacol 3:405
7. Tang C, Willingham MC, Reed JC, Miyashita T, Ray S, Ponnathpur V, Huang Y, Mahoney ME, Bullock G, Bhalla K (1994) Leukemia 8:1960
8. Whiterup KM, Look SA, Stasko MW, Ghiorzi TJ, Muschik GM, Cragg GM (1990) J Nat Prod 53:1249
9. Vidensek N, Lim P, Campbell A, Carlson C (1990) J Nat Prod 53:1609
10. Dubey KP (1997) Indian Forest 124:1150
11. Rikhari HC, Palni LMS, Sharma S, Nandi SK (1998) Environ Conserv 25:334
12. Su Z, Chen B (1999) Forest Res 12:23
13. Yang L, Xu J, Li L (1999) J Plant Res Env 8:39
14. Holton RA, Somoza C, Kim H-B, Liang F, Biediger RJ, Boatman PD et al (1994) J Am Chem Soc 116:1597
15. Nicolaou KC, Yang Z, Liu JJ, Ueno H, Nantermet PG, Guy RK et al (1994) Nature 367:630
16. Christen AA, Gibson DM, Bland J (1991) US Patent 5019504
17. Gibson DM, Ketchum REB, Christen AA (1993) Plant Cell Rep 12:479
18. Kim J-H, Yun J-H, Hwang Y-S, Byun SY, Kim DI (1995) Biotechnol Lett 17:101
19. Srinivasan V, Pestchanker L, Moser S, Hirasuna TJ, Taticek RA, Shuler ML (1995) Biotechnol Bioeng 47:666
20. Mirjalili N, Linden JC (1995) Biotechnol Bioeng 48:123
21. Mirjalili N, Linden JC (1996) Biotechnol Prog 12:110
22. Fett-Neto AG, Pennington JJ, DiCosmo F (1995) J Plant Physiol 146:584
23. Ketchum RE, Gibson DM, Croteau RB, Shuler ML (1999) Biotechnol Bioeng 62:97
24. Fett-Neto AG, Melanson SJ, Nicholson SA, Pennington JJ, DiCosmo F (1994) Biotechnol Bioeng 44:967
25. Bringi V, Kadkade P (1993) WO93/17121
26. Choi H, Kim S, Son J, Hong S, Lee H, Lee H (2000) Enzyme Microb Technol 27:593
27. Wang HQ, Yu JT, Zhong JJ (1999) Proc Biochem 35:479
28. Wang C, Wu J, Mei X (2001) Appl Microbiol Biotechnol 55:404
29. Wu J, Wang C, Mei X (2001) J Biotechnol 85:67
30. Wickremesinhe ERM, Arteca RN (1993) Plant Cell Tissue Organ Cult 35:181
31. Wickremesinhe ERM, Arteca RN (1994) J Plant Physiol 144:183
32. Yukimune Y, Tabata H, Higashi Y, Hara Y (1996) Nature Biotechnol 14:1129
33. Croom EM Jr (1995) Taxus for taxol and taxoids. In: Suffness M (ed) TAXOL science and applications. CRC Press, New York, p 37
34. Linsmair EM, Skoog F (1965) Physiol Plant 18:100
35. Wolter KE, Skoog F (1966) Am J Bot 53:263
36. Campbell RA, Durzan DJ (1975) Can J Bot 53:1652
37. Lloyd G, McCown B (1981) Int Plant Prop Soc Proc 30:421
38. Ahuja MR (1983) Silvae Genet 32:131
39. Saito A, Ide Y (1985) J Jpn For Soc 67:373

40. White PR (1963) The cultivation of animal and plant cells, 2nd edn. Ronald Press, New York
41. Nitch C, Nitch JP (1967) Planta 72:355
42. Schenk RU, Hildebrandt AC (1972) Can J Bot 50:199
43. Driver JA, Kuniyuki AH (1984) Hort Sci 19:507
44. Aitkin-Cristie J, Thorpe TA (1984) Clonal propagation, gymnosperm. In: Cell culture and somatic cell genetics of plants, vol 1. Academic Press, p 82
45. Chalupa V (1984) Biol Plant 26:374
46. Anderson WC (1984) J Am Soc Hort Sci 109:343
47. Sommer HE, Brown CL, Kormanik PP (1975) Bot Gaz 136:196
48. Gamborg OL, Miller RA, Ojima K (1968) Exp Cell Res 50:151
49. Harvey AE (1967) Can J Bot 45:1783
50. Slankis V (1948) Physiol Plant 1:278
51. Steinhart CE, Standifer LCJ, Skoog F (1961) Am J Bot 48:465
52. Anderson JW (1968) Phytochemistry 7:1973
53. Farmer EE, Ryan CA (1990) Proc Natl Acad Sci USA 87:7713
54. Lawton MA, Lamb CJ (1987) Mol Cell Biol 7:335
55. Memelink J, Linthorst HJM, Schilperoort RA, Hoge JHC (1990) Plant Mol Biol 14:119
56. Brederode FTh, Linthorst HJM, Bol JF (1991) Plant Mol Biol 17:1117
57. Creelman RA, Tierney ML, Mullet JE (1992) Proc Natl Acad Sci USA 89:4938
58. Albrecht T, Kehlen A, Stahl K, Knöfel H-D, Sembdner G, Weiler EW (1993) Planta 191:86
59. Falkenstein E, Groth B, Mithöfer A, Weiler EW (1991) Planta 185:316
60. Gundlach H, Müller MJ, Kutchan TM, Zenk MH (1992) Proc Natl Acad Sci USA 89:2389
61. Aerts RJ, Gisi D, Carolis ED, Luca VD, Baumann TW (1994) Plant J 5:635
62. Franceschi VR, Grimes HD (1991) Proc Natl Acad Sci USA 88:6745
63. Mizukami H, Tabira Y, Ellis BE (1993) Plant Cell Rep 12:706
64. Mandujano-Cháves A, Schoenbeck MA, Ralston LF, Lozoya-Gloria E, Chappell J (2000) Arch Biochem Biophys 381:285
65. Nojiri H, Sugimori M, Yamane H, Nishimura Y, Yamada A, Shibuya N, Kodama O, Murofushi N, Omori T (1996) Plant Physiol 110:387
66. Zhao J, Fujita K, Yamada J, Sakai K (2001) Appl Microbiol Biotechnol 55:301
67. Aoyagi H, Kobayashi Y, Yamada K, Yokoyama M, Kusakari K, Tanaka H (2001) Appl Microbiol Biotechnol 57:482
68. Vergopoulou S, Galanopoulou D, Markaki P (2001) J Agric Food Chem 49:3494
69. Dathe W, Rönsch H, Preiss A, Schade W, Sembdner G, Schreiber K (1981) Planta 153:530
70. Yamane H, Sugawara J, Suzuki Y, Shimamura E, Takahashi N (1980) Agric Biol Chem 44:2857
71. Yamane H, Takagi H, Abe H, Yokota T, Takahashi N (1981) Plant Cell Physiol 22:689
72. Miersch O, Meyer A, Volkefeld S, Sembdner G (1986) J Plant Growth Regul 5:91
73. Koda Y, Kikuta Y, Kitahara T, Nishi T, Mori K (1992) Phytochemistry 31:1111
74. Ueda J, Kato J (1982) Physiol Plant 54:249
75. Koda Y, Kikuta Y, Tazaki H, Tsujino Y, Sakamura S, Yoshihara T (1991) Phytochemistry 30:1435
76. Ueda J, Kato J, Yamane H, Takahashi N (1981) Physiol Plant 52:305
77. Birkett MA, Campbell CAM, Chamberlain K, Guerrieri E, Hick AJ, Martin JL, Matthes M, Napier JA, Pettersson J, Pickett JA, Poppy GM, Pow EM, Pye BJ, Smart LE, Wadhams GH, Wadhams LJ, Woodcock CM (2000) Proc Natl Acad Sci USA 97:9329
78. Helmchen G, Goeke A, Lauer G, Urmann M, Fries J (1991) Angew Chem 102:1079
79. Yukimune Y, Hara Y, Nomura E, Seto H, Yoshida S (2000) Phytochemistry 54:13
80. Vick BA, Zimmerman DC (1983) Biochem Biophys Res Commun 111:470
81. Vick BA, Zimmerman DC (1984) Plant Physiol 75:458
82. Vick BA, Zimmerman DC (1986) Plant Physiol 80:202
83. Vick BA, Zimmerman DC (1987) Plant Physiol 85:1073
84. Vick BA, Zimmerman DC (1989) Plant Physiol 90:125
85. Xu Y, Chang P, Liu D, Narasimhan ML, Raghothama KG, Hasegawa PM, Bressan RA (1994) Plant Cell 6:1077

86. Oldroyd GE, Engstrom EM, Long SR (2001) Plant Cell 13:1835
87. Shoji T, Nakajima K, Hashimoto T (2000) Plant Cell Physiol 41:1072
88. Tabata H, Higashi Y (2001) Catalysts Catalysis 43:207 (in Japanese)
89. Yu YB, Yang SF (1979) Plant Physiol 64:1074
90. Adams DO, Yang SF (1981) Ethylene the gaseous plant hormone: mechanism and regulation of biosynthesis. In: Trends in biochemical sciences. Elsevier/North-Holland Biochemical Press, New York, pp 161–163
91. Wang CY, Adams DO (1982) Plant Physiol 69:424
92. Fuhrer J (1982) Plant Physiol 70:162
93. Yang SF, Pratt HK (1978) The physiology of ethylene in wounded plant tissues. In: Kahl G (ed), Biochemistry of wounded plant tissues. de Gruyter, Berlin, p 595
94. Yang SF, Hoffman NE (1984) Ann Rev Plant Physiol 35:155
95. Ohkawa K, Sumitani K, Satoi S, Hayashi I, Yamamoto K (1987) Acta Hort 201:223
96. Guzman P, Ecker JR (1990) Plant Cell 2:513
97. Pan Z, Wang H, Zhong J (2000) Enzyme Microb Technol 27:714
98. Monacelli B, Pasqua G, Botta B, Vinciguerra V, Gacs-Baitz E, Monache GD (2002) Planta Med 68:764
99. Li SH, Zhan HJ, Yao P, Niu XM, Xiang W, Sun HD (2002) J Asian Nat Prod Res 4:147
100. Khan MS, Kumar I, Prasad JS, Nagarajan GR, Parthasarathy MR, Krishnamurty HG (1976) Planta Med 30:82
101. Das B, Rao SP, Srinivas KVNS, Yadav JS (1995) Phytochemistry 38:715
102. Arslanian RL, Bailey DT, Kent MC, Richheimer SL, Thornburg KR, Timmons DW, Zheng QY (1995) J Nat Prod 58:583
103. Shen YC, Chen CY, Lin YM, Kuo YH (1997) Phytochemistry 46:1111
104. Kobayashi J, Shigemori H (2002) Med Res Rev 22:305
105. Appendino G, Barboni L, Gariboldi P, Bombardelli E, Gabetta B, Viterbo D (1993) J Chem Soc Chem Commun 20:1587
106. Kobayashi T, Kurono M, Sato H, Nakanishi K (1972) J Am Chem Soc 94:2863
107. Zamir LO, Zhou ZH, Caron G, Nedea ME, Sauriol F, Mamer O (1995) J Chem Soc Chem Commun 5:529
108. Appendino G, Cravotto G, Enriu R, Jakupovic J, Gariboldi P, Gabetta B, Bombardelli E (1994) Phytochemistry 36:407
109. Sun DA, Nikolakakis A, Sauriol F, Mamer O, Zamir LO (2001) Bioorg Med Chem 9:1985
110. Sun DA, Sauriol F, Mamer O, Zamir LO (2001) Bioorg Med Chem 9:793
111. Hefner J, Ketchum REB, Croteau R (1998) Arch Biochem Biophys 360:62
112. Wildung MR, Croteau R (1996) J Biol Chem 271:9201
113. Walker K, Schoendorf A, Croteau R (2000) Arch Biochem Biophys 374:371
114. Schoendorf A, Rithner CD, Williams RM, Croteau RB (2001) Proc Natl Acad Sci USA 98:1501
115. Jennewein S, Rithner CD, Williams RM, Croteau RB (2001) Proc Natl Acad Sci USA 98:13595
116. Walker K, Croteau R (2000) Proc Natl Acad Sci USA 97:13591
117. Walker K, Croteau R (2000) Proc Natl Acad Sci USA 97:583
118. Walker K, Long R, Croteau R (2002) Proc Natl Acad Sci USA 99:9166
119. Walker K, Fujisaki S, Long R, Croteau R (2002) Proc Natl Acad Sci USA 99:12715
120. Ashby MN, Edwards PA (1990) J Biol Chem 265:13157
121. Joly A, Edwards PA (1993) J Biol Chem 268:26983
122. Tarshis LC, Proteau PJ, Kellogg BA, Sacchettini JC, Poulter CD (1996) Proc Natl Acad Sci USA 93:15018
123. Song L, Poulter CD (1994) Proc Natl Acad Sci USA 91:3044
124. Furuya T, Ushiyama K (1994) Ginseng production in cultures of Panax ginseng cells. In: Shargool P, Ngo TT (ed) Biotechnological applications of plant cultures. CRC Press, Boca Raton, FL, p 1
125. Wu JY, Zhong JJ (1999) J Biotechnol 68:89
126. Zhong JJ, Wang DJ (1996) J Biotechnol 46:69

127. Zhang YH, Zhong JJ (1996) Biotechnol Prog 12:567
128. Zhang YH, Zhong JJ (1997) Enzyme Microb Technol 21:59
129. Zhong JJ, Chen F, Hu WW (2000) Process Biochem 35:491
130. Liu S, Zhong JJ (1996) J Biotechnol 52:121
131. Hu WW, Yao H, Zhong JJ (2001) Biotechnol Prog 17:838
132. Honda Y, Inaoka H, Takei A, Sugimura Y, Otsuji K (1996) Phytochemistry 41:1517
133. Tan ZY, Thimann KV (1989) Physiol Plant 75:13
134. Hegarty PK, Smart NJ, Scragg AH, Fowler MW (1986) J Exp Bot 37:1911
135. Luo J, Yu F, Liu L, Wu CD, Mei XG (2001) Sheng Wu Gong Cheng Xue Bao 17:215
136. Tabata M, Fujita Y (1985) Production of shikonin by plant-cell cultures. In: Zaitlin M, Day P, Hollaender A (ed) Biotechnology in plant science. Academic Press, Orlando, FL, p 207
137. Yamakawa T, Kato S, Ishida K, Kodama T, Minoda Y (1983) Agric Biol Chem 47:2185
138. Hirasuna TJ, Shuler ML (1991) Plant Sci 78:107
139. Asada M, Shuler ML (1989) Appl Microbiol Biotechnol 30:475
140. Berlin J, Forche E, Wray V, Hammer J, Hosel W (1983) Z Naturforsch 38c:346
141. Morris P (1986) Planta Med 52:121
142. Ketcham REB, Tandon M, Gibson DM, Begley T, Shuler ML (1999) J Nat Prod 62:1395
143. Alder JD, Jarvis KP, Marsh KC, Klein LL, Clement JJ (1996) Br J Cancer 73:560
144. Klein LL, Li L, Maring CJ, Yeung CM, Thomas SA, Grampovnik DJ, Plattner JJ (1995) J Med Chem 38:1482

Received: May 2003

Adv Biochem Engin/Biotechnol (2004) 87: 25–59
DOI 10.1007/b94367

Submerged Cultivation of Medicinal Mushrooms for Production of Valuable Bioactive Metabolites

Jian-Jiang Zhong · Ya-Jie Tang

State Key Laboratory of Bioreactor Engineering, East China University of Science and Technology, 130 Meilong Road, Shanghai 200237, China
E-mail: jjzhong@ecust.edu.cn

Abstract Mushrooms are abundant sources of a wide range of useful natural products. Nowadays, commercial mushroom products are from mushrooms collected from field cultivation, which is a time-consuming and labor-intensive process. Submerged cultivation of mushrooms has significant industrial potential, but its success on a commercial scale depends on cost compared with existing technology. Increasing product yields and development of novel production systems that address the problems associated with this new technology will certainly facilitate expansion. This article outlines the major valuable metabolites produced by mushroom cultivation and advances in submerged culture of mushrooms, taking *Ganoderma lucidum*, a popular folk and an oriental medicine used to treat many diseases, as a typical example. Our latest data on mushroom cultivation for efficient production of bioactive ganoderic acids and *Ganoderma* polysaccharides in bioreactors are presented.

Keywords Medicinal mushroom · *Ganoderma lucidum* · Submerged culture · Static culture Scale-up · Bioactive compounds

1 Introduction

The number of types of mushroom on Earth is estimated at 140,000, yet maybe only 10% (approximately 14,000 named species) are known, of which 2000 are estimated to be edible; few have been studied thoroughly from the standpoint of their commercial potential. Less than 25 species of mushrooms are accepted widely as food and only very few species have attained the level of an item of commerce. Mushrooms are abundant yet largely untapped sources of a wide range of useful natural products and new compounds with interesting biological activity, including powerful new pharmaceutical products [1]. Historically, medicinal mushrooms (Basidiomycetes) have been shown to have profound health-promoting benefits and recent studies are now confirming their medical efficacy and identifying many of the bioactive molecules. Medicinal mushrooms are looked at as a rapidly developing area of biotechnology for cancer therapy and other bioactivity [2]. In particular, and most importantly for modern medicine, they represent an unlimited source of polysaccharides with antitumor and immunostimulating properties. Many, if not all, Basidiomycetes mushrooms contain biologically active polysaccharides in the fruit bodies, cultured mycelium, and culture broth [3]. Recently, a number of substances of higher Basidiomycetes mushroom origin, which have antitumor, immune modulating, cardiovascular, antihypercholesterolemia, antibacterial, antiviral, antiparasitic, hepatoprotective, and antidiabetic activity, have been isolated and identified [4].

Nowadays commercial mushroom products are mostly obtained from field-cultivated mushrooms, which is a time-consuming and labor-intensive process. It usually takes several months to cultivate the fruiting body of mushrooms and it is difficult to control the product quality during its soil cultivation. Submerged culture of edible and medical mushrooms is viewed as a promising alternative for efficient production of valuable metabolites and has received increasing attention around the world [1–3, 5–10]. Compared with research on fermentation with conventional filamentous microorganisms (streptomycetes and fungi), a literature survey indicates that cell culture of mushrooms is far from being thoroughly

studied; there are, in particular, few reports on their bioreactor cultivation [11–15]. Despite a great need for large-scale submerged cultivation of mushrooms for application in the food and health care sectors, there is a lack of related information on systematic bioprocess engineering studies.

2 Bioactive metabolites from mushrooms

Many types of useful metabolites have been isolated and identified from mushrooms. Some have unique biological activity. A brief list of major valuable metabolites produced by mushrooms is shown in Table 1 [5, 16].

Tanimoto et al. [17] reported a novel squalene synthase inhibitor, Schizostatin, produced by the mushroom *Schizophyllum commune*. Production of a variety of enzymes by mushrooms has also been reported, for example, cellulase production by the edible mushroom *Volvariella diplasia* [18], production of extracellular endo-α-mannanase by the mushroom *Volvariella volvacea* [19], and production

Table 1 Bioactive metabolites of mushrooms

Antifungal	Adustin, Aleurodiscal, Anisaldehyde, Clavilactones, Favolon, Fimicolon, Fomecins
Antibacterial	Anisaldehyde, Armillarin, Basidalin, Crinipellins, Frustulosin, Striatins, Panellon
Cytotoxic	Alliacols, Crinipellins, Flavidulols, Hebelomic acids, Illudins, Psathyrellons
Antitumor	Basidalin, Krestin, Schizophyllan
Antiviral	Clitocine, Collybial, Filoboletic acid, Nebularine
Anti-aggregation	Lagopodin, Naematolon, Omphalon, Panudial
Brain-protective	AMG-1
Phytotoxic	Agrocybin, Fasciculols, Hypnophilin, Mycenone, Omphalodin, Panellon, Siccayne
Insecticidal and Nematocidal	Anisaldehyde, Beauvericin, Cheimonophyllons, Ibotenic acid, Isovelleral, Linoleic acid
Inhibitors of:	
Aminopeptidase	Tyromycin
Cholesterol biosynthesis	Xerulins
Leukotriene biosynthesis	Allohedycariol, Blennins, Desozylactarorufin A
Isocitrate lyase	Mycenone
Reverse transcriptase	Clavicoronic acid, Hyphodontal, Kuehneromycins, Mniopetals, Podoscphic acid
Signal transduction	Paneoxydon, Tremediol
Phospholipases C or A_2	Caloporoside
Na^+-K^+-ATPase	Coriolin, Diketocoriolin B
Glycosidase	Cyclophellitol

of ligninolytic enzymes (laccase and manganese peroxidase) by *Pleurotus ostreatus* submerged cultures [20]. The cultivation of mushrooms on different lignocellulose-containing wastes is also a possible means of producing foods on polymer substrates of plant origin [21]. Mushrooms have also been used for production of natural pigments, such as yellow pigment (folic acid factor) by the mushroom *Coprinus lagopus* [22], the natural blue pigment indigo by the mushroom *Morchella rotunda* [23], and red pigments by submerged culture of edible mushroom *Paecilomyces sinclairii* [24].

It is well known that medicinal mushrooms are an important source of antitumor and immunomodulating polysaccharides. Mushroom polysaccharides prevent oncogenesis, have direct antitumor activity against various allogeneic and syngeneic tumors, and prevent tumor metastasis. Polysaccharides from mushrooms do not attack cancer cells directly, but produce their antitumor effects by activating different immune responses in the host [3]. There have been several reports on polysaccharide production by submerged cultivation of mushrooms. For example, Kim et al. [15] studied the optimum conditions for submerged culture of *Cordyceps militaris* C738 for production of mycelial biomass and exo-polysaccharides. In submerged cultures of a variety of edible mushrooms including *Ganoderma lucidum* and *Phellinus linteus* [25] and *Paecilomyces sinclairii* [26], the effects of different media on mycelial growth and exopolysaccharide production were investigated. Production of *Ganoderma* polysaccharide by submerged cultures of *Ganoderma lucidum* has also been reported [27–29].

3
Why submerged cultivation of *Ganoderma lucidum*?

Ganoderma lucidum (Fr.) Krast (Polyporaceae) is one of the most famous traditional Chinese medicinal herbs. It has been a popular folk and an oriental medicine used to treat many diseases, for example, hepatitis, hypertension, hypercholesterolemia, and gastric cancer [30, 31]. Studies on this mushroom have revealed many interesting biological activities, including antitumor activity [32, 33] and hypoglycemic activity of its polysaccharides (including ganoderans) [31, 34, 35]. The intracellular polysaccharides isolated from fruiting body and the mycelium culture of *G. lucidum* also have immunomodulating and antitumor activity [7, 30]. Recently, new ganoderic acids were isolated from the fruiting bodies of *G. lucidum* and their interesting biological activity such as anti-tumor and anti-HIV-1 has been reported [36–38].

However, it usually takes several months to cultivate the fruiting body of the mushroom, and it is also difficult to control product quality during soil cultivation. There is a great need to supply the market with a large amount of high-quality *G. lucidum* products. Nowadays the submerged cultivation of *G. lucidum* has received much attention in Asian regions as a promising alternative for efficient production of its valuable metabolites, especially polysaccharides and ganoderic acids. It is obviously necessary and important to develop a process for simultaneous production of these valuable metabolites in bioreactors.

There have been reports on liquid cultures of *G. lucidum* for production of polysaccharides [25, 39–44], ganoderic acids [45–47], and simultaneous produc-

tion of ganoderic acids and polysaccharides in flasks and bioreactors [6–8, 14, 27, 28]. The effects of culture conditions, such as inoculum preparation, medium components, pH and temperature, on the production of biomass and valuable metabolites have been reviewed [1, 9].

Because mushroom mycelia and pellets are shear-sensitive and culture viscosity usually increases during cultivation, the most serious problems in large-scale submerged cultures of mushrooms might be oxygen supply, shear stress, and scale up. Mushroom submerged cultivation has significant industrial potential, but its success on a commercial scale depends on cost compared with existing technology and whether industry sees an economic advantage. Increasing product yields and developing novel production systems that address the problems associated with this new technology will certainly facilitate expansion. In the following text we discuss our up-to-date results on effects of environmental factors (oxygen supply and shear stress), cultivation strategies (fed-batch and two-stage cultivation), process scale-up on a laboratory scale, and process modeling in improving metabolite production by mushroom cultures, taking liquid culture of *G. lucidum* for production of ganoderic acids and *Ganoderma* polysaccharides as an example.

4
Effects of oxygen supply and shear stress on metabolite production

4.1
Effect of oxygen supply

Submerged cultivation of mushrooms is characterized by an increase in broth viscosity with time, as a consequence of increased cell concentration, changes in cellular morphology, or the accumulation of extracellular products that alter the rheological characteristics of culture broth. After these changes there will be a series of problems that should be considered and solved, especially oxygen supply. Oxygen affects cell growth, morphology, nutrient uptake, and metabolite biosynthesis. Yoshida et al. [11–13] reported that in the submerged culture of *Lentinus edodes* small pellets grew more quickly than larger pellets, and that aspects of oxygen utilization by mycelia changed in accordance with the variation of the growth type (in fibrous mycelia suspension or in mycelia pellets suspension). We investigated the impacts of initial volumetric oxygen transfer coefficient (K_La) and dissolved oxygen tension (DO) on cultivation of *G. lucidum* to obtain useful information for large-scale production of *Ganoderma* polysaccharides and ganoderic acids by the bioprocess.

The bioreactor used was a 3.5-L (working volume) agitated bioreactor with two six-bladed turbine impellers (6.5 cm i.d.). Effect of initial K_La on *G. lucidum* cultures was studied by setting various initial K_La values. All cell cultures were agitated at 200 rpm and aeration rate was adjusted over a range of 220 to 3500 mL min^{-1} to produce the desired initial K_La values from 16.4 to 96.0 h^{-1}.

The initial K_La level affected the biomass accumulation, and its peak value of 15.6 g L^{-1} was obtained at an initial K_La value of 78.2 h^{-1} (Table 2). The results indicated that the initial K_La level had a significant effect on cell growth during cul-

Table 2 Effect of initial K_La on the cell growth and production of EPS, IPS, and GA

Initial K_La (h^{-1})	16.4	60.0	78.2	96.0
Maximum dry cells ($g\ L^{-1}$)	11.8 (day 8)[a]	14.1 (day 8)	15.6 (day 10)	13.6 (day 13)
Maximum EPS production ($g\ L^{-1}$)	0.97	0.69	0.92	0.92
EPS productivity ($mg\ L^{-1}\ day^{-1}$)	73.1	51.5	69.2	69.2
Maximum IPS content (mg/100 mg)	17.5	14.2	14.0	15.6
Maximum IPS production ($g\ L^{-1}$)	1.91	1.63	2.19	2.09
IPS productivity ($mg\ L^{-1}\ day^{-1}$)	189.0	161.0	217.0	207.0
Maximum GA content (mg/100 mg)	2.33	2.44	2.17	3.36
Maximum GA production ($mg\ L^{-1}$)	246	280	339	450
GA productivity ($mg\ L^{-1}\ day^{-1}$)	23.9	27.3	33.2	44.3

[a] Culture time when the maximum cell mass was reached.

tivation. The production and productivity of both extracellular polysaccharide (EPS) and intracellular polysaccharide (IPS) was relatively lower at an initial K_La value of 60.0 h^{-1} (Table 2). The data also showed that a relatively higher initial K_La value (78.2 and 96.0 h^{-1}) was favorable for polysaccharide production.

The maximum content (based on dry cell weight) of ganoderic acids (GA) in the cultures at initial K_La values of 16.4, 60.0, 78.2, and 96.0 h^{-1} was obtained for each case (Table 2). Although the highest biomass was obtained at an initial K_La value of 78.2 h^{-1}, the highest GA production of 450 mg L^{-1} was obtained at an initial K_La level of 96.0 h^{-1}, because of the high GA content obtained in the latter case (Table 2). An increase in initial K_La increased the production and productivity of GA, the amount of which at an initial K_La value of 96.0 h^{-1} was 1.8-fold that at an initial K_La level of 16.4 h^{-1}. It is clear that an initial K_La value of 96.0 h^{-1} was optimum for both GA production and productivity.

Figure 1 shows time courses of reactor operating conditions and two dissolved oxygen (DO) profiles during the submerged cultivation of *G. lucidum* in a turbine-agitated bioreactor. Compared with a low DO (around 10% of air saturation), the cells of *G. lucidum* grew more quickly when DO was kept at a higher level (i.e. around 25% of air saturation) (Fig. 2A). The results indicated that the cell growth of *G. lucidum* was significantly limited when DO was controlled around 10% of air saturation.

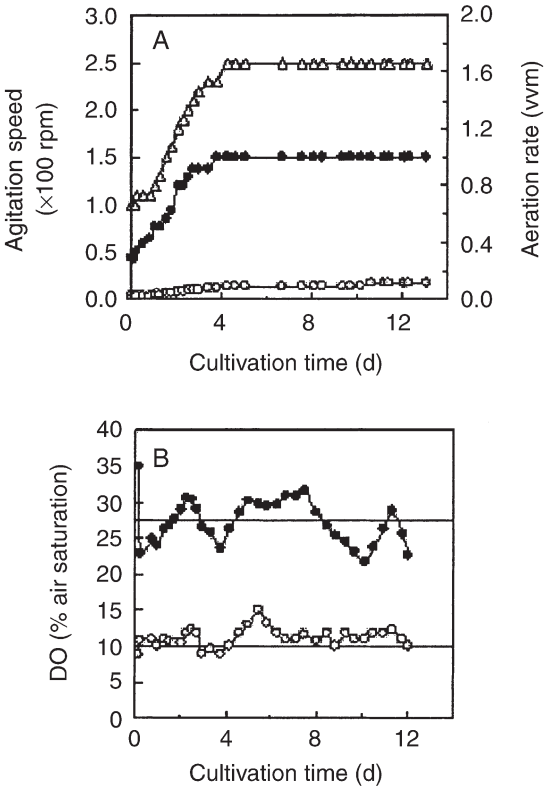

Fig. 1 Time courses of reactor operating conditions (**A**) and dissolved oxygen (DO; **B**) during submerged cultivation of *Ganoderma lucidum* in a turbine-agitated bioreactor. Symbols in Fig. 1A: *empty triangles*, agitation speed; *empty circles*, aeration rate corresponding to DO controlled at 10% of air saturation; *filled circles*, aeration rate corresponding to DO controlled at 25% of air saturation. Symbols for DO in Fig. 1B: *empty circles*, around 10% of air saturation; *filled circles*, around 25% of air saturation

The DO gradient in the mycelia pellet can be calculated according to the equation [48, 49]:

$$D\left(\frac{\mathrm{d}^2C}{\mathrm{d}r^2}+\frac{2}{r}\frac{\mathrm{d}C}{\mathrm{d}r}\right)=\rho(Q_{O_2})=\frac{\rho(Q_{O_2})_mC}{K_O+C} \quad (1)$$

Where C is the DO concentration over the pellet cross sections at a distance r from the pellet center, ρ is density of cells in the pellet, D is the coefficient of oxygen diffusion along the liquid channels inside the mycelia pellet, Q_{O_2} is the oxygen consumption rate per pellet volume, $(Q_{O_2})_m$ is the maximum oxygen consumption rate per pellet volume, and K_O is oxygen constant. When DO was controlled around 10% of air saturation, DO concentration was determined to be 2.44×10^{-2} mol m^{-3}, the radius of the mycelia pellet was about 1.9×10^{-4} m on average, the maximum specific oxygen uptake rate (SOUR) was measured as

1.85 mmol O_2 g^{-1} h^{-1}, the pellet density was 75 kg m^{-3}, D was assumed to be 1.9×10^{-9} m^2 s^{-1}, and K_O was 4.47×10^{-5} mol m^{-3} [49]. From Eq. (1), the DO in the center of mycelia pellet was estimated to be zero, which indicted that the cells in the mycelia pellet were under oxygen limitation.

The kinetics of EPS accumulation are indicated in Fig. 2B. After inoculation, a rapid increase of EPS concentration was observed. DO level affected the final production of EPS. EPS production and productivity obtained around 10% DO were higher than those around 25% DO. The IPS content (by dry cell weight) around 10% DO was also higher than that around 25% DO (Table 3). The results suggest that oxygen limitation was beneficial for the metabolic flux toward polysaccharide biosynthesis. Figure 2C shows the dynamic profiles of total IPS accumulation. The total IPS production and productivity were much higher at 25% DO than those at 10% DO.

The GA content around 10% DO was higher than that around 25% DO (Table 3). The data indicated that a relatively lower DO, in which the cells in the

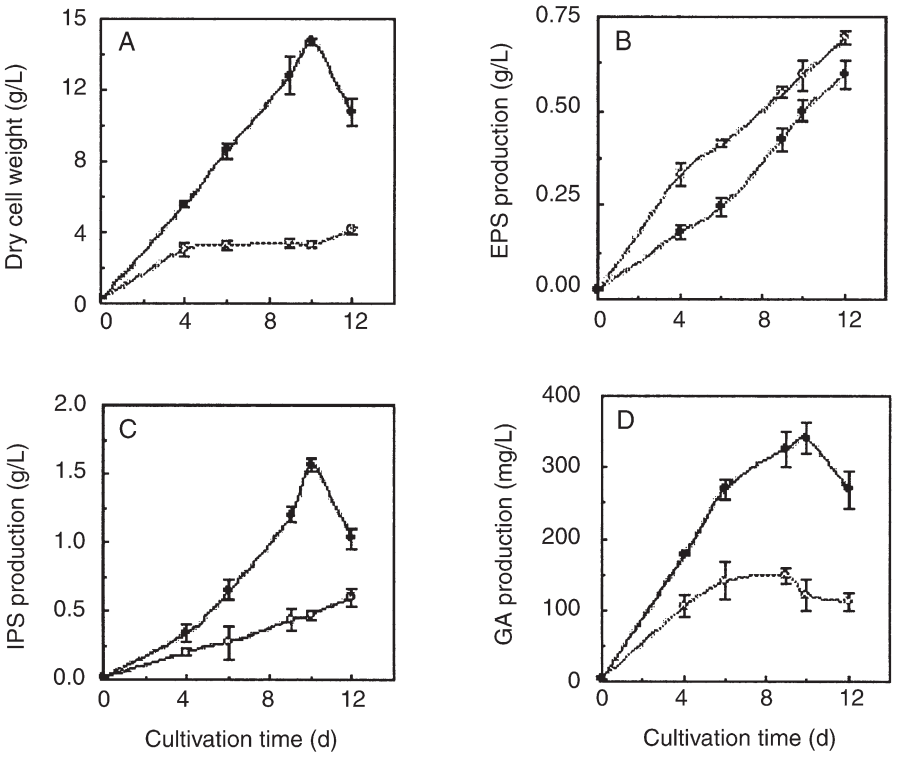

Fig. 2 Effect of DO on dry cell weight (**A**), production of extracellular polysaccharides (EPS; **B**), and intracellular polysaccharides (IPS; **C**), and total production of ganoderic acids (GA; **D**) during submerged cultivation of *G. lucidum* at different initial K_La levels in a turbine-agitated bioreactor. Symbols for DO: *empty circles*, around 10% of air saturation; *filled circles*, around 25% of air saturation. The error bars in the figure indicate maximum errors from two independent samples

Table 3 Effects of DO on the cell growth and production of EPS, IPS, and GA by *G. lucidum*[a]

DO (% air saturation)	10	25
Maximum dry cell weight (g L^{-1})	4.1±0.2 (day 12)	14.7±0.2 (day 10)[b]
Average growth rate[c] (day^{-1})	1.11±0.02	5.06±0.03
Yx/s (g g^{-1} lactose)	0.38±0.01	0.48±0.00
Maximum EPS production (g L^{-1})	0.70±0.02	0.60±0.04
EPS productivity (mg L^{-1} day^{-1})	56.3±0.3	48.0±2.0
Maximum IPS content (mg/100 mg)	14.7±0.6	10.6±0.8
Maximum IPS production (g L^{-1})	0.60±0.06	1.56±0.04
IPS productivity (mg L^{-1} day^{-1})	49.2±4.2	155.0±3.0
Maximum GA content (mg/100 mg)	4.39±0.25	3.22±0.14
Maximum GA production (mg L^{-1})	148±10	340±21
GA productivity (mg L^{-1} day^{-1})	16.0±0.7	33.7±1.8

[a] The error was calculated from two samples.
[b] Culture time when the maximum cell mass was reached.
[c] Average growth rate was calculated as: (maximum dry weight–initial dry weight)/initial dry weight/cultivation time.

center of mycelia pellet could be under oxygen limitation, was beneficial for GA biosynthesis. The results imply that oxygen limitation was beneficial for metabolic flux towards the GA biosynthesis. The kinetics of total GA production are shown in Fig. 2D. Total GA accumulation and productivity reached were much higher at a higher DO level. It is clear that a relatively high DO led to a higher GA production and productivity.

When DO was controlled around 10% of air saturation, the cells of mycelia pellet had relatively bigger sizes than those at 25% DO (data not shown), which were under oxygen limitation, as discussed above. They did not grow after day 4 (Fig. 2A) while maintaining cellular activity, and the metabolic flux was more shifted toward GA biosynthesis, which led to a higher GA content under this condition compared with at 25% DO (Table 3). Although a higher IPS and GA content (Table 3) was obtained at around 10% DO, a much higher cell density was obtained at around 25% DO (Fig. 2B), therefore higher total production of IPS and GA (Fig. 2C,D) was achieved in the latter case. The highest IPS and GA production was reached on the same day (day 10) as the biomass. The production and productivity of GA and IPS at around 25% DO were about twice those at around 10% DO. The results indicated that high cell density was desirable for total production of intracellular products to increase the metabolite productivity.

The above data reveal that oxygen supply significantly affected cell growth, cellular morphology, and metabolite biosynthesis during submerged cultivation of *G. lucidum* in a bioreactor. The experiments on both initial $K_L a$ values and DO were repeated, and the same conclusions were obtained. The results are considered useful for efficient production of the cell mass, *Ganoderma* polysaccharides, and ganoderic acids on a large scale.

4.2
Effect of shear stress

Hydrodynamic shear stress is well-known to be an important factor for shear-sensitive bioprocesses such as cultures of the cells of animals, insects, plants, and higher fungi. Mushroom cells are generally sensitive to shear environment, because of their morphological characteristics. Because investigation of the effect of shear on mushroom cultures is lacking, the influence of hydrodynamic shear on cell growth and production of ganoderic acids and polysaccharides by *G. lucidum* cells in bioreactors was studied.

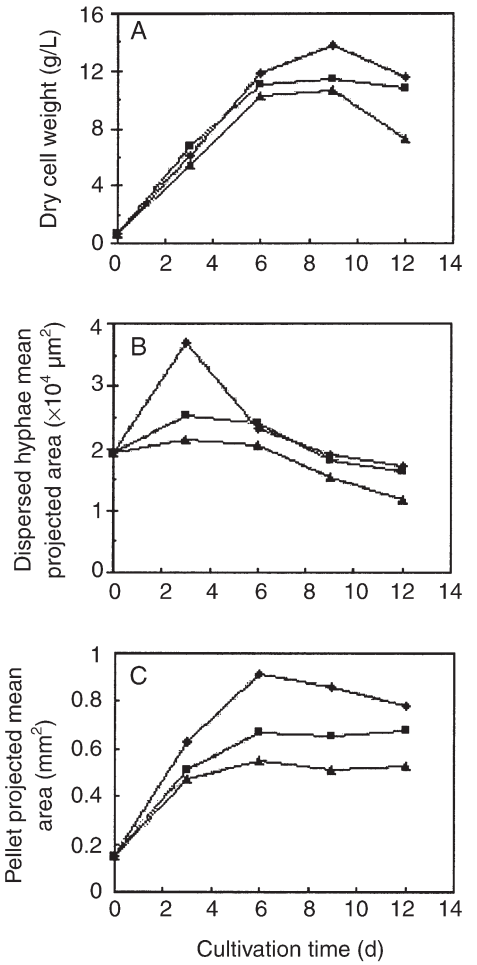

Fig. 3 Time profiles of dry cell weight (**A**) and mean projected area of dispersed hyphae (**B**) and pellets (**C**) under different shear conditions in *G. lucidum* cultures in a 5-L stirred bioreactor. Symbols for impeller tip speeds (m s^{-1}): 0.51 (*filled diamonds*); 1.02 (*filled squares*); 1.53 (*filled triangles*)

A 5-L stirred reactor [14] was used to study the hydrodynamic shear effect on mushroom cultures. Impeller tip speed was changed from 0.51 to 1.53 m s^{-1} while aeration rate was adjusted to keep the DO level above 25% of air saturation during cultivation. The shear stress was evaluated by impeller tip speed (ITS) as reported in other systems [50].

Figure 3A shows the cell growth kinetics at ITS of 0.51, 1.02, and 1.53 m s^{-1} in a 5-L stirred bioreactor. After 9-day cultivation a maximum cell density of 13.8 g L^{-1} by dry weight was obtained at an ITS of 0.51 m s^{-1}; it was only 10.6 g L^{-1} at 1.53 m s^{-1}. The results indicate that cell growth was inhibited by higher shear stress and that a low-shear environment was important to the mushroom cultivation.

The cellular morphology (dispersed hyphae and pellets) of *G. lucidum* was also affected by ITS (Fig. 3B). During the first three-day cultivation, the mean projected area of dispersed hyphae increased much more at an ITS value of 0.51 m s^{-1} than under other conditions. The maximum mean projected area of dispersed hyphae was 3.70, 2.54, and 2.13×10^4 μm^2 under ITS levels of 0.51, 1.02, and 1.53 m s^{-1}, respectively. Figure 3C shows the dynamic profiles of mean projected areas of pellets during cultivation. The pellet size at a relatively lower ITS (0.51 m s^{-1}) increased more rapidly than that at a higher ITS (1.02 or 1.53 m s^{-1}). The maximum mean projected area under these three conditions was 0.91, 0.67, and 0.55 mm^2, respectively. The results indicate that the hydrodynamic shear had a significant impact on the cellular morphology of *G. lucidum*, and smaller pellets and shorter mycelia were formed under a relatively high shear stress.

Figure 4A shows production of IPS and EPS at different ITS values. The data imply that a lower shear environment was favorable to IPS accumulation. EPS accumulation, on the other hand, was not much affected by ITS (Fig. 4A). For GA accumulation (Fig. 4B) an ITS value of 1.02 m s^{-1} seemed to be optimum. An optimum ITS value has been reported for production of anthocyanin pigment from cell cultures of *Perilla frutescens* in a bioreactor [50].

From these results it is apparent that a relatively high cell concentration of 13.8 g L^{-1} and higher production titer of IPS (2.64 g L^{-1}) and GA (306 mg L^{-1}) were obtained in a bioreactor under low shear conditions. The information is valuable for optimum operation and scale-up of the mushroom cell cultures for the metabolites production.

5
Strategies for enhancing metabolite production: fed-batch cultivation and two-stage cultivation

5.1
Fed-batch cultivation

The limited commercialization of mushroom cell cultures to date can essentially be attributed to matters of production cost – economic feasibility studies are unanimous in acknowledging productivity as a limiting factor. Because culture productivity depends on product yield, organism growth rate, and prevailing biomass levels [51, 52], high-density cell cultures offer the advantage of production of metabolites in a compact cultivation vessel with high volumetric production

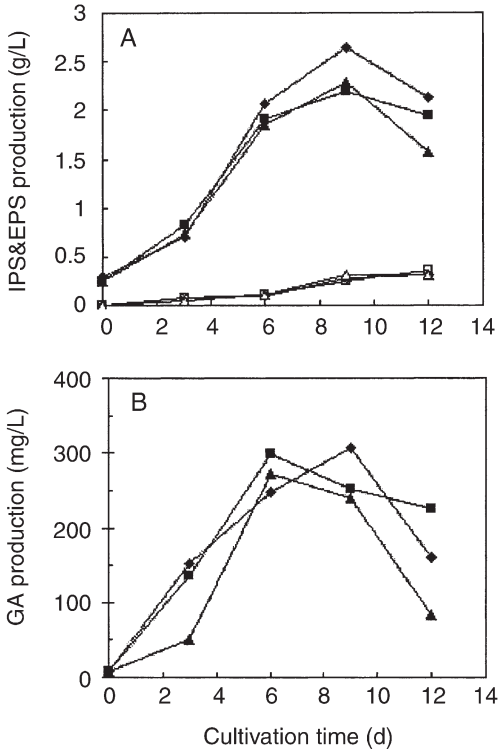

Fig. 4 Effect of impeller tip speeds on production of (**A**) intracellular (IPS) (*filled symbols*) and extracellular polysaccharide (EPS; *empty symbols*) and (**B**) ganoderic acids (GA). The symbols are the same as in Fig. 3

rate (productivity), especially for intracellular products [53, 54]. Here, a process was developed for efficient simultaneous production of bioactive *Ganoderma* polysaccharides and ganoderic acids by fed-batch cultivation of *G. lucidum*. The effects of carbon source and initial sugar concentration were investigated in an attempt to enhance final cell density and the productivity of the useful metabolites. By using a low level of initial lactose and its intermediate feed during cultivation, the inhibitory effect of a relatively higher level of initial lactose on GA biosynthesis was avoided, and process efficiency was greatly enhanced. The shake-flask process was successfully reproduced in a stirred bioreactor.

5.1.1 *Fed-batch cultivation in shake flasks*

On the basis of a preliminary study, feeding of lactose during cultivation was adopted to avoid the inhibitory effects of lactose on GA biosynthesis while increasing final cell density, metabolite accumulation, and productivity. Lactose feeding was tested on days 8, 10, and 12, when its residual level was 12.9, 6.0, and 3.3 g L^{-1}, respectively. The maximum cell density (by dry weight) of *G. lucidum*

Table 4 Effect of lactose feeding time on cell growth and production of EPS, IPS and GA

	Feeding time			
	Control (batch)	On day 8	On day 10	On day 12
Residual sugar level (g L^{-1})		11.2	6.6	2.9
Maximum dry cell weight (g L^{-1})	15.8±0.4 (day 14)[a]	20.0±0.6 (day 16)	20.1±0.3 (day 18)	20.0±0.4 (day 18)
Average growth rate[b] (day^{-1})	1.66±0.03	1.86±0.00	1.66±0.03	1.65±0.03
Yx/s (g g^{-1} lactose)	0.45±0.01	0.42±0.00	0.42±0.01	0.41±0.01
Maximum EPS production (g L^{-1})	0.57±0.05	0.96±0.03	0.80±0.02	0.76±0.02
EPS productivity (mg L^{-1} day^{-1})	38.2±0.9	46.1±0.4	34.8±0.6	39.9±0.7
Maximum IPS content (mg/100 mg)	10.8±0.3	9.85±0.30	11.3±0.6	9.83±0.30
Maximum IPS production	1.57±0.05	1.97±0.09	2.01±0.02	1.78±0.01
IPS productivity (mg L^{-1} day^{-1}) (g L^{-1})	86.7±0.1	122.3±0.1	142.9±0.1	97.9±0.2
Maximum GA content (mg/100 mg)	1.16±0.12	1.45±0.05	1.79±0.08	1.38±0.03
Maximum GA production (mg L^{-1})	170±12	258±0	334±11	270±24
GA productivity (mg L^{-1} day^{-1})	13.9±0.7	12.7±0.4	16.5±0.5	13.3±1.0

[a] Culture time when the maximum cell mass was reached.
[b] Average growth rate was calculated as: (maximum dry weight–initial dry weight)/initial dry weight/cultivation time.

at different feeding time was almost the same, i.e. around 20 g L^{-1}, whereas it was only 15.8±0.4 g L^{-1} (day 14) in batch cultures (Table 4). The average growth rate in fed-batch cultures was comparable with the control. It was clear that sugar addition during cultivation enhanced biomass accumulation. Although there was no obvious difference between maximum biomass values within the range of feeding time as investigated, the maximum cell density was reduced when lactose was fed at a later time (day 14) [28].

EPS production and productivity at feeding time of day 8 was 0.96 g L^{-1} and 46.1 mg L^{-1} day^{-1} as obtained on day 20, which was higher than under other conditions (Table 4). EPS yield against lactose at feeding time of day 8 was 19.9 mg g^{-1} lactose, which was higher than under the other conditions.

IPS production was highest at feeding time of day 10 – productivity was 142.9 mg L^{-1} day^{-1} (Table 4). In batch cultivation IPS production reached its peak

on day 18 with a productivity of 86.7 mg L^{-1} day^{-1}. The results indicated that fed-batch culture enhanced both the production and productivity of IPS, because of the relatively high cell density obtained under these conditions, and the optimum feeding time for IPS production was on day 10.

The GA content at feeding time of day 10 reached highest (1.79±0.08 mg/100 mg) on day 20 (Table 4). The results indicated that the GA content increased after lactose addition, and it reached the highest (1.79 mg/100 mg) when lactose was fed on day 10. The maximum production and productivity of GA at feeding time of day 10 was 334±11 mg L^{-1} and 16.5±0.5 mg L^{-1} day^{-1}, respectively (Table 4). The results indicated that the optimum feeding time for GA production was also on day 10.

These results revealed that fed-batch culture was an efficient means of enhancing the accumulation of biomass, EPS, IPS, and GA. It is considered that lactose should be fed at its residual concentration between 10 and 5 g L^{-1} (during days 8–12). Through this approach inhibition of GA biosynthesis by a relatively higher initial lactose level (>35 g L^{-1}) could be avoided and GA production improved markedly. Supplementation of lactose before or after this point was not so effective.

5.1.2
Batch and fed-batch cultivation in stirred bioreactors

Batch and fed-batch cultivation of *G. lucidum* in a 2.0-L (working volume) agitated bioreactor with two six-bladed turbine impellers were also studied. During batch culture, although the maximum dry cell mass was similar in both the reactor and the flask, the average cell growth rate in the bioreactor (1.51±0.05 day^{-1}) was a little higher than that in the flask (1.23±0.06 day^{-1}). Correspondingly, the lactose level in the reactor decreased faster than that in the flask [28], and the maximum dry cell mass was also reached earlier in the reactor. In the fed-batch culture the maximum dry cell mass obtained in both the bioreactor and shake flask was about 21 g L^{-1} (Table 5). The results indicated that fed-batch culture in the reactor was also very useful for efficient accumulation of cell mass. In addition, as confirmed by other experiments, the control of DO level over 20% of air saturation was very important for process operation [55].

During batch culture, the highest EPS production titer was 0.61 g L^{-1} in both bioreactors and flasks – obtained on days 12 and 18, respectively; their corresponding EPS productivity was 48.8 and 32.7 mg L^{-1} day^{-1} (Table 5). The highest EPS production titer in the fed-batch cultivation was 0.87 (bioreactor) and 0.75 g L^{-1} (flask) on days 20 and 18, respectively, and their corresponding EPS productivity was 42.3±1.4 and 40.2±1.3 mg L^{-1} day^{-1}. The maximum IPS content of the bioreactor reached about 13.1 mg/100 mg, which was almost 30% higher than that in the flask. IPS production in the reactor and flask reached its peak (about 1.7 g L^{-1}) on days 20 and 18, respectively. In fed-batch cultivation the maximum IPS content of the bioreactor reached 14.65±0.67 mg/100 mg, which was also higher than that in the flask (12.46±0.33 mg/100 mg). IPS production in both the reactor and flask reached approximately 2.4 g L^{-1} with a productivity of about 115 mg L^{-1} day^{-1}.

Table 5 Effect of fed-batch culture on the cell growth and production of EPS, IPS and GA in both shake flasks and bioreactors[a]

Culture vessel	Shake flask		Stirred bioreactor	
Culture mode	Batch	Fed-batch	Batch	Fed-batch
Maximum dry cell weight (g L^{-1})	16.2±0.4 (day 12)[b]	21.0±0.0 (day 14)	16.5±0.5 (day 10)	21.9±0.4 (day 12)
Average growth rate (day^{-1})	1.23±0.06	1.38±0.07	1.51±0.05	1.69±0.06
Y x/s (g g^{-1} lactose)	0.57±0.03	0.57±0.03	0.56±0.02	0.59±0.02
Maximum EPS production (g L^{-1})	0.61±0.04	0.75±0.05	0.61±0.00	0.87±0.05
EPS productivity (mg L^{-1} day^{-1})	32.7±0.7	40.2±1.3	48.8±1.7	42.3±1.4
Maximum IPS content (mg/100 mg)	10.8±0.4	12.5±0.3	13.1±0.3	14.7±0.7
Maximum IPS production (g L^{-1})	1.71±0.14	2.40±0.05	1.68±0.06	2.49±0.07
IPS productivity (mg L^{-1} day^{-1})	93.1±6.1	118.6±2.5	82.2±1.4	111.8±1.7
Maximum GA content (mg/100 mg)	1.40±0.03	1.54±0.13	2.05±0.20	1.85±0.01
Maximum GA production (mg L^{-1})	178±11	298±14	330±18	367±17
GA productivity (mg L^{-1} day^{-1})	16.7±0.1	14.3±0.1	31.9±0.7	29.6±0.5

[a] The error was calculated from two or three independent samples.
[b] Culture time when the maximum cell mass was reached.

GA content was higher in the reactor than in shake flask. During batch culture the highest production and productivity of GA in the bioreactor was 330±18 mg L^{-1} and 31.9±0.7 mg L^{-1} day^{-1}, respectively, which was almost twice the flask level. The highest GA production and productivity in fed-batch cultivation in the reactor and flask were 367±17 mg L^{-1} and 29.6±0.5 mg L^{-1} day^{-1} (for reactor), and 298±14 mg L^{-1} and 14.3±0.1 mg L^{-1} day^{-1} (for flask), respectively. Obviously, GA production in reactors was much higher than in flasks. The different GA accumulation in reactors and in flasks might be related to different DO levels in the two culture systems. Our preliminary experiments in bioreactors indicated that GA biosynthesis was affected by DO levels [55].

5.1.3 *Enzyme activity related to exopolysaccharide biosynthesis in fed-batch cultures*

In our preliminary work lactose was found to be a favorable carbon source for the submerged culture of *G. lucidum*. On the basis of previous reports on EPS biosyn-

thesis in bacteria [56–58], enzymes leading to EPS formation in *G. lucidum* can be divided into four groups (Fig. 5):

- enzymes responsible for the initial metabolism of a carbohydrate;
- enzymes involved in sugar nucleotide synthesis and interconversion;
- glycosyltransferases that synthesize the repeating unit attached to the glycosyl carrier lipid; and
- translocases and polymerases that synthesize the polymer.

The phosphoglucose isomerase (PGI) leading to lactate formation and α-phosphoglucomutase (α-PGM) leading to EPS formation are at the branch point between the Embden–Meyerhof–Parnas (EMP) pathway and the later part of EPS

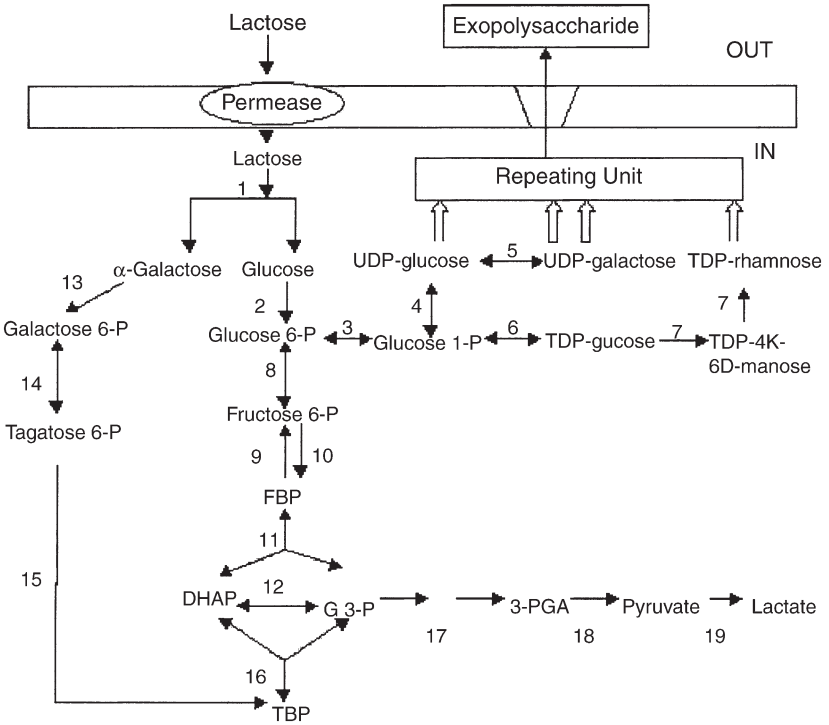

Fig. 5 Proposed pathway for EPS biosynthesis by *G. lucidum* based on related reports [56–58, 61]. *1*, β-galactosidase; *2*, glucokinase; *3*, α-phosphoglucomutase (α-PGM); *4*, UDP-glucose pyrophosphorylase; *5*, UDP-galactose-4-epimerase; *6*, TDP-glucose pyrophosphorylase; *7*, TDP-rhamnose biosynthetic system; *8*, phosphoglucose isomerase (PGI); *9*, 6-phosphofructokinase; *10*, fructose bisphosphatase; *11*, fructose-1,6-bisphosphate aldolase; *12*, triose phosphate isomerase; *13*, α-galactose kinase; *14*, galactose-6-phosphate isomerase; *15*, tagatose-6-phosphate kinase; *16*, tagatose-1,6-bisphosphate aldolase; *17*, glyceraldehyde-3-phosphate dehydrogenase and phosphoglycerate kinase; *18*, phosphoglyceromutase, enolase, and pyruvate kinase; and *19*, lactate dehydrogenase. Abbreviations: DHAP, dihydroxyacetone phosphate; FBP, fructose 1,6-biphosphate; G 3-P, glyceraldehyde 3-phosphate; P, phosphate; 3-PGA, 3-phosphoglyceric acid; TBP, tagatose 1,6-bisphosphate; TDP, thymidine diphosphate; TDP-4K-6D-manose, TDP-4-keto-6-deoxymannose; UDP, uridine diphosphate

biosynthesis. Another aspect is that substrate feeding is a useful strategy to enhance cell density and process productivity, because it can maintain the substrate below any inhibitory concentration it might have. The growing interest in *Ganoderma* polysaccharide for commercial application has triggered more studies of EPS biosynthesis. Here, we studied the effects of lactose feeding on the EPS production and related enzymes activity.

The maximum cell density of *G. lucidum* was 18.4±0.3 g L^{-1} in batch culture and 22.1±0.7 g L^{-1} in fed-batch culture [29], which indicated that lactose feeding enhanced cell growth. For the response of β-galactosidase activity, in batch culture, β-galactosidase reached its maximum activity after 10 days' growth but with lactose feeding its activity continued to increase until day 12 [29]. This suggests the existence of a lactose permease system in the cells of *G. lucidum* and the induction of β-galactosidase activity by lactose feeding. In *Streptococcus lactis*, Citti et al. [59] reported that β-galactosidase was effectively induced by lactose. Hickey et al. [58] showed there was a marked increase in the rate of β-galactosidase synthesis after addition of lactose to *Lactobacilli* cells grown on glucose or galactose.

Figure 6 shows the kinetics of α-PGM activity and EPS production in batch and fed-batch cultures of *G. lucidum*. Lactose addition caused an immediate increase of the α-PGM activity. The maximum α-PGM activity in fed-batch culture was 1.5-fold that in batch culture. Higher EPS production and productivity were obtained in fed-batch cultures than in batch cultures. Lactose feeding markedly improved both production and productivity of EPS. Compared with batch culture higher EPS production in fed-batch culture coincided with its higher α-PGM activity. Degeest and Vuyst [60] showed that α-PGM activity correlated with the amount of EPS produced by *Streptococcus thermophilus* LY03. Their data suggested that α-PGM might play a controlling role in the flux from glucose 6-phosphate to EPS biosynthesis. In contrast, another study of the same strain showed that α-PGM activity was not limiting for EPS production [61].

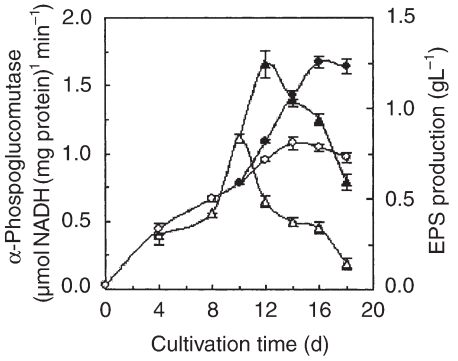

Fig. 6 Time courses of α-phosphoglucomutase (α-PGM) activity and exopolysaccharide (EPS) production in batch and fed-batch cultures of *G. lucidum* in stirred bioreactors. Symbols: *empty symbols*, batch culture; *filled symbols*, fed-batch culture; *triangles*, α-PGM activity; *circles*, EPS concentration. The error bars in the figure indicate the maximum errors calculated from two independent samples

Our work showed the positive response of α-PGM activity and EPS accumulation by *G. lucidum* to sugar feeding. The results suggest there might be a correlation between α-PGM activity and EPS biosynthesis by *G. lucidum*, and lactose addition might be useful in regulating cell metabolism and physiology in bioreactors.

With regard to the responses of PGI activity and lactate accumulation to lactose feeding, the PGI activity in fed-batch culture was lower than in batch culture; this was also true for lactate concentration [29]. The results indicated that in response to lactose addition the lactate accumulation level corresponded well to PGI activity.

5.2 Two-stage cultivation

Investigation of the impact of pellet size on cellular oxygen uptake and accumulation of ganoderic acids (GA) suggested the favorable effect of oxygen limitation on GA formation by the mushroom *G. lucidum* [8]. A two-stage cultivation process was thus proposed by combining conventional shaking cultivation with static culture (intentional limitation of oxygen supply) to enhance GA production. The two-stage culture process was conducted as follows. For shake flask cultivation 45-mL medium in a 250-mL flask was inoculated with 5-mL second-stage preculture broth (inoculum size 330 mg L^{-1}). The culture was incubated on a rotary shaker at 120 rpm. After 4, 8, or 12 days of shaking cultivation the flasks were transferred to static incubation.

Figure 7A shows the kinetics of the cell growth in static cultivation with shaking cultivation as a control. A higher final cell density of 20.9 g L^{-1} was obtained from 4-day shaking cultivation followed by 12-day static culture (Fig. 7A). The rate of consumption of glucose was also lower in this case than in the other three cases [8]; in all experiments the residual sugar was completely utilized before day 16. The cell yield on glucose (calculated between day 4 and the time of maximum biomass) was doubled by static cultivation. It suggests that sugar utilization might be more efficiently shifted to biomass formation in static cultures.

In Figs. 7B and 7C, time profiles of GA formation in static culture are compared with the shaking cultivation (as the control). The highest GA content (3.19 mg/100 mg) was obtained from 4-day shaking cultivation followed by a 12-day static culture; it was 2.3 times higher than that in shaking cultivation without static culture (Fig. 7B). The product titer was also much higher than previously reported (i.e. 0.46–1.0 mg/100 mg) [47]. Because of the very high final dry cell weight obtained in static cultivation, maximum GA production was as high as 582 mg L^{-1}, which was 2.7 fold higher than by shaking cultivation (214 mg L^{-1}) (Fig. 7C). The high production of GA might be related to the appearance of a thick mycelium layer on he liquid surface. In 4-day or 8-day shaking cultivation followed by static culture there was a thick mycelium layer and the GA content increased quickly at the same time. In 12-day shaking cultivation followed by static culture there was no thick mycelium layer and the GA content also did not change substantially. We also analyzed the GA content in the thick mycelium layer

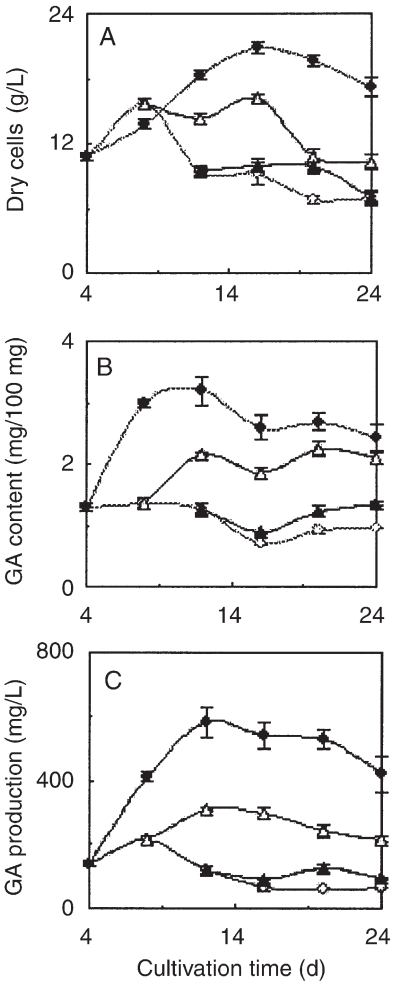

Fig. 7 Time courses of cell growth (**A**) and the content (**B**) and production (**C**) of ganoderic acids (GA) in static and shaking cultivation of *G. lucidum*. Static culture was started after day 4 (*filled circles*), day 8 (*empty triangles*) or day 12 (*filled triangles*) of shaking cultivation, while cultivation with shaking only was taken as a control (*empty circles*). The error bars in the figure indicate the standard deviations from three independent samples

and found it was 3.5±0.2 mg/100 mg, apparently higher than in the pellets from shaking cultivation. The results confirmed that GA accumulation was associated with morphological change of the pellets. It was concluded that a high cell density of 20.9 g L^{-1} was achieved by two-stage cultivation and that GA production in the new process was considerably enhanced, with its content increased from 1.36 (control) to 3.19 mg/100 mg.

6
Process scale-up and modeling

6.1
Scale-up of submerged cultures

A turbine-impeller reactor (STR) and a centrifugal impeller bioreactor (CIB) were used for cultivation. The diameter of six-bladed 5-L STR and 30-L STR was 6.5 and 9.5 cm, respectively. For a 30-L CIB, structure parameters of the centrifugal impeller were determined in accordance with previous work [62, 63]. The diameter of the centrifugal rotating pan, the inner diameter of the draft tube, and the length of draft tube were 162, 49, and 28 mm, respectively. Blade number and blade angle were 6 and 60° for each.

According to our previous work [14], at an initial K_La value of 80.3 h^{-1} or DO above 25%, cell growth and metabolite biosynthesis in a 5-L STR were comparable with or even better than those in shake flasks. Here, scale-up of *G. lucidum* cultures from a 5-L STR to a 30-L STR was first attempted on the basis of oxygen supply.

Cultivations in a conventional 30-L STR (working volume 21 L) were conducted under different conditions by setting the initial K_La level at 80.3 h^{-1}, or controlling DO>25% of air saturation during cultivation, or changing agitation speeds between 200 and 300 rpm with DO>25%. As it is apparent from the results summarized in Table 6, although EPS production was similar in both 5-L (control) and 30-L STR, maximum cell dry weight, IPS production, and GA production were all much lower in 30-L STR than in 5-L STR. In addition, it was observed that fluid mixing was never bad at agitation speeds of 200 rpm or 300 rpm. Therefore, initial K_La, DO, and mixing are not regarded as key factors in scale-up of *G. lucidum* cultures from 5-L to 30-L STR. We consider that hydrodynamic shear might be critical for process scale-up, because it was found to be significant to cell growth and metabolite production by the mushroom cultures as shown above.

Table 6 Summary of cultivations in a 30-L STR

Controlled condition	Dry cells ($g\ L^{-1}$)	Maximum IPS production ($g\ L^{-1}$)	Maximum EPS production ($g\ L^{-1}$)	Maximum GA production ($mg\ L^{-1}$)
DO level >25%	4.1	0.43	0.43	73
Initial K_La of 80.3 h^{-1}	4.7	0.49	0.63	91
Agitation speed at 300 rpm	4.2	0.42	0.57	77
Agitation speed at 200 rpm	4.8	0.42	0.66	83
Control (5-L STR)[a]	14.3±1.4	1.80±0.34	0.87±0.16	268±20

[a] Cultivations were conducted in various conditions in a 5-L STR.

In subsequent experiments a low-shear CIB [62, 63] was therefore applied to mushroom cultivation.

In 30-L CIB, agitation speed was set at 200 rpm and aeration rate was adjusted to keep DO above 25% of air saturation during cultivation. As shown in Fig. 8A, the maximum biomass in 5-L STR, 30-L CIB, and 30-L STR was 14.4, 11.9, and 4.1 g L^{-1}, on days 10, 10, and 4, respectively. The EPS accumulation titer was 0.57, 0.69, and 0.43 g L^{-1} in 5-L STR, 30-L CIB, and 30-L STR, respectively (Fig. 8B). Time profiles of IPS production are shown in Fig. 8C, and similar high IPS production was achieved in 5-L STR and 30-L CIB. The GA production titer was also higher in the 5-L STR and 30-L CIB than in the 30-L STR (Fig. 8D). It is clear that the cultivation results in 5-L STR could be well reproduced in 30-L CIB. The experiments on the scale-up were repeated, and the same conclusion was reached. The information obtained might be useful to large-scale cell cultures of medicinal and edible mushrooms. In submerged cultivation of a mushroom *Schizophyllum commune* for production of L-malic acid [64], rates of production of the acid in flask culture, a jar fermentor, an airlift column, and a standard bubble column were compared; the airlift column was found to be most suitable.

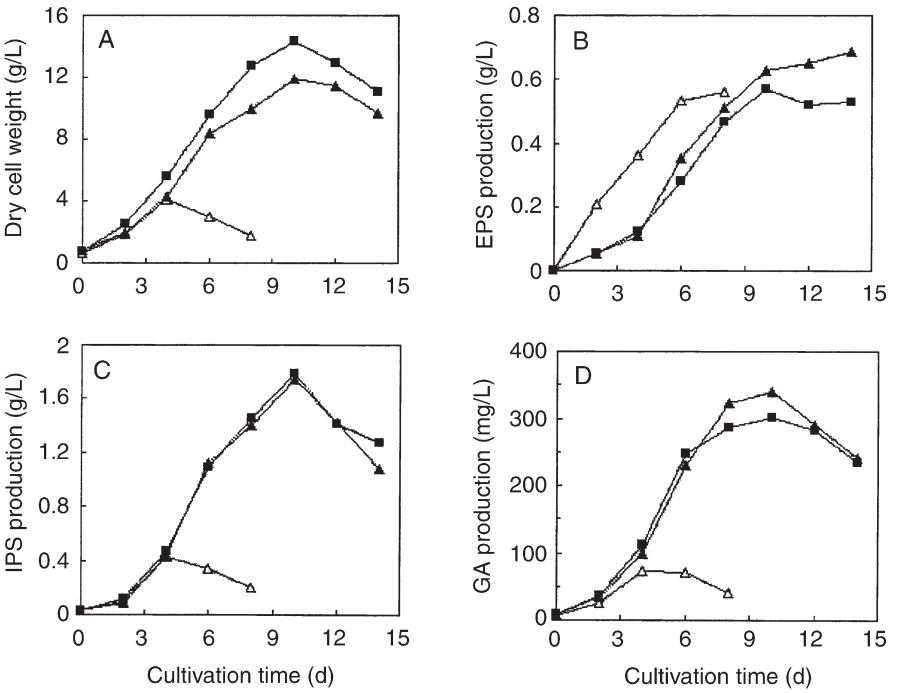

Fig. 8 Time profiles of dry cell weight (**A**), EPS production (**B**), IPS production (**C**), and GA production (**D**) during cultivation of *G. lucidum* in 5-L STR, 30-L STR, and 30-L CIB. Symbols: 5-L STR (*filled squares*), 30-L STR (*empty triangles*), and 30-L CIB (*filled triangles*)

6.2 Scale-up of liquid static cultures

Although there have been a few reports on liquid cultivation of mushrooms using small bioreactors [28, 65], there is a lack of reports on scale-up of mushroom cultivation processes [28]. Previous work in our laboratory demonstrated that the content and production of GA could be significantly enhanced by means of a two-stage culture process combining conventional shaking cultivation (first-stage) with static culture (second-stage) [8]. It is essential to study the scale-up of this novel process from a flask to a bioreactor for potential commercial application of the mushroom culture.

The first-stage culture of *G. lucidum*, which is similar to a conventional bacterial fermentation process, was recently successfully conducted in a laboratory reactor [28]. To scale-up the second-stage culture (liquid static culture), a systematic approach was then taken by performing a series of experiments to identify the potential factors that might be responsible for it. A multilayer static bioreactor was also designed for hyper-production of GA based on experimental findings. A multilayer static bioreactor is depicted in Fig. 9 and the geometric details of various static reactors used are summarized in Table 7. Compared with the one-layer static bioreactor a multilayer static bioreactor has multi-parallel growth surfaces, which provide a multi-fold culture area.

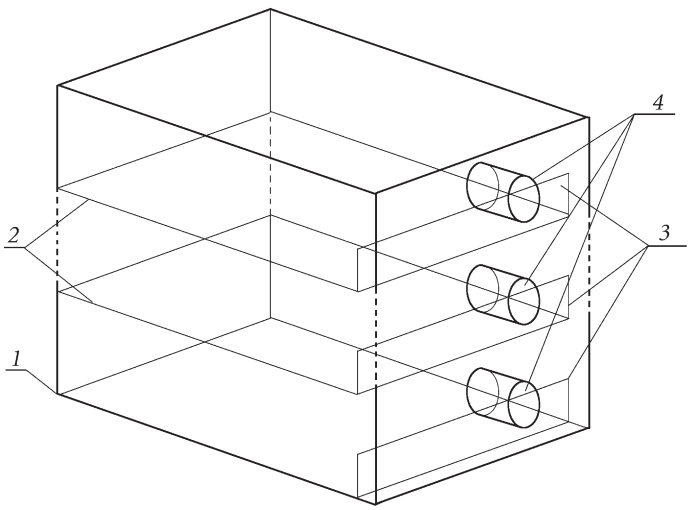

Fig. 9 Schematic diagram of a multilayer static bioreactor. *1*, Cuboid vessel; *2*, clapboard; *3*, fenderboard; *4*, inoculation port and sample port. The whole cuboid vessel is divided into multi-parallel growth surface by the clapboard. The *dashed lines* in the figure show that the vessel can be a single or multilayer static bioreactor

Table 7 Geometric details of static vessels used for *G. lucidum* cultures

Cultivation vessels	50-mL T-flask	One-layer static reactor	Two-layer static reactor	Three-layer static reactor	Large three-layer static reactor
Length of bioreactor (cm)	5.2	17.5	17.5	17.5	60
Width of bioreactor (cm)	3.5	11.3	11.3	11.3	38
Height of liquid (cm)	1.1	1.1	1.1	1.1	1.1
Working volume (mL)	20	218	436	654	7500

6.2.1 *Effect of initial K_La*

Oxygen transfer is generally one of the most important criteria for many culture processes [12, 66–68]. For scale-up of the static culture of *G. lucidum*, as a first step it is essential to study the influence of oxygen supply on cell growth and GA accumulation. Here, the effect of initial K_La levels, i.e. 16.4, 9.4, 3.2, and 2.1 h^{-1}, was investigated using 250-mL shake flasks.

At an initial K_La level of 2.1 h^{-1}, a thick layer of white mycelia was formed on the liquid surface in the static culture; this was not observed for the other three K_La levels [55]. Time courses of cell density in the liquid and on the liquid surface (based on total working volume) at an initial K_La value of 2.1 h^{-1} are compared in Fig. 10A. After inoculation cell density in the liquid increased until day 8, when a maximum value of 12.0±0.0 g L^{-1} was obtained. Later it decreased. Cell density on the liquid surface (based on total working volume, the same as below) increased from the appearance of white mycelial layer (day 9) to the end of cultivation (day 28), when a maximum value of 13.6±0.4 g L^{-1} was attained. As shown in Fig. 10B, the total cell density (i.e. cell density in the liquid plus that on the surface) reached 15.6±0.4, 18.5±0.4, 17.4±0.1, and 15.6±0.2 g L^{-1} on days 16, 12, 20, and 20 at initial K_La levels of 16.4, 9.4, 3.2, and 2.1 h^{-1}, respectively. Kinetics of lactose consumption are shown in Fig. 10C. Lactose consumption rate at initial K_La levels of 16.4 and 9.4 h^{-1} was much higher than that for the other two levels. It is evident that initial K_La significantly affected the cell growth and substrate consumption in the static culture.

Time profiles of GA content at different initial K_La levels are indicated in Fig. 11A. GA content was between 0.87 and 1.63 mg/100 mg at initial K_La values of 16.4, 9.4, and 3.2 h^{-1} whereas at an initial K_La level of 2.1 h^{-1} it was almost 2–3 times that at other levels. This suggests that oxygen limitation was beneficial for specific GA biosynthesis (i.e. content). A similar phenomenon was also observed in our previous study [14]. The dynamic profiles of GA production by cells in the liquid and on the surface at an initial K_La value of 2.1 h^{-1} are shown in Fig. 11B. After inoculation GA production by cells in the liquid increased until day 12, when a maximum value of 250±1 mg L^{-1} was attained. Later, it decreased. GA production by

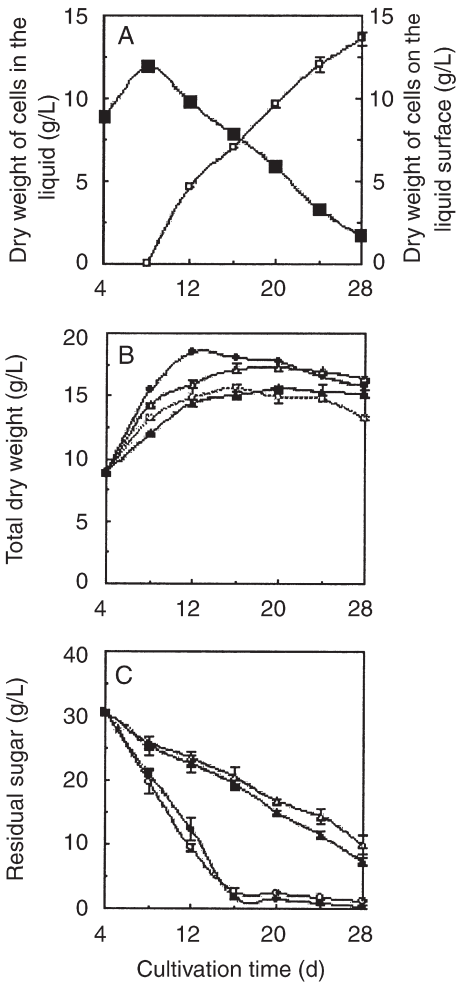

Fig. 10 Kinetics of cell growth and sugar consumption in static cultures of *G. lucidum* for different initial K_La levels. Symbols for Fig. 10A: cell density in the liquid (*filled squares*) and on the liquid surface (*empty squares*) for an initial K_La value of 2.1 h^{-1}. Symbols in Figs. 10B and 10C for initial K_La (h^{-1}): 16.4 (*empty circles*), 9.4 (*filled circles*), 3.2 (*empty triangles*) and 2.1 (*filled triangles*). The error bars in the figure indicate standard deviations from three independent samples

cells on the surface increased from the appearance of surface mycelial layer (day 9) to the end of cultivation (day 28), and a final concentration of 427±29 mg L^{-1} was reached. As shown in Fig. 11C, the total GA production (GA production by cells in the liquid plus that on the surface) reached the highest level of 516±17 mg L^{-1} at an initial K_La value of 2.1 h^{-1} with a corresponding GA productivity of 21.3±0.9 mg L^{-1} day^{-1}. Total GA production and productivity at an initial K_La of 2.1 h^{-1} were almost twice those under other conditions. As discussed previously [8], these data confirmed that oxygen limitation was favorable to the GA accumulation.

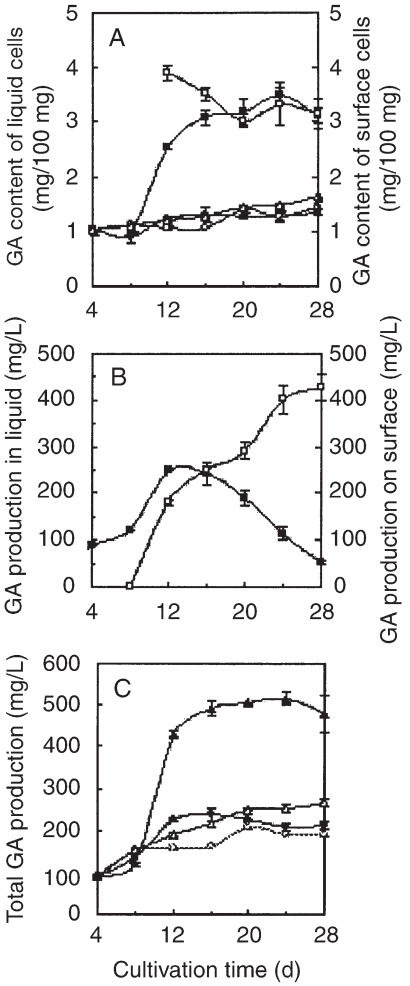

Fig. 11 Time courses of GA content of cells in the liquid and on the surface (**A**), GA accumulation by cells in the liquid and on the liquid surface (**B**), and total GA production (**C**) in static cultures of *G. lucidum* for different initial $K_L a$ levels. Symbols for cells: cells in the liquid (*filled squares*) and on the liquid surface (*open squares*) for an initial $K_L a$ value of 2.1 h^{-1}. Symbols for initial $K_L a$ values (h^{-1}): 16.4 (*empty circles*), 9.4 (*filled circles*), 3.2 (*empty triangles*), and 2.1 (*filled triangles*). Error bars in the figure indicate standard deviations from three independent samples

6.2.2 *Effect of liquid surface area per liquid volume*

Because not only the cells in the liquid but also those on the liquid surface made a significant contribution to total GA production, we investigated the impact of liquid surface area per liquid volume (A_s). In all experiments the white mycelia layer appeared on the liquid surface. The formation of white mycelia on the surface increased at larger A_s within the range investigated (0.24–1.53 cm^2 mL^{-1}) and

mycelial growth was significantly limited at an A_s of 0.24 cm^2 mL^{-1}. The maximum cell density in the liquid was 13.4±0.5, 16.0±1.3, and 13.4±0.5 g L^{-1} at A_s levels of 0.24, 0.90, and 1.53 cm^2 mL^{-1}, respectively, and the maximum cell density on the surface at A_s values of 1.53 and 0.90 cm^2 mL^{-1} was about twice that for A_s=0.24 cm^2 mL^{-1} (Table 8). At an A_s value of 0.24 its total cell density was relatively low (13.4 g L^{-1}) (Table 8). In agreement with the cell growth, an increase in A_s led to a higher lactose consumption rate [55].

The maximum GA production by cells in the liquid was 195±18, 318±14, and 236±11 mg L^{-1} on day 8 at A_s values of 0.24, 0.90, and 1.53 cm^2 mL^{-1}, respectively. The highest production and productivity of GA obtained were 667±6 mg L^{-1} and 28.2±0.3 mg L^{-1} day^{-1} at an A_s value of 0.90 cm^2 mL^{-1} (Table 8). These results indicated that A_s significantly affected cell growth and GA accumulation. The optimum A_s level in the static culture of *G. lucidum* was 0.90 cm^2 mL^{-1}. This information is also very important to the reactor design for large-scale cultivation of the mushroom.

Table 8 Effects of area of liquid surface per liquid volume on cell growth and GA production in static cultures[a,b]

Area of liquid surface per liquid volume (cm^2 mL^{-1})	0.24	0.90	1.53
Maximum dry cells in the liquid (g L^{-1})	13.4±0.5 (day 4)[c]	16.0±1.3 (day 8)	13.4±0.5 (day 4)
Maximum dry cells on the surface (g L^{-1})	9.2±0.9 (day 28)	17.6±0.3 (day 32)	19.1±0.4 (day 24)
Maximum total dry cells (g L^{-1})	13.4±0.5 (day 4)	22.2±0.6 (day 16)	21.0±1.2 (day 16)
Maximum GA content of cells in the liquid (mg/100 mg)	3.95±0.14	3.82±0.01	4.47±0.35
Maximum GA content of cells on the surface (mg/100 mg)	3.98±0.07	2.98±0.17	2.99±0.03
Maximum GA production by cells in the liquid (mg L^{-1})	195±18	318±14	236±11
Maximum GA production by cells on the surface (mg L^{-1})	344±13	477±13	545±4
Maximum total GA production (mg L^{-1})	440±31	667±6	620±13
Total GA productivity (mg L^{-1} day^{-1})	14.0±1.3	28.2±0.3	25.8±0.7

[a] The standard deviations were calculated from three samples.
[b] All data, unless otherwise indicated, were calculated between day 4 and the time of peak cell growth or metabolite production.
[c] The number in the parentheses refers to the time when the maximum dry cell weight was reached.

6.2.3
Cultivation in static bioreactors

Kinetics of cell growth (Fig. 12A) and lactose consumption in static bioreactors of different size were very similar (data not shown). After inoculation, cell density in the liquid increased until day 8, and it decreased sharply in the later stage. The cell density on the surface increased after appearance of the surface mycelial layer (day 6) until day 20, when a maximum level was attained. After that, it decreased slowly. The maximum total cell density was almost the same in different cultivation vessels (Table 9).

Time courses of GA content were similar in different static bioreactors [55]. After inoculation GA content increased until day 20, when the maximum content was obtained. Later, it began to decrease. The dynamic profile of GA accumulation was also very similar in different reactors (Fig. 12B). After 20 days of cultivation, the total GA production reached 940–980 mg L^{-1} in a variety of vessels, and their corresponding productivity was about 50 mg L^{-1} day^{-1} (Table 9).

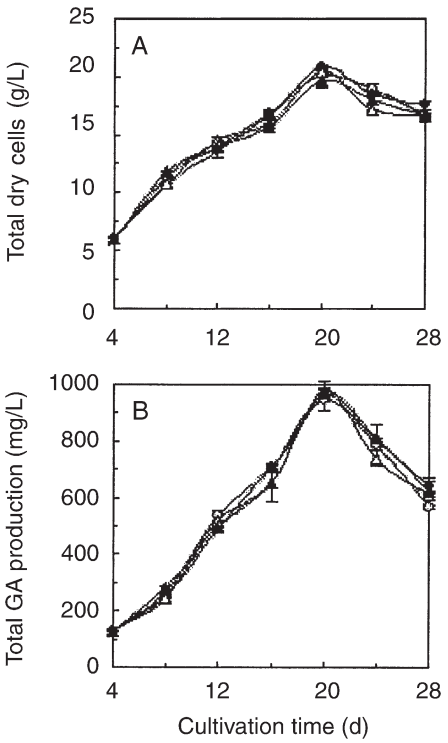

Fig. 12 Kinetics of total cell density (**A**) and total GA production (**B**) in different cultivation vessels. Symbols for different cultivation vessels: 50-mL T-flask (*empty circles*), one-layer static bioreactor (*filled circles*), two-layer static bioreactor (*empty triangles*), and three-layer static bioreactor (*filled triangles*). The error bars in the figure indicate standard deviations from three independent samples

Table 9 Cell growth and ganoderic acids (GA) accumulation by *G. lucidum* cells in different culture vessels

Cultivation system	50 mL T-flask	One-layer static reactor	Two-layer static reactor	Three-layer static reactor	Large three-layer static reactor
Total cell density[a] ($g\ L^{-1}$)	20.1	20.8	20.4	19.7	20.3
Maximum GA content (mg/100 mg)	4.88	4.64	4.81	4.96	4.67
Total GA production ($mg\ L^{-1}$)	944	963	976	970	937
Total GA productivity ($mg\ L^{-1}\ day^{-1}$)	50.9	52.1	52.9	52.5	50.4

[a] The maximum dry cell weight was reached on day 20 in all cases.

Table 10 The content and production of GA as reported in different cultivations of *G. lucidum*

GA content (mg/100 mg)	GA production ($mg\ L^{-1}$)	Process and scale	Refs.
0.46	Not reported	One-stage culture; flask scale	[47]
2.52	360	One-stage culture; reactor scale	[45]
1.86	267	One-stage culture; flask scale	[27]
2.05	367	One-stage culture; reactor scale	[28]
3.19	582	Two-stage culture; flask scale	[8]
4.96	976	Two-stage culture; reactor scale	[69]

A further study on the performance of static culture process of *G. lucidum* in a 7.5-L (working volume) three-layer static bioreactor was attempted. As summarized in Table 9, specific GA production (i.e. content) in a 7.5-L static bioreactor was similar to that in small static bioreactors. The maximum total dry weight of 20.3 $g\ L^{-1}$ and GA production of 937 $mg\ L^{-1}$ was achieved after 20 days of culture in a 7.5-L static bioreactor.

These results indicate that the static culture of *G. lucidum* for hyperproduction of GA was successfully scaled up from a T-flask (with a working volume of 20 mL) to a three-layer static bioreactor (with a working volume of 7.5 L). Initial $K_L a$ and area of liquid surface per liquid volume were identified as key factors in scaling up the static culture process. Both the GA content (4.96±0.13 mg/100 mg) and its production titer (976±35 $mg\ L^{-1}$) obtained here were higher than those in previous reports (Table 10).

6.3 Process modeling

Modeling cell culture processes might be useful for process control, optimization, and understanding process dynamics [70–74]. In mixed cultures, a mathemati-

cal model was developed to describe the dynamic behavior of mixed cultures by fitting model terms with experimental data [71]. A segregated model for heterologous amylase production by *Bacillus subtilis*, which could predict the transient behavior of *B. subtilis* in both batch and fed-batch cultures, was proposed [72, 73]. Compared with structured models, unstructured models do not offer much in terms of elucidating the exact nature of bioprocesses. However, structured models often involve introducing bioprocess variables that cannot be estimated reliably. Despite a great need for the development of large-scale mushroom cell culture processes for efficient production of useful metabolites, until now there have been no reports of their bioprocess modeling, except for the specific case of cell cultures of *G. lucidum*. In this work, modeling of the liquid static culture process was attempted.

According to the materials balance, the cell growth, substrate consumption, and GA production in the static culture of *G. lucidum* can be described by differential equations as follows:

$$\frac{dS}{dt} = -\mu \frac{X}{Y_{X/S}} \tag{2}$$

$$\frac{dX}{dt} = \mu X - k_d X \tag{3}$$

$$\frac{dP}{dt} = 1000\, r_p X \tag{4}$$

where S, X, P are the residual sugar concentration, cell concentration and GA production titer, respectively, μ is the specific growth rate, $Y_{X/S}$ is the biomass yield against lactose, k_d is the cell death rate, and r_p is the specific GA production rate.

Based on the kinetics of the mushroom cell growth [55], the specific growth rate could be represented by Monod model as follows:

$$\mu = \mu_{max} \frac{S}{K_S + S} \tag{5}$$

where μ_{max} is the maximum specific growth rate and K_S is the saturation constant.

The relationship between r_p and μ obtained from the static cultures [55] indicates that GA production followed segmental growth-associated kinetics during the cultivation. The specific GA production rate r_p was considered to be proportionately dependent on the segmental growth-associated product formation term. That is:

$$r_p = \alpha\mu + \beta \tag{6}$$

where α represents the growth-associated product formation constant and β is the non-growth-associated production formation constant.

Table 11 Estimated parameters for the unstructured kinetic model

Parameter	μ_m	k_s	$Y_{X/S}$	k_d	α	β
Estimated value	0.23 day^{-1}	17.52 g L^{-1}	0.78 g g^{-1}	0.036 day^{-1}	0.058	–0.0021 day^{-1}

6.3.1
Parameter estimation

Parameters in these differential equations were estimated by a non-linear least-squares routine (lsqnonlin.m) in the Optimization Toolbox of the Matlab environment [75]. The sum-of-squares error between model predictions and experimental data for residual sugar concentration, total cell concentration, and total GA production was minimized. Because minimization of the sum of squares for a general non-linear problem is quite dependent on the initial guesses for the parameters, various starting points were provided and the final parameter set that had the lowest sum-squared error was chosen. The initial conditions were given according to the experimental data in static cultures of *G. lucidum* at a one-layer bioreactor with a working volume of 218 mL, i.e. 30.8 g L^{-1} lactose (S), 6.1 g L^{-1} cell mass (X), and 130 mg L^{-1} total GA production (P). The values of the optimized parameters are summarized in Table 11.

6.3.2
Parameter sensitivity analysis

Parameter sensitivity analysis was also performed. Residual sugar concentration, total cell concentration, and total GA production were predicted by varying one condition while fixing all the others [73, 74]. Figure 13 shows the effects of perturbation on the model prediction by taking perturbation of α as a typical example. It can be seen that model prediction of residual sugar concentration and total cell concentration was not very sensitive to changes in α by 10% up or down; the prediction of total GA production was, however, quite sensitive to alteration in α by ±10% (Fig. 13C). To determine sensitivities of other parameters in the static cultures, residual sugar concentration, total cell concentration, and total GA production on day 20 were also predicted in the same way, i.e. by varying one condition while fixing the others. The predicted data in Table 12 indicate that increasing μ_m by 10% would cause a decrease of the residual sugar concentration (on day 20) by almost 40% whereas both cell concentration and GA production would increase by about 4% compared with the original prediction without alteration of μ_m. Table 12 also shows that the model was less sensitive to changes in k_d and β but was very sensitive to alterations in μ_m, K_S, $Y_{X/S}$ and α.

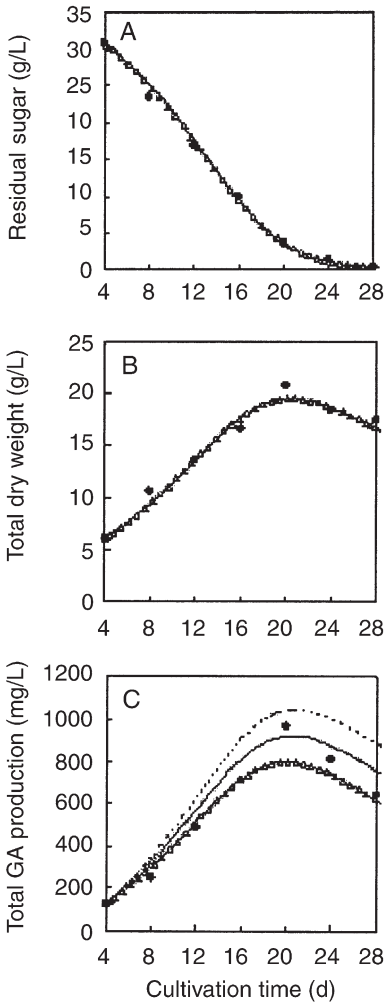

Fig. 13 Impact of perturbation of parameter α on model prediction of residual sugar concentration (**A**), cell concentration (by dry weight) (**B**), and GA accumulation (**C**). Symbols: *line*, original simulation results; *dashed line*, simulated data when parameter α was increased by 10%; *empty triangles*, simulated results when parameter α was decreased by 10%; *filled circles*, experimental data

6.3.3 *Model validation*

As mentioned above, a conventional unstructured kinetic model was used on the basis of the kinetics of the static culture of *G. lucidum* in a single-layer static bioreactor (working volume 218 mL). To test the validity of the established model parameters, model predictions were compared with experimental data from different laboratory-scale static bioreactors. As shown in Fig. 14, the model could

Table 12 Parameter sensitivity analysis

Parameter	Perturbation of parameter	Alteration of residual sugar	Alteration of cell concentration	Alteration of total GA production
μ_m	+10%	–41.2%	+3.6%	+4.3%
	–10%	+62.5%	–6.1%	–7.4%
K_s	+10%	+28.9%	–2.6%	–3.4%
	–10%	–27.2%	+2.6%	+3.2%
$Y_{x/s}$	+10%	+23.2%	+6.1%	+7.8%
	–10%	–21.6%	–7.1%	–8.6%
k_d	+10%	+9.2%	–4.1%	–0.2%
	–10%	–7.6%	+4.1%	+0.1%
α	+10%	+0.8%	0	+13.4%
	–10%	–2.0%	0	–13.4%
β	+10%	–2.0%	0	–4.7%
	–10%	+0.8%	0	+4.7%

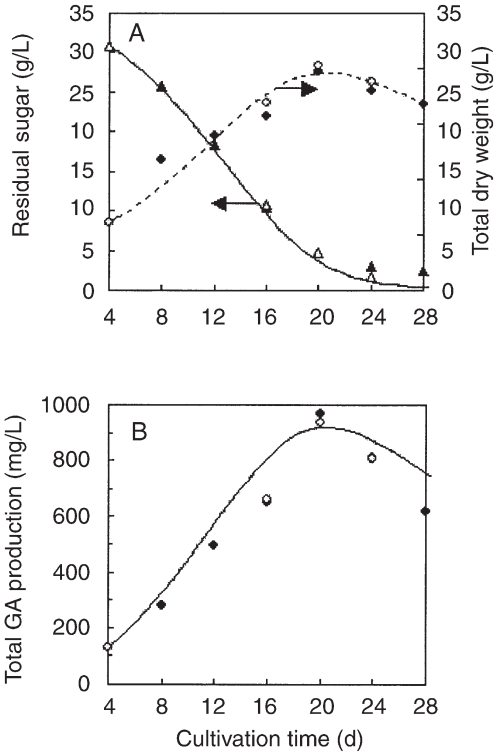

Fig. 14 Comparison of model predictions with the experiment data in three-layer static bioreactors with working volumes of 654 mL and 7.5 L. Experimental data are represented by *filled* (654-mL static bioreactor) and *open* symbols (7.5-L static bioreactor), and the *lines* show simulation results

predict the cell growth, lactose consumption, and GA accumulation quite well for three-layer static bioreactors with working volumes of 654 mL and 7.5 L. The performance of the static culture process in a T-flask (working volume 20 mL) and a two-layer static bioreactor (working volume 436 mL) could also be well described by using the above mathematical model [55].

The results demonstrate that the simple unstructured model could predict cell growth, lactose utilization, and GA production in the static culture of *G. lucidum* in a variety of laboratory-scale static bioreactors with working volumes from 20 mL to 7.5 L. Parameter sensitivity analysis indicated that the model was sensitive to changes in maximum specific growth rate (μ_m), the saturation constant (K_s), the biomass yield against lactose ($Y_{X/S}$) and the growth-associated product formation constant (α).

7 Conclusions

By taking submerged cultivation of *G. lucidum* as a typical example of mushroom cultures, significant effects of oxygen supply and hydrodynamic shear on the cell growth, morphology, and metabolite biosynthesis were demonstrated in shake flasks and bioreactors. These two important environmental factors should be well controlled to achieve a highly productive process on a large scale.

Production of ganoderic acids and *Ganoderma* polysaccharides could be reasonably enhanced by fed-batch cultivation. A two-stage cultivation strategy was also proposed; this was very useful for improving the production of ganoderic acids. Scale-up of submerged cultures of *G. lucidum* was successfully realized on a laboratory scale (30-L bioreactor) by using a low-shear centrifugal impeller bioreactor. For liquid static cultures both initial $K_L a$ level and liquid surface area per liquid volume were found to be key factors for the process scale-up. The results obtained are considered to be useful for the simultaneous, highly efficient production of the cell mass, *Ganoderma* polysaccharides, and ganoderic acids in large-scale bioreactors. The information might be also beneficial to other submerged cultivation processes of medicinal and edible mushrooms, which have wide utilization and application in the food and health-care sectors.

In addition, both cell growth and formation of ganoderic acids in a static culture process could be described mathematically using a simple unstructured kinetic model by fitting model parameters to the experimental data. The model identified might be useful in converting large-scale static culture processes to industrial application. Such work might also be helpful in the development of process modeling and the optimization of other mushrooms culture processes.

Acknowledgement We thank Mr Hai-Gang Gong and Mr Qing-Hua Fang for their contribution to this work. Financial support from the National Natural Science Foundation of China (NSFC project nos. 20076011 and 20236040) and the Key Discipline Development Project of Shanghai Municipality is appreciated. We are also grateful to the National Science Fund for Distinguished Young Scholars (NSFC project no. 20225619) and the Cheung Kong Scholars Program of the Ministry of Education of China.

8 References

1. Tang YJ, Zhong JJ (2000) In: Zhong JJ (ed) Advances in applied biotechnology. East China University of Science and Technology Press, Shanghai, p 104
2. Smith JE, Rowan NJ, Sullivan R (2002) Biotechnol Lett 24:1839
3. Wasser SP (2002) Appl Microbiol Biotechnol 60:258
4. Wasser SP, Weis AL (1999) Int J Med Mush 1:31
5. Tang YJ, Zhong JJ (2001) J East China Univ Sci Technol 27:704 (in Chinese)
6. Fang QH, Zhong JJ (2002) Process Biochem 37:769
7. Fang QH, Zhong JJ (2002) Biochem Eng J 10:61
8. Fang QH, Zhong JJ (2002) Biotechnol Prog 18:51
9. Wagner R, Mitchell DA, Sassaki GL, de Almeida Amazonas MAL, Berovic M (2003) Food Technol Biotechnol 41:371
10. Kim SW, Hwang HJ, Xu CP, Sung JM, Choi JW, Yun JW (2003) J Appl Microbiol 94:120
11. Yoshida T, Taguchi H, Teramoto S (1965) J Ferment Technol 43:325
12. Yoshida T, Shimizu T, Taguchi H, Teramoto S (1965) J Ferment Technol 43:901
13. Yoshida T, Shimizu T, Taguchi H, Teramoto H (1967) J Ferment Technol 45:1119
14. Tang YJ, Zhong JJ (2003) Enzyme Microb Technol 34:478
15. Kim S, Hwang H, Xu C, Sung J, Choi J, Yun J (2003) J Appl Microbiol 94:120
16. Lorenzen K, Anke T (1998) Curr Org Chem 2:329
17. Tanimoto T, Onodera K, Hosoya T, Takamatsu Y, Kinoshita T, Tago K, Kogen H, Fujioka T, Hamano K, Tsujita Y (1996) J Antibiot 49:617
18. Puntambekar US (1995) World J Microbiol Biotechnol 11:695
19. Khowala S, Sengupta S (1984) Can J Microbiol 30:657
20. Guillen-Navarro GK, Marquez-Rocha FJ, Sanchez-Vazquez JE (1998) Rev Iberoam Micol 15:302
21. Klappach G (1990) Zentralbl Mikrobiol 145:83
22. Ghosh AK, Sengupt S (1981) J Food Sci Technol (Mysore) 18:133
23. Eyal J, Spencer MG (1991) US Patent 5 077 201
24. Cho Y, Park J, Hwang H, Kim S, Choi J, Yun J (2002) Lett Appl Microbiol 35:195
25. Kim S, Hwang H, Park J, Cho Y, Song C, Yun J (2002) Lett Appl Microbiol 34:56
26. Kim S, Hwang H, Xu C, Na Y, Song S, Yun J (2002) Lett Appl Microbiol 34:389
27. Fang QH, Tang YJ, Zhong JJ (2002) Process Biochem 37:1375
28. Tang YJ, Zhong JJ (2002) Enzyme Microb Technol 31:20
29. Tang YJ, Zhong JJ (2002) Biotechnol Lett 24:1023
30. Mizuno T, Wang G, Zhang J, Kawagishi H, Nishitoba T, Li J (1995) Food Rev Int 11:151
31. Shiao MS, Lee KR, Lee JL, Cheng TW (1994) In: ACS Symp Ser 547, Food Phytochemicals for Cancer Prevention II. American Chemical Society, Washington DC, p 342
32. Miyazaki T, Nishijima M (1981) Chem Pharm Bull 29:2269
33. Sone Y, Okuda R, Wada N, Kishida E, Misaki A (1985) Agric Biol Chem 49:2641
34. Hikino H, Konno C, Mirin Y, Hayashi T (1985) Planta Med 4:339
35. Hikino H, Ishiyama M, Suzuki Y, Konno C (1989) Planta Med 55:423
36. El-Mekkaway SR, Meselhy M, Nakamura N, Tezuka Y, Hattori M, Kakiuchi N, Shimotohno K, Kawahata T, Otake T (1998) Phytochemistry 49:1651
37. Min BS, Gao JJ, Nakamura N, Hattori M (2000) Chem Pharm Bull 48:1026
38. Wu TS, Shi LS, Kuo SC (2001) J Nat Prod 64:1121
39. Yang FC, Ke YF, Kuo SS (2000) Enzyme Microb Technol 27:295
40. Yang FC, Liau CB (1998) Process Biochem 33:547
41. Lee KM, Lee SY, Lee HY (1999) J Biosci Bioeng 88:646
42. Li PZ, Xu R, Zhang KC (1998) J Wuxi Univ Light Ind 17(4):26 (in Chinese)
43. Li PZ, Zhang KC (2000) Weishengwu Tongbao 27(1):5 (in Chinese)
44. Li PZ, Xu R, Zhang KC (2000) Ind Microbiol 30(3):20 (in Chinese)
45. Li PZ, Xu R, Xia JH, Zhang KC (2000) Ind Microbiol 30(1):15 (in Chinese)
46. Li PZ, Xia JH, Zhang KC (1999) Zhongcaoyao 30:584 (in Chinese)

47. Tsujikura Y, Higuchi T, Miyamoto Y, Sato S (1992) Jpn Kokai Tokkyo Koho JP 04304890 (in Japanese)
48. Cui YQ, Van der Lans RGJM, Luyben KCAM (1998) Biotechnol Bioeng 57:409
49. Biryukov VV, Tarasova SS (1974) Biotechnol Bioeng Symp 4:573
50. Zhong JJ, Fujiyama K, Seki T, Yoshida T (1994) Biotechnol Bioeng 44:649
51. Kieran PM, MacLoughlin PF, Malone DM (1997) J Biotechnol 59:39
52. Zhong JJ (2001) Adv Biochem Eng Biotechnol 72:1
53. Zhong JJ, Yoshida T (1995) Enzyme Microb Technol 17:1073
54. Hu WW, Yao H, Zhong JJ (2001) Biotechnol Prog 17:838
55. Tang YJ (2003) PhD thesis, East China University of Science and Technology, Shanghai. (in Chinese)
56. Ramos A, Boels IC, Willem M. de Vos, Santos H (2001) Appl Environ Microbiol 67:33
57. Looijesteijn PJ, Boels IC, Kleerebezem M, Hugenholtz J (1999) Appl Environ Microbiol 65:5003
58. Hickey MW, Hillier AJ, Jago GR (1986) Appl Environ Microbiol 51:825
59. Citti JE, Sandine WE, Elliker PR (1965) J Bacteriol 80:937
60. Degeest B, Vuyst L De (2000) Appl Environ Microbiol 66:3519
61. Levander F, Radstrom P (2001) Appl Environ Microbiol 67:2734
62. Wang SJ, Zhong JJ (1996) Biotechnol Bioeng 51:511
63. Wang SJ, Zhong JJ (1996) Biotechnol Bioeng 51:520
64. Kawagoe M, Hyakumura K, Suye S, Miki K, Naoe K (1997) J Ferment Bioeng 84:333
65. Sinha J, Bae JT, Park JP, Song CH, Yun JW (2001) Enzyme Microb Technol 29:392
66. Tanase T, Ikeda Y, Iwama K, Hashimoto A, Kataoka T, Tokushima Y, Kobayashi T (1997) J Ferment Bioeng 83:499
67. Wang DIC, Cooney CL, Demain AL, Dunnill P, Humphrey AE, Lilly MD (1979) Fermentation and enzyme technology. Wiley, New York
68. Abel C, Linz F, Scheper T, Schügerl K (1994) J Biotechnol 33:183
69. Tang YJ, Zhong JJ (2003) Biotechnol Prog 19:1842
70. Tartakovsky B, Sheintuch M, Hilmer JM, Scheper T (1997) Bioprocess Eng 16:323
71. Katoh T, Yuguchi D, Yoshii H, Shi H, Shimizu K (1999) J Biotechnol 67:113
72. Huang H, Ridgway D, Gu T, Moo-Young M (2003) Enzyme Microb Technol 32:407
73. Huang HJ (2002) PhD dissertation, Ohio University, Ohio
74. Fordyce AP, Rawlings JB (1996) AIChE J 42:3241
75. Coleman T, Branch MA, Grace A (1999) Optimization toolbox – user's guide, vol 2. The MathWorks, Natick, MA

Received: September 2003

Adv Biochem Engin/Biotechnol (2004) 87: 61–96
DOI 10.1007/b94364

A Fibrous-Bed Bioreactor for Continuous Production of Monoclonal Antibody by Hybridoma

Shang-Tian Yang · Jun Luo · Chunnuan Chen

Department of Chemical Engineering, The Ohio State University, 140 West 19th Avenue, Columbus, Ohio 43210, USA
E-mail: yang.15@osu.edu

Abstract A fibrous-bed bioreactor (FBB) has been developed to culture hybridoma cells for long-term continuous production of monoclonal antibody (MAb). A non-woven polyester fibrous matrix was used to immobilize the cells to reach a high viable cell density of 3×10^8 cells cm^{-3} packed bed, which gave a high volumetric MAb productivity of 1 g L^{-1} day^{-1} under continuous feed conditions with the medium containing 10% serum. Reducing the medium serum content to 1% increased MAb production to 6.5 g L^{-1} day^{-1} in a repeated batch FBB culture. MAb production was higher at higher dissolved oxygen (DO) levels in the range between 10% and 70% of air saturation, although DO did not significantly affect glucose metabolism and lactate production. The medium LDH (lactate dehydrogenase) level increased dramatically when the DO level was decreased from 30% to 10%, suggesting that a critical DO level of ~30% is necessary for maintaining the FBB culture for long-term operation. Compared with suspension cultures in T-flasks and spinner flasks, the FBB culture had a lower lactate yield from glucose (0.80 vs. 0.91 g g^{-1}), produced MAb at a higher concentration (up to 442 mg L^{-1} vs. 83.5 mg L^{-1}), and was stable for continuous long-term operation (more than 1 month). The superior FBB performance was attributed to the highly porous fibrous matrix that enabled the efficient mass transfer, cell immobilization, and continued growth and regeneration that are critical to maintaining a high density of viable and productive cell populations. The cells immobilized in the fibrous matrix had high viability (>85%) even though many of them were in growth arrest (G1/G0 phase) as indicated by their smaller cell size (<10 μm). Scanning electron microscopic studies of the cell-matrix showed that the high density of cells formed large clumps within the interstitial spaces of the fibrous matrix. Their close contact and interaction with each other might have contributed to their ability to survive well under adverse conditions such as low DO and low serum content in the medium. It was also found that the cells present inside the fibrous matrix had a higher viability and lower apoptosis than those present in the liquid suspension, indicating that the fibrous matrix had selectively retained healthy, non-apoptotic cells and dislodged apoptotic and dead cells; this also might have contributed to the stability of the long-term culture. This work demonstrated that the FBB originally developed for microbial fermentation also gave excellent results in achieving high cell density, productivity, and product concentrations, and should have a good potential for industrial animal cell culture applications.

Keywords Hybridoma · Monoclonal antibody · Fibrous-bed bioreactor

Abbreviations

DO	Dissolved oxygen
FBB	Fibrous-bed bioreactor
LDH	Lactate dehydrogenase
MAb	Monoclonal antibody
RSV	Respiratory syncytial virus

Nomenclature

C	Concentration
D	Dilution rate (day^{-1})
Q	Volumetric reaction rate
Q_{MAb}	Volumetric production rate of MAb ($mg\ L^{-1}\ day^{-1}$)
Q_{glu}	Volumetric consumption rate of glucose ($g\ L^{-1}\ day^{-1}$)
Q_{gln}	Volumetric consumption rate of glutamine ($mmol\ L^{-1}\ day^{-1}$)
Q_{lac}	Volumetric production rate of lactate ($g\ L^{-1}\ day^{-1}$)
q_{MAb}	Cellular specific production rate of MAb ($\mu g/10^6 cells\ day^{-1}$)
t	time (day)

$Y_{lac/glu}$ Lactate yield on glucose (g g^{-1})
$Y_{MAb/gln}$ MAb yield on glutamine (mg $mmol^{-1}$)

Subscripts
f feed
i species
1, 2 time points 1 and 2

1 Introduction

Monoclonal antibodies (MAb) are widely used in biomedical research and in diagnostics, with an estimated annual sale of ~$4 billion in the US in 1998. Approximately 25,000 MAb are being produced by cell lines or clones obtained from animals that have been immunized with the corresponding antigen. Most of these antibodies are produced in small quantities (<0.1 g) for bench-related research purposes; however, some have gained commercial interest and require large-scale production, especially those for therapeutic purposes. Because MAb bind to specific cell-surface receptors, they can be used for treatment of transplant rejection, cancer, autoimmune and inflammatory diseases, and infectious diseases. By mid-2000, nine MAb products had been approved by the FDA for therapeutic applications, with more than $1.3 billion product sale in 1999. The launch of Synagis, a recombinant monoclonal antibody for respiratory syncytial virus (RSV), by MedImmune in the 1998/1999 RSV season was the most successful introduction of a biopharmaceutical product to date, generating $227 million [1]. Since then, worldwide sale of Synagis has increased at an annual rate of >20% to $668 million in 2002. Currently, MAb products comprise about 25% of all biotech drugs in clinical development. There is a major concern that the current industrial capacity for MAb production may not be sufficient to meet the fast growing market for antibody-based therapeutic products, which is estimated to reach $8 billion by 2004.

Current commercial MAb production uses two methods:

1. in-vivo cultivation in mouse or rabbit ascites, and
2. in-vitro cell culture in tissue flasks or bioreactors.

Economics and availability usually favor in-vivo production, especially for small to medium scale [2]. However, as the concern for animal welfare and the demand for MAb therapeutics increase, in-vitro production technology becomes more important. Production of MAb by in vitro culture of hybridoma cells has been studied for several decades [3]. Cells producing MAb are usually cultivated in suspension cell cultures on a batch or perfusion mode [4, 5]. The concentration of viable cells achieved in suspension cultures is usually low, ~10^6 cells mL^{-1} [6–11]. Consequently, MAb concentration (usually less than 100 mg L^{-1}) and volumetric productivity (usually 20–70 mg L^{-1} day^{-1}) are also low as compared with those from mouse ascites [12, 13]. These disadvantages of in-vitro tissue culture are mainly because hybridoma cells are usually difficult to culture in bioreactor suspension cultures, because of their sensitivity to shear and bubble damage, insufficient supplies of oxygen and other nutrients in the growth media, and in-

hibition by their own metabolites. Tissue-culture methods also require expensive media, and not all hybridoma cell lines can grow or produce sufficiently high or biologically functional MAb in the culture media. Although in-vitro tissue-culture methods have recently made tremendous progress, there is still a continuing need to develop an economical and scalable cell-culture process that is suitable for both small-to-medium and large scale production of MAb. Recent research efforts have focused on the development of bioreactor systems and feeding strategies that can give higher cell density, cell viability and productivity for mass production purpose [14, 15].

2 In-vitro MAb production in bioreactor

Commercial-scale production of MAb is generally for three applications–research and development of new therapeutic agents, diagnostics, and therapeutic drugs. Production scales of 0.1–10 g are regarded as small, 10–100 g as medium, and over 100 g as large [2]. Static flasks and roller bottles are usually used to produce up to 0.1 g antibody in about 30 days. For larger quantities four different types of cell culture bioreactor are available–stirred-tank, airlift, fixed-bed, and hollow fiber. Cells are usually suspended in stirred-tank and airlift bioreactors, and immobilized in hollow-fiber and fixed-bed bioreactors. These different types of bioreactor are compared in Table 1. The different growth environments in these bioreactors and operating modes contributed to different culture performance shown in Table 2.

Table 1 Comparison of four different types of bioreactor used for cell culture

	Stirred-tank	Airlift	Hollow-fiber	Fixed bed
Oxygenation	Mechanical agitation and gas sparging	Gas sparging	Diffusion and medium re-circulation	Diffusion and medium re-circulation
Cell density (mL^{-1})	10^6–10^7	10^6–10^7	$>10^8$	$>10^8$
Cell damage by shear stress	High, caused by agitation and gas sparging	Medium	Low	Low
Culture stability	High for continuous perfusion culture	High for continuous perfusion culture	Deterioration because of membrane fouling, cell clogging and accumulation of dead cells	Deterioration because of cell clogging and accumulation of dead cells
Scale up potential	High	High	Low–limited by oxygen supply	High, but might be limited by oxygen supply

Table 2 Comparison of MAb production in different culture systems

Reactor type and operating conditions	Cell density (10^6 mL^{-1})	MAb conc. (mg L^{-1})	Specific productivity (μg 10^{-6} cells h^{-1})	Volumetric productivity (mg L^{-1} day^{-1})	Ref.
T-flask					
T-150 flask, batch culture	0.7–0.9	160–180	4	67–86	[8]
Suspension culture in stirred tank bioreactor or spinner flask					
Batch culture	3–4	20	0.2–0.125	19.2	[11]
Fed-batch culture	6.3–17	2400	–	–	[17]
Continuous culture	1–2	41–55	1.0–1.5	72	[9]
Continuous culture	3–4	30	0.2–0.3	30	[90]
Continuous, with butyrate feeding	2–3	100–120	0.2–0.3	22	[7]
Continuous culture with optimum feeding strategy	0.7 g L^{-1}	200–250	–	–	[119]
Immobilized culture in stirred tank bioreactor or spinner flask					
PEG-alginate beads, batch culture	2.5–3	–	3.7 titer 10^{-6} h^{-1}	–	[14]
Perfusion culture	12	–	14 titer 10^{-6} h^{-1}	–	
Microcarriers (Cytoline 2)	0.6–1.4	20	0.08–0.17	5.7	[120]
Suspension culture in stirred tank bioreactor or spinner flask with cell retention or recycle					
Recycle by sedimentation	20–25	25–35	0.2–0.25	150	[20]
Recycle through a settling tube	0.1–0.5	20–50	0.6–1	12	[121]
Retention by using a spin filter	15.8	–	0.29	110	[21]
Recycle by ultrasonic cell separation	12.1	–	0.31	90	[21]
Retention by hollow fiber filtration	15–18	275 unit L^{-1}	–	275 U L^{-1} day^{-1}	[26]
Retention by hollow fiber filtration	4	80	0.4–0.7	67.2	[122]
Hollow fiber reactor[a]					
Perfusion culture	100	2500–6000	0.6–1.4	~3500	[41]
Perfusion culture	10–100	710–11100	–	500–2500	[12]
Perfusion with extra-capillary cycling	–	~2000	–	~1500	[51]
Packed bed bioreactor[b]					
Celligen with packed column	120	400–500	0.33	1050	[15]
with packed basket	–	150–200	–	–	
FBB continuous culture	300	106	0.14	994	This
batch with low serum medium	200	442	1.35	6500	study

[a] Cell densities and volumetric productivities are based on the extracapillary volume of the hollow fiber reactor; MAb concentrations are in the product streams.

[b] Cell densities and volumetric productivities are based on the packed reactor volumes.

2.1 Suspended culture

Stirred-tank and air-lift bioreactors are the norm for large-scale fermentation processes, because of their high scale-up potential, and are currently used in the animal cell culture industry for production of MAb therapeutics. Because of their fragile cellular structure, animal cells are sensitive to shear and bubble damage in the bioreactor environment. Cell damage and death caused by mechanical agitation and gas sparging [16] in stirred-tank and airlift bioreactors is a major concern in reactor design and scale up. In general, cell density is limited to 10^6–10^7 mL^{-1}, because of limited oxygenation at low agitation and aeration rates to avoid severe cell damage. With better medium design and feeding strategy [17] and continuous perfusion with cell recycle to remove toxic metabolic byproducts [18, 19], the cell density in conventional suspension cultures can be increased to 10^7 cells mL^{-1} with a significant improvement in MAb productivity (up to 150 mg L^{-1} day^{-1}) [20–26]. Also, shear damage to cells can be minimized and higher cell density and MAb production can be obtained with an improved impeller design [27].

MedImmune's recombinant paliviumab manufacturing process uses a stirred-tank fed-batch system with a stable cell line developed from a mruine myeloma cell line (NS0), which can produce about 1 g MAb per liter of culture medium [1]. The high titer of MAb production in this system was accomplished by extensive research and development work on cell-line improvement, medium optimization, and process optimization and control. The manufacturing process starts with a vial containing about 10 million frozen cells; these are cultured in a T-flask and then a spinner flask to expand the number of cells. These cells are then used in the larger-scale bioreactor process with the culture volume increased incrementally to the final volume of 10,000 L. After inoculation of the production bioreactor, the fermentation takes about 20 days to reach the final titer of the MAb product. It should be noted that MedImmune's process so far is the best known large-scale cell culture for MAb production. However, most hybridoma cell lines do not work well in stirred-tank bioreactors for reasons already mentioned.

2.2 Immobilized culture

Cell immobilization in a fixed bed or hollow fibers has also been studied as a better way of protecting cells from shear damage and to increase cell density and productivity [28–34]. The damaging effect of fluid-mechanical forces on cells can be reduced by cell immobilization [32–34]. A variety of immobilization techniques have been studied, including entrapping cells in agarose [35, 36], gelatin, and alginate beads [37, 38], in hollow fibers [39–44], between two membrane sheets [45, 46], in membrane-bound capsules [47], and by cell adhesion to, and entrapment in, fibers [15, 48]. Immobilized cell reactors can be easily perfused to receive a continuous supply of fresh culture medium, extending the productive lifetime of the cells and increasing the cell concentration obtained in the reactor. High cell densities of 10^7–10^8 cells mL^{-1} can thus be easily achieved in immobil-

ized cell cultures, and MAb productivity can be increased more than 20-fold compared with suspension cultures. Other advantages of cell immobilization include cell re-use, prevention of cell washout, and providing a favorable microenvironment for cell growth [49]. Also, products from such bioreactors are usually free from cells, thus reducing the burden on downstream processing.

Hollow-fiber bioreactors (HFB), in which cells are grown either in extracapillary or intracapillary space and the medium is circulated on the other side of the membrane, have been extensively studied as an alternative to murine ascites for MAb production [42, 50, 51]. In general, HFB can achieve a high cell density of $>10^8$ cells mL^{-1} with high MAb productivity; MAb are produced at a concentration comparable with or even higher than that in ascites [12, 13, 41, 44]. However, most studies were carried out with laboratory units for small-scale production and large-scale HFB units have encountered many operating difficulties, including mechanical failures and improper feed controls that could result in poor cell viability, poor process stability, and large diffusion gradients and product heterogeneity [12, 52, 53]. In general, hollow fibers are expensive and prone to membrane fouling, and are difficult to scale up for large-scale mass-production purposes. Their commercial uses are thus limited to small-to-medium scales and are mostly used for production of MAb needed for research and development of new therapeutic agents. The higher titers of MAb produced in hollow-fiber bioreactors are a consequence of the use of semi-permeable membranes that concentrate the product before they are harvested. For the same reason the products are usually contaminated with more dead cells and cell debris, requiring more vigorous and difficult pretreatments before final purification.

On the other hand, fixed bed bioreactors are easier to operate and have better scale-up potential. Fixed bed bioreactors, in which cells are immobilized and protected from shear stress within a carrier matrix, have been successfully used for both adherent and non-adherent cells. The microenvironment created by immobilized cells can be more favorable than that in the surrounding media. The high local cell density could reduce the serum requirement for cell growth, because the concentration of any intocrine growth factors can be high in the immobilized stage. Furthermore, immobilization can protect the cells from high shear stress, and cells are usually more sensitive to shear stress in low-serum and serum-free media. For these reasons, the possibility of using a low-serum or serum-free medium is higher in the immobilized culture than in the suspension culture. However, conventional fixed bed bioreactors with non-porous beads have low bed porosity (<60%) and usually suffer from a relatively low productivity and poor stability in long-term operation, and thus are not suitable for animal cell culture. Therefore, recent research has focused on fixed-bed bioreactors with porous carriers that can achieve high cell density and high productivity in immobilized culture systems [54–59].

Among porous carriers, fibrous matrices have been shown to be very efficient for cell immobilization, because of their three-dimensional (3D) structure, high surface to volume ratio, high void space, easy cell attachment and entrapment, and low resistance to flow and mass transfer [60–62]. Compared with other immobilized cell systems the main advantages of fibrous-bed bioreactors (FBB) include high mass-transfer efficiency, low pressure drop, easy to operate and scale

up, and low costs [15, 63]. Fibrous-bed bioreactors have been successfully used to immobilize and culture microorganisms [64–66], plant cells [67], insect cells [68], and mammalian cells [15, 31, 48, 54, 55, 69–73]. Chiou and his colleagues first developed a cell culture system that combined the features of air-lift, fiber-bed and packed bed with 24-μm glass fibers and achieved a high density of 5.1×10^7 CHO cells mL^{-1} [48]. Grampp and his colleagues used a ceramic-matrix bioreactor to culture βTC-3 cells [74]. With continuous perfusion the reactor achieved a cell density of ~5×10^8 cells mL^{-1} of pore volume after one month. New Brunswick Scientific (Edison, NJ, USA) developed a polyester basket in the packed-bed bioreactor (CelliGen) for which productivity could reach as high as 12-fold that in static and stirred suspension culture systems [15]. Non-woven fibers made of biodegradable polymers such as polyglycolic acid (PGA) and polylactic acid (PLA) have been widely used to culture a variety of anchorage-dependent cells such as smooth muscle (SM) cell in the tissue engineering field [75]. Non-woven polyester fibrous matrices also have been studied to support high-density cell culture (>3×10^8 cells mL^{-1} matrix) [54, 76]. The three-dimensional structure provided by a fibrous matrix has been shown to have profound effects on cell growth and protein production [31, 54, 61].

Table 2 compares cell density and MAb production in hybridoma cultures using various bioreactor systems. As is apparent from the Table 2, immobilized cultures, whether by entrapment in alginate beads or hollow fibers or via cell recycle, usually have higher cell densities and better MAb production than those in the T-flask cultures and suspended cultures in stirred-tank bioreactors. Perfusion cultures with hollow fiber bioreactors usually gave the highest cell density, MAb concentration, and productivity. However, hollow-fiber systems are difficult to scale up and have a relatively short operation life, because of accumulation of dead cells over time. Apparently, FBB would have many advantages for hybridoma cultures, although little has been done in scaling up the FBB and much work is still needed for a direct comparison of the FBB with other bioreactor systems, especially for hybridoma cultures.

To address the scale-up and long-term operation issues associated with conventional fixed-bed immobilized cell bioreactors we have developed a new, structured, fibrous-bed bioreactor, which contains a spiral wound fibrous sheet with spaces between wound layers to facilitate medium flow in the fibrous bed [64]. The spaces between fiber sheet layers are designed as free-flow channels for gases, liquids, and solids, which also allow continuous cell regeneration in the fibrous bed. More than tenfold increase in productivity with up to 1 year stable continuous operation has been obtained in several microbial fermentations using the spiral wound fibrous-bed bioreactor [64–66]. Two different designs of fibrous-bed bioreactor system can be used for cell cultures. As illustrated in the schematic diagrams shown in Fig. 1, the fibrous bed can be formed either inside a stirred-tank or airlift bioreactor or as an externally packed bed bioreactor with medium recirculation. The whole reactor system can be operated in either batch or continuous mode. Because of the high permeability of the fibrous matrix, the pressure drop for the fibrous bed is low, making it easy to scale up [61].

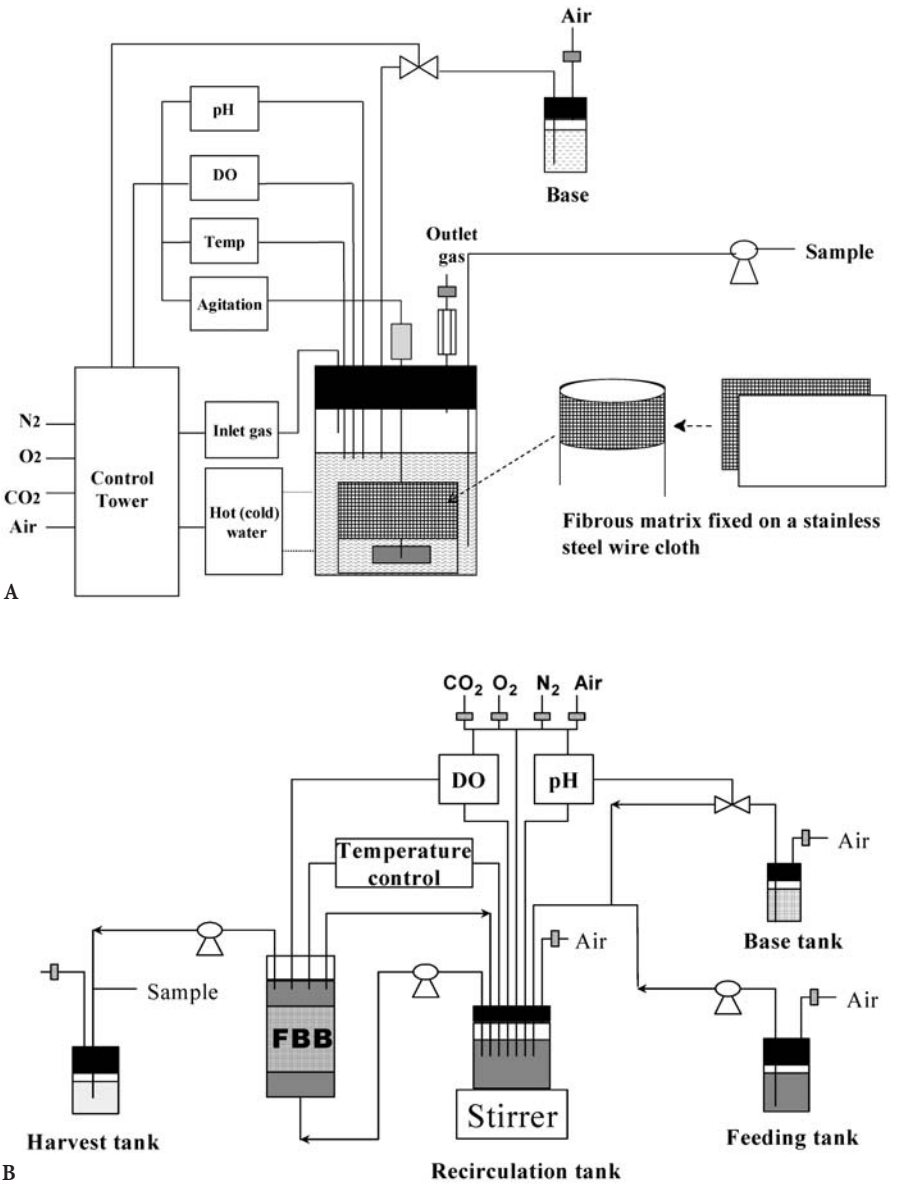

Fig. 1 Schematic diagrams of the FBB culture systems used in this study. (**A**) Fibrous bed inside the stirred vessel with temperature, DO, and pH control; (**B**) External fibrous bed with medium recirculation through the stirred vessel with temperature, pH, and DO control

3
Kinetic study of MAb production in FBB

In this study, a non-woven polyester fibrous matrix was used to culture hybridoma cells producing MAb against leptin-receptor, an important protein which has been studied for its potential use in obesity treatment and primitive hematopoietic stem-cell screening [77–79]. The kinetics of MAb production by the hybridoma cultured in T-flasks and spinner flasks were studied first for comparison purposes. Cells immobilized in fibrous matrices and cultivated in spinner flasks and FBBs under continuous and repeated batch conditions were then studied to evaluate their performance and feasibility for long-term MAb production. The effects of dilution rate, serum content, and DO (dissolved oxygen) on cell growth, glucose and glutamine consumption, lactate and MAb production, and cell density and reactor productivity were analyzed. Comparisons of FBB performance for MAb production with other types of animal cell bioreactor reported in the literature are also discussed. The reasons that FBB achieved high viable cell density and long-term stability for MAb production were also investigated by studying cell cycle and apoptosis of the cells cultured in the 3D fibrous matrix environment.

3.1
Cell line and medium

The mouse-rat hybridoma cell line AE-6 producing MAb against leptin-receptor was obtained from Progenitor (Menlo Park, CA). Unless otherwise noted, cells were cultured in Dulbecco Modified Eagle Medium (DMEM) supplemented with 10% (*v*/*v*) fetal bovine serum (FBS), both from Gibco Laboratories (Grand Island, NY, USA). The culture was maintained in T-75 flasks incubated in a humidified CO_2 incubator (Napco, 302) at 37 °C.

3.2
PET fibrous matrix

Non-woven polyethylene terephthalate (PET) fabrics (thickness 0.18 cm, fiber diameter ~20 μm, matrix density 0.11 g cm^{-3}, matrix porosity 92.5%) was used for cell immobilization [80]. The PET matrix was treated with 1% NaOH solution at boiling temperature for 1 h to reduce surface hydrophobicity and to increase biocompatibility by partially hydrolyzing PET to create carboxyl and hydroxyl groups on the PET surfaces [31]. The treated PET matrices were then used for cell immobilization.

3.3
Analytical methods

Cells in the fibrous matrix were removed by gently vortex mixing after trypsin–EDTA treatment. Cell number and viability were counted with 0.2% (*w*/*v*) trypan blue on a hemocytometer. The cell size and the number percentage distribution of cell size in the cell suspension were measured using a Coulter counter (Multisizer II, Coulter Electronics).

The concentrations of glucose, lactate, and glutamine in the medium were measured using YSI Biochemistry Select Analyzer (Yellow Spring, Ohio, USA) after removing suspended cells by centrifugation at 12,000 rpm and 4 °C for 5 min. LDH (lactate dehydrogenase) level in the medium was measured with a CytoTox 96 Assay kit (Promega) and determination of absorbance at 490 nm.

The monoclonal antibody concentration was analyzed using an enzyme linked immunosorbent assay (ELISA). Each of the 96 wells was coated with the primary antibody–goat anti-rat IgG (H+L) (KPL) at 4 °C overnight and blocked by 0.06 M Tris buffer (pH 7.5). Diluted rat IgG standard (Sigma) and sample solutions were added in duplicate to the plate and incubated for 2 h at 37 °C. Then, a second antibody–alkaline phosphatase-labeled goat anti-rat IgG (H+L) – was added and incubated for 2 h at 37 °C, followed by reaction with *p*-nitrophenylphosphate (pNPP, KPL). The absorbance at 405 nm was measured using a 96-well microplate reader (Molecular Device).

3.4 T-flask cultures

The culture kinetics were studied first in T-flasks. Unless otherwise noted, batch and fed-batch cultures were conducted in T-75 flasks. Each flask containing 40 mL medium was inoculated with 2×10^5 cells and incubated in a 5% CO_2 incubator at 37 °C. In fed-batch cultures glucose and glutamine were added on day 6 and day 8 to replenish consumed glucose and glutamine; meanwhile a 5% sodium bicarbonate solution was also added to restore the medium pH to ~7.1. Samples (1.0 mL) were taken once every day and the concentrations of glucose and lactate in the samples were measured after removing cells and cell debris by centrifugation. The supernatant was then stored in a freezer (–20 °C) for future analysis of glutamine and MAb.

Figure 2 shows typical kinetics of batch and fed-batch cultures in T-flasks. As is apparent from the figure, production of lactate and MAb followed glucose and glutamine consumption, respectively, with a lactate yield of 0.91 ± 0.02 g g^{-1} glucose consumed and MAb yield of 32.5 ± 7.9 mg g^{-1} glutamine consumed. In both batch and fed-batch cultures cell growth and lactate production stopped at ~3 g L^{-1} whereas MAb production continued until it leveled off at ~80 mg L^{-1}. Also, adding glucose and glutamine and adjusting the medium pH in the fed-batch culture did not significantly improve culture performance. There was no significant difference between either lactate formation or MAb production in the batch and fed-batch cultures, suggesting that accumulation of lactate and other byproduct(s) such as ammonium was the main cause of eventual termination of the culture. Similar culture inhibition by lactate and ammonia also have been reported for hybridoma and other animal cells [81, 82]. Reducing or selectively removing toxic metabolic byproducts is thus critical to improving MAb production by hybridoma cells [81, 83, 84]. It should be noted that some essential growth nutrients also might have been depleted during the batch culture. Thus, continuing perfusion to replenish the consumed nutrients is necessary to enable the culture to reach a higher cell density and to produce more MAb.

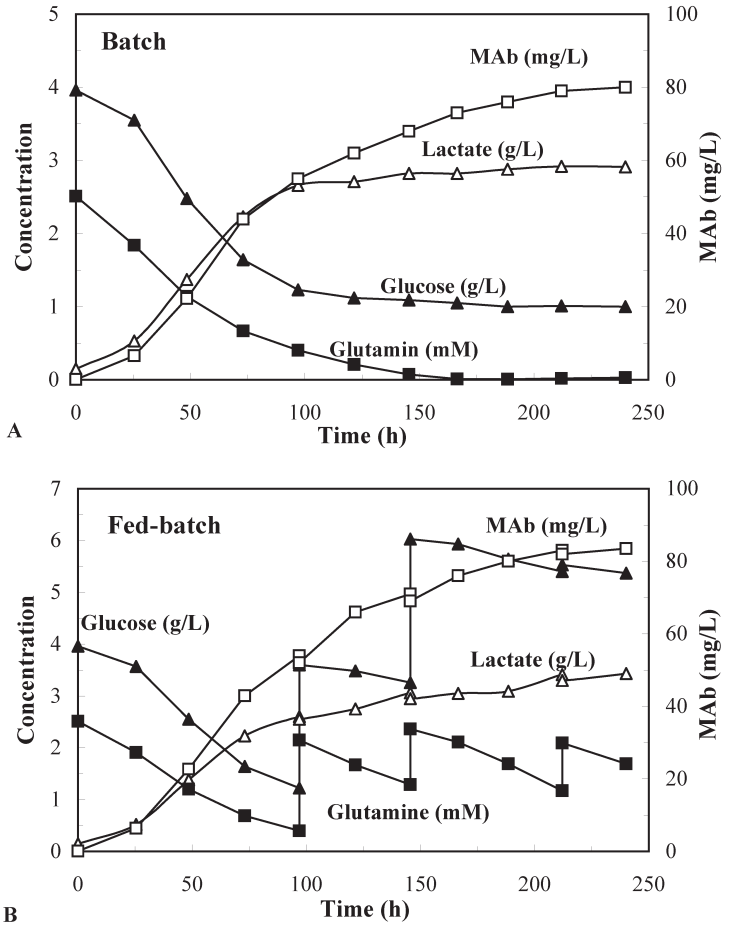

Fig. 2 Kinetics of T-flask cultures with 10% FBS: (**A**) batch culture, (**B**) fed-batch culture

3.5 Spinner flask cultures

The kinetics of suspended culture were also studied in a spinner flask (250 mL) containing 110 mL medium, agitated at 50 rpm, and incubated in a 5% CO_2 incubator at 37 °C. Samples were taken for analysis of glucose, lactate, MAb, and cell number and viability. For immobilized culture the PET matrix (20×2×0.18 cm^3) co-laminated with a stainless-steel wire cloth was wound into a hollow cylindrical shape (~6.5 cm in diameter; 2 cm in height) and then fixed around the agitator shaft in the spinner flask (Fig. 1A). Before use, the flask with the fibrous matrix in place was filled with PBS and autoclaved at 121 °C for 30 min. After sterilization, the flask was refilled with 110 mL fresh medium and then inoculated with cells to a density of 2×10^5 mL^{-1}. The culture was incubated in a 5% CO_2 incubator at 37 °C, agitated at 100 rpm, and operated in the repeated batch mode with

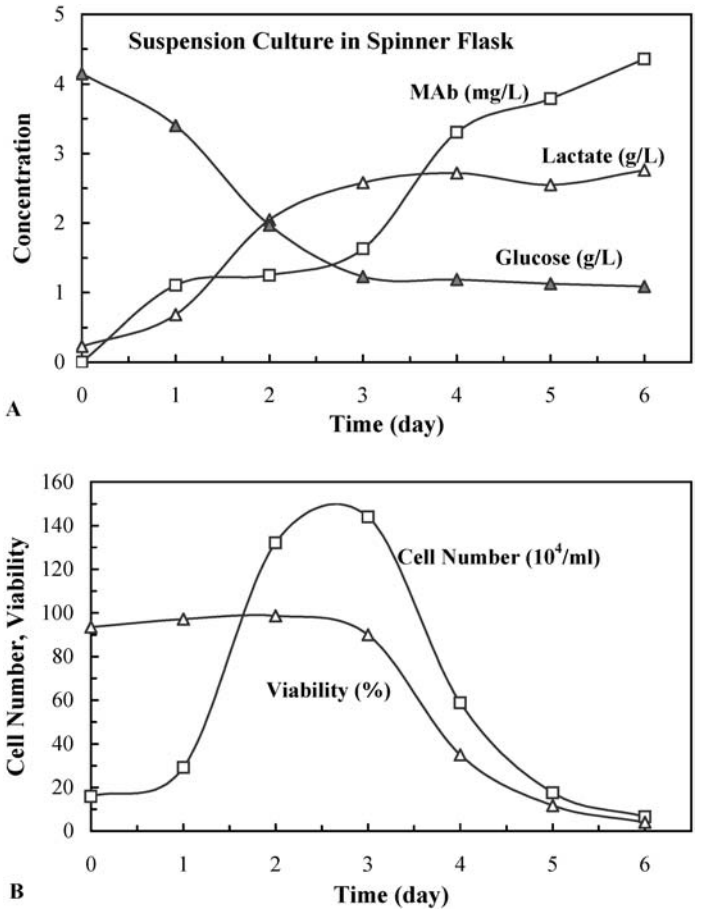

Fig. 3 Kinetics of batch suspension culture in the spinner flask with 5% FBS. Significant cell death occurred after the lactate concentration reached ~3 g L^{-1}

medium changes every one or two days for a total of five batches in 8 days. It was noted that almost no cells remained in suspension after ~12 h of incubation, indicating that most cells had been immobilized in the fibrous matrix. Samples were taken at the beginning and end of each batch for analysis of glucose, lactate, MAb, and lactate dehydrogenase (LDH).

The batch kinetics for suspended culture in the spinner flask is shown in Fig. 3. It was observed that severe cell damage and death occurred immediately after cell growth stopped. Also, MAb production was much lower than that in the T-flask cultures, perhaps because of cell death caused by severe shear damage in the suspended culture [11]. In contrast, when cells were protected by immobilization in the fibrous matrix stable MAb production was obtained in the spinner flask culture for an extended period operated under repeated batch mode (Fig. 4). As can be seen in this figure, both metabolic rates (glucose consumption and lactate

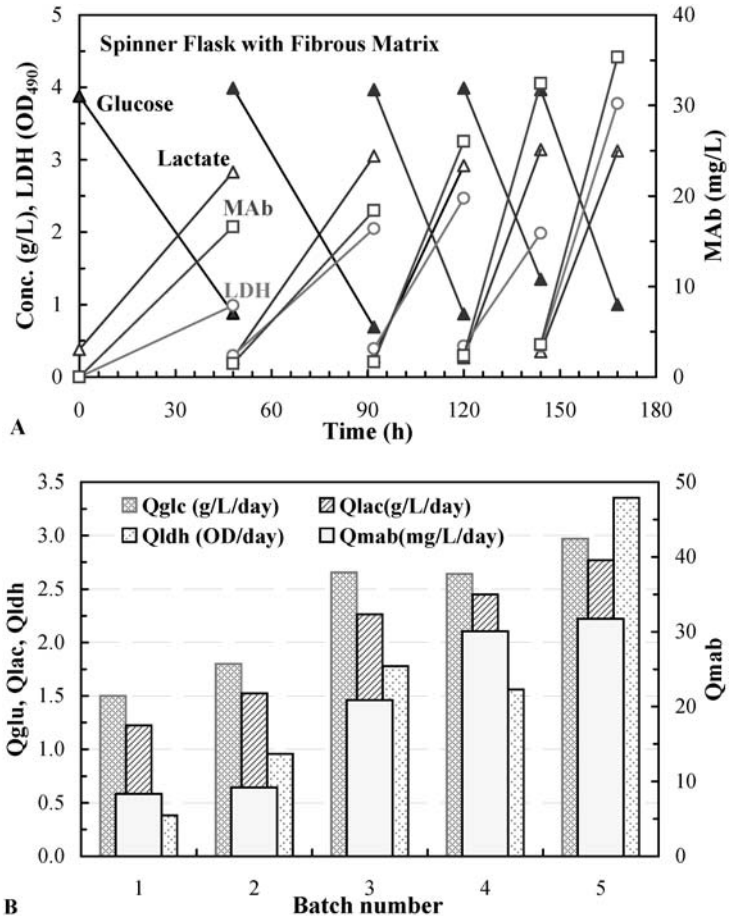

Fig. 4 Kinetics of repeated batch cultures with immobilized cells in the fibrous matrix in the spinner flask with 5% FBS. (**A**) concentrations of glucose, lactate, MAb, and LDH at the beginning and end of each batch; (**B**) Rates of glucose consumption and lactate, MAb, and LDH production (Q_{glu}, Q_{lac}, Q_{MAb} Q_{LDH}) in each batch

formation) and MAb production rate increased to stable levels after the first three batches. The total cell number in the reactor increased to 2.0×10^8 at the end of the fifth batch, corresponding to a cell density of approximately 2.75×10^7 cells cm^{-3} fibrous matrix. Clearly, the fibrous matrix was an effective support for cell immobilization and protection from shear damage.

However, the cell viability was only ~50% and the level of LDH, a cytotoxicity indicator, increased to a relatively high level at the end of the fifth batch, indicating an unhealthy cell population perhaps suffering from nutrient (oxygen) limitation. The low cell viability could be attributed to oxygen limitation in the system, especially with the high cell density in the fibrous matrix. Lack of oxygen is often the main limitation in immobilized cell culture because

oxygen has a low solubility and relatively high consumption rates by cells [85]. The spinner flask culture did not have proper aeration or DO control and there was probably oxygen starvation inside the fibrous matrix, as indicated by the relatively high lactate yield of 0.96 g g^{-1} glucose consumed, significantly higher than that in the suspended culture (0.83 g g^{-1}) and the T-flask cultures (0.91 g g^{-1}). Lactate is an anaerobic product of carbon (mainly glucose) metabolism [86], and a high lactate yield may indicate oxygen limitation in the cell culture [87].

3.6 FBB cultures

The fibrous-bed bioreactor (FBB) system used in this study is shown in Fig. 1B. The FBB was made of a jacketed glass cylinder (inner diameter 5 cm, length 10 cm) packed with 12 pieces of the PET matrix, each having a diameter slightly larger than 5 cm. The packed bed had a height of 2.1 cm and a void volume ratio of 95%. Silicone rubber stoppers were used to seal both ends of the glass cylinder. The bioreactor was connected to a well-mixed, jacketed flask (300 mL) which was agitated at a stirring rate of 100 rpm and had pH and DO probes installed for control and monitoring purposes. Another DO probe was installed at the outlet of the bioreactor. Before use, the whole system was sterilized by autoclaving at 121 °C for 30 min. After sterilization, the system was filled with 250 mL medium and inoculated with 9×10^7 cells from confluent T-75 flasks. The cells were left to grow and to establish themselves in the fibrous matrix for 5 days before continuous feeding was started at a dilution rate of 0.6 day^{-1}. Unless otherwise noted the FBB was operated with a continuous feed into the flask and medium recirculation through the FBB at a flow rate of 80 mL min^{-1} (or a superficial velocity of ~4 cm min^{-1}). The temperature in the bioreactor and the recirculation flask was controlled at 37.0±0.1 °C by circulating constant-temperature water through the jackets. The DO was controlled at 70% of air saturation and pH 7.05. The continuous culture was studied for a period of ~19 days, with the dilution rate varied between 0.6 and 1.8 day^{-1} according to the nutrient consumption rate. Samples (3.0 mL) were taken daily to monitor the reactor performance and stability.

To study the effects of the DO and FBS content of the medium on FBB performance, a similar reactor system with a smaller FBB (2 cm diameter; 8 cm long; packed with 18 pieces of PET matrices to a bed height of 3.2 cm, packed volume 10 mL) operated under repeated batch and fed-batch modes was used. The effect of DO was studied by reducing the DO level from 70% to 50%, 30%, and 10% after each batch culture, with the medium containing 4% FBS. The effect of serum was studied at 70% DO and the FBS content varied from 5% to 1%. The pH was controlled at 7.05 during these experiments.

At the end of the reactor study, the cell-matrix samples (0.5×0.5 cm^2) were removed from the FBB, fixed in 2.5% glutaraldehyde, dehydrated in 20–100% ethanol solution with ascending concentration of 10%, critical-point dried in CO_2, coated with gold/palladium, and then examined using a Philips XL 30 scanning electron microscope (Philips Electronics).

3.6.1
Continuous culture in the FBB

The historical concentration and metabolic rate profiles of glucose, lactate, glutamine, and MAb in the FBB, with the dilution rates used in feeding the reactor and the accumulated MAb production, over the entire period of 24 days studied are shown in Fig. 5. Continuous feeding was started at 131 h when glutamine in the reactor was almost depleted. The dilution rate was gradually increased to 1.8 day^{-1}. As can be seen in Fig. 5C, stable production of MAb was maintained for the entire continuous feeding period studied. However, when the dilution rate was increased to 1.8 day^{-1} at 417 h, there were rapid increases in glucose and glutamine concentrations and a significant drop in the MAb concentration in the FBB, indicating the "wash-out" effects of the high dilution rate. The culture was stabilized by lowering the dilution rate back to 1 day^{-1}, which was later increased to 1.5 day^{-1} to produce MAb stably at a high concentration of 106 mg L^{-1} and a high volumetric productivity of 160 mg L^{-1} day^{-1}, both of which were much higher than those obtained in the spinner flask culture. It is clear that stable long-term continuous production of MAb can be achieved with the FBB at a dilution rate between 1.0 and 1.5 day^{-1}. The good reactor performance was attributed to better pH and DO controls and maintenance of a high viable cell density in the FBB; this is discussed later in this paper.

3.6.2
Metabolic rates and yields

The concentration of substrate or product in a continuous, well-mixed culture changes with time as follows,

$$\frac{dC_i}{dt} = D(C_{i,f} - C_i) + Q_i \tag{1}$$

where C_i is the concentration in the bioreactor, $C_{i,f}$ is the feed concentration, D is the dilution rate, Q_i is the volumetric metabolic rate, and the subscript i stands for the various chemical species (glucose, glutamine, lactate, or MAb). Assuming that the metabolic rate Q_i is constant over a short time period between two time points, t_1 and t_2, the above equation can be integrated to obtain the equation:

$$Q_i = \frac{D\,(C_{i,2} - C_{i,f} - (C_{i,1} - C_{i,f})\exp\,(-D(t_2 - t_1)))}{1 - \exp\,(-D(t_2 - t_1))} \tag{2}$$

where the subscripts 1 and 2 denote the data points corresponding to the time points t_1 and t_2. Equation (2) and the concentration data shown in Fig. 5A were used to estimate the different metabolic rates during continuous FBB culture; the results are shown in Fig. 5B.

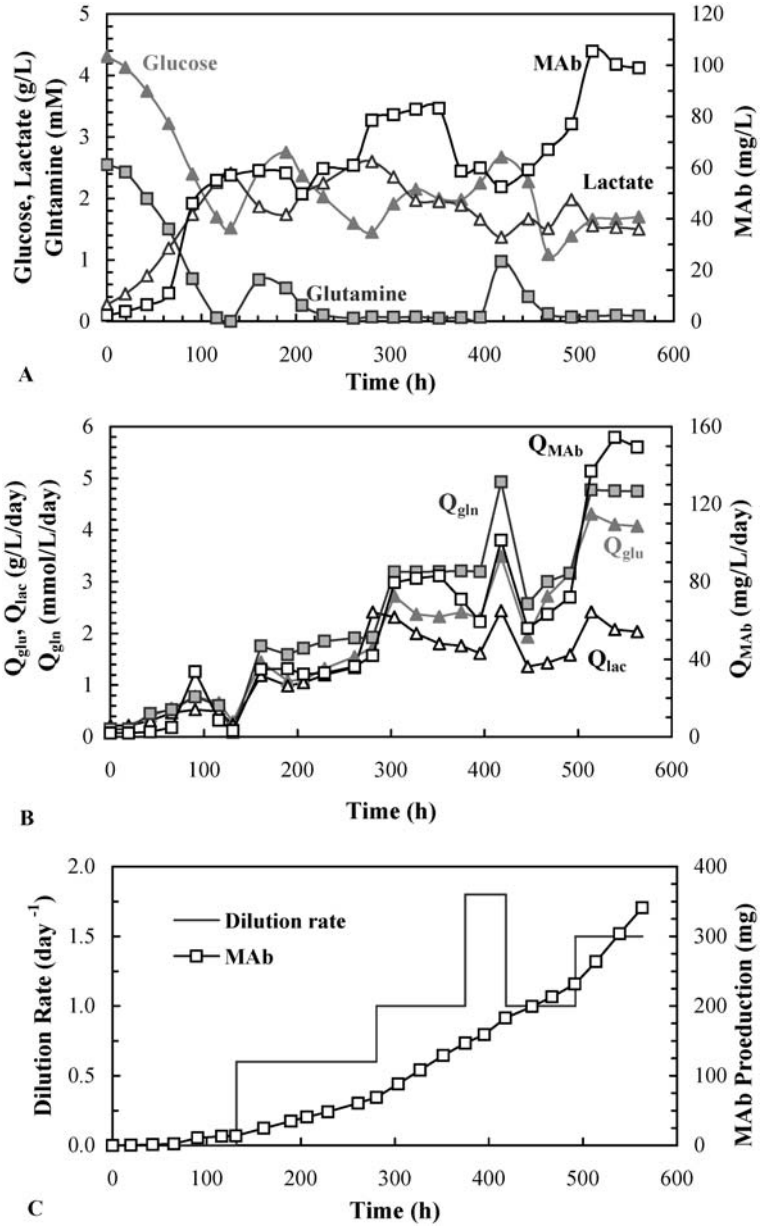

Fig. 5 Kinetics of continuous FBB culture operated under various dilution rates with 10% FBS. (**A**) concentration profiles for glucose, glutamine, lactate, and MAb; (**B**) metabolic rates for glucose and glutamine consumption and lactate and MAb production; (**C**) changes in dilution rate and cumulated MAb production

The lactate yield from glucose ($Y_{Lac/Glu}$) and MAb yield from glutamine ($Y_{MAb/Gln}$) in the continuous FBB culture can be estimated from the metabolic rate data as follows:

$$Y_{Lac/Glu} = \frac{Q_{Lac}}{Q_{Glu}} \tag{3}$$

$$Y_{MAb/Gln} = \frac{Q_{MAb}}{Q_{Gln}} \tag{4}$$

where the subscripts Lac, Glu, MAb, and Gln denote lactic acid, glucose, monoclonal antibody, and glutamine, respectively.

3.6.3
Effects of dilution rate

In general, cell growth and reactor productivity in a continuous culture are closely related to the dilution rate. The effects of dilution rate on FBB culture performance are shown in Fig. 6. Increasing the dilution rate up to 1.5 day^{-1} also increased glucose and glutamine consumption rates and MAb productivity. However, further increasing the dilution rate to 1.8 day^{-1} resulted in lower metabolic rates and MAb productivity. The product yields, $Y_{Lac/Glu}$ (0.80±0.06 g g^{-1} glucose consumed) and $Y_{MAb/Gln}$ (22.0±8.3 mg g^{-1} glutamine consumed) were not significantly affected by the dilution rate, indicating that cells remained in the same physiological state during the entire culture period.

3.6.4
Effects of dissolved oxygen

The dissolved oxygen (DO) concentration had profound effects on cell growth and metabolism for different animal cell cultures. In general, poor cell growth occurs at low DO, but high DO can cause cytotoxicity and damage cells [9]. The optimum DO levels for hybridoma culture depend on cell lines and culturing systems, and vary widely from as high as, e.g., 8–100% [88] and 60% [89] to 35% [90] and as low as 0.5% [91]. To optimize the FBB culture, the effects of DO on culture performance were studied in the repeated batch mode. Because it is difficult to harvest the immobilized cells inside the fibrous matrix without sacrificing the culture, the LDH level in the culture medium was used as an indicator of the health of cells immobilized in the matrix in the FBB. Figure 7 shows the concentration profiles of glucose, lactate, MAb and LDH in the medium containing 4% FBS in the FBB culture at different DO levels. It was found that the DO levels between 10% and 70% had no significant effect on glucose metabolism and lactate production. The lactate yield was not affected by the DO and remained at 0.81±0.03 g g^{-1} glucose consumed. However, as the DO level decreased MAb production also decreased whereas LDH increased. Apparently, low DO levels caused oxygen limitation, induced apoptotic cell death, and consequently, re-

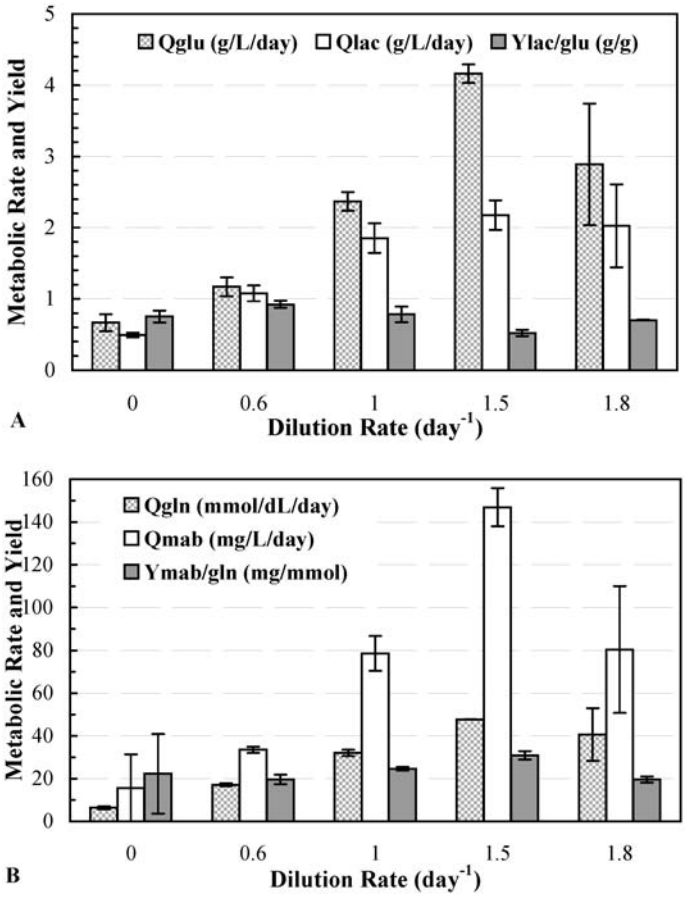

Fig. 6 Effects of the dilution rate on metabolic rates (Q_{glu}, Q_{lac}, Q_{gln}, Q_{MAb}) and product yields ($Y_{lac/glu}$, $Y_{del/gln}$) in the continuous FBB culture

duced MAb production. There was a dramatic increase in the LDH level when the DO level was reduced from 30% to 10%, suggesting that a critical DO level of ~30% is necessary for maintenance of the FBB culture. Below this DO level the culture cannot be sustained for long-term operation, because of oxygen limitation.

3.7 Effects of serum

Serum provides a complex mixture of hormones, growth factors, nutrients, and other trace elements and can enhance cell growth [37, 92], protect cells from fluid mechanical forces [93], and reduce cell death and apoptosis [29]. Therefore, fetal bovine serum and calve serum are often used in cell cultures. However, serum is a major cost in large-scale cultivation of animal cells. It also introduces

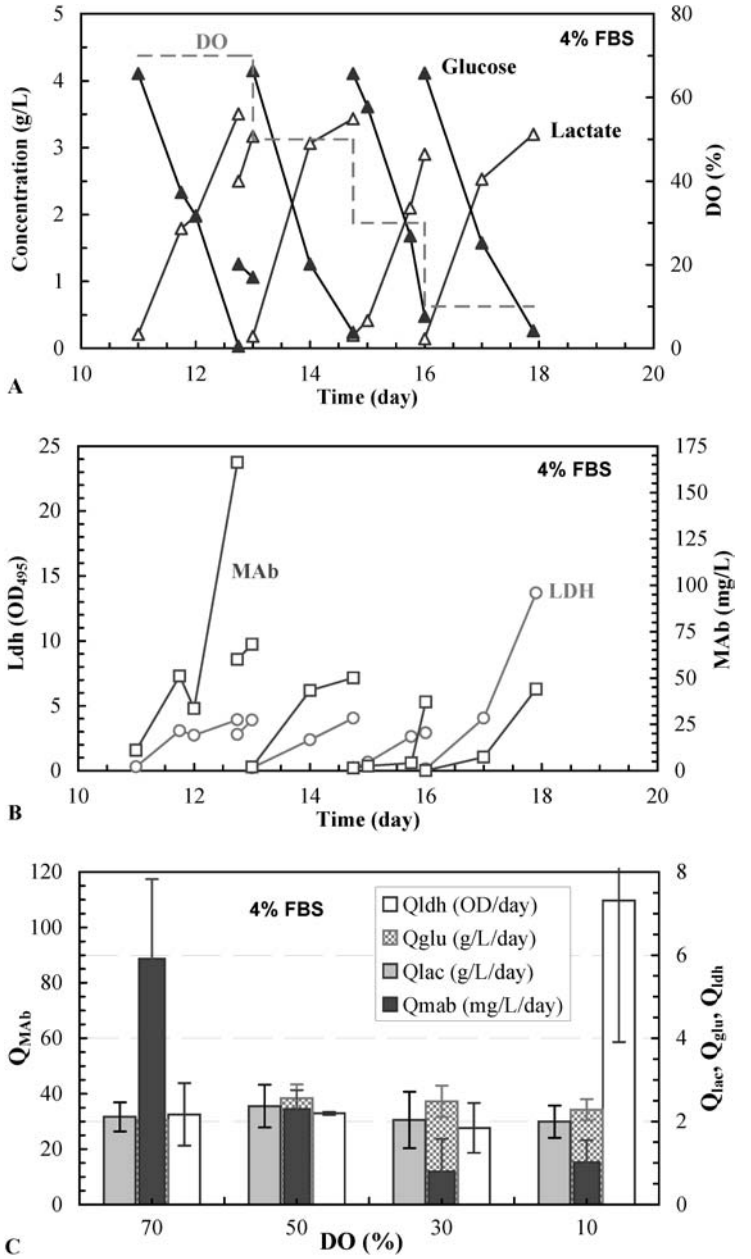

Fig. 7 Kinetics of repeated batch FBB cultures with 4% FBS at various DO levels. (**A**) Concentration profiles of glucose, lactate, and DO; (**B**) Concentration profiles of MAb and LDH. (**C**) Effects of DO on metabolic rates (Q_{glu}, Q_{lac}, Q_{MAb} Q_{LDH})

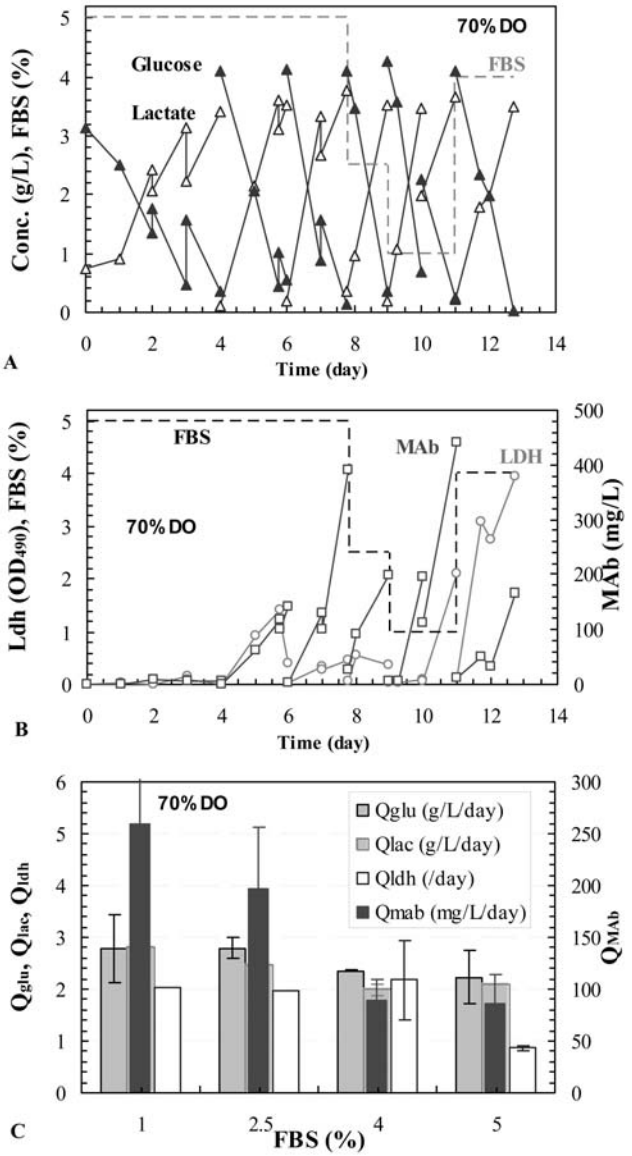

Fig. 8 Kinetics of repeated batch FBB cultures with different FBS content at 70% DO. (**A**) Concentration profiles of glucose, lactate and serum; (**B**) Concentration profiles of MAb, LDH and serum; (**C**) Effects of serum content on metabolic rates (Q_{glu}, Q_{lac}, Q_{MAb} Q_{LDH})

unknown proteins that make product purification difficult. It is thus desirable to reduce the serum content of the medium to a minimum level for the cell culture. The effects of serum on the FBB culture were studied in repeated batch mode; the results are shown in Fig. 8. In general, reducing the serum content from 5% to 1% increased MAb production but had no significant effects on glucose metabolism

and lactate production. The lactate yield remained unchanged at 0.83±0.03 g g^{-1} glucose consumed and MAb productivity increased from 90 mg L^{-1} day^{-1} to 260 mg L^{-1} day^{-1}. Reducing the serum content also had a minimal effect on LDH level, which remained below the low level of 4 OD units in the medium even at 1% FBS, indicating that cells remained healthy in the medium with low serum content. It is thus clear that a low-serum medium would be favorable for MAb production in the FBB culture.

Serum might affect cell metabolism and average cell size [94]. A lower serum content means lower concentrations of growth factors in the medium, which could arrest cell growth or cause the cells to stay in G0/G1 phase longer, favoring non-growth-associated MAb production by hybridoma cells [11, 95]. However, the effect of serum on protein production by cell cultures is complicated and often depends on the cell lines and other process factors. For example, Ozturk and Palsson [92] reported that production of MAb by two hybridoma cell lines increased with increasing the FBS content in the medium, because of increased viable cell number, but Lambert and Merten [96] found that MAb production was enhanced in a serum-free medium, because of increased specific MAb production rate. In attempts to use low-serum or serum-free medium to enhance recombinant protein production, many research efforts have been directed at genetic reconfiguration of the cell lines and applying different operation strategies and bioreactor systems [8, 9, 96]. In this study we concluded that the serum content of the medium for the FBB culture can be reduced to 1%, which is much lower than the 5–10% previously used in T-flask and spinner-flask cultures. Although it is also possible to adapt T-flask culture to a low-serum or serum-free medium, it would require many cell passages and transfers of culture to new flasks, which could take several weeks or months. With the FBB culture, adaptation to a low-serum medium was relatively easy and can be accomplished within one month, as was demonstrated in this study. Therefore, it is recommended that a high-serum medium be used initially to provide quick cell growth and obtain high cell density; thereafter the serum content of the medium can be reduced to reduce media cost and enhance MAb production during the long-term production stage.

3.8
Cell density and distribution in FBB

Figure 9 shows the high density of hybridoma cells immobilized in the fibrous matrix. These cells had typical spherical morphology in a three-dimensional culturing environment, and most cells were in contact with other cells and formed large clumps inside the fibrous matrix. The final cell density in the continuous FBB was 3×10^8 cells cm^{-3} packed bed with a cell viability of >85%. Only ~2.5% of the total cell population was in the suspension, and most of these were either dead or apoptotic cells [61]. It is clear that the fibrous matrix is effective and selective for immobilizing viable cells. Apparently, the culture adaptation/selection process in the FBB was aided by the retention of viable (healthy) cells and removal of dead and apoptotic cells from the fibrous matrix. Because cell–cell interactions can prevent cell death at the growth-arrested stage [97], the high cell

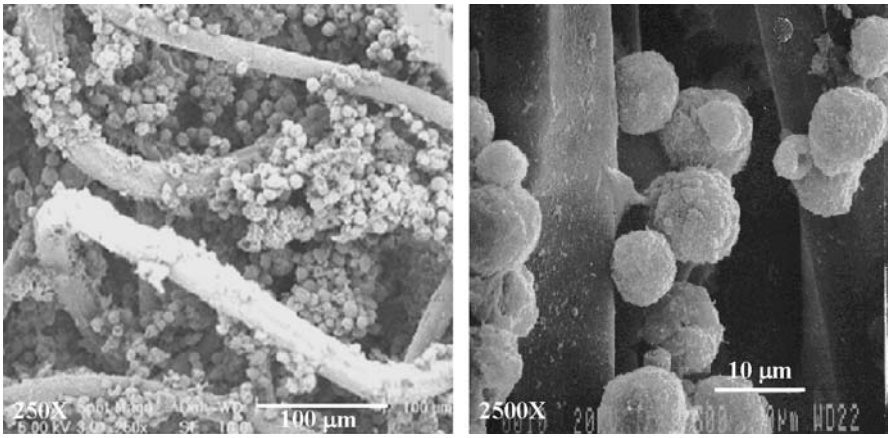

Fig. 9 Scanning electron micrographs of cells in the fibrous matrix in the continuous FBB. Cells grew around fibers and formed aggregates in the matrix

density and close cell–cell contacts in the fibrous matrix must also have protected cells from apoptotic and necrotic death.

Figure 10 shows cell size distributions for cells grown in the FBB and cells from the T-flask cultures. The cells grown in the 3D fibrous matrix, although highly viable, were much smaller than those grown on the 2D surface in the T-flask. On average, cells from the FBB culture had a smaller diameter of ~8.2 μm, compared with ~14.8 μm for cells from the T-flask culture. The large size difference between the FBB and T-flask cultures was also observed under the microscope and is consistent with our previous findings with osteosarcoma cells [54]. It was also noted that the suspended cells in the liquid medium in the FBB were significantly larger (average diameter ~12 μm) than the cells immobilized in the matrix. The smaller cell size for cells cultured in the FBB might be attributed to the 3D culture environment.

As seen in the SEM photos, cells in the 3D fibrous matrix formed large cellular clumps, perhaps because of limited accessible fiber surface area for cell spreading on the surface [31]. The small cell size could be a response to close cell–cell contacts and spatial limitation imposed on the cell aggregate. Under the high cell density conditions a smaller cell size would also give a larger specific cell surface area for better nutrient transport. In contrast, cells cultured on the 2D surface in the T-flask grew into a monolayer. They spread out on the surface to gain a maximum surface area for nutrient transport, and a large cell size becomes an advantage in this situation. It is well known that cell stretching and spreading on a surface is good if cells are to proliferate on 2D surfaces [98, 99]. It is also possible that the different cell-size distributions of cells cultured in the FBB and T-flask were because of their different cell cycle patterns [11, 100, 101]. Most cells in the long-term FBB culture were in the growth-arrest state (G1/G0 phase) [61], in which cell size is usually smaller than for cells in the other cell-cycle phases (S, M/G2) [100].

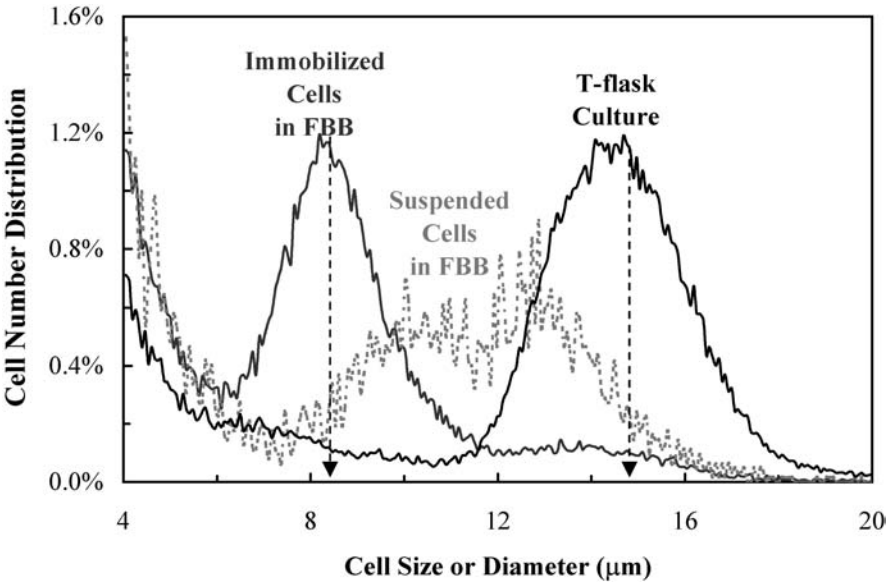

Fig. 10 Size distributions of the cells cultivated in the continuous FBB and T-flasks

3.9 Comparison of FBB with other systems

Table 3 summarizes and compares the performance of different culturing systems studied in this work. In general, the immobilized cultures in the spinner flask and the FBB had much higher volumetric metabolic rates and volumetric MAb productivity than those in the T-flask cultures, largely because of the higher cell density in the fibrous matrix. The overall cell density in the continuous FBB culture was 4.8×10^7 mL^{-1} on the basis of the total liquid volume in the reactor system (250 mL), which was about 50-fold higher than that in the T-flask cultures (10^6 mL^{-1}). Also, continuous perfusion in the FBB reduced metabolite inhibition, enhanced oxygen transfer, and thus enabled cells to produce more MAb for a longer period. The lactate yield from glucose was significantly lower in the FBB culture than in the T-flask and spinner flask cultures, because of better oxygen transfer and protection from shear stress. The apparently lower yield of MAb from glutamine in the FBB culture could be because of significant chemical decomposition of glutamine [54] that was not taken into account in the yield calculation.

Although the volumetric MAb productivity (Q_{MAb}) in the continuous FBB culture was ~10 times higher than that in the T-flask cultures, productivity on a per-cell basis for the FBB culture was ~5 times lower than in the T-flask culture. This was attributed to the much smaller cell size for the FBB culture, which was a factor of ~7.5 smaller than cells grown in the T-flask. If the cell size difference was considered in the comparison, cell productivity on a per cell-biomass basis for the FBB culture was higher than that for the T-flask culture. The results from

Table 3 Comparison of T-flask, spinner flask, and FBB cultures

	T75 flask[a]	Spinner flask[b]	FBB[c]	FBB[d]	
Culture mode	Fed-batch	Repeated batch	Continuous	Repeated batch	
FBS content (*v*/*v*, %)	10	5	10	5	1
Q_{glu} (g L^{-1} day^{-1})	0.78	2.97	2.8	2.3	
Q_{lac} (g L^{-1} day^{-1})	0.71	2.77	2.2	2.1	
Q_{gln} (mmol L^{-1} day^{-1})	0.48	–[f]	4.8	–[f]	
Q_{MAb} (mg L^{-1} day^{-1})	16.26	31.8	159	89	260
$Y_{lac/glu}$ (g g^{-1})	0.91±0.02	0.96±0.02	0.80±0.06	0.83±0.03	
$Y_{MAb/gln}$ (mg $mmol^{-1}$)	32.5±7.9	–[f]	22.0±8.3	–[f]	
Max. MAb conc. (mg L^{-1})	83.5	35.4	106	390	442
q_{MAb} (µg 10^{-6} cells day^{-1})	16.3	17.7	3.3	11.1	32.5
Total cell number[e]	4.0×10^7	2.0×10^8	1.2×10^{10}	2.0×10^9	
Cell density[e]					
(per mL liquid volume)	1.0×10^6	1.8×10^6	4.8×10^7	8.0×10^6	
(per mL packed volume)		2.75×10^7	3.0×10^8	2.0×10^8	
Cell viability[e]	>90%	~50%	>85%	>70%	
Cell diameter (µm)	~14.8	~9.5	~8.2	~8.0	

[a] Fed-batch culture in 75-cm^2 T-flask containing 40 mL medium.
[b] Fed-batch culture in spinner flask containing 110 mL medium and a fibrous matrix for cell immobilization.
[c] Continuous culture in the FBB containing 250 mL medium operated at 1.5 day^{-1} dilution rate. The packed fibrous bed volume was 40 mL.
[d] Repeated batch culture in the FBB containing 250 mL medium. The packed fibrous bed volume was 10 mL.
[e] The cell density and viability for the T-flask culture were measured at Day 4 when the maximum viable cell density had reached and before cells began to die. The cell density and viability in the fibrous matrix were measured at the end of the culture period.
[f] Not measured.

this study show that MAb production from the continuous FBB (250 mL stirred tank with 40 mL external packed matrix) is more than that of sixty 75-cm^2 T-flasks (40 mL media in each T-flask) combined. The productivity of the FBB culture could be greatly enhanced by packing more PET matrices into the reactor to support an even higher cell density. Based on the actual packed reactor volume the MAb productivity in the continuous FBB culture was ~1 g L^{-1} day^{-1}, which compared favorably with most other bioreactor systems reported in the literature (Table 2). As discussed above, reactor productivity can be further improved with a low serum medium. With the FBS content reduced to 1% in the medium, the volumetric productivity for the FBB culture increased to 260 mg L^{-1} day^{-1}, largely because of increased cell productivity (32.5 µg 10^{-6} cells day^{-1}). Based on the packed fibrous bed volume, the reactor productivity was ~6.5 g L^{-1} day^{-1} for the FBB batch culture. The batch FBB culture with the low-serum medium also had the advantage of producing MAb at a high concentration (442 mg L^{-1}). The reduced serum in the medium also greatly reduces medium cost and eases downstream processing.

4
Cell cycle and apoptosis

Most animal cells respond to stressful culture environments (e.g. nutrient limitation or low pH) by undergoing cellular suicide or apoptosis [21, 84, 102, 103]. Apoptosis or programmed cell death reduces the viability of cell culture and results in eventual cell death and productivity loss in the bioreactor [100, 104, 105]. It is thus important to reduce or prevent apoptosis and to remove apoptotic and nonviable cells from the bioreactor to maintain the culture for the purpose of long-term production.

It is also important to control the cell cycle of in-vitro culture in the bioreactor environment, because the molecular mechanisms that regulate cell cycle and apoptosis are inextricably linked [106] and production of a recombinant protein by animal cells is often cell-cycle dependent [107–110]. The cells in different stages of cell cycle have different properties with regard to their size, gene expression, metabolic rates, and shear sensitivity [101, 111]. For hybridoma cells, nongrowth or stressed conditions often result in increased specific production rates and there seems to be inverse relationship between growth rate and specific MAb productivity [86, 101, 110, 112]). It has been reported that cultures with slow growth rates or under growth arrest usually have a large portion of cell population in the G1 phase [14, 113]. Experimental confirmations of G1 expression of antibody in hybridoma cell cultures have also been reported [11, 114]. In general, cells can be growth-arrested in the G1 phase because of nutrient limitation [110]. However, nutrient limitation often also induces apoptotic cell death [115, 116]. How to prolong G1 phase without increasing apoptotic cell death is thus a key to maintaining a high rate of production of monoclonal antibody (MAb) by long-term hybridoma cultures.

As already discussed, the FBB culture had a good stability for continuous MAb production. We are interested to know whether the 3D growth environment in the FBB has any effects on cell cycle and apoptosis that might have contributed to the superior culture performance.

4.1
Flow cytometric analysis

Cells attached to fibrous matrices were removed by first rinsing with PBS and then soaking in a trypsin–EDTA solution for 5–10 min to detach cells, which were then collected by washing with PBS. The collected cells were fixed in formaldehyde solution and stored in 70% ethanol at –20 °C for flow cytometric analysis. Apoptosis was studied by use of the method of TDT-mediated BrdUTP nicked end labeling (TUNEL). APO-BrdU Kit (Pharmingen, San Diego, CA, USA) was used to quantitatively and qualitatively study the incidence of apoptosis via a flow cytometer and a fluorescence microscope, respectively. The assay enables incorporation of a fluorescent indicator (FITC) onto the end of fragmented DNA. Thus, only apoptotic cells were stained with FITC. Cells were also stained with propidium iodide (PI). The cell cycle distribution can also be obtained by flow cytometry after staining cells with PI. The linear DNA content data were pro-

cessed by use of the ModFit software package (Verity Software, Topsham, ME, USA) for cell-cycle analysis.

4.2 Effects of 3D culture in a fibrous matrix

As an anchorage-independent cell line, hybridoma can grow both in suspension and attached to the matrix. To examine if there were differences between cells present in these two different environments, cells in the 3D culture were separated into two parts, cells in suspension and cells immobilized in the fibrous matrix.

4.2.1 *Apoptosis*

It was observed that cells in suspension were more likely to be apoptotic than cells immobilized in the fibrous matrix. When visualized under the fluorescence microscope all cells stained by PI were red and apoptotic cells stained by FITC were green. As can be seen in Fig. 11, only a small fraction of the cells removed

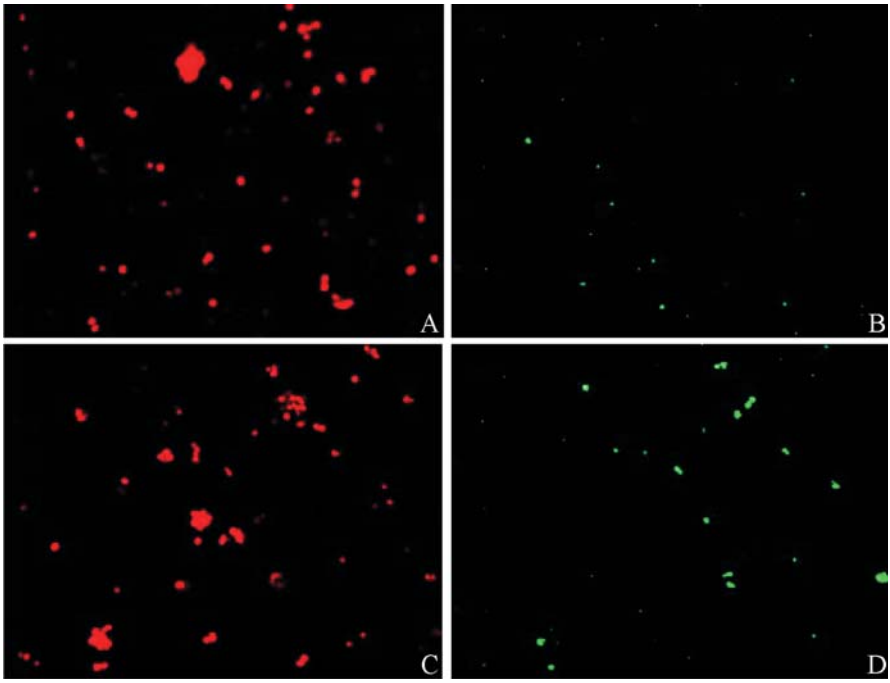

Fig. 11 Cell apoptosis visualized under a fluorescence microscope. The cells stained by PI were red, apoptotic cells stained by FITC were green: (**A**) total cells from the fibrous matrix, (**B**) apoptotic cells from the fibrous matrix, (**C**) total cells in suspension, and (**D**) apoptotic cells in suspension. The photographs shown here are from samples collected from batch cultures grown in multiwells containing fibrous matrices after incubation for 4 days. The culture conditions are described in Fig. 12

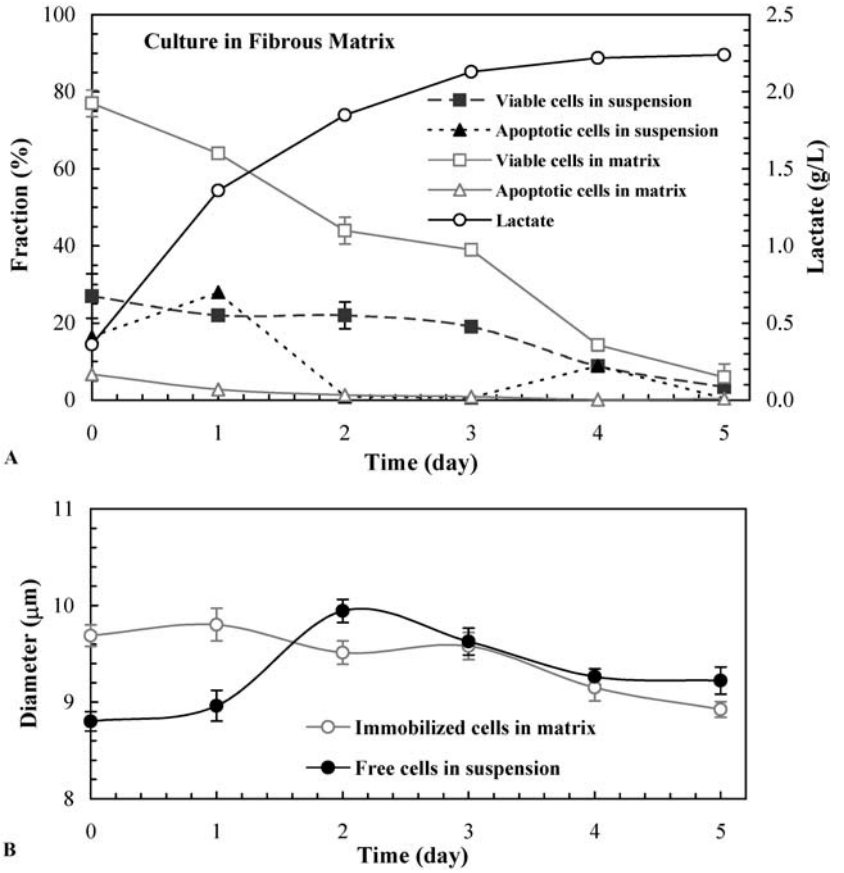

Fig. 12 Kinetics of batch 3D culture in multiwells containing fibrous matrices. (**A**) Cell viability, apoptosis, and lactate concentration; (**B**) Cell-size changes with culture time. Duplicate cell-matrix samples were taken daily by sacrificing the multiwell cultures. The cells removed from the fibrous matrix were regarded as immobilized cells in the fibrous matrix and cells remaining in the liquid medium were regarded as free cells in suspension

from the fibrous matrix was apoptotic (Figs. 11A, B), whereas more cells suspended in the culture medium were apoptotic (Figs. 11C, D). Apoptosis was further studied in a batch culture by flow cytometry after labeling. As shown in Fig. 12, immediately after inoculation most cells immobilized inside the fibrous matrix were viable and non-apoptotic whereas most of the cells remained in liquid suspension were non-viable and many were apoptotic. The explanation is that healthy cells are relatively larger and are more adhesive, and thus are more easily attached and entrapped inside the matrix. Consequently, the fibrous matrix selectively retains viable and non-apoptotic cells owing to stronger interactions between healthy cells and the matrix. Throughout the 6-day period of culture, viability was higher and apoptosis lower for the immobilized cells than for the suspended cells. These data indicate that the fibrous matrix can selectively

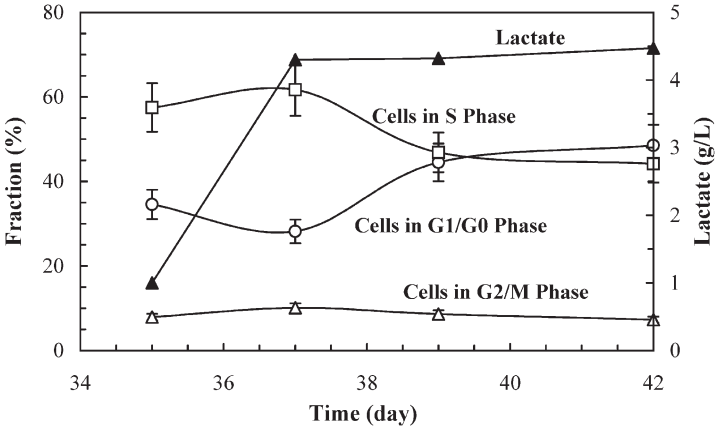

Fig. 13 Cell population distributions for long-term repeated-batch culture in multiwells with cells grown in fibrous matrices. The culture media were changed every 3–4 days during the first 35 days. After the last medium change on day 35, cell-matrix samples were collected every 2–3 days from duplicate wells to study the cell-cycle behavior in the long-term culture

retain healthy cells. At the end of the batch culture the cells became necrotic because of nutrient limitation and inhibition by metabolites.

4.2.2 *Cell cycle*

Cell-cycle distributions were also studied for cells immobilized in the fibrous matrix during batch and repeated batch cultures (Fig. 13). For cells entrapped inside the matrix, immediately after inoculation or media change G0/G1 percentage decreased because of new cell growth stimulated by adding fresh medium (more cells entered S phase). Then G0/G1 cells increased as the lactate concentration increased. The cells in the fibrous matrix tended to stay in the G0/G1 (growth arrest) phase, which might be attributed to the formation of cellular clumps within the fibrous matrix and the nutrient gradient inside the cell aggregates. Cells in clumps were in close contact with each other, resulting in "contact inhibition" or "density inhibition", which, in turn, arrested cells in a non-proliferating stage. After long-term culture the cells seemed to adapt themselves better in the adverse environment as indicated by the higher lactate concentration reached in the culture media–above 4 g L^{-1} (Fig. 13) compared with 2–3 g L^{-1} (Fig. 12).

4.2.3 *Cell size*

Cell size change during culture has been observed in our previous studies [54] and also by other researchers [11, 117, 118]. Cell size is critical to animal cells, because it is an indirect indicator of cell cycle stage and specific rate of nutrient consumption. It has been reported that cells in fast-growing culture were larger

than those in the slow growing stage. Slow growing cells take longer to synthesize the proteins necessary to satisfy cell-size criteria and pass the G1 and G2 checkpoints. As can be seen in Fig. 12B, initially, the average size of attached cells was bigger than that of suspended cells (~10 μm compared with 9 μm), confirming that larger cells were more easily entrapped inside the porous matrix or attached to fibers. Suspended cell-size increased with time, because of the growth of hybridoma cells in suspension. The final decrease of cell size was due to nutrient limitation and inhibition by toxic metabolites. On the other hand, the size of attached cells usually decreased with culture time and was smaller than the size of suspended cells after a sufficient culture period had passed. To exclude nutrient depletion as a possible reason for cell-size decrease, frequent changes of media were applied in spinner flasks with fibrous matrices. As a result the suspended cell size kept increasing but the immobilized cell size still decreased with culture time to ~8 μm in the fibrous bed culture, which was much smaller than the cells grown on the 2D surface in T-flasks (~14.8 μm) (Fig. 10). The smaller cell size for cells cultured in the fibrous matrix can be attributed to the 3D culture environment. Cells in the 3D fibrous matrix formed large cellular clumps, because of limited accessible fiber surface area for cell spreading on the surface [31]. The small cell size could be a response to close cell–cell contacts and spatial limitation imposed on the cell aggregate. The small cell size could also simply have resulted from the cell cycle [11, 100, 101]. Most cells in long-term culture were in the growth-arrest state (G1/G0 phase), for which the size is usually smaller than those of cells in the other cell cycle phases (S, M/G2) [100].

It should be noted that cell size can change substantially with growth conditions. More substrate is required per cell for cells in fast-growing culture than in slow-growing culture simply because the cells are larger in fast-growing culture [118]. For example, the oxygen consumption rate increased from 1 to 3.5×10^{-10} mmol O_2 h^{-1} $cell^{-1}$, simply because the cell volume increased from 500–600 μm^3 to 1000–1100 μm^3 [11]. The smaller cell size inside the matrix, after long-term culture reduced the nutrient requirement and gave the cells the possibility of achieving high density and keep long-term stability of cell culture. Under the high cell-density condition, a smaller cell size also would give a larger specific cell surface area for better nutrient transport. It is possible that the conducive environment created by cell–cell interactions made cells smaller and better adapted to survive under nutrient-limitation and other adverse conditions such as low serum in the medium, as discussed in the previous section.

5 Concluding remarks

The results from this study have suggested that the 3D fibrous matrix selectively retained healthy, non-apoptotic cells mostly in the growth-arrested stage (G1/G0 phase), which contributed to the superior culture performance for long-term MAb production by hybridoma cells immobilized in the fibrous matrix. Compared with other reactor systems reported in the literature (Table 2) the performance of the FBB is superior in terms of MAb concentration, reactor productivity, and long-term stability. One major advantage of the FBB is its stable

long-term performance. Unlike hollow fiber bioreactors, selective discharge of apoptotic and dead cells from the fibrous matrix into the perfusing liquid media enabled continuing renewal of the cell population in the bioreactor that also prevented the accumulation of nonproductive cells. The perfusion FBB also can reduce or remove toxic byproducts such as lactate and ammonia, increase oxygen transfer, and maintain uniform reaction conditions without causing excessive shear damage, all of which are important to the improvement of MAb production by hybridoma cells [119]. Consequently, both high cell density and high MAb productivity were obtained in the FBB culture, especially when the medium was optimized with a low serum content.

In conclusion, the FBB can be used as a continuous perfusion culture system for efficient production of MAb. The highly porous, non-woven polyester fibrous matrix is not only good for cell immobilization, but also can support a high density of viable cell population (of the order of 10^8 mL^{-1}) because of its high permeability for efficient mass transfer into the matrix. The low cost of the PET fibrous matrix, the simplicity of reactor construction, and ease in operation should enable the FBB system to be used as an alternative to hollow-fiber bioreactors for small-to-medium scale production of MAb. Scale up of the FBB to a larger production scale comparable with that currently achieved in stirred-tank bioreactors is likely to reduce the overall production costs of MAb, because of improved cell density and reactor productivity.

6 References

1. Rader RA (2003) Biopharma: Biopharmaceutical Products in the US Market, 2nd edn, Biotechnology Information Institute, Rockville Maryland
2. Anonymous (1999) Monoclonal antibody production, A Report of the Committee on Methods of Producing Monoclonal Antibodies, Institute for Laboratory Animal Research, National Research Council, National Academy Press, Washington DC
3. Kohler G, Milstein C (1975) Continuous cultures of fused cells secreting antibody of predefined specificity. Nature 256:495–497
4. Backer MP, Metzger LS, Slaber PL, Nevitt KL, Boder GB (1988) Large-scale production of monoclonal antibodies in suspension culture. Biotechnol Bioeng 32:993–1000
5. Lambert KJ, Boraston R, Thompson PW, Birch JR (1987) Production of monoclonal antibodies using large scale culture. Dev Ind Microbiol 27:101–106
6. Altshuler GL, Dziewulski DM, Sowek JA, Belfort G (1987) Continuous hybridoma growth and monoclonal antibody production in hollow fiber reactor-separator. Biotechnol Bioeng 28:646–658
7. Cherlet M, Marc A (2002) Stimulation of monoclonal antibody production of hybridoma cells by butyrate: evaluation of a feeding strategy and characterization of cell behavior. Cytotechnology 32:17–29
8. Hayter PM, Kirkby NF, Spier RE (1992) Relationship between hybridoma growth and monoclonal antibody production. Enzyme Microb Technol 14:454–461
9. Jan DCH, Petch DA, Huzel N, Butler M (1997) The effect of dissolved oxygen on the metabolic profile of a murine hybridoma grown in serum-free medium in continuous culture. Biotechnol Bioeng 54:153–164
10. Katinger H (1987) Principles of animal cell fermentation. Dev Biol Stand 66:195–209
11. Ramirez OT, Mutharasan R (1990) Cell cycle- and growth phase-dependent variations in size distribution, antibody productivity, and oxygen demand in hybridoma cultures. Biotechnol Bioeng 36:839–848

12. Jackson LR, Trudel LJ, Fox JG, Lipman NS (1996) Evaluation of hollow fiber bioreactor as an alternative to murine ascites production for small scale monoclonal antibody production. J Immunol Methods 189:217–231
13. Stoll T, Perregaux C, Von Stockar U, Marison IW (1995) Production of immunoglobulin A in different reactor configurations. Cytotechnology 17:53–63
14. Seifert DB, Phillips JA (1999) The production of monoclonal antibody in growth-arrested hybridomas cultivated in suspension and immobilized modes. Biotechnol Prog 15:655–666
15. Wang G, Zhang W, Jacklin C, Freedman D, Eppstein L, Kadouri A (1992) Modified Celligen-packed bed bioreactors for hybridoma cell cultures. Cytotechnology 9:41–49
16. Michaels JD, Mallik AK, Papoutsakis ET (1996) Sparging and agitation-induced injury of cultured animal cells: do cell-to-bubble interactions in the bulk liquid injure cells? Biotechnol Bioeng 51:399–409
17. Xie L, Wang DIC (1996) High cell density and high monoclonal antibody production through medium design and rational control in a bioreactor. Biotechnol Bioeng 51: 725– 729
18. Banik GG, Heath CA (1995) Hybridoma growth and antibody production as a function of cell density and specific growth rate in perfusion culture. Biotechnol Bioeng 48:289–300
19. Wen Z-Y, Teng X-W, Chen F (2000) A novel perfusion system for animal cell cultures by two step sequential sedimentation. J Biotechnol 79:1–11
20. Batt BC, Davis RH, Kompala DS (1990) Inclined sedimentation for selective retention of viable hybridoma in a continuous suspension bioreactor. Biotechnol Prog 6:458–464
21. Bierau H, Perani A, Al-Rubeai M, Emery AN (1998) A comparison of intensive cell culture bioreactors operating with hybridomas modified for inhibited apoptotic response. J Biotechnol 62:195–207
22. Broise DDL, Noiseux M, Massie B, Lemieux R (1992) Hybridoma perfusion systems: a comparison study. Biotechnol Bioeng 40:25–32
23. Hulscher M, Scheilber U, Onken U (1992) Selective recycle of viable animal cells by coupling of airlift reactor and cell settler. Biotechnol Bioeng 39:442–446
24. Linardos TI, Kalogerakis N, Behie LA, Lamontagne LR (1992) Monoclonal antibody production in dialyzed continuous suspension culture. Biotechnol Bioeng 39:504–510
25. Lu Z, Thompson BG, Sureah MR, Gray MR (1995) Cultivation of hybridoma cells in an inclined bioreactor. Biotechnol Bioeng 45:176–186
26. Yang J-D, Angelillo Y, Chaudhry M, Goldenberg C, Goldenberg DM (2000) Achievement of high cell density and high antibody productivity by a controlled-fed perfusion bioreactor process. Biotechnol Bioeng 69:74–82
27. Shi Y, Dewey DY, Park H (1992) Performance of mammalian cell culture bioreactor with a new impeller design. Biotechnol Bioeng 40:260–270
28. Bittinger F, Brochhausen C, Skarke C, Kohler H, Kirkpatrick CJ (1997) Reconstruction of peritoneal-like structure in three-dimensional collagen gel matrix culture. Exp Cell Res 236:155–160
29. Chen C (2000) Animal cell culture in a fibrous-bed bioreactor: protein production, cell immobilization, and cell cycle and apoptosis, PhD thesis, The Ohio State University, Columbus, Ohio
30. Ise H, Takashima S, Nagaoka M, Ferdous A, Akaike T (1999) Analysis of cell viability and differential activity of mouse hepatocytes under 3D and 2D culture in agarose gel. Biotechnol Lett 21:209–213
31. Ma T, Li Y, Yang S-T, Kniss DA (1999) Tissue engineering human placenta trophoblast cells in 3D fibrous matrix: spatial effects on cell proliferation and function. Biotechnol Prog 15:715–724
32. Lee GM, Palsson BO (1990) Immobilization can improve the stability of hybridoma antibody productivity in serum-free media. Biotechnol Bioeng 36:1049–1055
33. Nikolai TJ, Hu W-S (1992) Cultivation of mammalian cells on macroporous microcarriers. Enzyme Microb Technol 14:203–208
34. Portner R, Roessing S, Koop M, Luedemann I (1997) Kinetic studies on hybridoma cells immobilized in fixed bed reactors. Biotechnol Bioeng 55:535–541

35. Cadic C, Dupuy B, Piamat I, Merle M, Margerin C, Bezian JH (1992) In vitro culture hybridoma cells in agarose beads producing antibody secretion for two weeks. Biotechnol Bioeng 39:108–112
36. Nilsson K, Sheirer W, Merton OW, Ostberg L, Liehl E, Katinger HWD, Mosbach K (1983) Entrapment of animal cells for the production of monoclonal antibodies and other biomolecules. Nature 302:629–630
37. Lee GM, Varma A, Palsson B (1991) Production of monoclonal antibody using free-suspended and immobilized hybridoma cells: effect of serum. Biotechnol Bioeng 38:821–830
38. Sinacore MS (1984) Gel entrapment: Applications in production of biological and mass culturing animal cells. Karyon Technology News I, Karyon Technology, Norwood, Massachusetts
39. Altshuler GL, Dziewulski DM, Sowek JA, Belfort G (1987) Continuous hybridoma growth and monoclonal antibody production in hollow fiber reactor-separator. Biotechnol Bioeng 28:646–658
40. Brotherton JD, Chau PC (1995) Protein-free human-human hybridoma cultures in an intercalated-spiral alternate-dead-ended hollow fiber bioreactor. Biotechnol Bioeng 47: 384–400
41. Gramer MJ, Britton TL (2002) Antibody production by a hybridoma cell line at high cell density is limited by two independent mechanisms. Biotechnol Bioeng 79:277–283
42. Gramer MJ, Poeschl DM (1998) Screening tool for hollow-fiber bioreactor process development. Biotechnol Prog 14:203–209
43. Tharakan JP, Chau PC (1986) A radial flow hollow fiber bioreactor for the large-scale culture of mammalian cells, Biotechnol Bioeng 28:329–342
44. Valdes R, Ibarra N, Gonzalez M, Alvarez T, Garcia J, Llambias R, Perez CA, Quintero O, Fischer R (2001) CB.Hep-1 hybridoma growth and antibody production using protein-free medium in a hollow fiber bioreactor. Cytotechnology 35:145–154
45. Klement G, Scheier W, Katinger H (1987) Construction of a large membrane reactor system with different compartment for cells, medium and products, Dev Biol Stand 66:221–226
46. Scheirer W (1988) High-density growth of animal cells within cell retention fermentors equipped with membranes. In: Spier RE, Griffiths JB (eds) Animal Cell Biotechnology, vol 3. Academic Press, London, pp 263–281
47. Rupp RG (1985) Use of cellular micro-encapsulation in large-scale production of monoclonal antibodies. Large-scale mammalian cell culture. Academic Press, Orlando, pp 19–38
48. Chiou T-W, Murakami S, Wang DIC (1991) A fiber-bed bioreactor for anchorage-dependent animal cell cultures. Part I. Bioreactor design and operation. Biotechnol Bioeng 37:755–761
49. Emery AN, Lavery M, Williams B, Handa A (1987) Large scale hybridoma culture: animal and plant cells process possibilities. Ellis Horwood, Chichester, pp 137–146
50. Gramer MJ, Poeschl DM (2000) Comparison of cell growth in T-flasks, in micro hollow fiber bioreactors, and in an industrial scale hollow fiber bioreactor system. Cytotechnology 34:111–119
51. Gramer MJ, Poeschl DM, Conroy MJ, Hammer BE (1999) Effect of harvesting protocol on performance of a hollow fiber bioreactor. Biotechnol Bioeng 65:334–340
52. Dowd JE, Weber I, Rodriguez B, Piret JM, Kwok KE (1999) Predictive control of hollow-fiber bioreactors for the production of monoclonal antibodies. Biotechnol Bioeng 63:484– 492
53. Schweikart F, Jones R, Jaton J-C, Hughes GJ (1999) Rapid structural characterization of a murine monoclonal IgA α chain: heterogeneity in the oligosaccharide structures at a specific site in samples produced in different bioreactor systems. J Biotechnol 69:191–201
54. Chen C, Huang YL, Yang S-T (2002) A fibrous-bed bioreactor for continuous production of developmental endothelial locus-1 by osteosarcoma cells. J Biotechnol 97:23–39
55. Highfill JG, Haley SD, Kompala DS (1996) Large-scale production of murine bone marrow cells in an airlift packed bed bioreactor. Biotechnol Bioeng 50:514–520
56. Lee GM, Palsson BO (1993) Stability of antibody productivity is improved when hybridoma cells are entrapped in calcium alginate beads. Biotechnol Bioeng 42:1131–1135

57. Martens DE, Nollen EAA, Hardeveld M, Van Der Velden-De Groot CAM, De Gooijer CD, Beuvery EC, Tramper J (1997) Death rate in a small air-lift loop reactor of Vero cells grown on solid microcarriers and in macroporous microcarriers. Cytotechnology 23:61–75
58. Park S, Stephanopoulos G (1993) Packed bed bioreactor with porous ceramic beads for animal cell culture. Biotechnol Bioeng 41:25–34
59. Yang TH, Miyoshi H, Ohshima N (2001) Novel cell immobilization method utilizing centrifugal force to achieve high-density hepatocyte culture in porous scaffold. J Biomed Materials Res 55:379–386
60. Li Y, Yang S-T (2001) Effects of three-dimensional scaffolds on cell organization and tissue development. Biotechnol Biopr Eng 6:311–325
61. Luo J (2002) Three-dimensional culture of animal cells in a fibrous-bed bioreactor, PhD thesis, The Ohio State University, Columbus, Ohio
62. Ma T (1999) Fiber-based bioreactor systems in mammalian cell culture and tissue engineering human trophoblast cells, PhD thesis, The Ohio State University, Columbus, Ohio
63. Perry SD, Wang DIC (1989) Fiber bed reactor design for animal cell culture. Biotechnol Bioeng 34:1–9
64. Lewis VP, Yang S-T (1992) Continuous propionic acid fermentation by immobilized *Propiobaterium acidipropionici* in a novel packed-bed bioreactor. Biotechnol Bioeng 40:465–471
65. Yang ST, Huang Y (1995) A novel recycle batch immobilized bioreactor for propionate production from whey lactose. Biotechnol Bioeng 45:379–386
66. Yang ST, Zhu H, Li Y, Hong G (1994) Continuous propionate production from whey permeate using a novel fibrous-bed bioreactor. Biotechnol Bioeng 43:1124–1130
67. Archambault J, Volesky B, Kurz WGW (1990) Development of bioreactors for the culture of surface immobilized plant cells. Biotechnol Bioeng 35:702–11
68. Archambault J, Robert J, Tom L (1994) Culture of immobilized insect cells. Bioprocess Eng 11:189–197
69. Junker BH, Chiou T, Wang DIC, Buckland BC (1993) Cultivation of virus antigen in fibroblast cells using a glass fiber-bed reactor. Biotechnol Bioeng 42:635–642
70. Ma T, Li Y, Yang S-T, Kniss DA (2000) Effects of pore size in 3D fibrous matrix on human trophoblast tissue development. Biotechnol Bioeng 70:606–618
71. Motobu M, Matsuo S, Wang P-C, Kataoka H, Matsumura M (1997) High renin productivity of rCHO cells cultivated in radial-flow non-woven fabric mat packed-bed reactor with increasing circulating flow rate. J Ferment Bioeng 83:443–450
72. Murakami S, Chiou T-W, Wang DIC (1991) A fiber-bed bioreactor for anchorage-dependent animal cell cultures: part II. Scaleup potential. Biotechnol Bioeng 37:762–769
73. Robert J, Cote J, Archambault J (1992) Surface immobilization of anchorage-dependent mammalian cells. Biotechnol Bioeng 39:697–706
74. Grampp GE, Applegate Mark A, Stephanopoulos G (1996) Cyclic operation of ceramic-matrix animal cell bioreactors for controlled secretion of an endocrine hormone. A comparison of single-pass and recycle modes of operation. Biotechnol Prog 12:837–846
75. Kim B-S, Putnam AJ, Kulik TJ, Mooney DJ (1998) Optimizing seeding and culture methods to engineer smooth muscle tissue on biodegradable polymer matrixes. Biotechnol Bioeng 57:46–54
76. Zhu H (1995) Kinetics and analysis of a fibrous-bed bioreactor for mammalian cell cultures. PhD thesis, Ohio State University, Columbus, OH
77. Cioffi JA, Shafer AW, Zupancic TJ, Smith-Gbur J, Mickhail A, Platika D, Snodgrass HR (1996) Novel B219/OB receptor isoform: possible role of leptin in hematopoiesis and reproduction. Nat Med 2:585–589
78. Ghilardi N, Ziegler S, Wiestner A, Stoffel R, Heim MH, Skoda, RC (1996) Defective STAT signaling by the leptin receptor in diabetic mice. Proc Natl Acad Sci USA 93:6231–6235
79. Mikhail A, Beck EX, Shafer A, Barut B, Gbur JS, Zupancic T, Schweitzer AC, Cioffi JA, Lacaud G, Ouyang B, Keller G, Snodgrass RH (1997) Leptin stimulates fetal and adult erythroid and myeloid development. Blood 89:1507–1512

80. Li Y, Ma T, Yang S-T, Kniss DA (2001) Thermal compression and characterization of 3D non-woven PET matrices as tissue engineering scaffolds, J Biomater 22:609–618
81. Chen K, Liu Q, Xie L, Sharp PA, Wang DIC (2001) Engineering of a mammalian cell line for reduction of lactate formation and high monoclonal antibody production. Biotechnol Bioeng 72:55–61
82. Hansen HA, Emborg C (1994) Influence of ammonium on growth, metabolism, and productivity of a continuous suspension Chinese hamster ovary cell culture. Biotechnol Prog 10:121–124
83. Matsumura M, Nayve F, Rey P Jr (1995) Effects of ammonium ion removal on growth and MAb production of hybridoma cells. Cytotechnology 18:35–50
84. Singh RP, Al-Rubeai M, Gregory CD, Emery AN (1994) Cell death in bioreactors: a role for apoptosis. Biotechnol Bioeng 44:720–726
85. Fassnacht D, Pörtner R (1999) Experimental and theoretical considerations on oxygen supply for animal cell growth in fixed-bed reactors. J Biotechnol 72:169–184
86. Miller WM, Blanch HW, Wilke CR (1988) A kinetic analysis of hybridoma growth and metabolism in batch and continuous suspension culture: effect of nutrient concentration, dilution rate, and pH. Biotechnol Bioeng 32:947–965
87. Geaugey V, Pascal F, Engasser JM, Marc A (1990) Influence of the culture oxygenation on the release of LDH by hybridoma cells. Biotechnol Tech 4:257–262
88. Boraston R, Thompson PW, Garland S, Birch JR (1983) Growth and oxygen requirements of antibody-producing mouse hybridoma cells in suspension culture. Dev Biol Stand 55:103–111
89. Reuveny S, Velez D, Macmillan JD, Miller L (1986) Factors affecting cell growth and monoclonal antibody production in stirred reactors. J Immunol Methods 86:53–59
90. Ozturk SS, Palsson B (1990) Effects of dissolved oxygen on hybridoma cell growth, metabolism, and antibody production kinetics in continuous culture. Biotechnol Prog 6:437–446
91. Miller WM, Blanch HW, Wilke CR (1987) The effects of dissolved oxygen concentration on hybridoma growth and metabolism in continuous culture. J Cell Physiol 132:524–530
92. Ozturk SS, Palsson BO (1991) Growth, metabolic, and antibody production kinetics of hybridoma cell culture: 2. Effects of serum concentration, dissolved oxygen concentration, and medium pH in a batch reactor. Biotechnol Prog 7:481–494
93. Michaels JD, Petersen JF, McIntire LV, Papoutsakis ET (1991) Protection mechanisms of freely suspended animal cells (CRL 8018) from fluid-mechanical injury. Viscometric and bioreactor studies using serum, Pluronic F68 and polyethylene glycol. Biotechnol Bioeng 38:169–180
94. McDowell CL, Papoutsakis ET (1998) Serum increases the CD13 receptor expression, reduces the transduction of fluid-mechanical forces, and alters the metabolism of HL60 cells cultured in agitated bioreactors. Biotechnol Bioeng 60:259–268
95. Jang JD, Barford JP (2000) An unstructured kinetic model of macromolecular metabolism in batch and fed-batch cultures of hybridoma cells producing monoclonal antibody. Biochem Eng J 4:153–168
96. Lambert N, Merten O-W (1997) Effect of serum-free and serum-containing medium on cellular levels of ER-based proteins in various mouse hybridoma cell lines. Biotechnol Bioeng 54:165–180
97. Yasui K, Kada K, Hojo M, Lee JK, Kamiya K, Toyama J, Opthof T, Kodama I (2000) Cell-to-cell interaction prevents cell death in cultured neonatal rat ventricular myocytes. Cardiovasc Res 48:68–76
98. Chen CS, Mrksich HS, Whitesides GM, Ingber DE (1997) Geometric control of cell life and death. Science 276:1425–1428
99. Ruoslahti E (1997) Stretching is good for a cell. Science 276:1345–1346
100. Al-Rubeai M, Singh RP, Emery AN, Zhang Z (1995) Cell cycle and cell size dependence of susceptibility to hydrodynamic forces. Biotechnol Bioeng 46:88–92
101. Martens DE, de Gooijer CD, van der Velden-de Groot CAM, Beuvery EC, Tramper J (1993) Effect of dilution rate on cell growth, productivity, cell cycle and size, and shear sensitivity of a hybridoma cell in a continuous culture. Biotechnol Bioeng 41:429–439

102. Mercille S, Massie B (1994) Induction of apoptosis in nutrient-deprived cultures of hybridoma and myeloma cells. Biotechnol Bioeng 44:1140–1154
103. Simpson NH, Milner AE, Al-Rubeai M (1997) Prevention of hybridoma cell death by bcl-2 during suboptimal culture conditions. Biotechnol Bioeng 54:1–16
104. Perani A, Singh RP, Chauhan R, Al-Rubeai M (1998) Variable functions of bcl-2 in mediating bioreactor stress-induced apoptosis in hybridoma cells. Cytotechnology 28:177–188
105. Peshwa MV, Kyung YS, McClure DB, Hu WS (1993) Cultivation of mammalian cells as aggregates in bioreactors: effect of calcium concentration on spatial distribution of viability. Biotechnol Bioeng 41:179–187
106. Fussenegger M, Bailey JE (1998) Molecular regulation of cell-cycle progression and apoptosis in mammalian cells: implications for biotechnology. Biotechnol Prog 14:807–833
107. Gu MB, Todd P, Kompala DS (1993) Foreign gene expression (β-galactosidase) during the cell cycle phases in recombinant CHO cells. Biotechnol Bioeng 42:1113–1123
108. James RI, Elton JP, Todd P, Kompala DS (2000) Engineering CHO cells to overexpress a secreted reporter protein upon induction from mouse mammary tumor virus promoter. Biotechnol Bioeng 67:134–140
109. Kubbies H, Stockinger H (1990) Cell cycle dependent DHFR and tPA production in cotransfected, MTX amplified CHO cells revealed by dual-laser flow cytometry. Exp Cell Res 188:665–677
110. Simpson NH, Sigh RP, Emery AN, Al-Rubeai M (1999) Bcl-2 over-expression reduces growth rate and prolongs G1 phase in continuous chemostat cultures of hybridoma cells. Biotechnol Bioeng 64:187–193
111. Lloyd DR, Leelavatcharamas V, Emery AN, Al-Rubeai M (1999) The role of the cell cycle in determining gene expression and productivity in CHO cells. Cytotechnology 30:49–57
112. Cain SJ, Chau PC (1998) Transition probability cell cycle model with product formation. Biotechnol Bioeng 58:387–399
113. Moses H, Proper JA, Volkenant ME, Swartzendruber DE (1980) Growth arrest of AKR-2B cells maintained in the presence of epidermal growth factor or 12-o-tetradecanoylphorbol-13-acetate: evidence for two separate G1 arrest points. J Cell Physiol 102:367–378
114. Suzuki E, Ollis DF (1990) Enhanced antibody production at slowed growth rate: experimental determination and a simple structured model. Biotechnol Prog 6:231–236
115. Doverskog M, Ljunggren J, Ohman L, Haggstrom L (1997) Physiology of cultured animal cells. J Biotechnol 59:103–115
116. Wang J, Honda H, Park YS, Iijima S, Kobayashi T (1994) Effect of dissolved oxygen concentration on growth and production of biomaterials by animal cell culture. In: Proc Int Meeting on Animal Cell Technology: Basic Application Aspects, Japen Assoc. Animal Cell Technology, 6th Meeting 1993, pp 191–195
117. Zanghi JA, Fussenegger M, Bailey JE (1999) Serum protects protein-free competent Chinese hamster ovary cells against apoptosis induced by nutrient deprivation in batch culture. Biotechnol Bioeng 64:108–119
118. Nielsen LK, Reid S, Greenfield PF (1997) Cell cycle model to describe animal cell size variation and lag between cell number and biomass dynamics. Biotechnol Bioeng 56:372–379
119. Dhir S, Morrow KJJ, Rhinehart RR, Wiesner T (2000) Dynamic optimization of hybridoma growth in a fed-batch bioreactor. Biotechnol Bioeng 67:197–205
120. Voigt A, Zintl F (1999) Hybridoma cell growth and anti-neuroblastoma monoclonal antibody production in spinner flasks using a protein-free medium with microcarriers. J Biotechnol 68:213–226
121. Fong W, Zhang Y, Yung P (1997) Optimization of monoclonal antibody production: combined effects of potassium acetate and perfusion in a stirred tank bioreactor. Cytotechnology 24:47–54
122. Park SH, Ryu DY (1994) Cell cycle kinetics and monoclonal antibody productivity of hybridoma cells during perfusion culture. Biotechnol Bioeng 44:361–367

Received: August 2003

Adv Biochem Engin/Biotechnol (2004) 87: 97–150
DOI 10.1007/b13537

A Multi-Scale Study of Industrial Fermentation Processes and Their Optimization

Siliang Zhang · Ju Chu · Yingping Zhuang

State Key Laboratory of Bioreactor Engineering, East China University of Science and Technology, 130 Meilong Road, Shanghai 200237, China
E-mail: siliangz@163.net

Abstract In this article problems in multi-scale industrial fermentation processes are discussed. The problems are generated virtually, by using computer simulation on three different scales – the molecular scale (genetics), the cellular scale (metabolic regulation), and the reactor engineering scale. Inter-scale observation and operation are deemed to be crucial in the optimization of bioprocesses. Bioreaction engineering based on metabolic flux analysis and control is further elucidated. Optimization methodology for study of multi-scale problems in a fermentation process, based on correlation of data, and the scale-up technique for regulation of several bioprocess parameters are generalized by investigation of two typical fermentation processes. A novel bioreactor system was designed to monitor mass flux (for example substrates and (by-)products) in a fermentation process. It was successfully applied to the optimization and scale-up of an industrial fermentation process for penicillin, erythromycin, chlortetracyclin, inosine, and guanosine, and for production of recombinant human serum albumin and a malaria vaccine by use of the *Pichia* expression system. Substantial improvement of industrial fermentation productivity was achieved.

Keywords Bioreactor · Fermentation · Optimization · Scale-up · Metabolic flux

Abbreviations

AcCoA	Acetyl coenzyme A
Ala	Alanine
ADP	Adenosine diphosphate
AMP	Adenosine monophosphate
Arg	Arginine
ARX	Adaptive regression expansion
ATP	Adenosine triphosphate
Bioradar	Trademark of a software program for bioprocess monitoring and control
CER	CO_2 evolution rate
CIT	Citric acid
COM	Component object model
CSTR	Continuous stirred tank reactor
Cys	Cysteine
D	Dilution rate
DNA	Deoxyribonucleic acid
DO	Dissolved oxygen
E-4-P	Erythrose-4-phosphate
EMP	Embden–Mayerhof–Parnas
F	Air flow rate
F6P	Fructose-6-phosphate
FAD	Flavin adenine dinucleotide
FADH	Reduced flavin adenine dinucleotide
FS	Full-scale
G6P	Glucose-6-phosphate

G-6-PDH	Glucose 6-phosphate dehydrogenase
GAP	Glyceraldehyde-3-phosphate
GFP	Green fluorescence protein
GK	Glucokinase
Gln	Glutamine
Gly	Glycine
GMP	Guanosine monophosphate
GPC	Generalized predictive controllers
GS	Glutamine synthetase
HDE	Hybrid differential evolution
His	Histidine
HK	Hexokinase
HMP	Hexose monophosphate
HPLC	High-performance liquid chromatography
Ile	Isoleucine
Leu	Leucine
KES	Knowledge engineering system
Lys	Lysine
MAL	Malate
Matlab	A computer language used in computation
MDA	Metabolic design analysis
NAD	Nicotinamide adenine dinucleotide
NADH	Reduced nicotinamide adenine dinucleotide
NADP	Nicotinamide adenine dinucleotide phosphate
NADPH	Reduced nicotinamide adenine dinucleotide phosphate
OAA	Oxaloacetate
OGA	Oxoglutarate
OTR	Oxygen transfer rate
OUR	Oxygen uptake rate
PC	Personal computer
PEP	Phosphoenolpyruvate
PFK	Phosphofructokinase
PID	Proportional integral differential
PGA	3-Phosphoglyceric acid
PK	Pyruvate kinase
Pro	Proline
PRPP	Phosphoribosylpyrophosphate
Pur	Purine
PYR	Pyruvate
RHSA	Recombinant human serum albumin
R	Reynolds number
R-5-P	Ribose-5-phosphate
RQ	Respiratory quotient
RNA	Ribonucleic acid
RPM	Revolutions per minute
Ru5P	Ribulose-5-phosphate
sAMP	Adenyl succinate

Ser	Serine
SBR	Stirred bioreactor
TCA	Tetracarboxylic acid
TCP/IP	Transmission control protocol/internet protocol
Thr	Threonine
tRNA	Transfer ribonucleic acid
Tyr	Tyrosine
Val	Valine

Symbols

α_{gly}	Reciprocal yield of glycerol on ATP
α_{glu}	Reciprocal yield of glucose on ATP
a_h	Stoichiometry of oxidative phosphorylation
a_p	Reciprocal yield of product on ATP
a_x	Reciprocal yield of biomass on ATP
C	Concentration
C^*	Saturation concentration of oxygen in broth
C_{nx}	Nitrogen contents in biomass
C_{np}	Nitrogen content in product
f	Degrees of freedom
k_N	Constant in Monod equation related to the nitrogen sources
k_C	Constant in Monod equation related to the carbon sources
K_1 to K_9	Various reaction rate constants
K_{IN}	Conversion rate constant of soybean meal transformed to amino acids
K_La	Oxygen transfer coefficient
ND_I	Rate of stress
P/V_R	Power consumption per unit volume of broth
q_{gly}	Specific glycerol consumption rate
Q_p	Specific product synthesis rate
$\boldsymbol{r}$	Metabolic reaction rates vector
r_1 to r_{23}	Various metabolic reaction rates
r_{gly}	Glycerol consumption rate
r_c	Carbon dioxide evolution rate
r_{moh}	Methanol consumption rate
r_n	Ammonia consumption rate
r_o	Oxygen uptake rate
r_p	Product formation rate
r_x	Cell growth rate
$\boldsymbol{R}_E$	External flow vector
$\boldsymbol{R}_{E1}$	Primary external flow vector
$\boldsymbol{R}_{E2}$	Secondary external flow vector
R_{NH3}	Feed rate of ammonia
R_{GLU}	Feed rate of glucose
R_{MOH}	Feed rate of methanol
S_1	Concentration of starch
S_2	Concentration of glucose

S_3	Concentration of ammonium sulfate
S_4	Concentration of soybean meal
t_m	Mixing time
X	Biomass concentration
$x1$ to $x23$	Various metabolites
Y_{xs}	Macroscopic yield of biomass on substrate
Y_{ps}	Macroscopic yield of product on substrate
β_1 to β_3	Various coefficients describing the relation between product formation and cell growth
σ	Stoichiometric coefficient of the carbon source in anabolic or product formation reactions
γ	Degree of reduction
μ	Specific growth rate

1 Introduction

Fermentation technology for large-scale cell cultivation was recognized and exploited in ancient times. Fermentation has been used to produce medicine, food, and light industrial products, and in agricultural and environmental protection. Its applications can be divided into those of traditional biotechnology using conventional microorganisms and those of modern biotechnology involving engineered cells. To enhance fermentation productivity researchers often use their own way of thinking, based on their research background, to comprehend and analyze the characteristics of fermentation processes. They first consider strain breeding or the construction of an engineered strain, and investigate different methods for strain mutation and selection. Because of the rapid and profound development of biotechnology, it is now possible to improve industrial strains by using transformation or reconstruction of a gene encoded for the key enzyme of a biosynthetic pathway, and remarkable results have been achieved in this field. However, changes in the behavior of a culture which result from bioreactor engineering are often overlooked when dealing with the optimization of a bioprocess in the course of transferring a research achievement to industrial practice. Generally speaking, after obtaining a high-yield production strain in the laboratory, stepwise scale-up and optimization will follow. The main focus will be on the optimum means of controlling the process, and static operation is usually adopted, mainly on the basis of personal experience. Methods for optimization are largely based on orthogonal design. Optimization and scale-up of bioprocesses are always regarded as two sides of a complex problem in biochemical engineering, and are investigated from different points of view.

Furthermore, along with the rapid development of computer technology, most fermentation plants have been equipped with computers for on-line control and with a dissolved oxygen probe, a pH probe, a paramagnetic O_2 analyzer, and an infra-red CO_2 analyzer, to monitor the *DO* and pH of broth and the O_2 and CO_2 content of exhaust gas, and even with probes or sensors to measure broth ingredients. Nevertheless, the data obtained and their profiles do not reveal the multi-

scale characteristics of the bioprocess. For instance, during the fermentation what does a change of *DO* profile mean? Is this a problem arising from the genetic scale, from the cellular scale, or from the bioreactor engineering scale? Most process analyses rely on experience, because of lack of a theoretical basis. Consequently, they can be used to solve instability problems among different batches of a bioprocess by implementing feedback control of pH, *DO*, etc., and by introducing cascade control, but they fail to explain the high yields sometimes obtained from fermentation batches. It takes a long time before a new product can be put into production, and practical results obtained in the laboratory are always not fully realized on a larger scale. In view of these disadvantages, a method for optimized control of a fermentation process has been proposed on the basis of the estimated values of different conditions. Solving practical problems arising from industrial production processes is currently a critical task in the fermentation industry.

Along with intensive studies of large-scale cell culture techniques and an understanding of why conditions vary with time, the reasons for their diversity, the correlation between them, and their indeterminate nature, mathematical models based on process kinetics have been set up, and a series of modern control theories has been introduced by researchers with a professional background in automatic control. For instance, Rani and Rao [1] have reviewed bioreactor process control and Lee et al. [2] summarized control strategies for optimization of batch fermentation, including system recognition, dynamic optimization, adaptive control, use of expert systems and artificial neural networks, and studies of various chaos phenomena. In a review, Bellgardt [3] introduced the principles of modeling of biotechnical processes, focusing on models of the biological system within the entire bioprocess and stressing the importance of growth and product synthesis.

System recognition is a mathematical model for the fermentation process which is used to describe relationships among input, output, and the status of a process in a system, and to form the foundation for process control. Simon and Karim [4], using the ARX model as the basis achieved system recognition for an animal cell cultivation process. A generalized predictive controller (GPC) was adopted for *DO* control, and the results achieved were better than those obtained by use of the PID method. Ungarala et al. [5] applied modulating functions and spline models to identification of time-varying systems in fermentation processes, and verified that the functions and models were quite suitable for fermentation processes with time-varying systems. In their review, Luttmann et al. [6] introduced integration of on-line simulation methods with process-control systems for bioreactors. The technique relied on complete modeling of the bioreactor system and its replacement by a real-time simulator with duplicate I/O connections. This inexpensive method can be used to validate automation hardware and software, and to enable the development of complex processing strategies of advanced functions. Stephanopoulos et al. [7] presented a method for processing fermentation data to enable creation of a database of derivative process quantities representing global patterns, intermediate trends, and local characteristics of the process. The method has been implemented in user-friendly software which facilitates use of the method for efficient analysis of fermentation process data.

Optimization of a process can be conducted after the process has been modeled. Because of the time-varying performance of a fermentation process, it is quite difficult to optimize a process by using the traditional static method. Wang et al. [8] dynamically optimized a process for alcohol production using the hybrid differential evolution (HDE) method. As a result they established a rational feeding strategy. Balsa-Canto et al. [9, 10] discussed the application of restricted second-order information to the dynamic optimization of a bioprocess. Dhir et al. [11] achieved dynamic optimization of hybridoma growth in a batch-fed culture.

Self-adaptive control is an advanced control technique first applied to fermentation process control. In 1984 Dochain and Bastin [12] devised a simple self-modulated control system for regulation of substrate concentration and production rate for a bacterial fermentation. Ben Youssef and Guillou [13] adopted a self-adaptive control method for control of continuous lactate fermentation. Meleiro and Maciel [14] succeeded in applying self-tuning adaptive control to industrial large-scale ethanol production.

Expert systems were introduced in the mid-1960s. As their applications broadened they became more attractive. In the 1980s the expert system concept was introduced for control of fermentation processes. Many scholars, both experienced technicians and experts, have summarized knowledge about the optimization and control of bioprocesses. They set up knowledge bases which were described by rules (models). These rules were then used to deduce an optimum control method on the basis of measurable variables during the fermentation process. Shioya et al. [15] reviewed research progress in the development and operation of expert systems and their application to bioprocesses. Lennox et al. [16] discussed the application of an expert system to an industrial fermentation process and pointed out that the expert system could effectively show the operators that malfunction had occurred during fermentation. Ray et al. [17] developed a prototype expert system for diagnosis of Baker's yeast fermentation on the expert system shell called "knowledge engineering system-HT" (KES-HT), based on heuristic reasoning, for prompt detection of any malfunction in a bioprocess.

Fuzzy set theory has been developed very quickly and put to practical use. Researchers such as Mamdani [18] described concepts of fuzzy control which marked the formal emergence of fuzzy control theory. Although the relationships among the different variables in fermentation processes are difficult to describe precisely by use of mathematical models, it is possible to reflect their relevance during different periods of fermentation through fuzzy relationships. Hence, results inferred from fuzzy relationships can be used to supervise the optimum operation and control of the fermentation process [19, 20]. Fuzzy inference was applied by Horiuchi et al. [21] to identify the culture phase; it was also used for on-line fuzzy control of the production of glutamate, α-amylase, β-galactosidase, and vitamin B_2. Honda and Kobayashi [22] have published an overview of the application of fuzzy control to bioprocesses.

Study of the neural network technique has undergone a rather long history. Pioneering research on neuron models under excitement and inhibition was a result of cooperation between psychologist McCulloch and mathematician Pitts [23]; the amending rule for the connecting intensity of the neurons was introduced by Hebb [24]. Their research achievements have since been the

foundation of many neural network models. Many studies have focused on use of neural networks to describe fermentation processes. They can be used to forecast the status of a fermentation process, whether normal or abnormal [25], to predict its metabolic state, or to predict properties which are hard to measure directly, for example cell density, and substrate and product concentration [26]. Vlassides et al. [27] made use of an artificial neural network and archive information in a process for modeling wine properties; historical data were used to optimize the process.

Chaotic phenomena occur in diverse natural phenomena, from the simple falling of leaves to complicated weather patterns. From the viewpoint of certainty, the world can be divided into deterministic and non-deterministic systems. In a deterministic system evolution of system status is determined after the initial conditions have been given; a non-deterministic system is a stochastic and/or fuzzy system. Chaos seems to be random, but it is almost an ordered phenomenon. Its extent depends on the initial conditions of a system. A slight change in the initial conditions can lead to the entirely different evolution of a process – as the Chinese proverb says: "a nuance makes the distance thousands of miles apart". Fermentation processes are chaotic in nature [28]. The difference in the early phase of fermentation will have a substantial influence on the entire process and, eventually, on the production level of the process. Studies on the dynamic behavior of glycolysis [29] revealed that intricate oscillating behavior occurred in the pathway, and two types of chaotic phenomena were found. Fox and Hill [30] studied the topology and dynamic behavior of a metabolic network in a biochemical system. Their studies concentrated on the types of attractor, an excited branch point, the length of the cycle, etc. In general, chaotic phenomena in the course of fermentation are currently in the stage of exploration [31–33]. These kinds of research method adapted to the non-linear features of a fermentation process have greatly promoted intense studies of the technology used for large-scale cultivation of cells, and the amount of academic research has increased. However, it should be remembered that the application of chaotic phenomenon to practical production is still restricted, and results have been unsatisfactory.

Shioya et al. [34] and van Gulik et al. [35], respectively, applied on-line metabolic flux analysis to the fermentation process and to identification of a bottleneck in the biosynthesis of penicillin G. The latter developed detailed stoichiometric models for the growth of *Penicillium chrysogenum* and the production of penicillin-G. In dynamic analysis and process optimization Chae et al. [36] used the green fluorescence protein (GFP) fusion monitoring method to perform online optimization of the expression of recombinant protein in high-cell-density cultures of *E. coli*. They used a sequential quadratic programming optimization algorithm to estimate model data and to solve optimum open-loop control problems for the control of inducer feed rates that maximized productivity. Conejeros and Vassiliadis [37] studied the dynamic analysis of a biochemical reaction process and predicted the change of pathway. Using their framework they analyzed the production of penicillin V and identified the most sensitive reaction steps and the most significant constraints on the system by determination of the effects of the concentrations of intracellular metabolites on the activity of each enzyme. Cruickshank et al. [38] performed dynamic modeling and optimization

of the feeding strategy of batch-fed cultivation in a two-phase partitioning bioreactor. Zeiser et al. [39] investigated on-line monitoring of the growth of worm cells during cultivation and physiological data during the infection process. To obtain information on intracellular variables Schuster [40] reviewed a complementary approach which analyzed the microbial cells indirectly. The suitability of methods for online analyses of a bioprocess was discussed. Information obtained by use of the methods can be used to establish better knowledge as a basis for monitoring and control strategies.

Scale-up of fermentation processes can be regarded as suffering from two fundamental problems:

- investigation and design of fermentation conditions; and
- design of a reactor that meets these process conditions.

The first problem, in a sense, is the problem of the kinetics of a fermentation process; the second is the problem of transfer and mixing on the reactor engineering scale. Investigators with a chemical engineering background introduced a series of approaches for mathematical modeling of process scale-up, namely, dimensional analysis, empirical rules, time constants, and the association mechanism [13]. For example, the empirical approach integrated with the principle of similarity and dimensional analysis for scale-up puts forward the general principles of the equalities of power consumption per unit volume of culture broth (P/V_R), oxygen transfer coefficient ($K_L a$), rate of stress (ND_I), or mixing time (t_m). Scale-up has been achieved by mechanisms based on rate determination according to the characteristic time, and by comparison of time constants of different transfers in bioprocesses, such as substrate consumption, growth, mixing, flow, diffusion, mass transfer, and residence time.

A combined mathematical model for glutamate fermentation in an SBR, including mixing of fluid, oxygen transfer, and the kinetics of cell growth, substrate consumption, and product formation was constructed by Nagy et al. [41]; he then calculated the oxygen distribution in the bioreactor and the transient change of pH during process control and compared these with practical data from an industrial scale process. It should be recognized that unless a model is constructed by integrating entirely the reaction kinetics of the microorganism with the ambient transfer conditions, scale-up of the process is eventually based on the geometric similarity of a system or the similarity of flow dynamics or fluid kinetics. It is, in fact, impossible to meet these similar conditions simultaneously. Successful examples of scale-up of fermentation processes show that the process of interest should be investigated intensively to determine the control elements and investigate their local correlations before scale-up can be achieved. However, difficulties can occur if the results of investigations are regarded as criteria for scale-up, especially when study of a new process has been just started. As a result, the scale-up of fermentation processes still remains a perplexing problem, because different experimental results are obtained with shake flasks and fermenters from several liters to thousands of liters, even under the same operating conditions.

Intensive studies have been performed on regulation of metabolism on the cellular scale. In some studies cell growth and metabolism were calculated stoichiometrically [42–46] and numerous reports on metabolic engineering, some-

times studied in conjunction with control of fermentation processes, have been published. Bailey et al. [47] conceived the concept of inverse metabolic engineering, which comprises elucidation of a metabolic engineering strategy by identifying and constructing a desired phenotype, determining the genetic or the environmental factors, and endowing another strain with that phenotype by genetic or environmental manipulations. They succeeded in using the strategy to eliminate growth factors from mammalian cell cultures and to enhance the energetic efficiency of the respiration of microaerobic bacteria. Khetan and Hu [48] focused their studies on knowledge-based metabolic engineering for improvement of processes for biosynthesis of antibiotics, particularly penicillin and cephalosporin, with the conclusion that if major successes are to be achieved in this domain, progress in the quantitative characterization of basic and altered physiology of producer strains is critical. Herwig et al. [49] developed a method for determination of on-line stoichiometry and identification of the metabolic state under dynamic process conditions; they stated that the basis of the proposed method was the on-line availability of consistent stoichiometric coefficients which enabled significant speeding up of strain characterization and bioprocess development but using minimal knowledge of the metabolism. Kholoenko et al. [50] developed a method to determine the cell concentration; this is required to achieve the aim of increasing the production of valuable compounds. The method was termed "metabolic design analysis" (MDA). To employ MDA, only limited kinetic information about the pathway enzymes is needed. Feng and Glassey [51] demonstrated that data obtained from chemical fingerprinting methods, such as pyrolysis mass spectrometry, could be used to identify changes in physiological state during cultivation, and that the information obtained could be used to estimate the physiological state and enable physiological state-specific-model development for on-line bioprocess control.

Analysis of exocellular concentration and calculation of intracellular metabolite content have been performed by Shioya et al. [34]; the data obtained were used for state recognition and process control. They proposed three steps for modeling metabolism with on-line data – modeling, noise elimination, and flux analysis. In some circumstances the results obtained from flux partition could be used for recognition of the physiological state of cells. In another circumstance the model with time-variant properties based on estimated physiological state was applied to metabolic flux analysis. They established a universal approach for construction of an on-line flux-analysis system. Metabolic flux distribution was estimated by use of measurable rates and an extended Kalman filter and was applied to on-line estimation of specific growth rate and specific sugar consumption rate. The metabolic reaction model thus constructed was also used to calculate the molar flux distribution. A high-yield penicillin-producing strain, *Penicillium chrysogenum*, was used as a model system by van Gulik et al. [35] to study the effect of the interaction between primary metabolism and product formation on the supply of carbon precursors and reducing equivalents. Metabolic flux analysis was used for rational identification of the main nodes of primary metabolism, which had great influence on the distribution of flux. Subsequently, the effects of changing the growth rate in chemostat culture on the partition of the fluxes around the nodes were investigated. Metabolic flux analysis was further

applied to the production of penicillin G, by determination of the flux input and flux output of the cells. Chauvatcharin et al. [52] applied the acetone–butanol fermentation equations to metabolic analysis of the reaction network under different conditions and succeeded in on-line estimation of the state of the culture by coupling an automated measurement system with the models.

It should be admitted that studies of regulation of metabolism on the genetic and cellular scales have played an important role in enabling understanding of bioprocesses. Nevertheless, in practical operation of bioreactors the basis of optimization of fermentation technology is still a search for the optimum means of control of the bioprocess, for example medium formulation, temperature, pH, *DO*, etc., by use of kinetic studies.

The essential reason for this problem is, in our opinion, that some researchers often consider and analyze the characteristics of the fermentation process according to their own professional background, and based on one scale only. For instance, researchers who engage in strain breeding or gene construction regard the problem as that of changing the DNA on the molecular scale; those who deal with the problem of metabolic reactions merely focus on regulation of metabolism; and reactor engineers are mainly concerned with three kinds of transfer (momentum, mass, and heat) within the chemical engineering domain. Serious problems can occur when living cells are controlled by a traditional biological approach or chemical engineering method alone. As a matter of fact, the growth of living cells in a bioreactor should be performed on different scales, i.e. molecular genetics, regulation of cellular metabolism, and by bioreactor engineering. Relevant analyses of the living organisms on the three scales are the key elements of optimization of a bioprocess. This is the primary viewpoint of this review article.

After reviewing the basic idea – methods of optimization and scale-up of fermentation processes adopted by many researchers for quite a long time – the authors came to the conclusion that the static optimization method based on the kinetic concept with conventional optimum operating conditions is, in fact, only an extension of the kinetic concept of chemical engineering to the fermentation process in which the existence of cellular metabolic flux is always neglected. Thus, our opinion that control of bioreaction engineering should be based on metabolic flux analysis is emphasized in this article. By means of further experiments optimization of fermentation processes on several scales are realized, on the basis of data correlations and scale-up strategy with multi-variable modulation. With the development of process monitoring by use of sensors and computer technology a novel-concept bioreactor (FUS-50L) for fermentation process optimization and scale-up has been designed and constructed. This novel bioreactor, designed to enable measurement of material flux, has been successfully applied to the fermentation of penicillin, erythromycin, aureomycin, inosine, guanosine, recombinant human serum albumin, and malaria vaccine, etc. As a result, increases in titers from 30% to severalfold were achieved. The process can be directly scaled up from several hundred liters to hundreds of cubic meters.

2
Principles and methods

2.1
Fundamental principles

The problems of fermentation processes are basically on several levels. In the study of a system if a certain phenomenon on different scales is regarded as an object it is hard to discover the relevance among the different scales, because of difficulties with micro- and macro-statistical processing of the data. Nevertheless, once a relationship which can be followed has been discovered it is possible to trace the essence of the phenomenon, and changes might be made in the study and control of the process. Thus the multi-scale problem of a substance-processing system becomes a problem of interest and difficulties.

Through further studies the multi-scale features in terms of time and space are taken as the common features of all the complicated phenomena in process engineering. The term "multi-scale", and its study, originated early in the field of chemical engineering. The traditional approach, which took "unit operation" and "process transfer" as the attributes, could not meet the demand for solution of the problem of a system. Studies of behavior such as mobility, transfer, phase splitting, and reaction on different scales (ranging from molecules to rivers and even to the atmosphere) and the rule that these phenomena occur together on the same scale are currently the quantitative trend in chemical engineering [53, 54]. The primary characteristics of the multi-scale system, the method, and the key point of implementation procedures were further studied. Quantification of a complicated phenomenon can be achieved by studying on a separate scale and synthesizing on several scales [55–58]. This viewpoint and theory have been extended to many other fields. Guo et al. suggested that instead of using various domains to annotate chemical engineering it is better to use process engineering to describe modern chemical engineering more precisely. They use "process engineering" as a general term for all the processes by which the materials are transformed by chemical or physical processing; the structure on several scales represents the common essence of a complicated phenomenon in process engineering [59–61].

In large-scale cultivation of living cells things occur on the scales of molecular genetics, cellular metabolism, and technical control of a bioreactor, all of which are interrelated. The objects under investigation have vastly different geometric sizes, i.e. there is no simple thermodynamic statistical relationship but a correlation of a series of reactions varying in time and space, which is the characteristic of a living object. These are reflected by changes of information flux, material flux, and energy flux. They appear as a network with multi-inlet and multi-outlet correlation. This kind of network structure also manifests itself as interaction among different scales of the network, and the main metabolic flux becomes the kernel problem of such a network relationship. The main flux of the microorganisms is changing incessantly. Its direction, flux, and even the pathway of its flow can vary. This is the mobility of the main flux of metabolism, and it selects a pathway within the metabolism network. The basis of this mobility and

selection is the genetic material of the microorganisms and the path selected depends on the environmental conditions in which the microorganisms live. It is, therefore, unnecessary to investigate all the working pathways. These ideas offer us essential approaches and clues for multi-scale study of a bioreactor. The main point of these approaches is that study of the interdependence of changes of metabolic flux and alterations of the fluxes of materials in a bioreactor is an effective means of investigating the multi-scale problem in a bioreactor; discrimination of the different problems from the relevant characteristics should be considered before optimization of a fermentation process can be achieved efficiently.

On the basis of the characteristics of large-scale cultivation in bioreactors, multi-scale correlative analysis, i.e. molecular genetics, regulation of cellular metabolism, and engineering performance of a bioreactor is considered in this article to be the key point of optimization of a process. The significance of studies of the bioreactor from multi-scale considerations and the viewpoint of the bioreaction engineering on the basis of metabolic flux analysis and control as the kernel is presented below [62].

1. The dependence of the symptom of the phenomenon on changes of the cellular metabolic flux distribution must be fully taken into account.

Quantification of all the micro-particulars of the internal network of links generated in bioreactors on different scales is impossible and also unnecessary, because the complicated phenomena in process engineering are always non-linear and non-equilibrium in nature and it is hard to find a stable criterion adaptable to all the non-linear and non-equilibrium systems. It therefore becomes a difficult problem to seek to optimize a bioreactor system by use of static kinetics alone. This is because of the difficulty of establishing kinetic relationships between the different links, and identifying and treating boundary conditions for the different links, especially when dealing with a macro-system which is unstable because of its changing configuration; this is a handicap in judging the stability of the system.

Despite these difficulties, stabilized conditions or relevant features of many processes still can be sought through scale and process analysis, and from this a means of solving problems can be found. For this reason, we suggest that above all we must seriously take into account the acquisition of relevant data relating to changes in the cellular metabolic flux distribution, so that insight can be gained into the internal rules of a complicated process from start to completion.

2. Correlating the cellular metabolic flux with changes of the material flux is an effective way of studying multi-scale interrelated problems in a bioreactor, i.e. to distinguish problems on different scales from the relative characteristics. Process optimization can be realized by use of these strategies.

When dealing with a multi-scale system, solving an inter-scale problem is a tough task. To analyze an inter-scale problem, measures covering interdisciplinary and inter-technology are always necessary. If we want to control a certain phenomenon on one scale, it is generally necessary to determine an operational approach on another scale.

Each application has its own special major scale, but it should cooperate with other sub-scales in solving a problem under comprehensive consideration. Con-

sequently, study of the process theory and methodology of a bioreactor should not rest on traditional concepts; the emphasis of the study should be on interdependence among the various scales, to discover a feature of one scale from a phenomenon on another.

The changes of information flux, material flux, energy flux, or metabolic flux in a bioreactor can be analyzed efficiently only by use of measurable experimental data. However, because of the restrictions of analytical methods, especially during operation of a bioreactor, relevant information is usually acquired on the reactor engineering scale. We must seek an approach that can reflect the essence of a process, gain insight into its inherent rules, and apply the results to engineering without adding too much complexity.

3. The complexity, high non-linearity, and other properties, including the process characteristics, of a bioprocess endow the system with dynamic properties and make it difficult to predict. By use of a mathematical model with a linear or quasi-linear relationship, process status can be approximately reflected. It cannot, however, meet the cause–effect response relationship needed for control and optimization. The authors therefore suggest that a non-modeling processing method should first be adopted for optimization of large-scale fermentation processes, and the research method dealing with correlation of the data profiles of the fermentation processes, i.e. the so-called data-driving approach, should be stressed. By use of experimental research the authors suggest that an optimization technique based on the relevance of process data profiles on several scales and scale-up techniques using modulation of several parameters should be used.

2.2 Data acquisition system

With the development of process transducer techniques and of computer technologies, on the basis of the material flux principle, the laboratory- or production-scale bioreactors used were equipped with conventional monitoring and control devices, such as devices for measurement and control of temperature and stirrer speed, for foam removal, and for measurement of pH and dissolved oxygen (*DO*) tension. Apart from these, the actual volume of the fermentation broth, additions of substrate, precursor, antifoam agent, acid, and alkali by use of high-precision pumps, precise measurement of air flow rate and back pressure converted to an electronic signal, and the exhaust gas connected to CO_2 and O_2 analyzers were also monitored and controlled. The complete bioreactor was equipped with devices to monitor and control more than 14 on-line measurable and/or control data. A PC control and data-processing system which harvested off-line analytical data was set up. From this we could also measure indirect properties precisely, for assessing metabolic fluxes and engineered characteristics, for example oxygen uptake rate (*OUR*), CO_2 evolution rate (*CER*), respiratory quotient (*RQ*), volumetric oxygen transfer coefficient ($K_L a$), specific growth rate (μ), etc., all of which were necessary for optimization and scale-up of a fermentation process. On the basis of a study of the bioreactor, a commercial laboratory-scale bioreactor,

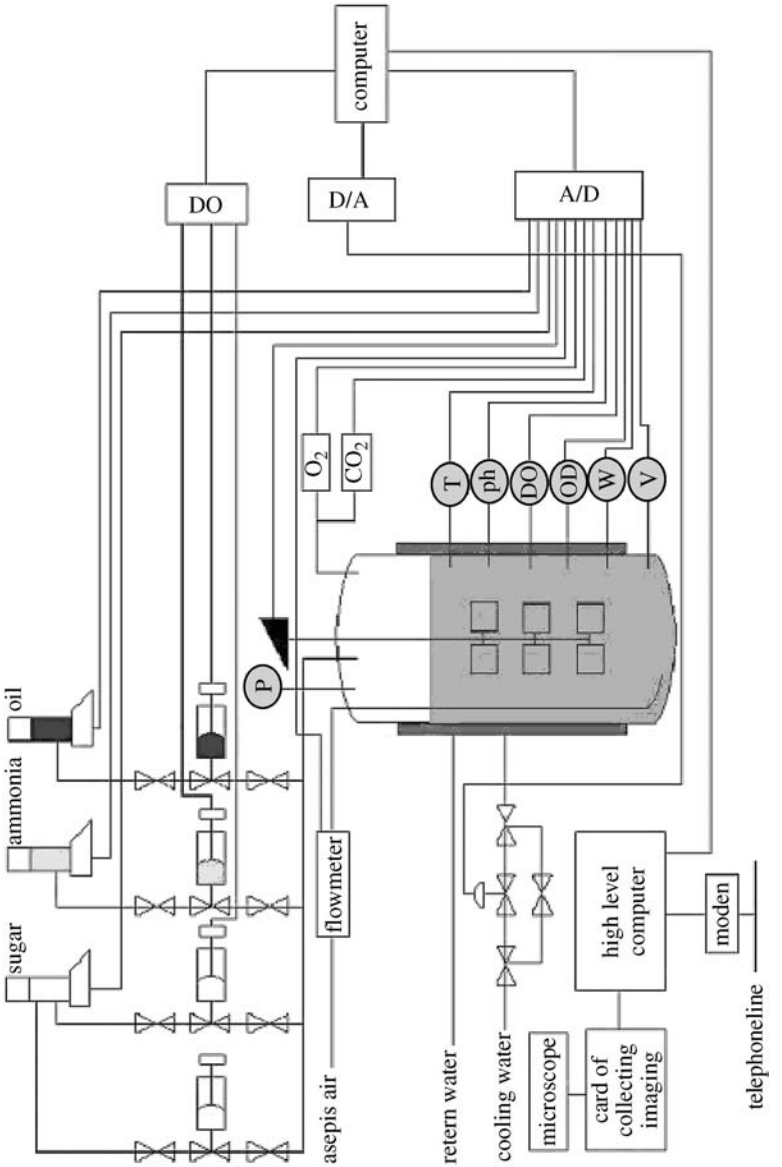

Fig. 1 Schematic diagram of the use of a PC for monitoring and control during fermentation

named FUS-50L(A) was developed [63]. Our affiliated company can manufacture bioreactors from 50 L to 100 m^3. Figure 1 shows a schematic diagram of the computer-aided bioreactor with data monitoring and control.

The interdependence of data is mainly apparent from the relationship between data profiles. From these profiles, the diversity, variation with time, relevance coupling, and indeterminacy of the data determined can be observed. Consequently, the demands for sensors, system configuration, precision, and drifting should be

considered. In programming applied software, attention should be paid to coordination and the entire objective. The configurations and demands are:

1. Selection of measurable parameters and deployment of sensors

The parameters monitored in bioprocess are conventional physical parameters, such as temperature, air flow rate, back-pressure etc. To investigate changes in metabolic flux distribution, to reflect the physiological performance of microbial cells and agitation transfer features in a bioreactor, and according to the objective demands of the studies of fermentation processes, additional properties are selected. These can be the biomass, intermediate metabolites, metabolic pathway enzymes, and energy carriers, even DNA, RNA, or proteins. Some of these are indirect results calculated on-line or off-line from the measured data. Generally speaking, data can be classified as direct, for example physical, chemical, and biological properties, or indirect, depending on its nature. More than a hundred properties can be selected [64]. A variety of sensors based on different principles was designed for on-line monitoring purposes; some of these have been further developed into commercial products. Data which cannot be determined on-line can be analyzed manually in a laboratory, and then integrated, acquired, and processed using a PC.

2. Demand for sensor performance

To enable precise determination of the characteristic properties of metabolic flux, changes due to the long-term cultivation of microbial cells, and tiny metabolic and physiological changes of parameters, and because of the sterile operation and high-temperature sterilization of bioreactors, special demands are placed on sensors with regard to precision, drift, response time, and linearity, etc.

3. Selection and calculation of indirect data [65]

One of the bottlenecks in data monitoring and control of a bioprocess is the lack of biosensors, such as those for *OUR* and *CER*, which reflect metabolic activity in the cultures; the specific growth rate, μ, the volumetric oxygen transfer coefficient, $K_L a$, the dilution rate, D, and the Reynolds number, R, are indirect properties reflecting the growth behavior of microbial cells, the engineering performance, the operationing features of a reactor, and fluid kinetics, respectively. These important data can be calculated only from measurable variables; this is accomplished by use of measurable information and estimated values of dominant variables (indirect data that cannot be measured directly). Reasonable selection and design of the configuration of indirect data can unambiguously reflect changes in the bioreactor on different scales; from this logical correlation can be obtained which can help us to distinguish further the relevant features of data from mechanisms based on different scales. This is of great significance in the optimization and scale-up of bioprocesses.

Because indirect data are obtained by assembly and calculation directly from measurable data, to ensure the precision of the calculations attention must be drawn to the synchronization of direct variable assignments. For example, asynchronous phenomena in determinations of *DO* concentration and the oxygen content of the exhaust gas caused by the lag in sampling from the exhaust gas

might lead to a significant change in the value of $K_L a$ estimated. In this case, suitable filtering measures should be adopted. With regard to the weighing system for feeding, which can be carried out steadily with a peristaltic pump, the feed rate is not strictly proportional to the revolving speed of the pump because of variation of the inner diameter of silicone rubber tubing and differential pressures between the inlets and outlets of the tubes. Consequently, an accurate weighing device with 0.1% FS and high stability was provided. The maximum feed rate and the sensitivity threshold are inconsistent with the use of different substrates. As a result differences among signal-to-noise ratios are great even under the same conditions. Therefore, identified measures should be prepared.

4. Deployment of secondary instruments and computer hardware

A PC-based configuration was adopted to place acquisition, processing, and analysis of data on a unified platform.

5. Design of the data-acquisition software package

The development of computer software which can reflect the relevant features of alteration of material fluxes in a bioreactor caused by the changes of cellular metabolic fluxes is of significance in research on the cellular- and engineering-scales, and is also the most important task for optimization and the scale-up of a process. In this paper, the computer software package consisted of control software mainly for process operation control; software mainly for analysis of process data was developed. In view of the situation we developed, meticulously, a software package which can be adapted to various bioreactors and which integrated several process theories and control principles. It is suitable for analysis of fermentation technology and process optimization. The software, named Bioradar, can also perform data transmission and analysis between two intercity locations by means of remote communications. Bioradar was designed under the Windows operating system by adopting the multi-thread principle, and by applying the Microsoft COM system to realize the interaction between the primary program and subprograms. The configuration of the multi-thread consists of a main thread, a sampling thread, a process analysis and control thread, an alarm thread, and a storage thread, and the priority is set for each. The system operates smoothly and responds immediately when the multi-thread technique has been adopted.

6. Remote data communications

In view of its complexity, studies of a fermentation process, particularly the principles and the methods involved in the process on different scales, are still under development. Considering that the scientific knowledge and professional techniques involved are quite broad, and that many research institutes and plants do not have the basics to tackle these kinds of problem, we designed a remote data communication system for data acquisition which was integrated with the ethernet interface, utilizing the TCP/IP protocol, to organize the local area network. We also made use of remote terminals, via the internet, for the experts to play their roles adequately. A special software package with password protection was designed to transmit process data, and to enable remote diagnosis of a fermentation process.

3
Problems on different scales and data correlation features

Qualitative and quantitative description of a production process by analysis of different data by automatic or manual methods must be conducted before the process can be controlled. One fundamental feature of a bioreaction process is that it is an open system or, in another words the organism takes nutrients from the outside environment, obtains the energy and materials necessary for survival, and, afterwards, the waste metabolites are discharged outside the cells. Figure 2

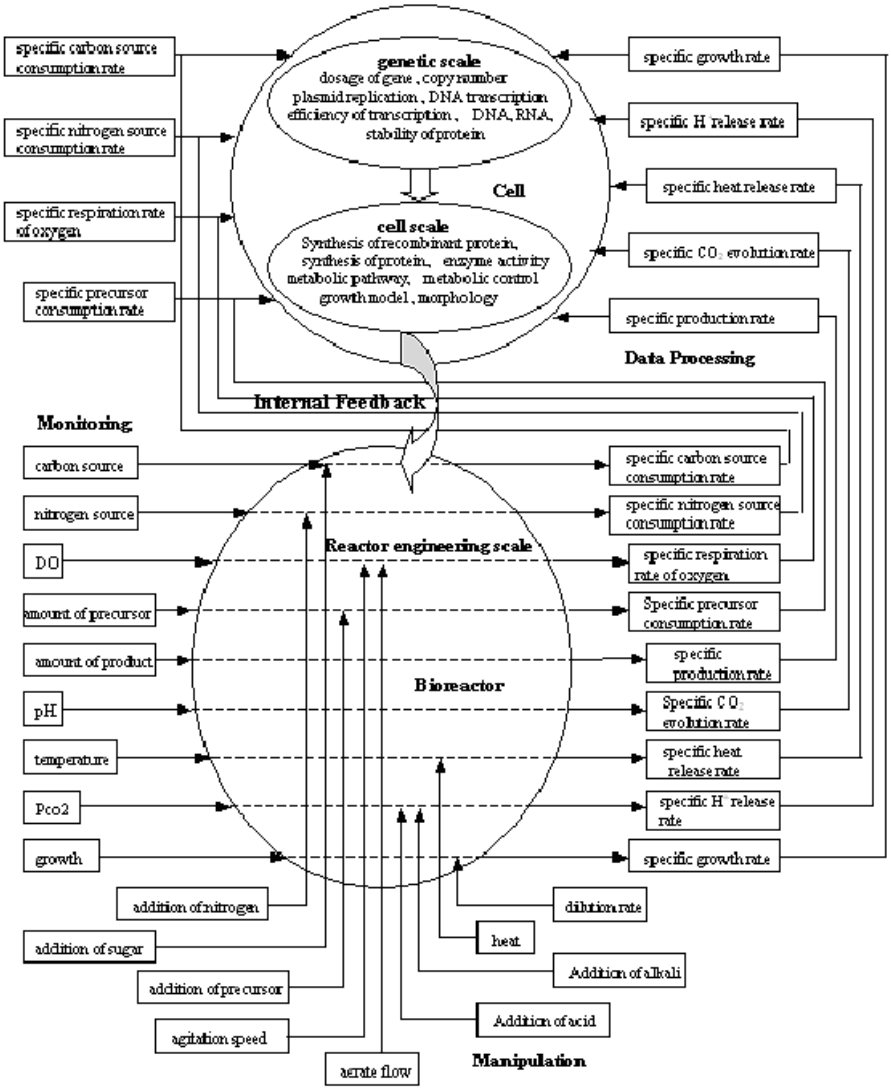

Fig. 2 Network of relationships between the different scales in a bioreactor

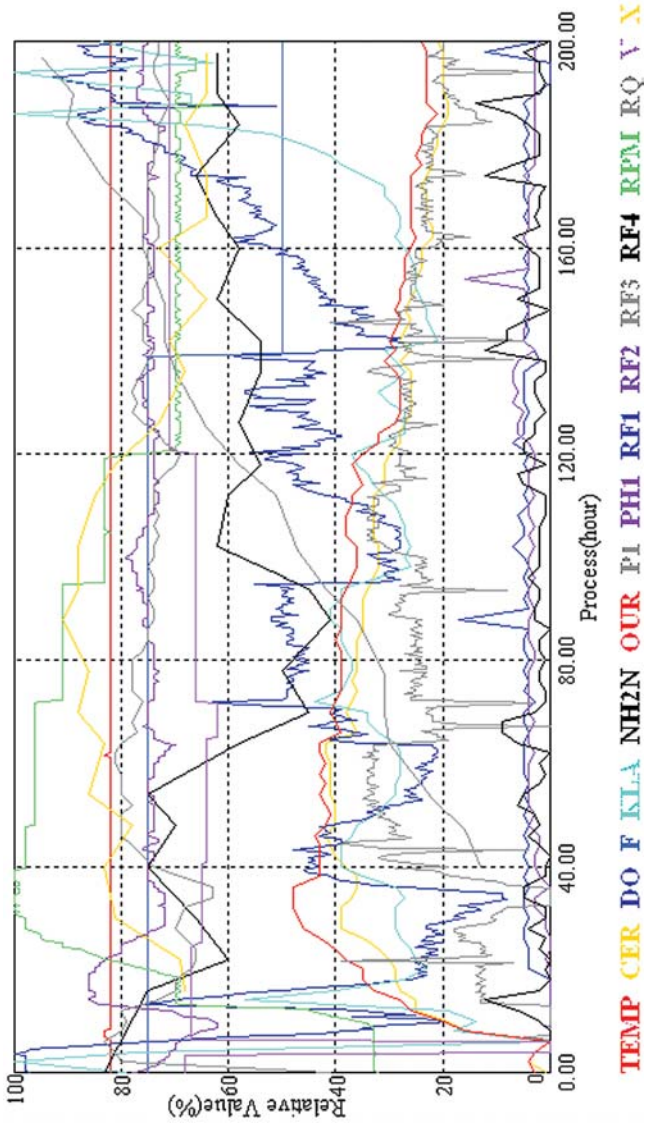

Fig. 3 Data profiles during erythromycin fermentation

depicts the essential schematic diagram illustrating the status of the process and its dependence on changes in the environmental conditions. The objects of process monitoring can only be the environmental status or the different values of the operating variables. By further analysis cellular or engineering problems of a bioreactor on different scales can be reflected.

Batch operation is usually used in the industry for large-scale cultivation of microorganisms. Various monitored data change with time during growth of the cells when the metabolism is changing. It is therefore necessary to perform a sequential synthetic study of the process with the help of a computer. Figure 3

shows the time course of erythromycin fermentation. From the profiles one can determine the diversity, variation with time, relevant coupling, and indeterminacy of the data estimated.

The multi-capacities and highly non-linear features of a fermentation process are reflected by the discreteness of the process variables estimated. In addition to the precision of the analytical method used, and the drift, such discreteness is also caused mainly by the high sensitivity of cell metabolism to changes in environmental factors, by the irreversibility of cell metabolism, and, occasionally, by the effects of initiation and expression on the genetic scale. The systems are sometimes also multi-polymorphic and unstable. This is the so-called chaotic aspect of a fermentation process. Owing to lack of knowledge about such phenomena, which are usually out of control, it is regarded as contributing to the indeterminacy of the data estimated and becomes a kind of noise. The authors believe that intensive study of the essence of the noise, particularly with regard to knowledge about biological mechanistic phenomena, might lead to a breakthrough in industrial fermentation.

The relationships between the variables means that the results estimated directly and indirectly, and manually, change during the course of fermentation processes, and can be correlated. We take this kind of correlation as a property of the materials and/or energy transfer, both conversion and balance and imbalance in a bioreactor. Although its microscopic cause might have happened on only one of the three scales – genetic, cellular, or engineering – it will eventually be reflected in the macroscopic process. This would provide us the clue to the application of the appropriate analytical approach to correlate the data from the different scales in a bioreactor.

We consider that correlated data can be classified into two basic types:

1. Physically or chemically dependent, meaning that the correlation results merely from changes in the physical or chemical properties of materials, e.g. the relationship between heat transfer and temperature, between acid or alkali and pH, or between stirrer speed and *DO* tension, and so on. These features are independent of changes in cell performance.
2. Biologically dependent, which means that correlation between the data is a consequence of the activity of biological cells. This is mainly manifested in two ways. One is a change in a property of the culture broth, caused by the growth and metabolism of the organisms, which results in data correlation – for instance, during the growth phase the viscosity of the culture broth increases and *DO* decreases. The other is a change of the metabolic activity of the cells and a shift of metabolic pathway.

These are the most important correlated data. We can now proceed to investigate measures for solving the relevance of these correlations on the different scales in a bioreactor. For instance, the oxygen uptake rate (*OUR*) is the most important physiological parameter, and characterizes the activity of microbial metabolism. There are two kinds of relationship between *OUR* and *DO* (Fig. 4): trans-correlation (A) and cis-correlation (B). The trans-form of the relationship between the two profiles represents consumption of O_2 merely as a material balance in a transfer process. The material balance of oxygen in the fermentation broth can

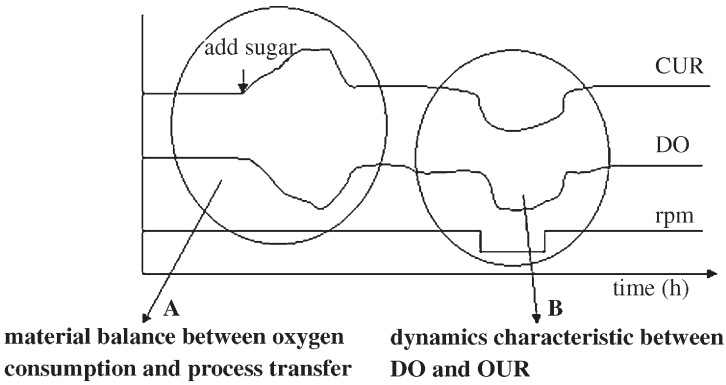

Fig. 4 Characteristics of basic correlations between *OUR* and *DO*

be described by the equation: $dc/dt=K_La(C^*-C)-OUR$. When cell metabolism is in its steady state the *DO* of the broth will also remain constant, i.e. $dc/dt=0$. If the *OUR* increases, then $dc/dt<0$, and *DO* will decrease. With decreasing *DO* the driving force for oxygen transfer (C^*-C) will gradually increase, which means that the oxygen transfer rate (*OTR*) will also improve, leading to an increase of *DO*. When the *OUR* and *DO* profiles are cis-correlated, cellular metabolic activity is directly influenced by the change of *DO*. When *DO* is below the critical value *OUR* declines with decreasing *DO*; the kinetic correlation for this kind of process is shown in Fig. 4.

The correlation between pH and *OUR*/*CER* during the early period of fermentation is shown in Fig. 5. After inoculation the pH gradually declined with growth of the mycelia, *OUR* and *CER* increased synchronously, while *DO* dropped rapidly. These phenomena showed that the glucose or the hydrolyzed starch was utilized by the culture. After approximately 9 h of fermentation the pH stopped declining for a while, and then started climbing. At the same time, *OUR* and *CER* almost kept constant (with a slight fall) and *DO* remained unchanged and even moved upward as *OUR* declined. These results showed that glucose was consumed rapidly by the culture, and that the concentration of glucose in dynamic balance in the culture broth had become restricted. After approximately 10 h of fermentation the pH elevation leveled off whereas *OUR* and *CER* started rising again. This meant that another carbon source was being utilized. However, a difference between the increases of *OUR* and *CER*, i.e. a branch off phenomenon, could be observed; this signified that the value of *OUR* was greater than that of *CER*. This kind of correlation indicated that a strongly reducible carbon source was utilized, and a change of cell metabolic performance occurred.

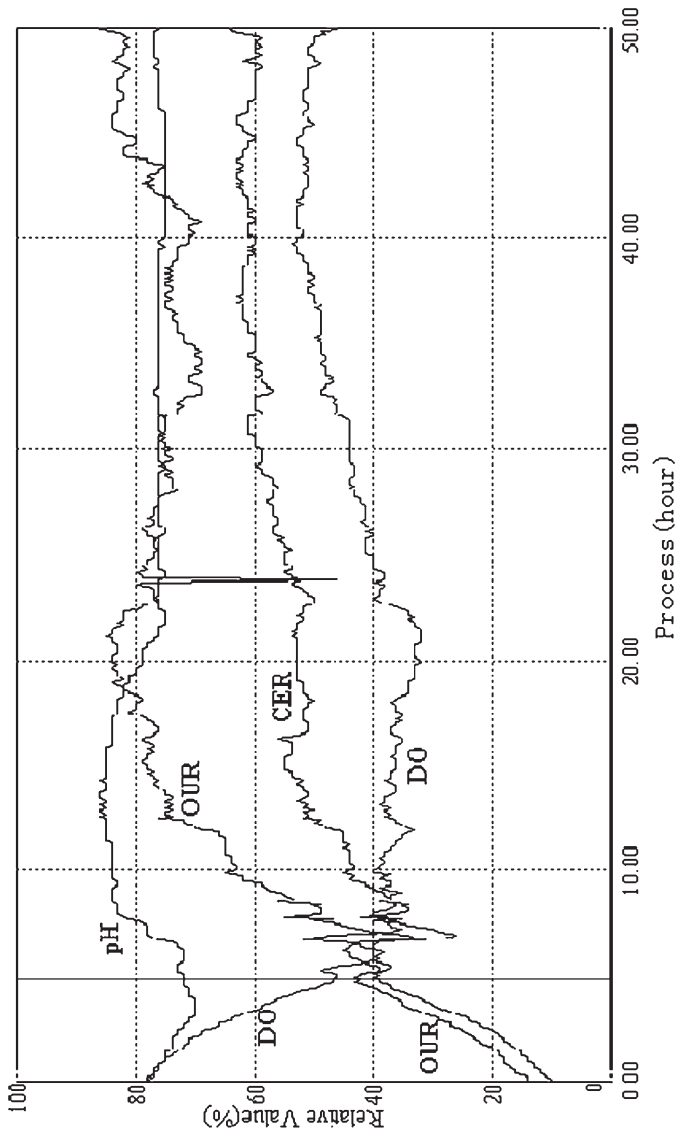

Fig. 5 Correlations among pH, *OUR*, *CER*, and *DO*

4
Results of process optimization for different species

4.1
Multi-scale studies on the optimization of the guanosine fermentation process

4.1.1
Observation of the metabolic flux shift

Guanosine, an essential ingredient of the bisodium ribonucleotide "I+G", is an expensive food additive [66]. In this review, studies of the guanosine fermentation process in a fully automatic, multi-variable monitoring and control fermenter, i.e. the model FUS-50(A) fermenter, are presented from a multi-scale point of view [67]. The results are shown in Fig. 6. It can be seen from the process profiles from various batches of fermentation experiments, with use of a PC for data correlation analysis, that the entire fermentation process could be divided into three phases. The 1st phase was the growth phase which lasted 12 h, in which almost no guanosine was produced. Thereafter the process entered the 2nd phase, which lasted 35 h, in which guanosine was produced quickly, and a substantial amount of the product was accumulated. In the second and third phases the decline of *OUR* and *CER* can be observed after approximately 40 h of fermentation; at the same time the rate of guanosine production decreased abruptly, while the rate of sugar consumption and the ammonia feed rate increased synchronously. From analysis of the carbon balance, and considering the synchronous increase of ammonia addition at the time, we believed that some intermediates of metabolism, possibly organic acids and/or amino acids or some other nitrogenous substances had accumulated. In other words, from analysis on the reactor engineering scale we observed shifts of metabolic fluxes occurring on the cellular scale.

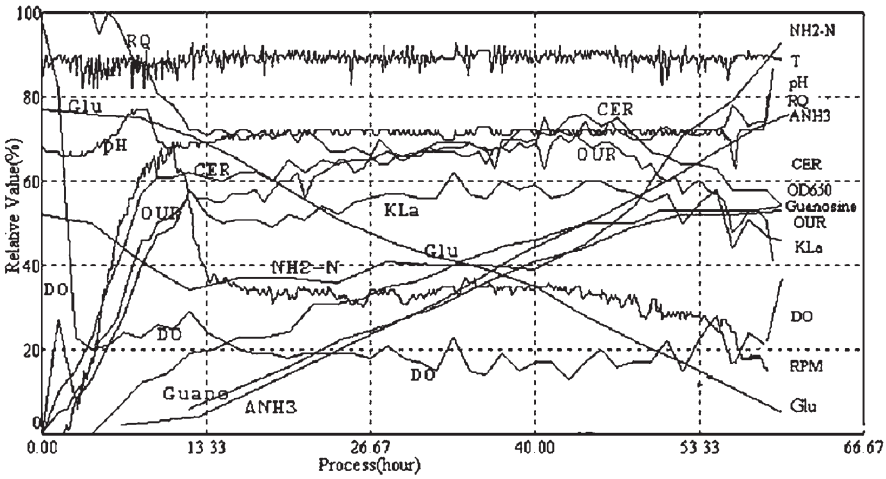

Fig. 6 Data profiles during guanosine fermentation

4.1.2
Determination of the accumulation of metabolic intermediates

By using paper chromatography accumulation of amino acids was detected. HPLC determination of the amino acids accumulating in the fermentation broth at different times of the fermentation furnished results in good agreement with those from paper chromatography. Amino acid analysis showed that alanine apparently started accumulating after apparently approximately 48 h of fermentation, and that the amount accumulated was 12.6 times the initial concentration, whereas amounts of the other amino acids were low (Fig. 7). The identities of the organic acids accumulated during the process were determined; the results in Fig. 8 show that accumulation of pyruvic acid occurred.

4.1.3
Metabolic flux shift and fermentation process optimization

To avoid the occurrence of the unfavorable situation described above, the operating conditions were altered and a regulation factor A was added to the medium. As a result we observed that *OUR* declined slowly and the rate of sugar

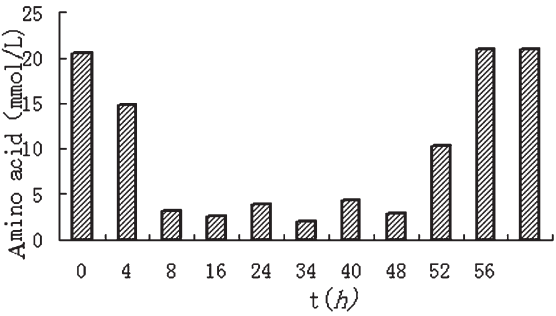

Fig. 7 Time course of total amino acid accumulation during fermentation

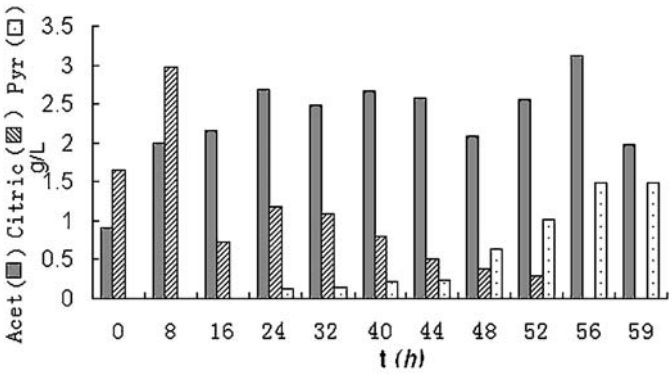

Fig. 8 Time courses of accumulation of organic acids during fermentation

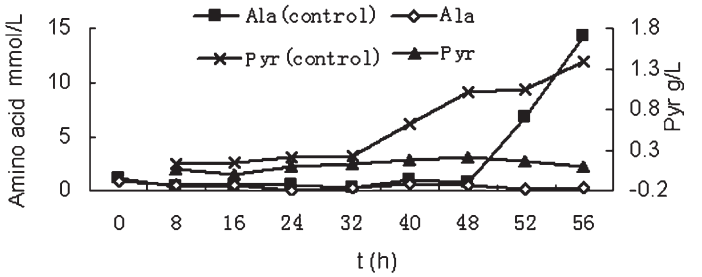

Fig. 9 Time courses of accumulation of alanine and pyruvate for use of two technologies

consumption also decreased, simultaneously with promotion of guanosine production. The change in the accumulation of the metabolic intermediates is apparent from Fig. 9. Investigation of the time of addition of factor A was conducted to establish a control strategy for feeding of factor A. The results showed that the fermentation level of guanosine increased by 70.05%, and the fermentation process was eventually optimized. From profiles obtained from the fermentation process it can be seen that, basically, the *OUR* did not decline at the late phase (40 h) whereas both sugar-consumption rate and ammonia feed rate decreased slowly. The improved technology was immediately scaled up from a fermenter capacity of 50 L to 100 m^3, in accordance with the relevant features of the profiles. As a result, production technology became more stable and guanosine productivity and yield increased by 49.50% and 16.62%, respectively. Because of the improvement of guanosine yield and the reduced consumption of raw materials, the costs of the raw materials and power consumption were reduced by 19.73%.

From this example it is evident that in the multi-scale study of guanosine fermentation optimization of the metabolic process was realized by implementation on the reactor engineering scale. What kind of relationship does this have to the primary scale? The distribution of cellular metabolic flux in guanosine production on a lower scale was studied in our laboratory.

4.1.4
Enzymatic evidence of metabolic flux shift

Figure 10 shows a schematic diagram of the synthetic pathway to guanosine from glucose [68]. Analysis of the intracellular metabolic pathway of glucose indicated that guanosine was synthesized through the purine pathway via the HMP route [69]. In this way the rational distribution of metabolic flux of glucose among the EMP, TCA, and HMP routes is the focus of product maximization. From the variation of the levels of amino acids and organic acids with time during the fermentation it can be seen that the major amino acid accumulated is alanine. Alanine is synthesized directly by conversion of pyruvate, which is not subject to feedback inhibition or repression. Thus, it is easy to understand that accumulation of pyruvate, caused by the increase in EMP flux, has resulted in the formation of alanine, which is the feedback inhibitor of GS. This inhibition, in

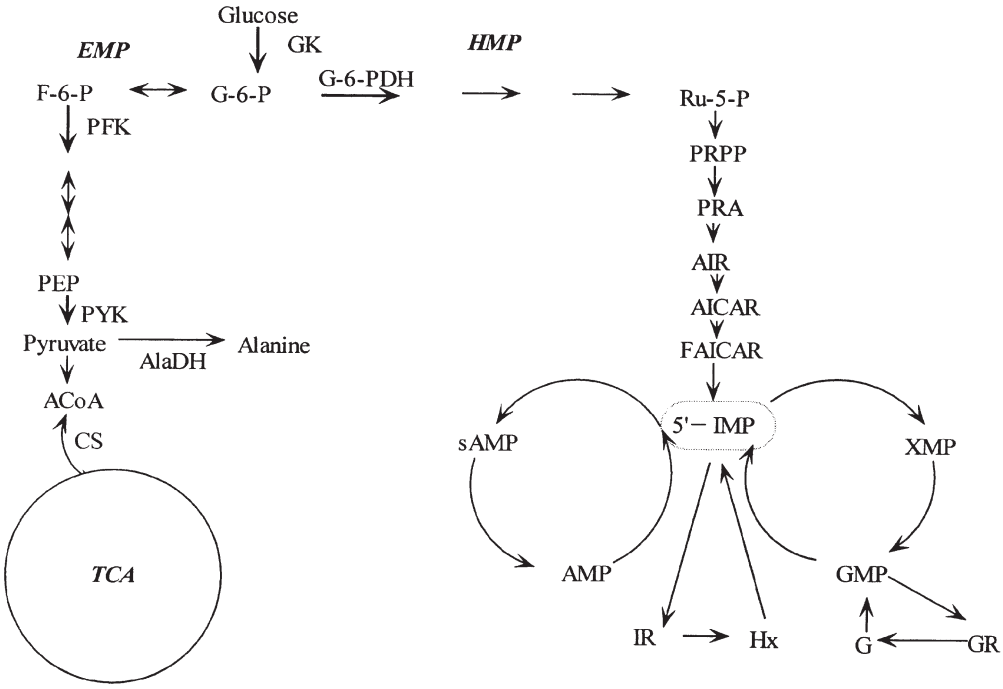

Fig. 10 Biosynthetic pathway of guanosine via the EMP and HMP pathways

turn, leads to a further decrease of HMP flux, which eventually causes a decrease in guanosine production rate.

The key regulating enzymes involved in the pathways have been clarified. Study of the dynamic activity of these enzymes, which is related to the flux of these pathways, is useful for understanding the process and its optimization. For this reason we determined the levels of the essential rate-limiting enzymes of the pathway, namely hexokinase (HK)/glucokinase (GK), phosphofructokinase (PFK), and pyruvate kinase (PK) of the EMP pathway, glucose 6-phosphate dehydrogenase (G-6-PDH), and citrate synthase. In addition, the metabolic intermediates accumulated and the key enzymes alanine dehydrogenase and inosine monophosphate dehydrogenase were also determined. Figure 11 shows the dynamic profiles of the activity of these enzymes during fermentation.

These enzymology studies of the main pathway of the process showed that the decline of the rate of product synthesis in the late phase could be attributed to metabolic flux shift to the EMP pathway. Further studies revealed that an "overflow" phenomenon occurred in the EMP pathway and in the TCA cycle, i.e. the activity of alanine dehydrogenase apparently increased during the late phase of the process and strengthened the enzyme's capacity to convert pyruvate to alanine. The results clearly demonstrated the roles of the time-varying enzymes in regulating metabolism in the process on the cellular scale, and presented immediate evidence of the metabolic flux shift.

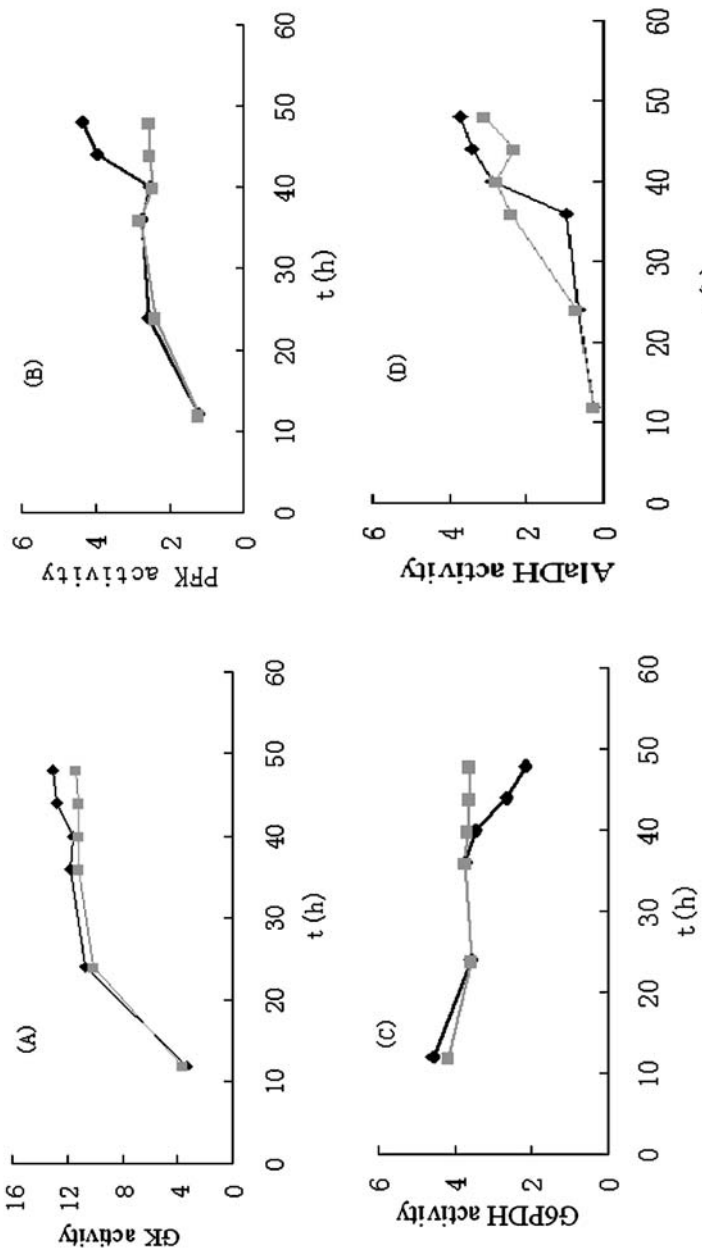

Fig. 11 Time courses of the activities of different enzymes during fermentation with original (*filled circles*) and new technology (*filled squares*)

In addition, by determination of the enzymes we also discovered the contradiction that the activity of inosine monophosphate dehydrogenase increased while the amount of guanosine, the product of the reaction, declined. This was because the metabolic flux of the central pathway changed (decreased). The increase of the flux of the subsequent branch routes is, therefore, insufficient to cope with the effect of decreasing metabolic flux through the central pathway. Thus, the significance of the role of the main metabolic pathway in the synthesis of the secondary product of metabolism must be understood when improving the strain by use of genetic engineering. If the key genes of the main metabolic pathway can be improved by genetic engineering, better results can be expected.

4.1.5 *Stoichiometric calculation of metabolic flux shift*

4.1.5.1 Overview

Many metabolic reactions occur inside the cells of a microorganism. The complicated metabolic network comprising these reactions is subject to strict regulation. The exchange of the materials, energy, and information between cytoplasm and organelle, the cell and its environment, through the metabolic network was investigated. To comprehend profoundly the metabolic behavior and its characteristics for the sake of optimizing the process and to point out the correct route of genetic construction, quantitative studies of the intracellular metabolic network should be performed.

It is currently impossible to study all the thousands of metabolic reactions in a cell one by one. Appropriate simplification is inevitable. The central metabolic pathways (including the EMP, HMP, and TCA cycles, etc.) occur widely in microorganisms. They provide precursors, reducing equivalents, and energy for cell growth and product synthesis. Identification of these is the important object of quantitative studies of the metabolic network. Study of metabolic flux distribution is of significance to in-depth comprehension of the regulation of cell metabolism.

There are several ways of studying metabolic flux [70–77]. If the metabolic reaction kinetics and related regulation information are unavailable we can make use of the mass conversion law of materials and the assumption of a quasi-steady-state of metabolic intermediates to calculate the distribution model of metabolic flux in the cell by determination of the growth rate, the rate of product formation, the rate of substrate consumption, and the rates of accumulation of other metabolites.

4.1.5.2 Metabolic network analysis

Figure 12 shows the simplified metabolic network of *B. subtilis*. It consists of five parts: the EMP and the HMP pathways, the TCA cycle, oxidative phosphorylation, and the accumulation of metabolites.

- Glycolysis (EMP). In glycolysis, 1 mol glucose is degraded into 2 mol pyruvate. It consists of five metabolic reactions: r_4, r_6, r_7, r_9, and r_{10}.
- The HMP pathway. This provides the precursors and reduced power necessary for cell growth and product synthesis. It comprises two metabolic reactions: r_2 and r_5.
- The TCA cycle. Its role is mainly to provide ATP by oxidative phosphorylation of NADH. It includes seven metabolic reactions: r_{12}, r_{14}, r_{15}, r_{16}, r_{17}, r_{18}, and r_{19}.
- Oxidative phosphorylation. In this process, NADH and FADH are oxidatively phosphorylated to ATP. It consists of three metabolic reactions: r_{21}, r_{22}, and r_{23}.
- Accumulation of metabolites. Six metabolic reactions are included: r_1, r_3, r_8, r_{11}, r_{13}, and r_{20}.

Tables 1 and 2 show the metabolic reaction equations and formulas, respectively. G6P, Ru5P, F6P, GAP, PGA, PEP, PYR, AcCoA, OAA, CIT, OGA, and MAL denote glucose-6-phosphate, ribulose-5-phosphate, fructose-6-phosphate, glyceraldehyde-3-phosphate, 3-phosphoglyceric acid, phosphoenolpyruvate, pyruvate, acetyl coenzyme A, oxaloacetate, citric acid, oxoglutarate, and malate, respectively.

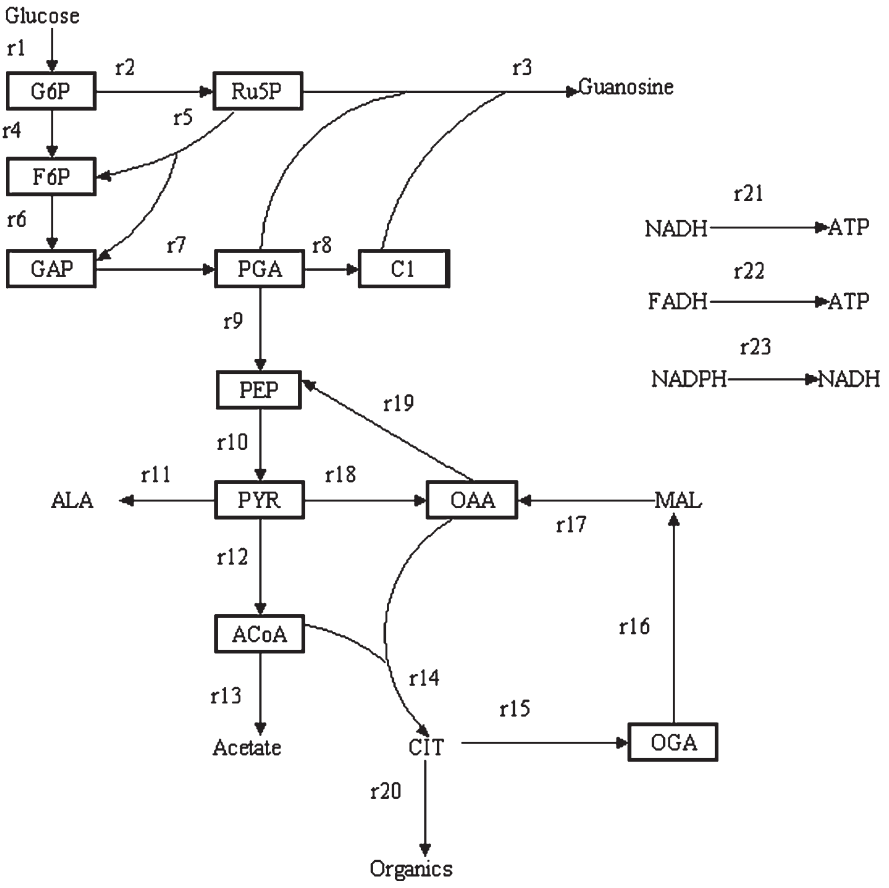

Fig. 12 Simplified metabolic network of *B. subtilis*

Table 1 Metabolic reactions of *B. subtilis*

r_1: Glucose→G6P
r_2: G6P→Ru5P+2NADPH+CO_2
r_3: Ru5P+PGA+Cl+CO_2+11ATP+2NADPH→Guanosine+3NADH
r_4: G6P→F6P
r_5: Ru5P→2/3 F6P+1/3 GAP
r_6: F6P+ATP→2GAP
r_7: GAP→PGA+ATP+NADH
r_8: PGA+NADPH→2Cl+CO_2+NADH
r_9: PGA→PEP
r_{10}: PEP→PYR+ATP
r_{11}: PYR+NADPH→ALA
r_{12}: PYR→ACoA+NADH+CO_2
r_{13}: ACoA→Acetate+ATP
r_{14}: ACoA+OAA→CIT
r_{15}: CIT→OGA+NADPH+CO_2
r_{16}: OGA→MAL+NADH+FADH+ATP+CO_2
r_{17}: MAL→OAA+NADH
r_{18}: PYR+CO_2+ATP→OAA
r_{19}: OAA+ATP→PEP+CO_2
r_{20}: CIT→Organics
r_{21}: NADH+1/2 O_2→1.3ATP
r_{22}: FADH+1/2 O_2→2/3 (1.3ATP)
r_{23}: NADPH→NADH

Table 2 Metabolic formulae for *B. subtilis*

x_1(Glucose):	$-r_1=\Delta$Glucose
x_2(G6P):	$r_1-r_2-r_4=154\times10^{-6}\Delta X$
x_3(F6P):	$r_4+2/3\ r_5-r_6=190\times10^{-6}\Delta X$
x_4(Ru5P):	$r_2-r_3-r_5=(816+308)\times10^{-6}\Delta X$
x_5(Guanosine):	$r_3=\Delta$Guanosine
x_6(GAP):	$1/3\ r_5+2r_6-r_7=194\times10^{-6}\Delta X$
x_7(PGA):	$-r_3+r_7-r_8-r_9=1395\times10^{-6}\Delta X$
x_8(Cl):	$-r_3+2r_8=156\times10^{-6}\Delta X$
x_9(PEP):	$r_9-r_{10}+r_{19}=711\times10^{-6}\Delta X$
x_{10}(PYR):	$r_{10}-r_{11}-r_{12}-r_{18}=2942\times10^{-6}\Delta X+\Delta$PYR
x_{11}(ALA):	$r_{11}=\Delta$ALA
x_{12}(ACoA):	$r_{12}-r_{13}-r_{14}=2132\times10^{-6}\Delta X$
x_{13}(Acetate):	$r_{13}=\Delta$Acetate
x_{14}(OAA):	$-r_{14}+r_{17}+r_{18}-r_{19}=1923\times10^{-6}\Delta X$
x_{15}(CIT):	$r_{14}-r_{15}-r_{20}=\Delta$CIT
x_{16}(OGA):	$r_{15}-r_{16}=1071\times10^{-6}\Delta X$
x_{17}(MAL):	$r_{16}-r_{17}=0$
x_{18}(CO_2):	$r_2-r_3+r_8+r_{12}+r_{15}+r_{16}-r_{18}+r_{19}=-2052\times10^{-6}\Delta X+\Delta CO_2$
x_{19}(O_2):	$-r_{21}-r_{22}=-2\Delta O_2$
x_{20}(NADPH):	$2r_2-2r_3-r_8+r_{15}-r_{23}=16333\times10^{-6}\Delta X$
x_{21}(NADH):	$3r_3+r_7+r_8+r_{12}+r_{16}+r_{17}-r_{21}+r_{23}=-3595\times10^{-6}\Delta X$
x_{22}(FADH):	$r_{16}-r_{22}=0$
x_{23}(Organics):	$r_{20}=\Delta$Organics

The 23 metabolites in Table 2 can be divided into three groups:

1. precursors for cell growth,
2. extracellular metabolites, and
3. intracellular metabolites.

The 1st group consists of 14 metabolites, including x_2, x_3, x_5, x_6, x_7, x_8, x_9, x_{10}, x_{12}, x_{14}, x_{16}, x_{18}, x_{20}, and x_{21}. For every gram of biomass the amounts of precursors needed are quoted from the relevant literature data. The 2nd group comprises x_1, x_5, x_{10}, x_{11}, x_{13}, x_{15}, x_{18}, x_{19} and x_{20}. The 3rd group consists of x_{17} and x_{22}.

In Table 2 the 23 unknown data and 23 equations are listed. Because r_{10}, r_{18} and r_{19} form a cycle, r_{18} and r_{19} can only occur alternately. Thus, there are only 22 unknown data. The equations have an optimum solution but to examine the validity of the solution of the set of metabolic equations, 22 equations were applied when solving the equation set, i.e. the 19th equation was retained to check the validity of the solution.

4.1.5.3
Solution of the metabolic equation set

During the fermentation on-line monitoring of air flow rate, fermentation broth volume, the O_2 and CO_2 content of the exhaust gas, and off-line analyses of the concentration of biomass, glucose, and products were undertaken. The concentration of organic acids, for example acetate, citrate, pyruvate, etc., were determined by use of HPLC, and 17 amino acids, for example alanine were analyzed. Making use of the Matlab language, solution of the metabolic equation sets under the new and old conditions was programmed. The normalized metabolic fluxes for the new and old technologies in different time periods, after fermentation for 24 h, with r_1 as a standard, are listed in Tables 3 and 4, respectively.

In the data processing described above the magnitude of the metabolic flux of the different pathways in vivo should be calculated with use of specific units of biomass. Because of the difficulty of estimating biomass concentration, errors were introduced. Calculation of metabolic flux in this work was carried out when the *DO* of the process was unchanged. In addition, the change of the partition of the metabolic flux into different pathways after glucose has entered the cell is stressed in this work. So, for the sake of simplicity in calculations, the consumption of every 100 mol glucose was taken as reference standard.

From the calculations above, with use of stoichiometry, it can be seen that during guanosine fermentation r_2 decreased with fermentation time, from 11.72 mol/100 mol glucose after 24 h to 0.52 mol/100 mol glucose after 52 h; r_4 increased simultaneously from 88.10 to 99.48 mol/100 mol glucose, which meant that the metabolic flux had shifted from the HMP pathway to the EMP pathway. This type of transfer and its energy requirement warrant further investigation.

Table 3 The metabolic flux distribution for original technology (units: mol/100 mol glucose)

Time (h)	24.00	32.00	40.00	44.00	48.00	52.00
r_1	100.00	100.00	100.00	100.00	100.00	100.00
r_2	11.72	16.27	5.60	4.75	2.67	0.52
r_3	10.41	14.42	4.75	4.75	1.56	0.52
r_4	88.10	83.47	94.28	95.25	97.17	99.48
r_5	0.00	0.00	0.00	0.00	0.00	0.00
r_6	87.88	83.16	94.14	95.25	96.99	99.48
r_7	175.54	166.00	188.13	190.51	193.78	198.96
r_8	5.30	7.34	2.43	2.37	0.86	0.26
r_9	158.21	141.94	179.90	183.39	189.98	198.17
r_{10}	157.38	140.77	179.36	183.39	189.28	198.17
r_{11}	–0.21	0.57	–0.70	0.58	7.54	7.80
r_{12}	130.34	132.12	128.20	126.29	136.30	132.27
r_{13}	–2.36	2.53	–1.62	–7.79	9.70	10.02
r_{14}	130.29	126.19	128.24	134.07	124.55	122.25
r_{15}	109.54	127.76	80.63	81.97	90.10	69.66
r_{16}	108.47	126.24	79.94	81.97	89.19	69.66
r_{17}	108.61	126.44	80.03	81.97	89.31	69.66
r_{18}	23.77	2.72	49.59	52.10	37.02	52.59
r_{19}	0.00	0.00	0.00	0.00	0.00	0.00
r_{20}	21.31	0.00	49.27	52.71	35.22	54.13
r_{21}	643.22	692.75	557.74	576.95	585.93	541.77
r_{22}	108.47	126.24	79.94	81.97	89.19	69.66
r_{23}	87.89	97.25	67.51	79.60	75.34	69.40
r_O[a]	383.63	456.73	263.32	260.39	307.80	233.95
Ratio-O[b]	1.02	1.12	0.83	0.79	0.91	0.77

[a] Oxygen uptake rate calculated directly from monitored data for the exhaust gas analyzer.
[b] The ratio of r_O to the oxygen consumption rate by oxidative phosphorylation ($(r_{21}+r_{22})/2$), which is the result from solution of the metabolic equations.

4.1.5.4 The role of the HMP pathway

In the metabolic reactions of the cell the HMP pathway plays two roles. One is to provide the precursors for macro-molecular synthesis (necessary for cell growth) and synthesis of products such as R5P and E4P; the other is to provide reducing power, NADPH, which is realized through reactions r_2 and r_5 of the series, i.e. for 1 mol G6P consumed, 2/3 mol F6P and 1/3 mol GAP were generated and 2 mol NADPH and 1 mol CO_2 were released. However, in the time period studied r_5=0, which implies that the second role of the HMP pathway has lost. Where, then, did the NADPH come from? We noticed that one of the reactions in the TCA cycle was the main source of NADPH. The rate of formation far exceeded the demand for cell growth and product synthesis. More than 80% of the NADPH was converted into NADH for the energy supply through the r_2 reaction. Consequently, the HMP pathway played the role of supplying the precursors for cell growth and product synthesis.

Table 4 The metabolic flux distribution for the new technology: (units: mol/100 mol glucose)

Time (h)	24	34	40	48	52
r_1	100.00	100.00	100.00	100.00	100.00
r_2	13.06	12.26	11.32	16.51	11.28
r_3	12.14	12.02	11.15	15.42	10.77
r_4	86.82	87.71	88.66	83.34	88.65
r_5	0.00	0.00	0.00	0.00	0.00
r_6	86.66	87.66	88.63	83.16	88.57
r_7	173.17	175.29	177.24	166.13	177.05
r_8	6.14	6.03	5.59	7.78	5.42
r_9	153.75	156.94	160.30	141.57	160.23
r_{10}	153.17	156.79	160.19	140.88	159.91
r_{11}	0.22	0.35	–0.12	–0.40	0.09
r_{12}	140.97	135.65	139.90	103.62	143.11
r_{13}	–3.59	–6.46	1.50	–30.95	–7.67
r_{14}	142.87	141.67	138.10	132.56	149.85
r_{15}	135.73	122.07	118.73	99.63	134.67
r_{16}	134.98	121.87	118.60	98.74	134.26
r_{17}	135.08	121.89	118.61	98.85	134.31
r_{18}	9.27	20.16	19.75	35.46	16.35
r_{19}	0.00	0.00	0.00	0.00	0.00
r_{20}	9.10	14.68	22.47	34.92	15.74
r_{21}	741.95	709.00	703.95	596.03	747.78
r_{22}	134.98	121.87	118.60	98.74	134.26
r_{23}	118.13	113.00	111.09	78.16	122.93
r_O[a]	458.24	400.63	399.84	308.62	447.11
Ratio-O[b]	1.05	0.96	0.97	0.89	1.01

[a] Oxygen uptake rate calculated directly from monitored data for the exhaust gas analyzer.
[b] The ratio of r_O to the oxygen consumption rate by oxidative phosphorylation ($(r_{21}+r_{22})/2$), which is the result from solution of the metabolic equations.

4.1.5.5 Dynamic feature of metabolic flux

Figure 13 shows the changes in the flow rates of r_2, r_3, and r_4 in different periods before and after improvement of the technology.

Determination of the accumulation of metabolic intermediates and the key enzymes of the pathway relating to guanosine fermentation after improvement of the technology confirmed that the metabolic flux had been transferred back to the HMP pathway. Figure 14 shows the metabolic flux distributions after 52 h of fermentation for the new and old technologies, calculated according to the stoichiometry. The latter was used as the control. It can be seen that after the glucose had been converted into G6P the amount of F6P generated after 52 h of fermentation from the old and new technologies were 99 and 89 mol/100 mol glucose, respectively. Only 1 mol Ru5P/100 mol glucose was formed in the old process whereas 11 mol Ru5P/100 mol glucose was produced in the new process; this means the flux entering the HMP pathway was almost 10 times that of the old process.

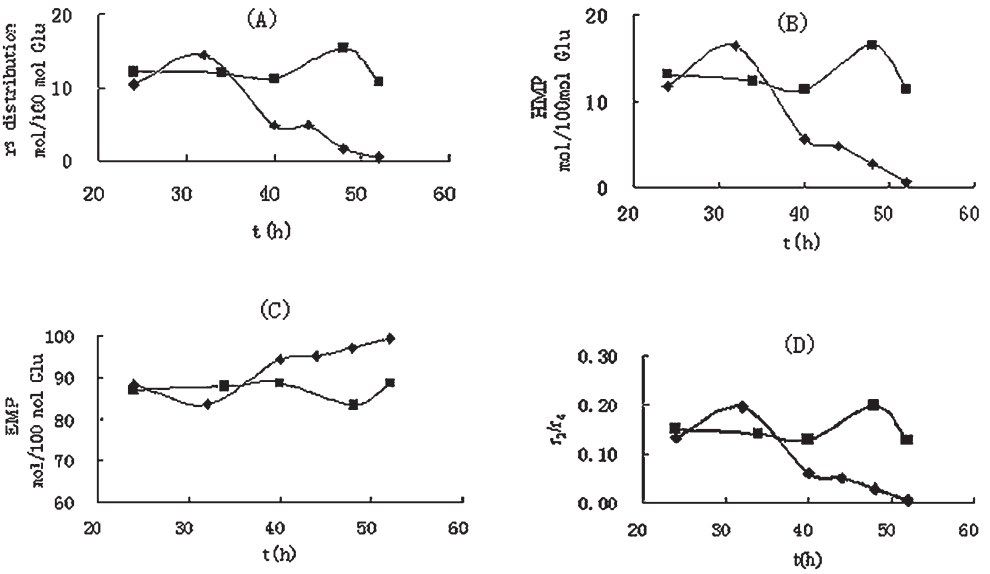

Fig. 13 Flux distributions for original (*filled circles*) and new technology (*filled squares*)

4.1.6
Genetic nature of the guanosine production strain and its phenotypic feature in a bioreactor

Under different bioreactor operating conditions, is the metabolic flux shift related to a problem on the genetic scale? We must further clarify the interesting problem in this study on the genomic scale, which seems to be well known already.

The purine synthetic pathway was studied intensively in the early 1960s and 1970s [78], and a detailed synthetic mechanism was worked out, with inosine monophosphate (IMP) as the core of the pathway. The key enzymes for process regulation are phosphoribosylpyrophosphate (PRPP) transamidase, IMP dehydrogenase, and adenyl succinate (SAMP) synthetase. Thus, the activities of these key enzymes in the producing stains at different productivity levels were compared in this study.

It was found that the wild-type (w) strain apparently had high SAMP synthetase activity, the low-yield inosine-producing strain (91) had rather low activity, and the guanosine producing strain (ng) lost SAMP synthetase activity entirely (data not shown). This shows its superiority in regulation of the pathway, which is in accordance with its high yield capability.

Along with intensive exploration of the genetic engineering technique, studies on the gene sequence encoding the key enzyme of synthetic pathway of guanosine have been carried out extensively. In 1990 sequencing of the *Bacillus subtilis* genome was started and it was accomplished in 1997. The whole genome sequence published in detail provides the genetic background for further studies of the genes encoding the key enzymes involved in the biosynthesis of inosine and guanosine and for the analysis of the inosine- and guanosine-producing strains.

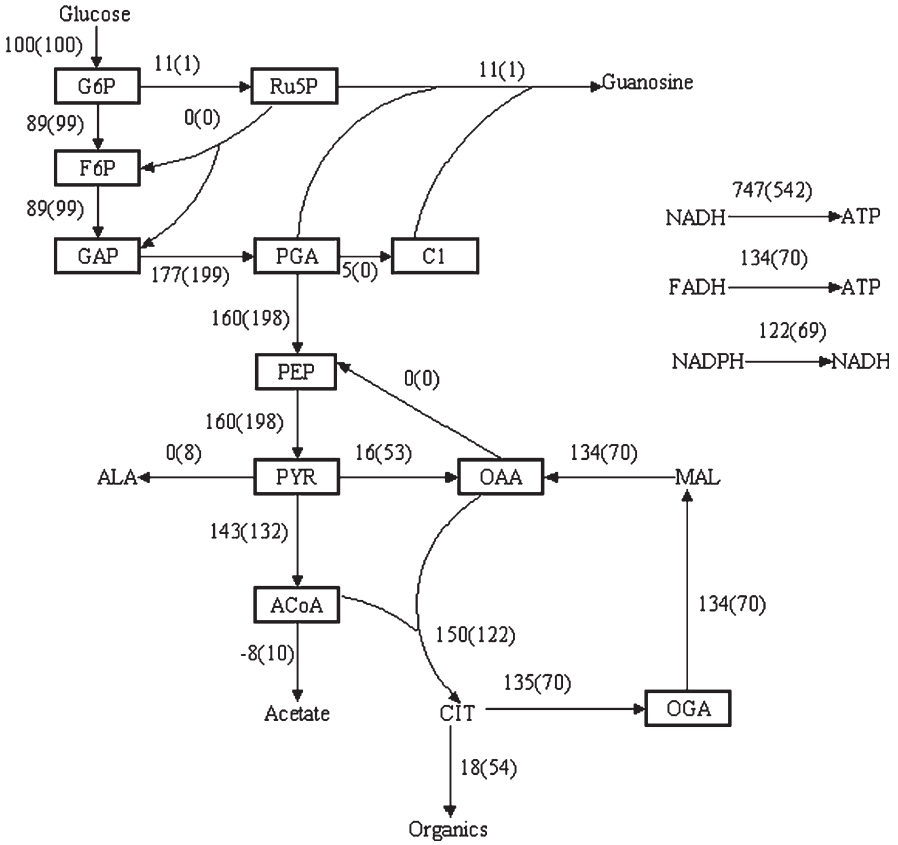

Fig. 14 Flux distributions for the two different technologies (the flux of the former technology is in *square brackets*) at t=52 h

In *B. subtilis*, synthesis of purine nucleotide starts from PRPP and produces guanosine and adenosine via two routes after the synthesis of IMP with multi-step catalysis. Figure 15 is the schematic diagram of the operon for regulation of the genes encoded for the synthesis of purine ribosome. In this synthetic pathway the genes encoding the IMP synthesis enzymes (12 enzyme proteins) are regulated by the *pur* operon.

Therefore, the pur operon's initiating sequence, the purA and the guaA genes, which encode for the SAMP and GMP synthetic enzymes located in the branch routes of the AMP and GMP synthetic pathways, respectively, were used as objects in this work, to analyze the partial genetic background relating to immediate synthesis of inosine and guanosine in the producing strains. In accordance to the genome sequence of *B. subtilis* published in the Genebank [79] and by concentrating on the three small sequences, and with an appropriate primer devised, sequencing of the genes was undertaken for four strains: *B. subtilis* wild-type (No. 160), the low-yield inosine-producing strain (No. 161), the current inosine-producing strain (No. 162), and the current guanosine-producing strain (No. 163).

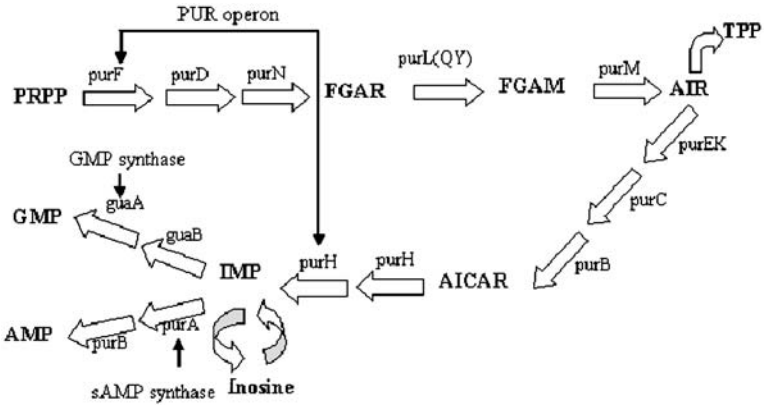

Fig. 15 Biosynthesis of purine nucleotides by *B. subtilis*

The analytical results for the partial sequence of the promoter of the pur operon were compared with those for *Bacillus subtilis* No. 168 published in the literature [80–83]. The sequence from strain No. 160 was the same as that from strain No. 168, and only one site of mutation was found in strain No. 161 (nucleotide No. 361) and in strain No. 162 (nucleotide No. 167), whereas in strain No 163, fifty one sites (Nos. 32, 35, 40, 41, 47, 50, 59, 68, 69, 77, 85, 118, 130, 131, 136, 145, 160, 177, 258, 259, 267, 268, 292, 293, 295, 297, 298, 299, 312, 313, 333, 340, 341, 343, 344, 374, 382, 384, 385, 386, 387, 392, 393, 399, 400, 401, 402, 412, 413, 421, and 432) were found mutated.

4.1.6.1
purA gene sequence

The initial codon was regarded as 1. Table 5 shows statistical results from mutations in the gene coding areas of the four strains. From these statistical results it can be seen that the DNA sequences of current inosine- and guanosine-producing strains at site 55 lost one base pair, which led to the shifting mutation caused by the shift of the rear DNA sequence, and eventually resulted in inactivation of the SAMP synthesis enzyme coded.

4.1.6.2
guaA gene sequence

The initial codon was regarded as 1. Table 6 shows statistical results from mutations in the purA gene of four *B. subtilis* strains, compared with the sequence from the wild strain No. 168. From Table 6 it is apparent that in all the four strains of *Bacillus subtilis* tested, 23 base pairs were different from those in the literature. The change involved 12 amino acids, but the changes all occurred simultaneously in the production strain, in the low yield strain, and in the wild type; this indicated that the activity of the GMP synthesis enzyme in the four strains should remain the same. Variation of the guaA gene of the producing strains did not

Table 5 Mutations of the purA gene of four *B. subtilis* strains

Sequence no. (site mutated)	Mutant	Wildtype (codon)	Mutant (codon)	Change of amino acid
1 (55)	162, 163	A (ATT)	delete	Frame shift mutation
2 (513)	160, 161	C (CTC)	T (CTT)	Leu→Leu (no change)
3 (579)	160, 161	A (GGA)	C (GGC)	Gly→Gly (no change)
4 (594)	160, 161	G (AAG)	A (AAA)	Lys→Lys (no change)
5 (734)	160, 161, 162, 163	–	G	
6 (743, 744)	160, 161, 162, 163	AG	GA	
7 (772)	160, 161, 162, 163	A	delete	
G-CGGTGTCACAGTCGGTTCTGGTGTCGGCCCGACCAAAAATC→GGCGGTGTCACGAT CGGTTCTGGTGTCGGCCCGACCAAAA-TC Ala Val Ser Gln Ser Val Leu Val Ser Ala Arg Pro Lys Ile→Gly Gly Val Thr Ile Gly Ser Gly Val Gly Pro Thr Lys Ile (734–772)				
8 (832)	160, 161	T (TTT)	C (TTC)	Phe→Phe (no change)
9 (842)	160, 161	C (CTG)	T (TTG)	Leu→Leu (no change)
10 (912, 913)	160, 161, 162, 163	CG (CCG)	GC (CGC)	Pro→Arg
11 (1004)	161	G (GCA)	A (ACA)	Ala→Thr
12 (1034, 1035)	160, 161, 162, 163	CG (CGG)	GC (GCG)	Arg→Ala
13 (1123)	160, 161	G (CCG)	A (CCA)	Pro→Pro (no change)
14 (1202)	162	T	C	
15 (1289)	162	A	G	

Table 6 Mutations in the guaA gene of four *B. subtilis* strains

Sequence no. (site)	Mutant	Wild-type (codon)	Mutant (codon)	Change of amino acid
1 (105)	160, 161, 162	G (CTG)	A (CTA)	Leu→Leu (no change)
2 (308, 309)	160, 161, 162, 163	CG (ACG)	GC (AGC)	Thr→Ser
3 (448, 9, 450)	160, 161, 162, 163	GCG (GCG)	delete	Ala delete
4 (488, 489)	160, 161, 162, 163	GC (GGC)	CG (GCG)	Gly→Ala
5 (502)	160, 161, 162, 163	C (CAC)	T (TAT)	His→Tyr
6 (504)	160, 161, 162, 163	C (CAC)	T (TAT)	
7 (587, 588)	160, 161, 162, 163	CG (TCG)	GC (TGC)	Ser→Cys
8 (646, 647)	160, 161, 162, 163	CA (CAG)	AC (ACG)	Gln→Thr
9 (674, 675)	160, 161, 162, 163	GC (GGC)	CG (GCG)	Gly→Ala
10 (726)	163	G (GCG)	A (GCA)	Ala→Ala (no change)
11 (739)	161	C (CTG)	T (TTG)	Leu→Leu (no change)
12 (784, 785)	160, 161, 162, 163	CG (CGT)	GC (GCT)	Arg→Ala
13 (1378)	160, 161, 162, 163	–	G	
14 (1382)	160, 161, 162, 163	–	C	
15 (1389)	160, 161, 162, 163	–	T	
1378–1389	-GAAT-CGCGCCGT-→GGAATCCGCGCCGTT (Glu Ser Arg Arg→Gly Ile Arg Ala Val)			

occur; it is, therefore, not the direct consequence that led to the high guanosine productivity of the strain.

Studies of the genetic sequence indicated that both the inosine- and guanosine-producing strains belonged to the purine auxotrophs, and their branch AMP synthesis pathways were repressed. In contrast with the wild type and the low-yield strain, deletion of one base pair in their purA gene at locus 55 occurred; this resulted in the frame-shift mutation of the subsequent sequence. Being translated, the protein has lost activity as a SAMP synthesis enzyme, and thus the AMP synthesis pathway was blocked. This might be why the two production strains (inosine-producing strain No. 162 and guanosine-producing strain No. 163) were auxotrophic; it might also explain the high production level of the two producing strains.

In addition, from the results of genetic analysis it can be observed that the 5′ non-coding area of the pur operon in inosine-producing strain No. 162 has only one base pair change whereas the guanosine-producing strain No. 163 has mutations in 51 base pairs. The rate of mutation was nearly 10%. This might effect the recognition and the binding affinity of the promoter sequence by AMP, ADP, or the other related transcription regulating factors. If their repression can be attenuated, production capacity might be enhanced.

4.1.7 *Summary*

From analysis of experimental results we realized that the decrease in the productivity of guanosine fermentation could be attributed to a shift of the central metabolic flux, and cellular metabolic regulation was thus regarded as the primary effect. However, because such a shift phenomenon was observed and optimization of metabolic process was achieved on the reactor engineering-scale, relationships among these inter-scale problems must be investigated on the basis of individual scale studies before effective control of the process can be implemented.

Correlation of problems on the genetic-scale and on the cellular metabolic regulation-scale was further studied, and the role of the functional gene of SAMP synthetase and the effect of the mutation of the pur operon on the biosynthesis of guanosine were disclosed in our laboratory. The expression of a gene is the process expressing the genetic information in a biological phenotype, but this transformation by no means has the same effect in different physiological periods. The activity and amount are subject to regulation. Taking guanosine fermentation as an example, our serial experimental data merely showed that even when the genetic characteristics did not change, the metabolic flux was shifted from the HMP pathway to the EMP pathway; this was attributed to a variety of factors under the bioreactor conditions. This kind of shift might be because of activation of enzymes in the metabolic pathway or a change in the amount of enzyme. Because exocellular environmental signals are not transferred to the regulatory protein, it might be a regulation problem on the transcription or translation of RNA scale, i.e. the functional gene and the phenotype on the RNA scale are not related [84–87].

This shows there is still a vague inter-scale relationship between the genetic constitutive and cellular metabolic scales. It also manifested itself in the asymmetry of the functional gene over the phenotype. Therefore, further study and exploration should be conducted, especially acquisition and study of genetic phenotypic data, including the acquisition and logging of data relating to gene transcription, protein, and metabolite aspects, and the metabolic flux distribution and shift using trace elements. A variety of quantitative analytical instruments with powerful functions are worth exploring. Consequently we are developing powerful chemometric tools for optimum assignment of gene functions on the basis of highly dimensional acquired phenotypic data [88–99]. There are many problems, from the collection of a large amount of genetic phenotypic data to the discovery of functional genes; further studies of optimization techniques for fermentation processes are also worth consideration.

4.2 Optimization and scale-up of erythromycin fermentation

Many research papers in the literature describe the biosynthesis of erythromycin by *Saccharopolyspora erythraea*. Study of biosynthetic pathways to erythromycin has made great progress, and has gone deep into the genome scale to elucidate the mechanisms of the biosynthetic pathways [100–104]. Nevertheless, application of the achievements of molecular studies to optimum control of a fermentation process is still a problem to be solved. For instance, experience from much production practice tells us that soybean meal is the best nitrogen source for highly productive erythromycin fermentation. However, in practical operation it is difficult to explain the mechanism of its effect, and it has to rely on trial and error experiments and experience. An optimization technique using data correlation was applied to this study, as shown in Fig. 3 in which multi-parameter metabolic profiles are displayed on a PC monitor with a user-friendly interface. In Fig. 3, *DO*, *OUR*, *CER*, K_La, *RQ*, and R_{GLU} are dissolved oxygen, oxygen uptake rate, CO_2 evolution rate, oxygen transfer coefficient, respiratory quotient, and glucose feed rate, respectively. An interesting point is that the *RQ* value decreased noticeably after approximately 9 h of fermentation, and the decrease lasted for more than 15 h. The decrease of *RQ* might perhaps be attributed to fixation of CO_2 to the propionyl-CoA by carboxylase, to give rise to methylmalonic acid. It is worthy of note that the decline of *RQ* occurred simultaneously with the fall of *CER*. If glucose was added during this period *RQ* would increase again. This implies that the decline of *RQ* is engendered by the highly reductive substrate which served as the carbon source. This can only be the soybean meal. This conclusion is deduced from correlation of data-trend curves. At this time amino-nitrogen decreased and biomass concentration increased rapidly. From the literature it is known that utilization of some amino acids favors the generation of methylmalonic acid. Results from on-line data acquisition with a computer showed that soybean meal might play a role in furnishing the carbon skeleton in the biosynthesis of the macrolide of erythromycin, by amino acid metabolism. Correlation analysis of data profiles also showed the time and manner of utilization of soybean meal and competitive utilization of another carbon source. As a consequence,

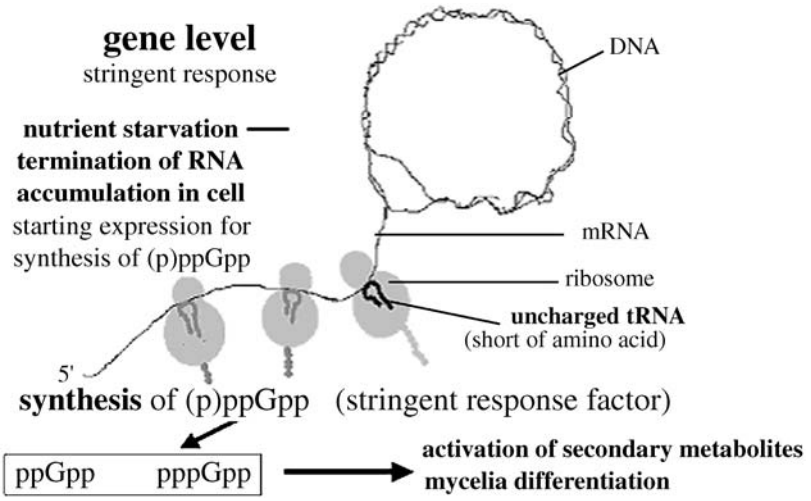

Fig. 16 The stringent response

the mechanism of the effect of the competitive utilization of soybean meal and glucose on secondary metabolism during the fermentation of erythromycin was disclosed. At this time, if control is inappropriate, erythromycin productivity might be substantially reduced, and the so-called chaos phenomenon will occur [105].

In the course of antibiotic fermentation investigated in our laboratory polymorphism and instability in the early period of fermentation were usually observed. Tiny changes in the initial conditions could lead to a great diversity of results. This is the so-called chaos phenomenon. Chaos is a kind of special mobile pattern in a non-linear system. In a deterministic system seemingly disordered and complicated movement is generated as a result of inner randomization. Study of the chaos phenomenon relied on discovery and characterization of chaotic phenomena in microbiological processes, and did not involve studies of microscopic mechanisms. As far as we know, the cause of any problem in terms of biological phenomena must be sought from cell biology. As a result of a preliminary study we believe that the mechanism of metabolic regulation (stringent response) prevalent in a prokaryote cell, shown in Fig. 16, might play a role in chaotic phenomena [106–109]. When levels of the amino acids in the culture broth became restricted, the level of the unloaded tRNA was increased and, after the unloaded tRNA entered the ribosome, the stringent response factor was initiated. Meanwhile, differentiation of mycelia occurred and secondary metabolism for product synthesis commenced. This kind of status reflects the changes in genetic phenotype and cellular metabolism. By controlling the chaos we can ensure the cells attain the desired physiological state. This might be of significance in promoting biosynthesis of the antibiotic. One phenomenon that attracted our attention was that after approximately 9 h of erythromycin fermentation peaks and corresponding valleys were observed in *CER*, *OUR*, pH and *DO* values.

The heights and the times of the peaks/valleys reflected the system characteristics of the early phase of fermentation. Such characteristics depend on a variety of factors and are also the essential basis for stabilization of a fermentation process.

These findings indicated that correlation analysis of related cell metabolic fluxes is of great significance in the studies of cell metabolism and process optimization in a bioreactor. This can be further deduced and quantified by using the material balance method. Take pH as an example. From the metabolic profiles (Fig. 3) we find that pH is an important control parameter. Alteration of pH would lead to changes in the activity of different enzymes, and hence would influence the utilization of substrates, and even the metabolic pathway, cell structure, and, finally, the formation of products. Moreover, it is worthy of note that a pH change is virtually the result of a change of the balance of protons. The result is related to the change of metabolic flux. Figure 17 shows a schematic diagram illustrating the balance of protons in the culture broth. S_1, S_2, S_3, and S_4 represent the concentrations of starch, glucose, ammonium sulfate, and soybean meal, respectively; K_1 to K_9 are various reaction rate constants, K_I is the enzyme activity coefficient of the starch, and its value is related to the amount and activity of cells, i.e. $K_I=\alpha X$; where K_2 is the rate constant for conversion of the reducing sugar into organic acids. The value of K_2 also depends on the amount and activity of the culture, i.e. $K_2=\beta X$. Similarly, it was assumed that $K_{IN}=rX$, where K_{IN} is the rate constant for conversion of soybean meal into amino acids.

When ammonium sulfate serves as a nitrogen source, the H^+ ion balance is:

$$\frac{dC_{H^+}}{dt} = \beta X(\alpha X S_{1t} + I_C) + K_3 k \frac{C_N}{k_N + C_N} \cdot \frac{C_C}{k_C + C_C} X + K_7 [CER - K_L a_{CO_2}(C_{CO_2} - C^*_{CO_2})] - K_4 m X - K_5 k \frac{C_N}{k_N + C_N} \cdot \frac{C_C}{k_C + C_C} X - K_6 \frac{dP}{dt} \quad (1)$$

where k_N and k_c are the constants in the Monod equation that are related to the nitrogen and carbon sources, respectively.

If soybean meal is used as a nitrogen source, then:

$$\frac{dC_{H^+}}{dt} = \beta \times (\alpha \times S_{1t} + I_C) + \theta k \frac{C_N}{k_N + C_N} \cdot \frac{C_C}{k_C + C_C} X + \frac{dC_N}{dt} - S_{4t} r X + K_7 [CER - K_L a_{CO_2}(C_{CO_2} - C^*_{CO_2})] - K_4 m X - K_5 k \frac{C_N}{k_N + C_N} \cdot \frac{C_C}{k_C + C_C} X - K_6 \frac{dP}{dt} \quad (2)$$

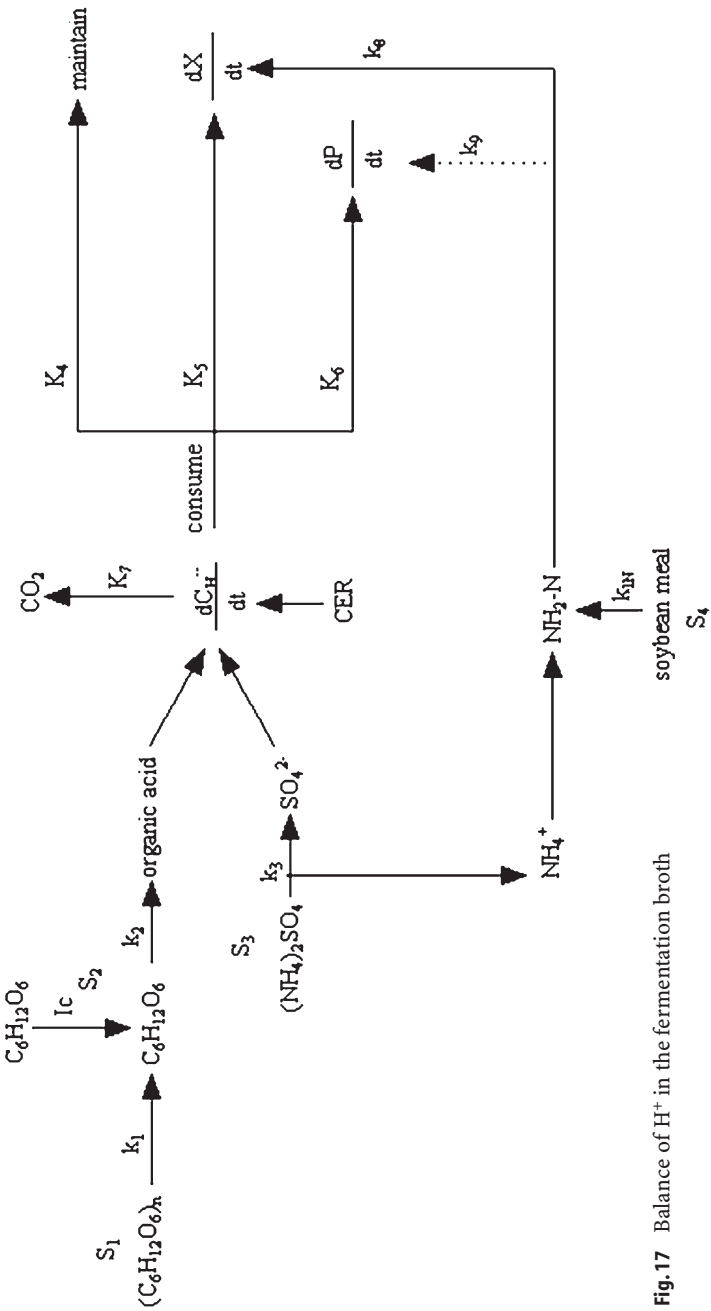

Fig. 17 Balance of H^+ in the fermentation broth

The change in the H^+ balance caused by the change of metabolic flux can be used as the guideline to optimize preparation of the basic medium, addition of sugar during the fermentation, and the settings for controlling pH, aeration rate, and some other operations.

4.3 Studies on the expression of recombinant human serum albumin by engineered *P. pastoris* in high-density culture

4.3.1 *Background*

In 1987 Cregg et al. [110] were the first to report that *Methylotrophic P. pastoris* could be used to express exogenous proteins. In view of its advantages – its high efficiency of expression, genetic stability, and capability of product excretion, etc. – it has become a very attractive host in gene expression in recent years. In less than 20 years more than 200 exogenous genes have been expressed by this system [111], most of which could be further developed into drugs. The production capacity of these drugs has reached 20 m^3. Progress in this study is of economic importance and social significance.

There are many reports of studies of the construction of the expression system of *P. pastoris*, for example the types of vector, secretion sequence, vector unit, etc. [112] Some of the studies have also concentrated on experimental research for optimization of fermentation processes. However, these studies did not consider the relationship among the problems of the process on the three scales discussed in this article.

In recent studies expression of recombinant human serum albumin (rHSA) has been achieved by using the expression system of *Pichia* yeast as host [113, 114]. The multi-variable metabolic profiles obtained from a 500-L FUS-50L(A) fermenter equipped with a PC and a user-friendly interface are shown in Fig. 18. After inoculation *DO* gradually declined while *OUR* increased. This reflected the features of the material balance in the bioreactor, which was characterized by mass transfer of the oxygen supply, and the oxygen uptake kinetics of microorganisms with oxygen as a substrate. The phenomenon also reflected the relevant features stirrer speed (RPM), air flow rate (F), and *DO*, and the effects of the operating variable oxygen supply on the oxygen transfer coefficient, $K_L a$, in the special circumstances of the rheological properties of the fermentation broth. It is worthy of note that after fermentation for 35.6 h, the agitation speed reached its highest value. At a high *OUR* value of 302 mol m^{-3} h^{-1} during high-density fermentation of the yeast *DO* approached zero, which showed that the *OUR* had far surpassed the *OTR*. Thus the conventional oxygen supply to the CSTR could not meet the demand of industrial production. Therefore, preventing zero *DO* level after fermentation for 36 h was the main problem to be solved. After analysis of the metabolic profiles by the data processing software of Bioradar, a rational basic medium was designed and used. As a result, *DO* rebounded within 20 min, i.e. after fermentation for approximately 36.7 h, and reached approximately 65% of air saturation. Thus the usual practice of using pure oxygen was avoided.

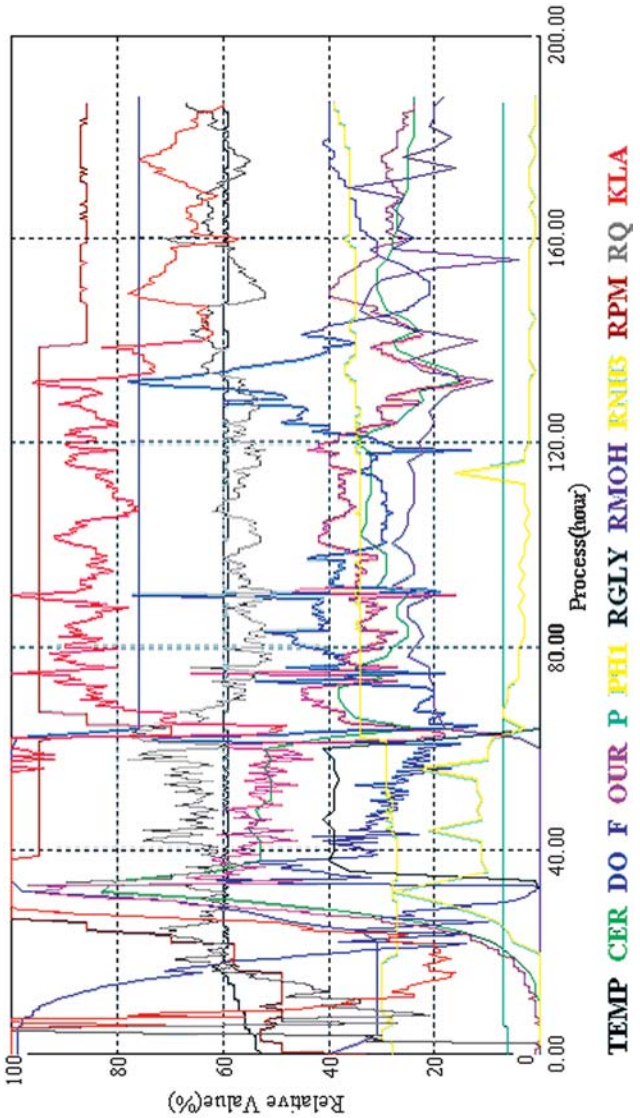

Fig. 18 Data profiles during rHSA fermentation

In a study of the utilization of nitrogen sources close correlation was observed among the conditions pH, and the feed rates of ammonia (R_{NH3}) and carbon sources (R_{GLU}, R_{MOH}). In this study a closed control loop consisting of pH and the ammonia feeding system was adopted in the FUS-50L(A) bioreactor. The pH was controlled at a fixed value. As shown in Fig. 18, automatic matching of the consumption of carbon and nitrogen sources during cultivation was achieved by regulation of the C/N ratio. This can also be seen from the different feed rates of ammonia during the growth phase and the product expression phase. As fermentation continued the expression rate declined, and R_{NH3} also decreased.

Addition of ammonia was then stopped, followed by product harvesting. Overfeeding of methanol during the expression phase led to serious disruption of cell metabolism, i.e. the so-called poisoning phenomenon emerged, and even transcription and translation terminated. In Bioradar, under the guidance of the curves produced by the data-processing software, the *OUR* would gradually ascend as the feed rate of methanol, R_{MOH}, was increased. Thus, avoiding the occurrence of methanol toxic effect is of significance for achieving the highest expression rate.

It can be seen that changing some of the distribution characteristics of the cell metabolic flux described above, and the transfer characteristics on the bioreactor engineering scale, provide critical clues for process optimization and scale-up. The material flux can further be applied to data processing and mathematical modeling through element balances and metabolic flux balances [115–117]. The rHSA fermentation process using *P. pastoris* as the host strain can be divided into the growth phase and the expression phase. In the growth phase, glycerol was used by *P. pastoris* as a carbon and energy source; in the expression phase methanol acted as both carbon and energy source and as an inducer. The amounts used can be calculated stoichiometrically, in accordance with data acquired from different phases.

4.3.2
Stoichiometric calculation in the growth phase [118]

Theoretically, the five measurable macroscopic reaction rates (n=5) are rate of glycerol consumption, r_{gly}, cell growth rate, r_x, ammonia consumption rate, r_n, oxygen uptake rate, r_o, and rate of carbon dioxide evolution, r_c. Consideration of the balance of three elements (m=3): carbon, nitrogen, and degree of oxidation or reduction (synthesized expression of oxygen and hydrogen) leads to the expression:

$$BR_E = 0 \tag{3}$$

where:

$$B = \begin{bmatrix} 1 & 1 & 0 & 0 & 1 \\ 0 & C_{nx} & 1 & 0 & 0 \\ \gamma_{gly} & \gamma_x & \gamma_n & \gamma_o & \gamma_c \end{bmatrix} \tag{4}$$

and where C_{nx} is the nitrogen content of the cell and R_E consists of five components. Equation (4) contains three linear equations, the number of degrees of freedom of the model is 2 (f=2). Therefore, only two of the components in R_E can change freely whereas the other three components may be calculated from Eq. (3). Letting $R_{E1}=[r_{gly}r_x]^T$, $R_{E2}=[r_n r_o r_c]^T$, and setting the two front rows of B to B_1, and the three remaining rows to B_2, Eq. (3) can be rewritten as:

$$[B_1\ B_2]\begin{bmatrix} R_{E1} \\ R_{E2} \end{bmatrix} = 0 \tag{5}$$

Thus

$$R_{E2} = -B_2^{-1}B_1B_{E1} \tag{6}$$

By combining the cell metabolic balance in vivo, the degrees of freedom can be further reduced. For instance, considering that during mycelia growth glucose and ammonia are converted into CO_2, glycerol into glucose, and glucose glycolysis and oxidative phosphorylation, etc., are used to produce the ATP necessary for growth and maintenance, the following equations can be written:

$$ZE = 0 \tag{7}$$

where: $E = [\text{Gly X Glu ATP NADH } NH_3\ O_2\ CO_2\ H_2O]^T$

$$Z = \begin{bmatrix} 0 & 1 & -\sigma_x & \sigma_x & \frac{1}{2}(\sigma_x \gamma_{glu} - \gamma_x) & -C_{nx} & 0 & \sigma_x - 1 & 0 \\ -1 & 0 & 1 & -\alpha_{gly} & \frac{1}{2}(\gamma_{gly} - \gamma_{glu}) & 0 & 0 & 0 & 0 \\ 0 & 0 & & \alpha_{glu} & \frac{1}{2}(\gamma_{glu}) & 0 & 0 & 1 & 0 \\ 0 & 0 & 0 & \alpha_h & -1 & 0 & -\frac{1}{2} & 0 & 1 \end{bmatrix} \tag{8}$$

Combined with Eq. (3), the relationship among r_x, r_n, r_o, r_c, and r_{gly} is expressed by:

$$\begin{bmatrix} r_x \\ r_n \\ r_o \\ r_c \end{bmatrix} = \begin{bmatrix} Y_{x/s} \\ -C_{nx}Y_{x/s} \\ \frac{1}{4}(\gamma_{gly} - \gamma_x Y_{x/s}) \\ -(1 + Y_{x/s}) \end{bmatrix} r_{gly} \tag{9}$$

Making use of the concept of metabolic flux, the mathematical models constructed with element balances and metabolic balances can overcome disadvantages such as the obscurity of data and difficulties explaining the relationship between input and output. These models have fully utilized a knowledge of biology and have universal applicability and flexibility. The method above was used to calculate the specific glycerol consumption rate, $q_{gly} = 0.05785 + 1.5184\mu$, i.e. the equation for the specific feed rate of glycerol. We took the advantage of this method to control the feed rate of glycerol, and succeeded in achieving the expected high expression results.

4.3.3
Stoichiometric calculation in the expression phase [119]

4.3.3.1
Element balances

During the expression phase of rHSA fermentation there are, theoretically, six macroscopic reaction rates to be determined – methanol consumption rate, r_{moh}, cell growth rate, r_x, product synthesis rate, r_p, ammonia consumption rate, r_n, oxygen uptake rate, r_o, and CO_2 evolution rate, r_c. Considering the balances of three elements (m=3): carbon, nitrogen, and the degree of oxidation and reduction, we obtain the expression:

$$BR_E = 0$$

$$B = \begin{bmatrix} 1 & 1 & 1 & 0 & 0 & 1 \\ 0 & C_{nx} & C_{np} & 1 & 0 & 0 \\ \gamma_{moh} & \gamma_x & \gamma_p & \gamma_n & \gamma_o & \gamma_c \end{bmatrix}, R_E = \begin{bmatrix} r_{moh} \\ r_x \\ r_p \\ r_n \\ r_o \\ r_c \end{bmatrix} \tag{10}$$

where C_{nx} and C_{np} represent the nitrogen content of biomass and albumin, respectively.

Letting $\boldsymbol{R}_{E1}=[r_{moh}r_x r_p]^T$, $\boldsymbol{R}_{E2}=[r_n r_o r_c]^T$, and setting the three front rows of $\boldsymbol{B}$ to $\boldsymbol{B}_1$, and the three remaining rows to $\boldsymbol{B}_2$ (f=3), we get:

$$R_{E2} = -B_2^{-1}B_1B_{E1} \tag{11}$$

4.3.3.2 Metabolic balances

According to the element balances, r_{moh}, r_x, and r_p can change freely, but in the expression phase of the rHSA fermentation process only r_{moh} can be controlled manually. Consequently, the degrees of freedom of the model must be further reduced to accommodate the metabolic balances inside the cell.

The metabolic pathway in *P. pastoris* in the expression phase can be simplified as shown in Fig. 19. The intermediate metabolites are HCHO, GAP, NADH, and ATP (i=4). The pathway consists of six main reactions – oxidation of methanol to formaldehyde, dissimilation of formaldehyde, assimilation of formaldehyde (xylulose cycle), cell growth, product synthesis, and oxidative phosphorylation (k=6).

The energy generated from oxidative phosphorylation is used for growth, maintenance, and product synthesis, and, meanwhile, operation of the xylulose cycle also consumes energy. Consequently, the efficiency of oxidative phosphorylation is the critical factor that influences product synthesis.

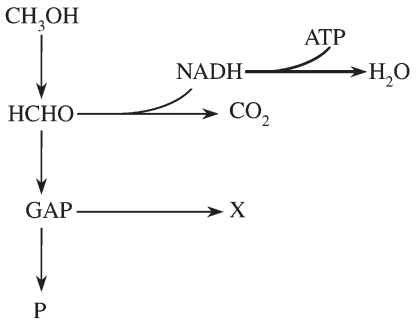

Fig. 19 Simplified metabolic scheme for *P. pastoris* expression phase

By setting E=[MOH X P ATP NADH HCHO GAP NH_3 O_2 CO_2 H_2O]^T, the six reactions above can be expressed as:

$$ZE = 0$$

$$Z=\begin{bmatrix} -1 & 0 & 0 & 0 & 0 & 1 & 0 & 0 & -\frac{1}{2} & 0 & 1 \\ 0 & 0 & 0 & 0 & 2 & -1 & 0 & 0 & 0 & 1 & 0 \\ 0 & 0 & 0 & -1 & 0 & -1 & 1 & 0 & 0 & 0 & 0 \\ 0 & 1 & 0 & -a_x & \frac{1}{2}(\sigma_x\gamma_{gap}-\gamma_x) & 0 & -\sigma_x & -C_{nx} & 0 & \sigma_x-1 & 0 \\ 0 & 0 & 1 & -a_p & \frac{1}{2}(\sigma_p\gamma_{gap}-\gamma_p) & 0 & -\sigma_p & -C_{np} & 0 & \sigma_p-1 & 0 \\ 0 & 0 & 0 & a_h & -1 & 0 & 0 & 0 & -\frac{1}{2} & 0 & 1 \end{bmatrix} \tag{12}$$

First, let us see whether the metabolic equation set above can be solved: g=f–k+i=3–6+4=1, which meets the second necessary condition of the metabolic equation, Eq. (13). By processing Eq. (12), we get the relational expression among various components in $\boldsymbol{R}_{E1}$:

$$\begin{aligned} &Z_3R_{E1} = 0 \\ &Z_3 = [2a_h \quad a_x+\sigma_x(2a_h+1)-\tfrac{1}{2}a_h(\sigma_x\gamma_{gap}-\gamma_x) \quad a_p+\sigma_p(2a_h+1) \\ &\qquad -\tfrac{1}{2}a_h(\sigma_p\gamma_{gap}-\gamma_p)] \triangleq [a_1 \;\; a_2 \;\; a_3] \end{aligned} \tag{13}$$

The number of degrees of freedom reduces to two after Eq. (13) is applied, i.e. two components of $\boldsymbol{R}_{E1}$ were able to change freely. However, in the expression phase of rHSA fermentation mycelia growth rate and product formation rate could not be controlled immediately, and only one component could be altered freely. Therefore, other restrictive conditions had to be introduced to reduce further the number of degrees of freedom of the process. In the course of fermentation with a microorganism there are relationships between product synthesis and mycelial growth. This has been regarded as a limited condition, which is introduced into the systematic equations. Applying:

$$r_p = \beta r_x$$

and solving with Eq. (13), we get:

$$\begin{bmatrix} r_x \\ r_p \end{bmatrix} = \begin{bmatrix} -\dfrac{a_1}{a_2+\beta a_3} \\ -\dfrac{\beta a_1}{a_2+\beta a_3} \end{bmatrix} r_{moh} \triangleq \begin{bmatrix} Y_{xs} \\ Y_{ps} \end{bmatrix} r_{moh} \tag{14}$$

The number of degrees of freedom reduces to 1 after the relationship between product synthesis and mycelial growth is introduced, i.e. only one component can change freely during the expression phase of rHSA fermentation. This is in accordance with the practical fermentation process.

Combining Eqs. (13) and (14), we obtained the following equation, which describes the expression phase of the rHSA fermentation process quantitatively:

$$\begin{bmatrix} r_x \\ r_p \\ r_n \\ r_o \\ r_c \end{bmatrix} = \begin{bmatrix} Y_{xs} \\ Y_{ps} \\ -(C_{nx}Y_{xs} + C_{np}Y_{ps}) \\ \frac{1}{4}(\gamma_x Y_{xs} + \gamma_p Y_{ps}) \\ -(Y_{xs} + Y_{ps}) \end{bmatrix} r_{moh} + \begin{bmatrix} 0 \\ 0 \\ 0 \\ \frac{1}{4}\gamma_{moh} \\ -1 \end{bmatrix} r_{moh} \tag{15}$$

4.3.3.3 Model identification

Equation (15), describing the expression phase of rHSA fermentation, does not take maintenance of the cells into account. Let:

$$a_x = a_x + m_x/\mu, \beta = \frac{\beta_1}{\mu} + \beta_2 + \beta_3\mu \tag{16}$$

When Eq. (16) is substituted into Eq. (15) and its sub-equations, we get a quantitative model describing the expression phase of rHSA fermentation, where a_h, m_x, a_p, β_1, β_2, and β_3 are six unknown terms, estimation of which was based on data acquired from the monitoring and control system using the optimization of multi-variables method. Owing to introduction of the maintenance coefficient and the relationship between product formation and mycelial growth, the model established here has a strong non-linear characteristic and solution of Eq. (15) can be realized only by the cyclic iterative method using a PC.

In the course of the rHSA fermentation, product formation can be divided into two periods:

The 1st period

The relative coefficient values between the specific production rate and the specific growth rate were calculated, and the results were: β_1=–3.7956, β_2=–0.0060, and β_3=0.0007. Curve fitting is shown in Fig. 20. The quadratic curve in Fig. 20 was further examined at μ=0.0008 h^{-1} for which there was a peak value, Q_p=0.0007 g g^{-1} h^{-1}. The shape of the quadratic curve in Fig. 20 showed that during the expression phase of rHSA fermentation the growth of the culture must be controlled. This does not mean that the faster the growth, the better the production. This is in accordance with our experience. In addition, we noticed that when the value of the specific growth rate became negative, i.e. the culture underwent autolysis, the concentration of albumin still increased; this might be attributed to the release of intracellular albumin after the cells lysed.

The 2nd period

Similar to the 1st period, the relative coefficient values were calculated and are listed below:

$$\beta_1 = -0.3939, \beta_2 = 0.0113, \beta_3 = -0.0003$$

$$a_h = 1.5013 \pm 0.8017; m_x = 0.2218 \pm 0.1438; a_p = 549.4991 \pm 223.85$$

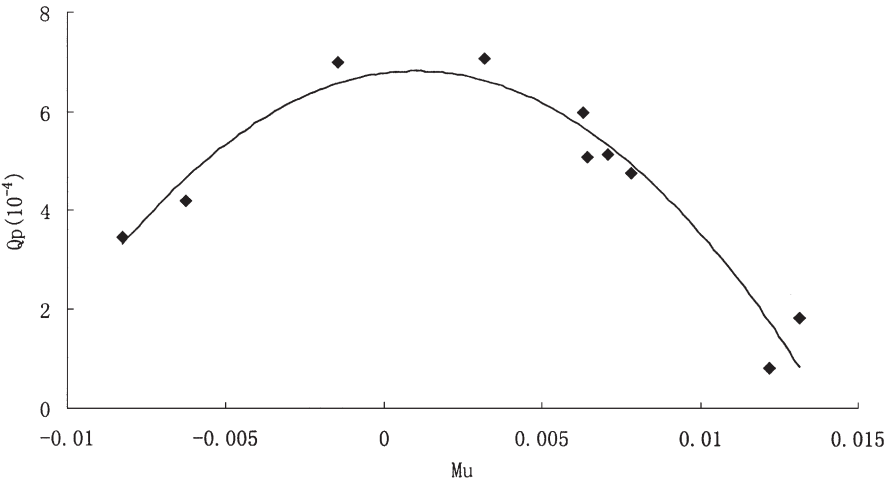

Fig. 20 Relationship between Q_p and μ in the first period of the expression phase

By comparing the metabolic coefficients, a_h, m_x, and a_p between the 1st and 2nd periods in the expression phase it can be observed that a_h and a_p are quite different, even though m_x is almost the same in both periods and a_h is the intracellular level of oxidative phosphorylation. Its value represents the amount of ATP generated per mole of NADH oxidized by the culture, which reflects the situation of energy supply inside the cells. The a_h of the 2nd period is about $^1/_3$ smaller than that of the 1st period, which means that the energy supply to the culture in the 2nd period might be insufficient. This was unfavorable to production. We also noticed that in the 2nd period the amount of ATP necessary per mole carbon for production of rHSA was greater than that in the 1st period by about 100 mol. This might be one reason for the reduced productivity. Why a_h and a_p make such a difference, how this difference affects synthesis of the product, and how to prevent this difference are still awaiting clarification by future investigation.

5 Conclusions

Space-time characteristics on several scales are a common feature of all the complicated phenomena in process engineering. The large-scale cultivation of microorganisms using living cells as an object was undertaken on the molecular-scale (genetics), the cellular-scale (metabolic regulation), and the reactor-scale (process control). It was shown that the relationship between space-time series reactions, a characteristic of living organisms only, manifests itself in changes of information flux, material flux, and energy flux, and behaves as a multi-input/output relationship of a network.

In industrial production expression of product on the genetic scale or the metabolic product on the cellular scale can be implemented only by large-scale cultivation of microorganisms in bioreactors. Modifying reactor equipment size

or changing the operating conditions can change the microscopic reaction conditions in cellular bioreactions and this can lead to different results.

The most important characteristic of a complicated system on multi-structural-levels, as for all industrial processes, is its "varying structure"; i.e. changing the scale might lead to an intricate change in the intra-structure of an equipment, and great diversification of material transformation. Qualitative changes on characteristic scales might occur in the subject observed. Consequently, when the dimensions of a bioreactor or the operating conditions are altered, the resulting change of material status cannot be described by a linear relationship or by an average statistical approach. In addition to the linear or kinetic factor, the cause of process variation is often attributed to the abrupt change of systematic structure, which leads to different results or serious deviations from the optimized process. This indicates that the scale effect in microbial reaction engineering is of great significance.

In studying and solving a multi-scale problem in process operation attention must be paid to the difficulties of inter-scale problems. In other words, if we want to control a phenomenon on a certain scale, we should usually seek an observable phenomenon and operable approach on another scale. Each application has its own special main scale, but it should cooperate with another related sub-scale under all-around consideration. Therefore, in optimizing a bioreaction process and in studying the main scale of cellular metabolism, we should pay attention to the inter-scale analysis and operation of reactor engineering, and also notice the correlation between the genetic scale and the cellular metabolic regulation scale. Thus, we have to make use of interdisciplinary knowledge and rely on inter-technical measures.

The most important development in current biochemical engineering is that in the rapid movement of biotechnology and the profound comprehension of the life process, chemical engineering is integrated intensively with biotechnology. In chemical engineering the transfer of mass, heat, momentum, and chemical reaction are the fundamental subjects. However, computational hydrodynamics and the life process, including the mechanisms of synthesis of various products, metabolic regulation, metabolic engineering, functional genes, gene mutation and recombination techniques, RNA regulation and control, etc., have all been studied systematically and intensively, and continue to lead to new discoveries. All these are important bases of this study on the analysis of sub-processes, and these related topics must be integrated appropriately into sub-scale studies.

Moreover, making use of a multi-scale research method, we can observe different scale phenomena with multi-scale problems on their individual scales. This might result in the discovery of a new biotechnological phenomenon which might not be uncovered by consideration of a single scale only – for instance, the shift in cellular metabolic flux, the asymmetry of a functional gene over phenotype in the course of a production, and biological discrepancy in the study of model biology, etc. To study these phenomena, combined use of interdisciplinary knowledge and inter-technique is also needed.

Acknowledgement Financial aid from the China State 9th and 10th Five Year Key Programs (Serial Nos. 96–C03–04–02 and 2001BA708B07–05), National Natural Science Foundation of China (Serial No. 29976013), and China National "863" Program (Serial No. 2002AA217021) is gratefully acknowledged. We are greatly indebted to Dr TY Gu of Ohio University (USA) for his helpful suggestions and comments on the chapter.

6 References

1. Rani KY, Rao VSR (1999) Bioprocess Eng 21:77
2. Lee J, Lee SY, Park S, Middelberg APJ (1999) Biotechnol Adv 17:29
3. Bellgardt KH (2000) Bioprocess models. In: Schugerl K, Bellgardt KH (eds) Bioreaction engineering, modeling and control. Springer, Berlin Heidelberg New York, p 44
4. Simon L, Karim MN (2001) Biotechnol Prog 17:634
5. Ungarala S, Co TB (2000) Comput Chem Eng 24:2739
6. Luttmann R, Gollmer K-U (2000) On-line simulation techniques for bioreactor control development. In: Schugerl K, Bellgardt KH (eds) Bioreaction engineering, modeling and control. Springer, Berlin Heidelberg New York, p 197
7. Stephanopoulos G, Locher G, Duff MJ, Kamimura R, Stephanopoulos G (1997) Biotechnol Bioeng 53:443
8. Wang FS, Su TL, Jang HJ (2001) Ind Eng Chem Res 40:2876
9. Balsa-Canto E, Banga JR, Alonso AA et al. (2001) Comput Chem Eng 25:539
10. Balsa-Canto E, Banga JR, Alonso AA, Vassiliadis VS (2000) Ind Eng Chem Res 39:4287
11. Dhir S, Morrow KJ, Rhinehart RR et al. (2000) Biotechnol Bioeng 67:187
12. Dochain D, Bastin G (1984) Automatica 20:621
13. Ben YC, Guillou V (2000) Control Eng Practice 8:1297
14. Meleiro LAC, Maciel RA (2000) Comput Chem Eng 24:925
15. Shioya S, Shimizu K, Yoshida T (1999) J Biosci Bioeng 87:261
16. Lennox B, Kipling K, Glassey J et al. (2002) Biotechnol Prog 18:269
17. Ray ID, Basu S, Chattopadhyay P (2001) J Food Sci Technol–Mysore 38:329
18. Mamdani EH (1975) Electron Lett 11:625
19. Horiuchi JI, Kishimoto M (2002) Fuzzy Set Syst 128:117
20. Horiuchi J, Hiraga K (1999) J Biosci Bioeng 87:365
21. Horiuchi JJ, Hiraga K (1998) Proc Comput Appl Biotechnol 7:25
22. Honda H, Kobayashi T (2000) J Biosci Bioeng 89:401
23. McCulloch WS, Pitts W (1943) Biophys 15:115–133
24. Hebb DD (1949) The organization of behavior. Wiley, New York, p 1
25. Karim MN, Yoshida T, Rivera SL et al. (1997) J Ferment Bioeng 83:1
26. Gonzalo A, Eric L, Catherine B et al. (1998) J Ferment Bioeng 85:615
27. Vlassides S, Ferrier JG, Block DE (2001) Biotechnol Bioeng 73:55
28. May RM (1975) J Theor Biol 51:511
29. Baier G, Muller M, Orsnes H (2002) J Phys Chem B 106:3275
30. Fox JJ, Hill CC (2001) Chaos 11:809
31. Letellier C (2002) Acta Biotheor 50:1
32. Goldbeter A, Gonze D, Houart G et al. (2001) Chaos 11:247
33. Min LQ, Yu N (2000) J Univ Sci Technol Beijing 7:305 (in Chinese)
34. Shioya S, Shimizu H, Takaguchi N (1999) On-line metabolic flux analysis for fermentation operation. In: Lee SY, Papoutsakis ET (eds) Metabolic engineering. Marcel Dekker, New York, p 227
35. Van Gulik WM, De Laat WTAM, Vinke JL, Heijnen JJ (2000) Biotechnol Bioeng 68:602
36. Chae HJ, Delisa MP, Cha HJ, Weigemd WA, Rao G, Bentley WE (2000) Biotechnol Bioeng 69:275
37. Conejeros R, Vassiliadis VS (2000) Biotechnol Bioeng 69:285
38. Cruickshank SM, Daugulis AJ, McLellan PJ (2000) Biotechnol Bioeng 67:224

39. Zeiser A, Elias CB, Voyer R, Jardin B, Kamen AA (2000) Biotechnol Prog 16:803
40. Schuster KC (1999) Adv Biochem Eng/Biotechnol 66:185
41. Nagy E, Neubeck M, Mayr B, Moser A (1995) Bioprocess Eng 12:231
42. Cooney CL, Wang HY, Wang DIC (1973) Biotechnol Bioeng 19:55
43. Minkevich IG (1983) Biotechnol Bioeng 25:1267
44. Stouthamer AH, Van Verseveld HW (1985) Comp Biotechnol 1:215
45. Stouthamer AH (1992) Quantitative aspects of growth and metabolism of microorganisms. Kluwer, London, pp 275–292
46. Stouthamer AH (1992) Quantitative aspects of growth and metabolism of microorganisms. Kluwer, London, pp 257–274
47. Bailey JE, Sburlati A, Hatzimanikatis V, Lee K, Renner WA, Tsai PS (1996) Biotechnol Bioeng 52:109
48. Khetan A, Hu WS (1999) Metabolic engineering of antibiotic biosynthesis for process improvement. In: Lee SY, Papoutsakis ET (eds) Metabolic engineering. Marcel Dekker, New York, p 177
49. Herwig C, Marison I, Von Stocker U (2001) Biotechnol Bioeng 75:345
50. Kholodenko BN, Cascante M, Hoek JB, Westerhoff HV, Schwaber J (1998) Biotechnol Bioeng 59:239
51. Feng M, Glassey J (2000) Biotechnol Bioeng 69:495
52. Chauvatcharin S, Siripatana C, Seki T, Takagi M, Yoshida T (1998) Biotechnol Bioeng 58:561
53. James HK (1996) Chem Eng News 74:10
54. Villermaux J (1996) New horizons in chemical engineering. In: Proc 5th World Congress of Chemical Engineering, Suu Deigu, USA. AIChE, p 6
55. Wel J (1990) Chem Eng Sci 45:1947
56. Lerou JJ, Ka MN (1996) Chem Eng Sci 51:1595
57. Guo MS, Li JH (2001) Chinese Prog Nat Sci 11:81
58. Xu G, Li J (1998) Chem Eng Sci 53:1349
59. Li JH, Guo MS (1999) Chinese Prog Nat Sci 9:1073 (in Chinese)
60. Guo MS, Li JH (2000) Chinese Prog Nat Sci 10:1078 (in Chinese)
61. Zhong T, Li XH, Wang LF (2001) Chem Eng Progr 4:1
62. Zhang SL (2001) Eng Sci 3:37 (in Chinese)
63. Zhang SL, Chu J, Zhuang YP (2002) Chinese J Antibiotic 27:572 (in Chinese)
64. Carleysmith SW, Fox RI (1984) Fermentation instrument and control. Advances in biotechnological processes 3:1
65. Swartz JR, Coony CL (1979) Indirect fermentation measurements as a basis for control. Biotechnol Bioeng Symp 9:95
66. Cai XP, Chu J, Zhuang YP, Zhang SL (2002) Food Ferment Ind 28:5 (in Chinese)
67. Cai XP, Chen SX, Chu J, Zhuang YP, Zhang SL (2002) Acta Microbiol Sinica 42:232 (in Chinese)
68. Shen T, Wang JY (1994) (eds) Biochemistry, vol 2, 2nd edn. Higher Education Press (in Chinese)
69. Nishikawa H, Momose H, Shiio I (1968) J Biochem 63:149
70. Savageau MA, Voit EO, Irvine DH (1987) Math Biosci 86:127
71. Fell DA (1992) Biochem J 286:313
72. Liao JC, Delgodo J (1993) Biotechnol Prog 9:221
73. Brand MD (1996) J Theor Biol 182:351
74. Heinrich R, Schuster S (1998) Biosystems 47:61
75. Simpson TW, Shimizu H, Stephanopoulos G (1998) Biotechnol Bioeng 58:149
76. Varner J, Ramkrishna D (1999) Curr Opin Biotechnol 10:146
77. Gombert AK, Nielsen J (2000) Curr Opin Biotechnol 11:180
78. Demain AL (1968) Prog Ind Microbiol 8:35
79. Ebbole DJ, Zalkin H (1987) J Biol Chem 262:8274
80. Ebbole DJ, Zalkin H (1989) J Bacteriol 171:2136
81. Ebbole DJ, Zalkin H (1989) J Biol Chem 264:3553
82. Weng M, Nagy PL, Zalkin H (1995) Proc Natl Acad Sci USA 92:7455

83. Shin BS, Stein A, Zalkin H (1997) J Bacteriol 179:7394
84. Raamsdonk LM, Teusink B, Broadhurst D et al. (2001) Nat Biotechnol 19:45
85. Cascante M, Boros LG, Comin-Anduix B (2002) Nat Biotechnol 20:243
86. Waite KA, Eng C (2002) Am J Hum Genet 70:829
87. Feder ME, Bennett AF, Huey RB (2000) Annu Rev Ecol Syst 31:315
88. Andrade MA, Sander C (1997) Curr Opin Biotech 8:675
89. Palsson BO (1997) Nat Biotechnol 15:3
90. Edwards JS, Palsson BO (1998) Biotechnol Bioeng 58:162
91. Poratais JC, Delort AM (2002) Fems Microbiol Rev 26:375
92. Fenselau C, Demirev PA (2001) Mass Spectrom Rev 20:157
93. Gombert AK, Nielsen J (2000) Curr Opin Biotechnol 11:180
94. Ryu DDY, Nam DH (2000) Biotechnol Prog 16:2
95. Johnson BM, Nikolic D, Van-Breemen RB (2002) Mass Spectrom Rev 21:76
96. Larsson L, Saraf A (1997) Mol Biotechnol 7:279
97. Ellis DI, Broadhurst D, Kell DB (2002) Appl Environ Microbiol 68:2822
98. Brandao PFB, Torimura M, Kurane R (2002) Appl Microbiol Biotechnol 58:77
99. McGovern AC, Ernill R, Kara BV (1999) J Biotechnol 72:157
100. Minas W, Brunker P, Kallio PT et al. (1998) Biotechnol Prog 14:561
101. Reeves AR, English RS, Lampel JS, Post DA, Vanden-Boom TJ (1999) J Bacteriol 181:7098
102. Weissman KJ, Bycroft M, Staunton J, Leadlay PF (1998) Biochemistry 37:11012
103. Gaisser S, Bohm GA, Doumith M, Raynal MC (1998) Mol Gen Genet 256:78
104. McPherson M, Khosla C, Cane DE (1998) J Am Chem Soc 120:3267
105. Fan T, Fu JL, Zhang M, Chu J, Zhang SL (2002) J East China Univ Sci Tech 28:43 (in Chinese)
106. Ochi K (1986) J Gen Microbiol 132:2621
107. Ochi K (1987) J Bacteriol 169:3608
108. Beppu T (1995) Trends Biotechnol 13:264
109. Chakraburtty R, Bibb M (1997) J Bacteriol 179:5854
110. Cregg JM, Tschopp JF, Stilman C et al. (1987) Bio/Technology 5:479
111. Wolf K (1996) (ed) Non-conventional yeast in biotechnology. Springer, Berlin Heidelberg New York, pp 203–290
112. Kobayashi K, Kuwae S, Ohya T, Ohda T et al. (2000) J Biosci Bioeng 90:280
113. Guo MJ, Chu J, Zhang SL et al. (2001) Acta Microbiol Sinica 41:617 (in Chinese)
114. Guo MJ, Chu J, Zhang SL et al. (2002) Acta Microbiol Sinica 42:62(in Chinese)
115. Van Gulik WM, Heijnen JJ (1995) Biotechnol Bioeng 46:681
116. Maria IK, Sung MP, Anthony JS, Gregory S (1999) Biotechnol Bioeng 82:375
117. Maria IK, Sung MP, Anthony JS, Gregory S (1999) Appl Biotechnol Bioeng 82:393
118. Huang MZ, Chu J, Zhang SL et al. (2000) Chinese J Biotechnol 16:631 (in Chinese)
119. Huang MZ, Chu J, Zhang SL et al. (2003) Chinese J Biotechnol 19:81 (in Chinese)

Received: May 2003

Adv Biochem Engin/Biotechnol (2004) 87: 151–171
DOI 10.1007/b13535

Industrial Application of Fuzzy Control in Bioprocesses

Hiroyuki Honda · Takeshi Kobayashi

Department of Biotechnology, School of Engineering, Nagoya University,
Nagoya 464-8603, Japan
E-mail: honda@nubio.nagoya-u.ac.jp, takeshi@nubio.nagoya-u.ac.jp

Abstract In a bioprocess, for example a fermentation process, many biological reactions are always working in intracellular space and the control of such a process is very complicated. Bioprocesses have therefore been controlled by the judgment of the experts who are the skilled operators and have much experience in the control of such processes. Such experience is normally described in terms of linguistic IF–THEN rules. Fuzzy inference is a powerful tool for incorporating linguistic rules into computer control of such processes. Fuzzy control is divided into two types–direct fuzzy control of process variables, for example sugar feed rate and fermentation temperature, and indirect control via phase recognition. In bioprocess control the experts decide the value of controllable process variables such as sugar feed rate or temperature as output data from several state variables as input data. Fuzzy control is regarded as a computational algorithm in which the causal relationship between input and output data are incorporated. In Japan fuzzy control has already been applied to practical industrial processes such as production of pravastatin precursor and vitamin B_2 and to the Japanese sake mashing process; these examples are reviewed. In addition, an advanced control tool developed from a study on fuzzy control, fuzzy neural networks (FNN), are introduced. FNN can involve complicated causality between input and output data in a network model. FNN have been proven to be applicable to a research in biomedicine, for example modeling of the complicated causality between electroencephalogram or gene expression profiling data and prognostic prediction. Successful results on this research will be also explained.

Keywords Fuzzy inference · Process control · Bioprocess · Fuzzy neural network · Gene expression profiling data · Prognostic prediction

1 Introduction

In large-scale chemical processes different optimization and control methods based on deterministic mathematical models have been proposed in attempts to meet process requirements. However, such methods have never been used successfully in practical industrial production by use of bioprocesses such as fermentation, because it is difficult to develop a mathematical model which can precisely describe the complex intracellular reactions of the microorganisms in a bioprocess. The operating conditions in industrial bioprocesses are often optimized by utilizing knowledge acquired during repeated operation under the control of the experts, who are highly skilled operators. Such empirical knowledge-based operation can be considered to be useful practically. Although the knowledge cannot be quantified, it is necessary for automatic control of bioprocess to bring them under computer control and incorporate them into traditional control systems.

Fuzzy set theory was at first developed by Zadeh [1]. Fuzzy control based on fuzzy set theory is a mathematical tool for dealing with qualitative information and linguistic expressions which has been applied in biotechnology for several years. Fuzzy control can easily incorporate empirical knowledge gained from skilled operators by employing membership functions and IF–THEN rules, and it has proved to be effective for simulation [2–4], in expert systems [5], and for on-line control of bioprocesses [6–10]. This contribution is a review of scientific papers, mainly published by Japanese researchers, in the field covered by the title of the chapter. Studies on fuzzy control can be categorized into two types. The first utilizes direct inference, in which the fuzzy inference determines directly the outputs from the knowledge base and on-line data. This method enables bioprocess control to be easily automated by using the knowledge of expert operators, and it simply transfers the operators' know-how into the control system. Nakamura et al. [6] reported the fuzzy control of sugar feeding rate in glutamic acid fermentation. Hosobuchi et al. [11] applied fuzzy control to the production of the pravastatin precursor. Horiuchi et al. [12] reported the fuzzy control of vitamin B_2 production. Those are examples in large-scale fermentation. Alfafara et al. [13] presented a method of applying fuzzy logic on a compensator in a feed-forward/feedback controller scheme to realize utilization of non-linearity for robustness of control, flexibility in use of multiple measurable variables, and easy and effective use of expert knowledge.

Another type is indirect inference in which fuzzy inference is first used to estimate the culture phase or physiological state, after which empirical control strategies are performed in each phase or state [7, 14–16]. Control values are determined on the basis of the inferred culture state. Shimizu et al. [17] developed a method for culture-state diagnosis and property estimation by using a fuzzy inference procedure in combination with molar-flux calculations based on a metabolic reaction model. These studies suggest the possibility of more flexible bioprocess control based on qualitative fermentation characteristics. Horiuchi et al. [18, 19] have also reported several laboratory-scale applications of phased control, using fuzzy inference, to fed-batch cultures for α-amylase production and recombinant β-galactosidase production.

Characteristics of these fuzzy control systems and the usefulness of fuzzy control for automatic control of bioprocess are reviewed.

An advanced control tool developed from study of fuzzy control, a fuzzy neural network (FNN), has been proposed. FNN have been proven to be applicable to research in biomedical fields, for example modeling of the complicated causality between electroencephalogram or gene expression profiling data and prognostic prediction. Successful results in this research are also reviewed.

2
Fuzzy control systems and their application in bioprocess control

2.1
Direct inference of process variables

Different process variables are often determined directly from fuzzy inference. As a process variable, glucose feed rate in fed-batch culture has received much attention. Nakamura et al. [6] reported the use of fuzzy control for determination of sugar feed rate in glutamic acid fermentation. The rate of consumption of ammonia in glutamic acid fermentation was correlated with the rate of consumption of sugar, and it was found that control of the sugar feed rate was important for glutamic acid production at low sugar concentrations in fed-batch culture. Fermentation was performed in a 1 kL bench-scale fermenter. This was the first application of fuzzy control in Japan in which the effectiveness of fuzzy control was proven in large-scale fermentation.

2.1.1
Feed rate

2.1.1.1
α-Amylase Production

Because catabolite repression of glucose and the inhibitory effect of by-products such as ethanol or lactate cannot be ignored in fermentation, it is important to maintain glucose and inhibitor concentrations at low levels. Figure 1 shows the effect of ethanol concentration on specific growth rate, μ, and the productivity in the fermentation of *Saccharomyces cerevisiae*. For this purpose a fuzzy control

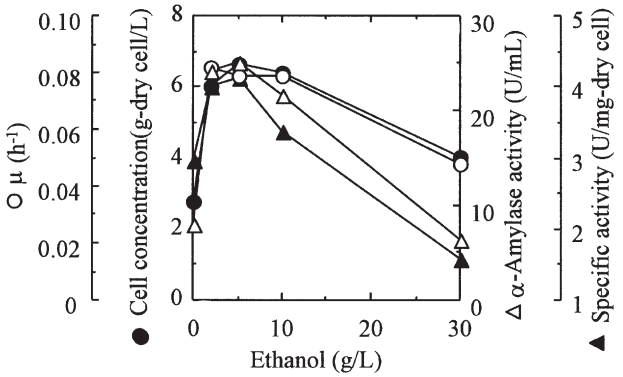

Fig. 1 Effects of ethanol concentration in batch culture of *S. cerevisiae* 20B-12/pNA3. Symbols: (*open circles*), specific growth rate (h^{-1}); (*filled circles*), cell concentration (g L^{-1}); (*open triangles*), α-amylase (U mL^{-1}); (*filled triangles*), specific α-amylase activity (U mg^{-1} dry cells)

strategy consisting of a feed forward and a feedback control [20] has been often used for feed rate control.

The dependence of feed-forward glucose feed rate, F^*, on the increasing cell concentration can be determined as follows:

$$F^* = \mu XV/Y_{x/s}S_o \tag{1}$$

where μ, X, S_o, and $Y_{x/s}$ denote the specific growth rate, concentrations of cell and feed glucose, and cellular yield from glucose, respectively. The previous determination of normal glucose feed rate is just a rough approximation. Because of changes in cell activity and environmental conditions, the feed rate must be corrected. This correction was noted as *DF* which was determined by the fuzzy control algorithm. Determination of *DF* was carried out by fuzzy inference.

$$F = F^* + DF \tag{2}$$

Table 1 shows the production rules. Membership functions for inputs and outputs are established as in Fig. 2. "S", "M", and "B" concentrations were set at 0.1, 0.2,

Table 1 Production rules of fuzzy control

DO concentration: M				DO concentration: B			
Ethanol	Glucose			Ethanol	Glucose		
	S	M	B		S	M	B
S	PM	PS	NS	S	PB	PM	ZE
M	PS	ZE	NM	M	PM	ZE	NS
B	NS	NM	NB	B	ZE	NS	NB

S: small, M: medium, B: large, P: positive, N: negative, ZE: zero.

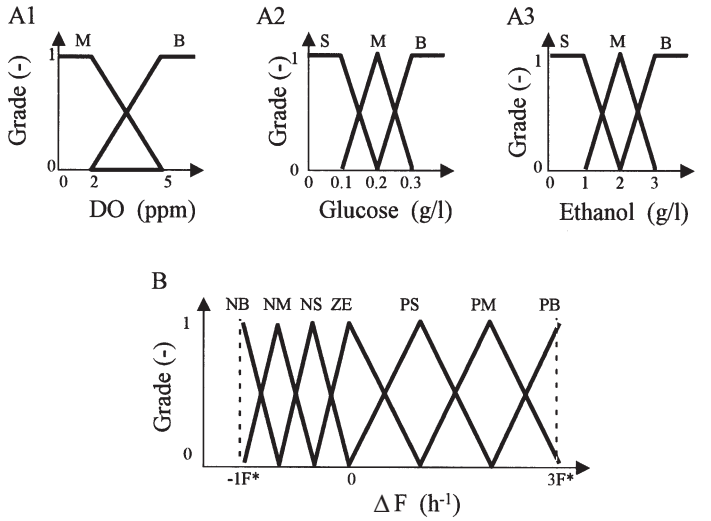

Fig. 2 Membership functions of DO **A1**, glucose **A2**, and ethanol **A3**, and output **B**. Characters: *B*, large; *M*, medium; *S*, small; *PB*, positive large; *PM*, positive medium; *PS*, positive small; *ZE*, zero; *NS*, negative small; *NM*, negative medium; *NB*, negative large

and 0.3 g L^{-1} for glucose and 1, 2, and 3 g L^{-1} for ethanol, respectively. Concerning DO concentration, only two memberships "M" and "B" were set in this research, because it did not much vary throughout fermentation. The inference procedure was carried out by use of Mamdani's min–max algorithm [21]. Defuzzification is then carried out using a simplified center-of-gravity method:

$$DF = \int DF g(DF) \mathrm{d}DF / \int g(DF) \mathrm{d}DF \tag{3}$$

Here, g is an output variable membership function. In this case, the value of DF is bound by $-1F^*(DF\mathrm{min})$ and $+3F^*(DF\mathrm{max})$ (Fig. 2b).

Cultivation results are shown in Figure 3. When glucose alone was controlled ethanol was accumulated and then α-amylase production was 120 U mL^{-1} (Fig. 3A). On the other hand, when ethanol and glucose were controlled by fuzzy inference as mentioned above, those concentrations were kept almost constant during cultivation because accumulated ethanol was consumed. At the end of fermentation 400 U mL^{-1} α-amylase was obtained (Fig. 3B).

2.1.2 *Temperature*

Japan's traditional sake brewing technology has been formulated through accumulation of various kinds of technical knowledge by sake-brewing experts (*Toji*). Steamed rice is added to a mashing (*moromi*) tank. Fungi and yeast are inoculated and saccharification and fermentation are carried out simultaneously. In the early *moromi* phase, temperature increases because of fermentation heat and the

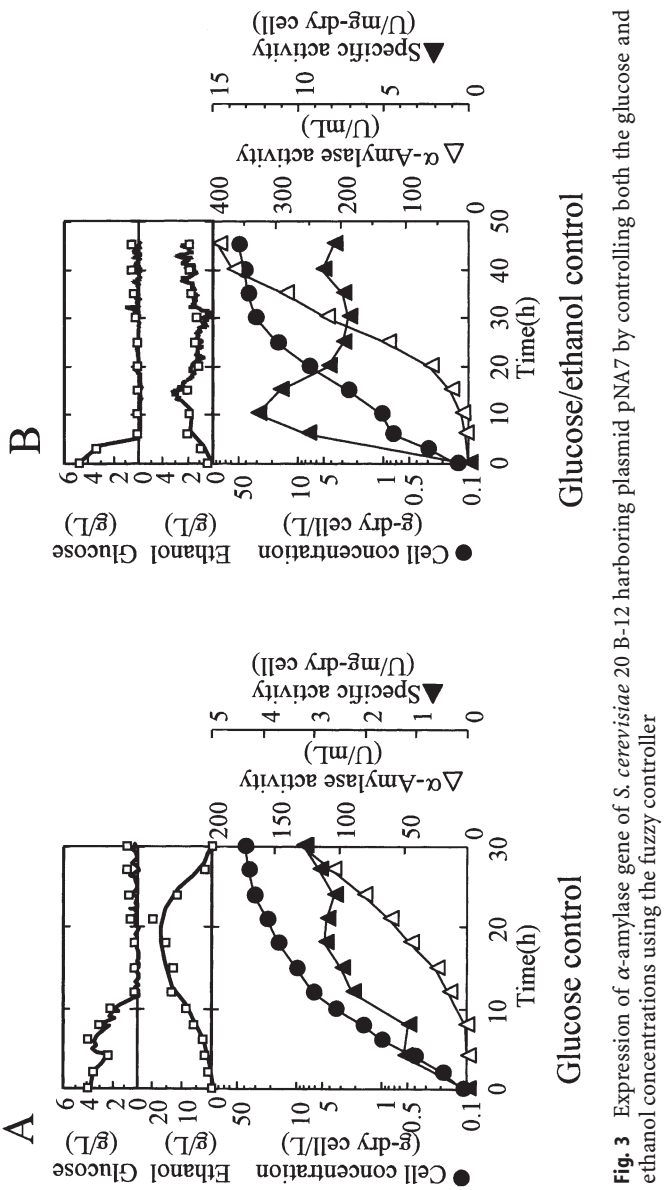

Fig. 3 Expression of α-amylase gene of *S. cerevisiae* 20 B-12 harboring plasmid pNA7 by controlling both the glucose and ethanol concentrations using the fuzzy controller

expert gradually decreases temperature in the late phase, depending on the *moromi* state, to increase the ester component. In the *moromi* phase, measurable state variables are alcohol concentration, specific gravity (Baumé), and temperature. To brew a sake of a desired quality, only temperature is precisely controlled by the *Toji*. There are many reports on temperature control of *moromi* by fuzzy inference [3, 22–25].

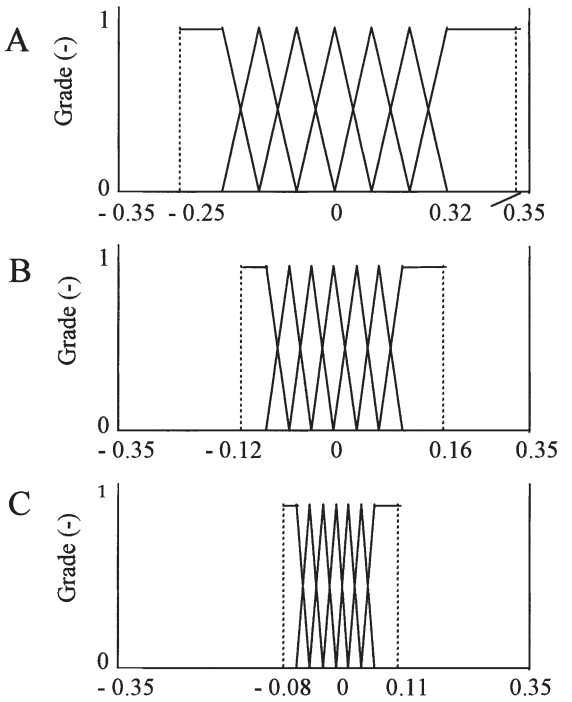

Fig. 4 Membership functions of *DB* for the different brewing periods. **A**, 5th day; **B**, 12th day; **C**, 15th day

2.1.2.1 Japanese sake fermentation

Oishi et al. [22] reported the fuzzy control of *moromi* process. The expert usually judges a change in *moromi* temperature (*CT*) by subjective evaluation of three properties:

- the difference between estimated and reference Baumé values at a future target time (*DB*);
- the difference between the decreasing rate of Baumé and that of the reference Baumé up to the present time (*DD*); and
- the alcohol concentration (*AL*) at the present time.

They constructed the fuzzy rules for temperature control by using *CT*, *AL*, *DB*, and *DD*. As shown in Figure 4, membership functions of *DB* were changed on the basis of the *moromi* period. In addition, production rules were also changed depending on alcohol concentration.

We have also reported the fuzzy control of *Ginjo* sake mashing [10, 26]. *Ginjo* sake has an extremely rich flavor and is categorized as a special grade. In this process an advanced fuzzy control algorithm – a fuzzy neural network (FNN) – was also applied (see below).

2.2 Identification of the culture phase

Phase recognition is one of the most important aspects of the precise control of process variables, because nutrient consumption rate or the product formation rate depends on the physiological condition of microorganism. Therefore, the fuzzy control strategy should be also changed in each culture phase, for example the lag phase, the early logarithmic phase, the late logarithmic phase, the production phase, and so on. The culture phase is identified by determination of state variables.

2.2.1 *Pravastatin precursor production*

ML-236B is the precursor of pravastatin sodium (trade name Mevalotin), a 3-hydroxy-3-methylglutaryl-CoA reductase inhibitor clinically applied in the treatment of hypercholesterolemia, which is produced by Sankyo Co. ML-236B is a fermentation product generated by *Penicillium citrinum*. Production of ML-236B depends strictly on culture broth pH, which can be regulated by adjusting the sugar concentration. Hosobuchi et al. [11] constructed the fuzzy controller for determination of the sugar feed rate. The cultivation period could be divided into five clustered phases. The feeding control strategy was altered for each phase.

The rules used by skilled operators to control the sugar feed rate in the production culture are as described in Table 2. These rules were expressed linguistically, and the control of feed rate by skilled operators was carried out sequentially. The membership function for each state variable and the method of control in each phase were constructed (Fig. 5). In this case, TCO (total CO_2 evolved) and PHV (pH value) are used for phase recognition. For example:

– If TCO=B and PHV=M, then phase=III.

Table 2 Rules for culture phase identification and selection of sugar feeding

1. If the concentration of the reducing sugar is more than 1% the culture is in phase 1 and no sugar is to be fed.
2. If the concentration of the reducing sugar is less than 1% during the period from 30 to 50 h after starting the culture the culture is in phase 2 and sugar feeding is to be maintained at a constant rate.
3. If the pH is less than 4.3 the culture is in phase 3 and the feed rate is to be gradually reduced.
4. If the pH is less than 4.0 and the slope of the pH begins to rise then the culture is in phase 4 and the feed rate should be gradually increased.
5. If the pH is around the set point then the feed rate should be decided in accordance with the relationship:

pH value	Sugar feed rate	Slope of pH	Sugar feed rate
High	Increase	Up	Increase
Low	Decrease	Down	Decrease

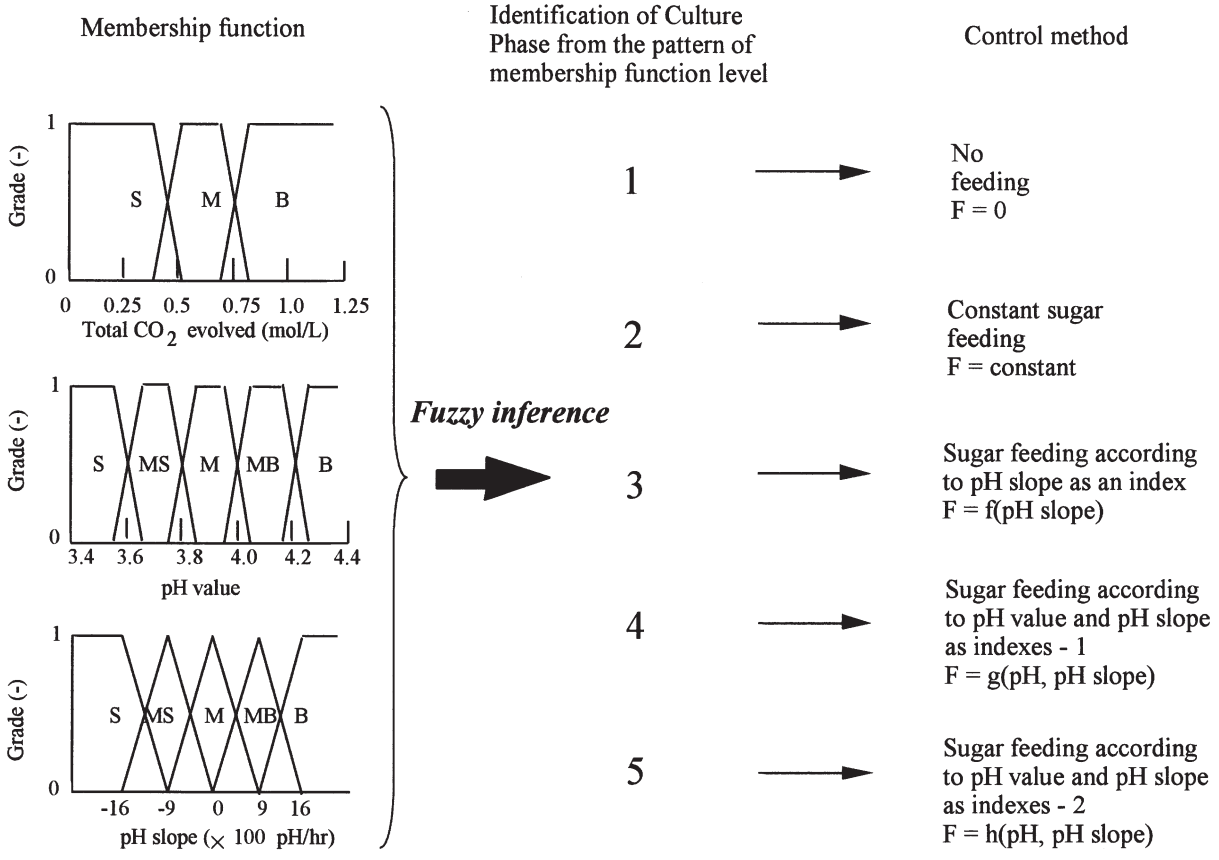

Fig. 5 The membership function for each state variable and the method of control in each phase

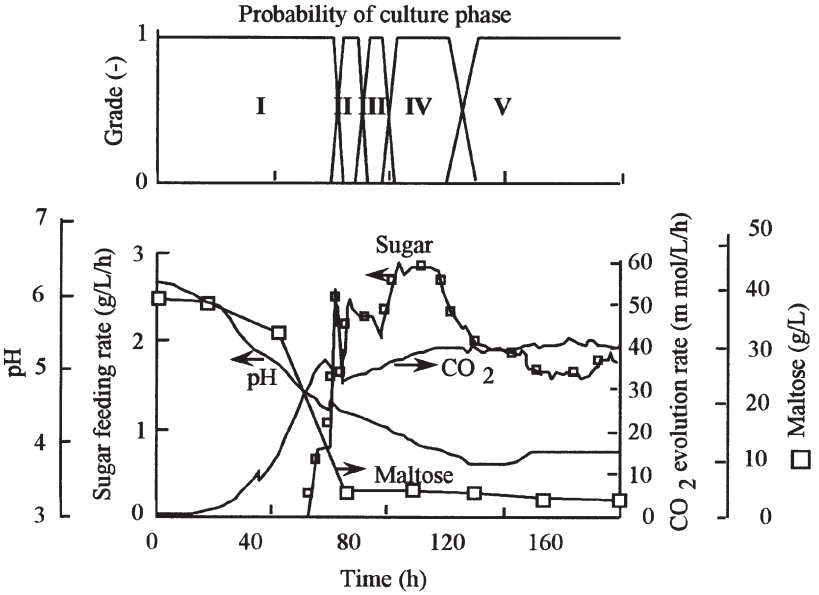

Fig. 6 Time courses of probability of culture phases in ML-236B production culture with fuzzy control of the sugar feed rate using a 30 L fermenter

The probability, p, that the measured state falls into phase i (i=I, II, III, IV or V) was calculated as follows:

– If p(TCO=B)=1 and p(PHV=M)=0.6, then p(phase III)=0.6

The value of the operating variable (sugar feed rate), F, was calculated for each situation. Sugeno's inference method III [27] was used for defuzzification. For example, the sugar feed rate in phase III, *FIII*, was defined as:

– If pH slope is *B*, then *FIII*=7.0
– If pH slope is *MB*, then *FIII*=6.0

When the value of pH slope was classified as intermediate between B and MB, *FIII* was defined as follows:

$$FIII = (pB \times 7.0 + pMB \times 6.0)/(pB + pMB) \quad (4)$$

The fuzzy controller was applied to the determination of sugar feed rate in the industrial production of ML-236B [11]. Figure 6 shows the time course of ML-236B production under fuzzy control using a 30-L fermenter. The time courses of the probability of the classified culture phases inferred by fuzzy rules are shown in the upper portion of the figure. Sugar feeding was started when the maltose concentration was about 10 g L^{-1}. The pH gradually decreased from 40 h to 80 h and was controlled at about 3.9 to 4.0 after 80 h of cultivation. This result indicated that the control system using the fuzzy clustering theory worked well in ML-236B culture. This control system has been scaled-up to industrial scale in order to automate pH control in the fermentation process.

In Sankyo Co., milbemycin production has been also performed by fuzzy control. In this case, low productivity of milbemycin was caused mainly by insufficient oxygen supply in a commercial-scale fermenter. Okada et al. [28] reported the problem could be overcome by the consistent and reliable actions of fuzzy control system. Over 100 cultivations on the industrial scale have been performed under fuzzy control.

2.2.2 *Vitamin B_2 (VB2) production*

Horiuchi and Hiraga [12] reported a fuzzy control system for large-scale recombinant VB2 production. The system was applied to the on-line control of the feed rate and pH for the fed-batch cultivation of *Bacillus* species to produce VB2.

Microbial VB2 production is a well-known process, but it has not been employed commercially, because of the high production costs compared with the conventional two-step process which comprises microbial conversion of glucose to D-ribose followed by chemical conversion of the ribose to riboflavin (VB2). Recently, however, Nippon Roche, Japan, has developed and commercialized single-step fermentative VB2 production using a recombinant *Bacillus* strain which effectively produces the VB2 directly from glucose in a fed-batch operation.

For phase identification four parameters (the culture time, CO_2 evolution rate, total CO_2 evolution, and DO) were selected as state variables on the basis of operating experiences and a simulation study. The control variables were the glucose feed rate and culture pH. On the basis of repeated operating experience the control variables were described as follows:

$$\text{Feed rate for A phase: } FA = aFA + bFA \times tA \tag{5}$$

$$\text{pH for A phase: } PHA = aPHA + bPHA \times tA \tag{6}$$

Here, a and b are the specific constants for each phase and t is the time from the beginning of the A phase. Accurate phase identification is therefore desired.

Figure 7 shows a typical set of results from a fed-batch culture for recombinant VB2 production under fuzzy control. Figure 7A displays the results of culture phase identification as the time courses of the average adaptabilities of the on-line data to the rules for each phase. The culture phase transitions from the lag phase to production phase 2, which are regarded as fuzzy sets, because they have ambiguous and overlapping boundaries, were properly recognized by the system. Identification of the culture phases by the inference system coincided almost exactly with identifications made by the experienced operators. Figures 7B and 7C show the glucose feed rate and pH as they were inferred and controlled by the system. Figure 7D shows the time courses of the optical density at 540 nm and VB2 concentration. As a result of appropriate feeding and pH control the final VB2 concentration reached the level of the maximum concentration achieved in a fed-batch culture manually controlled by experienced operators.

This fuzzy control system has been successfully operated in a large-scale main fermenter for more than 2 years, during which time over 200 batches have been

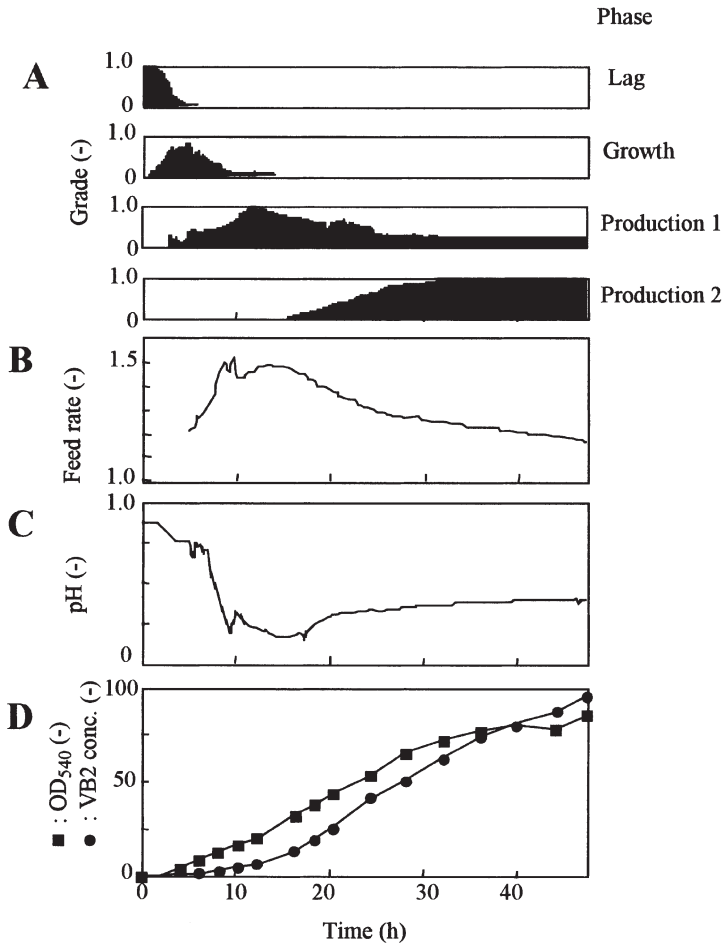

Fig. 7 Results from fuzzy control of a fed-batch culture for recombinant VB2 production. Time courses of: **A**, average adaptability of on-line data to the rule for each phase; **B**, glucose feed rate; **C**, pH; and **D**, cell concentration and VB2 concentration

completed. These results show that the system is able to successfully carry out these tasks in commercial-scale production. Fuzzy inference is a useful tool for realizing on-line control based on qualitative characteristics such as culture phases and empirical information gained from operators, both of which play significant roles in the daily operation of industrial fermentation processes.

2.3
Fuzzy neural network (FNN) as automatic fuzzy controller

Construction of the fuzzy controller takes usually a relatively long time to tune membership functions by trial and error or by simulation and much expert experience is necessary for identifying the rules.

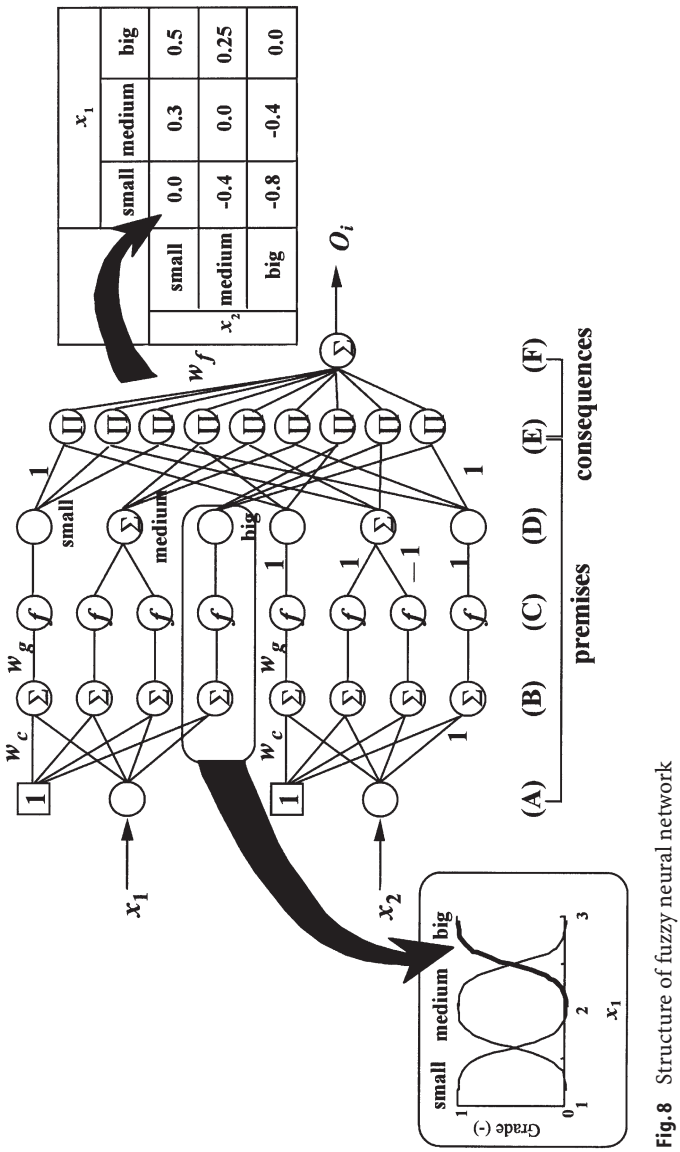

Fig.8 Structure of fuzzy neural network

Fuzzy neural networks (FNNs) have been studied as an advanced tool for fuzzy modeling [29–33]. FNNs have neural network structures in which fuzzy production rules and membership functions are automatically acquired and tuned from the numerical data collected. Hanai et al. [31] constructed an FNN model for temperature control of *Ginjo* sake mashings without manual tuning. Tuning and *Toji*' experience were not necessary for construction in this modeling method. The acquired fuzzy rules of the FNN can be linguistically compared with the experience of *Toji*.

The configuration of FNN "Type I" is shown in Figure 8. The FNN realizes a simplified fuzzy inference. The consequences of FNN are described with singletons. The inputs are non-fuzzy numbers. In Figure 8 the FNN has two inputs x_1 and x_2 and one output y^* and three membership functions in each premise. The symbols of the circle and square in Figure 8 mean units of the neural network and the symbols w_c, w_g, w_f, 1 and –1 denote the connection weights. The connection weights w_c and w_g determine the positions and gradients, respectively, of the sigmoid functions "f" in the units of the (C)-layer; the sigmoid functions "f" are defined as follows:

$$f(x) = 1/1 + \exp\{-w_g(x + w_c)\} \tag{7}$$

Each membership function consists of one or two sigmoid functions.

In the FNN, the membership functions in the premises are tuned and the fuzzy rules are identified by adjusting the connection weights w_c, w_g, and w_f by the back-propagation learning algorithm [34]. The connection weights w_c and w_g are initialized so that the membership functions in the premises are appropriately allocated equally. The value of w_f is initialized to be zero. This means that the FNN has no rules at the beginning of the learning.

After learning, acquired connection weights w_f can be described linguistically as follows:

– If x_1 is big and x_2 is small, then output variables should be 0.5.

Using this tool, fuzzy rules for the bioprocess can be acquired precisely without tuning of membership functions and from the fermentation results obtained so far, not by interviewing the expert. Moreover, if necessary, parameter determination method was incorporated in the modeling. This is called the "parameter increasing method (PIM)", in which suitable parameters were determined stepwise. By use of the PIM parameter combinations suitable for modeling can be decided (see Refs. on FNN, for example [30–33]).

For temperature control of *Ginjo* sake mashing an FNN model was constructed. The accuracy of the FNN model was confirmed from the results of the simulation, which were compared with average values from 25 *Ginjo* mashings. Using the FNN model, *Ginjo* sake mashings using 1500 kg total rice were performed by Sekiya Brewing Co. [33]. The time course pattern and the *Ginjo* sake produced were compared with those produced by the conventional method operated by a *Toji*.

Mashing results are described in Fig. 9. The time courses of Baumé and alcohol concentration coincided well with those of the conventional method throughout the mashing period. Temperature in the *moromi* mashing using the FNN model reached a maximum 2 days later than in the conventional process and was a little lower from the 20th to the 28th day. As shown in Table 3, the mashing period and all other values were in the same range as the other seven mashings performed conventionally by the *Toji*. The score for the flavor of the sake produced by FNN control was very similar to that of the conventional control. Therefore, it was confirmed that the mashing was performed well by use of the FNN model.

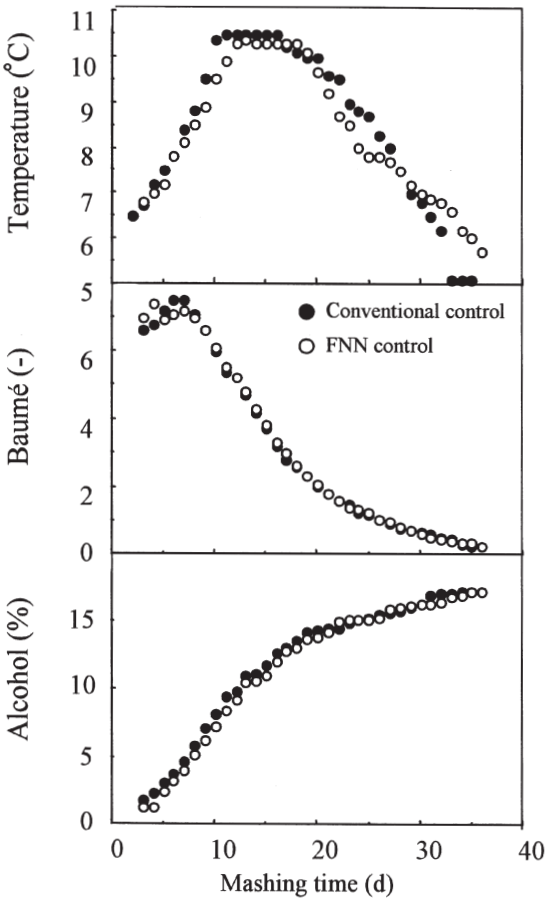

Fig. 9 Time courses of temperature, Baumé, and alcohol concentration

Table 3 Comparison of mashes on the finishing day

	FNN control	Conventional control	References[a]		
			Average	Minimum	Maximum
Mashing period (days)	36	35	34	33	36
Baumé (–)	0.20	0.25	0.16	0	0.30
Alcohol (%)	17.2	17.3	17.1	17.0	17.3
BMD (days)[b]	7.0	8.5	6.1	0	9.9
Acidity (mL)	1.5	1.5	1.5	1.4	1.6

[a] These data were obtained from seven other mashes operated under similar conditions.
[b] BMD means Baumé Multiple Day.

3
Application in biomedicine

The FNN model proposed by us has some benefits, because the model can be constructed automatically from data sets collected previously and does not need much time for tuning membership function compared with conventional fuzzy control. In addition, the rules acquired after learning can be described linguistically as IF–THEN rules which are so explicit as to be understood. FNN can involve a complicated causality between input and output data as network model. From this feature, FNN is applicable to modeling in other fields. In this section, two examples investigated by us are introduced.

3.1
Analysis of electroencephalogram

There are at present some 580 million people aged over 60 in the world, and it is estimated there will be almost 1970 million by 2050. Concomitant with this rapid growth in the elderly population, the number of dementia patients, which is now approximately 29 million, is predicted to rise to as many as 80 million within a few decades. For this reason, dementia is receiving much research attention. In current research [35], we have investigated a modeling system for assessing dementia of the Alzheimer type (DAT) from electroencephalogram (EEG) data by means of fuzzy neural networks (FNNs).

EEG data were collected using 15 electrodes (F_3, F_4, F_Z, C_3, C_4, C_Z, T_3, T_4, T_5, T_6, P_3, P_4, P_Z, O_1, and O_2) placed on the scalp in accordance with the international 10–20 system with bimastoid average reference. The power spectra were calculated by the fast Fourier transform. For each electrode, the power spectrum was divided into nine frequency bands (Table 4) and relative power values were calculated. The θ_1 (4.0–6.0 Hz), θ_2 (6.0–8.0 Hz), and α (8.0–13.0 Hz) band data were used as the network input values. DAT severity was assessed by the Mini-Mental State (MMS) examination administered to each patient and the results were used as the output. Subjects were twenty-six DAT outpatients of the Nagoya City Rehabilitation Center.

Table 4 Characterized electroencephalogram waves

Band number	Frequency	Wave name
Band 1	3.0–4.0 Hz	δ-wave
Band 2	4.0–6.0 Hz	θ_1-wave
Band 3	6.0–8.0 Hz	θ_2-wave
Band 4	8.0–9.0 Hz	α-wave
Band 5	9.0–11.0 Hz	
Band 6	11.0–13.0 Hz	
Band 7	13.0–15.0 Hz	β-wave
Band 8	15.0–20.0 Hz	
Band 9	20.0–25.0 Hz	

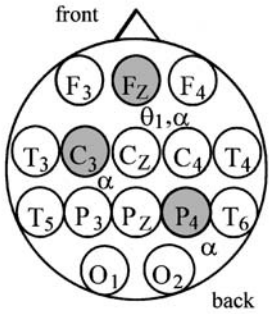

Fig. 10 Channels and frequency bands selected in the FNN models for DAT patient discrimination (*Top view*)

EEG data sets collected were applied to FNN modeling for DAT patient discrimination. The FNN model correctly distinguished 94% of the DAT patients from normal subjects. As shown in Fig. 10, four input variables were selected by the PIM for the FNN model: (F_Z:θ_1), (F_Z:α), (C_3:α), and (P_4:α). Next, we attempted to construct an FNN model to estimate the MMS scores from the EEG power spectrum. The relationship between actual value and estimated value is described in Fig. 11. The FNN model for severity estimation gave an average error of 2.57 points out of 30 in the MMS scores. Several rules expressed linguistically were acquired from the connection weights. An example of a rule in the DAT discrimination model is:

– IF (F_Z:θ_1) is "Big" AND (F_Z:α) is "Small" AND (C_3:α) is "Big" AND (P_4:α) is "Big" THEN the output is "Big" (non-DAT).

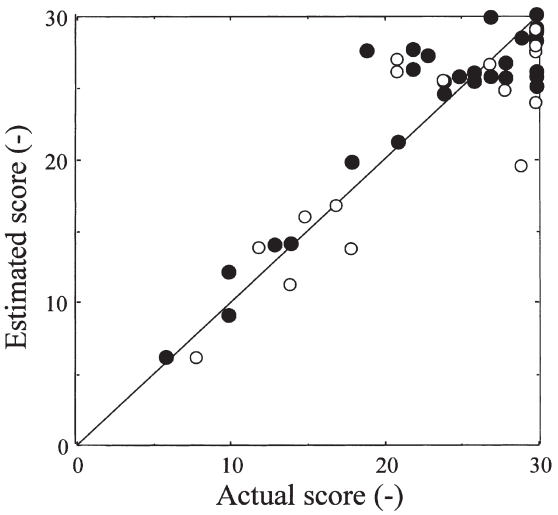

Fig. 11 Estimation of MMS scores by FNN: *filled circles*, learning data scores; *open circles*, evaluation data scores

The FNNs were found to be useful tools for discriminating DAT patients from normal subjects and for estimating quantitatively the severity of DAT symptoms from EEG data. It is expected the models will prove useful for diagnostic purposes and in the development of home-care systems, although many more data need to be accumulated to further improve their accuracy.

3.2 Analysis of gene expression profiling data

The recent development of microarray analysis provides a new tool for establishing prognoses of various diseases. With microarray data comparison of gene expression in tissues from distinct patient groups and their normal counterparts will lead to more comprehensive and detailed understanding of the molecular mechanisms of the disease than can be obtained from general data such as clinical stage and age of the patient. The causal genes among several thousand genes is hard to select and construction of an accurate model using those genes is also very difficult. Researchers are, therefore, still stranded in front of exhaustive data from a microarray. Because FNN are among the most convenient modeling tools for expressing complicated relationships, we used FNN to model input, gene expression data, and output, diagnosis or survival of a malignant disease [36–38].

Diffuse large B-cell lymphoma (DLBCL) is the largest category of aggressive lymphoma. Fewer than 50% of patients can be cured by combination chemotherapy. Microarray technologies have recently shown that the response to chemotherapy reflects molecular heterogeneity in DLBCL. On the basis of published microarray data we therefore attempted to develop a long-overdue FNN method for precise and simple prediction of survival of DLBCL. Expression data of 5857 genes in 40 DLBCL patients were taken from the Stanford Microarray Database (http://genome-www5.stanford.edu/MicroArray/SMD/). From these data the model identified four genes (*CD10*, *AA807551*, *AA805611*, and *IRF-4*) that could be used to predict prognosis with 93% accuracy. The relationship between the input of four genes and the output of the survival score is described as a fuzzy rule, shown in Figure 12. A poor outcome was predicted particularly when *CD10* expression was low and *IRF-4* expression was high. Furthermore, the FNN model also identified cases for which the prognosis was poor despite a high expression ratio of *CD10*. Correct identification of these cases was achieved by adding the expression information on the other two genes; outcomes for patients are poor even though *CD10* expression is high if *AA807751* is high and *AA805611* is low. Kaplan–Meier survival analyses indicated that patients predicted to live by the FNN model survived for longer than patients predicted to die (Fig. 13). This result indicates the existence of a gene-expression signature in DLBCL associated with better outcome. It was proven that FNNs are powerful tools for extracting significant biological markers affecting prognosis and can be applied to different kinds of expression profiling data for any malignancy.

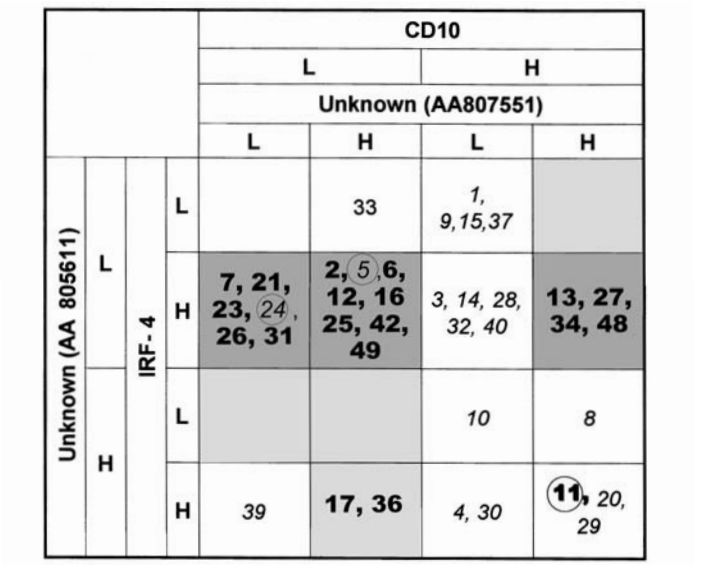

Fig. 12 Relationship among four input genes and predicted outcome. H and L refer to the high and low expression levels, respectively, of each gene. Because the expression level of each gene can be divided into either high or low groups according to fuzzy reasoning, this model comprised 16 ($=2^4$) fuzzy rules. *Light gray* areas represent predicted poorer prognosis by the FNN. *Dark gray* areas represent the poorest prognosis. Numbers in each matrix cell are the patients' numbers previously described by Alizadeh et al. (Nature 403:503–511 (2000)). *Bold* numbers indicate the patients dead within four years, *italic* numbers indicate live patients after four years. Patient numbers are placed in the matrix according to the expression levels of the four genes in that patient. Patient numbers in *circles* denote incorrect classification by the FNN

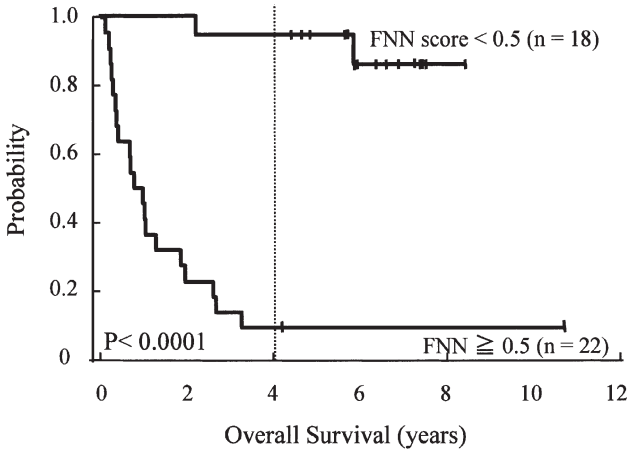

Fig. 13 Kaplan–Meier plot of the four-year overall survival for all patients grouped by FNN score. The *p*-value for the predicted outcome groups was computed using a log-rank test

4 Summary

Fuzzy control systems based on knowledge-base rules are categorized into two types – direct inference of process variables and indirect inference via phase identification. Even for direct inference, constructed fuzzy rules almost always change during the culture period used to realize precise control of process variables. This means that the fuzzy rules depend on the different culture phases, which depend on the physiological state of the microorganism. In many cases, no clear structure for phase recognition is included in the fuzzy controller. However, different physiological states implicitly imply the need for many fuzzy rules.

Construction of an algorithm for phase identification plays an important role when the control strategy is significantly different in each phase. In addition, identification of a phase and its indication during cultivation enables the system to be operator-friendly in use and increases the reliability of the operation.

In Japan, some industrial processes have been operated under fuzzy control. In this article, three examples were introduced – Mevalotin precursor production (Sankyo), vitamin B_2 production (Nippon Roche), and sake mashing (Sekiya Brewing, Gekkeikan, and Ozeki). For precise control of bioprocesses much skilled operator knowledge is very important. In almost all bioprocess, many rules on process operation should be acquired explicitly or implicitly. Fuzzy control is a useful tool for incorporating these linguistic rules into computer control. The fuzzy control systems will be established, moreover, and the application of fuzzy control will proceed widely in the field of bioprocess control.

Construction of the fuzzy controller takes usually a relatively long time to tune membership functions by trial and error or by simulation and much expert experience is necessary to identifying the rules. Fuzzy neural networks (FNNs) are an advanced tool for fuzzy modeling [29–33] in which fuzzy production rules and membership functions are automatically acquired and tuned from the numerical data collected. FNN modeling has been applied not only to monitoring and control [39, 40] and software sensing [41] of bioprocesses but also research to in other fields, for example biomedical engineering [35, 36, 42], biological science [43], environmental monitoring [44], or food engineering [45, 46]. Because FNN can involve complicated causality between input and output conditions as a network model, we expect attempts will be made to apply FNN to all scientific modeling.

5 References

1. Zadeh LA (1965) Inf Control 8:338
2. Filev DP, Kishimoto M, Sengupta S, Yoshida T, Taguchi H (1985) J Ferment Technol 63:545
3. Tsuchiya Y, Koizumi J, Suenari K, Teshima Y, Nagai S (1990) Hakkoukogaku Kaishi 68:123 (in Japanese)
4. Horiuchi J, Kishimoto M, Momose H (1995) J Ferment Technol 79:297
5. Kishimoto M, Moo-Young M, Allsop P (1991) Bioproc Eng 6:163
6. Nakamura T, Kuratani T, Morita Y (1985) Proc. IFAC Modeling and Control of Biotechnology Process. Pergamon Press, Oxford, p 211

7. Kishimoto M, Kitta Y, Takeuchi S, Nakajima M, Yoshida T (1991b) J Ferment Bioeng 72:110
8. Shi ZP, Shimizu K (1992) J Ferment Bioeng 74:39
9. Shiba S, Nishida Y, Park YS, Iijima S, Kobayashi T (1994) Biotechnol Bioeng 44:1055
10. Hanai T, Honda H, Takahasi N, Nishida T, Fukaya I, Kobayashi T (1994) Seibutsu-kogaku Kaishi 72:275 (in Japanese)
11. Hosobuchi M, Fukui F, Matsukawa H, Suzuki T, Yoshikawa H (1993) J Ferment Technol 76:482
12. Horiuchi J, Hiraga K (1998) Proc. 7th Int Conf Computer Application in Biotechnology – CAB7. IFAC Publications, Elsevier Science, Oxford, p 281
13. Alfafara C, Miura K, Shimizu H, Shioya S, Suga K, Suzuki K (1993) Biotechnol Bioeng 41:493
14. Konstantinov KB, Yoshida T (1989) Biotechnol Bioeng 33:1145
15. Konstantinov KB, Yoshida T (1990) J Ferment Bioeng 70:48
16. Konstantinov KB, Yoshida T (1990) J Ferment Bioeng 70:420
17. Shimizu H, Miura K, Shioya S, Suga K (1995) Biotechnol Bioeng 41:165
18. Horiuchi J, Kamasawa M, Miyakawa H, Kishimoto M (1993) J Ferment Bioeng 76:207
19. Horiuchi J, Kamasawa M, Miyakawa H, Kishimoto M, Momose H (1993) J Ferment Technol 76:382
20. Park YS, Shi ZP, Shiba S, Chantal C, Iijima S, Kobayashi T (1993) Appl Microb Biotechnol 38:649
21. Mamdani EH (1976) Int J Man–Machine Studies 8:669
22. Oishi K, Tominaga M, Kawato A, Imayasu S, Nanba S (1991) J Ferment Bioeng 72:115
23. Suenari K, Tsuchiya Y, Teshima Y, Koizumi J, Nagai S (1990) Hakkoukogaku Kaishi 68:131 (in Japanese)
24. Imayasu S, Suginami K, Abe Y, Kawado A, Oishi K (1993) Seibutsu-kogaku Kaishi 71:29 (in Japanese)
25. Matsu-ura K, Shiba H, Hirotsune M, Hamachi M (1995) J Ferment Bioeng 80:251
26. Hanai T, Nishida T, Ohkusu E, Honda H, Kobayashi T (1995) Seibutsu-kogaku Kaishi 73:283 (in Japanese)
27. Sugeno M (1988) (ed) Fuzzy control, 1st edn. Nikkan Kogyo Shinbunsha, Tokyo, p 88
28. Okada S (1995) Seibutsu-kogaku Kaishi 74:203 (in Japanese)
29. Ye K, Jin S, Shimizu K (1994) J Ferment Bioeng 77:663
30. Hanai T, Kakamu A, Honda H, Furuhashi T, Uchikawa Y, Kobayashi T (1996) Trans Soc Inst Cont Eng 32:1113
31. Hanai T, Katayama A, Honda H, Kobayashi T (1997) J Chem Eng Japan 30:94
32. Nishida Y, Hanai T, Katayama A, Honda H, Fukaya I, Kobayashi T (1997) J Brew Soc Japan 92:447
33. Honda H, Hanai T, Katayama A, Tohyama H, Kobayashi T (1998) J Ferment Bioeng 85:107
34. Rumelhart DE, Hinton GE, Williams RJ (1986) Nature 323:533
35. Hibino S, Hanai T, Nagata E, Matsubara M, Fukagawa K, Shirataki T, Honda H, Kobayashi T (2001) J Chem Eng Japan 34:936
36. Ando T, Suguro M, Hanai T, Kobayashi T, Honda H, Seto M (2002) J Cancer Res 93:1207
37. Ando T, Suguro M, Hanai T, Kobayashi T, Seto M, Honda H (2003) J Biosci Bioeng 96:161
38. Ando T, Suguro M, Hanai T, Kobayashi T, Seto M, Honda H (2003) Cancer Sci 94:906
39. Tomida S, Hanai T, Ueda N, Honda H, Kobayashi T (1999) J Biosci Bioeng 88:215
40. Tomida S, Hanai T, Honda H, Kobayashi T (2001) J Chem Eng Japan 34:369
41. Hibino S, Hanai T, Nagata E, Matsubara M, Fukagawa K, Shirataki T, Honda H, Kobayashi T (2001) Clinic Electroencephal 43:109
42. Imanishi T, Hanai T, Aoyagi I, Uemura J, Araki K, Yoshimoto H, Harima T, Honda H, Kobayashi T (2002) Biotechnol Bioprocess Eng 7:275
43. Noguchi H, Hanai T, Honda H, Harrison LC, Kobayashi T (2001) J Biosci Bioeng 92:227
44. Nagamori E, Honda H, Hanai T, Nakanishi K, Hata N, Masuda T, Kobayashi T (2001) J Chem Eng Japan 34:998
45. Tominaga O, Ito F, Hanai T, Honda H, Kobayashi T (2002) J Food Sci 67:363
46. Tominaga O, Ito F, Hanai T, Honda H, Kobayashi T (2002) Food Sci Technol Res 8:281

Received: May 2003

Adv Biochem Engin/Biotechnol (2004) 87: 173 – 194
DOI 10.1007/b94365

Production of Lactic Acid from Paper Sludge by Simultaneous Saccharification and Fermentation

Sang-Mok Lee[1] · Yoon-Mo Koo[1] · Jianqiang Lin[2]

[1] ERC for the Advanced Bioseparation Technology, Department of Biological Engineering, Inha University, Incheon 402-751, Korea
[2] State Key Laboratory of Microbial Technology, Shandong University, Jinan 250100, China
E-mail: ymkoo@inha.ac.kr

Abstract Production of lactic acid from paper sludge has been performed by simultaneous saccharification and fermentation (SSF). The SSF process design was based on experimental data obtained from cellulose hydrolysis and fermentation. The SSF process was employed to avoid an excessively dense solution when the sludge content of the feed was higher than 15%; this is one of several benefits of SSF. The enzyme system used for hydrolysis of paper sludge for production of glucose was optimized. CMCase and β-glucosidase with activities of 2.5 and 10 U mL^{-1}, respectively, were found to be optimum for hydrolyzing 5% sludge. In batch SSF 16 g L^{-1} lactic acid was produced from 5% paper sludge with an yield of 80%. Paper sludge which served as a feed seemed to have a buffering effect during SSF, probably because of the inorganic ash component in the sludge. The final product concentration by SSF was observed to be limited by the cellulose content of the system, which can probably be resolved by intermittent feeding of the paper sludge. SSF of paper sludge fed in batch mode, with intermittent feeding, produced lactic acid at 162 g L^{-1}, with a yield of 74% and a productivity of 1.4 g L^{-1} h^{-1}. The lactic acid production performance of the modified bioreactor improved after removal of indigestible solid materials from the upper compartment, which enabled the feed of paper sludge to be increased. A mathematical model is described which predicts glucose and subsequent lactic acid production on the basis of the rate expressions of each step of the SSF process. Saccharification kinetics were determined by experiments on enzymatic cellulose hydrolysis, by use of a Michaelis–Menten equation; growth kinetics of *L. rhamnosus* were determined by use of a Monod expression which incorporated lactic acid inhibition. The kinetic model is expected to predict the performance of the SSF process. For further use of the lactic acid, i.e. polylactic acid, it must be recovered and purified. Results from application of the simulated moving-bed (SMB) process for separation of lactic acid and acetic acid are given, as are several methods of lactic acid purification.

Keywords SSF (Simultaneous saccharification and fermentation) · Paper sludge · Cellulase · Cellulose · Lactic acid

List of abbreviations

B	Cellobiose concentration (g L^{-1})
S	Cellulose concentration (g L^{-1})
S^*	Oligosaccharide concentration (g L^{-1})
E	Enzyme concentration (g L^{-1})
G	Glucose concentration (g L^{-1})
K_1	Desorption rate (g L^{-1})
$E_{1.ad}$	Endoglucanase adsorbed on the cellulose (U g^{-1})
$E_{2.ad}$	Exoglucanase adsorbed on the cellulose (U g^{-1})
$E_{3.ad}$	β-Glucosidase adsorbed on the cellulose (U g^{-1})
$e_{1.ad}$	Saturated adsorption of endoglucanase (mg g^{-1})
$e_{2.ad}$	Saturated adsorption of exoglucanase (mg g^{-1})
$e_{3.ad}$	Saturated adsorption of β-glucosidase (mg g^{-1})
K	Glucose saturation constant (g L^{-1})
P	Product concentration (g L^{-1})
r	Rate of reaction (g L^{-1} h^{-1})
v	Maximum enzyme rate (g L^{-1} h^{-1})
X	Biomass concentration (g L^{-1})
Y	Biomass yield (g g^{-1})
α	Growth associated constant for product formation (g lactic acid g^{-1} biomass)
β	Non-growth associated constant for product formation (g lactic acid g^{-1} biomass h^{-1})
μ	Specific growth rate (h)
1	Endoglucanase reaction rate
2	Exoglucanase reaction rate
3	β-Glucosidase reaction rate
m	Maximum value
B	Cellobiose
E	Enzyme
G	Glucose
L	Lactic acid
V	Volume (L)
β_a	Constant representing the apparent activity of adsorbed β-glucosidase

1 Introduction

1.1 Conventional treatments of paper sludge

Increasing efforts are being made to recycle organic waste because of environmental concerns, government regulations, and economic considerations. The paper sludge generated by the waste water treatment units of paper mills is currently a major concern of the paper industry. It amounts to more than 1 million tons per year in Korea. Solid paper sludge waste is mostly disposed of by combustion or by landfilling. Some paper sludges are used as composts and building materials [1–4]. In terms of combustion treatment, paper sludge containing more than 60% water by weight should be incinerated in combustors with an auxiliary fuel. Land filling is expected to decrease because of the limitations of existing capacities, costs, and environmental concerns [1–3]. To be used as a compost, toxic materials must be removed. Currently, paper-sludge treatment costs about \$30 ton^{-1}, which is more than \$30 million $year^{-1}$ in Korea.

The paper sludge generated by paper companies is in the form of wet cake. Tables 1, 2, and 3 show the chemical composition of paper sludge generated by several paper companies. The water content of paper sludge is 60–70%. When dried sludge is burned at 550 °C, the average weight loss amounts to 35–70%. In other words, the non-flammable material in the dried sludge accounts for about

Table 1 Chemical composition of paper sludge (unit: %)

Company	Water	TS	VS (% of TS)	FS (% of TS)
A	60.6	39.4	37.3	62.7
B	59.5	40.5	55.7	44.3
C	67.9	32.1	48.2	51.8
D	70.0	18.0	71.5	28.5
E	75.6	24.4	48.1	51.9

TS: total solid.
VS: volatile solid.
FS: fixed solid.

Table 2 Organic composition of paper sludge (unit: % of TS)

Company	Hot water-extractable	Lignin	Hemi-cellulose	Cellulose
A	2.0	8.0	ND	30.6
B	3.1	11.8	ND	33.5
C	5.9	12.7	ND	30.3
D	16.4	16.2	3.5	28.9
E	9.4	5.6	–	28.3

ND: not detectable.

Table 3 Inorganic composition of paper sludge (unit: g kg^{-1})

Company	Al	Si	Ca	Cu	Fe	Mg	Mn	Cd	Ni
A	46.1	73.6	0.01	0.08	0.14	0.10	0.18	ND	ND
B	40.2	60.1	0.09	0.03	0.61	0.13	0.04	0.03	ND
C	11.9	18.6	1.29	0.06	0.40	0.17	0.01	ND	ND
D	20.0	64.1	0.23	0.04	0.35	0.10	0.02	ND	ND
E	31.3	47.8	0.10	0.03	0.93	0.24	0.33	ND	ND

ND: not detectable.

30–65% of its weight – the rest is flammable fiber. The cellulose fraction of the dried sludge is about 30%. The compositions of the raw materials are listed in Tables 2 and 3, which show that the major components of the ash are Al and Si.

1.2 Organic acid production from paper sludge

Biotechnology is often defined as a clean technology which produces valuable products from renewable resources. Cellulose waste from the pulp and paper industries is a fine biomass resource from which valuable products such as ethanol and organic acids can be fermented [5, 6]. Relatively little effort has been made to hydrolyze the cellulose waste of paper sludge, compared with research on the hydrolysis of starch. Mixed cellulase, consisting of endo/exo glucanase and β-glucosidase from *Trichoderma reesei* Rut C-30 and *Aspergillus niger*, respectively, can be used to hydrolyze the cellulose portion of paper sludge. The resulting hydrolysate can be used as a substrate for further fermentation to yield a variety of organic products (Fig. 1).

Carboxylic acids, including acetic, propionic, and butyric acids, are among the top-ranked commercial organic chemicals. Fermentation is an ideal way of producing carboxylic acids, because it is generally considered to be environmentally friendly and uses renewable resources. Acetic acid is an important chemical with an annual production of approximately 2 million metric tons in the USA in 1995. Acetic acid can be used to produce acetate deicer, an environmentally benign and non-corrosive agent that finds uses on airport runways, bridges, and strategic roads [7]. Recently, organic acids produced from organic wastes have been viewed favorably as sources for microbial production of biodegradable plastics [8]. To produce commodity chemicals, such as organic acids, it is necessary to use inexpensively and readily available raw materials. From this point of view large amounts of cellulosic materials are readily available, because they are

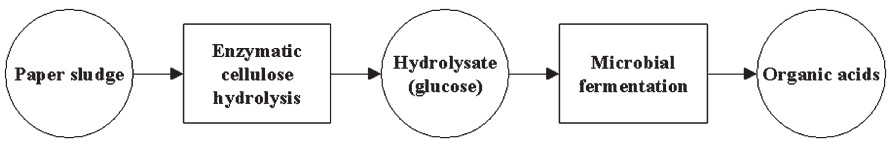

Fig. 1 Organic acid production from paper sludge using biological methods

Table 4 Industrial biopolymers in USA (1997)

Company	Capacity (1000 ton year^{-1})	Commercial name	Type
Eastman Chemical Company	1.1	Easter Bio	Copolyester 14766
Dupont	–	Biomax	PET-based
Planet Polymer Technologies	0.5	EnviroPlastic	Cellulose acetate
Cargill	4.5	ECO-PLA	PLA
Chronopol	1	HEPLON	PLA
Union Carbide	4.5	TONE	PCL
Bioplastics	<0.2	Envar	Starch and PCL
Uni-Star Industries	<0.5	StarKore	Starch
StarTech	<0.2		Starch
FP International	1	Flo-Pak Bio 8	Starch
American Excelsior	>2	Eco-Foam	Starch
Ecco/Green Packaging	<0.2	ReNature	Starch
EnPac	5	Enviromold	Starch (wheat-based)
Total	20		

Chemical Economics Handbook, 1998.
Bohlmann GM, Takei N (1998) Biodegradable polymers, CEH Marketing research report.
Earthshell examining product shipping sleeves, Chemical News Base, 1999.
Joint venture between Earth Shell Corp and Prairie Packing Inc; stage set for production of generation II products, Chemical News Base, 1999.

cheap and renewable. The worldwide demand for citric acid is met by fermentative production mainly by processes involving the filamentous fungus *Aspergillus niger* [9]. Oxalic acid has been shown to be the predominant organic acid produced by many white-rot fungi when grown in liquid medium or on lignocellulosic substrates, for example wheat straw [10]. Propionic acid and its salts are widely used as raw materials in different industries, and esters of propionic acid are used in the perfume industry, whereas cellulose propionate finds use as an important thermoplastic in the plastics industry [11].

Lactic acid is an organic acid found in many products of natural origin. It was first discovered in 1780 by the Swedish chemist Scheele. Lactic acid is an intermediate-volume specialty chemical (world production ~70,000 tons year^{-1} in 1997) [12, 13], which is used in a wide range of food processing and industrial applications. Lactic acid has the potential to become a very large-volume item, as a commodity-chemical intermediate produced from renewable carbohydrates, because it could be used as a feedstocks for biodegradable polymers, environmentally friendly clean solvents, and specialty chemical intermediates [13].

Lactic acid-based polymers (PLA) have previously been cited in several reviews. The first was published as early as 1948. Other, more recent, reviews concern its use in medical applications and biodegradation, its hydrolytic degradation in different environments, and its use in biopolymers and biocomposites [14]. During the last years of the 20th century several companies have attempted to produce large amounts of poly(lactide). The status of the main

industrial efforts to produce lactic acid and related compounds are indicated in Table 4. Cargill–Dow is a joint-venture between Dow Chemicals and Cargill, the largest poly(lactide) producing company, with a planned annual capacity of 140,000 metric tons, to be located in Blair, Nebraska, USA. PLA is currently produced by ring-opening polymerization; its main applications are in the fiber and packaging material industries. Moreover, lactic acid esters can be used as solvents. Research on lactic acid-related materials has attracted the attention of many institutes and universities in Europe, Asia, and the USA.

For lactic acid to be commercially attractive, economically efficient and environmentally sound manufacturing processes are needed for its production. Recent announcements of new lactic acid production plants by major chemical and agrochemical companies might usher in new technologies for the efficient, low-cost manufacture of lactic acid and its derivatives for new applications [13].

2
Lactic acid production from paper sludge

2.1
Enzymatic hydrolysis of paper sludge

Paper sludge has caused severe environmental problems. Utilizing the sludge as a raw material not only solves the environmental problem but also reduces production costs. The dried materials, comprising 40% of the paper sludge, are composed of 30 to 60% cellulose and 5 to 10% lignin, with the remainder being mainly inorganic ash. Cellulose in sludge can be hydrolyzed chemically or enzymatically to produce glucose, which in turn can be used as a substrate in fermentation for production of fuel [15, 16], organic acids [17], and other useful products. However, chemical hydrolysis of cellulose yields acid or alkaline waste, which will eventually lead to environmental pollution, whereas enzymatic hydrolysis is potentially free from this drawback. Many studies have been performed on the enzymatic hydrolysis of biomass such as different types of wood [18] and rice straw [19]. These natural materials must be pretreated to promote enzymatic attack [18–20]. Commercial development has been hindered, because these pretreatment processes require much energy [21, 22] and because of the high cost of the enzyme. Sludge, on the other hand, might require no pretreatment, because it has already been subject to a recycling process to remove lignin and hemicellulose, and is, therefore, much more susceptible to enzymatic hydrolysis [23]. In this research, the enzyme system was optimized to obtain high glucose yield with relatively low enzyme levels.

Cellulose is degraded by the synergistic action of three types of enzyme in the cellulase complex–endoglucanase, exoglucanase, and β-glucosidase. Endoglucanase acts randomly on the internal bonds of amorphous cellulose to fragment the polymer. Exoglucanase cuts the cellulose polymers from their non-reducing terminals producing cellobiose units. Exoglucanase is markedly inhibited by cellobiose, which is degraded by β-glucosidase into glucose, relieving the feedback inhibition of cellobiose on exoglucanase (Fig. 2). Because glucose, the final product, inhibits various steps in the cleavage of cellulose into glucose [24], it is

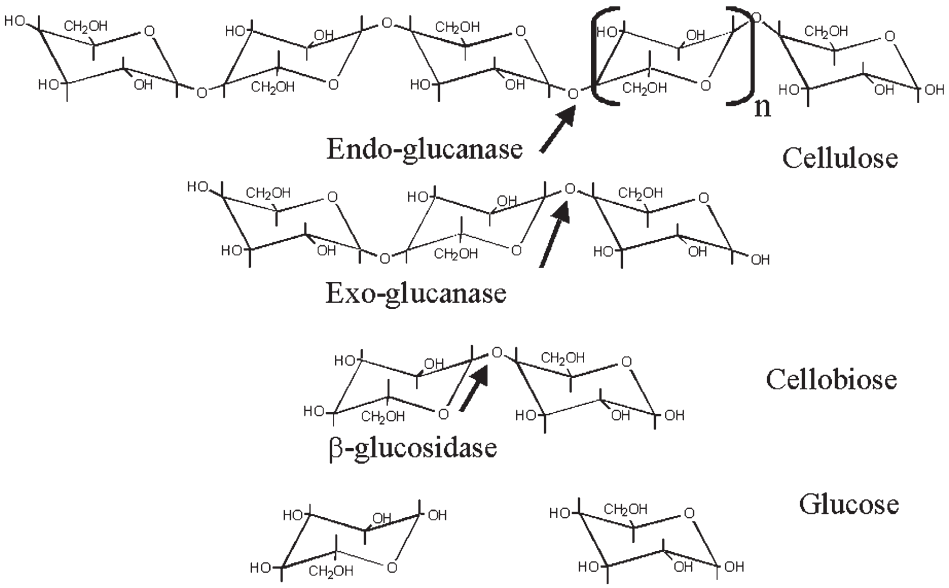

Fig. 2 Chemical structure of cellulose and reaction site (*diagonal arrow*) of cellulase

necessary to employ a balanced enzyme system containing appropriate relative amounts of the endo- and exo-types of glucanase, and β-glucosidase, to achieve efficient cellulose hydrolysis. In this research, we undertook to identify optimum conditions, especially with regard to the balance of the enzyme system for hydrolysis of paper mill sludge.

Raw cellulase powder, produced by *Trichoderma reesei* Rut C-30 (ATCC 56765), mixed with commercial β-glucosidase solution (Novozym 188, Novo Nordisk, Denmark) in different proportions was used in this research. Sludge and enzymes, at different levels, in 20 mL citrate buffer (pH 4.8), in 100 mL flasks, were incubated at 50 °C and 350 rpm in a shaking water bath (KMC Vision, Korea). Flasks containing the mixture of sludge and buffer solution were sterilized at 121 °C for 30 min and then cooled to about 50 °C before addition of the enzymes and antibiotics. The sludge was obtained from the Samwha Paper Company, Korea.

CMC- and FP-degrading activity, and avicelase and β-glucosidase activity were determined by the International Union of Pure and Applied Chemistry (IUPAC) method. One unit of enzyme activity was defined as the amount of enzyme releasing 1 μmol glucose min^{-1}. Glucose concentration in enzymatic hydrolysis experiments was measured by use of a glucose analyzer (YSI 2700, Yellow Springs Instrument Company, USA).

Cellulase and β-glucosidase were mixed in different combinations. Six levels of endoglucanase activity, 100, 50, 5, 2.5, 1.5 and 0.5 U mL^{-1}, (Fig. 3) and four levels of β-glucosidase activity, 20, 10, 1 and 0.25 U mL^{-1}, were used. All combinations of endoglucanase activity and β-glucosidase activity were used in experiments on the hydrolysis of 5% sludge in batch mode. On increasing the

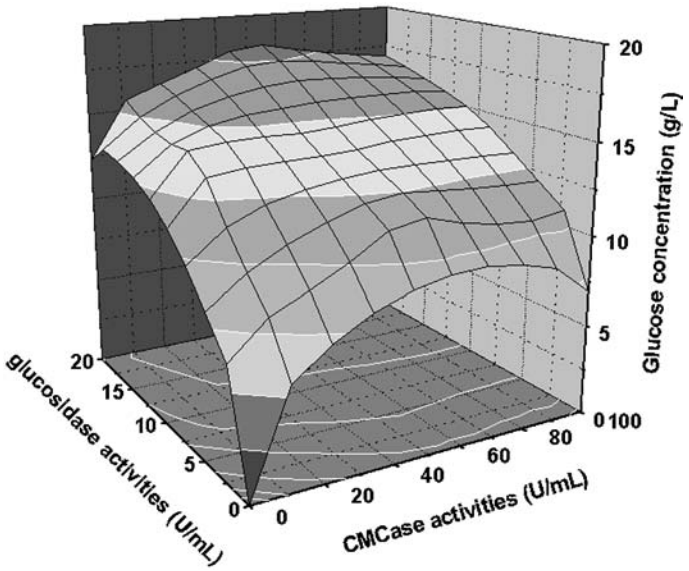

Fig. 3 Dependence of glucose production on CMCase and β-glucosidase activity

cellulase activity to 100 U mL^{-1}, glucose production increased and decreased depending on the amount of β-glucosidase – high glucose production was obtained at high β-glucosidase activity. CMCase activity at ca 2.5 U mL^{-1} and β-glucosidase activity at ca. 10 U mL^{-1} was an optimum condition for hydrolysis of 5% sludge.

2.2 SSF for lactic acid production

In the simultaneous saccharification and fermentation (SSF) process the normally consecutive processes of saccharification and fermentation were performed simultaneously in the same container [25–29]. In terms of lactic acid production from paper sludge, cellulose in the sludge can be hydrolyzed enzymatically to produce glucose, which in turn can be used as a substrate for lactic acid fermentation. The SSF process has the advantages of high conversion and rate of saccharification, because the resulting product, usually glucose, is consumed by the microbial fermentation. This also minimizes the inhibition of hydrolysis by glucose.

In SSF a substantial decrease in enzyme use per glucose unit produced is possible, because of the prolonged process time. SSF is important industrially because a faster saccharification rate can be achieved in a smaller reactor [25, 27].

In this study, the SSF process was used to produce lactic acid as a final product from paper sludge. The fermentation broth was analyzed by HPLC to identify all the organic acids present in the broth, which can compete for adsorption in the recovery process. The results are presented in Table 5. The conversion yield

Table 5 HPLC assay (g L^{-1}) offer mentation broth of *Lactobacillus rhamnosus* with glucose as a substrate

Organic acids	Flask[a] (200 mL)	Flask[b] (200 mL)	Flask[c] (200 mL)	Fermenter[d] (1 L)
Citric acid	2.11	1.66	2.13	5.97
Succinic acid	0	2.55	4.66	3.67
Lactic acid	95.1	86.5	63.4	104.7
Formic acid	0	0.62	1.71	0.88
Acetic acid	2.89	2.52	3.62	1.56
Propionic acid	1.30	7.50	8.54	4.76

[a] Glucose (100 g L^{-1}), 3% $CaCO_3$ powder as a buffer.
[b] Glucose (100 g L^{-1}), 4% $CaCO_3$ powder as a buffer.
[c] Glucose (90 g L^{-1}), no buffer.
[d] Glucose (140 g L^{-1}), 4% $CaCO_3$ powder as a buffer.

of glucose into lactic acid was more than 90%. Lactic acid was the major organic acid and acetic acid was the major impurity. The total amount of acetic acid and other organic acids was less than 10% of the lactic acid level.

Crude cellulase was produced from *Trichoderma reesei* fermentation. Novozym 188 was used for β-glucosidase. The MRS media for *Lactobacillus rhamnosus* culture had the composition: D-(+)-glucose, yeast extract, $(NH_4)_2SO_4$, KH_2PO_4, $MgSO_4 \cdot 7H_2O$, K_2HPO_4, $FeSO_4 \cdot 7H_2O$. Paper sludge was used as a carbon source. The microbial cell concentrations were measured spectrophotometrically at 600 nm (Genesys 5, Spectronic Instruments). Glucose and lactic acid were measured by means of a glucose analyzer (YSI 2700 Select, Yellow Springs Instrument Company, USA). Seed culture and preliminary SSF experiments were conducted out in an Erlenmeyer flask (100 mL) in a shaking incubator (150 rpm). A modified bioreactor was designed to remove solid materials from the fermentation broth by settling. SSF in a fed-batch mode was performed in a modified reactor (400 mL) and fermenter (3 L; KoBioTech). SSF was performed at 42 °C and pH 5.0. The optimum temperature and pH for the enzymatic hydrolysis and fermentation were 50 °C and pH 4.8, and 37 °C and pH 6.0, respectively. SSF was initiated by adding the enzyme mixture and the microbial inoculum at the same time.

The sludge content of the solution is an important factor in SSF. Although the sludge provides the feed material, cellulose, as its major component, it also causes a mixing problem as its content increases. The time course of glucose and lactic acid concentrations with varying paper sludge content are shown in Fig. 4. The enzyme loading was 5 and 2 U mL^{-1} for crude cellulase and β-glucosidase, respectively. The glucose concentration increased as enzymatic hydrolysis occurred, and decreased as a result of its consumption by fermentation. The maximum glucose concentration at 6 h is probably because of a lag phase in microbial growth, compared with the instant start of enzymatic hydrolysis. The lower glucose value at the higher sludge content is caused by insufficient mixing. Mixing was inadequate when the initial sludge content exceeded 15%. However, higher initial sludge content resulted in higher lactic acid production, because the solid content in the system decreased with time, resulting in a reduced mixing

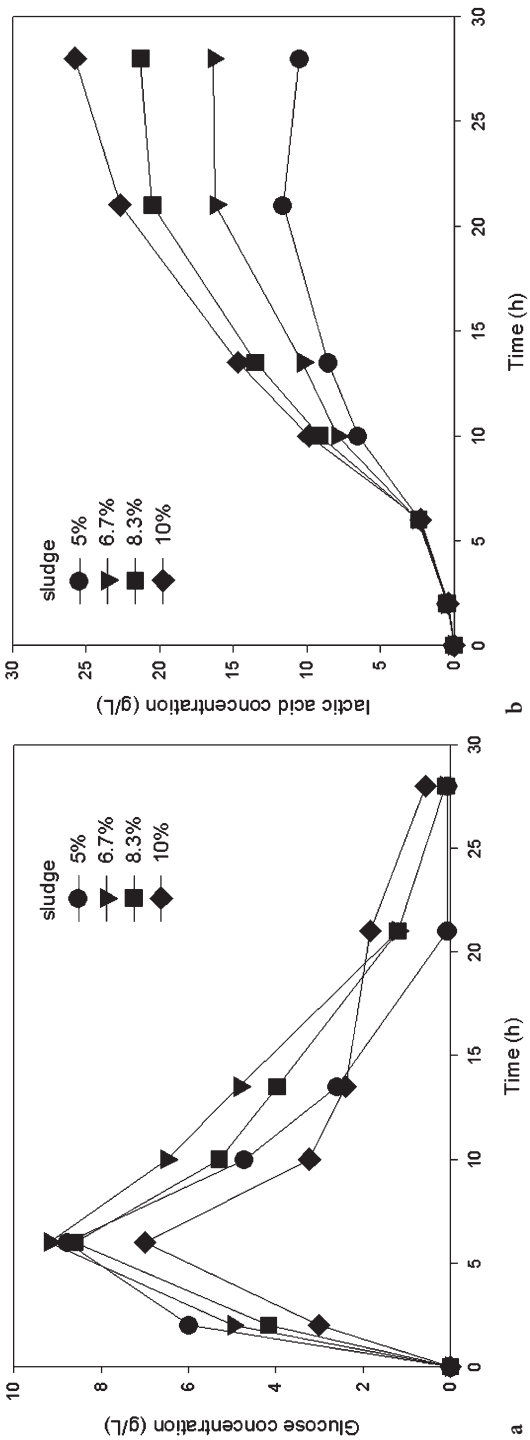

Fig. 4 Effect of sludge content on SSF: (**a**) glucose concentration; (**b**) lactic acid concentration

problem. During the latter stage of the reaction, high glucose and high lactic acid concentrations were observed at higher sludge content. Although maximum lactic acid concentration was obtained at an initial sludge content of 10%, a sludge content of 8% was chosen as optimum, considering the production rate.

The enzyme mixture for SSF consisted of crude cellulase and commercial β-glucosidase. The crude cellulase is mainly responsible for the conversion of cellulose to cellobiose, whereas β-glucosidase converts cellobiose into glucose. The composition of these cellulases in the enzyme mixture is an important factor for maximum hydrolysis of cellulose, and for efficient production of lactic acid. SSF experiments were conducted with enzyme mixtures containing different amounts of crude cellulase and a constant amount of β-glucosidase (Fig. 5).

The initial sludge content was 5%. SSF with higher levels of crude cellulase resulted in faster increases in glucose concentration. During the following period, in which microbial fermentation predominated, the glucose concentration dropped to almost zero, irrespective of sludge content. The final lactic acid concentration was about 16 g L^{-1}, which is equivalent to a conversion yield, from cellulose via glucose to lactic acid of about 80%. Note that the cellulose content in the dry sludge was about 35%. This high yield demonstrates the major advantage of SSF, that it can prevent the product (glucose) inhibition effect in the enzymatic hydrolysis reaction. In general, enzymatic cellulose hydrolysis is inhibited by glucose at concentrations higher than 10%. Similar trends for glucose and lactic acid concentrations were observed for SSF with enzyme mixtures containing different amounts of β-glucosidase (data not shown). A higher lactic acid production rate is expected for earlier fermentation, i.e. microbial growth, compared with enzymatic hydrolysis.

The maximum lactic acid concentration obtained by batch SSF was low around 30 g L^{-1}, because the initial sludge content was less than 10%, because of the mixing problem. To enhance the final lactic acid concentration, a certain amount of sludge was added intermittently (shown as b in Fig. 6) to the SSF system to make up for depleted cellulose in the fed-batch mode. The initial sludge content was 8%, and sludge at 35% *w*/*w* was added during the SSF to maintain the sludge content at 7%. With this intermittent addition of sludge, a constant supply of cellulose was possible without excessive addition of sludge in the beginning of the SSF process, which was carried out in an 100-mL Erlenmeyer flask. The initial enzyme loading was 10 and 4 U mL^{-1} for the crude cellulase and β-glucosidase, respectively. Crude cellulase and β-glucosidase of 5 and 1 U mL^{-1}, respectively, were also intermittently fed (shown as b in Fig. 6) to the reactor. In the early period the glucose concentration increased as enzymatic hydrolysis dominated microbial fermentation, i.e. microbial growth. In the period between 20 to 50 h lactic acid production was limited because of the lack of glucose in the system, even with addition of sludge. After 50 h microbial growth was in the stationary phase in which lactic acid production was maintained while glucose consumption decreased. With this intermittent feeding a high production of lactic acid with final concentration of around 90 g L^{-1} was obtained. Doubling the β-glucosidase content in the experimental range did not change the lactic acid production significantly. Without pH control SSF operated at around pH 4.5.

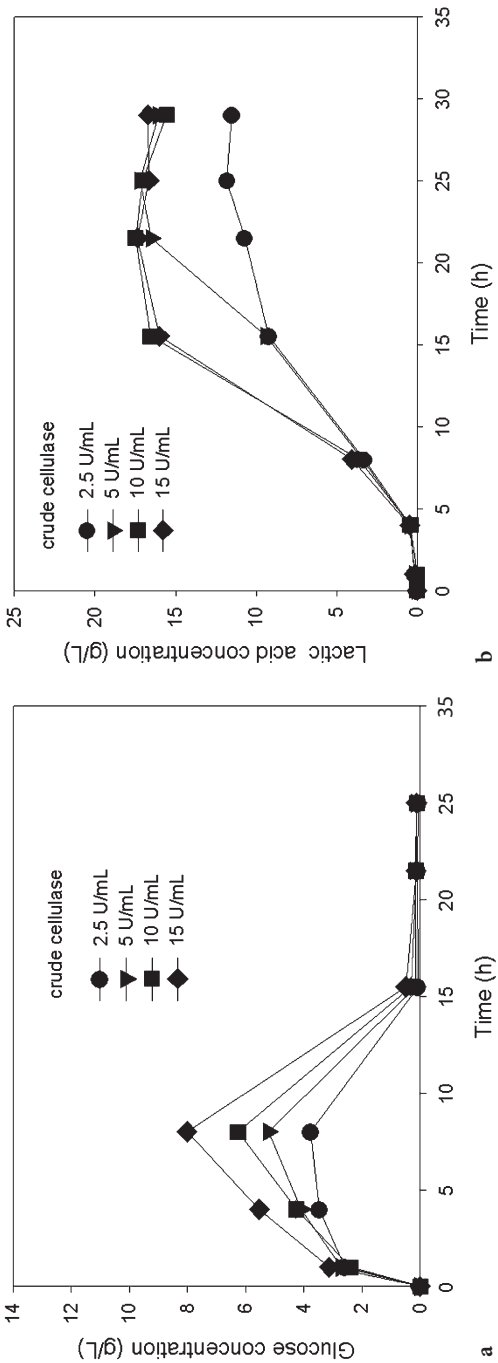

Fig. 5 Effect of crude enzyme content on SSF with a fixed amount of *β*-glucosidase: (**a**) glucose concentration; (**b**) lactic acid concentration

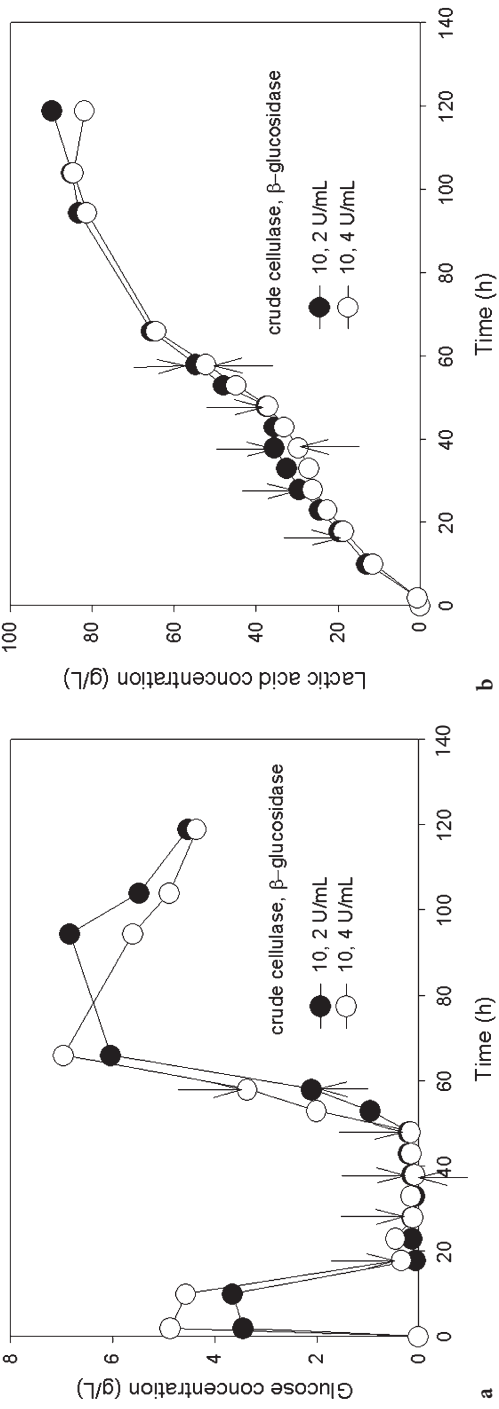

Fig. 6 Time course of SSF in flask (100 mL) with intermittent feeding of sludge (*downward pointing arrow*) and enzyme mixture (*upward pointing arrow*) (crude cellulase, *β*-glucosidase: 5, 1 U mL^{-1}). (**a**) glucose concentration, (**b**) lactic acid concentration

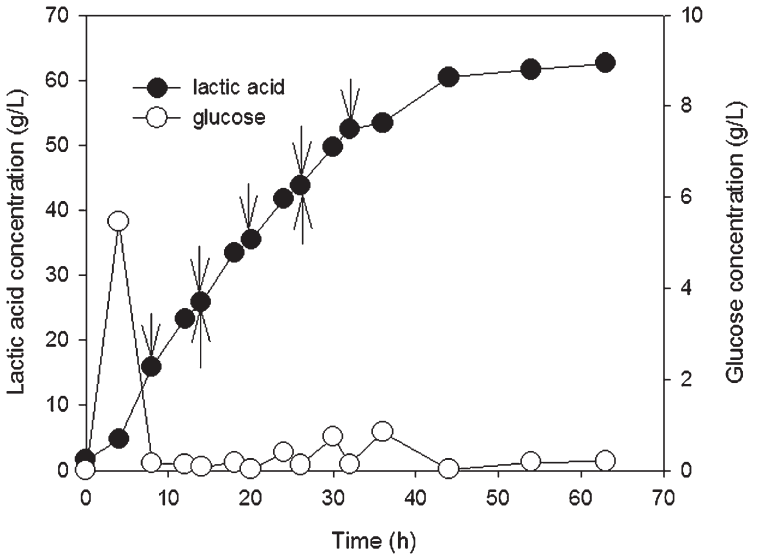

Fig. 7 Time course of SSF in fermenter (3 L) with intermittent feeding of sludge (*downward pointing arrow*) and enzyme mixture (*upward pointing arrow*) (crude cellulase, β-glucosidase: 5, 1 U mL^{-1})

This pH stability was ascribed to the fact that the inorganic ash components in the sludge buffered the system.

SSF was performed in a fermenter with the nominal volume of 3 L, with most operating conditions maintained as described for Erlenmeyer flask SSF, except for the timing of intermittent feeding and pH control.

As shown in Fig. 7, the first intermittent feeding was performed after 8 h to avoid limitation of lactic acid production as a result of the lack of glucose during the exponential microbial growth phase. The arrows in the figure have the same meaning as those in Fig. 6. The pH of the solution was controlled at 5.0 by use of 5 mol L^{-1} NH_4OH. The final lactic acid concentration was 62 g L^{-1} with a conversion yield of 80%. Lactic acid productivity during the first 32 h was calculated to be 1.64 g L^{-1} h^{-1}, which is higher than that achieved in the Erlenmeyer flask of 0.98 g L^{-1} h^{-1}.

During the SSF process insoluble materials from paper sludge accumulated. These components, mostly silica, alumina, and lignin, affected mass transfer in the fermentation broth as the viscosity of solution increased. A modified bioreactor was designed to remove solid materials from the fermentation broth by allowing settlement into the lower compartment beneath the perforated divider. As shown in Fig. 8, the final lactic acid concentration was 162 g L^{-1} and the conversion yield was 74%. The arrows in the figure have the same meaning as those in Fig. 6. The extra sludge of 35% *w/w* was fed intermittently at 30–40 g per addition. Lactic acid productivity during the first 86 h was calculated to be 1.40 g L^{-1} h^{-1}, which is lower than was achieved in the fermenter (1.64 g L^{-1} h^{-1}). The higher lactic acid production and productivity were explained by more

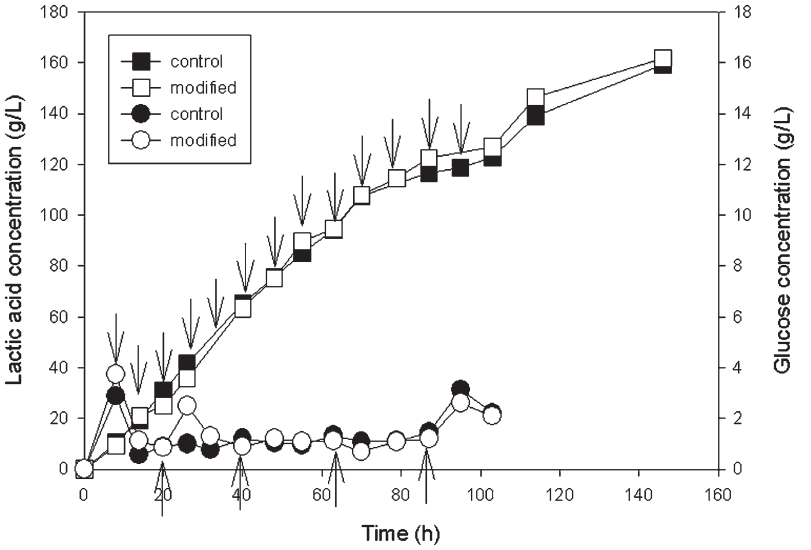

Fig. 8 Time course of SSF in modified bioreactor with intermittent sludge (*downward pointing arrow*) and enzyme mixture (*upward pointing arrow*) feeding (crude cellulase, β-glucosidase: 5, 1 U mL^{-1}): *circles*, glucose, *squares*, lactic acid

optimum feeding times and amounts. The modified bioreactor had a slightly better performance in terms of lactic acid production because of the removal of solid materials from the lower compartment. Further optimization of the design of the bioreactor, i.e. compartment volume, perforated divider, and stirring speed, would improve lactic acid production. The optimum operating conditions for SSF can be predicted by model simulation, based on detailed knowledge about each SSF element.

2.3 Mathematical modeling

The saccharification of cellulose by the cellulase enzyme system has been studied in detail by various workers [19, 20, 25–29]. Glucose strongly inhibits the various steps involved in the cleavage of the cellulose molecule to glucose. The study carried out by Ghosh and Das et al. demonstrated that both glucose and cellobiose inhibit cellulase [20]. The inhibition is competitive for both glucose and cellobiose. Detailed modeling performed by Philippidis et al. addressed these inhibitory effects.

The kinetics of simple saccharification were extended to a model of SSF by incorporating the growth kinetics of the microorganisms. In SSF the glucose formed by saccharification is consumed by *Lactobacillus* sp. [26]. Mathematical modeling is important for understanding the characteristics of the SSF process and for process optimization. In terms of the enzymatic hydrolysis of cellulose the glucose yield decreases with increasing cellulose concentration, possibly

because of an imbalance in the composition of the enzyme mixture which results from adsorption of the components on the solid substrates.

Although the adsorption of endoglucanase by cellulose is necessary for the hydrolytic reaction to proceed, the enzyme must then desorb and relocate on the cellulose molecule, because the enzyme molecule is unable to move along the cellulose molecule. It is believed that the reaction speed is much faster than the adsorption/desorption speed and the desorption speed is less than or equal to the adsorption speed. Therefore, the reaction rate of endoglucanase is controlled by the desorption speed of endoglucanase from cellulose.

Most of the oligosaccharides produced by endoglucanase are soluble and are, therefore, suitable for reaction with exoglucanase in its dissolved form. The apparent activity of adsorbed exoglucanase and β-glucosidase is very low. It can be concluded from these observations that the higher desorption speed of endoglucanase and the higher concentrations of free exoglucanase and β-glucosidase are important for cellulose hydrolysis. The rate equation for the desorption speed of endoglucanase can be expressed as:

$$r_{1'} = (K_1 \cdot E_{1.\mathrm{ad}} \cdot C)/(K_{1\mathrm{m}} + C) \tag{1}$$

where C is the cellulose concentration (g L^{-1}), K_1 is the desorption rate (h^{-1}), and $K_{1\mathrm{m}}$ is a constant. $E_{1.\mathrm{ad}}$ is the amount of endoglucanase adsorbed by cellulose (U g^{-1}), which is given by:

$$E_{1.\mathrm{ad}} = e_{1.\mathrm{ad}} \cdot E_1/(k_1 + E_1) \tag{2}$$

where $e_{1.\mathrm{ad}}$ is the saturated amount of endoglucanase adsorbed by cellulose (mg g^{-1}), E_1 is the soluble endoglucanase concentration (U mL^{-1}), and k_1 is a constant. The reaction rate of endoglucanase is also inhibited by cellobiose, as shown by:

$$r_1 = r_1'/(1 + B/K_{1B}) \tag{3}$$

where B is the concentration of cellobiose (g L^{-1}) and K_{1B} is a constant (g L^{-1}). The conversion rate of oligosaccharides to cellobiose is given by:

$$r_2 = (K_2 \cdot E_2 \cdot S^*)/(K_{2\mathrm{m}} \cdot (1 + B/K_{2B}) + S^*) \tag{4}$$

where E_2 is the soluble endoglucanase concentration (U mL^{-1}), K_2 is the maximum reaction rate (h^{-1}), $K_{2\mathrm{m}}$ and K_{2B} are constants (g L^{-1}), and S^* is the concentration of oligosaccharides (g L^{-1}). The adsorption of exoglucanase can be expressed as:

$$E_{2.\mathrm{ad}} = e_{2.\mathrm{ad}} \cdot E_2/(k_2 + E_2) \tag{5}$$

where $e_{2.\mathrm{ad}}$ is the saturated amount of exoglucanase adsorbed by cellulose (mg g^{-1}), E_2 is the apparent activity of exoglucanase in solution (U mL^{-1}), and k_2 is a constant. E_2 is calculated from

$$E_2 \cdot V = E_{2.0} \cdot V - E_{2.\mathrm{ad}} \cdot S + a \cdot E_{2.\mathrm{ad}} \cdot S \tag{6}$$

Then:

$$E_2 = E_{2.0} - (1 - a) \cdot E_{2.\mathrm{ad}} \cdot S \tag{7}$$

where $E_{2.0}$ is the exoglucanase added to the reaction system (U mL^{-1}) and α is a constant, representing the apparent activity of the adsorbed exoglucanase.

The conversion rate of cellobiose to glucose is given by:

$$r_3 = (K_3 \cdot E_3 \cdot B)/(K_{3m} \cdot (1 + G/K_{3G}) + B) \tag{8}$$

where E_3 is the apparent β-glucosidase concentration in the solution (IU mL^{-1}), K_3 is the maximum reaction rate (h^{-1}), and K_{3m} and K_{3G} are constants (g L^{-1}). The adsorption of β-glucosidase is obtained from:

$$E_{3.ad} = e_{3.ad} \cdot E_3/(k_3 + E_3) \tag{9}$$

where $e_{3.ad}$ is the amount of β-glucosidase adsorbed on cellulose at saturation (mg g^{-1}), E_3 is the apparent activity of β-glucosidase in solution (U mL^{-1}), and k_3 is constant. Similarly, E_3 is calculated using:

$$E_3 = E_{3.0} - (1 - \beta_a) \cdot E_{3.ad} \tag{10}$$

where $E_{3.0}$ is the initial amount of β-glucosidase added to the reaction system (U mL^{-1}) and β_a is a constant representing the apparent activity of adsorbed β-glucosidase. The conversion rates of cellulose, oligosaccharides, β-glucosidase, and glucose are given by:

$$dS/dt = -r_1 \tag{11}$$

$$dS^*/dt = r_1 - r_2 \tag{12}$$

$$dB/dt = 1.056 \cdot r_2 - r_3 \tag{13}$$

$$dG/dt = 1.053 \cdot r_3 - r_4 \tag{14}$$

As the glucose remains at a low concentration in the SSF process, only product inhibition may be included in the mathematical model. The rate equations for SSF are:

$$\mu = \mu m/EXP(-P/k_i)/(k_s + S) \tag{15}$$

$$dVS/dt = -r_1 V \tag{16}$$

$$dVS^*/dt = (r_1 - r_2)V \tag{17}$$

$$dVB/dt = (1.056\, r_2 - r_3)V \tag{18}$$

$$dVX/dt = \mu VX \tag{19}$$

$$dVP/dt = (a\mu + \beta)VX \tag{20}$$

$$dVG/dt = 1.053 r_3 V - r_4 \cdot Y_{P/G} V\, dP/dt \tag{21}$$

The prediction of lactic acid fermentation by the mathematical model developed in this study, as described above, is shown in Fig. 9.

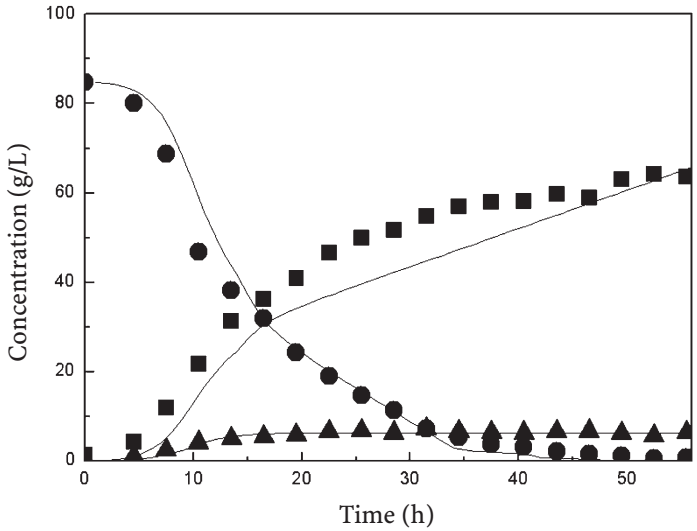

Fig. 9 Comparison of model prediction (*lines*) and experimental data (*symbols*) for the number of cells (*circles*) and the concentrations of lactic acid (*squares*) and cellulose (*triangles*) in SSF

3 Lactic acid recovery and purification

Lactic acid obtained by fermentation must be separated from the fermentation broth, and usually purified, to be suitable for polymerization. Several different approaches and combinations have been applied. To this end, neutralization with a base, followed by filtration, concentration, and acidification is traditionally used to manufacture highly pure lactic acid. Many other separation methods such as adsorption, electrodialysis, membrane filtration, ion exchange, and aqueous two-phase system extraction have been studied [30–37].

Calcium and zinc lactate are important chemicals in the pharmaceutical, food, and chemical industries. They are widely used as nutrients in foods and as medicines for calcium and zinc deficiency [30, 31]. Recently the solubility of calcium and zinc lactates in water and ethanol–water was reported [32]. Ultrasonification was found to reduce the induction time required to crystallize DL-(±)-calcium lactate to one sixth to one eighth of that required without ultrasonification [33].

Reactive extraction has been investigated as an alternative to the conventional process. Extraction processes do not affect the thermal stability of bioproducts, and the energy demand is very low. Compared with physical liquid–liquid extraction, the selectivity of separation is enhanced remarkably, because amino-based extractants favorably separate acids. The reactive substance forms a reversible complex with lactic acid, which promotes the phase transfer of the polar acid from the aqueous phase to the non-polar organic phase [35].

Membrane bioreactors have been used with some success in numerous publications and have appeared in several patents; their main drawback is, never-

Table 6 Comparison of design and experimental results of SMB separation (unit: %)

	$Purity_{Acetate}$	$Purity_{Lactate}$	$Yield_{Acetate}$	$Yield_{Lactate}$
Design[a]	99.5	99.7	99.9	97.1
Run[b]	100	96.4	100	99.6

[a] All values calculated from VERSE simulator [38].
[b] All values calculated from experimental results.

theless, the loss of a carbon source in the permeate because of the non-selectivity of the ultrafiltration and microfiltration membranes used. Nanofiltration is a pressure-driven membrane process with a molecular weight cut-off situated between those of reverse osmosis and ultrafiltration. The nanofiltration of lactic acid fermentation broth has been investigated to develop a model capable of predicting lactic acid rejection [34].

Adsorption on to ion-exchange resins is an industrially used method, because it is economical and straightforward. In particular, the separation method can be coupled with the fermentation process. King et al. separated carboxylic acids from carboxylic salt solutions at pH close to or above their pK_a values [36].

Electrodialysis is an attractive and rapid process with effective removal of non-ionic molecules, high concentration of the product, and no by-product generation. A two-stage electrodialysis method, desalting of lactate salt from fermentation broth and acidification of the purified lactate salt by water-splitting electrodialysis, has been used to recover lactic acid from fermentation broth [37].

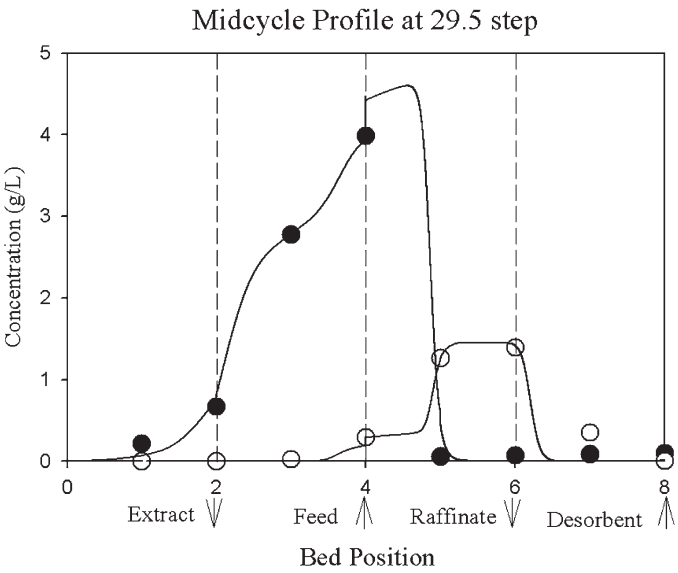

Fig. 10 The mid-cycle profile of SMB model prediction (*lines*) and experimental data (*symbols*) for separation (after 3322 min) of lactic acid (*filled circles*) from acetic acid (*empty circles*)

Simulated moving bed (SMB) is a continuous chromatographic separation process which is gaining in importance industrially. A SMB unit consists of a number of chromatographic columns divided into four zones with two inlet and two outlet ports. The four ports are moved periodically by one column length along the desorbent flow direction, which achieves a countercurrent movement between the adsorbent and the fluid. Compared with batch chromatography SMB achieves higher yields and purity, and lower desorbent consumption. In this study SMB experiments using poly(4-vinylpyridine) (PVP) resin were performed to fractionate two organic acids, i.e. lactic acid and acetic acid. For both operational design and numerical simulations variables such as adsorption isotherms and mass-transfer data were determined by single-column experiments. To confirm the data numerical simulations were performed.

Experimental and design data are compared in Table 6 and in Figure 10. The experimental results agree well with the design data.

4 Concluding remarks

A variety of renewable biomasses, such as corn and its stover, have been regarded as useful feedstocks for starch and cellulose, respectively. They can be converted to produce value-added products, such as ethanol and different organic acids. The paper sludge waste generated by the paper industry was found in this study to be a consistent source of cellulose with excellent enzymatic digestibility.

The SSF process was used to produce lactic acid from the cellulose in paper sludge. This process can prevent product inhibition of enzymatic cellulose hydrolysis and alleviate the mixing problem which results from its high sludge content. When SSF was used in a fed-batch mode lactic acid production was 162 g L^{-1} at 42 °C with an yield of 74%. Lactic acid productivity during the first 87 h was calculated to be 1.40 g L^{-1} h^{-1}, and the optimum conditions for the SSF process were 42–45 °C and pH 5.

A bioreactor was designed to remove solid materials from the fermentation broth by allowing settling into a stagnant compartment beneath the perforated divider. This modified bioreactor was found to perform better in terms of lactic acid production by removing indigestible solid materials from the upper compartment and by enabling additional paper sludge feed.

A predictive model was studied for SSF by combining the kinetics of saccharification and fermentation. The saccharification kinetics were determined by means of experiments on enzymatic cellulose hydrolysis. The saccharification kinetics were described by use of a Michaelis–Menten type equation and the growth kinetics of *L. rhamnosus* fitted a Monod expression incorporating lactic acid inhibition. These kinetic models were used to predict the performance of the SSF process for lactic acid production.

The model solutions for lactic acid and acetic acid were separated by conventional four-zone SMB with eight columns (Fig. 10). The adsorption properties affect the performance of SMB, for example, the yield, purity, and sensitively. The SMB devised design can be extended to separation of other organic acids. Pre-

cipitation and reactive distillation are being studied for large-scale production of lactic acid. The economics of lactic acid production depend significantly on the efficiency of the SSF and recovery processes.

Acknowledgements The authors are grateful for the support of KOSEF and of the Engineering Research Center for Advanced Bioseparation Technology.

5 References

1. Yu YH, Kim SD, Lee JM, Lee KH (2002) Kinetic studies of dehydration, pyrolysis and combustion of paper sludge. Energy 27:457
2. Trevor GP, George CB (1998) Responses of invertebrates to paper sludge application to soil. Appl Soil Ecol 9:393
3. Phillips VR, Kirkpatrick NI, Scotford M, White RP, Burton RGO (1997) The use of paper-mill sludges on agricultural land. Bioresour Technol 60:73
4. Liaw CT, Chang HL, Hsu W-C, Huang C-R (1998) A novel method to reuse paper sludge and co-generation ashes from paper mill. J Hazard Mater 58:93
5. Lark N, Xia Y, Qin C-G, Gong CS, Tsao GT (1997) Production of ethanol from recycled paper sludge using cellulase and yeast, *Kluveromyces marxianus*. Biomass Bioenergy 12:135
6. Bisaria VS, Ghose TK (1981) Biodegradation of cellulosic materials: substrates, micro-organisms, enzymes and products. Enzyme Microb Technol 3:90
7. Huang YL, Wu Z, Zhang L, Cheung CM, Yang ST (2002) Production of carboxylic acids from hydrolyzed corn meal by immobilized cell fermentation in a fibrous-bed bioreactor. Bioresour Technol 82:51
8. Horiuchi JI, Shimizu T, Tada K, Kanno T, Kobayashi M (2002) Selective production of organic acids in anaerobic acid reactor by pH control. Bioresour Technol 82:209
9. Haq IU, Ail S, Iqbal J (2003) Direct production of citric acid from raw starch by *Aspergillus niger*. Process Biochem 38:921
10. Makela M, Galkin S, Hatakka A, Lundell T (2002) Production of organic acids and oxalate decarboxylase in ligin-degrading white rot fungi. Enzyme Microb Technol 30:542
11. Goswami V, Srivastava AK (2000) Fed-batch propionic acid production by *Propioibacterium acidipropionici*. Biochem Eng J 4:121
12. Wilke D (1999) Chemicals from biotechnology. Appl Microb Biotechnol 52:135
13. Datta R, Tsai S-P, Bonsignore P, Moon S-H, Frank JR (1995) Technological and economic potential of poly(lactic acid) and lactic acid derivatives. FEMS Microb Rev 16:221
14. Södergard A, Mikael S (2002) Properties of lactic acid based polymers and their correlation with composition. Prog Polym Sci 27:1123
15. Ooshima H, Sakata M, Harano Y (1983) Adsorption of cellulase from *Trichoderma viride* on cellulose. Biotechnol Bioeng 25:3103
16. Withers SG, Tull D, Gebler J, Braun C, Aebersold R, Wang Q, Warren T, Kilburn D, Gilkes N, Suominen P, Reinikainen T (1993) (eds) Mechanistic studies on cellulases. In: Proc 2nd TRICEL Symp on *Trichoderma reesei* cellulases and other hydrolases, Espoo, Finland
17. Nazhad M, Ramos M, Paszner LPL, Saddler JN (1995) Structural constraints affecting the initial enzymatic hydrolysis of recycled paper. Enzyme Microb Technol 17:68
18. Eklund R, Galbe M, Zacchi G (1990) Optimization of temperature and enzyme concentration in the enzymatic saccharification of steam pretreated willow. Enzyme Microb Technol 12:225
19. Philippidis GP, Smith TK, Wyman CE (1993) Study of the enzymatic hydrolysis of cellulose for production of fuel ethanol by the simultaneous saccharification and fermentation process. Biotechnol Bioeng 41:846
20. Ghosh TK, Das K (1971) Kinetics of hydrolysis of insoluble cellulose by cellulase. Adv Biochem Eng 1:49

21. Mansfield SD, Mooney C, Saddler JN (1999) Substrate and enzyme characteristics that limit cellulose hydrolysis. Biotechnol Prog 15:804
22. Ooshima H, Burns DS, Converse AO (1990) Adsorption of cellulase from *Trichoderma reesei* on cellulose and liginacious residue in wood pretreated by dilute sulfuric acid with explosive decompression. Biotechnol Bioeng 36:446
23. Ghose TK, Panda T, Visaria VS (1985) Effect of culture phasing and mannanase on production of cellulase and hemicellulase by mixed culture of *Trichoderma reesei* D1–6 and *Aspergillus wentii* Pt 2804. Biotechnol Bioeng 27:1353
24. Parajo JC, Alonso JL, Santos V (1996) Development of a generalized phenomenological model describing the kinetics of the enzymatic hydrolysis of NaOH-treated pine wood. Appl Biochem Biotechnol 56:289
25. Abe S, Takagi M (1991) Simultaneous saccharification and fermentation of cellulose to lactic acid. Biotechnol Bioeng 37:93
26. Venkatesh KV (1997) Simultaneous saccharification and fermentation of cellulose to lactic acid. Bioresour Technol 62:91
27. Takagi M (1984) Inhibition of cellulase by fermentation products. Biotechnol Bioeng 26:1506
28. Anuradha R, Suresh AK, Venkatesh KV (1999) Simultaneous saccharification and fermentation of starch to lactic acid. Process Biochem 35:367
29. Stenberg K, Galbe M, Zacchi G (2000) The influence of lactic acid formation on the simultaneous saccharification and fermentation (SSF) of softwood to ethanol. Enzyme Microb Technol 26:71
30. Xue XX, Liu HY (1993) Experimental research of nutrient–zinc lactate. Food Sci 161:26
31. Zhang SP, Zhu J, Wang XC (1994) Development of a novel nutrient–zinc lactate. Res Dev Food 3:28
32. Kricheldorf HR, Damrau DO (1998) ZnL-lactate-catalyzed polymerizations of 1,4-dioxan-2-one. Macromol Chem Phys 199:1089
33. Jin QR, Zhang JM, Xu Q (1994) (eds) Fermentation technology of organic acids. Light Industrial Press of China, Beijing
34. Jeantet R, Boyaval JLP (1996) Semicontinuous production of lactic acid in a bioreactor coupled with nanofiltration membranes. Enzyme Microbiol Technol 19:614
35. Tamada JA, King CJ (1990) Extraction of carboxylic acids with amine extractants. 3. Effect of temperature, water coextraction, and process consideration. Ind Eng Chem Res 29:1333
36. King CJ, Tung LA (1992) Sorption of carboxylic acid from carboxylic salt solutions at pHs close to or above the pK_a of the acid, with regeneration with an aqueous solution of ammonia or low-molecular-weight alkylamine. US Patent 5 132 456
37. Lee EG, Moon SH, Chang YK, Yoo IK, Chang HN (1998) Lactic acid recovery using two-stage electrodialysis and its modelling. J Membr Sci 145:55
38. Mallmann T, Burris BD, Ma Z, Wang N-HL (1998) Standing wave design of nonlinear SMB systems for fructose purification. AIChE J 22:2628

Received: August 2003

Adv Biochem Engin/Biotechnol (2004) 86: 195–268
DOI 10.1007/b94369

Developing a Sustainable Bioprocessing Strategy Based on a Generic Feedstock

C. Webb · A. A. Koutinas · R. Wang

Satake Centre for Grain Process Engineering, Department of Chemical Engineering, UMIST PO Box 88, Manchester, M60 1QD, UK
E-mail: c.webb@umist.ac.uk

Abstract Based on current average yields of wheat per hectare and the saccharide content of wheat grain, it is feasible to produce wheat-based alternatives to many petrochemicals. However, the requirements in terms of wheat utilization would be equivalent to 82% of current production if intermediates and primary building blocks such as ethylene, propylene, and butadiene were to be produced in addition to conventional bioproducts. If only intermediates and bioproducts were produced this requirement would fall to just 11%, while bioproducts alone would require only 7%. These requirements would be easily met if the global wheat yield per hectare of cultivated land was increased from the current average of 2.7 to 5.5 tonnes ha^{-1} (well below the current maximum). Preliminary economic evaluation taking into account only raw material costs demonstrated that the use of wheat as a generic feedstock could be advantageous in the case of bioproducts and specific intermediate petrochemicals. Gluten plays a significant role considering the revenue occurring when it is sold as a by-product. A process leading to the production of a generic fermentation feedstock from wheat has been devised and evaluated in terms of efficiency and economics. This feedstock aims at providing a replacement for conventional fermentation media and petrochemical feedstocks. The process can be divided into four major stages – wheat milling; fermentation of whole wheat flour by *A. awamori* leading to the production of enzymes and fungal cells; glucose enhancement via enzymatic hydrolysis of flour suspensions; and nitrogen/micronutrient enhancement via fungal cell autolysis. Preliminary costings show that the operating cost of the process depends on plant capacity, cereal market price, presence and market value of added-value by-products, labour costs, and mode of processing (batch or continuous).

Keywords Bioprocessing · Chemicals · Generic feedstock · Wheat · *Aspergillus awamori*

1 Introduction

Up to the beginning of the 20th century renewable agricultural carbohydrates constituted the raw materials for fuel, chemical and material production. They were gradually substituted by environmentally hazardous fossil hydrocarbons because of fewer processing steps, higher yields, and, most of all, favourable economics of production. The development of today's chemical industry was motivated by this second wave of industrialization, based on booming petroleum exploration and refining and advances in conventional organic chemistry. The associated integration of chemistry with engineering principles led to the creation of the discipline of chemical engineering. Likewise, nowadays, the integration of biosciences (biotechnology, biochemistry, biology) with engineering principles (chemical and biomolecular engineering) has led to the development of biochemical engineering as an academic discipline and profession.

It is common knowledge that sustainable development and green processing is essential for the sake of humanity. The establishment of a biobased future is also stimulated by the depletion of petroleum resources, advancing biotechnologies, and the globalized market. In today's market companies are challenged to survive under extremely competitive conditions. Deregulation of market areas such as energy and telecommunications that until recently used to be monopolies run by the public sector, strategic mergers of multinational giants, dislocation of environmentally hazardous chemicals, strict regulations imposed on the industry over environmental issues, and globalization of service provision and commodity distribution change the rules of the market. The faster the companies comply with the pattern of free market economy and globalized society the faster they will grow and outstrip their rivals. In this context, innovative biotechnologies provide notable prospects for faster growth and add value to our everyday lives.

Generally, a bioprocess can be divided into three stages (Fig. 1):

1. upstream processing,
2. bioconversion, and
3. downstream processing.

The bottlenecks in upstream processing are the expensive raw materials and the limited microorganisms that can achieve high conversion yields from saccharide to product. Conventional batch bioconversion results in low volumetric productivities. Downstream processing has been adopted predominantly from the chemical industry and is expensive because it is not flexible, it contains many processing steps and produces large amounts of wastes. Thus, the use of today's bioprocessing for fuel and chemical production is expensive and inefficient.

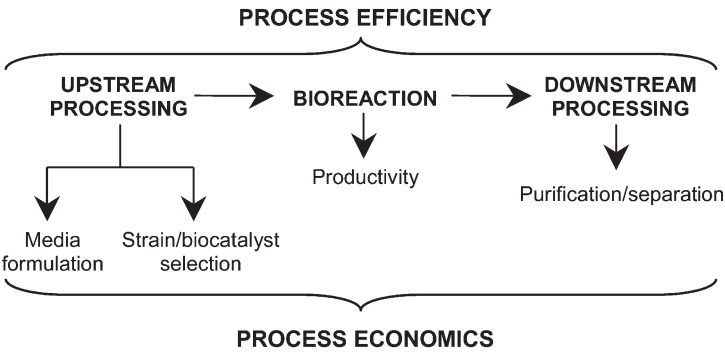

Fig. 1 General layout of bioprocessing and major problems encountered

Paraphrasing the *Bioscience Engineering* report (BBSRC review of biochemical engineering, http://www.bbsrc.ac.uk/tools/download/bio_eng/bio_eng.doc, July 1999), the main task for a biochemical engineer is to achieve breakthrough solutions in biological and engineering challenges of process scale-up in an economical manner, always in accordance with strict safety and environmental regulations, to enable bioprocessing to provide the globalized society with added-value bioproducts. To achieve this the development of cost-competitive and highly efficient processing strategies is necessary in upstream, bioconversion and downstream processing.

This review focuses on the current situation of bioprocessing and envisages its future potential in chemical production. It also presents a novel upstream processing strategy, which will lead to the production of a cost-competitive and nutrient-complete generic feedstock from cereals suitable for numerous microbial bioconversions.

2 Upstream processing

The term "upstream processing" represents the preparation stages for the bioconversion step. It can be practically divided into:

1. the formulation and sterilization of the bioconversion medium, and
2. the selection and modification (e.g. mutation, genetic engineering) of the case-specific microorganism.

The latter is subject to the individual bioprocess. The bioconversion media though, have a more generic use, because the nutrient requirements (e.g. glucose as carbon/energy source, amino acids as nitrogen source) of most microorganisms are more or less the same. In many bioprocesses the feedstock cost constitutes the major cost of the process. This can be justified considering that the expenditure for fermentation media accounts for:

- 10–50% of the total production cost in the speciality sector, such as around 10% for penicillin, 30–50% for organic acids, lysine, and vitamin B_{12} [1, 2].
- 50–90% of the total production cost in the commodity sector [2, 3].

2.1 Feedstocks in today's petrochemical industry

More than 95% of the world's petrochemical production is derived from oil or natural gas [4]. Generally, petrochemicals can be classified according to their position along the manufacturing process from crude oil to end-product. Initially, the oil refinery process fractionates the crude oil through atmospheric distillation into natural gas liquids, naphtha, jet fuel, light fuel oil, heavy fuel oil, and feed for vacuum distillation. Predominantly naphtha together with natural gas and coal are used to produce the primary products (ethylene, propylene, butadiene, butenes, benzene, toluene, xylenes, and methane), which are the feedstocks for the chemical industry. The most important are ethylene and propylene, which are derived either from naphtha or from natural gas through steam cracking, and benzene, which is derived from naphtha through catalytic reforming. In 1995, approximately 82 billion kg (out of a total 204 billion kg) of chemicals and polymers in the USA were produced from ethylene alone [5]. The next group is the intermediates (e.g. vinyl chloride, styrene), which are produced by combining primary products and/or making these react with other chemical compounds. The final group is finished products, such as plastics, pharmaceuticals, and detergents. Figure 2 presents predominant production routes, capacities, and unit cost of major organic chemicals and plastics in the mid-1990s. The current worldwide capacity of these chemicals is quite similar to those presented in Fig. 2 due to the economic recession that occurred in 2001. Chemical prices refer to the year 2001 and were taken from the journal *Chemical Market Reporter* [6].

The depletion of fossil fuels is unavoidable but not within the next half century or more [7]. Therefore, there is little point in waiting for fuel prices to rise significantly. Additionally, the chemical industry utilizes only 7% of the global oil refinery output, while the rest is consumed for the production of gasoline and other fuels, which means that the current resources are more than adequate to feed the chemical industry for many more years [5]. Thus, bioprocesses will dominate over chemical processing only by improving their capital and operating cost requirements.

2.2 Feedstocks in today's bioindustry

Biological systems can be quite fastidious in respect of their nutrient requirements for growth, maintenance, and synthesis of metabolic products. Bioconversion media can be either chemically defined or undefined (complex) (Table 1). The former type is confined mainly to laboratory-scale fermentations due to unfavourable economics. However, they are used industrially when product yield and process consistency are of prime importance (e.g. pharmaceuticals). Complex media constitute the core feedstocks of today's bioindustry and are produced as by-products of meat, cheese, grain, and fibre processing [8]. Table 2 shows that many of these provide more than one nutrient.

The most widely used complex media are molasses – a by-product of the sugar-refining industry – sugar and starch derivatives [1, 9]. Until 1986, cane or

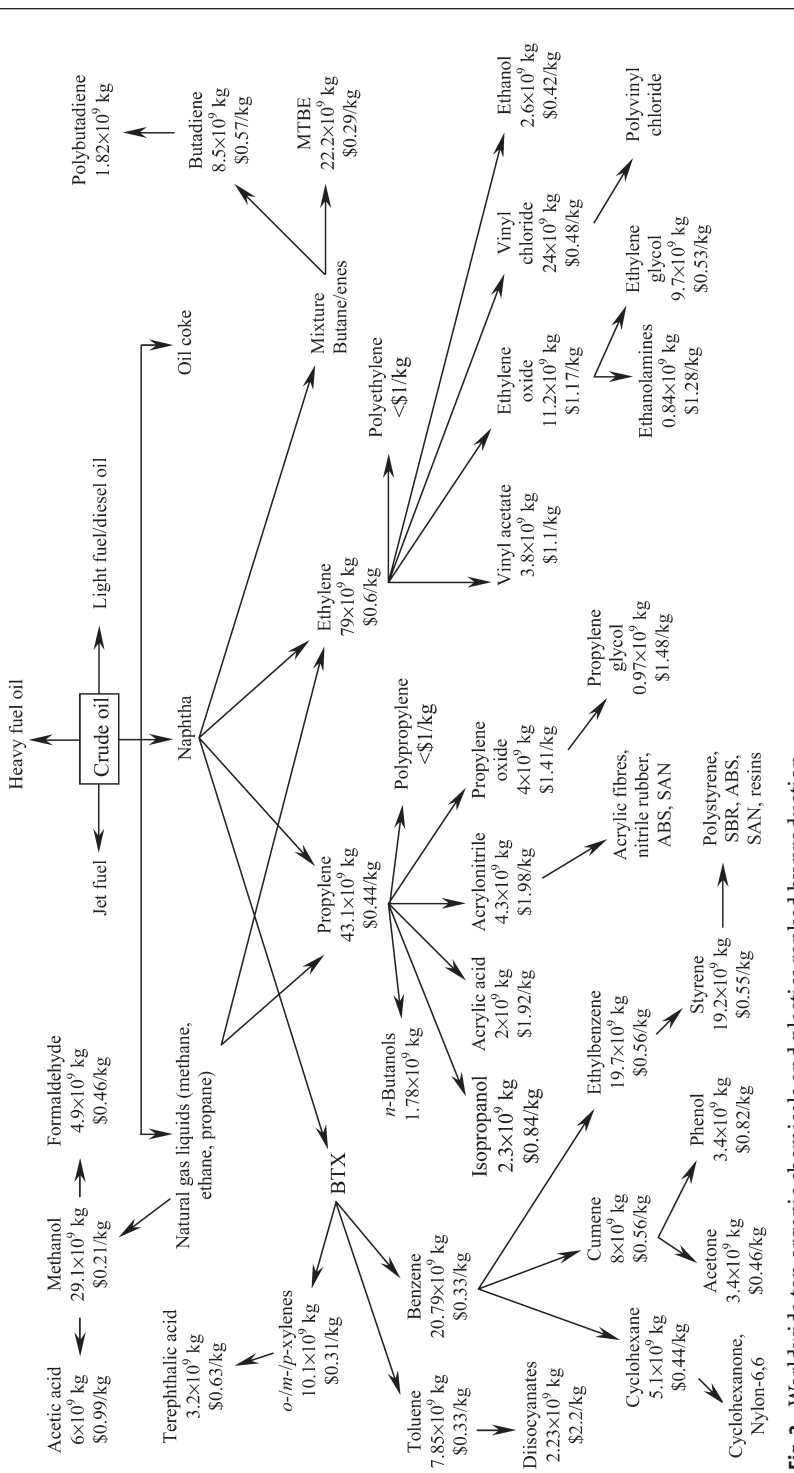

Fig. 2 Worldwide top organic chemicals and plastics ranked by production

Table 1 Raw materials commonly used in commercial bioprocesses grouped by their major nutritional value for cellular activity (adapted from Ref. [8])

Carbon sources:	Dextrose (commercial glucose)
	Glycerol
	Molasses (Beet or cane)
	Oils (soybean, corn and cottonseed)
	Starch, glucose syrups
	Starch hydrolysates
	Whey (65% lactose)
	Alcohols (such as methanol)
Nitrogen sources:	Cottonseed flour
	Soybean meal, flour, or grits
	Peanut meal
	Dried distillers' grains
	Whole yeast, yeast extract
	Yeast hydrolysates
	Corn steep liquor or its powders
	Corn gluten meal
	Linseed meal
	Fish meal
	Urea
	Ammonium sulfate
	Ammonia gas

beet molasses was almost the sole feedstock used in the EU fermentation industry [1]. Molasses has been widely utilized due to its low price, but its high impurity content, variable composition, limited production, high production of wastes, and low assimilation by microorganisms will eventually lead to its substitution by more efficient raw materials. Since 1986, starch and sugar derivatives have become more popular due to regulations enforced by the EU in an attempt to save the European fermentation industry from bankruptcy, as they could not compete with their non-EU counterparts [10].

2.2.1 *Starch production and processing*

Starch is a mixture of two different polymers of glycopyranose (amylose and amylopectin), whose only building block is glucose ($C_6H_{12}O_6$), linked by predominantly α-1,4 glycosidic bonds. It is predominantly present in cereals and potato. In EU countries starch is primarily extracted from wheat and maize (corn) and is mainly used in the food industry. Dry and wet milling techniques are applied to fractionate cereal grains into their components and produce a great diversity of foodstuffs. Wheat is processed by dry milling where the coarse grains are separated from straw/impurities, tempered to increase moisture content, and reduced by a series of break and reduction roller mills into various flour streams of varying particle size and starch, gluten, and bran composition. Current wheat flour mills operate at up to 80% grain to flour conversion efficiency; the remaining 20% comprises mainly bran, which is used as animal feed [11]. Starch

Table 2 Fermentation media ingredient analysis (adapted from [8])

Nutrient source	Major components						Mineral content				Vitamin content				Amino acids				
	Dry matter (%)	Protein (%)	Carbohydrates (%)	Fat (%)	Fibre (%)	Ash (%)	Calcium (%)	Magnesium (%)	Phosphorus (%)	Sulfur (%)	Biotin (mg kg^{-1})	Niacin (mg kg^{-1})	Riboflavin (mg kg^{-1})	Thiamine (mg kg^{-1})	Arginine (%)	Lysine (%)	Methionine (%)	Phenylalanine (%)	Tryptophan (%)
Carbon sources:																			
Corn	82.0	9.9	69.2	4.0	2.2	1.3	0.02	0.11	0.28	0.08	–	22.0	1.1	–	0.5	0.2	0.17	0.5	0.1
Molasses, beet	77.0	6.7	65.1	0.0	0.0	5.2	0.16	0.23	0.02	0.47	–	39.6	2.2	–	–	–	–	–	–
Whey, dried	95.0	12.0	68.0	1.0	0.0	9.6	0.9	0.13	0.75	1.04	–	11.0	19.8	3.96	0.4	1.0	0.4	0.5	0.2
Nitrogen sources:																			
Corn germ meal	93.0	22.6	53.2	1.9	9.5	3.3	0.3	0.16	0.5	0.32	–	41.8	3.74	–	1.3	0.9	0.57	–	0.18
Corn gluten meal, 41%	91.0	42.0	40.2	2.5	4.3	2.0	0.14	0.05	0.46	0.5	–	77.0	2.2	0.1	1.9	1.0	1.9	–	0.25
Corn steep liquor	50.0	24.0	5.8	1.0	8.8	–	–	–	–	0.88	–	–	0.88	0.4	0.2	0.5	0.3	–	
Corn steep powder	95.0	48.0	–	0.4	–	1.7	0.06	1.5	3.3	0.58	–	0.16	0.01	0.01	3.3	2.5	1.9	44	–
Dried distillers solubles	92.0	26.0	45.0	9.0	4.0	8.0	0.3	0.65	1.3	0.37	2.86	110.0	15.4	5.5	1.0	0.9	0.6	1.5	0.2

Table 2 (continued)

Nutrient source	Major components						Mineral content				Vitamin content				Amino acids				
	Dry matter (%)	Protein (%)	Carbohydrates (%)	Fat (%)	Fibre (%)	Ash (%)	Calcium (%)	Magnesium (%)	Phosphorus (%)	Sulfur (%)	Biotin (mg kg^{-1})	Niacin (mg kg^{-1})	Riboflavin (mg kg^{-1})	Thiamine (mg kg^{-1})	Arginine (%)	Lysine (%)	Methionine (%)	Phenylalanine (%)	Tryptophan (%)
Fish meal (anchovy), 65%	92.0	65.0	–	3.8	1.0	21.3	4.0	0.25	2.6	0.54	–	93.5	9.46	–	3.6	4.7	1.9	2.37	0.7
Linseed meal	92.0	36.0	38.0	0.5	9.5	6.5	0.4	0.56	0.9	0.39	–	35.2	3.08	8.8	2.5	1.0	0.8	1.8	0.7
Peanut meal and hulls	90.5	45.0	23.0	5.0	12.0	5.5	0.15	0.32	0.55	0.28	–	167.2	5.28	7.26	4.6	1.3	0.6	2.3	0.5
Pharmamedia (cottonseed flour)	99.0	59.2	24.1	4.02	2.55	6.71	0.25	0.74	1.31	0.6	1.52	83.3	4.82	3.99	12.3	4.49	1.52	5.92	0.95
Soybean meal	90.0	42.0	29.9	4.0	6.0	6.5	0.25	0.25	0.63	0.32	–	26.4	3.3	–	3.2	3.0	0.65	2.14	0.63
Yeast, brewers	95.0	43.0	39.5	1.5	1.5	7.0	0.1	0.25	1.4	0.49	–	498.3	35.2	74.8	2.2	3.4	1.0	1.8	0.8
Yeast, hydrolysate	94.5	52.5	–	0.0	1.5	10.0	–	–	–	–	–	–	–	–	3.3	6.5	2.1	3.7	1.2

is currently extracted by fractionating flour streams into gluten, bran, and starch. It is obvious that throughout this long operation from coarse grain to starch many components/nutrients are lost, while at the same time the high number of processing steps increases the final purchase cost of the starch.

Corn is mainly processed by wet milling in which it is initially soaked in an aqueous solution of sulfur dioxide (steeping) causing kernel swelling and transfer of some nutrients to the liquid fraction (steep liquor), which is drawn off and concentrated. The corn steep liquor is frequently used as a nitrogen and nutrient source for media formulations in the fermentation industry. After steeping the corn germ is removed from the kernel and processed to remove the corn oil. In the final stage, the remaining components of the kernel (starch, gluten, and bran) are separated. The bran is either mixed with the steep liquor to form wet corn gluten feed or dried to form dry corn gluten feed.

For most industrial bioprocesses, starch has to be hydrolysed into glucose. Before the 1970s, industrial starch hydrolysis was carried out by chemical processing. Nowadays, chemical degradation of starch is less often used because it has been substituted by enzymatic hydrolysis. Starch derivatives obtained by enzymatic hydrolysis can be categorized into four groups: maltodextrins with dextrose equivalent (DE) <20, glucose syrups (20<DE<80), starch hydrolysates (DE>80), and crystalline dextrose. The term dextrose equivalent refers to the extent of hydrolysis to the monomer and represents the relative reducing power of the hydrolysed starch slurry, calculated on a dry basis (db), with anhydrous dextrose given the value 100. The industrial process (Fig. 3) for the enzymatic hydrolysis of starch is divided into three stages: liquefaction, saccharification, and separation/purification [12]. The appropriate level of purification of starch derivative for a bioprocess depends on the microorganism to be used and the desired end-product. For instance, the low chloride and low inorganic levels of demineralized syrups have advantages in the brewing and pharmaceutical industries [12].

In many microbial bioprocesses, only the first two steps (i.e. liquefaction and saccharification) of starch hydrolysis are necessary. Figure 4 presents a schematic representation of the current production routes for the production of fermentation media from corn and wheat. Processes 1 and 2 utilize the starch derived from the conventional fractionation of wheat and starch, respectively. Process 3 utilizes the whole grain. Apart from α-amylase and glucoamylase, the use of proteases could be necessary if a polymeric nitrogen source (e.g. gluten) is present in the raw material.

2.2.2 *Sugar (sucrose) production and processing*

The disaccharide sucrose ($C_{12}H_{22}O_{11}$) consisting of one mole D-glucose and one mole D-fructose is the second most widely used carbohydrate, after starch, in bioprocesses. It is industrially available in the crystalline form or as aqueous solutions and syrups. The sucrose world market is supplied with 67% cane sugar and 33% beet sugar. The latter is the dominant source of sucrose in EU countries. The production of sugar from sugar beet is divided into the following processing stages:

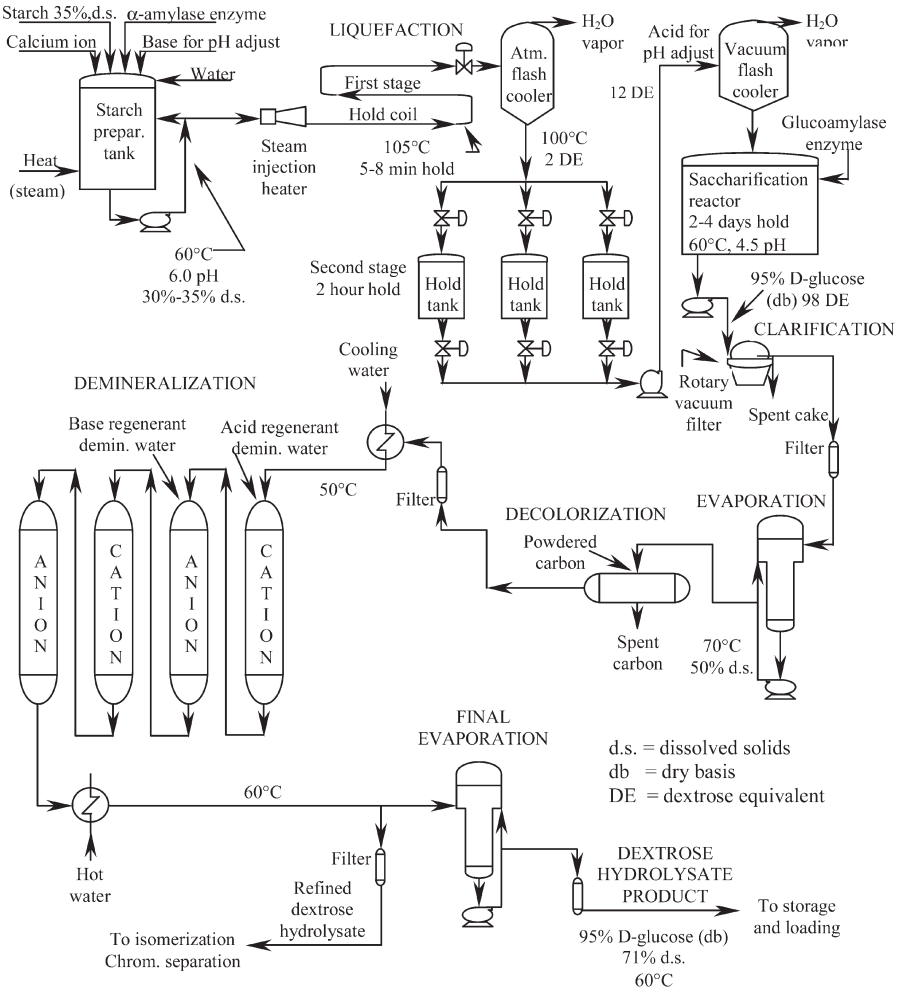

Fig. 3 Process flow sheet of a typical starch process producing various starch derivatives (adapted from [8])

1. cutting the beet to chips,
2. water treatment at 70–75 °C,
3. purification of the raw juice (12–15% sucrose) by filtration and treatment with slaked lime, CO_2, and ion-exchange,
4. concentration of the thin juice (11–14% sucrose) to 65–70%,
5. crystallization, and
6. centrifugation to separate the brownish raw sugar from the mother liquor, which is recycled [13].

Steps five and six are repeated three times and the mother liquor of the last crystallization step is sucrose molasses. For white sugar production the raw sugar in

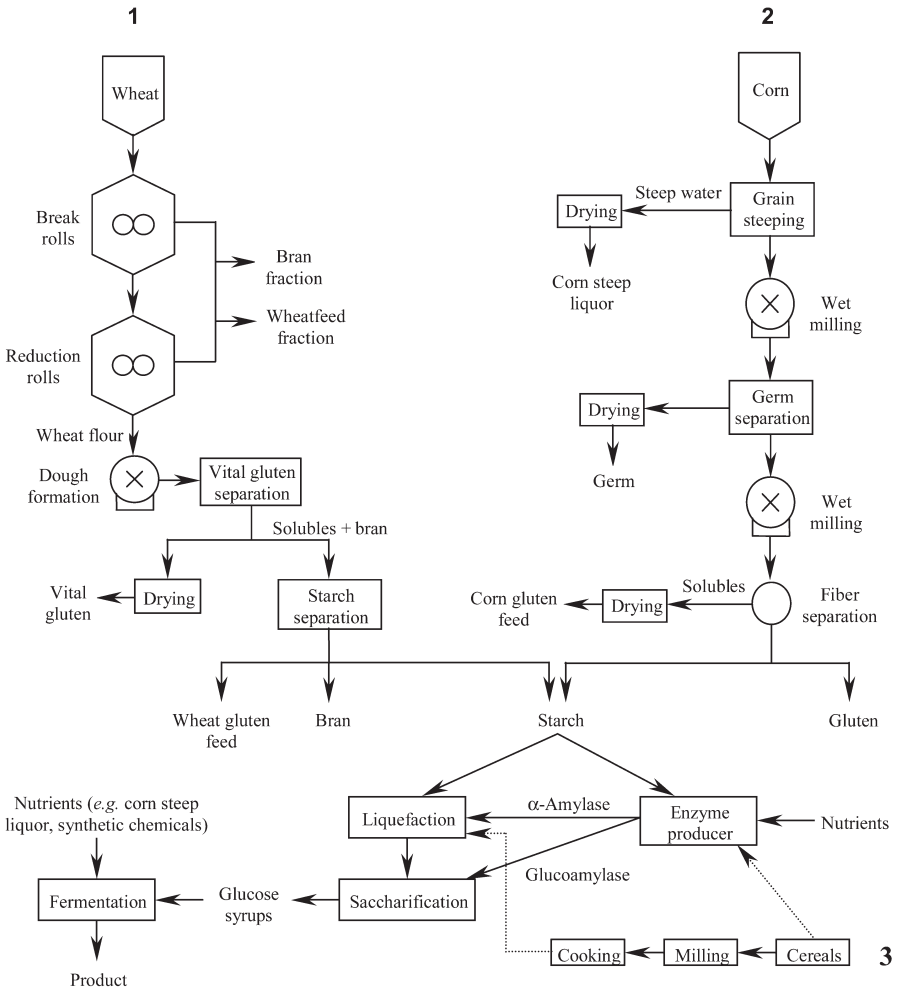

Fig. 4 Schematic diagram of current processing of wheat and corn for the production of fermentation media

the centrifuge is processed by stripping with hot water and drying. Subsequent steps include dissolution of the white sugar, purification with silica, treatment with activated carbon/decolorizing resins, concentration, crystallization and drying. The refined sucrose has the same sucrose content as white sugar but less moisture and minerals.

2.2.3
Burdens caused by current raw materials

Nowadays, it is clear that starch and sugar derivatives may provide higher yields than molasses but they are still too expensive and hamper the growth of bio-

processing. Biotechnology may have grown remarkably in the past ten years but one reason for its failure to dominate chemical processing is the type of raw material used. Price is the major barrier to development. European prices of fermentation feedstocks are not competitive in comparison with world market prices and fossil fuel sources of carbon. In addition, the need for cheap and efficient raw materials for bioprocessing is increasing rapidly and the carbohydrate (i.e. starch and sugar) extraction industry is unable to meet such requirements because it is largely based on old technology with high energy requirements. The development of improved extraction technologies or even the introduction of novel technologies is urgently needed to offer cost savings, improved environmental practice, and the ability to cope with the increasing productivity and range of product types. Apart from cost increases, the primary processing of agricultural crops, such as cereals, in the food industry leads to the partitioning to their components, such as starch, fibres, oil, and protein, resulting in the loss of essential fermentable materials. Last but not least, the major consumer of the carbohydrate extraction industry is the food sector, which diminishes the outlets for bioprocessing. This renders necessary the introduction of novel renewable raw materials and the development of production lines that will modify them and provide the fermentation industry with fermentable feedstocks of high efficiency and low cost. In turn, the development of a process to produce a generic fermentation feedstock could create a new market from which agriculture and the bioindustry can simultaneously benefit.

2.3 Future feedstocks for bio-industry

There is no doubt that the ideal bioconversion media in terms of economics would be those derived from low/no-cost lignocellulosic materials. These include various agricultural residues (e.g. wheat straw, hulls, stems, and corn stalks), wood, municipal solid wastes, wastes from the paper, food, and pulp industry and specifically grown crops (e.g. hybrid poplar and willow) [14, 15].

Lignocellulosic raw materials consist of three closely associated natural polymers: cellulose 35–50%, hemicellulose 20–35%, and lignin 10–25% [14]. Cellulose is a linear homopolymer of glucose linked by β-1,4-glycosidic bonds. Hemicellulose is an heteropolymer intimately associated with the cellulose chains which contributes to the strength of cell walls and consists mainly of three hexoses – glucose, mannose, and galactose – and two pentoses – xylose and arabinose – together with some uronic acids [16]. Lignin, the most complex natural polymer, is deposited in the walls of specific cells during the final stages of their differentiation. It plays a fundamental role in the mechanical support, solute conductance, and disease protection of higher plants. It consists of three hydroxyphenyl propenol building blocks.

Prior to fermentation, lignocellulosic raw materials are subject to some kind of pretreatment, including physical treatment (e.g. mechanical size reduction, pyrolysis), physicochemical treatment (e.g. steam explosion, ammonia fibre explosion, CO_2 explosion), chemical treatment (e.g. ozonolysis, acid hydrolysis,

alkaline hydrolysis, oxidative delignification), biological treatment and various combinations of such pretreatment processes [17, 18]. Chemical pretreatment has been found to be effective and economical [19]. Pretreatment optimization is necessary so as to maximize subsequent bioconversion yields, reduce costs and minimize the formation of inhibitory compounds [20]. One of the objectives of these pretreatment steps is to separate the lignin fraction. Lignin separation opens the lignocellulosic pore structure increasing the susceptibility of cellulose and hemicellulose to enzymatic hydrolysis. Lignin could also be regarded as a valuable by-product which can be either converted to low-molecular weight chemicals (e.g. vanillin, phenol and phenol derivatives, benzene and benzene derivatives and catechols) or used as raw material in the manufacture of a variety of polymeric materials [14].

The next stage is the hydrolysis of cellulose into reducing sugars. Enzymatic hydrolysis has less utility cost and is more environmentally friendly than acidic/alkaline hydrolysis [21]. The final stage is the fermentation of mixed hexoses and pentoses to produce the product of interest. Recombinant DNA technology could lead to the construction of genetically engineered microorganisms with the ability to hydrolyse the polymers and consume all the sugars for production of numerous end-products [15].

2.3.1
Burdens caused by lignocellulosics

Despite their low purchase cost, lignocellulosics cannot be used in the bioindustry, at least at the moment, because of the high costs of pretreatment and solids handling [22]. Biodegradation of lignocellulosics is a complicated procedure for four reasons [23]:

- Lignocellulosics are insoluble and highly crystalline, rendering the glycosidic bonds inaccessible to enzymes.
- Monomers in cellulose are linked with β-1,4 chemical linkages, which are more resistant to hydrolysis than the α-1,4 linkages in starch.
- Purified enzyme solutions (cellulase, hemicellulase) are currently expensive, while existing microbes cannot produce sufficient amounts of such enzymes in-situ.
- Hemicellulose and lignin are tightly associated with cellulose, hindering cellulose biodegradation.

3
Chemical production via bioconversion

A bio-based chemical industry will restructure the current petroleum-based industry because:

1. the chemical composition of biomass differs from that of petroleum, and
2. microbial metabolism leads to the production of primary chemicals that are different from the primary building blocks of the chemical industry.

In most bioconversions, the most important nutrient is the carbon source, which most of the time is also the energy source. Glucose, which is the most favourable carbon source for the metabolism of many microorganisms, is the predominant monomer in starchy and lignocellulosic raw materials. Figure 5 presents the great diversity of metabolic products that can be derived directly from glucose via fermentation. In turn, these products can be used either as end-products or as intermediates for the production of other chemicals.

In general, biotechnologies can lead to the production of either existing chemicals or new ones with added-value performance characteristics (e.g. biopolymers, biopesticides). In the former case markets for product disposal have been created long ago and competition with conventional production pathways will be strictly on the basis of price. In the latter case, however, the public may be prepared to pay a higher premium because of the special attributes provided by the product. However, the establishment of such novel products is not an easy task because there are no existing markets for their disposal and, therefore, extensive product development, research, and market evaluation is a prerequisite for their commercialization.

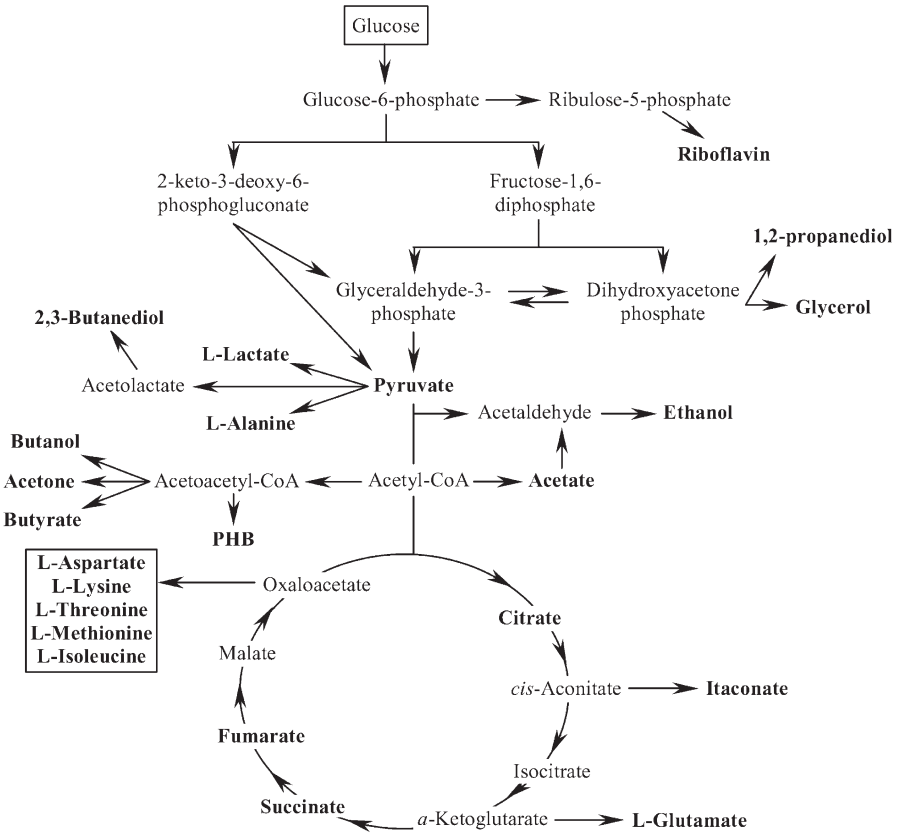

Fig. 5 Metabolic products from glucose

3.1
Current status of industrial bioprocessing

In general, chemical products can be classified into two major groups, according to their production volume and market value.

- *Commodity products*. Such products are produced in bulk quantities and are sold on price, rather than quality.
- *Speciality or higher value products*. These are produced in lower quantities and usually command a high price. They are sold on physical and chemical performance and not on price.

The relationship between value and price cannot be described easily because it depends on several factors. In an inflated economy value is inversely proportional to quantity and directly proportional to price, considering that higher productivity naturally leads to a lower price. If, however, a speciality product has specific performance characteristics then the price may still remain relatively high even at higher production capacities. In addition, a speciality product may turn into commodity and vice-versa depending on social needs and political decisions. For instance, the agricultural sector is often favoured by governmental subsidies and protection against imports. An example is ethanol production in the USA and Brazil, which has become economically feasible on a large scale because of government subsidies.

Large-scale bioproduction of most chemicals demands significant improvements in process economics and major technological advances. But even if these have been achieved survival of a bioprocess in the market depends on secondary factors such as the number of applications and their efficiency/cost margins, restructuring, the entry of competitors, and growth prospects. These observations suggest that bioprocessing is currently suitable only for manufacturing of speciality products. The widespread application of bioprocessing for the production of commodities is strictly dependent on politics, and government support is necessary to restructure today's chemical industry.

Bioprocessing already dominates and grows steadily in key speciality sectors (e.g. pharmaceuticals), while it is gradually expanding in some others (e.g. agrochemicals, flavour and fragrances, food additives, dyes) [24, 25]. Industrialists spend significant amounts of venture capital on research and development (R&D) to replace chemical processing with bioprocesses [26–28]. In 1998, more than 200 organic chemicals (over half of which were specialities) were produced by fermentation by approximately 3000 biotech companies worldwide (mainly in the USA and the UK) [29]. Figure 6 illustrates the growth of dedicated biotech companies in the EU and USA from 1997 to 2001 [30]. Current estimates predict that by the year 2005 the European biotechnology market could be worth over €100 billion and that by the end of the decade global biomarkets could amount to over €2,000 billion [30]. Last, but not least, government support of the biosciences has been increasing steadily.

Some examples of governmental initiatives are listed below:

- The £13 million BIOWISE program was launched by the UK Department of Trade and Industry (DTI) as a comprehensive source of expert advice, pro-

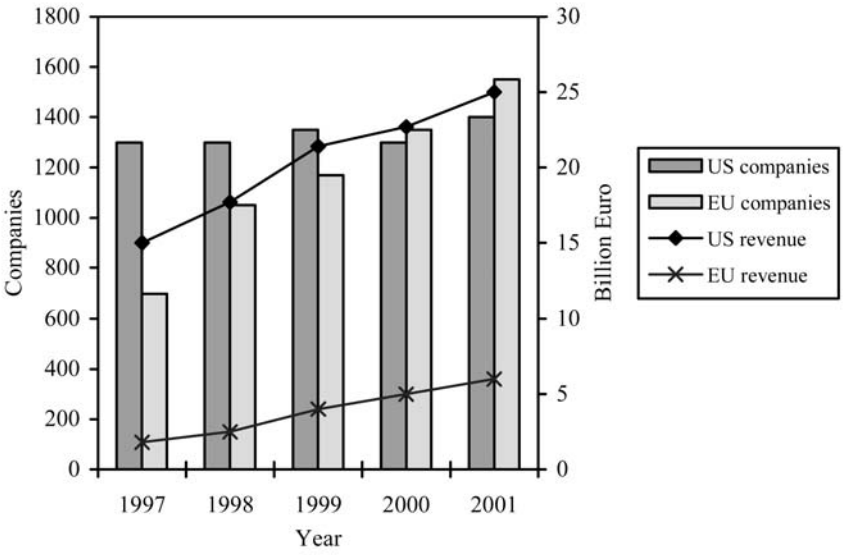

Fig. 6 Biotech companies and markets in EU and USA (adapted from Ref. [30])

vided free of charge, focussing on promoting industrial bioprocessing in the UK's manufacturing industry [31]. It was identified that more than 70,000 UK manufacturing companies could benefit by adopting bioprocessing through cost reductions and profitability improvement.

- The UK Pro-Bio Faraday Partnership aims at developing a more sustainable and vibrant chemical and pharmaceutical sector through interdisciplinary (e.g. biological sciences, chemistry, engineering) collaborations [32].
- Between 1994–1998, the EU commissioned €595.5 million for the Biotechnology program (BIOTECH 2) during the Fourth Framework program with the aim of improving basic biological knowledge of living systems and increasing productivity in a sustainable fashion, with regard to applications in agriculture, industry, health, nutrition, and the environment. This effort continues through the fifth (1998–2002) and sixth (2002–2006) framework programs [30].
- In 1999, the US government introduced the "INEEL Bioenergy Initiative", which embraces the vision of "Whole Crop Utilization" aiming at replacing fossil with renewable carbon for the production of fuels, power and materials [33]. The term "Whole Crop Utilization" can be translated in two ways:

  1. to use the entire crop to produce food, feed, fibre, energy and value-added products, and
  2. to revitalize agricultural growth by providing an additional outlet to farmers.

Table 3 presents the global magnitude and market value of chemicals that are already produced through bioprocesses. In the following sections a literature review of a selection of products that are already produced, or present a great potential to be produced, by bioprocessing is presented.

Table 3 Global quantity, substrate and value of major fermentation products

Organic Chemical	Global production (10^3 kg/yr)	Current feedstock used for fermentative production	Value (10^6 $/yr)
Bioethanol	13,000,000	Corn/sugar cane	5,460
Organic acids			
Citric acid	600,000	Molasses/starch hydrolysates	1,400
L-Lactic acid	100,000	Sucrose/glucose syrups	150
Gluconic acid	40,000	Glucose syrups/starch hydrolysates	93
Itaconic acid	15,000	Molasses or starch hydrolysates	60
Vitamins			
C (Ascorbic acid)[a]	80,000	Glucose syrups	600
B_2 (Riboflavin)	3,000	Molasses	207
B_{12} (Cyanocobalamin)	3	Molasses	71
Amino acids			
L-Glutamic acid	1,000,000	Molasses/glucose syrups	1,143
L-Lysine	300,000	Molasses/glucose syrups	600
L-Phenylalanine	13,000	Glucose syrups	198
L-Aspartic acid	8,800	Not found	43
L-Threonine	2,500	Glucose syrups	Not found
L-Isoleucine	400	Not found	Not found
Miscellaneous			
Antibiotics	50,000	Sucrose/glucose syrups	28,000
Xanthan gum	33,000	Sucrose/glucose syrups	408
Nucleotides	10,100	Not found	350
Biopesticides	4,600	Not found	160
PHB	1,000	Sucrose/glucose syrups	16,000

[a] Partly synthetic process (chemical+bioconversion).

3.1.1 *Biofuels*

Bioethanol, which is used as an oxygenated chemical added to gasoline, to make it burn more easily, is the main biofuel currently produced on a large scale (about 13 million tonnes per year). The fuel of the future, hydrogen, could also be produced through bioprocessing but the research for its bioproduction is in its infancy.

3.1.1.1 Bioethanol

Unlike most chemicals derived through bioprocessing, industrial bioethanol costs less than \$1.00 kg^{-1}. After a decade-long competition with methyl *tert*-butyl ether (MTBE), bioethanol, although more expensive, has become the preferred gasoline additive for environmental reasons – MTBE leakage from gasoline storage tanks can severely contaminate underground water resources [34, 35].

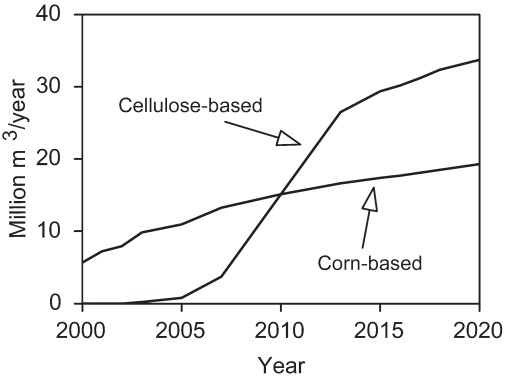

Fig. 7 Projections for bioethanol production in USA by cellulose and starch based processes until 2020 (adapted from Ref. [36])

Glucose and sucrose are the most common carbon sources for current bioethanol production in the USA/EU and Brazil, respectively. Glucose is derived from starch, which is extracted from corn, potatoes, and wheat. Current fermentation processes, most frequently involving *Saccharomyces cerevisiae*, yield 10–12% ethanol by volume under optimum conditions after 5 days. The major step in downstream processing for bioethanol recovery is steam distillation, while the remaining stillage can be further processed into animal feed. In recent years new bioprocesses are being developed aiming at producing bioethanol from lignocellulosics (Fig. 7). However, lignocellulosics do not provide a cost-effective feedstock due to the cost of the enzymes needed to convert the biomass into sugars. If enzyme costs were less than \$0.033 kg^{-1} ethanol, compared with \$0.15 today, the cost of production would drop enough to make this form of biomass an economical feedstock [36].

Iogen Corporation (Canada) is scaling up a bioethanol production process which utilizes cellulosic materials instead of corn-derived glucose [37]. The conversion of cellulose to fermentable sugars has been maximized by utilizing bio-optimized cellulase and production costs are expected to be competitive with the cost of gasoline produced from oil when a barrel costs \$25.

Cost reduction in bioethanol production could be achieved by using hydrolysates of cheap renewable carbohydrates (e.g. lignocellulosics, whole grain), but this endeavour faces bigger obstacles [38]:

- Traditional high-yield bioethanol producers such as *Saccharomyces* species and *Zymomonas mobilis* metabolize a limited range of carbon sources.
- Several bacteria such as *E. coli*, *Klebsiella*, *Erwinia*, *Lactobacilli*, *Bacilli*, and *Clostridia* utilize a wider variety of carbon sources, but conversion results in limited ethanol yield because mixed acids and solvents are also produced by their metabolism.

Classical mutagenesis and selection without genetic engineering cannot achieve the required results. Two approaches have been widely used by pathway engineers [15]:

- Expand pentose utilization capacities of the hosts (*Saccharomyces*, *Zymomonas*), which are already efficient in converting hexoses to ethanol.
- Divert carbon flow from the native fermentation products to ethanol in the hosts (*E. coli*, *Klebsiella*, *Erwinia*), which are already efficient in utilizing mixed sugars.

3.1.1.2 Hydrogen

Hydrogen is a renewable and CO_2-neutral energy source because it produces only water vapour as end-product and can be easily converted to electricity by fuel cells, producing large amounts of energy per unit mass (122 kJ g^{-1}). Large-scale economic fuel cells utilizing hydrogen could soon be used in residential housing, buses, and cars [39]. Current natural gas and petroleum based production routes (45×10^9 kg in 1988) via steam reforming spoil the environmentally benign nature of hydrogen. In addition, renewable hydrogen production by photovoltaic-electrolysis, thermal cracking with nuclear process heat, and gasification of biomass is still an expensive alternative [4, 40]. For this reason, research into cost-competitive biohydrogen production has revived in the last decade especially in Japan, Germany, and the USA. Biological processing can be divided into photosynthetic and fermentative production routes (Table 4). In all cases, hydrogen is the final product of reductant disposal from hydrogenase or nitrogenase activity. Ferredoxin acts as the primary electron donor for both enzymes receiving electrons from the reduced products of glycolysis, NADH or NADPH [41, 42].

3.1.1.2.1 Direct–indirect biophotolysis

Despite wide research undertakings for development of economical photosynthetic biohydrogen operations, most studies proved to have limited viability in large-scale applications [40]. Photosynthetic processes for hydrogen production can be divided into direct and indirect biophotolysis, microbial photoheterotrophic fermentation, and microbial shift reaction. The term "direct biophotolysis" describes direct electron transfer from water to hydrogen ions by combining the water splitting and ferredoxin-reducing reactions of photosynthesis with a hydrogen-producing hydrogenase [40]. Direct biophotolysis using microalgae (e.g. *Chlamydomonas* sp. and various mutants) have been studied extensively but simultaneous oxygen and hydrogen generation restricts its efficiency [43]. The enzyme hydrogenase that catalyses water reduction is inhibited by oxygen generated during photosynthesis. Thus, compartmentalization of direct biophotolysis reactions in two stages is necessary. The first stage would involve photosynthesis (CO_2 fixation and O_2 production) by one microorganism and the other, degradation of carbohydrates by another organism (indirect

Table 4 Biological hydrogen production routes

A. Photosynthetic production routes

1. *Direct biophotolysis*

$6H_2O+6CO_2 \xrightarrow{light} C_6H_{12}O_6+6O_2+$cellular energy

$H_2O \xrightarrow{light} H_2+0{,}5O_2$

Constraints:
1) enzyme inhibition by O_2 generation,
2) low solar conversion efficiency,
3) expensive photobioreactors

2. *Indirect biophotolysis*

$6H_2O+6CO_2 \xrightarrow{light} C_6H_{12}O_6+6O_2+$cellular energy

$C_6H_{12}O_6 \xrightarrow{light}$ cells+cellular energy+CO_2+H_2

Constraints:
1) need for separate steps for CO_2 fixation and O_2 production – H_2 production,
2) low solar conversion efficiencies due to inefficient nitrogenase,
3) expensive photobioreactors

3. *Bacterial photosynthesis*

Organic acids→cells+cellular energy+CO_2+H_2

Max. theor. yield: $CH_3COOH+2H_2O \rightarrow 4H_2+2CO_2$ (ΔG_0=+104.6 kJ mol^{-1})

Constraints:
1) inexistent organic acid waste streams,
2) inefficient nitrogenase

4. *Microbial shift reaction*

$CO+H_2O \rightarrow CO_2+H_2$

Constraints:
1) CO dehydrogenase inefficient,
2) expensive photobioreactors

B. Fermentation of carbohydrates (no light requirements)

Carbohydrates→cells+cellular energy+organic acids+CO_2+H_2

Theoretical yields: $C_6H_{12}O_6+2H_2O \rightarrow 2CH_3COOH+2CO_2+4H_2$

$C_6H_{12}O_6 \rightarrow CH_3CH_2CH_2COOH+2CO_2+2H_2$

Constraints:
1) low H_2 production yields,
2) costs of carbohydrates

biophotolysis). For instance, Miura et al. proposed hydrogen production in a light/dark cycle where starch is formed by CO_2 fixation during day-time and hydrogen and organic acids/alcohols are formed from starch under anaerobic conditions during night-time [44]. However, to develop a viable large-scale process utilizing biophotolysis, the yield for H_2 production should be increased by a factor of ten or more [45]. In addition, 10% solar energy conversion efficiency is necessary to develop biophotolysis processes competitive with alternative sources of renewable hydrogen [40]. Last but not least, another major problem is the currently expensive photobioreactors, and economical designs are required.

Photosynthetic H_2 production by nitrogen-fixing blue–green algae (cyanobacteria) using nitrogenase is not an efficient production route. The main disadvantages of such a process are inhibition of nitrogenase by NH_3 and O_2, high energy requirements, low solar conversion efficiency, and a turnover rate 1000 times lower than hydrogenase. Benemann [40] stated that even with additional R&D the nitrogen-fixing cyanobacteria will never achieve the necessary efficiency goals required by preliminary economics of production.

3.1.1.2.2
Photoheterotrophic fermentation

Photosynthetic bacteria (especially *Rhodopseudomonas* and *Rhodobacter*) can produce hydrogen by anoxygenic photosynthesis by utilizing organic compounds (e.g. alcohols and/or acetic, lactic, succinic, and butyric acids) as electron donors. The main advantages of using bacteria are:

1. the wide knowledge of their physiology, enabling genetic engineering, and
2. the low light-energy requirements resulting in simpler photobioreactor design and reduced cost.

Nevertheless, in such a system the hydrogen evolution rate is low because the photosystem of the cell becomes light-saturated at low light intensities [46]. For this reason, the level of light saturation of the system should be increased to increase light-energy conversion.

Another problem is that hydrogen production in many photosynthetic bacteria is catalysed by inefficient nitrogenase, resulting in high light-energy losses. A possible solution is the use of engineered bacteria that reduce energy losses [43]. In addition, wastes containing large amounts of organic acids are rare, hindering large-scale operations. Profitable process economics could be achieved by coupling H_2 production with another process of environmental importance (e.g. wastewater treatment) [47] or the production of another added-value chemical (e.g. microbial biodegradable plastics) [48, 49].

Photosynthetic bacteria can also be used to shift CO and H_2O into H_2 and CO_2 in darkness and at room temperature [50]. Jung et al. reported that a heterotrophic bacterium, *Citrobacter* sp. Y19, can catalyse the water-gas shift reaction producing H_2 at a maximum rate of 33 mmol H_2 (g cells)$^{-1}$ h^{-1} for about 200 h under anaerobic conditions [51]. However, further improvements in CO dehydrogenase are necessary [46].

3.1.1.3 Fermentation of carbohydrates (no light requirements)

In heterotrophic fermentation anaerobic bacteria produce hydrogen and organic acids from carbohydrates. Its main advantage over photosynthetic processes is that it does not rely on light availability and the transparency of the mixed broth [52]. Pure bacterial cultures such as *Clostridia*, *Alcaligenes*, *Bacillus* sp., and *Enterobacteria* have been widely used [53]. Recently, mixed communities have been tested for fermentative hydrogen production [54, 55]. One of the difficulties with mixed cultures is the co-existence of hydrogen-producing and hydrogen-consuming microorganisms, such as methanogens. To overcome this obstacle mixed bacterial cultures are heat-treated to inhibit hydrogen-consuming methanogens and to enrich spore-forming, hydrogen-producing acidogens [39, 55, 56].

The major obstacle faced in fermentative hydrogen production is the low yield. The theoretical maximum yield (Table 4) is 4 mol H_2/mol glucose (corresponding to 0.467 L H_2/g COD), in the case that all of the substrate is converted into acetic acid. In practice, the substrate is consumed for cell growth, maintenance, and synthesis of various metabolic products (e.g. butyric, formic, lactic acids, alcohols) resulting in a lower hydrogen yield. For this reason, reported hydrogen yields by pure or mixed cultures vary from 0.37 (over 60 days semi-continuous culture of *Bacillus licheniformis*) [57] to 3.02 mol H_2/mol glucose (continuous culture of *Enterobacter aerogenes* growing on agro-industrial residues in a packed column) [58]. No microbiological route has been reported to produce the maximum of 4 mol H_2/mol glucose. However, Woodward et al. achieved 97% conversion efficiency using an enzyme solution [59].

In order to achieve higher H_2 production yield, Miyake et al. introduced a two-step process utilizing anaerobic and photosynthetic bacteria to convert sugars into organic acids and hydrogen in the first stage and organic acids into hydrogen in the second [60]. In such a process, the theoretical conversion is 12 mol H_2/mol glucose. Zhu et al. enhanced H_2 production (160% higher than the single entrapped culture of the anaerobic bacterium) by using an entrapped co-culture of *Rhodobacter sphaeroides* and *Clostridium butyricum* [61]. A two step reaction consisted of:

1. a mixed batch culture of *Clostridium butyricum* and *Enterobacter aerogenes* grown in a medium consisting of sweet potato starch residue/waste and 0.1% polypeptone/corn steep liquor, and
2. a photosynthetic fermentation carried out by *Rhodobacter* sp. M-19 in the supernatant of the culture broth derived from the first step, which resulted in a high overall H_2 yield of 7.0–7.2 mol H_2/mol glucose [62, 63].

Another way to increase H_2 yields is to use facultative anaerobic bacteria instead of strict anaerobes, exploiting the TCA cycle and re-oxidizing the $FADH_2$ generated in the electron-transport system, resulting in a maximum of 10 mol H_2/mol glucose [64].

This combination of dark and photosynthetic fermentation is attempted because conversion of organic acids (acetate) to CO_2 and H_2 by dark fermentative

bacteria is thermodynamically unfavourable (Table 4) at moderate temperatures [50]. This reaction would be feasible under high H_2 partial pressure (10–100 Pa) and temperature (≥40 °C) conditions [46]. In this respect the use of thermophilic organisms could achieve the oxidation of organic acids to CO_2 and H_2 at high temperatures (around 70 °C) where this conversion is thermodynamically feasible [65].

Because of low H_2 yields, the only way to develop economic large-scale operations based on heterotrophic fermentation is to reduce capital investment and operating costs (e.g. continuous instead of batch operation, raw material, energy requirements). Continuous fermentation will not only reduce capital investment but it will also keep low the partial hydrogen pressure in the gas phase, decreasing the growth rate and shifting from acetate to lactate or alanine production, hence decreasing hydrogen yield [46]. The raw materials used should be inexpensive wastes/by-products from agriculture and the food industry. Waste starch has been used effectively in some studies [63, 66] but no-cost lignocellulosic wastes should be the targeted raw materials. In this respect, major breakthroughs could be achieved by using extreme thermophiles. Such microbes can secrete a wide range of enzymes (e.g. cellulolytic, amylolytic, proteolytic) enabling the use of complex agricultural/forestry wastes for H_2 production. In addition, high temperature would avoid the need for sterilization and favour hydrogen production by inhibiting the production of other end-products [46]. Thermophylic microorganisms belonging in the genus *Thermotogales* can utilize a wide variety of feedstocks, including complex carbohydrates and proteins, at high temperatures (≥40 °C) leading to efficient H_2 production [67]. Metabolic engineering could also assist H_2 production yields, though only limited studies have so far been carried out [68].

Process optimization is necessary depending on the biological system used. Various fermentation conditions (e.g. pH, residence time, substrate concentration, nitrogen gas sparging) should be optimized to achieve higher productivities and yields [56, 66, 69, 70]. For instance, optimum pH may vary from 4.0–9.0 (extreme values) depending on the culture used [70].

3.1.2 *Organic acids*

Bioprocessing has long been the basis for production of citric acid. In recent years, large-scale bioprocesses for lactic, gluconic, and itaconic acid production have also been developed. Succinic acid is a likely next candidate for large scale bioproduction.

3.1.2.1 Citric acid

Citric acid fermentation has been recorded as the first established industrial filamentous fungal bioprocess [71]. Current worldwide demand is about 6×10^8 kg year^{-1} [72]. It is an edible acidifier, a strong chelating agent, highly soluble, palatable, with low toxicity. Because of all these characteristics the acid has been applied

as condiment, preservative, antioxidant, and pH adjuster, while its sodium, potassium, and calcium salts are used as chelating agents and food dyes. Citric acid is also used in pharmaceutical manufacturing.

The filamentous fungus *Aspergillus niger* is the most commonly used microorganism in industrial fermentations, which are carried out either in the submerged or solid state. Fermentation lasts 5–12 days, depending on the specific process [73]. The glucose to citric acid conversion yields can reach values of 90–100% on a weight basis. Common carbon sources in fermentation media are sucrose, glucose syrups, starch, and molasses. Fermentative citric acid overproduction is achieved when:

1. aconitate dehydrogenase together with all the enzymes of the TCA cycle apart from citrate synthetase are deactivated, and
2. the feedback inhibition of phosphofructokinase by citric acid is bypassed [71].

These targets are industrially met by formulating fermentation media deficient in iron and manganese. Iron increases the activity of aconitate dehydrogenase causing citric acid to convert into aconitate. In turn, manganese causes an increase in cell growth, while sugar consumption diminishes and acidogenesis decreases drastically. Manganese deficiency results in:

1. the repression of the anaerobic and TCA cycle enzymes with the exception of citrate synthetase, and
2. the accumulation of intracellular NH_4, which reverses phosphofructokinase inhibition by citric acid [73, 74].

Another factor that contributes to high citric acid production is the low pH optimum conditions (1.7–2.0) because higher pH levels lead to the production of oxalic and gluconic acids instead of citric acid [74].

Recovery of citric acid is achieved industrially by neutralization of citric acid with lime, separation of the tricalcium citrate deposit by filtration, a double-decomposition reaction between tricalcium citrate and sulfuric acid, disposal of calcium sulfate by filtration, carbon and ion exchange treatment of the mother liquor containing dissolved citric acid, and, finally, purification of citric acid by evaporation, crystallization, separation, and drying [73].

3.1.2.2 Lactic acid

Lactic acid (2-hydroxypropionic acid) is the most extensively occurring hydroxycarboxylic acid. Lactic acid finds applications in the food and textile industries as an acidulant, a flavouring, a pH buffering agent, an ingredient for emulsifying agent formulation, and an inhibitor of bacterial spoilage [75]. With ethyl lactate it has long been used in pharmaceutical and cosmetic applications and formulations. Recently lactic acid has received much attention due to its use for polylactate polymers [76]. For instance, Cargill Dow has already commercialized polylactic acid (PLA) under the trade name NatureWorks with initial markets in clothing fibre and packaging materials [77]. Cargill Dow Polymers (CDP) is constructing a plant to produce 1.4×10^8 kg year^{-1} of PLA in Blair (Nebraska, USA).

The company is currently producing lactic acid from corn starch, but research is focussed on the use of lignocellulosics.

In industry, lactic acid is manufactured either by chemical synthesis or by fermentation. Fermentative lactic acid production is more beneficial, because of the direct production of the desired stereoisomer L-lactic acid, the high yield achieved, and the low power and cooling requirements, because lactic acid fermentation is an anaerobic process. The existing industrial production processes use homolactic microorganisms (e.g. *Lactobacillus delbrueckii*, *L. bulgaricus*, *L. leichmanii*), which are fed with either sucrose or glucose syrups. Nitrogen and other nutrients are supplied by corn steep liquor, yeast extract, and soy hydrolysate. Lactic acid fermentation is conducted batchwise, lasting 4–6 days. The initial carbohydrate concentration is around 15% (*w*/*v*) and the conversion from total carbohydrate to lactate is more than 90% (*w*/*w*) [75]. As in all organic acid fermentations the pH is adjusted by addition of base during fermentation and this causes lactate formation. Fermentation economics are currently poor, because of the high cost of fermentation media and the production of a relatively low concentration of lactic acid, because of its inhibitory effect on the growth of lactic acid bacteria [78].

Downstream processing involves broth filtration to remove cells, carbon treatment, evaporation and acidification with sulfuric acid to convert the lactate into lactic acid and an insoluble by-product, such as calcium sulfate, which is removed by filtration. Further purification is achieved through carbon columns, by ion exchange, and finally evaporation to produce technical and food-grade lactic acid. Heat-stable and highly pure lactic acid, essential for the production of biodegradable polymers, is derived by esterification of the technical-grade lactic acid with ethanol or methanol and subsequent recovery of the desired product by distillation, water hydrolysis, and evaporation. Downstream processing is currently expensive because of the complex and prolonged recovery and purification processing steps and the large amount of by-product produced by the addition of sulfuric acid [75].

The impending future use of lactic acid as an intermediate in chemical synthesis is the main reason for the increased interest amongst the scientific community in the fermentative production of lactic acid. On-going research using lactic acid bacteria is mainly focused on:

- the formulation of more competitive and efficient fermentation media from cereals, potatoes, various protein sources, and agricultural or food-industry wastes [76, 78–87]; and
- the improvement of downstream processing aiming to reduce the total operating cost, eliminate the production of by-products, separate various impurities alongside the primary purification process and develop an effective and cost-competitive secondary purification process [87, 88].

Apart from lactic acid bacteria, recent research has shown that the fungus *Rhizopus oryzae* can produce significant quantities of almost optically pure L-(+)-lactic acid [89–101]. In these studies, emphasis was given to the improvement of process efficiency and minimization of process costs. The morphology of *R. oryzae* during lactic acid fermentation is very important because the production

of high lactic acid concentrations, glucose to lactic acid conversion rates, and productivities depends on oxygen transfer. The formation of large pellets, free mycelia, or clumps increases the viscosity of the fermentation broth hampering the transfer of oxygen, which results in long fermentation times, formation of unwanted end-products such as ethanol, because of the localized anaerobic conditions, and low glucose to lactic acid conversion yield. The importance of *R. oryzae* morphology during lactic acid fermentation has led to research on the development of favourable morphologies aiming at process optimization [92, 94, 100].

Promising results for the commercialization of lactic acid production by *R. oryzae* have been published by Kosakai et al. [92]. In this study, lactic acid production was enhanced by altering the fungal morphology from a pellet-like cake to a cotton-like appearance. This was achieved by creating mycelial flocs, which were formed by the addition of 3 g L^{-1} mineral support and 5 ppm polyethylene oxide. This morphology facilitated oxygen transfer in the culture broth and improved the fluidity of the culture broth in the fermenter. Batch fermentation conducted using this technique resulted in lactic acid concentration and yield of 103.6 g L^{-1} and 0.86 g g^{-1}, respectively, using a fermentation medium that contained a glucose concentration of 120 g L^{-1}. The creation of cotton-like mycelial flocs by addition of 3 g L^{-1} mineral support and 5 ppm polyethylene oxide was also used in fermentations in an airlift reactor resulting in lactic acid concentration and yield of 104.6 g L^{-1} and 0.87 g g^{-1}, respectively [94].

Bai et al. studied the effect of $CaCO_3$ addition, inoculum size, NH_4NO_3 concentration, agitation speed, and rate of aeration on mycelial morphology, growth, and lactic acid production [100]. Initiation of $CaCO_3$ addition after fermentation for 8 h resulted in the formation of uniform sized mycelial pellets (diameter 1–2 mm). An inoculum spore concentration around 3×10^6 spores mL^{-1} resulted in the formation of small mycelial pellets. A maximum L-(+)-lactic acid concentration of 76.2 g L^{-1} was produced after fermentation for 36 h, which was operated at 300 rpm agitation speed and 0.6 vvm aeration rate. In this fermentation, *R. oryzae* formed pellets with an average diameter of 1.4 mm. Fungal pellets were reused in six successive batch fermentations resulting in average L-(+)-lactic acid concentration, yield and productivity of 75.6 g L^{-1}, 75.6%, and 3.52 g L^{-1} h^{-1}, respectively.

Immobilization techniques and integrated production/separation processes have been used to enhance process efficiency and economics. Lin et al. developed a process where lactic acid fermentation, which was carried out by *R. oryzae* immobilized on a rotating disk contactor, was coupled with lactic acid separation by means of ion-exchange resins [91]. This process resulted in a conversion ratio of glucose to L-lactic acid of 0.7 g g^{-1}. Xuemei et al. developed another simultaneous fermentation-separation process where fermentation was carried out in a three-phase fluidized bed bioreactor with *R. oryzae* immobilized on calcium alginate beads and separation was conducted by electrodialysis [98].

The fermentative production of lactic acid by *R. oryzae* could outstrip lactic acid bacteria in terms of economics if a bioprocess utilizing starch instead of glucose is developed. In a study conducted by Yin et al. it was shown that it is possible to produce a lactic acid concentration and a glucose to lactic acid conversion yield of 102 g L^{-1} and 77%, respectively, in fermentations conducted by *R.*

oryzae NRRL395 in a 3-L air-lift bioreactor using a microbial medium that contained 120 g L^{-1} corn starch, 1.35 g L^{-1} ammonium sulfate, and small amounts of mineral salts (potassium phosphate, magnesium sulfate, and zinc sulfate) [90]. Attempts to reduce bioprocessing costs have also been made by using hydrolysates of lignocellulosic raw materials (e.g. *Pinus taeda* chips) as microbial media for lactic acid fermentation by *R. oryzae*, but the sugar to lactic acid conversion yields (about 25%) and lactic acid concentrations (around 20 g L^{-1}) were very low [99].

Bioprocessing economics for lactic acid production could be significantly improved by developing continuous submerged or solid-state cultivation. Sun et al. developed a continuous bioprocess that was carried out in an airlift bioreactor with immobilized *R. oryzae* in polyurethane foam cubes [97]. In this fermentation, the productivities of lactic acid were in the range of 1.0–6.2 g L^{-1} h^{-1} at dilution rates between 0.04–0.2 h^{-1}. However, glucose to lactic acid conversion yields and lactic acid concentrations were rather low. Even at dilution rates as low as 0.035 h^{-1} the lactic acid concentration did not exceed 50 g L^{-1} when an initial glucose concentration of 102 g L^{-1} was used. In addition, approximately 10 g L^{-1} of glucose was still present in the fermenter effluent.

Promising results were published by Soccol et al. who used solid state cultivation for lactic acid fermentation by *R. oryzae* [101]. In this study, fermentations were carried out on sugar-cane bagasse impregnated with a nutrient solution containing glucose and $CaCO_3$. A comparative study was also conducted on submerged and solid-state cultures containing optimized initial glucose concentrations of 120 g L^{-1} and 180 g L^{-1}, respectively, resulting in lactic acid concentrations of 93.8 and 137.0 g L^{-1}, respectively. These final lactic acid concentrations correspond to similar glucose to lactic acid conversion rate (about 77%) for both processes. The productivities were 1.38 g L^{-1} h^{-1} and 1.43 g L^{-1} h^{-1} in submerged and solid cultures, respectively.

3.1.2.3 Succinic acid

Succinic acid ($HOOCCH_2CH_2COOH$) and its anhydride have many unique properties (e.g. halogenation, Stobbe condensation of succinic diesters with aldehydes and ketones, Friedel–Craft reactions, esterification, oxidation, and degradation reactions), which are mainly attributed to the so-called succinoyl grouping, –(O:)C-CH_2-CH_2-C(O:)–. Because of its versatile properties, succinic acid is classified as an important intermediate in the manufacture of pharmaceuticals and a valuable ingredient in the synthesis of various specialities such as elastomers, protective coatings, electrical insulation, foods, detergents, surfactants, corrosion inhibitors, and cosmetics. The combined market size of these uses is more than $\$4\times10^8$ per year [102]. Bioderived succinate could be catalytically converted into 1,4-butanediol (a precursor of polybutylene terephthalate resin), tetrahydrofuran (solvent), γ-butyrolactone (intermediate and ingredient of paint removers and textile products), maleic acid, fumaric acid, adipic acid (the precursor of Nylon-6,6), succinimide, *N*-methylpyrrolidone (a recyclable alternative to the common solvent dichloromethane) and linear aliphatic esters with a worldwide market in

excess of 275×10^6 kg year^{-1} [102]. It can also provide a source for bioplastics production. For instance, Bionelle is an ester comprising succinic acid and 1,4-butanediol [103].

Currently, succinic acid is predominantly produced petrochemically; maleic anhydride production via butane oxidation, hydration of maleic anhydride to maleic acid, and hydrogenation to succinic acid. Petrochemically-based succinic acid production exceeds 15×10^6 kg year^{-1} and the purchase price is between \$5.90 and \$8.80 kg^{-1} depending on purity [102]. This price renders succinic acid a speciality product.

Succinic acid is an intermediate in the tricarboxylic acid (TCA) cycle and therefore is a major end-product of energy metabolism in many anaerobic and facultative microbes. *Anaerobiospirillum succiniproducens* isolated from the mouth of the beagle dog is a well-studied succinic acid-producing strain [103, 104]. It has been reported that it can yield 0.83–0.88 g succinic acid/g glucose at 19–38 g L^{-1} glucose during a continuous bioprocess [103]. However, the development of continuous bioprocessing using this microbe may not be feasible because it is not resistant to high succinate salt concentrations. Genetically engineered species of *E. coli* have been developed producing succinic acid up to 99.2 g L^{-1} with an overall yield of 110% [105], but they also have no tolerance to high succinate salt concentrations. The most promising succinic acid producing microbe is *Actinobacillus succinogenes* 130Z because:

1. it can produce naturally high succinic acid concentrations (110 g L^{-1}),
2. it has a single succinic acid-producing pathway,
3. it is an osmophile and facultative strain, and
4. it has high tolerance of succinate salts [102].

In *Anaerobiospirillum succiniproducens* and *Actinobacillus succinogenes* the succinic acid metabolic pathway consists of four reaction steps catalysed respectively by phosphoenolpyruvate (PEP) carboxykinase, malate dehydrogenase, fumarase, and fumarate dehydrogenase [106]. However, the PEP can also be converted to pyruvate leading to other end-products (lactic acid, ethanol, acetic acid). The glucose to succinic acid conversion yield can be increased at high CO_2 and H_2 concentrations [104, 106, 107]. CO_2 functions as an electron acceptor altering the flux of PEP, which is metabolized to pyruvate and lactate/ethanol at low CO_2 levels (10 mol CO_2/100 mol glucose) but makes succinate at high CO_2 levels (100 mol CO_2/100 mol glucose). Hydrogen has been shown to increase the succinate to acetate ratio, because in the presence of hydrogen the hydrogenase of *A. succinogenes* generates low-redox-potential electrons causing fumarate reduction to succinate, avoiding the need for pyruvate oxidation that leads to acetic acid. The consumption of CO_2 and H_2 increases the theoretical conversion yield from glucose to succinic acid from 0.78 g g^{-1} to 1.31 g g^{-1}.

The consumption of the notorious greenhouse gas CO_2 during the glucose bioconversion to succinate constitutes a crucial performance characteristic upgrading this bioprocess into a novel green technology. The integration of any microbial bioprocess with a succinate fermentation not only reduces carbon losses but also offers opportunities for further improvements in the process economics of both processes and helps turn bioprocessing into even greener technology.

The bioproduction of succinic acid has not yet been established on a large scale, because of the high raw material cost, low production yields, and expensive product separation, concentration, acidification and purification steps. In addition, the large quantities of by-product produced during acidification causes serious waste disposal and environmental concerns. However, industrially-based research has introduced advances in conventional bioconversion and separation/purification processing steps leading to succinic acid production at substantially lower cost [108]. With the adoption of new technology, the production of succinic acid by microbial bioconversion could be more economical than conventional petrochemical production routes that can produce succinic acid only as a speciality chemical. Bioprocessing could therefore turn succinic acid into a commodity chemical at a price of less than \$0.55 kg^{-1} [102].

As for other organic acids, current research is focused on the exploitation of various raw materials (e.g. whey, glycerol) to reduce processing costs [109–111]. Lee et al. reported that by growing *A. succiniproducens* anaerobically on glycerol and yeast extract a higher succinic acid yield (160%) and a 7.9 times higher ratio of succinic acid to acetic acid, compared with production on glucose, can be achieved [111].

3.1.3 *Amino acids*

Bioprocessing has been widely used for the production of L-glutamic acid and L-lysine, while some other amino acids (e.g. L-phenylalanine, L-aspartic acid, L-threonine, L-isoleucine) are gradually gaining importance. Traditional amino acid fermentation processes have been improved significantly by strain selection, rDNA technology, and mutagenesis techniques, leading to the construction of bacterial strains capable of producing: 100 g L^{-1} threonine, 40 g L^{-1} isoleucine, 34 g L^{-1} leucine, 31 g L^{-1} valine, 28 g L^{-1} phenylalanine, 55 g L^{-1} tryptophan, 26 g L^{-1} tyrosine, 100 g L^{-1} proline, and 100 g L^{-1} arginine [74].

3.1.3.1 Glutamic acid

L-Glutamic acid was one of the first primary metabolites produced industrially by fermentation, providing an exception to the general perception that primary microbial metabolites were produced at insufficient concentration to be economic [112]. Worldwide production of the flavour enhancer exceeds 10^9 kg $year^{-1}$ [113]. It is produced by various species of the genera *Corynebacterium* and *Brevibacterium*. In industry the bacterial overexcretion of glutamic acid is achieved by biotin limitation, which results in the construction of a phospholipid-deficient cytoplasmic membrane, because the industrially used glutamic acid bacteria are biotin auxotrophs [74]. Fermentation lasts 40–60 h and the accumulated glutamic acid reaches concentrations higher than 150 g L^{-1}. Product purification and separation steps include biomass separation by centrifugation or ultrafiltration, concentration by evaporation, crystallization, filtration, and drying [114].

Current research is aimed at explaining and improving glutamic acid overproduction by *Corynebacterium* or *Brevibacterium* species. The addition of surfactants, instead of biotin, resulted in the production of 100 g L^{-1} glutamic acid by *C. glutamicum* and *B. lactofermentum* when it was grown on molasses [115, 116]. Glutamate production of 80 and 85 g L^{-1} has been achieved by controlling the temperature between 33 and 39 °C during fermentation of *C. glutamicum* on glucose [117, 118]. Finally, glutamate overproduction can be achieved by genetically modifying the chemical and physical properties of the cytoplasmic membrane [113].

3.1.3.2 Lysine

Worldwide almost 80% of lysine is produced by fermentation. Its supplementation in cereal or cassava products provides a balanced human food, especially in third-world countries, and animal feed [119]. Apart from its use as a feed supplement, L-lysine finds pharmaceutical applications. As a member of the aspartate family, it is produced in bacteria (mainly *Corynebacteria* and *Brevibacteria*) by a branched biosynthetic pathway together with methionine, threonine, and isoleucine (Fig. 8). The fermentative production of lysine has been improved by undirected mutagenesis and screening of several microbes (e.g. *C. glutamicum, B. flavum, B. lactofermentum*) aiming at increased productivity. In this way, industrial processes produce around 60–120 g L^{-1}L-lysine with a 0.3–0.4 molar yield. In 1992 Kim et al. reported the highest L-lysine concentration (140 g L^{-1}) produced by fermentation; at higher concentrations self-inhibition of L-lysine was observed [120]. Recombinant DNA technology can also be used to improve lysine production by genetic removal of homoserine dehydrogenase from a glutamate-producing *Corynebacterium* [74]. As shown in Fig. 8, the result of such a modification is to restrict the production of threonine and methionine, bypassing the feedback inhibition of aspartate kinase. Industrial downstream processing of lysine is characterized by removal of microbial cells by ultrafiltration, absorption of lysine in an ion exchange step, and crystallization/spray drying as L-lysine hydrochloride [114].

Several industrial fermentations have been improved significantly by use of traditional whole-cell mutation techniques. However, the results of such techniques are not always successful, because they can lead to underperformed mutations that are inferior to the parental strain. A novel method that could overcome such problems is "genome-based strain reconstruction", which can identify desired mutations by comparative genomic analysis and reconstitute them in a single wild-type background [121]. Such a technique has been applied to improve L-lysine fermentation by *C. glutamicum* leading to a concentration of 80 g L^{-1} after only 27 h, corresponding to the highest reported productivity (3 g L^{-1} h^{-1}) [121].

In June 2000, a $100 million plant (Midwest Lysine LLC) began operation in Blair (Nebraska, USA) producing 75×10^6 kg $year^{-1}$ of the amino acid lysine [25]. The conventional fermentation route produces L-lysine hydrochloride by a multistep process utilizing *Corynebacteria* or *Brevibacteria*. The novel bioprocess changed raw materials (it currently utilizes dextrose) and fermentation process,

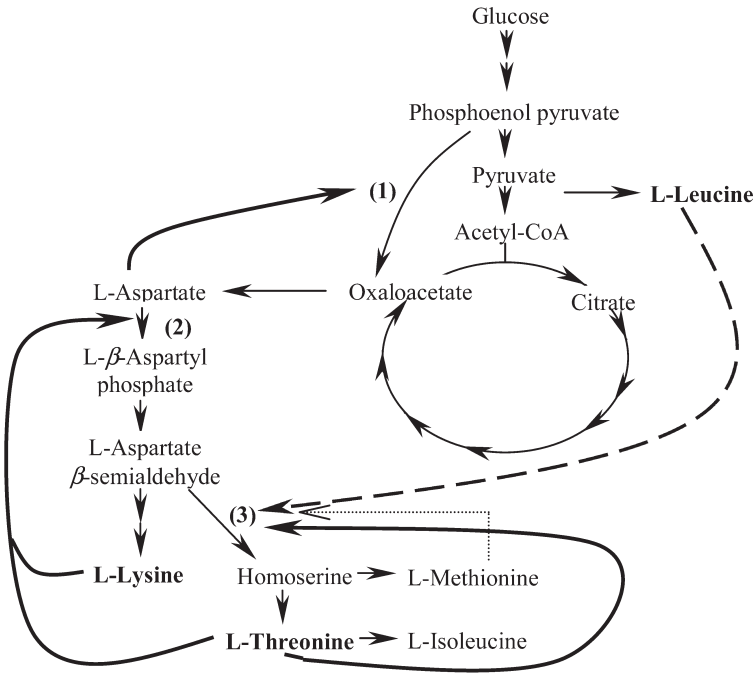

Fig. 8 Regulation of L-lysine biosynthesis in *C. glutamicum*; enzymes (coding gene): (*1*) phosphoenolpyruvate carbo-xylase, (*2*) aspartate kinase and (*3*) homoserine dehydrogenase; ⟶ feedback inhibition, ⋯⟶ repression, - - ⟶ activation (adapted from Ref. [114])

reducing wastes and downstream processing steps. This is an example where advances in bioprocessing made possible the reduction of the production costs of a bulk chemical.

3.1.4 *Vitamins*

The vitamins currently produced by fermentation are vitamin C (L-ascorbic acid), vitamin B_2 (riboflavin), vitamin B_{12} (cyanocobalamin), niacin, and biotin. In recent years, industrialists realized the overwhelming benefits of biotechnology for vitamin production and are gradually switching their production processes from chemical to biological [24, 36].

3.1.4.1 Ascorbic acid (vitamin C)

Worldwide L-ascorbic acid production is of the order of 8×10^7 kg year^{-1} (3–4% annual growth rate) with a fluctuating price between \$6–\$8 kg^{-1} and a global market between \$500 and $\$650\times10^6$ [122]. Ascorbic acid is mainly used as a vitamin supplement, an antioxidant in foods, and in pharmaceutical formulations,

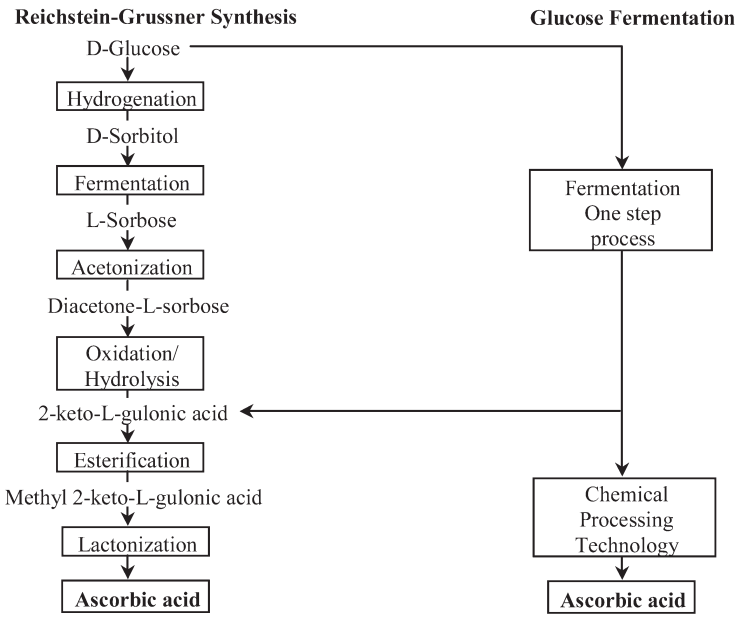

Fig. 9 Process routes to ascorbic acid (adapted from Ref. [38])

cosmetics, beverages, and animal feeds [38]. The predominant industrial process is the seven-step Reichstein process, which includes a single fermentation step for oxidation of D-sorbitol to L-sorbose within a series of chemically-based unit operations (Fig. 9). The low ascorbic acid production yield (about 50%) and the high energy requirements has motivated research into the development of an economic bioprocess [123].

Genencor and Eastman Chemical have developed a one-step fermentation producing 2-ketogulonic acid from glucose, which is subsequently converted into ascorbic acid by chemical esterification and lactonization reactions (Fig. 9) [25]. The commercialization of such a process might result in the reduction of capital costs by half, creation of new markets for ascorbic acid, and a significant reduction in its price. This process has been improved by genetic engineering – engineered strains of *Erwinia citreus*, *Pantoea citrea*, and *Gluconobacter oxydans* are capable of converting either sorbitol or glucose into 2-keto-L-gulonate with high efficiency [74, 123].

3.1.4.2 Riboflavin (vitamin B_2)

Riboflavin is of great importance in the electron transport chain in cells, acting as a coenzyme for respiratory enzymes. It is also important in the metabolism of amino acids, carbohydrates, and fatty acids. Worldwide production is more than 3×10^6 kg year^{-1}, of which 60% is used in animal feed, 25% in medical formulations, and 15% as food/feed supplements [124].

Riboflavin production began shifting towards bioprocess routes, utilizing mainly glucose, about 15 years ago. Bioprocessing is gradually replacing what is now considered the uncompetitive multistep chemical route [36, 125]. Chemical synthesis is only used for pharmaceutical formulations [124]. Microorganisms used for bio-production of riboflavin are *Ashbya gossypii*, *Candida famata*, *Eremothecium ashbyii*, and *Bacillus subtilis*.

A recent technological innovation in riboflavin production involves a 20% productivity increase from the riboflavin fungal overproducer *Ashbya gossypii*, which can naturally produce concentrations greater than 20 g L^{-1}, by identifying the key enzymes participating in the respective synthetic pathway [36]. In addition, Hoffmann La-Roche (Germany) has replaced the conventional six-step chemical process for vitamin B_2 production with a one-step bioprocess utilizing a metabolically engineered strain of *Bacillus subtilis* [25]. By innovations in downstream processing final products of 96% (animal feed-grade) or even 98% (food/pharma grade) purity can be obtained [126]. This has led to a 75% reduction in the use of non-renewable raw materials, 50% reduction in emissions of volatile organic compounds, and 50% reduction in operating costs.

Current research is focused on bioprocess optimization by understanding and controlling metabolic pathways and application of mutation and genetic engineering [126–130].

3.1.5 *Industrial enzymes*

The world enzyme market has grown from $\$1\times10^9$ in 1995 to around $\$1.5\times10^9$ in 2000 [131], and it is expected to grow to $\$2\times10^9$ by 2005. Commercially, enzymes are treated as fine chemicals because of the huge potential of biotransformations that can be achieved either by using microbial cells that employ specific enzymes as biological catalysts of chemical reactions or by using purified enzymes as end-products [132]. In recent years, developments in protein engineering and directed evolution have made possible the development of new enzymes with improved properties for established technical applications or tailor-made ones for entirely new applications in which enzymes have not previously been used [133]. Bulk uses of enzymes include detergents (37%), textile treatments (12%), starch processing (11%), baking (8%) and animal feed (6%). Table 5 lists some of the most commercially important enzymes.

Industrial enzymes can be produced either by using the wild-type organism excreting the desired enzyme or by expressing the gene encoding the desired enzyme in a recombinant expression system, such as *E. coli*. The former technique is dominant in today's industry, though the latter offers advantages because it provides enzyme overproduction relative to the primary microbial source and the option to modify the enzymes, improving their properties (e.g. greater thermal/pH tolerance, altered catalytic function) [132, 134]. However, further advances in enzyme technology and bioengineering are still required to develop this method to its full potential [135].

Industrial enzymes are mainly produced by the fungi from the genera *Aspergillus*, *Trichoderma*, and *Streptomyces* and the bacterial genus *Bacillus*. Most

Table 5 Identified and commercially available enzymes

Enzyme type	Source	Applications
1. *Hydrolase* (636 identified and 125 commercially available)		
α-Amylase, β-amylase	*Bacillus subtilis*, *Aspergillus niger*	Textiles, starch syrups, detergents, detergents, paper desizing, fermentation ethanol, animal feed
Glucoamylase	*Aspergillus niger*, *Rhizopus* sp., *Endomyces* sp.	Manufacture of dextrose syrup and high-fructose syrup
Hemicellulase/ pentosanase/xylanase	*Thermomyces lanuginosus*, *Penicillium simplicissimum*	Baking, fruit juice manufacture, wood pulp processing
Protease	*Bacillus subtilis*, *Bacillus licheniformis*, *Aspergillus oryzae*	Detergents, leather, baking, protein processing, chemicals
Lipase	*Rhizopus* sp.	Cleaners, leather and fur, dairy, chemicals
2. *Oxidoreductase* (650 identified and 90 commercially available)		
Alcohol dehydrogenase	*Saccharomyces cerevisiae*, *Thermoanarobium brockii*	Chiral synthesis
Catalase	*Aspergillus niger*	Food
Peroxidase	Not known	Personal care, laundry and wood pulp bleaches
3. *Transferase* (720 identified and 90 commercially available)		
Cyclodextrin glycosyltransferase	Not known	Manufacture of cyclodextrins from starch
4. *Lyase* (225 identified and 35 commercially available)		
Acetolactate decarboxylase	Not known	Brewing industry
Aspartic β-decarboxylase	Not known	Manufacture of L-alanine from L-aspartic acid
5. *Isomerase* (120 identified and 6 commercially available)		
Glucose isomerase	*Bacillus* sp.	Fructose syrup production
6. *Ligase* (80 identified and 5 commercially available)		

industrially used microbes have been genetically modified to overproduce the desired enzyme, preventing the production of undesired end-products. Enzyme production is achieved either in submerged (SmB) or solid state bioprocesses (SSB). The latter often results in higher enzyme production but it has not been applied extensively in industry because further technological and engineering advances are necessary [119]. Studies have revealed the enormous economic benefits that can be achieved by enzyme production by SSB. Tengerdy compared SmB

with SSB for cellulase production and found that the production cost in SmB is about \$20 kg^{-1} whereas for SSB is only \$0.2 kg^{-1} [136]. Castilho et al. performed an economic analysis for lipase production by *Penicillium restrictum* by SmB and SSB and concluded that SmB requires 78% higher capital investment than SSB [137]. They also calculated that for a production scale of 100 m^3 the unit production cost for SmB was 68% higher than the lipase selling price, whereas for SSB the unit production cost was 47% lower than the lipase selling price [137]. Soccol et al. evaluated three strains of *Rhizopus* growing on raw and cooked cassava in SmB and SSB for α-amylase and glucoamylase production and concluded that the SSB gave higher enzyme production than SmB [138].

After the production step, extracellular enzymes are purified by filtration/centrifugation to remove solids, ultrafiltration to remove proteins, and ion-exchange chromatography. Downstream processing constitutes one of the biggest hurdles in enzyme production because:

1. removal of all unwanted proteins is very difficult, and
2. there is an approximate 20% loss of enzymatic activity after each processing step.

Some recent major process improvements achieved in industry by use of enzymes are presented below [25].

- During the past 30 years Tanabe Seiyaku (Japan) has been developing enzyme immobilization techniques for the production of amino acids. Recent advances in surface immobilization and reuse led to a 40% cost saving. Genetically engineered microorganisms optimized the performance of the enzymes increasing productivity 15-fold and reducing organic waste materials.
- Mitsubishi Rayon Company (Japan) replaced the chemical process for acrylamide production by a bioprocess (uses the enzyme nitrile hydratase to catalyse the reaction) increasing energy savings by 80%, reducing costs, and increasing purity.
- Baxenden Chemicals introduced a novel bioprocess for polyester production which uses lipase from the bacterium *Candida antarctica* to catalyse the polymerization reaction at a much lower temperature (60 °C) than the conventional chemical process (200 °C), eliminating the use of organic solvents and inorganic acids, improving polyester properties, and increasing energy savings by 2000 MW annually at full industrial scale operation.
- Windel (Netherlands) uses the enzyme catalase to reduce the energy and time required to wash hydrogen peroxide bleach from textiles before dying, resulting in 9–14% energy savings, 17–18% water savings, and an overall cost saving of 9%.
- Domtar (Canada) and Oji Paper (Japan) are using xylanase as an auxiliary brightening agent for wood pulp in paper-making and for bleaching chemicals, respectively. Improvements in enzyme production cost and performance have been achieved by genetic engineering of the fungus from which it is extracted and by producing xylanase on-site by fermentation. The use of xylanase resulted in reduction of organically bound chlorine in wastewater by 60% and cost reductions by 10–15%.

– M-I and British Petroleum Exploration (UK) introduced a bio-based drilling fluid containing mixtures of bio-organic polymers (e.g. xanthan gum, starch, cellulose) avoiding the problems of conventional drilling muds. Enzymes such as cellulase, hemicellulase, amylase, and pectinase are also used, increasing efficiency and preventing equipment corrosion and environmental pollution. Although the use of bio-organic drilling fluid systems is in its early days, it seems in a number of cases that their performance is satisfactory and cost savings are of the order of $75,000–$80,000 per well drilled.

3.1.6 *Biopesticides*

The increasing need for agricultural products has resulted in increased use of pesticides. Chemical pesticides cause serious environmental damage, because they do not degrade easily and accumulate in soil, air, and water, and their extensive use has caused insecticide resistance in more than 500 species of insects and mites [139]. Bioprocessing can provide an alternative tool for development of highly efficient, environmentally benign, and low-cost biopesticides as substitutes for chemical pesticides. They can also improve rural economics by reducing production costs and increasing the competitiveness of domestic agriculture in the globalized market. In 2001 there were approximately 195 registered biopesticide active ingredients and 780 products [140]. Paulitz and Belanger reported that in the UK the biological control of greenhouse insects predominates over chemical control [141]. Biopesticides can be classified into three groups [140]:

– biochemical pesticides, which include naturally occurring substances that control pests by non-toxic mechanisms;
– plant incorporated protectants, which include pesticidal substances produced by plants through genetic material that has been added to the plant; and
– microbial pesticides, where the microorganism (e.g. bacteria, viruses, fungi, microscopic nematode worms, sub-cellular parts of microorganisms) is the active ingredient.

3.1.6.1 Bacterial biopesticides

The most widely used biocontrol agents are derived by fermentation of a gram-positive, spore forming, facultative soil bacterium *Bacillus thuringiensis*. During sporulation, *B. thuringiensis* produces a protein crystal (endotoxin protein) that specifically inhibits the normal function of the digestive process in pests, resulting in their death [142]. The most well-known *B. thuringiensis* proteins are classified as CryI, CryII and CryIII. The global biopesticide market has grown from $\$71\times10^6$ in 1991 to $\$119\times10^6$ in 1995 and about $\$160\times10^6$ in 2000, of which over 90% was due to sales of *B. thuringiensis* products.

The fermentative production of the pesticidal proteins by *B. thuringiensis* is accomplished in two phases. In the first phase the organism is supplied with a nu-

trient-complete fermentation medium and grows into a vegetative phase. Although glucose is the preferred carbon source in most large scale *B. thuringiensis* fermentations, glucose concentrations higher than 40 g L^{-1} can be inhibitory to growth and further research is required to evaluate the affect of glucose on growth [143]. Research has also focussed on identification of cheap and highly efficient nitrogen sources containing mainly amino acids. During the growth phase, glucose is gradually consumed and acetate is formed. The second phase occurs when a critical nutrient becomes depleted, causing sporulation and simultaneous synthesis of pesticidal protein [143]. Nitrogen depletion seems to be the reason for sporulation.

In China and Cuba *B. thuringiensis* production is carried out by SSB. Aranda et al. proposed the development of SSB using available local wastes or by-products directed to small farmers for production aimed at increasing competitiveness with synthetic pesticides and cost reduction [144].

B. thuringiensis may provide the most inexpensive source of microbial pesticides but process economics should be improved further if it is ever to compete with chemical pesticides [142]. This can be achieved by reducing the cost of fermentation media and increasing production yields. Therefore, research incentives focus on optimization of various fermentation conditions (e.g. bioreactor design, metabolic heat flux, inoculum, nutrient requirements, oxygen, temperature, metabolic inhibition) [143, 145–147]. Various raw materials (e.g. defatted soybean, groundnut seed meal extracts) have been screened for *B. thuringiensis* fermentation [148–150]. Genetic engineering should aim at protein stabilization, production of multiple specific toxin proteins capable of targeting more insects, and optimization of fermentation by increasing growth yield and spore formation [142, 151].

Other registered bacteria for biopesticide formulations are strains of *Burkholderia cepacia*, *Pseudomonas chlororaphis*, *Bacillus subtilis*, *Pseudomonas syringae*, *Streptomyces griseoviridis*, *Bacillus cereus*, and *Bacillus sphaericus* [140].

3.1.6.2 Fungal biopesticides

Some fungal strains have been registered as potent biopesticides in agriculture (e.g. *Trichoderma polysporum*, *Trichoderma harzianum*, *Lagenidium giganteum*, *Gliocladium virens*, *Metarhizium anisopliae*, *Ampelomyces quisqualis*, *Coniothyrium minitans*, *Gliocladium catenulatum*, *Beauveria bassiana*) [140]. Specific emphasis is given on the development of biopesticides based on chitinolytic enzymes [152]. Such enzymes play a key role in autolysis, spore germination, branching and mycelial development, hyphal growth, cell separation, nutrition, and parasitism [153]. It has been demonstrated that microorganisms producing chitinases could be the basis for future biopesticide formulations [154]. One of the most extensively studied fungal strains for chitinase production is *T. harzianum* because this fungus produces large amounts of chitinases that are active over a wide range of environmental conditions and phytopathogens [153]. The naturally occurring *T. harzianum* Rifai Strain T-22, was registered in 2001 as a biopesticide targeting various fungi that cause seed rot, diseases of plant roots,

and other plant diseases [155]. Another strain, strain T-39 was registered in 2000 as a biopesticide to protect crops from the harmful grey mould, *Botrytis cinerea* [156]. The large scale production of *T. harzianum* Rifai has become the focus of research and industrial development aiming at reducing costs and increasing biomass production of high quality and quantity [157].

Although *C. minitans* was described for the first time in 1947 [158], its commercialization as a biocontrol agent was very slow, because bioprocesses were not profitable enough to produce sufficient amounts of fungal material to be used in field and glasshouse trials [159]. Current research incentives concentrate on the development of cost-effective large-scale bioprocesses [160]. SSB seems to provide an efficient and low-cost solution for mass production of *C. minitans* spores. In contrast with SmB, in which spore production does not exceed 6×10^{10} spores L^{-1} medium, SSB may produce up to 10^{12} spores L^{-1} medium [160, 161]. In addition, SSB provides a large surface area facilitating scale up and satisfying applications to thousands or millions of hectares [162]. The naturally occurring strain of *Coniothyrium minitans* strain CON/M/91–08 was registered in 2001 as a biopesticide to treat the common plant pathogens, *Sclerotinia sclerotiorum* and *Sclerotinia minor,* which cause white mould, pink rot, and water soft rot [163]. The plant pathogen *S. sclerotiorum*, commonly known as white mould, causes major losses in oilseed and pulse crops and no effective plant resistance has been identified so far [164].

3.1.6.3 Nematode biopesticides

Another kind of biopesticide is the nematode-bacteria complex, in which entomopathogenic nematodes (e.g. *Steinernema*, *Heterorhabditis*) kill insects with the aid of mutualistic bacteria [165]. This biocontrol agent can be produced either in-vivo or in-vitro. The latter can be achieved either by SmB or SSB. Shapiro-Ilan and Gaugler advocated that SmB is the most cost-efficient process but it requires further advances in media development, nematode recovery, and bioreactor design in order to reduce start-up capital and improve nematode quality [165]. Wilson et al. used flow-assisted wet sieving and a novel cross-flow sieving technique to separate adult nematodes (waste material) from infective juveniles (effective bioinsecticides) proving that this is a viable alternative for nematode recovery to the conventional settling and/or centrifugation removal techniques [166].

3.1.7 *Biodegradable plastics*

About 5×10^{11} kg plastics are produced each year. Disposal constitutes a major environmental challenge and conventional disposal techniques (e.g. incineration, recycling, landfill) cannot resolve critical problems (e.g. high costs, diversity of disposed plastics, increasing amount of plastic disposal). The substitution of non-degradable plastics by biodegradable ones offers a potential solution to all these problems. Many biodegradable polymers have been identified, including starch and cellulose (and their derivatives), polyhydroxyalkanoates (PHAs),

poly(vinyl alcohol), polycaprolactone, and poly(lactic acid) [103]. The chemical transformation of fermentatively produced monomers succinic acid, propanediols, and lactic acid into polymers has been extensively investigated [103]. For instance, Genencor and DuPont cooperate on the development of a bioprocess for 1,3-propanediol (PDO) production using an engineered bacterium. DuPont has already started a pilot plant producing 90,000 kg year^{-1} of bio-PDO and is planning to enter the PDO-market by 2003 [25].

3.1.7.1 Polyhydroxybutyric acid (PHB)

PHAs are energy and/or reducing power storage materials that are accumulated intracellularly by many bacteria under conditions of nitrogen, phosphorus, sulfur, oxygen, or magnesium limitations and in the presence of excess carbon source [103]. Because of their inability to produce sufficient exoenzymes, plastic-producing bacteria rely on simple sugars, usually glucose, as carbon source and small organic nitrogen compounds, frequently amino acids and short chain peptides, as nitrogen source [167].

The most well-known PHA polymer is polyhydroxybutyric acid (PHB). Many microorganisms can produce intracellular PHB, but *Alcaligenes eutrophus* emerges as the favourite because it accumulates large amounts of PHB and grows easily. Microbial PHB production can be divided into three essential steps:

1. bacterial growth aiming at the production of large amounts of cells,
2. accumulation of large amounts of intracellular PHB, and
3. recovery of PHB from the cells.

The economic viability of the whole process is determined by cell-growth rate, the intracellular PHB content, and recovery efficiency. High cell-growth rate depends on a properly balanced medium and optimum incubation conditions. Efficient PHB accumulation, on the other hand, results from imbalanced nutrient conditions, which is usually achieved by use of an excess of carbon source and a limiting nutrient [168]. Conventional strategies encourage batch growth in medium of imbalanced glucose and nitrogen or by fed-batch incubation, supplying extra glucose after the exhaustion of nitrogen. The bacteria interpret the lack of nitrogen as a sign of inhospitable conditions ahead and subsequently devote the carbon resource to producing PHB. In addition to difficulties in precise process control, the efficiency of these processes is much lower than continuous processes owing to the long down time between batches.

The separation of intracellular PHB granules requires cell disruption. Current processes include solvent extraction, chemical reagent or enzyme digestion, and high-pressure homogenization [169]. The high price of biodegradable PHB associated with the cost of the nutrient sources, the low production efficiency, and complicated recovery process, impedes the development of a real market for this alternative to petroleum-based plastics. Current research incentives aim at developing approaches to reduce the processing cost of raw materials and increase PHB production yields and recovery efficiency in order to supply PHB at an acceptable price.

3.2 Future trends in bioprocessing

The chemicals presented above are only a fraction of the chemicals that can be produced by bioprocessing. Future bioprocesses using carbohydrates as feedstocks would substitute petrochemical synthesis in two ways:

- Direct one-step biotransformation using whole cells. This is similar to traditional fermentation in which microorganisms that incorporate the required biochemical pathways are grown under optimum conditions to produce the desired metabolic end-product (Fig. 5). In addition to the products presented above, in the section *Current status of industrial bioprocessing*, Table 6 presents some more bioprocesses that seem promising for future production of specific chemicals.
- Multi-step biotransformations using combinations of whole cells, cell-free enzymes, and conventional catalysts. As an indication of the enormous potential of biocatalysts it could be feasible in the future to design bioreactors in which immobilized layers of several enzymes in the proper sequence can perform the equivalent of a complex, multistep, thermochemical reaction sequence in a single, small-volume reactor [179].

Some two-step bioprocesses are gradually appearing in the literature. In one of these 1,3-propanediol is produced in a two-step fermentation process in which initially glucose is converted into glycerol by use of a glycerol-producing yeast and this glycerol is subsequently converted into 1,3-propanediol by *Klebsiella pneumoniae* without intermediate isolation and purification of the glycerol [180]. Another two step process is the production of acrylic acid from lactic acid, which is initially produced by lactic acid bacteria from glucose. This is subsequently converted into acrylic acid by *Clostridium propionicum*, if the propionyl-CoA dehydrogenase has been sufficiently inhibited to prevent propionate production, and the accumulation of reduction equivalents (e.g. ferredoxin, NADH) has been prevented by finding ways to regenerate them [181]. The use of 3-butynoic acid as an inhibitor of propionyl-CoA dehydrogenase might have inhibited propionate production but the accumulation of reduction equivalents limited acrylic acid production to 1% conversion from the initial substrate concentration. The regeneration of reduction equivalents could be achieved by incorporation of a hydrogenase gene into *C. propionicum* [181].

Another possible two-step bioprocess could be the production of succinic acid from glucose using as intermediate step the fermentative production of glycerol. Glucose can be converted to glycerol by *Candida glycerinogenes* at a conversion ratio close to 60% (Table 6). Subsequently the glycerol can be converted to succinic acid by *Anaerobiospirillum succiniproducens* at a conversion ratio of 160% [111].

Table 6 Some organic chemicals that can be produced through direct fermentation

Chemical	Substrates	Microorganisms	Bioprocess specifics	Theoretical yield	Demonstrated yield
ABE (Acetone, butanol, ethanol)	Starch	*Clostridium acetobutylicum*, *Clostridium beijerinckii* [170]	Batch process	Approx. 0.5 g total solvent g^{-1} glucose	Approx. 0.25 g total solvent g^{-1} glucose
	Glucose	*Clostridium beijerinckii* mut. [171]	Batch process with product separation by pervaporation		0.43 g total solvent g^{-1} glucose
Acetic acid	Various sugars (e.g. glucose, xylose)	*Clostridium thermoaceticum* [172]	Spore forming, thermophilic bacterium (55–60 °C), new mutant strains are necessary for industrial application	1 g g^{-1} glucose	0.85 g g^{-1} glucose
	Cellulose	*Clostridium lentocellum* SG6 [173]	Optimum fermentation conditions: 0.8% cellulose, 0,4% yeast extract, 37 °C and pH 7.2	1 g g^{-1} glucose	0.67 g g^{-1} glucose
2,3-Butanediol (BDL)	Various pentoses and hexoses	*Aerobacter aerogenes. Bacillus polymyxa, Bacillus polymyxa, Klebsiella oxytoca, Aeromonas hydrophyla* [174]	Initial substrate conc. and aeration influence BDL yield, productivity and by-product formation	0.5 mol BDL g^{-1} glucose	0.3–0.35 g BDL g^{-1} glucose 60–70% of theoretical yield for xylose

Table 6 (continued)

Chemical	Substrates	Microorganisms	Bioprocess specifics	Theoretical yield	Demonstrated yield
Glycerol (GL)	Glucose	*Saccharomyces cerevisiae* [175]	Sulfite or alkaline process	0.51 g GL g^{-1} glucose	0.2–0.35 g GL g^{-1} glucose
		Candida glycerinogenes [176]	50 m^3 airlift bioreactor (29–33 °C, pH 4–6, 200 g L^{-1} glucose) – 30 g GL/(L day), 110–120 g GL L^{-1}	1 g GL g^{-1} glucose	0.58 g GL g^{-1} glucose
Pyruvic acid (PA)	Glucose	*Torulopsis glabrata* WSH-IP303 (multi-vitamin auxotrophic strain) [177]	5 L bioreactor, $CINH_4$ as the sole nitrogen source, 69 g L^{-1} PA, 56 h	0.98 g PA g^{-1} glucose	0.62 g PA g^{-1} glucose
Itaconic acid (IA)	Glucose, sucrose, molasses	*Aspergillus terreus* [178]	Phase 1: 150 g L^{-1} glucose, pH, 37 °C or higher, Phase 2: phosphate limitation, pH around 3,71 g L^{-1} IA, 4 days, 1 g (Lh)	0.72 g IA g^{-1} glucose	0.45–0.54 g IA g^{-1} glucose

4 Downstream processing

The establishment of a cost-competitive bulk commodity bioindustry requires the development of separation and purification technologies tailor-made for specific bioprocesses aimed at cost reduction and efficiency improvement [182].

Integrated bioconversion and product separation receives extensive attention because of the major improvements that could be achieved (e.g. lower capital costs, prevention of product inhibition, higher productivities and yields) [183]. Membrane technology plays a crucial role in integrated bioprocesses. For instance, alcohols (e.g. ethanol, butanol) can be separated from fermentation broths by pervaporation. Nakamura et al. reported that the use of pervaporation could provide a higher ethanol concentration (e.g. 50 g L^{-1}) when *Pichia stipitis* was grown on a rice straw hydrolysate, which had been pretreated by steam explosion and enzymatic hydrolysis [184]. A technical disadvantage of pervaporation is that it separates only the volatile components, while the non-volatile ones (higher alcohols) accumulate in the fermentation broth causing growth inhibition [183].

Extractive bioprocesses using a two-liquid phase partitioning bioreactor for product or substrate separation are also of great importance but the major difficulty is to find a low-cost solvent with low toxicity for microbial growth [185, 186].

The growth of bacteria in organic acid fermentations is inhibited by high product concentrations, while conventional downstream processing of organic acids results in large amounts of by-products that have to be disposed. To overcome this problem membrane separation, electrodialysis in particular, seems to provide a potentially viable solution [187].

Some novel bioseparation techniques are: aqueous two-phase extraction, reverse micellar extraction, cloud point extraction, and magnetic and electrophoretic separation [188].

5 Wheat as a potential feedstock

In previous sections it was made clear that bioprocessing will become dominant in industry only if major advances are accomplished in strain selection, bioconversion technology, downstream processing, and media development. All are subject to the individual bioprocess but the growth of bioprocessing is strongly dependent on the availability of raw materials. Can cereals sustain the establishment of bioprocessing for chemical production?

5.1 Critical review of wheat as bioconversion feedstock

Wheat contains large amounts of starch, protein, various micromolecules, and vitamins and therefore, in essence, constitutes a self-sufficient feedstock for most microbes [189]. However, wheat contains nutrients in the form of natural polymers, while many microorganisms need monomers to grow efficiently. By hy-

drolysing these polymers, a versatile bioconversion feedstock can be produced which does not contain impurities and does not usually require further nutrient supplementation.

To demonstrate the feasibility of using wheat for chemical production, a preliminary evaluation has been conducted on the capacity of world wheat production required to manufacture major commodity chemicals. This evaluation was based on the requirements of microbial bioconversions for carbon source (glucose), which is the most important factor for microbial growth. The glucose required for each chemical was subsequently translated to starch and this to wheat. The theoretical yield from glucose to each individual product has always been used. Although theoretical yields are not currently feasible, they remain targets for the future, awaiting improvements via genetic engineering and more sophisticated bioprocessing techniques.

To convert glucose volume to the starch equivalent, the stoichiometry of the hydrolysis of starch (1.11 kg glucose kg^{-1} starch) and a conversion of 95% are assumed. The polysaccharide content of wheat is assumed to be 62.1% of the total wheat, on a wet basis. In 2000 global wheat production and yield per hectare were 584×10^9 kg and 2.7 tonnes, respectively [190].

This preliminary evaluation showed that 82.1% of current world wheat production would be required for production of ethylene, propylene, and butadiene (Fig. 10a), 11% for major petrochemicals (Fig. 10b) and 7.35% for major fermentation products (Fig. 11). All of the world's current production would therefore be needed to produce the full range of products, leaving none for food! More importantly, though, these results illustrate that, although wheat usage for the production of chemical feedstocks is prohibitive, its utilization for the production of major fermentation products is feasible.

The establishment of wheat as bioconversion feedstock will only be achieved if sufficient supplies are available. This can be achieved by increasing the amount of cultivated land and/or the yield per hectare. This is not an unrealistic goal, because the global wheat yield per hectare cultivated land is 2.7 whereas in some parts of Europe (e.g. the UK) it is around 6 to 8. Just by increasing the productivity of wheat to 3.5 t ha^{-1}, surplus production would be sufficient to supply the bioproduction of the chemicals listed in Figs. 10b and 11. In turn, by increasing the wheat productivity to 5.5 t ha^{-1} even production of the most important building blocks – ethylene, propylene and butadiene – would be feasible. However, governmental support and significant advances in technology (including genetic engineering) will be necessary if this is ever to become feasible.

5.2 Preliminary economic evaluation

In every bioprocess evaluation a preliminary economic analysis will determine the feasibility of the specific endeavour. For this reason, a preliminary economic analysis was carried out for wheat by using two equations – the fraction of revenue from feedstock (FRF) and the raw material cost ratio (RMCR) [3, 191].

It must be stressed that this is a preliminary economic evaluation and certain discrepancies from reality are inevitable. For instance, this analysis was based

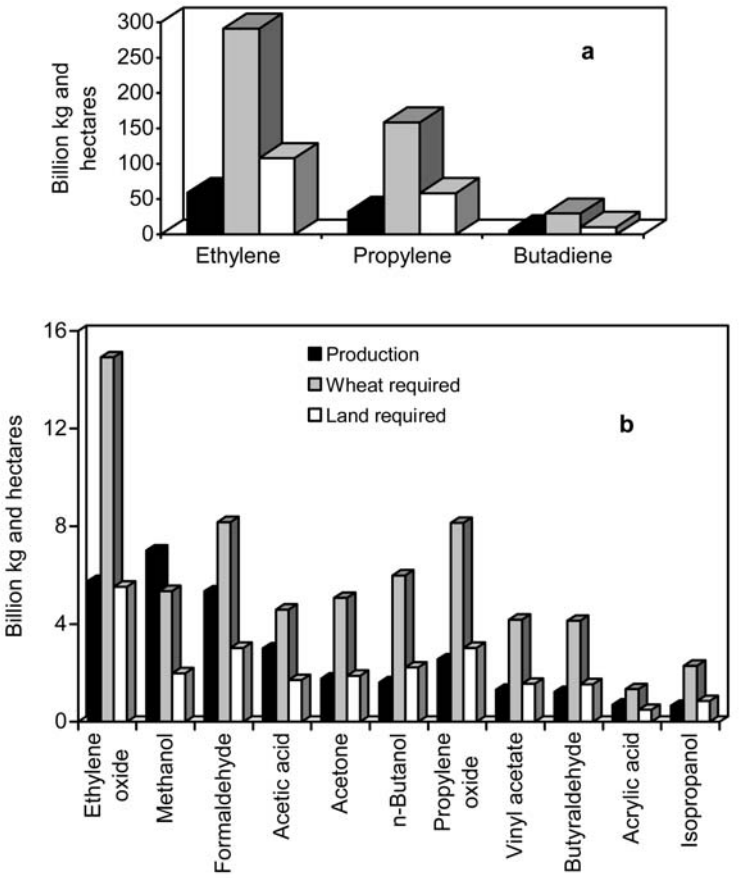

Fig. 10 Land area and quantity of wheat required for the production of major fermentation products

only on feedstock costs, which constitute a fraction of the overall process economics. Feedstock prices tend to fluctuate, influencing process economics. The purchase price of wheat will be a fraction of the final feedstock formulation because processing expenditure is bound to alter the overall cost significantly.

5.2.1 *Equation 1: fraction of revenue from feedstock (FRF)*

The FRF equation represents the ratio of feedstock cost to the value of products derived from that feedstock. According to this equation, the lower the FRF the more likely will be the feasibility of using wheat as a feedstock. Clearly, the FRF must be significantly below unity for a process to stand a chance of being feasible.

$$\text{FRF} = (\text{Cost of wheat/Value of products}) = (C_f / \sum x_i \beta_i y_i \alpha_i V_i) \quad (1)$$

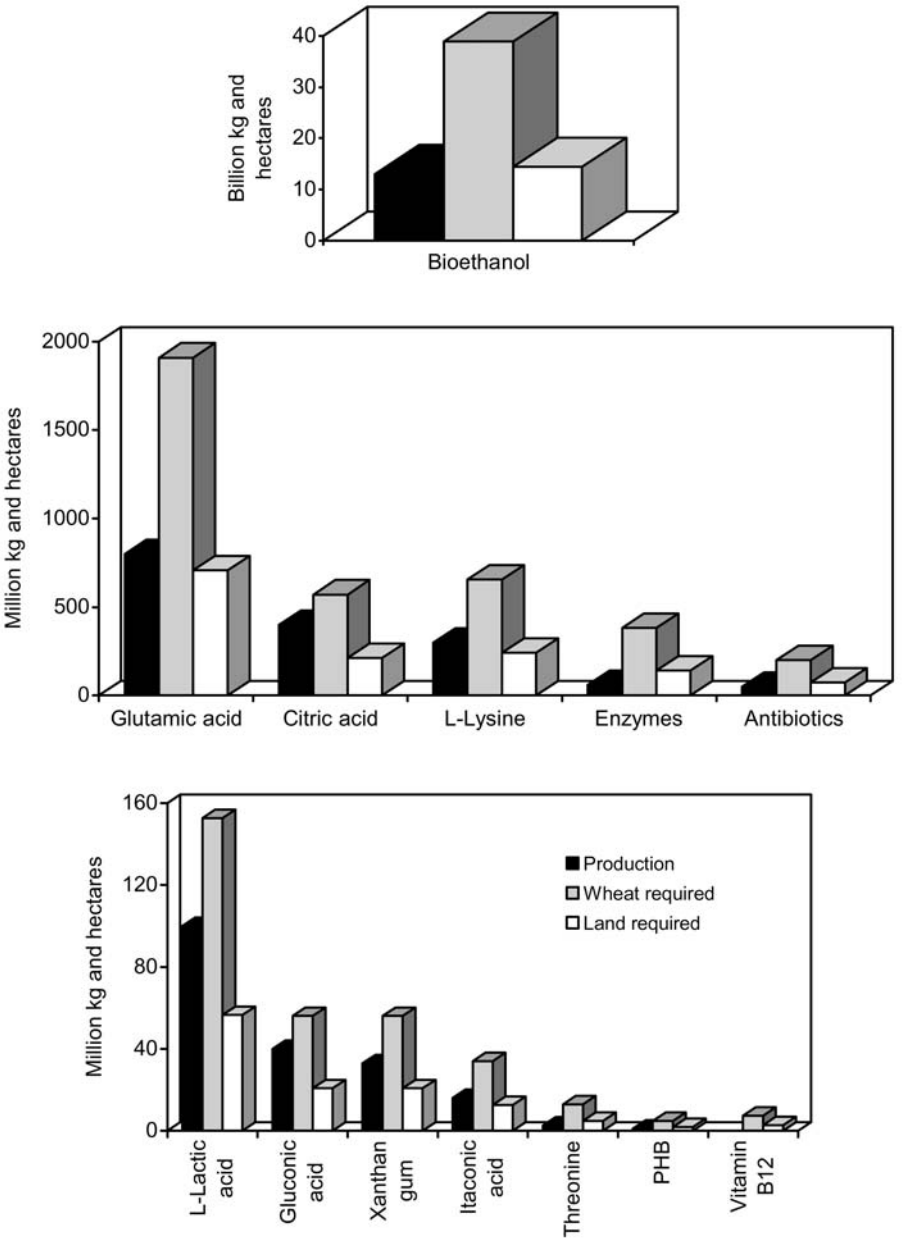

Fig. 11 Land area and quantity of wheat required for the production of some major petrochemicals

where, i represents each of the major components of wheat (starch, gluten and bran), C_f is the unit cost of the feedstock, α_i is the fraction of the maximum theoretical yield of product from component i, y_i is the theoretical maximum yield of product derived from component i, V_i is the value of the product derived from component i, x_i is the fraction of component i in the feedstock, and β_i is the hydrolysis weight gain conversion factor (1.11 from starch to glucose).

In calculations using Eq. (1), only the starch and gluten components have been included. No data could be found for yields from bran but they are, in any case, likely to be very low. Nevertheless, if they proved to be significant they would increase the total value of product and hence improve the feasibility of using wheat as the feedstock. The unit cost of the feedstock, C_f, was taken as \$0.145 kg^{-1}, the average UK price for wheat since 1985. The fractions of starch and gluten in wheat (x_i) were taken as 62.1% and 11.9% on a wet basis (10% moisture content), respectively. The value of gluten (V_{gluten}) was taken as \$1.16 kg^{-1}. The theoretical maximum yield (y_i) used for all but one of the products was the stoichiometric yield based on glucose. For threonine, however, in the absence of a simple stoichiometric equation, y_i was based on a demonstrated yield. The fraction, α_i, of theoretical maximum yield was always taken as 95%. This is regarded as an upper limit rather than an accurate estimate and is therefore useful only as part of a preliminary evaluation. Product prices (V_i) were taken from the journal *Chemical Market Reporter* [6].

Figure 12 presents the results from the FRF calculations. According to the calculated FRF values for each chemical, wheat usage could be economically attractive for traditional fermentation products, for which FRF values are very low. On the other hand, the FRF calculated for petrochemical replacements is much higher, especially for ethylene, propylene, and butadiene, and wheat does not seem to be an attractive raw material for further investigation. It is important to

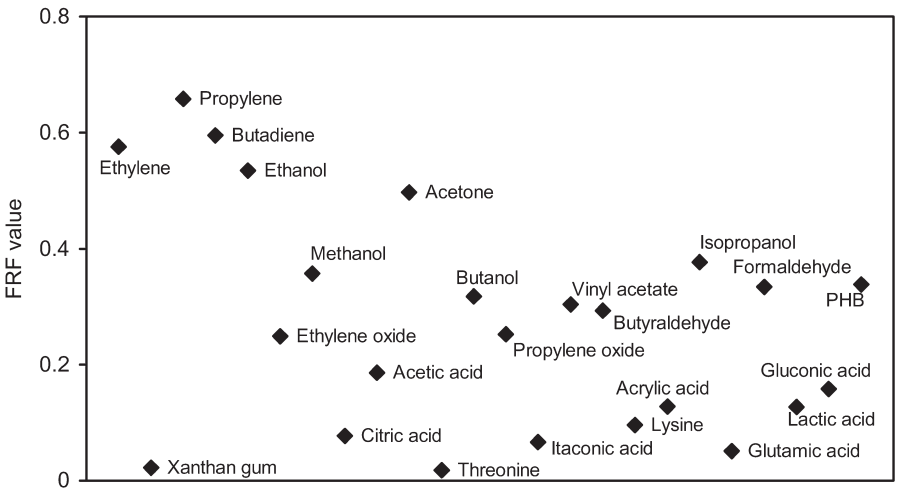

Fig. 12 Economic feasibility of wheat as feedstock for chemical production using the FRF equation. The lower the FRF the greater is the potential of wheat for the specific chemical

mention that these results could change in the future due to process improvements, reductions in wheat price, and increases in product values.

5.2.2 *Equation 2: raw material cost ratio (RMCR)*

The RMCR (Eq. 2) is the ratio of the estimated cost of the traditional feedstock in a conventional process to the estimated cost of wheat for the equivalent bioprocess, modified by a risk factor of 1.3 to compensate for possible problems and unknowns in the bioprocess [191]. The RMCR provides a preliminary comparison between the conventional feedstock and wheat to detect whether the substitution is likely to be feasible. If the RMCR is greater than unity then wheat is a potential substitute for the conventional feedstock, whereas below unity wheat cannot easily compete with the conventional feedstock. It is assumed that, for each product, the cost of both conventional and wheat feedstocks represents an approximately equal fraction of the total operating cost for the alternative processing schemes.

$$\text{RMCR} = \frac{\text{Estimated cost of feedstock for conventional process}}{\text{Estimated cost of wheat for intended bioprocess} \times \text{Risk factor}} \quad (2)$$

The estimated feedstock cost for a conventional fermentation process is the market price per kg glucose equivalent divided by the demonstrated yield from glucose to the product. In Table 7, wheat is compared with various conventional fermentation feedstocks (molasses, glucose syrup, corn, sucrose). According to the calculated RMCR values wheat has a potential economic advantage when compared with glucose syrup. For molasses and sucrose the results fluctuate depending on the product. Wheat does not compete with corn for bioethanol production, except where its purchase cost is higher (as in the UK where corn is not a major cereal crop) or where restrictions on the production of corn-based hydrolysates exist (as throughout the EU).

The estimated cost of the feedstock for a conventional petrochemical process is the market price per kg divided by the attainable yield. The estimated cost of wheat feedstock for the potential alternative bioprocess is the cost per kg glucose equivalent divided by the theoretical maximum yield for each product, divided by 0.95 (to adjust for the uncertainty in converting bench- or pilot-scale yield data to production scale) [191]. In Table 8, wheat is compared with petrochemical feedstocks. Most of the calculated RMCR values for petrochemicals are below unity. Therefore, wheat cannot usually compete with petrochemical feedstocks yet. The general conclusion that can be drawn from this table though is that the RMCR fluctuates around 1 depending on the chemical product. The advancement of bioprocesses in combination with further reduction in wheat prices will eventually promote wheat as a highly competitive feedstock in comparison with its petrochemical rivals.

Table 7 Comparative RMCR analysis between wheat and conventional raw materials used in the fermentation industry

Fermentation products	Industrial yield (kg kg^{-1} glucose)	Theoretical yield (kg kg^{-1} glucose)	RMCR of various Feedstocks and wheat[f]			
			Molasses[b]	Glucose syrup[c]	Corn[d]	Sucrose[e]
Bioethanol	0.459	0.51			0.611	0.957
Glutamic acid	0.63	0.64	0.875	2.419		
Citric acid	0.9	1.07	1.024	2.831		
Lysine	0.5	0.7	1.206	3.333		
Enzymes	0.24	0.24[a]		2.381		0.861
Lactic acid	0.95	1		2.506		0.907
Antibiotics	0.38	0.38[a]		2.381		0.861
Gluconic acid	0.9	1.09		2.883		
Xanthan gum	0.625	0.9				1.240
Itaconic acid	0.65	0.72	0.954	2.637		
Threonine	0.297	0.297		2.381		
PHB	0.317	0.48		3.605		1.304
Vitamin B_{12}	0.000617	0.000617[a]	0.861			

[a] Demonstrated yield.
[b] Molasses (50% sucrose) has a 10 year average cost of \$0.261 kg^{-1} fermentable sugars.
[c] Glucose syrup (80.4% DS, 80 DE) has an EU five-year average cost of \$0.721 kg^{-1} glucose.
[d] Corn has an approximate USA cost of \$0.167 kg^{-1} glucose.
[e] Sucrose has a 10 year average cost of \$0.261 kg^{-1}.
[f] Wheat has an approximate UK cost of \$0.221 kg^{-1} glucose.
A sterling to dollar exchange rate of 1.45 has been assumed.

Table 8 Comparative analysis between wheat and conventional raw materials used in the petrochemical industry by RMCR calculation

Product	Conventional feedstock	Feedstock price yield (\$ kg^{-1})	Industrially achieved yield (kg kg^{-1} feedstock)	Theoretical yield (kg kg^{-1} glucose)	RMCR
Ethylene	Natural gas liquids			0.31	
Propylene	Natural gas liquids			0.31	
Butadiene	Butane/enes	0.62	0.6	0.3	1.02
Ethylene oxide	Ethylene	0.60	0.75	0.59	1.55
Methanol	CO/H_2 (synthesis gas)	0.15	0.6	2	1.69
Formaldehyde	Methanol	0.21	0.9	1	0.77
Acetic acid	Methanol/CO	0.21	0.99	1	0.70
Acetone	Cumene	0.56	0.91	0.53	1.08
n-Butanol	Propylene/CO	0.44	0.95	0.41	0.63
Propylene oxide	Propylene	0.44	0.9	0.48	0.78
Vinyl acetate	Ethylene	0.60	0.95	0.48	0.99
Butyraldehyde	Propylene/CO	0.44	0.67	0.45	0.98
Acrylic acid	Propylene	0.44	0.7	0.8	1.66
Isopropanol	Propylene	0.44	0.95	0.44	0.67

6
A continuous process to produce a generic bioconversion feedstock from wheat

As mentioned in the section *Upstream processing*, conventional processing routes from cereal grain to fermentation media frequently commence with the extraction of starch (and consequent removal of proteins and loss of potentially valuable products in waste streams), which is subsequently hydrolysed using commercial enzyme formulations. These enzymes are produced by individual fermentation processes and lead to relatively expensive processing routes to products such as glucose syrups. Bioindustries use these starch hydrolysates and mix other nutrients (which might well have existed in the unprocessed grain) with them to produce complete media for the production of chemicals via cultivation of microorganisms. Exploitation of the starch component of grain and its subsequent bioconversion – the current focus of grain processors – are not the most cost-effective or environmentally benign processes and lead to a lack of flexibility and independence and, most importantly, cost increases for bioindustries (see the section *Burdens caused by current raw materials*). A viable solution to this problem could be provided by developing a process that can directly convert cereal grain into a nutrient-complete and low-cost bioconversion medium. In this way, all the intermediate processing steps from agriculture to the bioprocess would be bypassed, reducing costs and loss of fermentable materials. In addition, the exploitation of whole cereal grain by bioindustries will give them the opportunity to extract valuable chemical compounds present in the grain (e.g. β-glucan, oil, gluten) that are not useful in microbial bioprocesses. The extraction of such added-value components will create new market outlets and, most importantly, improve overall production economics. Apart from bioindustries, farmers would also benefit by being able to dispose their harvest to a wider range of buyers.

Research in the Satake Centre for Grain Process Engineering (UMIST, UK) has shown that it is possible to short-circuit the conventional processing route from grain to fine chemicals by using filamentous fungi to convert whole grain flour into a generic microbial feedstock [189, 192–197]. These publications describe the analytical assays used to measure process variables and provide extensive information about this process. This review will only concentrate on highlighting the most important processing steps and achievements. Overall, the process (Fig. 13) can be divided into four main steps.

- Wheat grain is milled for production of whole wheat flour, which is separated into two streams. The first is used for gluten extraction via the Martin method, while the second provides the substrate for a continuous bioconversion process. The amount of gluten removed is controllable and depends on the nitrogen requirements of the subsequent target microbial system.
- Continuous bioconversion of *A. awamori* on whole wheat flour for the production of glucoamylase and fungal cells. The fermentation solids, which comprise fungal cells and undigested wheat particles, are removed from the fermentation effluent by filtration. The resulting effluent filtrate and solid sediment are used separately in subsequent processing stages.

- The effluent filtrate, which contains an enzyme complex among which glucoamylase is predominant, is used for the further hydrolysis of wheat flour (glucose enhancement). The liquid stream collected after the remaining solids are filtered from the reaction mixture constitutes a glucose-rich solution (Liquid 1).
- The fungal cells, which are contained in the fermentation solids, are disrupted under specific conditions of oxygen and substrate starvation (to release nitrogenous compounds). It should be stressed that the fungal cells need not be separated from the undigested wheat components because some of these will also be hydrolysed during this stage. After filtration of the reaction mixture, the resulting nitrogen-rich liquid stream (Liquid 2) contains various nitrogen-sources, phosphorus, vitamins, minerals, and other compounds essential or desirable for secondary fermentations.

The specific combination of the two product streams (Liquids 1 and 2) can provide a versatile feedstock for numerous fermentations. For instance, when microbial formation of the targeted product requires a certain amount of nitrogen in the initial fermentation medium, such as amino acids and single cell protein, the formulated feedstock can contain the appropriate amount of the nitrogen-rich stream.

The benefits derived from the biorefinery concept presented in Fig. 13 can only be illustrated by comparing this process with conventional formulation routes of bioconversion media that were presented in Fig. 4 (processes 1, 2, and 3):

- Process 1 has been developed specifically for the food industry and includes many processing steps, which increase the overall cost significantly. The biorefinery concept presented in Fig. 13 shows that only one milling stage is re-

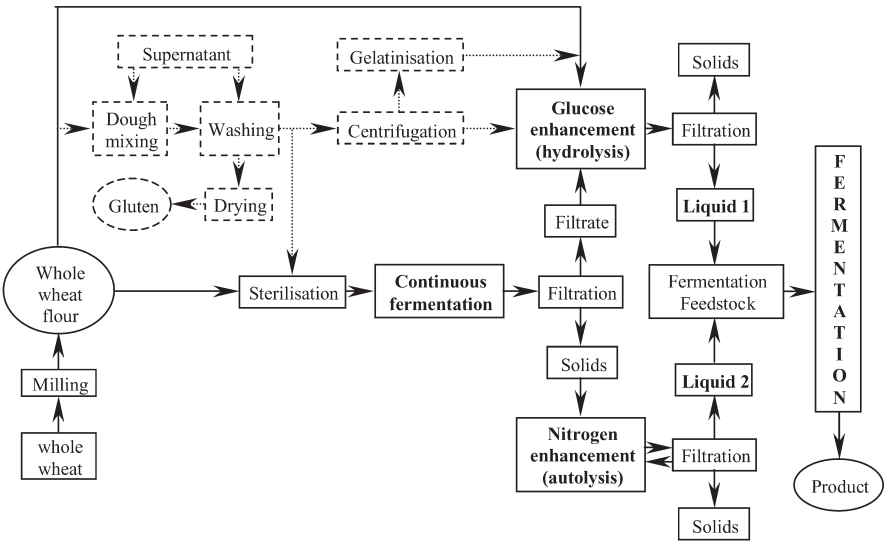

Fig. 13 Schematic diagram of the process to produce a generic fermentation feedstock

quired and the application of the Martin process for gluten separation. Hence, it can directly connect the agriculture with the bioindustry, circumventing the food processor.
- Process 2 cannot always be applied because of restrictions (e.g. in EU countries) on corn utilization.
- Process 3 produces only a low-value by-product (fermentation solids), which has very limited use (e.g. as animal feed). In addition, fermentations conducted at high solids concentration may cause operational difficulties reducing overall production yields.
- In contrast with processes 1, 2, and 3, in the proposed biorefinery by-product (gluten) separation can be optimized to retain the amount of nitrogen source required in subsequent microbial bioconversions.
- The single fermentation stage by *A. awamori* produces an enzyme complex that contains all the enzymes (e.g. α-amylase, glucoamylase, protease) that processes 1, 2, and 3 have to purchase as commercial enzyme preparations. These commercial preparations are produced from similar fermentations as that carried out in the proposed biorefinery and their market price incorporates the costs of production, purification and profit to the enzyme supplier.
- In the glucose enhancement stage (Fig. 13), the gluten-free wheat flour is hydrolysed by the enzyme complex into glucose and other micronutrients (e.g. amino acids, phosphorus) in a single stage, while in processes 1, 2, and 3 two stages are required (i.e. liquefaction and saccharification). In addition, the higher temperatures required in the liquefaction stage increase processing costs.
- The nitrogen enhancement stage produces a nutrient-rich liquor (Liquid 2), which is equivalent to yeast extract. Hence, especially for fastidious microorganisms (e.g. lactic acid bacteria), it can achieve superior production yields in comparison with the conventional nutrient sources (e.g. synthetic chemicals) used in the fermentation stages of processes 1, 2, and 3. Alternatively, Liquid 2 could be sold as a by-product.
- The proposed biorefinery introduces a novel concept of "drainless added-value total processing of cereals". It aims at converting whole grain into commodity chemicals with minimum, or even no, production of waste streams.

6.1 Raw materials

Wheat was selected as the pilot raw material to develop this process because it is the most abundant cereal grain in the EU and, at the same time, contains adequate amounts of nutrients to sustain a microbial bioprocess [189, 197]. In addition, the high-value gluten by-product that can be extracted from wheat provides significant revenue to the process. The high flexibility of this process rests on the fact that any cereal grain (e.g. oats, barley, rice) can replace wheat with limited changes in the whole process.

Apart from whole grain, by-products from flour milling plants can also be used, reducing processing costs further. Milling plants produce many products and by-products with various prices and uses. In the UK approximately 20%

(1125×10^6 kg $year^{-1}$) of the wheat processed in the year 1999/2000 for flour production was used as animal feed (wheatfeed) and commercial bran [198]. Worldwide, the amount of coarse grain used for feed purposes in the same year reached a total of 96.9×10^9 kg [199].

The continuous cultivation of flour milling by-products and feed grain with a consortium of fungal microorganisms could facilitate the creation of raw materials with versatile end uses. Fungi are robust enzyme producers capable of degrading either completely or at least partly the natural polymers (starch, protein, cellulose and hemicellulose) present in cereal grain. Thus, the liquor from such a fungal bioconversion process will constitute a nutrient-complete microbial feedstock rich in fermentable sugars and other nutrients capable of producing a range of added-value chemicals. The solid residues containing undigested flour components and fungal cells would provide a protein-enriched animal feed free from phytic acid, contributing to the reduction of phosphorus pollution. Such a process can benefit simultaneously the environment, bioindustries, and agriculture.

6.2 Fungal bioconversion

The fermentation of *A. awamori* on whole wheat flour constitutes the cornerstone of this process because it produces the enzyme complex and fungal cells necessary in the subsequent glucose and nitrogen enhancement stages. *A. awamori* produces a great diversity of enzymes such as glucoamylases, proteases, and many others, including pectinases, lipases, tannases and phosphatases, xylanases, and other cellulases [189].

Batch fermentations were conducted initially to:

1. confirm the suitability of whole-wheat flour for the growth of *A. awamori*, and
2. determine the flow rate in continuous operation by measuring the maximum specific growth rate in the exponential growth phase of the fungus.

The latter was hindered by the presence of bran and gluten in whole-wheat flour. Thus, the maximum specific growth rate of *A. awamori* (0.0365 h^{-1}) was measured in a fermentation of bran-free and gluten-free flour. Continuous bioconversions led from the initial residence time of 27.4 h to the optimized 16.67 h. The optimization was decided on the basis of:

1. the complete digestion of the aleurone layer in wheat bran releasing various vitamins and minerals into the fermentation medium, and
2. the complete hydrolysis of starch into glucose.

As mentioned earlier, starch, gluten, and bran are the major constituents of wheat with gluten being the major protein source. To increase the cost-competitiveness of the process only 8% of the available gluten was included in the raw material for fungal bioconversion, the remainder being extracted as a by-product. It should be stressed that the amount of gluten available as by-product depends on the nitrogen requirements of the subsequent microbial bioconversion.

Gluten concentration in the medium affects free amino nitrogen (FAN) and glucose concentration in the continuous effluent (Fig. 14). Figure 14 shows that

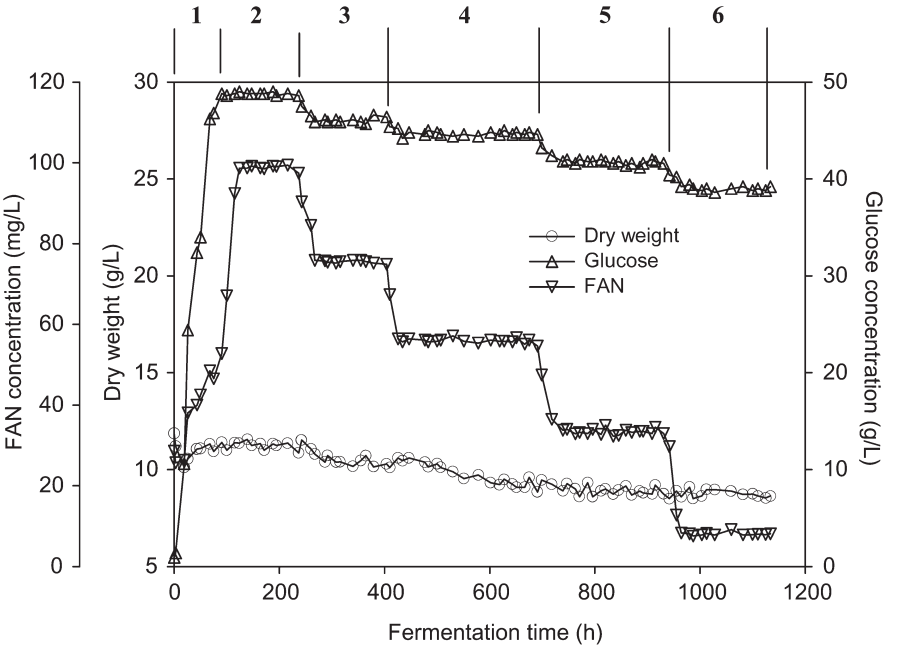

Fig. 14 Effects of gluten content on the output of continuous fermentation using soft wheat flour. (*1*) batch mode; (*2*) whole wheat flour; (*3*) 25% gluten removed; (*4*) 50% gluten removed; (*5*) 75% gluten removed; (*6*) gluten-free flour

gradual removal of gluten from the feed results in gradual reduction of the glucose concentration from 49 g L^{-1} to 39 g L^{-1}. This occurs because gluten is also a carbon source, so its absence from the medium means that more of the starch-derived glucose must be consumed. Furthermore, some starch is lost during gluten extraction. The constant biomass levels during each steady state represent the dynamic equilibrium between accumulation of cells and digestion of wheat solids.

Laboratory scale fermentations could not be carried out at flour concentrations higher than 8% (*w*/*v*, on a dry basis), because of the high viscosity of the sterilized flour suspension. Industrial scale experiments would require higher flour concentrations providing higher operating efficiency. To predict results for higher flour concentrations, the effects of flour input on component output in the effluent were investigated in another long-term continuous fermentation. It was observed that the average concentrations of all components analysed in the effluent filtrate during steady state increased after the increase in medium flour concentration. Whole-wheat flour suspension of 10% could result in an effluent containing approximately 59 g L^{-1} glucose, 118 mg L^{-1} FAN, 173 mg L^{-1} dissolved phosphorus and 0.9 g L^{-1} total nitrogen.

6.3 Glucose enhancement

The continuous fermentation of *A. awamori* on whole-wheat flour can provide glucose concentrations up to around 50 g L^{-1} only, because of the limitations in handling whole wheat flour suspensions. This glucose concentration is much lower than the desired level for many microbial bioprocesses. To increase this value, experiments on glucose enhancement were carried out using filtered effluent as a source of enzymes to hydrolyse added flour. This hydrolytic reaction produced a glucose-rich stream with a concentration up to approximately 320 g L^{-1}. The flour suspensions were gelatinized before the reaction to increase enzyme susceptibility and reduce reaction time. The main disadvantages of the so-called glucose enhancement stage were the long reaction times (48–72 h) and the solidification of the flour suspensions after gelatinization. Although the long reaction times are similar to those tolerated in conventional starch hydrolysis processes, it was considered necessary to reduce them to improve overall economics. It was observed that when the flour suspensions were not gelatinized the residence time required was prolonged further (up to 120 h).

These problems were tackled by mixing 40% (*v*/*v*) of the enzyme solution with the wheat flour suspensions before gelatinization. The gelatinization was carried out at 75 °C and lasted only 20 min and, therefore, the enzymes were not deactivated, while at the same time they hydrolysed starch granules preventing the flour suspensions from solidifying. After the gelatinization had been completed, the temperature was adjusted to the optimum for hydrolysis (60 °C) and the rest of the filtrate (enzyme solution) was added to the reaction mixture. In this way, the overall reaction time was reduced to less than 24 hours.

Figure 15 presents experimental data from glucose enhancement reactions at different flour concentrations. The major difference between Figs. 15a and 15b was the addition of effluent filtrate (Fig. 15b) to the flour suspensions to prevent flour solidification during gelatinization. It is obvious that the addition of fermentation effluent filtrate during gelatinization of flour suspensions diminishes significantly the overall reaction time.

By using the gelatinized gluten-free flour from a 35% whole wheat flour suspension (Fig. 15b) more than 250 g L^{-1} glucose were produced. This glucose concentration corresponds to more than 94% starch conversion ratio in just 12 h reaction. Taking into consideration that the glucose content of the fermentation broth is around 40 g L^{-1}, it is therefore possible to produce a glucose-rich stream with a concentration around 270 g L^{-1} in approximately 12 h. This residence time is around one-fifth that required in a glucose enhancement reaction using the gelatinized gluten-free flour without enzyme addition during gelatinization. When a 40% flour suspension was used ungelatinized (Fig. 15a) the production of 300 g L^{-1} glucose took 120 hours.

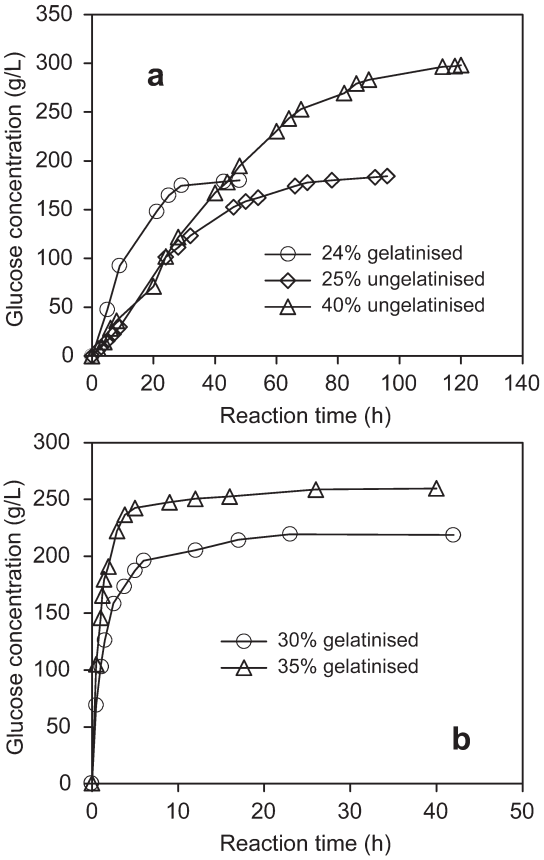

Fig. 15 Glucose production during glucose enhancement hydrolytic reactions using gluten-free wheat flour. (**a**) Experimental results without enzyme addition during gelatinization; (**b**) Experimental results with enzyme addition during gelatinization

6.4 Nutrient enhancement

Continuous fermentation on 8% whole soft wheat flour produced an effluent containing 51.4 g L^{-1} glucose and 99 mg L^{-1} FAN, on average. After glucose concentration had been increased to much higher levels by the glucose enhancement operation, the comparatively low concentration of assimilable nitrogen source became the main challenge to the production of a suitable generic fermentation feedstock. During fermentation, the fungus assimilated various nutrients from the medium to support cell growth. A material balance revealed that 65% of the total Kjedahl nitrogen (TKN) and 52.1% of the phosphorus initially present in wheat remained in the fermentation solids after the removal of effluent filtrate. Most, if not all, were incorporated into the *A. awamori* cells. Cell disruption via cell autolysis and a combined cell autolysis–bead milling process were evaluated as potential approaches for the conversion of *A. awamori* cells or cell components

into digestible materials for secondary microbial bioprocesses. Any remaining undigested wheat components present in the fermentation solids were not separated from the fungal cells because they could also be hydrolysed during the nutrient-enhancement stage.

6.4.1 *Cell autolysis*

Experimental work showed that pH in the range of 3–7 had little effect on either FAN production or dry weight reduction, while temperature in the range of 25–55 °C had substantial effect, with higher temperature leading to higher reaction rate. The autolysis of *A. awamori* cells was initiated on exhaustion of dissolved oxygen from the reaction mixture. In a slurry of fermentation solids, concentrated by centrifugation from the fermentation effluent, the initiation of cell autolysis was signalled by the decrease in dry weight and the increase in the production of various components in the liquid phase. The process of cell autolysis released significant amounts of phosphorus and proteinaceous components into the liquid phase.

It has been reported that cell self-degradation takes place not only in the cytoplasm [200] but also in the cell wall [201]. The cell wall structure will eventually be damaged, resulting in the leakage of lytic enzymes into the surrounding liquid phase. This should eventually provide the autolysate with some hydrolytic capability so that autolysis of fresh solids in this autolysate would be accelerated. A set of eight trials was carried out to test the effects of autolysate re-circulation. Fresh solids were suspended in tap water to initiate the first trial. In subsequent trials fresh solids from the same steady state were suspended in the autolysate from the previous trial to form a new slurry (Fig. 16). Compared with single-batch autolysis accumulation of the lytic enzymes reduced reaction times from 72 h to 40 h for achievement of a similar dry weight reduction ratio. Table 9 compares the nutrient value of the final autolysate with yeast extract.

Further research is in progress to confirm that autolysis of fungal biomass comprising one or more fungal species grown on cereal-based medium can provide an alternative way of producing a nutrient-rich fungal extract [202].

6.4.2 *Combined cell autolysis and bead milling*

An alternative process scheme for the production of the nitrogen rich stream has been proposed – combination of cell autolysis with mechanical disruption of fun-

Table 9 Nutrient value of the autolysate after the seventh re-circulation

Component	Pre-circulation	Post-circulation	Nutrient equivalence
FAN (g L^{-1})	0.005	1.58	31 (g yeast extract L^{-1})
Total nitrogen (g L^{-1})	0.031	5.34	54.5 (g yeast extract L^{-1})
Phosphorus (g L^{-1})	0.004	0.51	2.24 (g $KH_2PO_4L^{-1}$)
Glucose (g L^{-1})	1.82	33.2	

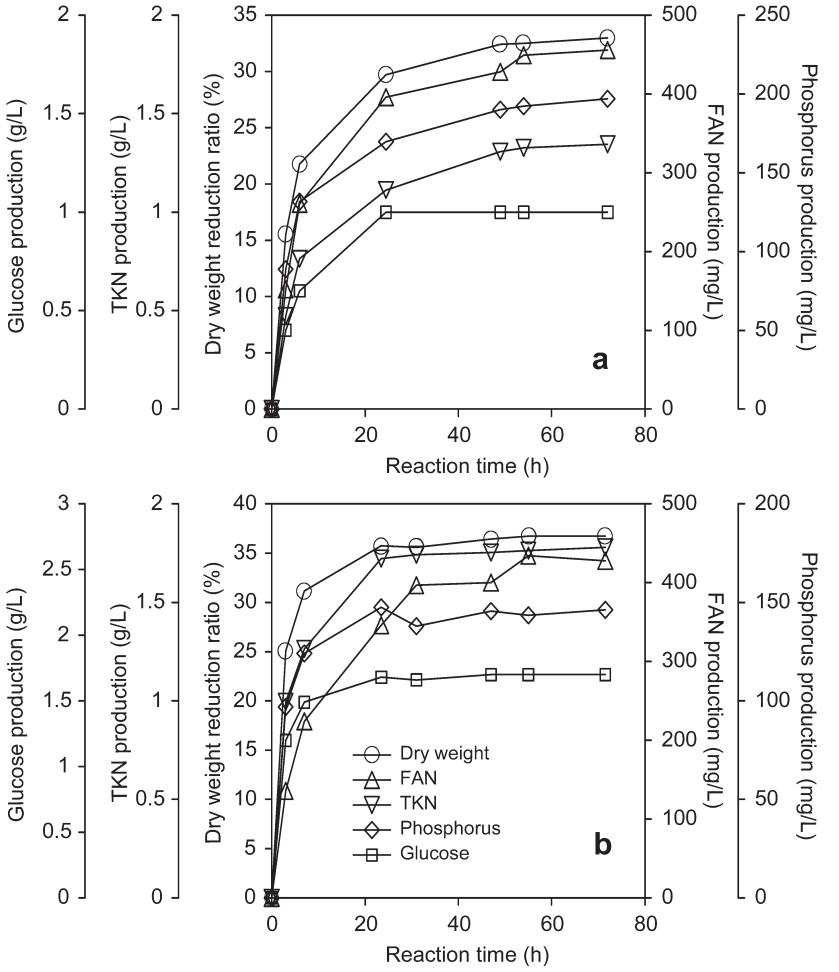

Fig. 16 Dry weight reduction and component production during cell autolysis experiments. (**a**) Single autolysis stage on the exhaustion of dissolved oxygen at 55 °C; (**b**) Autolysis during the seventh recycling of autolysate at 55 °C

gal cells by bead milling. Initially cell autolysis was induced at 55 °C and pH 4.5. The solid suspension was maintained under these conditions for 10 h to induce production of lytic enzymes by the cells. Taking into consideration that the structure of the fungal cells was not fundamentally affected during autolysis [189], a bead milling process was used to disrupt the cell wall and release the enzymes and protein contained in the cytoplasm. It lasted for 15 min and fundamentally affected the structure of the fungal cells [197].

The duration of milling was minimized to avoid contamination of the solution. After the bead milling stage the slurry was returned to the autolytic conditions to investigate the production of components and the reduction of dry weight.

Figure 17 shows that the mechanical disruption of fungal cells by bead milling has a significant effect on FAN and TKN production. Prior to bead milling (0–10 h reaction), the concentrations of FAN and TKN in the liquid phase increased in a similar pattern as in the single autolysis reaction presented in Fig. 16. After bead milling (broken lines in Fig. 17), the concentration of TKN in the liquid phase was significantly higher. This can be explained by the extensive damage that the cells have undergone during the milling process. Thus, the disruption of the cell walls resulted in large amounts of protein being released from the cell cytoplasm into the liquid. The gradual increase in FAN concentration, after cell autolysis had been resumed, revealed that the proteolytic enzymes were still active and had not been severely damaged during bead milling. The final FAN concentration was 700 mg L^{-1} at 62 h reaction, which corresponds to almost 55% production ratio increase compared with the single cell autolysis reaction (Fig. 16a).

6.5 Evaluation of the feedstock

The nutrient composition of the continuous fermentation effluent, Liquids 1 and 2 (Fig. 13) are presented in Table 10. Also presented in this table is the micronutrient composition of Liquid 1 when whole wheat flour is used in the glucose-enhancement stage. The feedstock was evaluated in terms of both its nutritional significance in actual microbial bioprocesses and its relative cost in relation to sugar and starch derivatives.

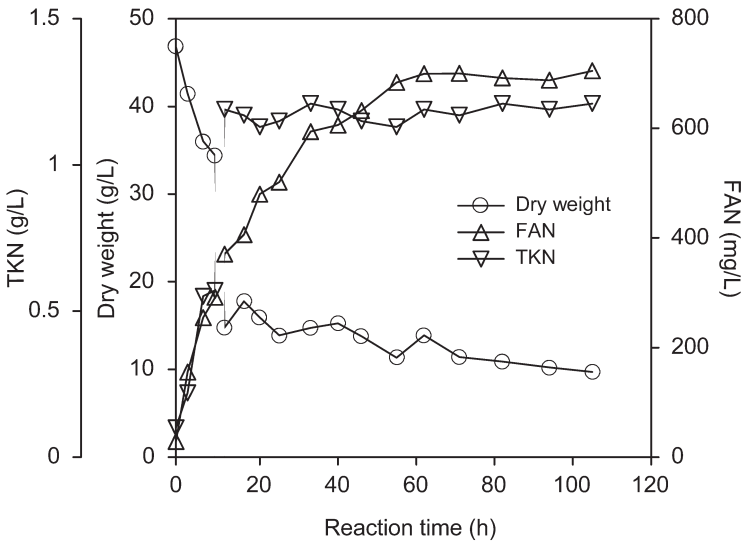

Fig. 17 Time profiles of dry weight reduction and FAN and TKN production during a combined cell autolysis and bead milling experiment

6.5.1 *Microbial bioconversions using the feedstock*

Microbial bioconversions including yeast, ethanol, lactic acid, glycerol, and pigment production verified the versatility of the generic feedstock. Detailed information about microbial strains used in each of these fermentations, analytical assays and in depth discussion are presented in other studies [189, 197, 203–206].

6.5.1.1 Yeast growth and ethanol production

The nutritional value of the nitrogen-rich stream (Liquid 2 in Fig. 13) was validated by growing yeast *S. cerevisiae* aerobically on a medium constituted of pure glucose of constant concentration (19 g L^{-1}) and various fractions of Liquid 2 (10%, 20%, 30%, 40%, *v*/*v*, corresponding to 37, 75, 101, and 144 mg L^{-1} FAN, respectively). Glucose was consumed completely only in the fermentation with the highest Liquid 2 fraction (40% *v*/*v*) indicating that this liquid stream provides a nutrient-rich solution that balances glucose consumption and yeast cell growth. In an equal mixture of the glucose-rich stream and the nitrogen-rich stream, *S. cerevisiae* consumed all the available glucose and FAN in less than 72 h at 30 °C and under aerobic conditions (Fig. 18). The conversion yield of 0.3 g dry yeast per g glucose is close to the industrial standard.

Table 10 Output of each unit operation in the process to produce a generic fermentation medium

Unit operation	Intermediate	Component	Concentration (g L^{-1})
Continuous fermentation	Continuous effluent	Glucose	45.8
		FAN	0.098
		TKN	0.77
		Phosphorus	0.14
		Solids	13.41
Glucose enhancement using gluten-free flour	Glucose-rich solution (Liquid 1 in Fig. 13)	Glucose	258.2
		FAN	0.58
		TKN	2.02
		Phosphorus	0.78
		Solids	46.58
Glucose enhancement using whole wheat flour	Glucose-rich solution (Liquid 1 in Fig. 13)	Glucose	260.8
		FAN	1.10
		TKN	3.54
		Phosphorus	0.89
		Solids	96.03
Cell autolysis (with autolysate recycling)	Nitrogen-rich solution (Liquid 2 in Fig. 13)	Glucose	33.2
		FAN	1.58
		TKN	5.34
		Phosphorus	0.51
		Solids	25.13

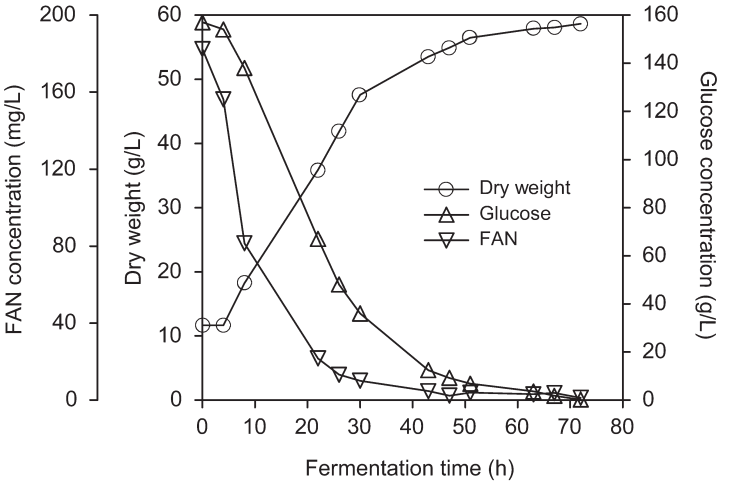

Fig. 18 Profiles of *S. cerevisiae* fermentation using the generic feedstock

Anaerobic fermentation for ethanol production was carried out by *S. cerevisiae* on the same medium composition (50:50) of Liquids 1 and 2 as in the best case of yeast production. The glucose to ethanol yield reached 0.49 g g^{-1}, equivalent to 96% of the theoretical value of 0.51. Compared with aerobic incubation, the increase in total dry weight was much smaller (2.52 g L^{-1}), whereas the FAN concentration at the end of the fermentation remained higher (about 40% of initial FAN remained in the broth). This indicated that for ethanol fermentation wheat provided more than sufficient nitrogen and partial separation of wheat gluten as a co-product would benefit process economics significantly without harming process efficiency.

6.5.1.2 Lactic acid production

The strain of *Lactobacillus plantarum* used in lactic acid fermentations produces a racemate of equal quantities of L- and D-lactic acid stereoisomers when it is grown on glucose. This microbe was used to demonstrate the ability of the feedstock to support lactic acid fermentation. Three lactic acid fermentations were conducted in Media 1, 2, and 3 composed of different combinations of Liquids 1 and 2 (Medium 1: 100 g L^{-1} total reducing sugars (TRS), 92.5 mg L^{-1} FAN, and 0.3 g L^{-1} TKN; Medium 2: 100 g L^{-1} TRS, 142.4 mg L^{-1} FAN, and 0.46 g L^{-1} TKN; Medium 3: 150 g L^{-1} TRS, 222.3 mg L^{-1} FAN and 0.71 TKN). In all fermentations, lactic acid was produced during both the exponential and stationary phases of microbial cell growth. Nevertheless, the yield and volumetric productivity throughout all fermentations followed different patterns which depended on the nutrient composition of the feedstock used (Fig. 19).

The fermentation on Medium 1 ended prematurely in less than 70 h due to the low availability of nutrients. A concentration of 28 g L^{-1} TRS was still present in the

fermentation broth at the end of the fermentation, indicating that a higher content of FAN was necessary to prolong microbial growth and lactic acid production. This was confirmed by fermentation on Medium 2; addition of higher concentration of Liquid 2 accelerated lactic acid production and resulted in almost complete glucose consumption (98%). The yield in the fermentation on Medium 2 was the highest achieved (Fig. 19) reaching a value of 95% at 78 h, although it gradually decreased to 84% toward the end of the fermentation (138 h). Fermentation on Medium 3 gave the highest volumetric productivity (2.1 g L^{-1} h^{-1} between 20 and 30 h), lasted approximately the same time (about 140 h) as that on Medium 2, and produced 33% higher lactic acid concentration than Medium 2 (108 g L^{-1} and 81 g L^{-1}, respectively). These experiments led to the conclusion that the composition of nutrients plays a crucial role and further study on nutrient optimization is necessary.

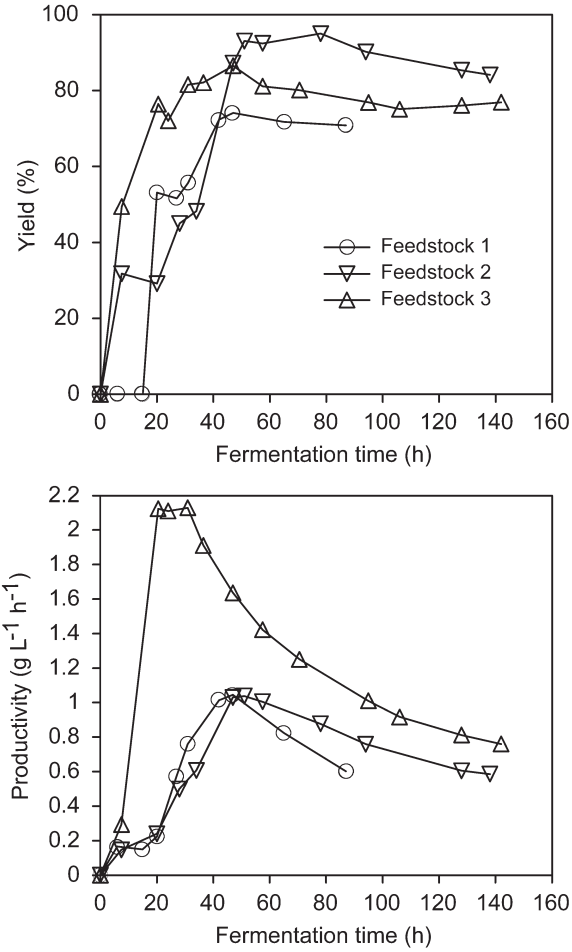

Fig. 19 Lactic acid yield and volumetric productivity as a function of time during fermentations on three media

6.5.1.3 Glycerol production

The feedstock was also tested for glycerol production in a fermentation using 10% Na_2CO_3 as steering agent and an osmophilic yeast *Pichia farinosa*. Preliminarily experiments were carried out in shake flasks and then in a 2 L bioreactor with air provision and on-line pH control. Shake flask experiments on media of various combinations of Liquids 1 and 2 identified an optimum C:N ratio of 396 g g^{-1} (where C:N corresponds to the ratio of the carbon in glucose to the FAN content in the fermentation broth) for the production of 40.5 g L^{-1} glycerol. Glucose consumption increased and fermentation time decreased when FAN supplementation increased. However, high FAN concentrations resulted in decreased glycerol production. Similar observations were made by Onishi, who concluded that high nitrogen concentrations in a fermentation by *P. miso* on glucose caused a drastic fall in glycerol production, despite high sugar consumption [207]. On the other hand, ethanol production was favoured by higher FAN concentrations. This can be attributed to the fact that higher FAN concentration induced cell growth causing a gradual greater need for oxygen. At increased cell population, the oxygen requirements could not be met and this favoured ethanol production, reducing glycerol production.

Aerobic incubation (1 vvm, 350 rpm agitation speed) in a bioreactor with a working volume of 1.5 L improved oxygen transfer. In feedstock with a C:N ratio of 322 g g^{-1}, glycerol concentration in the fermentation broth was significantly enhanced (Fig. 20) compared with the incubations in shake flasks, reaching a maximum of 72.7 g L^{-1} and a glycerol yield from glucose of 24.2%.

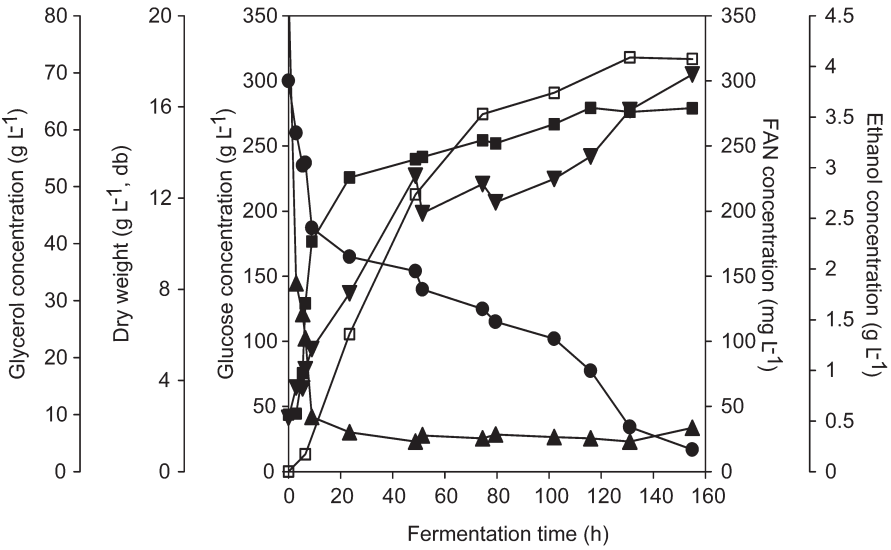

Fig. 20 Profiles of glycerol production using the generic feedstock in a 2 L bioreactor: (*filled circle*) glucose concentration; (*filled triangle*) FAN concentration; (*filled inverted triangle*) ethanol concentration; (*filled square*) dry weight; (*open square*) glycerol concentration

6.5.1.4 Production of Monascus pigments

To verify the wide range of applications of the feedstock, fermentations for dye production by *Monascus purpureus* were conducted. Fermentation media contained glucose at concentrations in the range 13.5–40.7 g L^{-1}, while the FAN concentration was adjusted to deliver eight desired C:N ratios covering the range from 8 g g^{-1} to 139 g g^{-1}. Fungal cell production was found most prolific when the medium C:N ratio was in the range from 20 g g^{-1} to 38 g g^{-1}. The concentrations of red and yellow dyes increased when the C:N ratio was increased from 8 g g^{-1} to 38 g g^{-1}. Both biomass and pigment productivity were reduced when the C:N ratio was higher than 38 g g^{-1}. In a medium containing 33.5 g L^{-1} glucose and 349 mg L^{-1} FAN the maximum colorant production reached 5.38 g L^{-1} and 0.164 g L^{-1} for red and yellow dyes, respectively.

6.5.2 *Preliminary cost estimation of the process*

The process to produce the generic feedstock can either be commercialized separately or integrated into an existing bioprocess plant. The feedstock can be generally used as a substitute for conventional fermentation media. However, the cost required to produce the generic feedstock is still unknown. Thus, after the development of the technical know-how, the most important factor that will determine the feasibility of the process is the cost estimate. Preliminary economic analysis will provide an approximate estimate (accuracy of estimate up to ±30%) of the capital investment required to construct the plant and the operating cost to manufacture the product. This preliminary analysis also provides the ability to change certain unit operations or certain variables of the process, test alternative technologies, and evaluate the effect of scale-up from laboratory to industrial size equipment.

The generic feedstock production plant was designed assuming 330 days per year and 24 h per day operation, producing 100 m^3 glucose-rich stream per day (Liquid 1). Evaporation stages for Liquids 1 and 2 have been included to reduce expenditure on transport and storage capacity/costs. A glucose concentration of 500 kg m^{-3} was produced after evaporation of the glucose-rich stream. The estimate of the fixed and total capital investment was based on the technique described by Blanch and Clark [208]. The costs of processing equipment were calculated from case-specific equations given by Blanch and Clark [208], while charts for equipment cost estimates were taken from various books [209–212] and one article [213]. To update the calculated costs in current prices, the Marshall and Swift equipment cost index was used.

Operating costs were calculated according to the mass and energy balances, which indicated the requirements for raw material, energy, electricity, process, and cooling water and waste treatment, while estimating factors that were involved in the calculation of the other components were taken from Coulson et al. [214]. The unitary costs of utilities were also taken from Coulson et al. [214] allowing for inflation (based on that in the UK) at 2% per year. The operating

labour was estimated by taking into consideration the labour requirements for each piece of process equipment according to the guidelines given by Reisman [215]. The credit from the gluten revenue was subtracted from the total operating cost. The operating cost has been calculated per m^3 generic feedstock produced in order to compare it with fixed purchased prices of conventional raw materials.

Figure 21 presents a preliminary comparison of the production costs for the generic feedstock and for starch hydrolysate (based on the process presented in Fig. 3) at various plant capacities (20–1000 m^3 day^{-1}). The separation and purification steps included in the design presented in Fig. 3 were not included in cost estimation because in most fermentations the starch hydrolysate is used without purification. A starch purchase price of £0.2 kg^{-1} has been assumed, which is far below the UK and EU ten-year average. The purchase price of glucoamylase and α-amylase were assumed to be £2 kg^{-1}. The procedure that was followed in this case was the same as that followed for the calculation of the cost of the proposed biorefinery concept. Thus, a plant operating 330 days per year and 24 h per day, producing 100 m^3 day^{-1} starch hydrolysate containing a glucose concentration of 320 kg m^{-3} (500 kg m^{-3} after evaporation) was assumed.

According to Fig. 21 the operating cost of the process producing the starch hydrolysate is lower than that required for production of the generic feedstock at plant capacities lower than 200 m^3 day^{-1}. It must, however, be taken into consideration that the price of starch used in this comparison is much lower than those in UK and EU markets. It should be also stressed that the feedstock is a formulated substrate ready for use in any bioprocess, while the starch hydrolysate requires substantial nutrient supplementation.

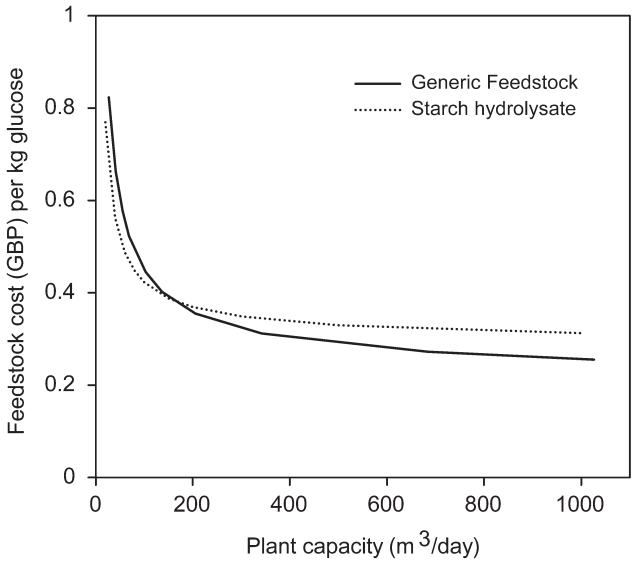

Fig. 21 Influence of scale on the production costs of wheat-based feedstock compared with starch hydrolysate produced via the process outlined in Fig. 3

The operating cost of the proposed biorefinery was also compared with purchased prices of conventional raw materials (glucose, glucose syrup, starch, and molasses). General methods were used to estimate raw material market prices as their costs fluctuate with time. The price of purified dextrose (£0.6 kg^{-1}) was determined by multiplying the price of starch by two [1]. The price of wheat/maize/potato starch (£0.3 kg^{-1}) may be considered low in relation to 1996 prices, which is close to £0.4 kg^{-1}, but is considered to represent the average price level achieved by the industry over recent years [10]. The price of glucose syrup (£0.498 kg^{-1} glucose) corresponds to an EU five-year average price for a product with a DE value of 80. The price of molasses (£0.155 kg^{-1} glucose equivalent) was estimated by dividing the world price of sugar by two [1]. All prices were converted to raw material costs per kg glucose content, because all these raw materials have different glucose equivalent concentrations. According to Fig. 21, the operating cost of the generic feedstock is lower than the purchase price of purified dextrose and glucose syrup (42 DE) in any plant capacity above 90 m^3 day^{-1}, while it is lower even than the starch price when the plant capacity exceeds 550 m^3 day^{-1}. On the other hand, it does not become as low as the purchase price of molasses.

The operating cost of the generic feedstock can be reduced further if the process is integrated into an existing fermentation plant, where evaporation is not necessary and major equipment is already installed (e.g. boiler, cooling tower). Furthermore, integration of glucose and nitrogen enhancement steps into a single continuous stage could reduce both capital and operating expenses significantly. In addition, a cereal grain that is cheaper than wheat (e.g. oats) could reduce costs further, particularly if it contains valuable by-products (e.g. proteins, antioxidants, β-glucan).

7 Conclusions

This review has presented various technological advances in the production of a spectrum of microbial metabolites. It has also proposed a novel processing scheme for production of a nutrient-complete bioconversion feedstock from wheat, with a high degree of adaptability according to the needs of a case-specific microbial bioprocess (e.g. lactic acid, glycerol, ethanol, pigments, yeast cell growth).

The next step should be to minimize processing costs further by developing continuous processes for glucose and nitrogen enhancement stages, using low-cost cereal grains, and extracting added-value chemicals contained in cereal grain. The nutritional significance of the feedstock should be evaluated by identifying the content of specific nutrients (e.g. amino acids, peptides, trace elements). In this way, case-specific bioprocessing obstacles could be solved.

The generic feedstock should justify its versatility and significance in the production of more bioproducts, for example microbial biodegradable plastics (e.g. PHB), biopesticides, succinic acid, and glutamic acid. Such research incentives should include economic considerations about the profitability of the generic feedstock, maximization and optimization of its nutrient composition, strain selec-

tion/screening, and development of efficient and cheap downstream processing routes.

More ambitious research planning could entail the use of the feedstock as the basis for the production of bulk, commodity petrochemical substitutes. In the section *Wheat as a potential feedstock* it was illustrated that wheat could be cost-competitive for production of specific intermediate petrochemicals (e.g. acrylic acid, isopropanol, butyraldehyde, and vinyl acetate). Such an endeavour is more difficult, because production of many petrochemicals cannot be accomplished by single-step microbial bioprocesses. However, in the future, the chemical industry will be dominated by clean bioprocessing routes and, therefore, the time has come to look into alternative solutions even for bulk chemical production.

Acknowledgements The authors gratefully acknowledge the generous contribution of the Satake Corporation of Japan in providing financial support for much of the work presented in this paper.

8 References

1. Leveque F (1992) Case study on non-food uses of European agricultural production, Cerna
2. Wilke D (1999) Appl Microbiol Biotechnol 52:135
3. Schilling LB (1995) FEMS Microbiol Rev 16:101
4. Weissermel K, Arpe H–J (1997) (eds) Industrial organic chemistry, 3rd edn. VCH, Weinheim
5. Wittcoff HA, Reuben BG (1996) (eds) Industrial organic chemicals. Wiley, New York
6. Anonymous (2001) Chem Market Rep, September 3, http://www.chemexpo.com
7. Himmel ME, Adney WS, Baker JO, Elander R, McMillan JD, Nieves RA, Sheehan JJ, Thomas SR, Vinzant TB, Zhang M (1997) ACS Symp Ser 666:2
8. Greasham RL (1993) Media for microbial fermentations. In: Rehm H–J, Reed G, Puhler A, Stadler P, Stephanopoulos G (eds) Biotechnology – Bioprocessing, VCH, New York
9. Carruthers SP, Miller FA, Vaughan CMA (1994) Crops for industry and energy, Centre for Agricultural Strategy, CAS report 15
10. Entwistle G, Bachelor S, Booth E, Walker K (1998) Ind Crops Prod 7:175
11. Anonymous (2001) Wheat usage by flour millers and flour production, Flour Advisory Bureau, http://www.fabflour.co.uk/prod_by_type.xls
12. Mulvihill PJ (1992) Crystalline and liquid dextrose products: production, properties and applications. In: Schenck FW, Hebera RE (eds) Starch hydrolysis products – worldwide technology production and applications, VCH, New York
13. Zoebelein H (1997) (ed) Dictionary of renewable resources. VCH, New York
14. Saha BC, Bothast RJ (1997) ACS Symp Ser 666:46
15. Aristidou A, Penttila M (2000) Curr Opinion Biotechnol 11:187
16. Kuhad RC, Singh A (1993) Crit Rev Biotechnol 13:151
17. Kim SB, Lee YY (2002) Biores Technol 83:165
18. Sun Y, Cheng J (2002) Biores Technol 83:1
19. Pandey A, Soccol CR, Nigam P, Soccol VS (2000) Biores Technol 74:69
20. Ballesteros I, Oliva JM, Negro MJ, Manzanares P, Ballesteros M (2002) Process Biochem 38:187
21. Duff SJB, Murray WD (1996) Biores Technol 55:1
22. McMillan JD (1997) Renew Energy 10:295
23. Webster LC, Anastas PT, Williamson TC (1996) ACS Symp Ser 626:198

24. Stinson SC (1998) Chem Eng News 76(3):49
25. Anonymous (2001) Sustainable development: the application of biotechnology to industrial sustainability, Organisation for Economic Co-operation and Development (OECD), http://www.oecd.org/sti/biotechnology
26. Stinson SC (1997) Chem Eng News 75(25):38
27. McCoy M (1998) Chem Eng News 76(25):13
28. Anonymous (2002) Biotechnology and pharmaceuticals, Department of Trade and Industry (DTI), http://www.dti.gov.uk/sectors_biotechnology.html
29. Layman PL (1998) Chem Eng News 76(19):14
30. Anonymous (2002) Communication from the commission to the council, the European parliament, the economic and social committee and the committee of the regions, life sciences and biotechnology – a strategy for Europe, Commission of the European Communities, http://europa.eu.int/eur-lex/en/com/cnc/2002/com2002_0027en01.pdf
31. Anonymous (2002) Biotechnology at work, BIOWISE, http://www.biowise.org.uk
32. Anonymous (2002) Faraday partnerships: advanced biotechnology for the chemical and pharmaceutical industries, http://www.faradaypartnerships.org.uk/Partners/Probio.html
33. Anonymous (2002) Energy efficiency and natural resources – bioenergy initiative, INEEL, http://www.inel.gov/energy/bioenergy
34. Hogue C (2000) Chem Eng News 78(19):40
35. Watkins K (2001) Chem Eng News 79(30):21
36. Thayer AM (2001) Chem Eng News 79:27
37. Anonymous (2002) Bioethanol process, http://www.iogen.ca/2101.html
38. Chotani G, Dodge T, Hsu A, Kumar M, LaDuca R, Trimbur D, Weyler W, Sanford K (2000) Biochim Biophys Acta 1543:434
39. Logan BE, Oh S, Kim IS, Van Ginkel S (2002) Environ Sci Technol 36:2530
40. Benemann JR (2000) J Appl Phycol 12:291
41. Glass TL, Bryant MP, Wolin MJ (1977) J Bacteriol 31:463
42. Bryant FO, Adams MWW (1989) J Biol Chem 264:5070
43. Miyamoto K (1997) (ed) Renewable biological systems for alternative sustainable energy production. FAO, Rome, Italy
44. Miura Y, Ohta S, Mano M, Miyamoto K (1986) Agric Biol Chem 50:2837
45. Ghirardi ML, Zhang L, Lee JW, Flynn T, Seibert M, Greenbaum E, Melis A (2000) Trends Biotechnol 18:506
46. Claassen PAM, van Lier JB, Contreras AML, van Niel EWJ, Sijtsma L, Stams AJM, de Vries SS, Weusthuis RA (1999) Appl Microbiol Biotechnol 52:741
47. Rocha JS, Barbosa MJ, Wijffels RH (2001) Hydrogen production by photosynthetic bacteria: culture media, yields and efficiencies. In: Miyake J, Matsunaga T, San Pietro A (eds) Biohydrogen II: an approach to environmentally acceptable technology. Elsevier, Oxford, UK, p 3
48. Yigit DO, Gunduz U, Turker L, Yucel M, Eroglu I (1999) Progr Ind Microbiol 35:125
49. Noparatnaraporn N, Takeno K, Sasaki K (2001) Hydrogen and poly(hydroxy) alkanoate production from organic acids by photosynthetic bacteria. In: Miyake J, Matsunaga T, San Pietro A (eds) Biohydrogen II: an approach to environmentally acceptable technology. Elsevier, Oxford, UK, p 33
50. Benemann J (1996) Nat Biotechnol 14:1101
51. Jung GY, Kim JR, Jung HO, Park J-Y, Park S (1999) Biotechnol Lett 21:869
52. Hart D (1997) Hydrogen power: the commercial future of the ultimate fuel. Financial Times Energy Publishing, London.
53. Nandi R, Sengupta S (1998) Crit Rev Microbiol 24:61
54. Fang HHP, Zhang T, Liu H (2002) Appl Microbiol Biotechnol 58:112
55. Sung S, Raskin L, Duangmanee T, Padmasiri S, Simmons JJ (2002) Hydrogen production by anaerobic microbial communities exposed to repeated heat treatments, Proc 2002 US DOE Hydrogen Program Review NREL/CP-610–32405
56. van Ginkel S, Sung S, Lay J (2001) Environ Sci Technol 35:4726
57. Kumar A, Jain SR, Sharma CB, Joshi AP, Kalia VC (1995) World J Microbiol Biotechnol 11:156

58. Palazzi E, Fabiano B, Perego P (2000) Bioproc Eng 22:205
59. Woodward J, Orr M, Cordray K, Greenbaum E (2000) Nature 405:1014
60. Miyake J, Mao X, Kawamura S (1984) J Ferment Technol 62:531
61. Zhu H, Wakayama T, Asada Y, Miyake J (2001) Int J Hydrogen Energy 26:1149
62. Yokoi H, Saitsu A, Uchida H, Hirose J, Hayashi S, Takasaki Y (2001) J Biosci Bioeng 91:58
63. Yokoi H, Maki R, Hirose J, Hayashi S (2002) Biomass Bioenergy 22:389
64. Tanisho S (2001) A scheme for developing the yield of hydrogen by fermentation. In: Miyake J, Matsunaga T, San Pietro A Biohydrogen II: an approach to environmentally acceptable technology. Elsevier, Oxford, UK, p 131
65. Lee MJ, Zinder SH (1988) Appl Environ Microbiol 54:124
66. Lay J-J (2000) Biotechnol Bioeng 68:269
67. van Ooteghem SA, Beer SK, Yue PC (2002) Appl Biochem Biotechnol 98/100:177
68. Sode K, Yamamoto S, Tomiyama M (2001) Metabolic engineering approaches for the improvement of bacterial hydrogen production based on *Escherichia coli* mixed acid fermentation. In: Miyake J, Matsunaga T, San Pietro A (eds) Biohydrogen II: an approach to environmentally acceptable technology. Elsevier, Oxford, UK, p 195
69. Mizuno O, Dinsdale R, Hawkes FR, Hawkes DL, Noike T (2000) Biores Technol 73:59
70. Fang HHP, Liu H (2002) Biores Technol 82:87
71. Roehr M, Kubicek CP, Kominek J (1996) Citric acid. In: Roehr M, Rehm H-J, Reed G, Puhler A, Stadler P Biotechnology – products of primary metabolism, VCH, New York
72. Kilic M, Bayraktar E, Ates S, Mehmetoglu U (2002) Process Biochem 37:759
73. Grewal HS, Kalra KL (1995) Biotechnol Adv 13:209
74. Demain AL (2000) Biotechnol Adv 18:499
75. Datta R, Tsai S, Bonsignore P, Moon S, Frank JR (1995) FEMS Microbiol Rev 16:221
76. Hofvendahl K, Akerberg C, Zacchi G, Hahn-Hagerdal B (1999) Appl Microbiol Biotechnol 52:163
77. Anonymous (2002) Cargill Dow LLC, http://www.cdpoly.com/home.asp
78. Akerberg C, Zacchi G (2000) Biores Technol 75:119
79. Cheng P, Mueller RE, Jaeger S, Bajpai R, Iannoti EL (1991) J Ind Microbiol 7:27
80. Linko YY, Javanainen P (1992) Enzyme Microbiol Technol 19:118
81. Tsai SP, Moon S-H (1998) Appl Biochem Biotechnol 70–72:417
82. Anuradha R, Suresh AK, Venkatesh KV (1999) Process Biochem 35:367
83. Akerberg C, Hofvendahl K, Zacchi G, Hahn-Hagerdal B (1998) Appl Microbiol Biotechnol 49:682
84. Hsieh CM, Yang F-C, Iannotti EL (1999) Process Biochem 34:173
85. Wenge F, Mathews AP (1999) Biochem Eng J 3:163
86. Fitzpatrick JJ, Ahrens M, Smith S (2001) Process Biochem 36:671
87. Milcent S, Carrere H (2001) Sep Purif Technol 22–23:393
88. Varadarajan S, Miller DJ (1999) Biotechnol Prog 15:845
89. Yang CW, Lu ZJ, Tsao GT (1995) Biotechnol Bioeng 51/52:57
90. Yin P, Nishina N, Kosakai Y, Yahiro K, Park Y, Okabe M (1997) J Ferment Bioeng 84:249
91. Lin JP, Chen B, Wu JP, Cen PL (1997) Chin J Chem Eng 5:49
92. Kosakai Y, Park YS, Okabe M (1997) Biotechnol Bioeng 55:461
93. Longacre A, Reimers JM, Gannon JE, Wright BE (1997) Fungal Gen Biol 21:30
94. Park EY, Kosakai Y, Okabe M (1998) Biotechnol Progr 14:699
95. Du JX, Cao NJ, Gong CS, Tsao GT (1998) Appl Biochem Biotechnol 70/72:323
96. Lin JP, Ruan SD, Cen PL (1998) Chem Eng Commun 168:59
97. Sun Y, Li YL, Bai S (1999) Biochem Eng J 3:87
98. Xuemei L, Jianping L, Mo'e L, Peilin C (1999) Bioproc Eng 20:231
99. Woiciechowski AL, Soccol CR, Ramos LP, Pandey A (1999) Process Biochem 34:949
100. Bai DM, Jia MZ, Zhao XM, Ban Rui, Shen F, Li XG, Xu SM (2003) Chem Eng Sci 58:785
101. Soccol CR, Marin B, Lebeault J-M, Raimbault M (1994) Appl Microbiol Biotechnol 41:286
102. Zeikus JG, Jain MK, Elankovan P (1999) Appl Microbiol Biotechnol 51:545

103. Lee SY, Park SH, Hong SH, Lee Y, Lee SH (2001) Fermentative production of building blocks for chemical synthesis of polyesters. In: Doi Y, Steinbuchel A (eds) Biopolymers. Polyesters II: properties and chemical synthesis, vol 3B, Wiley–VCH, New York
104. Lee PC, Lee WG, Kwon S, Lee SY, Chang HN (1999) Enzyme Microbiol Technol 24:549
105. Vemuri GN, Eiteman MA, Altman E (2002) J Ind Microbiol Biotechnol 28:325
106. van der Werf MJ, Guettler MV, Jain MK, Zeikus JG (1997) Arch Microbiol 167:332
107. Samuelov NS, Lamed R, Lowe S, Zeikus JG (1991) Appl Biochem Biotechnol 63–65:565
108. Ponnampalam E (2000) Integrating emerging technologies with biomass refining, MBI International, http://bioproducts-bioenergy.gov/pdfs/bcota/abstracts/12/z137.pdf
109. Lee PC, Lee WG, Lee SY, Chang HN (1999) Process Biochem 35:49
110. Lee PC, Lee WG, Kwon S, Lee SY, Chang HN (2000) Appl Microbiol Biotechnol 54:23
111. Lee PC, Lee WG, Lee SY, Chang HN (2001) Biotechnol Bioeng 72:41
112. MacKintosh TD (1987) ChemSA Dec:333
113. Nampoothiri KM, Hoischen C, Bathe B, Mockel B, Pfefferle W, Krumbach K, Sahm H, Eggeling L (2002) Appl Microbiol Biotechnol 58:89
114. Leuchtenberger W (1996) Amino acids – technical production and use. In: Roehr M, Rehm H-J, Reed G, Puhler A, Stadler P (eds) Biotechnology – products of primary metabolism. VCH, New York
115. Marquet M, Uribelarrea JL, Huchenq A, Laneelle G, Goma G (1986) Appl Microbiol Biotechnol 25:220
116. Shiratsuchi M, Kuronuma H, Kawahara Y, Yoshihara Y, Miwa H, Nakamori S (1995) Biosci Biotechnol Biochem 59:83
117. Delaunay S, Gourdon P, Lapujade P, Mailly E, Oriol E, Engasser JM, Lindley ND, Goergen J-L (1999) Enzyme Microbiol Technol 25:762
118. Gourdon P, Lindley ND (1999) Metab Eng 1:224
119. Pandey A, Soccol CR, Mitchell D (2000) Process Biochem 35:1153
120. Kim SS, Lee HW, Pan JG, Lebeault JM (1992) On the maximum productivity of L-lysine in the continuous culture of *Corynebacterium glutamicum*. In: Rao G, Tanner RB (eds) Ninth Int Biotechnology Symp and Exposition: Harnessing Biotechnology for the 21st Century, American Chemical Society, Washington, DC
121. Ohnishi J, Mitsuhashi S, Hayashi M, Ando S, Yokoi H, Ochiai K, Ikeda M (2002) Appl Microbiol Biotechnol 58:217
122. Hancock RD, Viola R (2001) Appl Microbiol Biotechnol 56:567
123. Hancock RD, Viola R (2002) Trends Biotechnol 20:299
124. Kalingan AE, Liao C-M (2002) Biores Technol 82:219
125. Stahmann K-P, Revuelta JL, Seulberger H (2000) Appl Microbiol Biotechnol 53:509
126. Bretzel W, Schurter W, Ludwig B, Kupfer E, Doswald S, Pfister M, Van Loon APGM (1999) J Ind Microbiol Biotechnol 22:19
127. Koizumi S, Yonetani Y, Maruyama A, Teshiba S (2000) Appl Microbiol Biotechnol 53:674
128. Bacher A, Eberhardt S, Eisenreich W, Fischer M, Herz S, Illarionov B, Kis K, Richter G (2001) Vitam Horm 61:1
129. Pujari V, Chandra TS (2001) J Microbiol Biotechnol 11:552
130. Dauner M, Sonderegger M, Hochuli M, Szyperski T, Wüthrich K, Hohmann H-P, Sauer U, Bailey JE (2002) Appl Environ Microbiol 68:1760
131. McCoy M (2000) Chem Eng News 19:23
132. Stinson SC (2000) Chem Eng News 79(49):35
133. Kirk O, Borchert TV, Fuglsang CC (2002) Curr Opin Biotechnol 13:345
134. Roberts SM, Turner MK (1998) Enantiomer 3:9
135. Panke S, Wubbolts MG (2002) Curr Opin Biotechnol 13:111
136. Tengerdy RP (1998) Solid substrate fermentation for enzyme production. In: Pandey A (ed) Advances in biotechnology. Educational Publishers and Distributors, New Delhi
137. Castilho LR, Polato CMS, Baruque EA, Sant'Anna Jr GL, Freire DMG (2000) Biochem Eng J 4:239
138. Soccol CR, Iloki I, Marin B, Raimbault M (1994) J Food Sci Technol 31:320
139. Higley LG, Zeiss MR, Wintersteen WK, Pedigo LP (1992) Am Entomol 38:139

140. Anonymous (2002) Biopesticides, United Stated Environmental Protection Agency, EPA, http://www.epa.gov/pesticides/biopesticides
141. Paulitz TC, Belanger RR (2001) Annu Rev Phytopathol 39:103
142. Kaur S (2000) World J Microbiol Biotechnol 16:781
143. Yang X-M, Wang SS (1998) Biotechnol Appl Biochem 28:95
144. Aranda E, Lorence A, del Refugio TM (2000) Entomop Bact 317
145. Moser A. (1991) Biotechnol Bioeng 37:1054
146. Lachhab K, Tyagi RD, Valero JR (2001) Process Biochem 37:197
147. Anderson RKI, Jayaraman K, Voisard D, Marison IW, von Stockar U (2002) Thermochim A 386:127
148. Zouari A, Dhouib A, Ellouz R, Jaoua S (1998) Appl Biochem Biotechnol 69:41
149. Vora D, Sethna YI (1999) World J Microbiol Biotechnol 15:747
150. Wu WT, Chen S, Hong JY (2001) Biotechnol Progr 17:778
151. Thompson MA, Schnepf HE, Feitelson JS (1995) Gen Eng 17:99
152. Elad Y, Chet I, Henis Y (1982) Can J Microbiol 28:719
153. Felse PA, Panda T (2000) Biochem Eng J 4:115
154. Herrera-Estrella A, Chet I (1999) EXS 87:171
155. Anonymous (2001) Biopesticide fact sheet, *Trichoderma harzianum* Rifai Strain T-22 (ATCC # 20847) (119202), Issued: August/2001, United Stated Environmental Protection Agency, EPA, http://www.epa.gov/pesticides/biopesticides/factsheets/fs119202e.htm
156. Anonymous (2000) Biopesticide Fact Sheet, *Trichoderma harzianum* Rifai Strain T-39 (119200), Issued May/2000, United Stated Environmental Protection Agency, EPA, http://www.epa.gov/pesticides/biopesticides/factsheets/fs119200e.htm
157. Jin X, Taylor AG, Harman GE (1996) Biol Control 7:267
158. Campbell WAA (1947) Mycologia 39:190
159. de Vrije T, Antoine N, Buitelaar RM, Bruckner S, Dissevelt M, Durand A, Gerlagh M, Jones EE, Luth P, Oostra J, Ravensberg WJ, Renaud R, Rinzema A, Weber FJ, Whipps JM (2001) Appl Microbiol Biotechnol 56:58
160. Ooijkaas LP, Buitelaar RM, Tramper J, Rinzema A (2000) Biotechnol Bioeng 69:292
161. Ooijkaas LP, Wilkinson EC, Tramper J, Buitelaar RM (1999) Biotechnol Bioeng 64:92
162. Oostra J, Tramper J, Rinzema A (2000) Enzyme Microbiol Technol 27:652
163. Anonymous (2001) Biopesticide Fact Sheet, *Coniothyrium minitans* CON/M/91–08 (028836), Issued: July/2001, United Stated Environmental Protection Agency, EPA, http://www.epa.gov/pesticides/biopesticides/factsheets/fs028836e.htm
164. Machida K, Trifonov LS, Ayer WA, Lu Z-X, Laroche A, Huang HC, Cheng KJ, Zantige JL (2001) Phytochemistry 58:173
165. Shapiro-Ilan DI, Gaugler R (2002) J Ind Microbiol Biotechnol 28:137
166. Wilson JA, Pearce JD, Shamlou PA (2001) Biotechnol Bioeng 75:733
167. Ackermann JU, Babel W (1998) Polym Degrad Stab 59:183
168. Ryu HW, Cho KS, Kim BS, Chang YK, Chang HN, Shim HJ (1999) J Microbiol Biotechnol 9:751
169. Shen Z, Yin J, Li H (1997) Huagong Shikan 11:40
170. Gutierrez NA, Maddox IS, Schuster KC, Swoboda H, Gapes JR (1998) Biores Technol 66:263
171. Qureshi N, Blaschek HP (1999) Biotechnol Prog 15:594
172. Danner H, Braun R (1999) Chem Soc Rev 28:395
173. Ravinder T, Swamy MV, Seenayya G, Reddy G (2001) Biores Technol 80:171
174. Syu M-J (2001) Appl Microbiol Biotechnol 55:10
175. Taherzadeh MJ, Adler L, Liden G (2002) Enzyme Microb Technol 31:53
176. Wang Z-X, Zhuge J, Fang H, Prior BA (2001) Biotechnol Adv 19:201
177. Li Y, Chen J, Lun S-Y (2001) Appl Microbiol Biotechnol 57:451
178. Willke Th, Vorlop K-D (2001) Appl Microbiol Biotechnol 56:289
179. Klass DL (1998) Biomass for renewable energy, fuels and chemicals. Academic Press, San Diego
180. Huang H, Gong CS, Tsao GT (2002) Appl Biochem Biotechnol 98–100:687
181. Danner H, Urmos M, Gartner M, Braun R (1998) Appl Biochem Biotechnol 70–72:887
182. Keller K, Friedmann T, Boxman A (2001) Trends Biotechnol 19:438

183. Schugerl K (2000) Biotechnol Adv 18:581
184. Nakamura Y, Sawada T, Inoue E (2001) J Chem Technol Biotechnol 76:879
185. Malinowski JJ (2001) Biotechnol Adv 19:525
186. Gu T (2000) Liquid–liquid partitioning methods for bioseparations. In: Ahuja S (ed) Handbook of bioseparations. San Diego, Academic Press, p 329
187. Bailly M, Balmanna HR, Aimar P, Lutin F, Cheryan M (2001) J Membr Sci 191:129
188. Karumanchi RSMS, Doddamane SN, Sampangi C, Todd PW (2002) Trends Biotechnol 20:72
189. Wang R–H (1999) Continuous production of a generic fermentation feedstock from whole wheat flour. PhD thesis, UMIST, UK
190. Anonymous (2000) World Grain 18(11):41
191. Landucci R, Goodman B, Wyman C (1994) Appl Biochem Biotechnol 45–46:677
192. Webb C, Wang R (1997) Development of a generic fermentation feedstock from whole wheat flour. In: Campbell GM, Webb C, McKee SL (eds) Cereals: novel uses and processes. Plenum press, New York, p 205
193. Webb C, Wang RH (1999) The development of a process for the production of a universal cereal-based fermentation medium, Proc 6th Symposium on Renewable Resources, Landwirtschaftsverlag, Munster, p 291
194. Wang R–H, Koutinas A, Webb C (2001) Cereals and sustainable chemicals production. Proc 6th World Congr Chemical Engineering, Melbourne, Australia, September 2001
195. Webb C, Wang R, Koutinas A (2001) Design and economic evaluation of a process producing a generic fermentation feedstock. Proc 3rd Int Congr Materials from Renewable Natural Resources, Erfurt, Germany, September 2001, paper 312
196. Koutinas AA, Wang R, Webb C (2002) Evaluation of wheat as generic fermentation feedstock for chemical production. 3rd Int Congr and Trade Show Green-Tech 2002 with 5th European Symposium Industrial Crops and Products, Floriade (Amsterdam), The Netherlands, 24–26 April 2002
197. Koutinas AA (2002) Evaluation of a process to produce a generic fermentation feedstock from wheat, PhD thesis, UMIST, UK
198. Anonymous (2001) IENICA: Summary report for European Union: carbohydrate crops, http://www.csl.gov.uk/ienica/national_reports/BIG%20CARBS.pdf
199. Anonymous (2002) OECD Agricultural Outlook: 2002/2007–2002 edn, Organisation for Economic Co-operation and Development (OECD), http://www.oecd.org/xls/M00031000/M00031936.xls
200. Isaac S, Gokhale AV (1982) Trans Br Mycol Soc 78:389
201. Mitchell R, Sabar N (1966) J Gen Microbiol 42:39
202. Wang R, Webb C (1998) Autolysis of *Aspergillus awamori*: An approach to nutrient regeneration. IchemE Research Event, Newcastle, 7–8 April
203. Leonard K (1995) Glycerol production from a whole wheat flour broth, MSc dissertation, UMIST, UK
204. Dominguez-Espinoza RM, Webb C (1998) Production of monascus pigments through bioconversion of wheat flour. Proc ADEBIO Symp on *Monascus* Culture and Applications, Toulouse, 8–10 July
205. Domingez-Espinoza R (2000) Submerged culture production of *Monascus* pigments from cereal raw materials. PhD thesis, UMIST, UK
206. Wang R, Dominguez-Espinoza RM, Leonard K, Koutinas A, Webb C (2002) Biotechnol Progr 18:1033
207. Onishi H (1963) Adv Food Res 12:53
208. Blanch HW, Clark DS (1997) (eds) Biochemical engineering. Marcel Dekker, New York, p 643
209. Perry RH, Green DW, Maloney JO (1984) (eds) Perry's Chemical Engineers' Handbook. McGraw–Hill, New York
210. Ulrich GD (1984) (ed) A guide to chemical engineering process design and economics. Wiley, New York, p 286

211. Garrett DE (1989) (ed) Chemical engineering economics. Van Nostrand Reinhold, New York, p 256
212. Peters MS, Timmerhaus KD (1991) (eds) Plant design and economics for chemical engineers. McGraw–Hill, New York
213. Maiorella BL, Blanch HW, Wilke CR (1984) Biotechnol Bioeng 26:1003
214. Coulson JM, Richardson JF, Sinnott RK (1999) (eds) Chemical engineering – design, vol 6. Butterworth and Heinemann, Oxford, p 242
215. Reisman HB (1988) (ed) Economic analysis of fermentation processes. CRC Press

Received: August 2003

Adv Biochem Engin/Biotechnol (2004) 87: 269–305
DOI 10.1007/b13533

Whole-Cell-Based Biosensors for Environmental Biomonitoring and Application

Man Bock Gu · Robert J. Mitchell · Byoung Chan Kim

National Research Laboratory on Environmental Biotechnology, Kwangju Institute of Science and Technology (K-JIST), 1 Oryong-dong, Puk-gu, 500-712 Gwangju, Republic of Korea
E-mail: mbgu@kjist.ac.kr

Abstract A variety of whole-cell-based biosensors has been developed using numerous native and recombinant biosensing cells. The use of reporter genes, for example bacterial luciferase and *gfp*, to monitor gene expression is discussed in terms of each reporters' benefits and disadvantages, including their possible use on-line, their sensitivity, the need for extra substrate, etc. All biosensing cells in use can be classified into two groups in terms of their biosensing mechanisms – constitutive expression and stress- or chemical-specific inducible expression. In this review several examples of each are presented and discussed. The use of recombinant whole-cell biosensors in the field requires three components – biosensing cells, a measurement device, and a signal-transducing apparatus, the last two depending on the first and the final applications of the system. The use of different immobilization techniques in several studies to maintain the cells and their viability is also discussed, in particular their use in the development of both high-throughput and chip-based biosensing systems. Finally the application of whole-cell-based biosensors to different environmental media, such as water, soil, and atmospheric monitoring is discussed; particular attention is given to their use for detection of various stressors, including dioxins, endocrine-disrupting chemicals, and ionizing radiation.

Keywords Whole-cell biosensor · Bioluminescence · Fluorescence · In-situ biomonitoring · Stress-specific · Chemical-specific

Abbreviations

BBIC	Bioluminescent-bioreporter integrated circuit
BEWS	Biological early warning system
BTEX	Benzene, toluene, ethylbenzene, or xylene
CERCLA	Comprehensive environmental response, compensation, and liability act
EDCs	Endocrine-disrupting chemicals
ELISA	Enzyme-linked immunosorbent assay
GECBB	Genetically engineered cell-based biosensor
GEMs	Genetically engineered microorganisms
GFP	Green fluorescent protein
IC	Integrated circuit
MDS	Minimum detectable signal
MEMS	Micro electromechanical systems
MUG	Methylumbelliferyl-β-D-galactopyranoside
NEMS	Nano electromechanical systems
ONPG	*o*-Nitrophenol β-D-galactopyranoside
PAH	Polycyclic aromatic hydrocarbon
TCDD	2,3,7,8-Tetrachlorodibenzo-*p*-dioxin

1 Introduction

Human activities have, without a doubt, had a negative impact on the environment both near and far, resulting in the contamination of water, the atmosphere, and soil both with naturally occurring toxicants, for example heavy metals, and with recalcitrant xenobiotics. In general, two methods – physicochemical and

biological – are available for measuring and quantifying the extent of pollution. Physicochemical methods involve the use of analytical equipment, for example GC–MS or HPLC, and provide important information about the chemical nature of the sample being tested. The major limitations of analytical methods include their cost and the lack of hazard and toxicological information; this necessitates the use of bioassays alongside traditional physical and chemical methods [1]. They are also very expensive, because of the complexity of the samples and the expertise of the operators needed to conduct the analysis. On the other hand, even with information obtained by use of analytical methods, the effects of such an environment on an organism or ecosystem might not be reliably inferred.

For these reasons, the use of environmental biosensors has found a place in monitoring for evaluation of a sample and its ecological toxicity. However, because of costs, time constraints, and public outcry, the use of whole organisms has been limited. In addition, because of health concerns, much emphasis in environmental monitoring has been given to water and water systems. Therefore, to study water-borne toxicity the use of aquatic organisms offers the most compatibility and possibly eventual on-line application in natural waterways. To this end, numerous aquatic organisms have been tested; of these several have been found to be useful and sensitive to the presence of deleterious compounds, including algae [2–5], *Daphnia* [4, 5], and various fish, including Japanese medaka [6–8] and rainbow trout.

The water flea, i.e. *Daphnia Spp.*, is a small (0.2–6 mm) aquatic crustacean, one of the orders of the *Branchiopoda*. Because of their rapid maturity, only a few days, ease of handling and culture, and sensitivity, daphnia have been used in numerous studies that determine the toxicity of a water sample on the basis of their behavior, reproduction, or mortality [4, 5]. Although the daphnia assay provides vital information about the toxicity of a water sample, it offers no information on the mode of toxicity, that is, where and how the contaminant is causing damage within the organism; it also requires a long detection time, has a relatively low sensitivity, and is poorly reproducible, in common with most whole-organism-based technologies in which the behavior and the mortality of the organism are the main variables observed.

Whole-cell biosensors utilizing microorganisms address and overcome many of the concerns raised with other conventional methods, because they are usually cheap and easy to maintain while offering a sensitive response to the toxicity of a sample. Also, public concern over the use of bacteria, yeast, and other single-cell systems in research has rarely been voiced. These aspects of whole-cell-based biosensors have led to the development of numerous strains and cell-lines capable of detecting and reporting on chemicals and stresses as diverse as organic compounds, xenobiotics, metals, radiation, changes in pH and even sugars. Also, because of their simple nature, the use of whole-cell-based biosensors has expanded to the monitoring of soil, water, and atmospheric conditions.

Generally speaking, "biosensor" is a general term that refers to any system that detects the presence of a substrate by use of a biological component which then provides a signal that can be quantified. Some examples of molecular-level biosensors are the ELISA test, which uses antibodies to a specific macromolecule, and enzyme-based techniques, including submerged dissolved-oxygen sensors.

However, this review will focus only on whole-cell-based biosensors and their applications.

2 Design and construction of biosensing cells

Before presenting an overview of the more commonly used reporter genes in whole-cell biosensors, it is necessary to explain their purpose within biosensors, and the purpose of the biosensors. The two main assay types commonly employed when using whole cells for biosensing utilize constitutive and inducible expression. These systems have different benefits and limitations in biosensing.

Constitutive expression typically uses a promoter that is highly expressed under normal conditions, leading to a high basal level expression of the reporter. Under harmful or toxic conditions this basal level is reduced and the reduction is measured and correlated as the toxicity of the sample. Therefore, constitutive systems offer a "large-picture" view of the metabolic state of individual cells or a culture and anything that reduces the growth rate or results in cytotoxicity will reduce the intensity of the reporter signals compared with those of the control (Fig. 1). Constitutive systems, however, give only a result for total toxicity and no information about the toxicity experienced by the cells. Inducible expression systems, on the other hand, pursue a low-level basal expression, that is increased in the presence of a certain compound or inducer, which includes stress responses.

In inducible systems, fusion of an inducible promoter, such as that responding to specific stresses or chemicals, to a reporter gene provides a means by which the expression levels of the gene native to the promoter can be measured. A higher expression level indicates the presence of the inducer, which might also indicate that the cells or culture are experiencing stressful conditions or responding to the presence of a chemical inducer. With the mapping and cloning of the genes responding to certain stresses it is possible to clone the promoter of these genes and fuse it with any number of reporters. Within cells bearing these fusions the presence of chemicals or conditions leading to increased promoter activity can

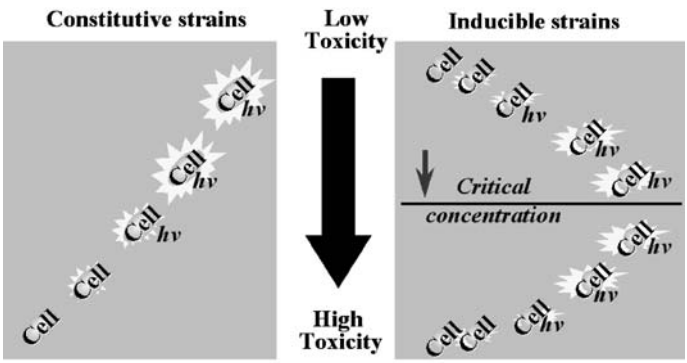

Fig. 1 Response characteristics for constitutive and inducible biosensors over a range of toxicity

be monitored as increased reporter production (Fig. 1). In addition, because of the specificity of the promoters, numerous combinations of promoters and reporters have been used for a wide variety of inducers. Traditional methods for finding an appropriate promoter were long and arduous; with the advent of computer-assisted DNA and protein microarray technology selection and evaluation of multiple candidates promises to be quicker and more fruitful in the future. Inducible systems offer the specificity lacking in constitutive systems but it is this very attribute that limits their performance, because in the absence of specific inducers no response is seen, even when other potentially harmful or serious compounds are present.

2.1 Reporters commonly used in whole-cell-based biosensing

2.1.1 *LacZ/β-galactosidase*

The gene for β-galactosidase, commonly referred to as *lacZ*, has been studied intensively and is the model of a typical repressor-inducer system within *Escherichia coli*. The protein encoded for, β-galactosidase (β-gal), forms a tetramer and is responsible for the cleavage of lactose into galactose and glucose; it is also slightly promiscuous, resulting in enzymatic cleavage of other substrates. One such substrate that has been used to monitor gene expression patterns is *o*-nitrophenol β-D-galactopyranoside (ONPG). β-Galactosidase levels within cells can be measured approximately by using the time it takes for a reaction mixture to change in color, from clear to yellow, as a result of cleavage of ONPG. Researchers have therefore used this simple colorimetric reaction to determine differences between expression levels from a given promoter under different conditions by fusing the promoter with the *lacZ* gene. However, because of the low sensitivity of this reaction, typically around 100 pg [9], other procedures using several other substrates have been developed [10]. Fluorimetric analysis of β-gal protein levels use the substrate methylumbelliferyl-β-D-galactopyranoside (MUG) [9, 11–13] whereas fluorescein-di-β-D-galactopyranoside has been used in laser-induced fluorescence detection [14]. Both of these analyses have led to greater sensitivity but further enhancement can be achieved by use of 1,2-dioxetane substrates and a luminescence-based assay, which lowers the detection limit of β-gal to 2 fg, from about 100 pg when using the colorimetric assay, and is about three times more sensitive than the fluorescence assay [15]. The limitations of this reporter are the lysis of the cells required, which preclude its application on-line, and the need for addition of expensive chemicals.

2.1.2 *Fluorescent proteins*

Fluorescent proteins absorb light within one wavelength range and emit it at an entirely different maximum. Within bio-applications the most popular and well-known fluorescent protein is green fluorescent protein (GFP). GFP is a

protein comprising 238 amino acids that has been isolated from coelenterates, for example the Pacific jellyfish, *Aequoria victoria* [16], in which its role is to transform the blue chemiluminescence of aequorin into green fluorescent light. The wild-type apo-protein has two absorbance/excitation peaks – a maximum at 395 nm and a minor peak at 475 nm – and an emission maximum at 508 nm. It has been also shown that GFP photoisomerizes when irradiated with UV light [17].

The cloning of GFP's cDNA and proof that GFP can be expressed within other organisms [18] has paved the way for researchers in a variety of disciplines to investigate cell, developmental, and molecular biology, with application of GFP spanning bacteria [18], yeast [19], slime mold [20], plants [21], *drosophila*, zebrafish [22], and mammalian cells [23]. Additionally, because of the availability of *E. coli* clones that express GFP, extensive mutational analyses of the GFP protein and the functions of individual amino acids have been conducted.

With the positive mutations listed in the literature the use of GFP as a bioreporter gene has become easier, because of increases in the thermotolerance and intensity and shifts within the fluorescence spectra. In addition, the almost universal application of GFP to highly different organisms and the fact that it requires no substrate for activity make it the reporter of choice in many experiments, especially for eukaryotic cells or organisms. However, GFP typically requires a long time for the fluorophore to form, after which more time is needed to evaluate differences between the expression levels of samples. This might restrict the use of GFP in on-line applications. Furthermore, use of GFP within constitutive systems is also limited, because the hardy character of the protein limits its denaturation by addition of chemicals. This might be a special problem in studies in which cell death might have occurred, because the GFP protein continues to fluoresce long after the cell has died.

2.1.3 *Prokaryotic luciferases*

The *lux* operons of bioluminescent bacteria consist of at least five required genes, *luxCDABE*. There are also two regulatory proteins, *luxR* and *luxI*, upstream of this operon that work via a quorum-sensing mechanism. The result is that within the native bioluminescent bacteria bioluminescence is induced when the culture achieves a certain cell density; below this, however, the operon is expressed at a low basal level. Two good reviews about quorum sensing and bioluminescence can be found elsewhere [24, 25].

2.1.3.1 Use of luxAB

Of the five genes within the *lux* operon, only *luxA* and *luxB* are required for bioluminescence, albeit with the addition of the substrate to the media. The LuxA and LuxB proteins form a dimer structure that catalyzes the formation of fatty acids from long-chain aldehydes. During this reaction a reduced flavin mono-

nucleotide ($FMNH_2$) is oxidized to FMN – an unstable high-energy oxide bond is formed and with its breakdown a photon of blue light (maximum $\lambda \approx 485$–490 nm) is emitted. The light produced by the culture can be measured and correlated with the amount of *luxAB* transcription. One study stated that the use of these two genes, as opposed to the entire *luxCDABE* operon, produced more significant bioluminescence [26], possibly because of the lower substrate level with the *luxCDE* genes, especially at lower expression levels, whereas addition of fatty aldehydes results in an obvious over abundance of the substrate. In addition, in their natural hosts, tetradecanal seems to be the substrate of choice but shorter-chain aldehydes, such as decanal, which is typically added to the cultures when using only the LuxA and B sub-units, have been found to give a greater bioluminescence intensity [27, 28]. However, aldehydes of lengths from 7-C to 16-C can effectively be used in the reaction [29]. Furthermore, to facilitate the sub-cloning of the *luxA* and *luxB* genes and the development of biosensors, these two genes were linked, providing a single protein that has the activity of the two separate subunits [30–34]. Because this protein incorporated both luciferase units within one gene, it made the use of bacterial luciferase within eukaryotic hosts a reality [33, 34], because eukaryotic organisms do not use an operon organization within their genomes. However, many of these fusions are heat-labile and are non-functional at temperatures above 30 °C, making their use impractical, especially in mammalian cells [27]. It was also necessary to add decanal to the media, which was recently found to be highly toxic to yeast and *Caenorhabditis elegans* [35], and therefore limits the effectiveness of using bacterial *luxAB* within eukaryotes. However, the same publication clearly stated that bacteria, in particular *E. coli*, are relatively unaffected by decanal addition. Numerous bacterial biosensing cells have been constructed using both the individual and fused genes and a variety of promoters, and some of these will be covered later. However, the required addition of decanal makes the use of biosensing cells using only these two *lux* genes impractical for on-line field applications.

2.1.3.2 Use of luxCDABE

Although the use of the LuxAB proteins may provide a greater bioluminescence, employing the entire operon within bacterial hosts greatly simplifies the measurement process. The LuxC, D, and E proteins are responsible for diverting fatty acyl chains from membrane formation into the luciferase reaction [36, 37]. These three proteins catalyze the production of fatty aldehydes from the fatty acyl groups and these aldehydes are then transferred to the LuxAB units where they are oxidized in the presence of $FMNH_2$ and molecular oxygen to their corresponding fatty acids. The fatty acids can then be reconverted to their aldehyde form through the reactions catalyzed by LuxE and LuxC. The obvious benefit of using the entire operon lies in the fact that aldehyde needs not be added. This simplifies the reaction and enables cells using the entire *luxCDABE* operon to be used on-line and, possibly, in-situ, because the bioluminescence reaction would enable fully automated monitoring requiring limited operator interaction. This is discussed more in depth in the later sections.

2.1.4 *Eukaryotic luciferases*

Because of the complexity of using a whole organism and in the hope of developing a variety of biosensing cells, eukaryotic luciferases were cloned using the cDNA of the organisms and have been adopted for use within bacteria, yeast, and mammalian cells. As with bacterial bioluminescence, eukaryotic luciferases were found to use the production of an unstable intermediate that, when it degrades, leads to the production of a photon of light [38]. Unlike their bacterial counterparts the luciferase protein is a monomer that does not require $FMNH_2$ and the substrates are much more complex.

Firefly luciferase (61 kDa) is one of the most commonly used of the bioluminescent reporters [39, 40]. The popularity of firefly luciferase as a genetic reporter is due both to the sensitivity and convenience of the enzyme assay, and to the tight coupling of protein synthesis with enzyme activity; there is, in addition, no need for any post-translational modifications [39], thereby providing a nearly instantaneous measure of the total reporter concentration in the cell. It catalyzes a two-step oxidation reaction to yield light generally in the green to yellow region of ~550–570 nm [41]. After mixing the substrates with the cell lysate, an initial burst of light is produced by the firefly luciferase that decays for about 15 s to a lower sustained luminescence and is thought to be due to the slow release of the enzymatic product, which limits the catalytic turnover after the initial reaction.

Different procedures have been evaluated in the hope of generating a stable luminescence signal to make the use of firefly luciferase more convenient for routine laboratory use. The incorporation of coenzyme A to yield a luminescence intensity that slowly decays over several minutes was the most successful [42, 43].

Renilla luciferase is a 31 kDa monomeric enzyme that catalyzes the oxidation of coelenterazine to yield a blue light of 480 nm and its gene has been sub-cloned via cDNA and is referred to as *Rluc* [44]. *Renilla reniformis*, the host organism, is a coelenterate that creates bright green flashes by association of the luciferase with a green fluorescent protein. Although *Renilla* luciferase has many of the same benefits as firefly luciferase, it has no particular advantages over the use of firefly luciferase. Along with a somewhat more limited assay chemistry there is a primary limitation – the presence of a low-level non-enzymatic luminescence. Although *Renilla* luciferase is not generally preferred over firefly luciferase, it has recently gained popularity in situations where two reporters are needed. Tests have shown that both of these reporters are detectable at subattomole concentrations and that they provide linear responses, correlated with their respective concentrations, over five (*Renilla*) and seven (firefly) orders of magnitude. The main drawback of using these reporters is their need for substrate addition and cell lysis, which contribute significantly to the cost and complexity, and therefore human error, of the assay. In addition, the requirement of substrate addition makes practical on-line field applications of these biosensing cells very difficult.

2.2 Biosensing mechanisms

2.2.1 *Constitutive systems*

As stated earlier, the benefit of constitutive systems stems from their lack of specificity. Constitutive systems seek to determine the apparent toxicity of a sample by monitoring reduced reporter expression or level after a certain time of exposure. The most famous constitutive system is the Microtox kit [45, 46], which uses the bacterium *V. fischeri*. In this kit, the bacteria are freeze-dried and a sample is added to reconstitute them whereas a pure water sample is added to the control. The simplicity and convenience of the test has led to its successful application in numerous studies, including some on metal complexation [47] and evaluation of site or sample detoxification [48, 49]. One limitation in the Microtox system is, however, the required use of salt water, because *V. fischeri* is a marine bacterium; this might affect the sensitivity or results. The result is that the reproducibility for multiple samples is low, resulting in a fairly large error. However, behind these constitutive systems lies one important aspect, the correlation of the signal with the metabolic state of the organism. Irrespective of the reporter, a lower concentration or activity should correlate with a lower metabolic activity, or even the death of the organism.

To overcome this the genes required for bioluminescence were cloned from several bioluminescent bacteria and transferred to other more applicable bacterial species, in particular, *E. coli*, on plasmids [50–53]. One example is the use of a fusion in the construction of a thermostable *luxCDABE* constitutive strain. This *lux* operon then had many of its internal restriction sites removed to facilitate transfer of the *lux* operon to other fusions [51, 52]. In addition, another common fusion is that with the *lacZ* promoter, because of its high level of transcription and its widespread use in plasmids. Constitutive systems, however, are not limited to the use of *luxCDABE* nor are they limited to a reduced reporter activity. Lampinen et al. [54] used the induction of the strong lambda P_L promoter, by shifting growing cultures to 42 °C for a short time to denature the cI857(ts) repressor, to study the effects of various chemicals on protein production. Using fusions of the P_L promoter with the *luxAB* genes from both *V. harveyi* and *Photorhabdus luminescens* and the *lucGR* gene from the click beetle *Pyrophorus plagiophthalamus*, they showed that addition of chemicals such as phenol, chloramphenicol, and mercuric chloride shortly before induction of the phage promoter had an adverse effect on the amount of protein produced, rather than reducing the activity of reporter proteins present before toxicant addition.

Constitutive systems also are not limited to bacteria. One recent publication used a mammalian cell line constructed using the plasmid pEGFP-N2 from Clontech, where the GFP gene is under the transcriptional control of the CMV promoter [55, 56]. By use of this cell line the toxicity of numerous chemicals to mammalian cells were characterized. To use the *GFPuv* gene as a reporter they employed a longer exposure time, because under harmful or toxic conditions the

consequence would be a lower growth rate and metabolism, which would result in lower a fluorescence value.

Other eukaryotic constitutive systems have been developed on the basis of the same principles. Hollis et al. [57] reported the construction of a *S. cerevisiae* that used the firefly luciferase as a reporter. Firefly luciferase requires the presence of ATP to produce bioluminescence, a fact that limits the production of bioluminescence to living cells. Consequently, they used a constitutive promoter to control luciferase production and measured the firefly luciferase activity after addition of the test chemicals. As was expected, greater toxicity, according to the concentration of the compound being tested, resulted in lower bioluminescence, because of a larger amount of damage and cell death.

The main drawback of constitutive systems, however, is their lack of specificity. Although they provide important information about the overall toxicity of a sample, they cannot offer information on how and where within the organism the chemicals have an effect. The use of stress- or chemical-specific inducible system might be able to provide additional specificity information.

2.2.2 *Inducible systems*

The inducible systems, with published studies, can be separated into two groups – stress-specific and chemical-specific (Fig. 2). For stress responses, such as when the cells experience oxidative or DNA damage, the number of genes that are induced varies between the stresses, whereas highly specific recognition systems exist for classes of chemicals, such as in BTEX monitoring, and even for one or two very specific antagonists, for example metal ions.

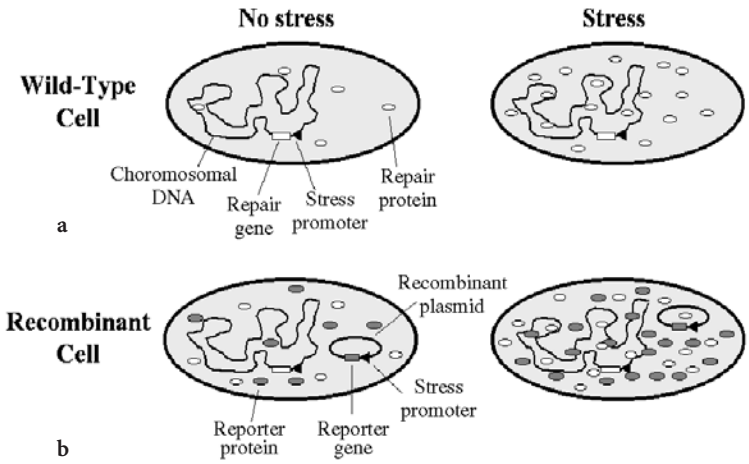

Fig. 2 Schematic representation of (**a**) wild-type and (**b**) recombinant inducible cells under ambient and toxic conditions

2.2.2.1 Stress-specific inducible systems

Within every organism exist several response regulons that are induced under stressful conditions in the hope of repairing the damage done by stress and reducing further damage to the organism. Table 1 lists some of the more common stress-response regulons of bacteria and some of the genes they control. In each of these regulons the presence of some inducer, for example the hydroxyl or superoxide radical or ssDNA, which is indicative of cellular damage or the possibility thereof, is required before the regulon is induced. Presented below are the cellular mechanisms involved in the induction of two *E. coli* stress regulons. These two regulons are just examples of the known regulons within bacteria. Using the genes listed above and numerous others (Table 1) a wide variety of stress-inducible systems has been developed using the different reporter genes. The benefit of these stress-inducible systems is that they provide a measurable response to specific stresses. Previous researchers interested in measuring the carcinogenic nature of a compound relied on the Ames test. With advances in molecular genetics, biosensing cells are more sensitive, faster, and capable of classifying a compound on the basis of the manner in which DNA is damaged and they are not limited in the chemical make-up of the sample, as was the Ames test. Also, with the use of reporter genes, application in-situ is a possibility, something that was impossible for the Ames test. It is, therefore, possible to classify chemical compounds on the basis of the stress induced and to evaluate the relative toxicity of similar compounds. One study recently reported the use of several of these stress-responsive biosensors to develop a type of "toxicity fingerprint" to reliably identify the chemical present and its concentration [62, 93].

One of the most thoroughly studied stress regulons for bacteria is the SOS regulon. The basic precepts of this regulon are activation of the RecA protein by recognition of single stranded DNA resulting from damage to the chromosome, and subsequent aid in the auto-cleavage of the LexA repressor protein (Fig. 3). With the cleavage of LexA, the promoters that it was bound to and repressing are then expressed, and each downstream gene product participates in the repair of the damaged DNA. One of these genes is the *lexA* gene and thus, as time

Table 1 Some stress responses and the genes involved

Stress	Gene	Refs.
Heat shock	*rpoH*, *grpE*, *lon*	[58–62, 93]
Cold shock	*cspA*	[63, 64]
Oxidative damage – hydroxyl	*katG*, *oxyR*	[61, 62, 65–67, 93]
Oxidative damage – superoxide	*sodA*, *soxRS*	[67–70, 94]
DNA damage	*recA*, *lexA*, *umuDC*	[62, 71–79, 93]
DNA alkylation	*ada*, *alkA*	[76, 80]
Membrane synthesis/damage	*fadR*, *fabA*, *micF*	[61, 62, 81–86, 93]
Osmotic stress	*rpoS*, *osmY*, *micF*	[61, 86–89]
Growth inhibition	*uspA*	[61, 90–92]

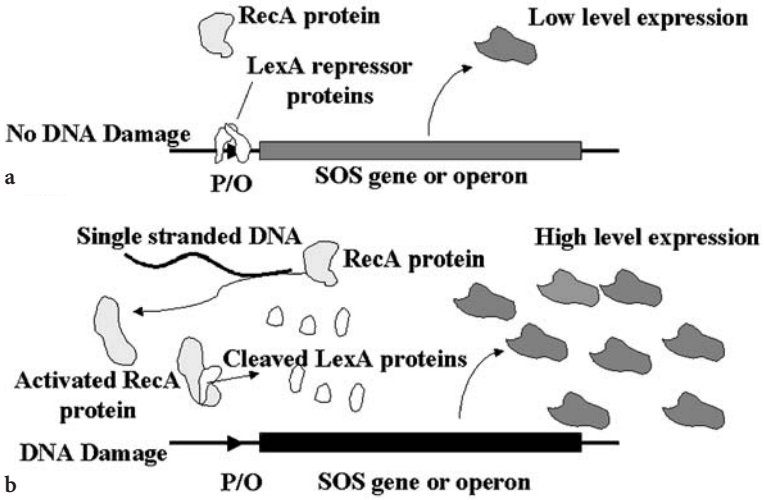

Fig. 3 Induction of the SOS response regulon genes. (**a**) Non-genotoxic conditions. (**b**) Genotoxic conditions leading to high-level expression of the SOS genes

progresses, the number of repressor proteins will increase and expression of the SOS genes will be blocked once again.

Damage to DNA has been found to occur by two possible means – directly or indirectly. Direct damage involves covalent binding to DNA by a chemical, as when mitomycin C, a powerful mutagen used in cancer treatment, is present, or by breaking the DNA strand, as when an organism is exposed to gamma rays. Indirect damage occurs by production of reactive species which then alter the structure of the base nucleotides. An example of this is the damage induced by addition of hydrogen peroxide. One study on this clearly showed, by use of a *recA*::*luxCDABE* fusion bacterial strain, that the responses of the SOS regulon differ for these two cases and that mutagens can be classified as direct or indirect on the basis of the expression kinetics of the *recA* gene [75].

In living systems, heat shock is a general term for any condition that leads to significant protein damage or unfolding; the name originates from the fact that higher temperatures lead to protein denaturation. Under such conditions, a variety of genes is induced. In bacteria, more particularly *E. coli*, this induction is facilitated by the $\sigma 32$ transcriptional factor, which recognizes a consensus sequence in the –10 region of the heat-shock promoters, binds it, and then aids in the binding of RNA-polymerase to the promoter. This leads to a greater transcriptional level of the genes downstream of these promoters. The proteins these genes encode for can be categorized into three groups – chaperone proteins, proteases, and effectors – and 17 different genes have been identified in *E. coli*. The chaperone proteins, such as GrpE, DnaJ and DnaK, recognize denatured proteins and aid their refolding. Proteases, such as the Lon protease, degrade the denatured and foreign proteins by cleaving them into smaller pieces, which are then further broken down and the amino acids recycled into the cellular metabolite processes. The effectors are responsible for activating the heat shock response.

All these proteins, chaperones, proteases, and effectors, have also been classified into five groups on the basis of their molecular weights. The σ32 regulon includes two chaperone teams, the DnaK-DnaJ-GrpE and the GroEL-GroES teams. Because these genes are induced when exposed to high temperatures, the over-expression of the GroEL and GroES proteins enables *E. coli* to grow at temperatures up to 40 °C whereas over-expression of both teams is needed for growth at 42 °C [58–62].

Recent work by the Alon lab has also shed some light on the broad transcriptional effects of regulon induction. Their work focused on the development of network motifs in the transcriptional regulation of *E. coli* [95–97]. They found that three general motifs are employed – the feedforward, single-input module (SIM) and dense overlapping regulons. The feedforward motif is defined as having a transcriptional factor that regulates a second factor, and these two jointly regulate a third gene or operon. An example of this type of motif is the arabinose utilization system. The SIM motif is defined as a set of operons controlled by a single regulator, either an inducer or repressor. An example of an SIM is the arginine regulon. The last motif, the dense overlapping regulons, is characterized by the presence of numerous transcriptional regulators for a given gene or operon. Their work found that the presence of such motifs in *E. coli* was much more common than would be expected within a randomized network. Furthermore, using different fusion with the GFP gene they were not only able to order the expression of various genes expressed in a given function, such as the formation of flagella [98], but were able to calculate the kinetic parameters for each of the genes and evaluate their transcriptional control based upon the model, as for the SOS regulon [97]. Such work will enable researchers to investigate the controls regulating the expression of a new gene or operon simply by comparing the responses given with those of known genes, while providing a fail-safe evaluation by also indicating the presence of possible other regulatory factors affecting the expression.

2.2.2.2 Chemical-specific inducible systems

Another class of inducible systems includes those that can sensitively detect a single compound or group of compounds. These differ from the stress-specific inducible systems in that they do not measure the toxicity or stress induced, but rather the presence of specific compounds, or inducers, both toxic and non-toxic (Fig. 4). The literature reports the construction of a variety of biosensing cells capable of recognizing chemically very diverse compounds, ranging from metals to sugars and from alkanes to aromatic hydrocarbons. Table 2 lists a few examples of bacterial genes induced in the presence of specific chemicals and, in particular, metal ions and xenobiotics. Much attention has been devoted to these chemicals, because of their characteristics, such as their tendency to bioaccumulate or their recalcitrant nature. Natural genetic and protein mechanisms to counteract or degrade them have therefore been studied in depth.

Recalcitrant organic compounds are generally human in origin and are degraded in natural biosystems at a very low rate. Some examples are polycyclic hydrocarbons (PAHs), dioxins, and various phenolic compounds and benzene

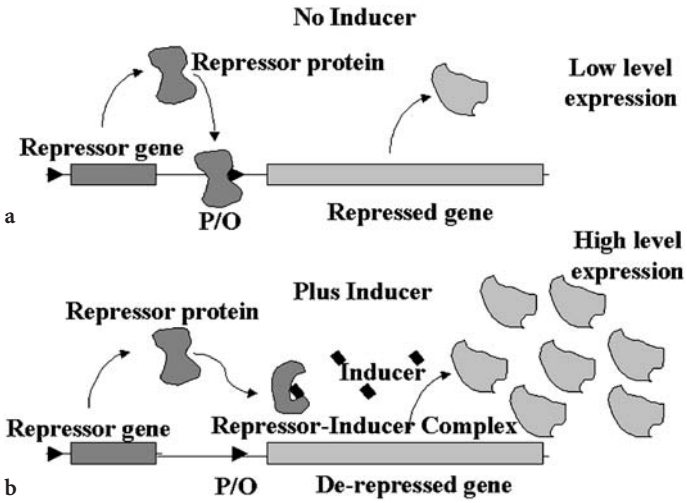

Fig. 4 Mechanism for the de-repression of a chemical-specific promoter in the presence of an inducer. (**a**) Repressed promoter system. (**b**) De-repressed promoter and high-level expression of the response genes

Table 2 Bacterial genes involved in chemical-specific resistance and sensing

Chemical(s) detected	Gene(s)	Refs.
Organics		
Alkanes	*alkB*	[99]
BTEX compounds	*xylR*, *todR*, *ipbR*	[100–106]
Phenolic compounds	*dmpR*, *mopR*, *tfdRP*(*DII*)	[107–110]
Naphthalene/salicylate	*nahR*, *nagR*	[111–118]
Chlorobenzoates	*fcbA*	[119]
Tetracyclines	*tetA*	[120–124]
Acyl homoserine-lactones	*luxR*	[125–126]
Nitrate	*narL-narG*	[127]
Metals		
Arsenic/antimonite	*arsR*	[128–134, 154]
Cadmium	*cadD*, *czcCBAD*, *smtA*, *zntA*	[132, 135–142]
Chromate	*chrA*	[143]
Cobalt/nickel	*cnr*, *czcCBAD*	[135, 136, 144, 145]
Copper	*copA*, *cueR*, *cusR*, *smtA*	[141, 146–149]
Lead	*zntA*	[134, 141]
Mercury	*merR*, *zntA*	[141, 150–153]
Zinc	*czcCBAD*, *smtA*, *zntA*	[134–136, 139, 141]

derivatives. Because of their persistence and potential bioaccumulation, many of these compounds can be found on the US EPA's priority chemical list, and some are within the Comprehensive Environmental Response, Compensation, and Liability Act (CERCLA) Priority List of Hazardous Substances top ten listing. It is natural, therefore, that their detection is interest to researchers and, as a result, numerous biosensing cells have been constructed for many of these chemicals or their classes. Many of these cells utilize a protein which specifically recognizes one or a group of these chemicals; one example of these is the NahR protein.

The NahR protein is the transcriptional activator of the *nahG* promoter of a variety of *Pseudomonas* strains and recognizes derivatives of salicylic acid. The degradation of naphthalene by these strains leads to the formation of salicylic acid as one of the central metabolites, which then, along with the NahR protein, actively induces the production of the genes needed for degradation via feedback loop regulation. Two pathways are necessary for complete conversion of naphthalene to pyruvic and acetic acid, the upper consisting of *nahABCDEF* and the lower of *nahGHIJ* [155]. The genes from the upper pathway are responsible for the degradation of naphthalene to salicylic acid whereas those of the lower pathway are necessary for its further degradation to tricarboxylic acid derivatives. Several other cells have been developed for sensing both naphthalene and salicylic derivatives using this protein and the promoters, P_{nah} and P_{sal}, that it recognizes [114–116]. In one study, a luminescent *Pseudomonas fluorescens*, strain HK44, was developed that was able to detect the presence of salicylic acid, and naphthalene, albeit through its degradation [156–158]. Using this strain, the researchers demonstrated its ability to respond with increased bioluminescence whenever salicylic acid or naphthalene was present in the sample [156].

Another class of organic toxicants that has received much attention from researchers is the BTEX group – benzene, toluene, ethylbenzene, and xylene. *Pseudomonas putida* strain mt-2 harbors a plasmid, pTOL, for degradation of toluene and the transcriptional activator for the degradative genes is the XylR protein, which recognizes toluene, or a similar compound, and then increases the promoter's activity by binding the region just upstream. Using a fusion of the P_u promoter, i.e. the promoter activated by the XylR protein, with the firefly luciferase gene within *E. coli*, one research group was able to sensitively detect toluene-like compounds and to assess their concentration within a deep aquifer that was contaminated [159]. Another group used the construction of a chromosomally integrated *todR*::*luxCDABE P. putida*, strain TVA8, to detect BTEX compounds [100]. As with XylR, the TodR protein recognizes BTEX chemicals and activates the promoter controlling the genes required for their degradation and, therefore, this strain responds to the presence of BTEX compounds by production of bioluminescence. Use of these cells to measure the water-soluble components of JP-4 jet fuel demonstrated its characteristic ability to detect these compounds in complex samples.

The priority list includes not only organic compounds but also some metal ions. In biological systems toxic metal ions are dealt with in one, or both, of two ways, namely detoxification of the ion and/or the transport of the ion out of the cell via an efflux pump. One example of metal detoxification is the *mer* operon,

which confers resistance to mercury (Hg(II)). When HgII passes through the outer membrane it is recognized by MerP protein in the periplasm. MerP then passes the ion to MerT, which transverses the inner membrane. The MerR protein is the repressor-transcriptional activator of the *mer* genes. Under ambient conditions the MerR protein binds the DNA in the region of the promoter and causes it to bend over on itself, thereby blocking transcription. When bound to an Hg(II) ion, however, the MerR protein changes its conformation and becomes a transcriptional activator. This character of the MerR protein has made use of its gene and the *merT* promoter prominent within metal toxicity biosensing cells. Fusions with reporter genes include *luxCDABE*, *GFP*, and *luc* [152, 154].

Metal efflux systems, on the other hand, utilize a protein channel that specifically recognizes some metals within the cytosol and pumps them out into the surrounding media. One such efflux system that has been studied extensively is that conferring arsenic resistance. Arsenic occurs in two oxidation states, +3 and +5. This metal is chemically related to phosphate, as is apparent from its oxidation states, and so interferes with normal metabolic pathways by mimicking phosphate. To deal with this bacteria have evolved a response operon, the *arsRDABC* operon. Arsenite (AsO_2^-) within the cytoplasm is transported out through an efflux pump, which consists of both ArsA, a membrane bound ATPase, and ArsB, the channel sub-units. This pump can drive the elimination of arsenite by ATP hydrolysis active transport or passive transport. However, arsenate (AsO_4^{2-}) cannot be transported through the channel. Therefore, the function of the ArsC protein is to reduce arsenate to the more toxic arsenite (AsO_2^-). An additional function of this pump is its ability to also remove antimonite (SbO_2^-), which is electrochemically equivalent to arsenite. Several biosensing cells have been developed with this response operon and are capable of recognizing arsenite and antimonite down to subattomole concentrations [133, 154].

The purpose of constructing these, and any, biosensing cells is to apply them to real fields as a key component in a whole-cell-based biosensor. Therefore, the next two sections will focus on different whole-cell-based biosensors that can be directly implemented in real fields.

3 Whole-cell-based biosensors

Whole-cell-based biosensors are measurement systems combining analytical devices and whole cells that produce biological signals as the recognition element [160, 161]. These record the metabolic activity of the cells in response to the samples to be analyzed [162]. Especially, bioluminescent and fluorescent cells, which produce signals proportional to the stimuli, can easily be combined with a measurement system using an appropriate immobilization method and/or the use of fiber optic probes, after which the signals can be transferred to the devices [162–165] (Fig. 5). The unique feature of using whole-cell biosensors is that functional information about the effect of a stimulus on a living system can be obtained and that a living component is used to obtain analytical information, such as the toxicity, quality, or load of water, soil, or gas samples. In addition, another feature is that the systems are easily automated and, because they involve

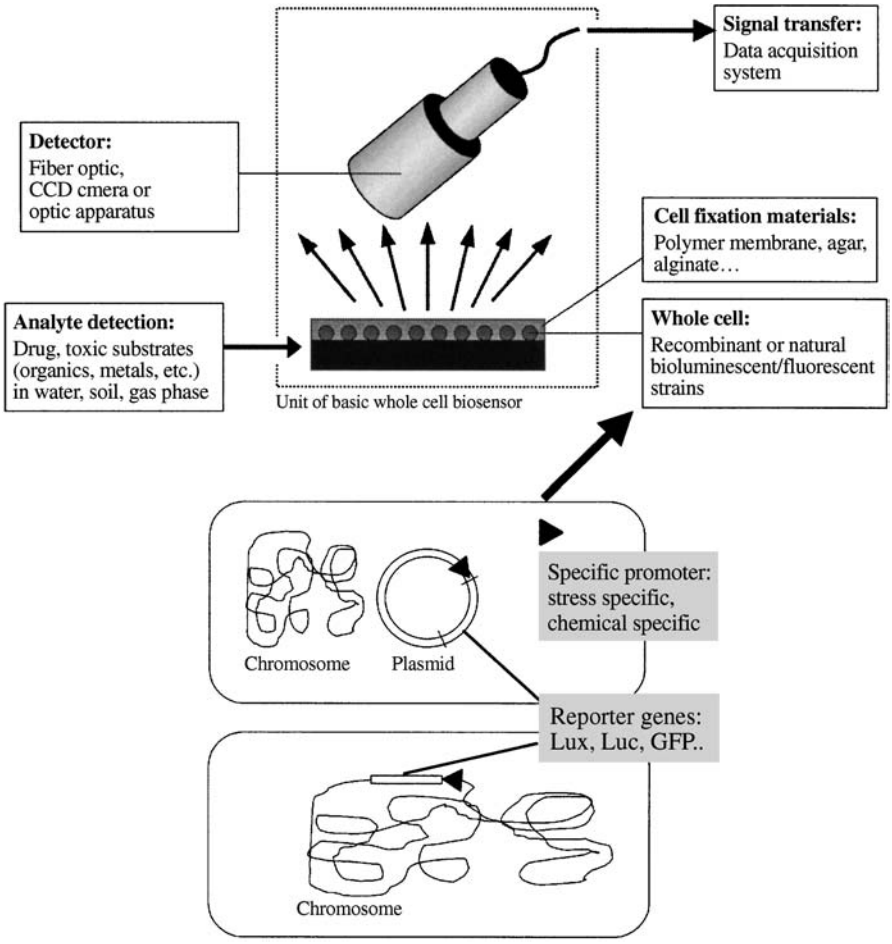

Fig. 5 Concept of a basic whole-cell biosensor

whole cells, they do not require extraction of enzymes or antibodies for the analysis [160, 162, 166, 167].

Because of their characteristics, whole-cell-based biosensors can respond to various ranges of changes in their environment or conditions and are suitable for use in eco-toxicity tests and environmental monitoring where the source and nature of toxicants and pollutants cannot be predicted [168] and, thus, most whole-cell-based biosensors have been implemented in the area of environmental toxicity monitoring [169–171].

This review, therefore, will focus on the types and applications of whole-cell-based biosensor systems in different environmental media, i.e. water, soil, and atmosphere, using natural or genetically engineered organisms.

3.1 Basic whole-cell biosensors

3.1.1 *Immobilized biosensors*

Many whole-cell biosensors applied to the toxicity screening of samples use bioluminescence or fluorescence as the reporter [172, 173]. Because bioluminescence or fluorescence signals can be transferred through fiber optic probes, they can be assessed with a luminometer or fluorimeter by use of immobilization methods. Therefore, by combining such biosensing cells with a fiber optic or other unit, many systems have been developed using whole cells [174, 175] and immobilization methods to affix the cells to the units. Such fiber-optic probe systems, generally referred to as basic whole-cell-based biosensor systems [163], can be applied to different environmental media, including studies on water, air, and soil quality, or for toxicity monitoring.

3.1.1.1 Water-quality biomonitoring

Numerous whole-cell-based biosensors have been applied to water quality monitoring [176–179]. Because the use of whole cells provides a rapid response to analytes in the environment, they are suitable for development of biological early warning systems, by-passing the need for whole organisms. Over the past couple of decades aquatic organisms, for example fish, daphnia, or fluorescent algae, have been used in biological water monitoring [161, 180–184]. Such monitoring focuses on the toxicity of the test samples and these organisms and whole-cell biosensors can both detect potential toxicity that instrumental and analytical techniques cannot. Also, biological detection provides information about unknown materials and evaluates the toxic action of mixtures in the aquatic environment [161]. In fact, Carins and Mount noted that only living material could be used to measure toxicity [185]. In terms of toxicity, therefore, whole-cell-based biosensors are key measurement systems for water environments.

For consistent monitoring of water quality using living organisms, a system should consist of three components: a test organism, an automated detection system, and an alarm system which enables the system to be implemented as a biological early warning system (BEWS) [161, 186]. These components are essential parameters for all biosensors, irrespective of whether they are for water, gas, or soil biosensing.

Biosensor systems should also be operated continuously, without system shut-down, and offer sensitivity appropriate for the monitoring needs. For this reason higher organisms, for example fish or daphnia, are limited in their application to continuous water monitoring [187]. The response time of systems using higher organisms is long and, if significant pollution were encountered, the indicator organisms would die. Such an incident would require complete system shut-down and re-establishment. Therefore, strictly speaking, true continuous monitoring is impossible with higher organisms and, therefore, microorganisms such as

green algae and bacteria which can be cultured and easily handled are the primary candidates for use in real-time monitoring.

Algae live in most surface waters that are exposed to sunlight and green algae, in particular, are a major component of the phytoplankton population [188]. Monitoring systems that use algae work by measuring changes in chlorophyll fluorescence after introduction of potentially toxic water samples. Algae, because of their phototrophic nature, are highly susceptible to herbicides, which inhibit their photosynthetic mechanisms. By use of this characteristic herbicide-biosensing systems have been developed using immobilized green algae [189–191]. An optical biosensor has also been developed to respond to herbicides present in aquatic samples using *Chlorella vulgaris*, a variety of alga [192, 193]. The algal cells were entrapped in the small pores of the membrane filter. Five of these membranes, which are easily removed, were located on a rotating disk and a fiber optic bundle was located above one of them. In a 10-mL home-made flow cell each of the membranes was in constant contact with the water sample and was under the fiber optic bundles for 1 min and then in the dark for 4 min, i.e. while one membrane was under the fiber optic bundle the other four membranes were in stand-by position in the dark until the disk was rotated again. By use of this arrangement the sensor was able to detect ppb levels of herbicides continuously, because the membrane-bound algal units were refreshed regularly. Another study showed that use of alginate to immobilize algae can be been applied to the in-situ biomonitoring of flowing waters and that it facilitated the site-specific assessment of eutrophication in running waters and the prediction of ecosystem response to an altered nutrient input [194]. It was also found that immobilization of the algae increased the rate of their response.

Polyak et al. [175] screened genotoxicants in water samples by use of genetically engineered cells connected to an optical fiber. The genetically modified *E. coli* strain, which emits bioluminescence in the presence of genotoxicants, was immobilized on to the exposed core of an optical fiber by use of an alginate matrix. The performance of this biosensor system was optimized with regard to gel-matrix volume, cell density, the numerical aperture of the fiber optic core, and the working temperature; under the optimized conditions this biosensor had a lower detection limit of 25 $\mu g\ L^{-1}$ mitomycin C.

Although many systems using algae or microorganisms have already been optimized and developed for toxicity monitoring, a truly continuous water-monitoring system that can handle a severely toxic sample has yet to be developed.

3.1.1.2 Atmospheric quality biomonitoring

Developments in the use of biosensors that exploit living organisms or biological materials have led to the expansion of their use to applications in the sensing and measurement of gas-based toxicity. Some examples include the use of immobilized enzymes and corresponding electrochemicals [195–197] or of whole cells [198–201]. They are generally highly sensitive with high selectivity, a rapid response, and can be used to detect many gases, ranging from CO_2 and O_2 to a variety of toxic vapors, for example benzene.

Many toxic materials occur in the form of gases or suspended particles. Because of the nature of gases they should be monitored continuously and a response should be provided within short time to ensure that human health and the surrounding atmosphere are being protected. For assessment of global atmospheric toxicity biosensors are more effective than physicochemical methods [195]. For applications in in-situ field studies, however, serious consideration should be given to the instrumentation and experimental set-up. Also, for affixing the biosensing cells to the instrumentation, an appropriate immobilization or pretreatment procedure is needed. Immobilization is an easy means of supporting biosensor devices, because the cells are entrapped by use of a matrix, such as agar, alginate, or a polymer. However, the most important aspects to consider when selecting an immobilizing material is that it be non-toxic and sufficiently permeable [52, 160].

One example of the use of immobilization is a study in which an algal biosensor was designed to determine the presence and toxicity of the vapor of solvents and organic compounds [198, 202]. The system was constructed from algae immobilized on a membrane associated with an oxygen electrode. This electrode measured the oxygen produced during the photosynthetic activity of the algae and the differences were used to measure the toxicity of methanol, which was used as a test volatile solvent. Inhibition of oxygen production by methanol vapor was the direct-determination property used in this study to determine toxicity.

Another gas-phase biosensor was developed using a cyanide-degrading bacteria, *P. fluorescens* NCIMB 11764. This system also used an oxygen electrode to measure the oxygen produced. The basic precept of the system was that the cyanide ion inhibits the production of oxygen, which then leads to a lower measured current in the electrode [199].

For detection of airborne chemicals and warfare agents biosensors using immobilized photosynthetic microorganisms have been developed [200]. These sensors measure the fluorescence from the algae directly and signal output is based on induction of fluorescence by living photosynthetic cyanobacteria and algae. The cyanobacteria and algae are immobilized on Millipore fiberglass filter disks and the sensory cell chamber is a closed-system aeration apparatus designed to infuse bench air through the fiberglass. A hand-held fluorimetric detector is connected to the cell chamber and used to measure the photochemical efficiency of the green algae and cyanobacteria. By use of this system the toxicity of chemical-warfare agents such as tabun, sarin, mustard gas, tributylamine, or dibutyl sulfide have been tested.

Genetically engineered bioluminescent or fluorescent whole-cell biosensors have also been used to detect a variety of gas-based toxicity [100, 201, 203, 204]. In particular, these biosensors were constructed to detect the volatile organic compounds benzene, toluene, ethylbenzene, or xylene (BTEX). To achieve this, one group constructed a *tod-luxCDABE*-based fusion and integrated it into the chromosome of *P. putida* F1. As discussed earlier, this strain can sensitively detect BTEX compounds and responds with an increase in its bioluminescence in the their presence [100]. A green fluorescent protein-based *Pseudomonas fluorescens* strain A506 has also been constructed to detect BTEX compounds.

This whole-cell biosensor is based on a plasmid carrying the toluene–benzene utilization pathway transcriptional activator, TbuT, from *Ralstonia pickettii* PKO1 and a transcriptional fusion of its promoter *PtbuA1* with a promoterless *gfp* gene on a broad-host-range promoter probe vector [203].

The bioluminescent character of other recombinant cells can also be used to develop fiber optic-based detection systems. Such systems are applicable in the development of different biosensors. One example is the development of a biosensor for detection of benzene gas toxicity using a bioluminescent *E. coli* immobilized within an LB agar matrix [201]. The cells and matrix were left to solidify inside a small plastic tube and this was then fixed to the end of a fiber optic probe so the bioluminescence could be measured continuously. Immobilization of the cells within the LB agar was done to prolong the activity of the microorganisms and to enable the detection of chemicals by direct contact with the gas. Further tests to enhance the sensitivity of the biosensor investigated the effect glass beads and the thickness of the immobilized agar matrix. It was found that sensitivity was enhanced both by addition of glass beads to the matrix, which increased gas diffusion through the agar medium, and use of a thinner matrix [204].

3.1.1.3 Soil-contamination biomonitoring

Biosensors that use living organisms or enzymatic materials have also been employed in the detection of toxic chemicals extracted from soil samples or for direct assessment of soil bioremediation. For instance, heavy metal ions [205–208], polyaromatic hydrocarbons [156, 209, 210], and phenolic compounds [110] extracted from soil have been detected by use of bioluminescent biosensors. Immunosensors have also been applied to the detection of herbicides [211] and pesticides [212].

One example of a fiber optic-based soil biosensor used the genetically engineered *P. putida* strain RB1353, which carries a plasmid-borne fusion of the genes for salicylate degradation (*nah*) and luminescence (*lux*) [174]. This strain was used to examine the relationship between microbial activity and the resulting impact on biodegradation and transport of salicylate in porous media. In this study, the biosensor consisted of a sample cell, optical fiber, detector, conditioning circuit, and signal processor. The maximum luminescence of the biosensing cells was linearly correlated with salicylate concentration and the minimum detection level, in a homogeneous porous medium, was 6.7 mg L^{-1}. Another naphthalene/salicylate sensor, *Pseudomonas fluorescens* HK44, which has a fusion of the *nahG* promoter and the *luxCDABE* operon from *V. fisheri*, was developed by Heitzer et al. [156]. This strain was immobilized on an optical liquid light guide using alginate and was found to be responsive to the presence of salicylate and naphthalene in waste streams for longer than 10 h. This system was also used to track these compounds in soil contaminated with naphthalene and salicylate.

However, application of the above whole-cell indicators to in-situ field studies with soil extracts should be done using the appropriate equipment. To accomplish this, a bioluminescent biosensor that uses constitutive bioluminescence to

detect the toxicity of polycyclic aromatic hydrocarbon (PAH) in contaminated soils was developed and applied, along with a fiber optic system, to assess a bioremediation process [210]. The system utilized a biosurfactant, rhamnolipids, to extract the PAHs, phenanthrene in this case, because it was found to be nontoxic while enhancing the bioavailability of hydrophobic compounds by increasing their rate of mass transfer from the sorbed soil particles to the aqueous phase. Monitoring of phenanthrene toxicity and, therefore, its concentration, was achieved by observing the decrease in bioluminescence when a sample extracted with the biosurfactant was injected into a sealed bioreactor, where it was exposed to the immobilized sensor. This study showed that aqueous-phase concentrations of phenanthrene and other PAHs correlated well with the corresponding toxicity data obtained with this biosensor kit [209, 213].

3.1.2
Suspension culture-based biosensors

Suspension cultures, such as those in batch or bioreactor-based experiments, can be applied to the continuous monitoring of water most easily if appropriate unit systems are developed.

One of the first examples of the use of genetically engineered bacteria in a continuous water-monitoring system was that of Gu et al. [214] in their study of the detection of heat-shock-inducible materials. Furthermore, a two-stage continuous monitoring system evolved from the design for the one stage system, providing the theoretical basis for a truly continuous system [215]. In this system the first mini-bioreactor, in which the bioluminescent strains are cultured, is connected to the second mini-bioreactor and fresh cells are continuously pumped from the first mini-bioreactor to the second. The second bioreactor is where biosensing occurs, with toxic chemicals being pumped into the bioreactor through a different port. The use of a fiber optic port also enabled autonomous measurement of the bioluminescence by connecting the reactor with a luminometer. The major breakthrough of this system is that, because fresh cells are continuously pumped into the second mini-bioreactor, the system can be maintained without system shut-down even when significant toxicity is experienced.

The sensitivity of the two-stage system was then optimized for each of the strains tested by varying the rate of dilution of each mini-reactor [216]. This system was then expanded into a multi-channel (four-channel) system that enabled several different recombinant bioluminescent bacteria to be used concurrently [217] (Fig. 6). Using this system, the potential toxicity of a field water sample can be classified within a few hours, providing information about the modes of toxicity according to the specificity of the different bioluminescent bacteria cultured in each reactor [187, 217]. Another application of the continuous bioreactor system is that of an early warning system for wastewater or contaminated sites; it can also be used to track pollution using an on-line, in-situ arrangement.

Another application of suspension-based biosensing cells is in the monitoring of bacterial cell growth. One study monitored the light emission of a strain genetically engineered to give constitutive bioluminescence; the simple sensor

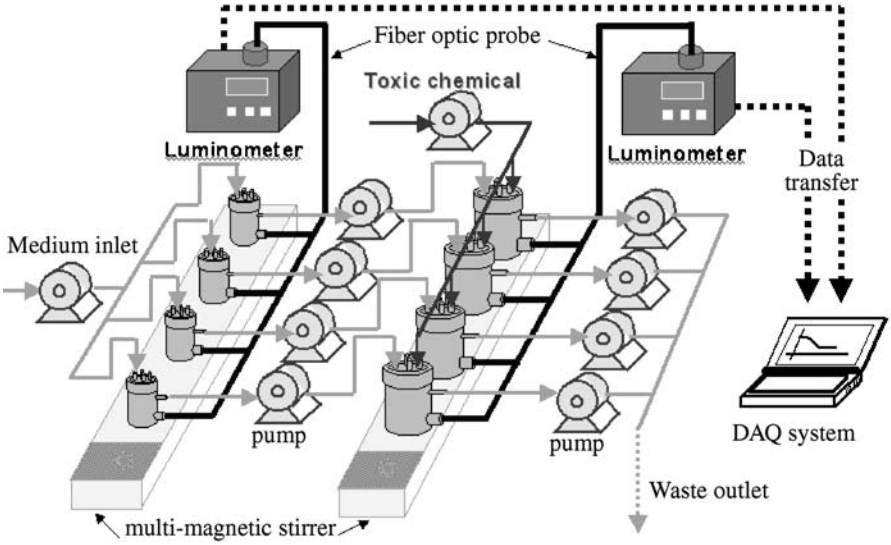

Fig. 6 Multi-channel continuous system for water toxicity monitoring

set-up used consisted of a photodiode, a photo-detector amplifier, and a recorder [218]. The changes in the bioluminescence and cell-forming units (CFU) of the cultures were found to correlate well with each other and were in proportion to the growth phase of cultures when grown at temperatures between 28 °C and 40 °C. The on-line technology used in this study can be used to observe specific cell growth when exposed to different water conditions. Although biosensors of this type are limited in their use as continuous monitoring tools, they can still be used as diagnostic tools for a quick, easy, and inexpensive detection of environmental contaminants.

Many suspension-based systems use the simple procedure of adding the test sample directly to the growing culture of the biosensing cells, albeit if there are no solvent effects. One example is the *lux*-based biosensors constructed with pUCD607 to determine the toxicity of heavy metals (Cd, Cu) using inhibition of bioluminescence from *P. fluorescens* 10586s and *Rhizobium leguminosarum* bv *trifolii* F6 [205]. By use of similar procedures the toxicity of Zn and Cu ions in a soil extract was determined by use of a Rhizobium-based luminescence biosensor [206]. In another study, after random insertion of *P. fluorescens* strain DF57 with a Tn5::*luxAB* promoter probe transposon, a mutant induced by copper was selected and used to assess bioavailable copper in soil solutions [207]. The toxicity of mercury and arsenite in soil extracts was also determined by using *P. fluorescens* OS8 (pTPT11) and *P. fluorescens* OS8 (pTPT13), respectively [208]. Three different soil types (humus, mineral, and clay) were initially spiked with mercury and arsenite to determine the efficacy of these strains with the different soil characteristics. The results of the tests showed that these mercury and arsenite biosensors were capable of detecting these metals, irrespective of the type of soil. In some studies, the cells were initially freeze-dried

to develop portable biosensors [84, 85]. To provide long-term storage of the cells before field application one study looked at four different cryoprotectants, trehalose, sucrose, sorbitol, and mannitol; trehalose and sucrose resulted in the best freeze-drying efficiency [84]. From this optimization study, portable biosensors were then developed [85]. The portable biosensor kit developed alongside these freeze-dried cells consisted of three sections – the freeze-dried biosensing strain (within a vial), a small light-tight test chamber, and an optical fiber connecting the sample chamber to a luminometer. This portable biosensor, with its very simple procedure of just adding 1 mL test water and monitoring the bioluminescence for an extended time, was proposed for use in field sample analysis and for in-situ monitoring of water systems.

In all these studies, however, the responses need to be optimized by manipulation of the procedure, e.g. determining the optimal aeration, optical density, solvent concentration and dilution rate. Also, each experiment provides information about a specific stress, chemical, or sample, a limitation inherent in all suspended cultures. Therefore, researchers have sought a procedure that will provide a more condensed survey of a sample, one that gives more information with little or no extra preparation or time. What they have come up with is high-throughput biosensor systems.

3.2 High-throughput biosensors

A variety of methods that utilize whole-cell-based biosensors have contributed to the development of high-throughput screening techniques [93, 219–222]. This development also stemmed from one of the merits of using whole cells – a researcher can easily perform high-throughput screening of chemical toxicity or for potentially beneficial drugs.

High-throughput systems typically use multi-well platform techniques. Such systems contain living cells and differ mainly in the supporting material and media used but offer an immense amount of data, especially for chemical studies. This type of system has been developed over a wide range of sizes, from a standard 96-well plate to a miniature transparent chip. Bioluminescence or fluorescence signals of multiple living cells from each well or spot can be detected and measured over time. When different types of cell are used within the same system the different response kinetics can be used to simultaneously measure and correlate the effects of compounds on multiple pathways [223].

One study applied four different stress-responsive bioluminescent *E. coli* strains within a high-throughput toxicity classification kit by immobilizing each within an LB-agar matrix in a single 96-well plate [93]. This kit was optimized according to the optical density of the cells, the storage time, and the specificity of each strain so that all strains could sensitively and simultaneously detects the test chemical. By use of this kit classification of different potential toxicity in aqueous samples was found to be possible, because of the high-throughput capability of this biosensor (Fig. 7). The responses of this system to phenolic compounds were compared to those of *Daphnia magana*, commonly used in aquatic monitoring systems [224].

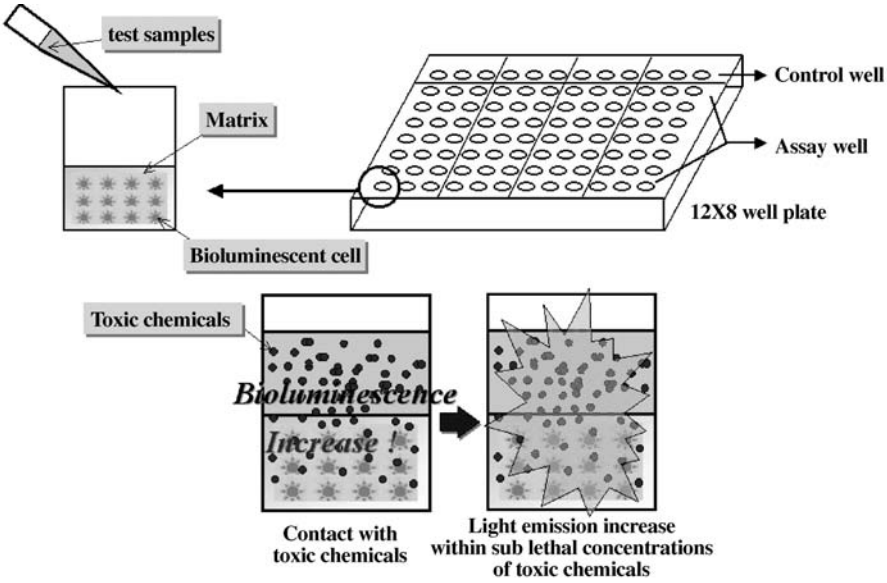

Fig. 7 High throughput bioluminescent whole-cell biosensor

Another study looked at the use of a sol–gel for immobilization to fabricate a basic biosensor system for the high-throughput screening of chemical toxicity [164]. By use of this method several bioluminescent *E. coli* strains were immobilized in thick silicate films. Heat shock-, oxidative stress-, fatty acid-, peroxide-, and genotoxicity-reporting bacteria were incorporated in the sol–gel silicate and the patterns of the bioluminescent emission were compared with those of non-immobilized cells. The encapsulated bacteria retained favorable biological properties better than their non-immobilized counterparts in terms of repeatability, shelf-life stability, sensitivity, and a broad-range response to a wide class of toxic compounds when tested with different chemicals.

In addition, a *lux*-array system was developed by Van Dyk et al. to perform high-throughput transcriptional analysis of *Escherichia coli* [225]. Each fragment of the *E. coli* genome was fused with the *Photorhabdus luminescence luxCDABE* operon and transformed back into *E. coli*. More than 1000 *E. coli* strains containing different reporter gene fusions were printed on to a membrane and used to detect the response of different genes to various compounds. The greatest merit of this system is that a transcriptional profile of a large part of the *E. coli* genome can be analyzed at one time in response to environmental stresses.

3.3 Chip-based biosensors

Another type of application that is becoming more popular is the use of cell chips. In these the cells are immobilized on to circuits so that their metabolic state and/or reporter synthesis can be monitoring by means of electric pulses.

One example, and a noteworthy application of stress- or chemical-specific responsive bioluminescent cells, is the development of the bioluminescent-bioreporter integrated circuit (BBIC) with its highly sensitive whole-cell biosensors [226, 227]. This system consists of two components – the cell immobilization matrix and the IC. Initially specific biosensing cells are constructed; these are then affixed to the integrated circuit (IC) by spraying a mixture of the cells and a liquid polymer on to the IC surface. When the cells come into contact with specific chemicals at or below the critical concentration (Fig. 1), the bioluminescence intensity increases. Although the surface of the IC is not in direct contact with the cells it can still measure the intensity of the photons, i.e. the bioluminescence, from the entrapped cells. The photons are recognized by the surface components of the IC and the generated signal can be analyzed and provide information, such as the minimum detectable signal (MDS) [228]. Because of its small size and ease of operation, under optimized conditions this system can be implemented as a highly sensitive tool for monitoring specific stresses or chemicals.

Aravanis et al. [229] developed a unique genetically engineered cell-based biosensor (GECBB) for functional classification of agents using an electrode. The cellular signal used in the GECBB was the spontaneous beat rate of two cardiomyocyte syncitia, which was measured with microelectrode arrays. This biosensor was found to be very sensitive and might be applied for many practical uses. The use of such an uncommon reporter suggests the possibility of a plethora of possible fusions between viable cells and electronic circuitry and clearly shows that biosensors can use any measurable response, even the beating of heart muscle cells.

4
Distinct applications of whole-cell-based environmental biosensors

Because of their diversity and simple nature, whole-cell-based biosensors can be used to monitor a variety of environmental pollutants and circumstances. The potential of these whole-cell sensors enables their application to a variety of unique and distinct areas of environmental contamination and for monitoring and assessment of environmental hazards.

4.1
EDCs and dioxins

Some chemicals disturb the endocrine system in eukaryotes, including humans, which has different effects on health as a result of interference with endogenous hormones in the organisms [230]. Such compounds are commonly referred to as endocrine-disrupting chemicals (EDCs). Harmful effects of EDCs have been monitored by use of biomarkers such as vitellogenin [231], choliogenin [232], and a DNA binding assay [233]. Mammalian cell-based assays are based on the binding reaction between endocrine-related triggers (or promoters) and EDCs [234]. Because EDCs are related to the endocrine system, most EDCs toxicity assays are performed with higher organisms. Recently, however, genetically engineered bioluminescent *E. coli*, which are sensitive to oxidative, DNA,

Table 3 Detection of EDCs and dioxins by use of recombinant bioluminescent *E. coli* [79, 237]

	Chemicals	Minimal detectable concentration (response ratio: 2.5)				EC_{20}
		DNA damage (*recA*::*lux*)	Membrane damage (*fabA*::*lux*)	Oxidative damage (*katG*::*lux*)	Protein damage (*grpE*::*lux*)	General damage (*lac*::*lux*)
EDCs	17-Estradiol	–[a]	–	–	–	–
	Bisphenol A	100	–	–	–	20,000
	Nonylphenol	–	25,000	15,000	25,000	100,000
	Styrene	–	–	20,000	–	–
	Phthalate	–	–	–	–	N.T.[b]
Dioxins	2,3,7,8-TCDD	0.05	–	–	–	0.1
	1,2,3,4,-TCDD	0.05	0.5	0.5	0.5	5
	2,8-DD	–	–	–	–	10
	2,3,7,8-TCDF	5	–	5	1	50
	PCBs	5	5	0.5	5	2
	PBDEs	0.5	–	1	1	2

Unit: ppb
[a] No response.
[b] Not tested.

membrane, or protein damage, have been applied to EDC toxicity monitoring and classification [79] (Table 3). Although this study focused on the toxic effects of EDCs to bacteria, not estrogenic effects, the compounds were found to be classifiable into several groups on the basis of the mechanisms of their toxic action.

Increases or decreases in the fluorescence from two recombinant fluorescent mammalian cells have also been used to monitor EDC toxicity [57]. Both the CMV promoter and the *c-fos* promoter were fused with the GFP gene and the resulting plasmids, pEGFP-N1 or pKCFG, respectively, were transfected into Chinese hamster ovary cells. The green fluorescence from these recombinant mammalian cells decreases or increases under toxic conditions as a result of inhibition of CMV promoter expression or activation of *c-fos* promoter expression, respectively. They were characterized with nonylphenol, ziram, and methyl bromide, all known EDCs. When the responses of the two mammalian cells were compared the pKCFG cell line was generally more sensitive. Comparisons also showed that these cell lines were 2- to 50-fold more sensitive to the test EDCs than were recombinant bacterial cells.

Because of their eukaryotic nature and their occurrence as single-cell organisms, yeast enable potentially quick analysis of EDCs and their effects. Several studies have highlighted this and have constructed different recombinant yeast strains to detect estrogenic effects [235–240], typically using a two-hybrid system with β-galactosidase as the reporter. Lee et al. studied not only the estrogenic effects of γ-hexachlorocyclohexane but also its degradation by-products; they found the estrogenic activity of 2,5-dichlorohydroquinone and chlorohydro-

quinone was similar to that of the original chemical whereas hydroquinone, a later stage metabolite, had no activity [240]. Toxic chemicals, for example chlorinated dibenzo-*p*-dioxins, are released into the environment mostly from combustion processes and move into the different environmental media as a result of a partitioning equilibrium based upon the physical and chemical properties of the chemicals. The monitoring of dioxin levels and temporal viability is therefore important for assessing and maintaining human health and the safety of ecosystems. Chemical analyses of these chemicals are sensitive and specific, but cannot provide information about the actual or potential biological activity of the contaminants [241]. Studies on the hazardous effects of dioxins have also been conducted using mammals, mostly in in-vitro or in-vivo bioassays [242–244].

A recombinant bioluminescent mammalian cell line has recently been used to assay the 2,3,7,8-tetrachlorodibenzo-*p*-dioxin (TCDD)-like activity of halogenated and polycyclic aromatic hydrocarbons [245]. Induction equivalents were determined by direct comparison of the EC50 and EC20 values from the dose – response curves for each petroleum product with those obtained with TCDD.

However, dioxins pose a toxic threat to all living organisms. Therefore, a recent study used several genetically engineered bioluminescent *E. coli* strains that are sensitive to different stresses to test the toxicity of different dioxin congeners and classify them on the basis of the responses [246] (Table 3).

4.2
Ionizing radiation and acoustic damage

The effect of ionizing radiation on microorganisms has been investigated by use of bacterial cells, in a test similar to the Ames test, to monitor genotoxic stress [247–250]. The genotoxic stress to microorganisms caused by ionizing and UV radiation was recently monitored by use of genetically engineered *E. coli* containing a plasmid bearing a fusion of a stress promoter and the *lux* operon or other genes, including *lacZ* [251, 252]. Min et al. [253] tested the effect of ionizing radiation (0.1–500 Gy) on three recombinant *E. coli*, which had the *recA*, *grpE* or *katG* stress promoter fused to the *lux* operon. The minimum dose of gamma-irradiation detected by the *recA* strain was about 1.5 Gy whereas the maximum bioluminescent response was obtained with 200 Gy. No specific responses were observed for the other strains. Ptitsyn et al. [254] have shown that an SOS *lux* system detected gamma-irradiation effects down to 2.56 Gy. Both of these studies clearly showed that ionizing radiation seriously damages DNA. Some of the more revolutionary work being done is, however, study of DNA damage and repair in space.

Horneck and Baumstark-Khan have co-authored numerous papers on their studies of the effects of space radiation and micro-gravity on the repair of damaged DNA [255–259]. In one of their studies they studied the effects of soil particles and meteorite composition on the protection of bacterial spores and found survival rates were very high (nearly 100%) when spores within a meteorite were exposed to space for two weeks [258], adding weight to the theory of Panspermia of the seeding of other worlds from one with life. In other studies

they investigated the use of fluorescence to study DNA unwinding, when broken by ionizing radiation, and cellular responses, measured through GFP production, in micro-gravity after exposure to ionizing radiation [255, 259].

Another type of damage to which living organisms are exposed is acoustic damage. To understand the effects of megahertz frequency ultrasound studies using *Escherichia coli* were performed with a panel of stress-responsive bioluminescent bioreporter strains. The results of the study showed that short pulses of 1-MHz ultrasound can induce stress responses, including membrane damage, heat shock, and the SOS response, in *E. coli* and, under some conditions, cause bacterial death. The most apparent damage attributed to ultrasound waves was the heat shock stress. Stationary-phase cultures were more resistant to acoustic effects than cells in the exponential phase [260].

4.3 Field and other applications

P. fluorescens HK44 has been approved for field-testing in the USA and subsequently used in bioremediation processes [210]. This strain has the *lux* genes fused within the naphthalene degradative pathway and, thus, produces bioluminescence as it degrades specific polyaromatic hydrocarbons, for example naphthalene. HK44 was inoculated into the vadose zone of intermediate-scale, semi-contained soil lysimeters contaminated with PAHs. For monitoring and controlling bioremediation the population dynamics were followed over an approximate two-year period. HK44 was found to survive in both hydrocarbon-contaminated and uncontaminated soils and was recoverable from soils 660 days post inoculation. Bioluminescence approaching a fourfold induction was detected in fiber optic-based biosensor devices responding to volatile polyaromatic hydrocarbons, compared with HK44 in uncontaminated soil. This first application of genetically engineered microorganisms (GEMs) in field applications offered hope they would be a viable option for in-situ determination of environmental contamination, bioavailability, and biodegradation process monitoring and control.

Biosensing using bioluminescent or fluorescent cells is not limited solely to chemical analysis. A simple in-vitro model of the population of a biofilm culture of bioluminescent *Pseudomonas aeruginosa* (pGLITE – the plasmid containing the *luxCDABE* operon of *Xenorhabdus luminescens*) was used for real-time monitoring of the antibacterial effects of ciprofloxacin [261]. Biofilms were grown using a Sorbarod filter plug, which consists of a cylindrical paper sleeve encasing a concertina of cellulose fiber. Each sorbarod was inoculated with exponentially growing *P. aeruginosa* pGLITE cells. Pseudo-steady state biofilms were exposed to 0.3 mg L^{-1} ciprofloxacin in the perfusing medium for 1 h. The viability of membrane-associated and eluted cells was assessed by means of viable cell counts and by monitoring the bioluminescence as a measure of metabolic activity. The use of bioluminescent bacteria proved to be a rapid and sensitive method for measurement of real-time antibacterial effects on a bacterial biofilm. Bioluminescence mutants of *Yersinia enterocolitica* were generated by transposon mutagenesis using a promoterless *lux* operon derived from *Photohabdus luminescens*,

and their bioluminescence during the production of cheese was monitored. The bioluminescence of the reporter mutant was significantly regulated by its environment, and by the growth phase, via the promoter fused to the *lux* operon. This is the first time a pathogen has been monitored in situ, in real time, and according to the status of a real product [262].

5 Concluding remarks

Whole cell- or organism-based biosensors have been continuously developed and updated in terms of their size, detection time, and field applicability by introduction of new technologies such as advances in signal measurement, visualization, and optical techniques. As shown in Fig. 8, organism-based biosensors are quite limited in their usage, detection time, and reproducibility. These limitations have been overcome with the use of whole-cell-based biosensors. The adoption of naturally bioluminescent bacterial cells as a means of detecting toxicity have reduced the detection time and size of the biosensors greatly, but the issues of reproducibility and classification of toxicity issues remain.

With the introduction of recombinant DNA technology cells have been designed and manipulated to develop very specific whole-cell-based biosensors, such as constitutive and stress- or chemical-specific whole-cell biosensors. As is apparent from Fig. 8, three different features, i.e. classification of the toxicity, applicability, and reproducibility, have been clearly improved compared with the simple use of naturally bioluminescent bacteria.

Whole-cell-based biosensors utilizing constitutive and stress- or chemical-specific promoters fused to reporter genes have been implemented in the field for environmental biomonitoring and other applications, since recombinant molecular technology, along with characterized genetic information, has been available. This type of approach accelerated when bacterial bioluminescence was

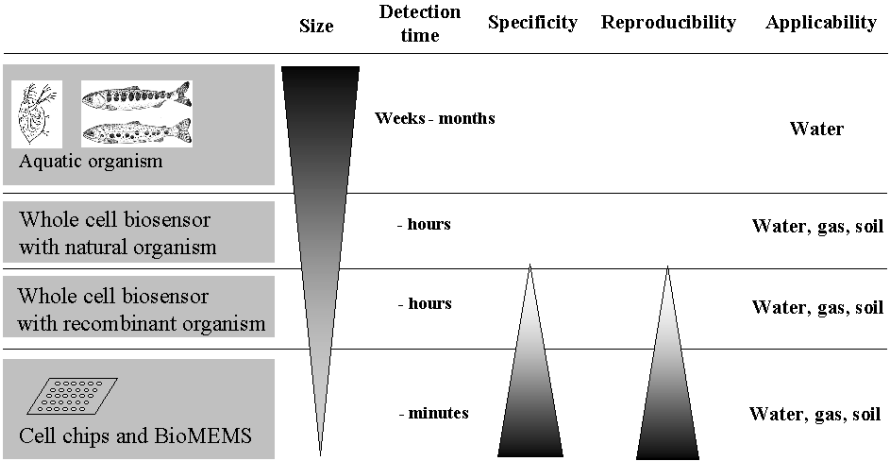

Fig. 8 Comparison of whole-organism and cell-based biosensors

introduced as a reporter gene, because there is no need to supply extra substrates or break down the cells to measure the reporting signal from the cells. One very unique and distinct merit of using bacterial bioluminescence is the possibility of on-line, in-situ monitoring of such biosensing cells. In this review the design and construction of these biosensing cells and their implementation and application into whole-cell-based biosensors were discussed. Furthermore, distinct and field application of these whole-cell biosensors for environmental biomonitoring have also been reviewed, with a few examples.

As shown in Fig. 8, whole-cell-based biosensors might possibly be further improved and their use might increase substantially in two different directions purely on the basis of the adoption of so-called micro electromechanical systems (MEMS) or nano electromechanical system (NEMS), to reduce the size of existing biosensors, and the implementation of DNA microarrays or protein chips, in the search for different chemical- or stress-specific inducible promoters. Whole-cell-based biosensors might be further reduced in size, with an increase in their functions, with high-throughput features, by adopting bioMEMS and bioNEMS technology. The development of bioMEMS- or bioNEMS-based whole-cell biosensors is expected. The design and construction of biosensing cells is receiving a boost from the use of DNA microarrays (and protein chips). The selection of constitutive or inducible promoters as possible candidates for signal switches has been solely based on genetic information obtained from studies performed previously (or trial-and-error-based search). However, with the high-throughput screening features of DNA microarrays based on snap shots of differential gene expression, this selection step for appropriate promoters is substantially simplified and shortened. It is truly a huge stepping-stone to the development of a variety of different biosensing cell batteries, which should result in partial or full development of cell chip-based biosensors with expanding features.

Acknowledgement This work was supported by the National Research Laboratory (2001 NRL) Program of Korea Institute of Science and Technology Evaluation and Planning (Project No. M10104000094–01J000004100).

6 References

1. Scheller F, Schmid RD (1991) GBF Monographs 17:419
2. Franklin NM, Stauber JL, Lim RP (2001) Environ Toxicol Chem 20:160
3. Riches CJ, Robinson PK, Rolph CE (1996) Biochem Soc Trans 24:174S
4. Cotelle S, Ferard JF (1996) Ecotoxicol Environ Saf 33:137
5. Orvos DR, Versteeg DJ, Inauen J, Capdevielle M, Rothenstein A, Cunningham V (2002) Environ Toxicol Chem 21:1338
6. Leung TS, Bulkley RV (1979) Bull Environ Contam Toxicol 23:236
7. Walker WW, Manning CS, Overstreet RM, Hawkins WE (1985) J Appl Toxicol 5:255
8. Chen HC, Pan IJ, Tu WJ, Lin WH, Hong CC, Brittelli MR (1996) Toxicol Pathol 24:696
9. Jain VK, Magrath IT (1991) Anal Biochem 199:119
10. Naylor LH (1999) Biochem Pharmacol 58:749
11. Ishikawa E, Kato K (1978) Scand J Immunol 8:34
12. Imagawa M, Yoshitake S, Ishikawa E, Endo Y, Ohtaki S, Kano E, Tsunetoshi Y (1981) Clin Chim Acta 117:190

13. Labrousse H, Guesdon JL, Ragimbeau J, Avrameas S (1982) J Immunol Methods 48:133
14. Craig D, Arriaga EA, Banks P, Zhang Y, Renborg A, Palcic MM, Dovichi NJ (1995) Anal Biochem 226:147
15. Bronstein L, Martin CS, Fortin JJ, Olesen CE, Voyta JC (1996) Clin Chem 42:1542
16. Morin J, Hastings J (1971) J Cell Physiol 77:313
17. Cubitt A, Heim R, Adams S, Boyd A, Gross L, Tsien R (1995) TIBS 20:448
18. Chalfie M, Tu Y, Euskirchen G, Ward W, Prasher D (1994) Science 263:802
19. Kahana J, Schapp B, Silver P (1995) Proc Natl Acad Sci USA 92:9707
20. Moores S, Sabry J, Spudich J (1996) Proc Natl Acad Sci USA 93:443
21. Casper S, Holt C (1996) Gene 173:69
22. Amsterdam A, Lin S, Moss L, Hopkins N (1996) Gene 173:99
23. Ludin B, Doll T, Meill R, Kaech S, Matus A (1996) Gene 173:107
24. Bassler BL (2002) Cell 109:421
25. Fuqua C, Parsek MR, Greenberg EP (2001) Annu Rev Genet 35:439
26. Meighen EA (1991) Microbiol Rev 55:123
27. Lewis JC, Feltus A, Ensor CM, Ramanathan S, Daunert S (1998) Anal Chem 70:579A
28. Ramanathan S, Ensor M, Daunert S (1997) Trends Biotechnol 15:500
29. Meighen EA (1992) Encyclo Microbiol 1:309
30. Boylan MO, Pelletier J, Dhepagnon S, Trudel S, Sonenberg N, Meighen EA (1989) J Biolumin Chemilumin 4:310
31. Escher A, O'Kane DJ, Lee J, Szalay AA (1989) Proc Natl Acad Sci USA 86:6528
32. Olsson O, Escher A, Sandberg G, Schell J, Koncz C, Szalay AA (1989) Gene 81:335
33. Kirchner G, Roberts JL, Gustafson GD, Ingolia TD (1989) Gene 81:349
34. Almashanu S, Musafia B, Hadar R, Suissa M, Kuhn J (1990) J Biolumin Chemilumin 5:89
35. Hollis RP, Lagido C, Pettitt J, Porter AJ, Killham K, Paton GI, Glover LA (2001) FEBS Lett 506:140
36. Billard P, DuBow MS (1998) Clin Biochem 31:1
37. Stewart GS, Williams P (1992) J Gen Microbiol 138:1289
38. Wilson T, Hastings JW (1998) Annu Rev Cell Dev Biol 14:197
39. de Wet JR, Wood KV, Helinski DR, DeLuca M (1985) Proc Natl Acad Sci USA 82:7870
40. de Wet JR, Wood KV, DeLuca M, Helinski DR, Subramani S (1987) Mol Cell Biol 7:725
41. Wood, K (1995) Photochem Photobiol 62:662
42. Airth RL, Rhodes WC, McElroy WD (1958) Biochim Biophys Acta 27:519
43. Wood KV (1991) In: Stanley PE, Kricka LJ (eds) Bioluminescence and chemiluminescence: current status. Wiley, Chichester, p 11
44. Lorenz WW, McCann RO, Longiaru M, Cormier MJ (1991) Proc Natl Acad Sci USA 88:4438
45. Bulich AA, Isenberg DL (1981) ISA Trans 20:29
46. Chang JC, Taylor PB, Leach FR (1981) Bull Environ Contam Toxicol 26:150
47. Morel JL, Bitton G, Koopman B (1988) Arch Environ Contam Toxicol 17:493
48. Symons BD, Sims RC (1988) Arch Environ Contam Toxicol 17:497
49. Middaugh DP, Resnick SM, Lantz SE, Heard CS, Mueller JG (1993) Arch Environ Contam Toxicol 24:165
50. Xi L, Cho KW, Tu SC (1991) J Bacteriol 173:1399
51. Marincs F, White DW (1994) Appl Environ Microbiol 60:3862
52. Voisey CR, Marincs F (1998) Biotechniques 24:56
53. Van Dyk TK, Rosson RA (1998) Methods Mol Biol 102:85
54. Lampinen J, Virta M, Karp M (1995) Appl Environ Microbiol 61:2981
55. Bi JX, Wirth M, Beer C, Kim EJ, Gu MB, Zeng AP (2002) J Biotechnol 93:231
56. Kim EJ, Lee Y, Lee JE, Gu MB (2002) Water Sci Technol 46:51
57. Hollis RP, Killham K, Glover LA (2000) Appl Environ Microbiol 66:1676
58. Lipinska B, King J, Ang D, Georgopoulos C (1988) Nucleic Acids Res 16:7545
59. Calendar R, Erickson JW, Halling C, Nolte A (1988) J Bacteriol 170:3479
60. Kitagawa M, C Wada, S Yoshioka, Yura T (1991) J Bacteriol 173:4247
61. Belkin S (1998) Methods Mol Biol 102:247
62. Ben-Israel O, Ben-Israel H, Ulitzur S (1998) Appl Environ Microbiol 64:4346

63. Goldstein J, Pollitt NS, Inouye M (1990) Proc Natl Acad Sci USA 87:283
64. Tanabe H, Goldstein J, Yang M, Inouye M (1992) J Bacteriol 174:3867
65. Hassan HM, Fridovich I (1978) J Biol Chem 253:6445
66. Belkin S, Smulski DR, Vollmer AC, Van Dyk TK, LaRossa RA (1996) Appl Environ Microbiol 62:2252
67. Belkin S (1998) Methods Mol Biol 102:189
68. Touati D (1983) J Bacteriol 155:1078
69. Compan I, Touati DJ (1993) Bacteriology 175:1687
70. Kogama T, Farr SB, Joycee KM, Natvig DO (1988) Proc Natl Acad Sci USA 85:4799
71. Weiseman JM, Weinstock GM (1985) J Bacteriol 163:748
72. Shinagawa H, Kato T, Ise T, Makino K, Nakata A (1983) Gene 23:167
73. Smith CM, Koch WH, Franklin SB, Foster PL, Cebula TA, Eisenstadt E (1990) J Bacteriol 172:4964
74. Weiseman JM, Weinstock GM (1991) Biochimie 73:457
75. Ptitsyn LR, Horneck G, Komova O, Kozubek S, Krasavin EA, Bonev M, Rettberg P (1997) Appl Environ Microbiol 63:4377
76. Vollmer AC, Belkin S, Smulski DR, Van Dyk TK, LaRossa RA (1997) Appl Environ Microbiol 63:2566
77. Min J, Kim EJ, LaRossa RA, Gu MB (1999) Mutat Res 442:61
78. Gu MB, Min J, LaRossa RA (2000) Biochem Biophys Methods 45:45
79. Gu MB, Min J, Kim EJ (2002) Chemosphere 46:289
80. Kenyon CJ, Walker GC (1980) Proc Natl Acad Sci USA 77:2819
81. Henry MF, Cronan JE Jr (1992) Cell 70:671–679
82. DiRusso CC, Metzger AK, Heimert TL (1993) Mol Microbiol 7:311
83. Bechor O, Smulski DR, Van Dyk TK, LaRossa RA, Belkin S (2002) J Biotechnol 94:125
84. Gu MB, Choi SH, Kim SW (2001) J Biotechnol 88:95
85. Choi SH, Gu MB (2002) Biosens Bioelectron 17:433
86. Forst SA, Delgado J, Inouye M (1989) J Bacteriol 171:2949
87. Anderson J, Forsk SA, Zhao K, Inouye M, Delihas N (1989) J Biol Chem 264:17961
88. Csonka LN (1989) Microbiol Rev 53:121
89. Yim HH, Brems RL, Villarejo M (1994) J Bacteriol 176:100
90. Nystrom T, Neidhardt FC (1992) Mol Microbiol 6:3187
91. Nystrom T, Neidhardt FC (1994) Mol Microbiol 11:537
92. Van Dyk TK, Smulski DR, Reed TR, Belkin S, Vollmer AC, LaRossa RA (1995) Appl Environ Microbiol 61:4124
93. Kim BC, Gu MB (2003) Biosens Bioelectron 18:1015–1021
94. Lee HJ, Gu MB (2003) Appl Microbiol Biotechnol 60:577–580
95. Milo R, Shen-Orr S, Itzkovitz S, Kashtan N, Chklovskii D, Alon U (2002) Science 298:824
96. Ronen M, Rosenberg R, Shraiman BI, Alon U (2002) Proc Natl Acad Sci USA 99:10555
97. Shen-Orr SS, Milo R, Mangan S, Alon U (2002) Nat Genet 31:64
98. Kalir S, McClure J, Pabbaraju K, Southward C, Ronen M, Leibler S, Surette MG, Alon U (2001) Science 292:2080
99. Sticher P, Jaspers MC, Stemmler K, Harms H, Zehnder AJ, van der Meer JR (1997) Appl Environ Microbiol 63:4053
100. Applegate BM, Kehrmeyer SR, Sayler GS (1998) Appl Environ Microbiol 64:2730
101. Inouye S, Nakazawa A, Nakazawa T (1983) J Bacteriol 155:1192
102. Inouye S, Nakazawa A, Nakazawa T (1985) J Bacteriol 163:863
103. Spooner RA, Lindsay K, Franklin FC (1986) J Gen Microbiol 132:1347
104. Ikariyama Y, Nishiguchi S, Koyama T, Kobatake E, Aizawa M, Tsuda M, Nakazawa T (1997) Anal Chem 69:2600
105. Applegate B, Kelly C, Lackey L, McPherson J, Kehrmeyer S, Menn FM, Bienkowski P, Sayler G (1997) J Ind Microbiol Biotechnol 18:4
106. Kelly CJ, Bienkowski PR, Sayler GS (2000) Biotechnol Bioeng 69:256
107. Wise AA, Kuske CR (2000) Appl Environ Microbiol 66:163
108. Shingler V, Moore T (1994) J Bacteriol 176:1555

109. Abd-El-Haleem D, Ripp S, Scott C, Sayler GS (2002) J Ind Microbiol Biotechnol 29:233
110. Hay AG, Rice JF, Applegate BM, Bright NG, Sayler GS (2000) Appl Environ Microbiol 66:4589
111. Zhou NY, Fuenmayor SL, Williams PA (2001) J Bacteriol 183:700
112. Cebolla A, Sousa C, de Lorenzo V (1997) J Biol Chem 272:3986
113. Burlage RS, Sayler GS, Larimer F (1990) J Bacteriol 172:4749
114. Schell MA, Poser EF (1989) J Bacteriol 171:837
115. Schell MA, Wender PE (1986) J Bacteriol 166:9
116. Yen KM, Gunsalus IC (1985) J Bacteriol 162:1008
117. Schell MA (1985) Gene 36:301
118. Grund AD, Gunsalus IC (1983) J Bacteriol 156:89
119. Rozen Y, Nejidat A, Gartemann KH, Belkin H (1999) Chemosphere 38:633
120. Korpela MT, Kurittu JS, Karvinen JT, Karp MT (1998) Anal Chem 70:4457
121. Kurittu J, Karp M, Korpela M (2000) Luminescence 15:291
122. Kurittu J, Lonnberg S, Virta M, Karp M (2000) J Agric Food Chem 48:3372
123. Kurittu J, Lonnberg S, Virta M, Karp M (2000) J Food Prot 63:953
124. Pellinen T, Bylund G, Virta M, Niemi A, Karp M (2002) J Agric Food Chem 50:4812
125. Winson MK, Swift S, Fish L, Throup JP, Jorgensen F, Chhabra SR, Bycroft BW, Williams P, Stewart GS (1998) FEMS Microbiol Lett 163:185
126. Andersen JB, Heydorn A, Hentzer M, Eberl L, Geisenberger O, Christensen BB, Molin S, Givskov M (2001) Appl Environ Microbiol 67:575
127. Prest AG, Winson MK, Hammond JR, Stewart GS (1997) Lett Appl Microbiol 24:355
128. San Francisco MJ, Hope CL, Owolabi JB, Tisa LS, Rosen BP (1990) Nucleic Acids Res 18:619
129. Wu J, Rosen BP (1991) Mol Microbiol 5:1331
130. Rosenstein R, Peschel A, Wieland B, Gotz F (1992) J Bacteriol 174:3676
131. Corbisier P, Ji G, Nuyts G, Mergeay M, Silver S (1993) FEMS Microbiol Lett 110:231
132. Ramanathan S, Shi W, Rosen BP, Daunert S (1997) Anal Chem 69:3380
133. Tauriainen S, Virta M, Chang W, Karp M (1999) Anal Biochem 272:191
134. Rosen BP (2002) Comp Biochem Physiol A Mol Integr Physiol 133:689
135. Nies DH, Nies A, Chu L, Silver S (1989) Proc Natl Acad Sci USA 86:7351
136. Nies DH (1992) Plasmid 27:17
137. Nies DH (1992) J Bacteriol 174:8102
138. Nies DH (1995) J Bacteriol 177:2707
139. Erbe JL, Adams AC, Taylor KB, Hall LM (1996) J Ind Microbiol 17:80
140. Crupper SS, Worrell V, Stewart GC, Iandolo JJ (1999) J Bacteriol 181:4071
141. Riether KB, Dollard MA, Billard P (2001) Appl Microbiol Biotechnol 57:712
142. Bontidean I, Berggren C, Johansson G, Csoregi E, Mattiasson B, Lloyd JR, Jakeman KJ, Brown NL (1998) Anal Chem 70:4162
143. Peitzsch N, Eberz G, Nies DH (1998) Appl Environ Microbiol 64:453
144. Grass G, Grosse C, Nies DH (2000) J Bacteriol 182:1390
145. Tibazarwa C, Wuertz S, Mergeay M, Wyns L, van der Lelie D (2000) J Bacteriol 182:1399
146. Lee SM, Grass G, Rensing C, Barrett SR, Yates CJ, Stoyanov JV, Brown NL (2002) Biochem Biophys Res Commun 295:616
147. Outten FW, Huffman DL, Hale JA, O'Halloran TV (2001) J Biol Chem 276:30670
148. Grass G, Rensing C (2001) J Bacteriol 183:2145
149. Fong ST, Camakaris J, Lee BT (1995) Mol Microbiol 15:1127
150. Ross W, Park S, Summers AO (1989) J Bacteriol 171:4009
151. Condee CW, Summers AO (1992) J Bacteriol 174:8094
152. Smith T, Pitts K, McGarvey JA, Summers AO (1998) Appl Environ Microbiol 64:1328
153. Selifonova O, Burlage R, Barkay T (1993) Appl Environ Microbiol 59:3083
154. Hakkila K, Maksimow M, Karp M, Virta M (2002) Anal Biochem 301:235
155. Dunn NW, Gunsalus IC (1973) J Bacteriol 114:974
156. Heitzer A, Malachowsky K, Thonnard JE, Bienkowski PR, White DC, Sayler GS (1994) Appl Environ Microbiol 60:1487
157. Ford CZ, Sayler GS, Burlage RS (1999) Appl Microbiol Biotechnol 51:397

158. Bundy JG, Campbell CD, Paton GI (2001) J Environ Monit 3:404
159. Willardson BM, Wilkins JF, Rand TA, Schupp JM, Hill KK, Keim P, Jackson PJ (1998) Appl Environ Microbiol 64:1006
160. Bousse L (1996) Sens Actuators B 34:270
161. van der Schalie WH, Shedd TR, Knechtges PL, Widder MW (2001) Biosens Bioelectron 16:457
162. Heim S, Schnieder I, Binz D, Vogel A, Bilitewski U (1999) Biosens Bioelectron 14:187
163. Wolfbeis OS (2002) Anal Chem 74:2663
164. Prekumar JR, Rosen R, Belkin S, Lev O (2002) Anal Chim Acta 462:11
165. Yolcubal I, Piatt JJ, Pierce SA, Brusseau ML, Maier RM (2000) Anal Chim Acta 422:121
166. Riedel K (1994) Exp Techn Phys 40:63
167. Daunert S, Barrett G, Feliciano JS, Shetty RS, Shrestha S, Smith-Spencer W (2000) Chem Rev 100:2705
168. Bentley A, Atkinson A, Jezek J, Rawson DM (2001) Toxicol in Vitro 15:469
169. Rawson DM, Willmer AJ, Turner AP (1989) Biosensors 4:299
170. van der Lelie D, Corbisier P, Baeyens W, Wuertz S, Diels L, Mergeay M (1994) Res Microbiol 145:67
171. Shear JB, Fishman HA, Allbritton NL, Garigan D, Zare RN, Scheller RH (1995) Science 267:74
172. Rabbow E, Rettberg P, Baumstark-Khan C, Horneck G (2002) Anal Chim Acta 456:31
173. Weitz HJ, Campbell CD, Killham K (2002) Environ Microbiol 4:422
174. Yolcubal I, Piatt JJ, Pierce SA, Brusseau ML, Maier RM (2000) Anal Chim Acta 422:121
175. Polyak B, Bassis E, Novodvorets A, Belkin S, Marks RS (2001) Sens Actuators B 74:18
176. Sluyts H, van Hoff F, Cornet A, Paulussen J (1996) Environ Toxicol Chem 15:1317
177. Twist H, Edwards AC, Codd GA (1997) Water Res 31:2066
178. Benecke G, Falke W, Schmidt C (1982) Bull Environ Contam Toxicol 28:385
179. Gu MB, Dhurjati PS, Van Dyk TK, LaRossa RA (1996) Biotechnol Prog 12:393
180. Shedd TR, van der Schalie WH, Widder MW, Burton DT, Burrows EP (2001) Bull Environ Contam Toxicol 66:392
181. Sloof W (1979) Bull Environ Contam Toxicol 23:517
182. Diamond JM, Parson MJ, Gruber D (1990) Environ Toxicol Chem 9:3
183. Schmitz P, Krebs F, Urmer U (1994) Water Sci Technol 29:215
184. Kikuchi M, Wakabayashi M (1997) Bull Japanese Soc Sci Fish 63:627
185. Carins J Jr, Mount DI (1990) Environ Sci Technol 24:154
186. Gerhardt A (1999) Environ Sci Forum 9:95
187. Gu MB, Kim BC, Cho J, Hansen PD (2001) Environ Monit Assess 70:71
188. Rodriguea M, Sanderrs CA, Greenbaum E (2002) Biosens Bioelectron 17:843
189. Samson G, Popovic R (1988) Ecotoxicol Environ Saf 16:272
190. Conrad R, Büchel C, Wilhelm C, Arsalane W, Berkaloff C, Duval JC (1993) J Appl Phycol 5:505
191. Van der Heever JA, Grobbelaar JU (1998) Arch Environ Contam Toxicol 35:281
192. Védrine C, Leclerc J-C, Durrieu C, Tran-Minh C (2003) Biosens Bioelectron 18:457–463
193. Nessens M, Leclerc J-C, Tran-Minh C (2000) Ecotoxicol Environ Saf 46:181
194. Twist H, Edwards AC, Codd GA (1997) Water Res 31:2066
195. Dennison MJ, Hall JM, Turner APF (1995) Anal Chem 67:3922
196. Hammerle M, Hall EAH (1996) Biosens Bioelectron 11:239
197. Kaisheva A, Iliev I, Christov S, Kazareva R (1997) Sens Actuators B 44:571
198. Naessens M, Tran-Minh C (1998) Biosens Bioelectron 13:341
199. Lee JI, Karube I (1996) Biosens Bioelectron 11:1147
200. Sanders CA, Rodriguez M Jr, Greenbaum E (2001) Biosens Bioelectron 16:439
201. Gil GC, Mitchell RJ, Chang ST, Gu MB (2000) Biosens Bioelectron 15:23
202. Naessens M, Tran-Minh C (1998) Anal Chim Acta 364:153
203. Stiner L, Halverson LJ (2002) Appl Environ Microbiol 68:1962
204. Gil GC, Kim YJ, Gu MB (2002) Biosens Bioelectron
205. Palmer G, McFadzean R, Killham K, Sinclair A, Paton GI (1998) Chemosphere 36:2683

206. Chaudri AM, Lawlor K, Preston S, Paton GI, Killham K, McGrath SP (2000) Soil Biol Biochem 32:383
207. Tom-Petersen A, Hosbond C, Nybroe O (2001) FEMS Microbiol Ecol 38:59
208. Petänen T, Romantschuk M (2002) Anal Chim Acta 456:55
209. Gu MB, Chang ST (2001) Biosens Bioelectron 16:667
210. Ripp S, Nivens DE, Ahn Y, Werner C, Jarrell J IV, Easter JP, Cox CD, Burlage R, Sayler GS (2000) Environ Sci Technol 34:846
211. Anis RBW, Eldefrawi ME (1993) Anal Chim Acta 279:141
212. Kumaran S, Morita M (1995) Talanta 42:649
213. Lee HJ, Villaume J, Cullen DC, Kim BC, Gu MB (2003) Biosens Bioelectron 18:571–577
214. Gu MB, Dhurjati PS, Van Dyk TK, LaRossa RA (1996) Biotechnol Prog 12:393
215. Gu MB, Gil GC, Kim JH (1999) Biosens Bioelectron 14:355
216. Gu MB, Gil GC, Kim JH (2002) J Biotechnol 93:283
217. Gu MB, Gil GC (2001) Biosens Bioelectron 16:661
218. Marincs F (2000) Appl Microbiol Biotechnol 53:536
219. Fernandes PB (1998) Curr Opin Chem Biol 2:597
220. Mistelli T, Spector DL (1997) Nat Biotechnol 15:961
221. Kain SR (1999) Drug Discov Today 4:304
222. Deb KK, Srivastava KK, Srivastava R, Srivastava BS (2000) Biochem Biophys Res Commun 279:457
223. Giuliano KA, Taylor DL (1998) Trends Biotechnol 16:135
224. Kim BC, Park KS, Kim SD, Gu MB (2003) Biosens Bioelectron 18:821–826
225. Van Dyk TK, DeRose EJ, Gonye GE (2001) J Bacteriol 183:5496
226. Simpson ML, Sayler GS, Patterson G, Nivens DE, Bolton EK, Rochelle JM, Arnott JC, Applegate BM, Ripp S, Guillorn MA (2001) Sens Actuators B 72:134
227. Bolton EK, Sayler GS, Nivens DE, Rochelle M, Ripp S, Simpson ML (2002) Sens Actuators B 85:179
228. Simpson ML, Sayler GS, Applegate BM, Ripp S, Nivens DE, Paulus MJ, Jellison GE (1998) Trends Biotechnol 16:332
229. Aravanis AM, DeBusschere BD, Chruscinski AJ, Gilchrist KH, Kobilka BK, Kovacs GTA (2001) Biosens Bioelectron 16:571
230. Gascon J, Qubina A, Barcelo D (1997) Trend Anal Chem 16:554
231. Hansen PD, Dizer H, Hock B, Marx A, Sherry J, McMaster M, Blaise CH (1998) Trend Anal Chem 17:448
232. Omowunmi AS, Diane MW (1999) Environ Sci Technol 33:368A
233. Nishikawa J, Saito K, Goto J, Dakeyama F, Matsue M, Nishihara T (1999) Toxicol Appl Pharmacol 154:76
234. Zacharewski T (1997) Environ Sci Technol 31:613
235. Gaido KW, Leonard LS, Lovell S, Gould JC, Babai D, Portier CJ, McDonnell DP (1997) Toxicol Appl Pharmacol 143:205
236. Graumann K, Breithofer A, Jungbauer A (1999) Sci Total Environ 225:69
237. Masuyama H, Hiramatsu Y, Kunitomi M, Kudo T, MacDonald PN (2000) Mol Endocrinol 14:421
238. Taneda S, Hayashi H, Sakata M, Yoshino S, Suzuki A, Sagai M, Mori Y (2000) Biol Pharm Bull 23:1477
239. Witters HE, Vangenechten C, Berckmans PP (2001) Water Sci Technol 43:117
240. Lee HS, Miyauchi K, Nagata Y, Fukuda R, Sasagawa S, Endoh H, Kato S, Horiuchi H, Takagi M, Ohta A (2002) J Biochem (Tokyo) 131:399
241. Park JS, Kim JG (2002) Chemosphere 49:755
242. Hahn ME (2002) Sci Total Environ 289:49
243. Schneider UA, Brown MM, Logan RA, Millar LC, Bunce NJ (1995) Environ Sci Technol 29:2595
244. Sinclair PR, Walton HS, Gorman N, Jacobs JM, Sinclair JF (1997) Toxicol Appl Pharmacol 147:171
245. Ziccardi MH, Gardner IA, Mazet JAK, Denison MS (2002) Mar Pollut Bull 44:983

246. Min J, Pham CH, Gu MB (2003) Environ Toxicol Chem 22:233–238
247. Kozubek S, Krasavin EA, Amirtayev KG, Tokarova B, Soska I, Drasil V, Bonev M (1989) Mutat Res 210:221
248. Isiladar M, Bakale G (1984) Radiat Res 100:396
249. Kozubek S, Ogievertskaya MM, Krasavin EA, Drasil V, Soska J (1990) Mutat Res 230:1
250. Quillardet P, Frelat G, Nguyen VD, Hofnung M (1989) Mutat Res 216:251
251. Kozubek S, Ogievertskaya MM, Krasavin EA, Drasil V, Soska J (1990) Mutat Res 230:1
252. Nunoshiba T, Nishioka H (1991) Mutat Res 245:71
253. Min J, Lee CW, Moon SH, LaRossa RA, Gu MB (2000) Radiat Environ Biophys 39:41
254. Ptitsyn LR, Horneck G, Komova O, Kozubek S, Krasavin EA, Bonev M, Rettberg P (1997) Appl Environ Microbiol 63:4377
255. Baumstark-Khan C, Hellweg CE, Palm M, Horneck G (2001) Phys Med Suppl 1:210
256. Horneck G, Rettberg P, Kozubek S, Baumstark-Khan C, Rink H, Schafer M, Schmitz C (1997) Radiat Res 147:376
257. Horneck G, Rettberg P, Baumstark-Khan C, Rink H, Kozubek S, Schafer M, Schmitz C (1996) J Biotechnol 47:99
258. Horneck G, Rettberg P, Reitz G, Wehner J, Eschweiler U, Strauch K, Panitz C, Starke V, Baumstark-Khan C (2001) Orig Life Evol Biosph 31:527
259. Baumstark-Khan C, Hentschel U, Nikandrova Y, Krug J, Horneck G (2000) Photochem Photobiol 74:477
260. Vollmer AC, Kwakye S, Halpern M, Everbach EC (1998) Appl Environ Microbiol 64:3927
261. Parveen A, Smith G, Salisbury V, Nelson SM (2001) FEMS Microbiol Lett 199:115
262. Maoz A, Mayr R, Bresolin G, Neuhaus K, Francis KP, Scherer S (2002) Appl Environ Microbiol 68:5737

Received: May 2003

Author Index Volumes 51 – 87

Author Index Volumes 1 – 50 see Volume 50

Subject Index